PB90-164526

Evaluation of the RADM (Regional Acid Deposition Model) Gas-Phase Chemical Mechanism

California Univ., Riverside

Prepared for:

Environmental Protection Agency, Research Triangle Park, NC

Feb 90

U.S. Department of Commerce
National Technical Information Service

PB90-164526

EPA/600/3-90/001
February 1990

EVALUATION OF THE RADM GAS-PHASE CHEMICAL MECHANISM

by

William P. L. Carter

Statewide Air Pollution Research Center
University of California
Riverside, California 92521

and

Fredrick W. Lurmann

Lurmann Associates
1819 State St., Suite D
Santa Barbara, California 93103

Cooperative Agreement No. CR-814558-01-0

Project Officer

Marcia C. Dodge

Chemical Processes and Characterization Division
Atmospheric Research and Exposure Assessment Laboratory
Research Triangle Park, North Carolina 27711

ATMOSPHERIC RESEARCH AND EXPOSURE ASSESSMENT LABORATORY
OFFICE OF RESEARCH AND DEVELOPMENT
U. S. ENVIRONMENTAL PROTECTION AGENCY
RESEARCH TRIANGLE PARK, NC 27711

REPRODUCED BY
U.S. DEPARTMENT OF COMMERCE
NATIONAL TECHNICAL INFORMATION SERVICE
SPRINGFIELD, VA. 22161

TECHNICAL REPORT DATA
(Please read Instructions on the reverse before completing)

1. REPORT NO. EPA/600/3-90/001	2.	3. RECIPIENT'S ACCESSION NO. PB 90 164526 /AS
4. TITLE AND SUBTITLE EVALUATION OF THE RADM GAS-PHASE CHEMICAL MECHANISM		5. REPORT DATE February 1990
		6. PERFORMING ORGANIZATION CODE
7. AUTHOR(S) W. P. L. Carter and F. W. Lurmann		8. PERFORMING ORGANIZATION REPORT NO.
9. PERFORMING ORGANIZATION NAME AND ADDRESS Statewide Air Pollution Research Center University of California Riverside, California 92521		10. PROGRAM ELEMENT NO. N104/C/05/05-7139 (FY-89
		11. CONTRACT/GRANT NO. CA 814558
12. SPONSORING AGENCY NAME AND ADDRESS Atmospheric Research & Exposure Assessment Lab Office of Research and Development U.S. Environmental Protection Agency Research Triangle Park, North Carolina 27711		13. TYPE OF REPORT AND PERIOD COVERED Final (9/87 - 1/89)
		14. SPONSORING AGENCY CODE EPA/600/09

15. SUPPLEMENTARY NOTES

16. ABSTRACT

Results are presented of a program to independently evaluate the gas phase mechanism developed for use in the second version of the Regional Acid Deposition Model (RADM-II). The RADM mechanism was tested by comparing predictions against results of over 550 environmental chamber experiments carried out at the University of California at Riverside and at the University of North Carolina. Statistical summaries of the overall results and results for individual experiments are presented and discussed. A series of 90 test problems for use in sensitivity calculations to assess effects of alternative assumptions for gas-phase mechanisms used in regional models was also developed and used to test several condensation approaches for the RADM mechanism. As a result of the evaluation against chamber data and the sensitivity test calculations, recommendations were made for modifications to the RADM mechanism. Two modified RADM mechanisms, one involving primarily changes in parameter values and one where more extensive changes and use of fewer model species are involved, were developed. These modified mechanisms and their performance in simulating the chamber data and the sensitivity test problems are discussed.

17. KEY WORDS AND DOCUMENT ANALYSIS

a. DESCRIPTORS	b. IDENTIFIERS/OPEN ENDED TERMS	c. COSATI Field/Group

18. DISTRIBUTION STATEMENT RELEASE TO PUBLIC	19. SECURITY CLASS *(This Report)* UNCLASSIFIED	21. NO. OF PAGES 408
	20. SECURITY CLASS *(This page)* UNCLASSIFIED	22. PRICE

EPA Form 2220-1 (9-73)

NOTICE

The information in this document has been funded by the United States Environmental Protection Agency under Cooperative Agreement No. CR-814558-01-0 to the University of California at Riverside. It has been subject to the Agency's peer and administrative review, and it has been approved for publication as an EPA document. Mention of trade names or commercial products does not constitute endorsement or recommendation for use.

PREFACE

This final report describes an independent evaluation of the gas-phase mechanism developed by Dr. William R. Stockwell of the State University of New York at Albany for use in the Regional Acid Deposition Model (RADM). Although the authors are solely responsible for the preparation of this report and the development of its conclusions, the work described herein includes significant contributions by Dr. Stockwell and several other scientists. Dr. Stockwell participated in this effort by providing data files necessary to implement the several versions of the mechanism that were evaluated. He also evaluated the reviews and recommendations made by the authors throughout the program, incorporating many of these recommendations into the mechanism and generally keeping the authors informed on the continuing evolution of his mechanism and its implementation into RADM. In addition, Stockwell assisted our evaluation of the effects of peroxy radical approximations by providing us with a detailed mechanism to use as the standard. Without his cooperation and participation, the utility of this program to the overall assessment of the RADM model would have been highly limited.

In addition to Dr. Stockwell, several other scientists provided valuable assistance in this program. Dr. Paulette Middleton of the National Center of Atmospheric Research solicited our advice and participation in the development of the RADM emissions processing system and is responsible for many of the ideas discussed in Section 3.2 of this report. Dr. Harvey E. Jeffries and co-workers at the University of North Carolina, as subcontractors to this program, prepared the data files used to implement their new light characterization model for the UNC chamber, reviewed the input files we used when modeling the UNC chamber runs, and provided us with data for UNC runs we had not modeled previously. Dr. Roger Atkinson of the Statewide Air Pollution Research Center (SAPRC) at U. C. Riverside provided valuable assistance in the initial review of the RADM gas-phase mechanism for consistency with current chemical data and the results of the latest data evaluations. Finally, the authors wish to acknowledge the role played by Dr. Marcia C. Dodge of EPA/AREAL in conceiving of the need for an independent evaluation of the RADM gas-phase mechanism, and providing leadership in its overall direction, and her active interest in its progress.

The authors also wish to acknowledge the SAPRC staff members who provided major assistance in the preparation of this report. Ms. Minn P. Poe is responsible for the preparation of many of the figures, and also provided computer programming assistance throughout this program. Ms. Christy J. LaClaire is responsible for most of the word processing for this report.

ABSTRACT

Results are presented of a program to independently evaluate the gas phase mechanism developed for use in the second version of the Regional Acid Deposition Model (RADM-II). This work consisted of the following: (1) An initial review of the 1987 version of the RADM mechanism was carried out and several modifications were made to the mechanism prior to the major evaluation effort described in this report. (2) Assistance was provided to the RADM team in developing methods for processing emissions input for the RADM model and for representing aggregated VOCs in the model. (3) The RADM mechanism was tested by comparing predictions against results of over 550 environmental chamber experiments carried out at the University of California at Riverside and at the University of North Carolina (UNC). The testing using the UNC experiments incorporated an improved chamber light characterization model developed at UNC. Statistical summaries of the overall results and results for individual experiments are presented and discussed. (4) A series of 90 test problems for use in sensitivity calculations to assess effects of alternative assumptions for gas-phase mechanisms used in regional models were developed, and these were used to test several condensation approaches for the RADM mechanism. (5) As a result of this evaluation against the chamber data and the sensitivity test calculations, recommendations were made for modifications to the RADM mechanism concerning the representation of the gas-phase chemistry of the aromatics and the condensation of the representation of the higher alkanes. Two modified RADM mechanisms, one involving primarily changes in parameter values, and one where more extensive changes and use of fewer model species are involved, were developed. These modified mechanisms and their performance in simulating the chamber data and the sensitivity test problems are discussed. The version of the mechanism involving primarily parameter changes has been adopted by the RADM team for implementation into the model.

It is concluded that the RADM mechanism, as modified as a result of this program, represents the state-of-the-art in gas-phase atmospheric reaction mechanisms and is suitable for use in the regional acid deposition model. However, there are still major uncertainties in our understanding of atmospheric chemistry. Also, available chamber data are not sufficient for evaluating the ability of mechanisms to represent the low NO_x conditions characteristic of much of the regional modeling domain, nor for evaluating their prediction of peroxide species or organic acids. The major areas of uncertainty and needs for future research are discussed.

CONTENTS

Page

Tables....vii

Figures....xi

1. Introduction....1

2. The March 1988 RADM and Recommended Modified RADM Gas-Phase Chemical Mechanisms....5

  2.1 The March 1988 RADM Mechanism....6
  2.2 Recommended Modifications to the RADM Mechanism....29
    2.2.1 Recommended Modifications to the Aromatic Mechanism....29
    2.2.2 Condensed Higher Alkane Representation....37
    2.2.3 Modifications to the XNO2 Reactions....38
    2.2.4 Omitted OLN Reactions....40
    2.2.5 Parameter Modifications Resulting from Updated Emissions Assignments....40
  2.3 The Recommended Modified Mechanism (RADM-M)....41
  2.4 The Modified Parameter Mechanism (RADM-P)....42

3. Aggregation and Representation of Organic Emissions in RADM....57

  3.1 Introduction....57
  3.2 Aggregation of VOC Emissions Input for RADM....58
    3.2.1 Development of a Mechanism-Independent VOC Emissions Classification System....59
    3.2.2 Recommended Extensions to the VOC Emissions Classification System....73
    3.2.3 Aggregation of Emissions into the RADM Mechanism....76
  3.3 Derivation of Kinetic and Mechanistic Parameters for Lumped Model Species in RADM....87
    3.3.1 Mechanistic Parameters for Lumped Alkanes....93
    3.3.2 Mechanistic Parameters for Lumped Aromatics....97
    3.3.3 Mechanistic Parameters for Lumped Alkenes....99

4. Evaluation Against Environmental Chamber Data: Characterization and Lumping Procedures....100

  4.1 Introduction....100
  4.2 Characterization of Chamber Conditions....102
    4.2.1 Light Characterization....103
    4.2.2 Representation of Other Chamber-Dependent Effects....112
  4.3 Representation of Organics in Chamber Experiments....138

CONTENTS
(continued)

Page

5. Evaluation Against Environmental Chamber Data: Results............142

5.1 Organization of the Evaluation....................................143
5.2 Measures of Model Performance....................................146
5.3 Performance on Characterization Runs.............................149
5.4 Performance of the RADM Mechanism on Single Organic Runs.......155
  5.4.1 Carbonyl-NO_x Runs....................................155
  5.4.2 Alkene-NO_x Runs......................................162
  5.4.3 Alkane-NO_x Runs......................................169
  5.4.4 Aromatic-NO_x Runs....................................175
  5.4.5 Natural Hydrocarbon Runs................................184
  5.4.6 Performance in Simulations of Formaldehyde Yields......190
  5.4.7 Performance in Simulations of PAN Yields...............192
5.5 Performance of the RADM Mechanism on Runs with Organic Mixtures...195
5.6 Tests of the RADM VOC Aggregation Approach.......................218
5.7 Performance of the Recommended Modified Mechanisms...............219

6. Evaluation of Alternative Chemical Assumptions.......................242

6.1 Test Problems for Sensitivity Analysis...........................242
6.2 Presentation of Sensitivity Test Results..........................256
6.3 Treatment of Peroxy Radical Reactions.............................258
6.4 Lumping of Higher Alkanes...290
6.5 The Recommended vs. the March 1988 RADM Mechanisms...............292

7. Summary and Conclusions..310

7.1 Evaluation of Kinetic and Mechanistic Parameters.................312
7.2 Development of the Linkage Between the VOC Emissions Inventory and the RADM Mechanism...314
7.3 Mechanism Evaluation Against Chamber Data.........................315
7.4 Sensitivity Testing of Alternate Mechanistic Assumption........320
7.5 Recommendations..322
  7.5.1 Longer Term Research Needs.............................323
  7.5.2 Shorter Term Needs.....................................325

References..328

APPENDICES

A Selected Results of Simulations of All Experiments Modeled Using the RADM Mechanism................................333

B Selected Results of Simulations of All Organic-NO_x Experiments Modeled Using the RADM-M Mechanism.................356

C Selected Results of Simulations of All Organic-NO_x Experiments Modeled Using the RADM-P Mechanism.................373

TABLES

Table Number | Page

1. Model Species Employed in the March 1988 Version of the RADM Gas-Phase Chemical Mechanism........8

2. Listing of Reactions in the March 1988 Version of the RADM Gas-Phase Chemical Mechanism........11

3. Absorption Coefficients and Quantum Yields Used in Versions of the RADM Gas-Phase Chemical Mechanism Evaluated in this Study........19

4. Organic Model Species Employed in the Recommended Modified Version of the RADM Gas-Phase Chemical Mechanism (RADM-M)........43

5. Listing of the Organic Reactions in the Recommended Modified Version of the RADM Gas-Phase Chemical Mechanism (RADM-M)........45

6. Listing of the Organic Reactions in the Modified Parameter Version of the RADM Gas-Phase Chemical Mechanism (RADM-P)........51

7. Summary of the Emissions Groupings Using the 32-Class Scheme, Amounts of Each Emitted in the NAPAP Total U.S. Inventory, and Estimated Amounts Reacted in Conditions Representative of RADM Applications........71

8. Assignments of Emissions Groups to RADM Model Species........77

9. Averages of Parameters for Emissions Groups Lumped as C_{3+} Alkanes and for RADM Lumped Alkane Model Species, Derived Using the NAPAP Total U.S. Emissions Inventory........89

10. Averages of Parameters for Emissions Groups Lumped as Aromatics and for RADM Lumped Aromatic Model Species, Derived Using the NAPAP Total U.S. Emissions Inventory........90

11. Averages of Parameters for Emissions Groups Lumped as Non-Ethene Alkenes and for RADM Lumped Non-Ethene Alkene Model Species, Derived Using the NAPAP Total U.S. Emissions Inventory........91

12. Averages of Parameters for Emissions Represented by the Combined Higher Alkane (HC5 + HC8) Model Species Recommended for the RADM-M Mechanism........98

13. Summary of Chamber-Dependent Parameters Used in the Model Simulations of the SAPRC EC Chamber Runs........117

14. Summary of Chamber-Dependent Parameters Used in the Model Simulations of the SAPRC ITC Chamber Runs........119

TABLES
(continued)

Table Number | Page

15. Summary of Chamber-Dependent Parameters Used in the Model Simulations of the SAPRC OTC Chamber Runs.........................121

16. Values of the Continuous Chamber Radical Input Parameter, k_{RS}, used in Modeling SAPRC ITC and OTC Chamber Runs, and Averages of Measured Values Used to Derive Them............................124

17. Summary of Chamber-Dependent Parameters Used in the Model Simulations of the UNC Chamber Runs...............................125

18. Values of Adjustable Chamber-Dependent Parameters Employed in the Simulations of UNC Chamber Runs............................127

19. Selected Performance Statistics in the RADM Simulations of the NO_x-Air, CO-NO_x-Air, Pure Air, and Carbonyl-Air Runs...........150

20. Performance Statistics on Maximum Ozone and on NO Oxidation and Ozone Formation Rates in the Simulations of the Organic-NO_x-Air Runs Using the RADM Mechanism.....................156

21. Performance Statistics on Maximum Formaldehyde in the Simulations of the Organic-NO_x-Air Runs Using the RADM Mechanism...191

22. Performance Statistics on Maximum PAN in the Simulations of the Organic-NO_x-Air Runs Using the RADM Mechanism.................193

23. Comparison of Average Normalized Biases and Errors in Simulations of Chamber Experiments using the RADM Mechanism with Run-to-Run Adjustment of Rate Constants with Simulations using the Standard RADM VOC Aggregation Procedure..................220

24. Performance Statistics on Maximum Ozone and NO Oxidation and Ozone Formation Rates in the Simulations of Organic-NO_x-Air Runs Using the RADM-M Mechanism...................224

25. Performance Statistics on Maximum Ozone and NO Oxidation and Ozone Formation Rates in the Simulations of Organic-NO_x-Air Runs Using the RADM-P Mechanism...................226

26. Performance Statistics on Maximum Formaldehyde in the Simulations of Organic-NO_x-Air Runs Using the RADM-M Mechanism...228

27. Performance Statistics on Maximum Formaldehyde in the Simulations of Organic-NO_x-Air Runs Using the RADM-P Mechanism...229

TABLES
(continued)

Table Number | Page

28. Performance Statistics on Maximum PAN in the Simulations of Organic-NO_x-Air Runs Using the RADM-M Mechanism....................230

29. Performance Statistics on Maximum PAN in the Simulations of Organic-NO_x-Air Runs Using the RADM-P Mechanism....................231

30. Comparisons of Average Normalized Biases and Errors in Maximum Ozone and NO_x Oxidation Rates in the Simulations of Organic-NO_x-Air Runs Using the RADM, RADM-M, and RADM-P Mechanisms.........232

31. Environmental Conditions Used in Test Problems for Sensitivity Calculations..244

32. Compositions of ROG Surrogate Mixtures Used in Test Calculations..249

33. Compositions of ROG Surrogates Used in the Test Calculations for the RADM Mechanism...252

34. Summary of Conditions of Test Calculations Used for Sensitivity Studies..253

35. Organic Peroxy + Organic Peroxy Reactions Used in Stockwell's "Detailed Radical" Version of the RADM Mechanism..................262

36. Listing of the Organic Reactions in the Modified RADM Mechanism Incorporating the 1986 SAPRC Approach for Representing Reactions of Organic Peroxy Radicals.................270

37. Results of Sensitivity Test Calculations Using the Evaluated RADM Mechanism as the Test Mechanism, Relative to the "Detailed Radical" Mechanism as the Standard......................277

38. Results of Sensitivity Test Calculations for the Version of the RADM Mechanism Using the 1986 SAPRC Peroxy Radical Representation as the Test Mechanism, Relative to the "Detailed Radical" Mechanism as the Standard......................282

39. Results of Sensitivity Test Calculations Using the Version of the RADM Mechanism with the Higher Alkane Species HC5 and HC8 Lumped Together, Relative to the Standard RADM Mechanism...........293

40. Summary of Results of Sensitivity Test Calculations Using the Recommended Modified (RADM-M) and the Recommended Modified Parameter (RADM-P) Mechanisms, Relative to the March 1988 RADM Mechanism as the Standard...................................298

TABLES
(continued)

Table Number | Page

41. Results of Sensitivity Test Calculations of Urban Ozone Formation Using the Recommended Modified (RADM-M) and the Recommended Modified Parameter (RADM-P) Mechanisms, Relative to the March 1988 RADM Mechanism as the Standard....................301

42. Results of Sensitivity Test Calculations of Urban H_2O_2 Formation Using the Recommended Modified (RADM-M) and the Recommended Modified Parameter (RADM-P) Mechanisms, Relative to the March 1988 RADM Mechanism as the Standard....................304

FIGURES

Figure Number | | Page

1. Comparison of Fits of RADM and Modified RADM Simulations to Results of Toluene and Xylene-NO_x-Air Chamber Experiments........36

2. Experimental and Calculated Concentration-Time Plots for Selected Species in the UNC Formaldehyde-NO_x-Air Run AU0279B.......113

3. Experimental and Calculated Concentration-Time Plots for Selected Species in the UNC Complex Mixture-NO_x-Air Run ST1682B...114

4. Experimental and Calculated Concentration-Time Plots for Selected Species in the UNC Complex Mixture-NO_x-Air Run ST2981R...115

5. Comparison of Results of UNC Characterization Simulations Using Various Mechanisms and Chamber and Light Characterization Models...129

6. Hierarchy of Species for Mechanism Testing........................144

7. Calculated vs Experimental Changes in [NO] in NO_x-Air and CO-NO_x-Air Runs...151

8. Calculated vs Experimental Changes in [NO_2] in NO_x-Air and CO-NO_x-Air Runs...151

9. Calculated vs Experimental Maximum Ozone in the Pure Air and Carbonyl-Air Runs...153

10. Calculated vs Experimental Rate of Ozone Formation in the Pure Air and Carbonyl-Air Runs.....................................153

11. Histogram of Normalized Biases in Maximum Ozone in Pure Air and Carbonyl-Air Runs...154

12. Normalized Biases in Maximum Ozone vs HC/NO_x Ratios in Carbonyl-Air Runs...154

13. Calculated vs Experimental Maximum Ozone in Carbonyl-NO_x Runs...159

14. Calculated vs Experimental Rates of NO Oxidation and Ozone Formation in the Carbonyl-NO_x Runs................................159

15. Histogram of Normalized Biases in Maximum Ozone in Carbonyl-NO_x Runs...160

16. Normalized Bias in Maximum Ozone vs HC/NO_x Ratio in Carbonyl-NO_x-Runs..160

FIGURES
(continued)

Figure Number		Page
17.	Experimental and Calculated Concentration-Time Plots for Selected Species in Simulations of UNC Acetaldehyde-NO_x Run AU2482B	161
18.	Calculated vs Experimental Maximum Ozone in the Alkene-NO_x Runs for the RADM Mechanism	163
19.	Calculated vs Experimental Rates of NO Oxidation and Ozone Formation in the Alkene-NO_x Runs for the RADM Mechanism	163
20.	Histogram of Normalized Biases in Maximum Ozone in Alkene Runs for the RADM Mechanism	164
21.	Normalized Bias in Maximum Ozone vs HC/NO_x in Alkene Runs for the RADM Mechanism	164
22.	Experimental and Calculated Concentration-Time Plots for Selected Species in Simulations of UNC Ethene-NO_x Run OC0584B	165
23.	Experimental and Calculated Concentration-Time Plots for Selected Species in Simulations of the Propene-NO_x Run EC-216	166
24.	Experimental and Calculated Concentration-Time Plots for Selected Species in Simulations of UNC Propene-NO_x Run JL2983B	167
25.	Experimental and Calculated Concentration-Time Plots for Selected Species in Simulations of UNC 1-Butene-NO_x Run ST2583B	168
26.	Calculated vs Experimental Maximum Ozone in the Alkane-NO_x Runs for the RADM Mechanism	170
27.	Calculated vs Experimental Rates of NO Oxidation and Ozone Formation in the Alkane-NO_x Runs for the RADM Mechanism	170
28.	Histogram of Normalized Biases in Maximum Ozone in Alkane Runs for the RADM Mechanism	171
29.	Normalized Bias in Maximum Ozone vs HC/NO_x in Alkane Runs for the RADM Mechanism	171
30.	Experimental and Calculated Concentration-Time Plots for Selected Species in Simulations of n-Butane-NO_x Run EC-130	172

FIGURES
(continued)

Figure Number		Page
31.	Experimental and Calculated Concentration-Time Plots for Selected Species in Simulations of n-Octane-NO_x Run ITC-552........	173
32.	Experimental and Calculated Concentration-Time Plots for Selected Species in Simulations of UNC 2,3-Dimethylbutane -NO_x Run OC1789R..	174
33.	Calculated vs Experimental Maximum Ozone in the Aromatic-NO_x Runs for the RADM Mechanism....................................	176
34.	Calculated vs Experimental Rates of NO Oxidation and Ozone Formation in the Aromatic-NO_x Runs for the RADM Mechanism..........	176
35.	Histogram of Normalized Biases in Maximum Ozone in Aromatic Runs for the RADM Mechanism.....................................	177
36.	Normalized Bias in Maximum Ozone vs HC/NO_x in Aromatic Runs for the RADM Mechanism..	177
37.	Experimental and Calculated Concentration-Time Plots for Selected Species in Simulations of the Benzene-NO_x Run ITC-562..	178
38.	Experimental and Calculated Concentration-Time Plots for Selected Species in Simulations of the Toluene-NO_x Run EC-327...	179
39.	Experimental and Calculated Concentration-Time Plots for Selected Species in Simulations of the UNC Toluene-NO_x Run JL3080R..	180
40.	Experimental and Calculated Concentration-Time Plots for Selected Species in Simulations of the m-Xylene-NO_x Run ITC-702..	181
41.	Experimental and Calculated Concentration-Time Plots for Selected Species in Simulations of the UNC o-Xylene-NO_x Run JL3080B..	182
42.	Experimental and Calculated Concentration-Time Plots for Selected Species in Simulations of the Mesitylene-NO_x Run EC-901...	183
43.	Calculated vs Experimental Maximum Ozone in the Natural Hydrocarbon Runs for the RADM Mechanism..........................	185

FIGURES
(continued)

Figure Number | Page

44. Calculated vs Experimental Rates of NO Oxidation and Ozone Formation in the Natural Hydrocarbon Runs for the RADM Mechanism....185

45. Histogram of Normalized Bias in Maximum Ozone in the Natural Hydrocarbon Runs for the RADM Mechanism....186

46. Normalized Bias in Maximum Ozone vs HC/NO_x in the Natural Hydrocarbon for the RADM Mechanism....186

47. Experimental and Calculated Concentration-Time Plots for Selected Species in Simulations of the Isoprene-NO_x Run ITC-811....187

48. Experimental and Calculated Concentration-Time Plots for Selected Species in Simulations of the UNC Isoprene-NO_x Run JL1680B....188

49. Experimental and Calculated Concentration-Time Plots for Selected Species in Simulations of the UNC α-Pinene-NO_x Run JL1580B....189

50. Calculated vs Experimental Maximum Formaldehyde in the Single Organic-NO_x Runs for the RADM Mechanism....192

51. Calculated vs Experimental Maximum PAN in the Single Organic-NO_x Runs for the RADM Mechanism....194

52. Calculated vs Experimental Maximum Ozone in the Simple Mixture Runs for the RADM Mechanism....196

53. Calculated vs Experimental Rates of NO Oxidation and Ozone Formation in the Simple Mixture Runs for the RADM Mechanism....196

54. Histogram of Normalized Biases in Maximum Ozone in the Simple Mixture Runs for the RADM Mechanism....197

55. Normalized Bias in Maximum Ozone vs HC/NO_x in the Simple Mixture Runs for the RADM Mechanism....197

56. Calculated vs Experimental Maximum Ozone in the Surrogate Mixture Runs for the RADM Mechanism....198

57. Calculated vs Experimental Rates of NO Oxidation and Ozone Formation in the Surrogate Mixture Runs for the RADM Mechanism....198

FIGURES
(continued)

Figure Number | Page

58. Histogram of Normalized Biases in Maximum Ozone in the Surrogate Mixture Runs for the RADM Mechanism......................199

59. Normalized Bias in Maximum Ozone vs HC/NO_x in the Surrogate Mixture Runs for the RADM Mechanism................................199

60. Normalized Bias in Maximum Ozone vs Initial NO_x in the Surrogate Mixture Runs for the RADM Mechanism......................200

61. Normalized Bias in Maximum Ozone vs Initial HC in the Surrogate Mixture Runs for the RADM Mechanism......................200

62. Experimental and Calculated Concentration-Time Plots for Selected Species in Simulations of the UNC Mixed Alkene Run OC1278R...201

63. Experimental and Calculated Concentration-Time Plots for Selected Species in Simulations of the 7 Hydrocarbon Surrogate Run EC-237...202

64. Experimental and Calculated Concentration-Time Plots for Selected Species in Simulations of the 8 Hydrocarbon Surrogate, Multi-Day Run ITC-630..................................203

65. Experimental and Calculated Concentration-Time Plots for Selected Species in Simulations of the 8 Hydrocarbon Surrogate, Multi-Day Run ITC-633..................................204

66. Experimental and Calculated Concentration-Time Plots for Selected Species in Simulations of the 8 Hydrocarbon Surrogate, Multi-Day Run ITC-637..................................205

67. Experimental and Calculated Concentration-Time Plots for Selected Species in Simulations of the 8 Hydrocarbon Surrogate, Multi-Day Run OTC-192B.................................206

68. Experimental and Calculated Concentration-Time Plots for Selected Species in Simulations of the 8 Hydrocarbon Surrogate, Multi-Day Run OTC-195A.................................207

69. Experimental and Calculated Concentration-Time Plots for Selected Species in Simulations of the 8 Hydrocarbon Surrogate, Multi-Day Run OTC-202B.................................208

70. Experimental and Calculated Concentration-Time Plots for Selected Species in Simulations of the 8 Hydrocarbon Surrogate, Multi-Day Run OTC-224B.................................209

FIGURES
(continued)

Figure Number | Page

71. Experimental and Calculated Concentration-Time Plots for Selected Species in Simulations of the UNC 3 Hydrocarbon Surrogate Run JN1483R....210

72. Experimental and Calculated Concentration-Time Plots for Selected Species in Simulations of the UNC Miscellaneous Surrogate Run AU2681B....211

73. Experimental and Calculated Concentration-Time Plots for Selected Species in Simulations of the UNC Synurban Surrogate Run JN2685R....212

74. Experimental and Calculated Concentration-Time Plots for Selected Species in Simulations of the UNC Synauto Surrogate Run AU0684R....213

75. Experimental and Calculated Concentration-Time Plots for Selected Species in Simulations of the UNC Auto Exhaust Run AU1183R....214

76. Calculated vs Experimental Maximum Formaldehyde in the Simple Mixture Runs for the RADM Mechanism....216

77. Calculated vs Experimental Maximum Formaldehyde in the Surrogate Mixture Runs for the RADM Mechanism....216

78. Calculated vs Experimental Maximum PAN in the Simple Mixture Runs for the RADM Mechanism....217

79. Calculated vs Experimental Maximum PAN in the Surrogate Mixture Runs for the RADM Mechanism....217

80. Plots of Maximum Ozone Yields in Simulations of Organic Mixture Experiments using the RADM Mechanism with Run-to-Run Adjustment of Rate Constants Against Yields Calculated Using the Standard RADM VOC Aggregation Procedure....222

81. Calculated vs Experimental Maximum Ozone in the Surrogate Mixture Runs for the RADM-M Mechanism....235

82. Calculated vs Experimental Maximum Ozone in the Surrogate Mixture Runs for the RADM-P Mechanism....235

83. Calculated vs Experimental Maximum Ozone in the Alkane-NO_x Runs for the RADM-M Mechanism....236

84. Calculated vs Experimental Maximum Ozone in the Alkane-NO_x Runs for the RADM-P Mechanism....236

FIGURES
(continued)

Figure Number | Page

85. Calculated vs Experimental Maximum Ozone in the Aromatic-NO_x Runs for the RADM-M Mechanism....237

86. Calculated vs Experimental Maximum Ozone in the Aromatic-NO_x Runs for the RADM-P Mechanism....237

87. Comparisons of Maximum Ozone Calculated using the RADM-M and the Unmodified RADM Mechanisms for Simple and Surrogate Mixture Runs....240

88. Comparisons of Maximum Ozone Calculated using the RADM-P and the Unmodified RADM Mechanisms for Simple and Surrogate Mixture Runs....240

89. Concentration-Time Plots for Selected Species Calculated Using the RADM, RADM-M, and RADM-P Mechanisms for the Summer Surface Static Urban Test Problem with Initial NO_x of 67 ppb and a ROG/NO_x Ratio of 10....307

90. Concentration-Time Plots for Selected Species Calculated Using the RADM, RADM-M, and RADM-P Mechanisms for the Winter Surface Static Urban Test Problem with Initial NO_x of 67 ppb and a ROG/NO_x Ratio of 10....308

1. INTRODUCTION

The Regional Acid Deposition Model (RADM) plays a central role in the National Acid Precipitation Assessment Program's (NAPAP) plan to develop an understanding of source-receptor relationships for acidifying pollutants in the United States. This model is needed to formulate appropriate and cost-effective emission control policies to mitigate the potentially damaging effects of acid deposition. While transport, deposition, and chemistry all play important roles in the acid deposition phenomenon, the chemistry plays a particularly important role in determining the response of the acid deposition system to major changes in NO_x and SO_x emissions. The chemistry submodel is the only component of the overall modeling system that is capable of predicting nonlinearly in the relationship between source emissions and acid deposition. Thus, it is critically important that any chemical mechanism incorporated into the RADM model be fully evaluated using the best available data and that it be recognized by the scientific community as representing the current state-of-the-art in our understanding of atmospheric chemistry.

Although the full RADM model must incorporate both gas phase and aqueous phase chemistry, the study described in this report addresses only the gas phase portion of the chemistry module. As presently implemented, only the gas phase species are transported within the model, and their concentrations at each time step are used to drive the aqueous phase chemistry, based on stationary state approximations. Therefore, the gas phase chemistry module contributes substantially to any non-linearities predicted by the model. The gas phase chemistry module is also important because, as implemented in the first version of the RADM model (RADM-I), approximately 75% of the computer time is consumed in calculating the gas phase transformations. This is with a smaller version of the gas phase chemical mechanism (Stockwell, 1986) than the one proposed for use in the second version of this model. Thus, clearly the efficiency and appropriateness of the level of detail in the gas phase transformation mechanism, as well as its accuracy and scientific validity, is an important issue which needs to be addressed.

Because of computer constraints, the gas-phase chemistry module in the first version of the RADM model (Stockwell, 1986) was highly condensed and contained a number of approximations that were chemically unrealistic. With the expanded memory capacities of the newer computers, a new, more detailed gas-phase chemical mechanism was proposed for use in the second version of the RADM model (designated RADM-II) which is now under development (NCAR, 1987). Although in terms of chemical detail and consistency with current knowledge, this new RADM gas-phase mechanism is an improvement over the previous version, it had not undergone the external review and comprehensive evaluation that is necessary for such an important component of a model which will be used in making policy decisions. For example, this new mechanism had undergone only limited testing against the results of a small number of environmental chamber experiments. In contrast, the mechanisms most recently developed for use in oxidant and EKMA models have been tested against results of hundreds of experiments carried out in several different chambers (Carter et al., 1986; Gery et al., 1988). The December 1986 EPA workshop on evaluation and documentation of chemical mechanisms for use in air quality simulation models concluded that an extensive testing program against chamber data is an important part of the overall evaluation process for such mechanisms (EPA, 1987). In addition, the new RADM mechanism had not undergone external review for consistency with available laboratory data and current chemical knowledge. Such a review and evaluation would be particularly useful prior to the implementation of the mechanism in RADM, when any problems can be more readily corrected. To address this need, the EPA contracted the Statewide Air Pollution Center (SAPRC) at the University of California at Riverside to carry out an independent review and evaluation of this new proposed gas-phase chemical mechanism for RADM, and to make suggestions and recommendations concerning areas where the mechanism might be improved.

This evaluation program was a cooperative effort involving the authors of this report at SAPRC and Lurmann and Associates, Dr. Harvey Jeffries and his group at the University of North Carolina (UNC), Dr. William Stockwell at the State University of New York (SUNY), and Dr. Paulette Middleton at the National Center for Atmospheric Research (NCAR). The evaluation itself was carried out at SAPRC with the assistance of Lurmann and Associates. Dr Jeffries and his group assisted in this effort by reviewing the input data used when testing the mechanism against results of UNC chamber experiments and preparing input data to implement a new model for light characterization in that chamber (Jeffries et al., 1989a). Dr. Stockwell, the principal developer of the RADM-II mechanism and the member of the RADM team ultimately responsible for the gas-phase mechanism which will be used in RADM-II, provided the initial and modified versions of the mechanism which were evaluated in this program, and served as an overall consultant on this project. Dr. Middleton is responsible for preparing the emissions input for the RADM model and as part of this program, SAPRC worked with her in developing appropriate procedures for processing organic emissions data for use with this mechanism. This report describes primarily the work on this evaluation effort carried out by SAPRC and Lurmann and Associates.

This evaluation effort involved several separate, though related, tasks: (1) SAPRC carried out an initial review of a preliminary version of the RADM-II mechanism (NCAR, 1987) to determine its consistency with current data and data evaluations and made recommendations for modifications. As a result of these recommendations, Stockwell made some modifications in the RADM-II mechanism prior to its implementation on SAPRC computers for further evaluation. (2) SAPRC also made recommendations regarding organic emissions processing procedures and methods used in the mechanism to represent organic emissions. Most of these recommendations were subsequently implemented in the RADM-II mechanism and in emissions processing procedures developed for it. (3) With the assistance of UNC, modifications were made in the light characterization and chamber effects models used when testing mechanisms against UNC chamber data. (4) The predictions of the RADM-II mechanism, as modified by Stockwell as a result of the initial review, was tested against the results of approximately 550 UNC and SAPRC chamber runs, and a statistical analysis of the results was carried out. Other modified versions of the RADM mechanism were tested against these chamber data as well. (5) A number of alternative mechanistic assumptions and condensation approaches for the RADM mechanism were tested using a series of 90 test problems representing a range of conditions expected in regional model applications. (6) Additional recommendations for modifications of the RADM mechanism were made as a result of the simulations of the chamber experiments and the test calculations. Stockwell incorporated some of these recommendations in a "final" version of the RADM mechanism, which, as of this writing, is expected to be the version which will be implemented into the RADM-II model. This mechanism is included among those which were simulated in the chamber experiments and test calculations.

This report is organized into seven sections. Following this introductory section, Section 2 describes and lists the version of the RADM-II mechanism which was evaluated in the model simulations carried out in this study, and two modified versions which were recommended as a result of this program. Section 3 describes the work carried out in this program concerning aggregation and representation of organic emissions data for use with the RADM-II mechanism. Section 4 describes the procedures used when evaluating the mechanisms against the chamber data, with emphasis particularly on the changes in the procedures and input data used, compared with previous studies. Section 5 presents the results of the simulations of the evaluated and recommended modified RADM mechanisms against the chamber data, including statistical summaries of the performance of the mechanisms and representative concentration-time plots. Section 6 describes the test calculations carried out to test alternative mechanistic assumptions and degrees of condensation, including a discussion of the 90 simulations employed, the mechanistic alternatives tested, and the results obtained. Finally, Section 7 gives a summary of the results from this program and the conclusions.

2. THE MARCH 1988 RADM AND RECOMMENDED MODIFIED RADM GAS-PHASE CHEMICAL MECHANISMS

In this section, we summarize and list the versions of the RADM-II chemical mechanisms which were evaluated during this study, and describe the modifications to the mechanism which are recommended as a result of this program. At the start of this program, the current RADM-II mechanism was the version documented in the NCAR (1987) report. However, as indicated earlier, Stockwell modified this mechanism shortly after this program began as a result of an initial review we carried out on this mechanism. This modified mechanism, which was dated March 30, 1988, is the version that was implemented at SAPRC for evaluation purposes. Therefore, the March 1988 version, and not the 1987 mechanism, is the version of the mechanism whose evaluation is discussed in this report. A listing of this mechanism is presented in Section 2.2. In the subsequent discussion, this version of the mechanism will be designated simply as the "RADM" or the "March 1988 RADM" mechanism.

The results of our evaluation efforts, described in more detail in Sections 3, 5 and 6 of this report, indicated several areas where improvements to the RADM mechanism were warranted. These included changes in the representation of the unknown aspects of the aromatic photooxidation mechanisms to improve its performance in simulations of the chamber data while reducing the number of species involved, a condensation in the representation of the alkanes, some changes in rate constant and product yield parameters for lumped species to better correspond to our most recent analysis of emissions data, correction of an error in the methylglyoxal quantum yields, addition of a few reactions omitted from the NO_3 + alkene mechanism, and minor improvements in the chemistry of the condensed representations of the reactions of nitrophenols. The modifications we recommended to the RADM mechanism are described in Section 2.2, and the resulting modified mechanism is listed in Section 2.3. In the subsequent discussion, this modified version of the RADM-II mechanism is designated as the "recommended modified," or simply as the "RADM-M," mechanism.

By the time we completed the evaluation effort and formulated our recommendations for modifying the mechanism, much of the work in implementing the RADM mechanism in the overall RADM-II model software had already been carried out. Although Stockwell and the RADM team were willing to implement our recommendations, we were informed that modifications involving more than just changes in kinetic or mechanistic parameters (i.e., rate constant values, product yield coefficients, or absorption coefficient and quantum yield data) would be difficult to implement without adversely impacting the RADM-II development schedule. Therefore, we developed a set of recommendations for modifications of the RADM mechanism that involved only changes in parameter values. These changes included revising the aromatics mechanism, updating the rate constants and product yield parameters for lumped species based on the most recent analysis of emissions data, and correcting the methylglyoxal quantum yields. In addition, the RADM team was willing to add the few reactions which were omitted from the NO_3 + alkene mechanism, so this change was also incorporated into this version of the mechanism. This second modified version of the RADM mechanism is designated as the "modified parameter," or simply the "RADM-P," mechanism. It is described and listed in Section 2.4.

The RADM team has accepted the recommendations for modifications which were incorporated in the RADM-P mechanism, and this version of the mechanism is now being implemented into the RADM-II model (Stockwell, private communication, 1989).

2.1 The March 1988 RADM Mechanism

The RADM gas-phase chemical mechanism that was used as the starting point in this evaluation effort is the March 1988 update of the RADM-II mechanism described in the NCAR (1987) report. This is a condensed mechanism which updated and extends the earlier mechanism of Stockwell (1986), with the representation of the reactions of the aromatics based on that of Lurmann et al. (1986). However, this mechanism has a more detailed representation of the reactions of the alkanes, organic acids, organic hydroperoxides, and the radical-radical reactions occurring in the absence of NO_x. The increased level of detail for the acids, organic peroxides, and radical-radical reactions is appropriate for a mechanism to be used for acid deposition modeling.

The modifications made to the NCAR (1987) mechanism included some relatively minor changes in some of the rate constants to be consistent with the latest evaluations of NASA (1987) and IUPAC (1988). Changes were also made in the representation of glycolaldehyde, an acetaldehyde oxidation product, and in the representation of lumped higher alkanes to be more consistent with observed organic nitrate yields from such compounds (Carter and Atkinson, 1985). Some changes in rate constants and product yields for lumped species based on results of a preliminary analysis of emissions data (see Section 3) were also made. The absorption coefficients and quantum yields for the photolysis reactions were not changed. Most of the changes made to the mechanism were relatively minor; the basic characteristics, approaches, and types of chemical approximations employed in this version are the same as the version documented in the NCAR (1987) report.

The model species employed in the RADM mechanism are listed in Table 1. There are a total of 18 inorganic species, 14 species representing the various types of organic oxidation products, 11 species representing emitted hydrocarbons, and 15 species representing reactive organic intermediates. The set of inorganic species is the same as that employed in most other state-of-the-art mechanisms. Like the Lurmann et al. (1986) mechanism and the more recent mechanisms developed at SAPRC (Carter et al., 1986, 1987; Lurmann et al., 1987; Carter, 1988), but unlike the Carbon Bond mechanisms (Gery et al., 1988), the reactions of the organics are represented on the molecular level, with some species being represented explicitly, and others being represented using either the "surrogate species" or the "lumped molecule" lumping approaches. The organic species represented explicitly in RADM are methane, ethane, ethene, formaldehyde, formic acid, methyl hydroperoxide, and isoprene. The surrogate species approach involves using a single representative compound to represent reactions of other compounds assumed to have similar mechanisms or reactivity. For example, the surrogate acetaldehyde (denoted as ALD) is used to represent all C_{2+} aldehydes. The lumped molecule approach involves representing mixtures of compounds by pseudo-molecules whose rate constants and perhaps other mechanistic parameters are determined based on the mixture they are used to represent. This lumping technique is used to represent C_{3+} alkanes and alkenes and (to some extent) the aromatic hydrocarbons. No attempt is made to conserve carbon in this mechanism, as is the case for most other current molecularly-based mechanisms.

Table 1. Model Species Employed in the March 1988 Version of the RADM Gas-Phase Chemical Mechanism

Name	Description
Transported Inorganic Species	
SO2	Sulfur Dioxide
O3	Ozone
H2O2	Hydrogen Peroxide
NO	Nitric Oxide
NO2	Nitrogen Dioxide
N2O5	Nitrogen Pentoxide
HONO	Nitrous Acid
HNO3	Nitric Acid
HNO4	Peroxy Nitric Acid
CO	Carbon Monoxide
Inorganic Radical and Atomic Intermediates	
HO	Hydroxyl (OH) Radicals
HO2	Hydroperoxyl Radicals
NO3	Nitrate Radicals
O3P	$O(^3P)$ Atoms
O1D	$O(^1D)$ Atoms
Constant Inorganic Species	
O2	Oxygen
N2	Nitrogen
M	Air
H2O	Water
Non-Reacting Inorganic Species	
H2	Hydrogen
CO2	Carbon Dioxide
SULF	Sulfuric Acid (or sulfates)
Organic Hydrocarbons	
CH4	Methane
ETH	Ethane
HC3	C3+ Alkanes with kOH $< 5 \times 10^3$ (a)
HC5	Alkanes with kOH Between 0.5 and 1.0×10^4
HC8	Alkanes with kOH $> 1.0 \times 10^4$
OL2	Ethene
OLT	Terminal Monoalkenes
OLI	Internal Alkenes, Terpenes, Conjugated Dialkenes
ISO	Isoprene
TOL	Aromatic Hydrocarbons with kOH $< 2 \times 10^4$
XYL	Aromatic Hydrocarbons with kOH $> 2 \times 10^4$

(continued)

Table 1 (continued) - 2

Name	Description
Organic Oxidation Products	
HCHO	Formaldehyde
ALD	Lumped Higher Aldehydes
KET	Ketones
GLY	Glyoxal
MGLY	Methyl Glyoxal
DCB	Uncharacterized Reactive Aromatic Fragmentation Products
CSL	Phenols and Cresols
PAN	Acyl Peroxy Nitrates (other than those formed from DCB)
TPAN	Acyl Peroxy Nitrates Formed from DCB
ONIT	Other Organic Nitrates (primarily alkyl nitrates)
OP1	Methyl Hydroperoxide
OP2	Higher Organic Hydroperoxides
ORA1	Formic Acid
ORA2	Higher Organic Acids (other than peroxy acetic acid)
PAA	Peroxy Acetic Acid
Organic Radicals	
MO2	Methyl Peroxy Radicals
ETHP	Ethyl Peroxy Radicals
HC3P	Peroxy Radicals from OH + HC3
HC5P	Peroxy Radicals from OH + HC5
HC8P	Peroxy Radicals from OH + HC8
OL2P	Peroxy Radicals from OH + Ethene
OLTP	Peroxy Radicals from OH + Isoprene and Terminal Alkenes
OLIP	Peroxy Radicals from OH + Internal Alkenes
KETP	Peroxy Radicals from OH + Ketones
TOLP	Peroxy Radicals from OH + Benzene and Monoalkyl Benzenes
XYLP	Peroxy Radicals from OH + Xylenes and More Reactive Aromatics
OLN	Peroxy Radicals from NO_3 + Alkenes
XO2	Chemical "Operator" Used to Account for NO-to-NO_2 Conversions due to Secondarily Formed Organic Peroxy Radicals
ACO3	Acyl Peroxy Radicals (other than those formed from DCB)
TCO3	Acyl Peroxy Radicals Formed from DCB
XNO2	Chemical Operator Used to Account for NO_x Loss Due to Reactions of NO_3 with Phenols and Cresols.

(a) kOH is the OH radical rate constant at 300 K in $ppm^{-1}\ min^{-1}$.

The RADM mechanism includes a relatively detailed, though still approximate, representation of the reactions of peroxy radical intermediates. This representation involves significantly more reactions than used for these processes in most other current lumped mechanisms. It also uses more model species to represent the products of these reactions in the absence of NO_x, with separate representations of methyl and higher hydroperoxides, formic and higher acids, and separate representation of peroxyacetic acid. Most of the reacting primary organics and organic products have separate representations of their peroxy radical products, and the mechanism includes explicit representation of the reactions of these radicals with NO, with NO_2 (for acyl peroxy radicals), with HO_2, with methyl peroxy (MO2), and with acetylperoxy (ACO3) radicals. In representing explicitly almost all of the possible peroxy + MO2 and peroxy + ACO3 reactions, this mechanism is more detailed in this regard than most other current mechanisms, which either ignore most of these processes (Gery et al., 1988), or uses approximations involving chemical "operators" to represent them (Carter et al., 1986; Lurmann et al., 1987; Carter, 1988). However, this mechanism omits the reactions of the peroxy species OLN (formed in the NO_3 + alkene reactions) with MO2 and ACO3, and ignores peroxy + peroxy reactions not involving MO2 and ACO3. The effects of alternative representations of peroxy radical reactions in this mechanism are discussed in Section 6.3.

Table 2 gives a listing of the reactions and the thermal rate constants used in the March 1988 RADM mechanism, and Table 3 gives the absorption coefficients and quantum yields used for its photolysis reactions. The reactions and thermal rate constants were obtained from Stockwell in computer readable format, along with input data and results of a test calculation employing constant photolysis rates. This mechanism was implemented on the computers at SAPRC and Lurmann and Associates (which each use different model calculation software), and the results of test problem were duplicated. The absorption coefficients and quantum yields used in this mechanism for atmospheric simulations were transmitted to us separately, and we used these to calculate photolysis rates as a function of zenith angle for the solar spectrum used in the test problems described in Section 6.1 of this report. Computer-readable data files implementing this mechanism are available from the authors of this report upon request (with update information available from Stockwell at SUNY).

Table 2. Listing of Reactions in the March 1988 Version of the RADM Gas-Phase Chemical Mechanism

Rxn. Label (a)	Kinetic Parameters (b)				Reactions (c)
	k(300)	A	Ea	B	
					Inorganic Reactions (d)
001	(Phot. Set = NO2R)				NO2 + HV = 03P + NO
002	(Phot. Set = 0301DR)				03 + HV = 01D + 02
003	(Phot. Set = 0303PR)				03 + HV = 03P + 02
004	(Phot. Set = HONOR)				HONO + HV = HO + NO
005	(Phot. Set = HNO3R)				HNO3 + HV = HO + NO2
006	(Phot. Set = HNO4R)				HNO4 + HV = HO2 + NO2
007	(Phot. Set = NO3NOR)				NO3 + HV = NO + 02
008	(Phot. Set = NO3NO2R)				NO3 + HV = NO2 + 03P
009	(Phot. Set = H202R)				H202 + HV = HO + HO
022	2.16E-05	2.16E-05	0.00	-4.30	03P + 02 + M = 03
023	1.42E+04	9.54E+03	-0.24	-1.00	03P + NO2 = NO + 02
024	3.82E+04	2.64E+04	-0.22	-1.00	01D + N2 = 03P + N2
025	5.93E+04	4.70E+04	-0.14	-1.00	01D + 02 = 03P + 02
026	3.23E+05	3.23E+05	0.00	-1.00	01D + H20 = HO + HO
027	2.76E+01	2.94E+03	2.78	-1.00	03 + NO = NO2 + 02
028	1.02E+02	2.35E+03	1.87	-1.00	03 + HO = HO2 + 02
029	3.05E+00	1.61E+01	0.99	-1.00	03 + HO2 = HO + #2 02
030	1.21E+04	5.43E+03	-0.48	-1.00	HO2 + NO = NO2 + HO
031	2.00E+03	(Falloff Kinetics)			HO2 + NO2 = HNO4
		6.46E-03	0.00	-5.20	(k0)
		6.90E+03	0.00	-2.40	(kinf)
		F= 0.60 n= 1.00			
032		(Equilibrium with 031)			HNO4 = HO2 + NO2
	3.24E-03	1.95E+13	21.66	1.00	(Keq)
033A	2.55E+03	3.23E+02	-1.23	-1.00	HO2 + HO2 = H202
033B	1.79E-03	6.82E-05	-1.95	-2.00	HO2 + HO2 + M = H202 + M
034A	1.34E-01	1.11E-05	-5.60	-2.00	HO2 + HO2 + H20 = H202
034B	9.38E-02	2.34E-06	-6.32	-2.00	HO2 + HO2 + H20 = H202
035	2.49E+03	4.84E+03	0.40	-1.00	H202 + HO = HO2 + H20
036	7.05E+03	(Falloff Kinetics)			NO + HO = HONO
		2.51E-02	0.00	-4.60	(k0)
		2.20E+04	0.00	-1.50	(kinf)
		F= 0.60 n= 1.00			
037	6.93E-10	1.19E-10	-1.05	-2.00	NO + NO + 02 = #2 NO2
038	4.94E-02	2.06E+02	4.97	-1.00	03 + NO2 = NO3
039	4.11E+04	2.50E+04	-0.30	-1.00	NO3 + NO = NO2 + NO2
040	6.08E-01	3.67E+01	2.44	-1.00	NO3 + NO2 = NO + NO2 + 02
041	3.67E+03	3.67E+03	0.00	-1.00	NO3 + HO2 = HNO3 + 02
042	1.85E+03	(Falloff Kinetics)			NO3 + NO2 = N205
		7.90E-02	0.00	-6.30	(k0)
		2.20E+03	0.00	-1.50	(kinf)
		F= 0.60 n= 1.00			

(continued)

Table 2 (continued) - 2

Rxn. Label (a)	Kinetic Parameters (b)				Reactions (c)
	k(300)	A	Ea	B	
043		(Equilibrium with 042)			N2O5 = NO2 + NO3
	2.27E-03	3.72E+13	22.26	1.00	(Keq)
044	2.94E-06	2.94E-06	0.00	-1.00	N2O5 + H2O = #2 HNO3
045	1.66E+04	(Falloff Kinetics)			HO + NO2 = HNO3
		9.34E-02	0.00	-5.20	(k0)
		3.52E+04	0.00	-2.30	(kinf)
		F= 0.60	n= 1.00		
046	2.16E+02	2.16E+02	0.00	-1.00	HO + HNO3 = NO3 + H2O
047	6.77E+03	1.91E+03	-0.75	-1.00	HO + HNO4 = NO2 + H2O
048	1.45E+05	6.75E+04	-0.46	-1.00	HO + HO2 = H2O + O2
049	1.29E+03	(Falloff Kinetics)			HO + SO2 = SULF + HO2
		1.08E-02	0.00	-5.30	(k0)
		2.20E+03	0.00	-1.00	(kinf)
		F= 0.60	n= 1.00		
050A	2.20E+02	2.20E+02	0.00	-1.00	CO + HO = HO2 + CO2
050B	1.31E-04	1.31E-04	0.00	-2.00	CO + HO + M = HO2 + CO2
					Organic Photolysis Reactions
010		(Phot. Set = HCHOMR)			HCHO + HV = H2 + CO
011		(Phot. Set = HCHORR)			HCHO + HV = HO2 + HO2 + CO
012		(Phot. Set = ALDR)			ALD + HV = MO2 + HO2 + CO
013		(Phot. Set = OPR)			OP1 + HV = HCHO + HO2 + HO
014		(Phot. Set = OPR)			OP2 + HV = ALD + HO2 + HO
015		(Phot. Set = PAAR)			PAA + HV = MO2 + CO2 + HO
016		(Phot. Set = KETR)			KET + HV = ACO3 + ETHP
017		(Phot. Set = GLY2R)			GLY + HV = #.13 HCHO + #1.87 CO
018		(Phot. Set = GLY1R)			GLY + HV = #.45 HCHO + #1.55 CO + #.80 HO2
019		(Phot. Set = MGLYR)			MGLY + HV = ACO3 + HO2 + CO
020		(Phot. Set = DCBR)			DCB + HV = #.98 HO2 + #.02 ACO3 + TCO3
021		(Phot. Set = ONITR)			ONIT + HV = #.20 ALD + #.80 KET + HO2 + NO2
					Organic + OH Reactions
051	1.29E+01	9.23E+02	2.54	1.00	CH4 + HO = MO2 + H2O
052	4.11E+02	1.81E+03	0.88	1.00	ETH + HO = ETHP + H2O
053	3.76E+03	2.28E+04	1.07	-1.00	HC3 + HO = #.90 HC3P + #.10 HO2 + #.014 HCHO + #.069 ALD + #.026 KET + H2O
054	7.86E+03	2.79E+04	0.75	-1.00	HC5 + HO = HC5P + #.27 XO2 + H2O

(continued)

Table 2 (continued) - 3

Rxn. Label (a)	Kinetic Parameters (b)				Reactions (c)
	k(300)	A	Ea	B	
055	1.66E+04	5.87E+04	0.75	-1.00	HC8 + HO = HC8P + #.78 XO2 + H2O
056	1.24E+04	3.16E+03	-0.82	-1.00	OL2 + HO = OL2P
057	3.82E+04	7.12E+03	-1.00	-1.00	OLT + HO = OLTP
058	9.24E+04	1.48E+04	-1.09	-1.00	OLI + HO = OLIP
074	1.46E+05	3.74E+04	-0.81	-1.00	ISO + HO = OLTP
059	9.02E+03	3.08E+03	-0.64	-1.00	TOL + HO = #.84 TOLP + #.16 CSL + #.16 HO2
060	4.54E+04	3.08E+04	-0.23	-1.00	XYL + HO = #.83 XYLP + #.17 CSL + #.17 HO2
063	1.32E+04	1.32E+04	0.00	-1.00	HCHO + HO = HO2 + CO + H2O
064	2.37E+04	1.01E+04	-0.51	-1.00	ALD + HO = ACO3 + H2O
065	1.47E+03	1.76E+04	1.48	-1.00	KET + HO = KETP + H2O
066	1.69E+04	1.69E+04	0.00	-1.00	GLY + HO = HO2 + #2 CO + H2O
067	2.50E+04	2.50E+04	0.00	-1.00	MGLY + HO = ACO3 + CO + H2O
061	5.87E+04	5.87E+04	0.00	-1.00	CSL + HO = #.1 HO2 + #.9 XO2 + #.9 TCO3
062	5.28E+04	5.28E+04	0.00	-1.00	CSL + HO = CSL
068	4.11E+04	4.11E+04	0.00	-1.00	DCB + HO = TCO3 + H2O
069	1.47E+04	1.47E+04	0.00	-1.00	OP1 + HO = #.5 MO2 + #.5 HCHO + #.5 HO
070	1.47E+04	1.47E+04	0.00	-1.00	OP2 + HO = #.5 HC3P + #.5 ALD + #.5 HO
071	1.47E+04	1.47E+04	0.00	-1.00	PAA + HO = ACO3 + H2O
072	2.06E+02	9.06E+02	0.88	1.00	PAN + HO = HCHO + NO3 + XO2
073	3.76E+03	2.28E+04	1.07	-1.00	ONIT + HO = HC3P + NO2
					Organic + NO3 Reactions
093	9.23E-01	8.81E+02	4.09	-1.00	HCHO + NO3 = HO2 + HNO3 + CO
094	3.65E+00	2.06E+03	3.78	-1.00	ALD + NO3 = ACO3 + HNO3
095	9.23E-01	8.81E+02	4.09	-1.00	GLY + NO3 = HNO3 + HO2 + #2 CO
096	3.65E+00	2.06E+03	3.78	-1.00	MGLY + NO3 = HNO3 + ACO3 + CO
097	3.65E+00	2.06E+03	3.78	-1.00	DCB + NO3 = HNO3 + TCO3
098	3.23E+04	3.23E+04	0.00	-1.00	CSL + NO3 = HNO3 + XNO2 + #.5 CSL
099	1.72E-01	2.94E+03	5.81	-1.00	OL2 + NO3 = OLN
100	2.33E+01	1.47E+04	3.84	-1.00	OLT + NO3 = OLN
101	1.84E+03	4.74E+04	1.94	-1.00	OLI + NO3 = OLN
102	8.53E+02	8.53E+02	0.00	-1.00	ISO + NO3 = OLN
					Organic + O3 Reactions
103	2.72E-03	1.76E+01	5.23	-1.00	OL2 + O3 = HCHO + #.42 CO + #.4 ORA1 + #.12 HO2

(continued)

Table 2 (continued) - 4

Rxn. Label (a)	Kinetic Parameters (b)				Reactions (c)
	k(300)	A	Ea	B	
104	1.74E-02	1.94E+01	4.18	-1.00	OLT + O3 = #.53 HCHO + #.50 ALD + #.33 CO + #.20 ORA1 + #.20 ORA2 + #.23 HO2 + #.22 MO2 + #.10 HO + #.06 CH4
106	3.02E-01	1.33E+01	2.26	-1.00	OLI + O3 = #.18 HCHO + #.72 ALD + #.10 KET + #.23 CO + #.06 ORA1 + #.29 ORA2 + #.09 CH4 + #.26 HO2 + #.14 HO + #.31 MO2
106	2.20E-02	1.81E+01	4.00	-1.00	ISO + O3 = #.53 HCHO + #.50 ALD + #.33 CO + #.20 ORA1 + #.20 ORA2 + #.23 HO2 + #.22 MO2 + #.10 HO
					Organic Peroxy + NO2 Reactions
075	7.52E+03	4.11E+03	-0.36	-1.00	ACO3 + NO2 = PAN
076	2.90E-02	1.17E+18	26.91	0.00	PAN = ACO3 + NO2
077	6.90E+03	6.90E+03	0.00	-1.00	TCO3 + NO2 = TPAN
078	2.90E-02	1.17E+18	26.91	0.00	TPAN = TCO3 + NO2
					Organic Peroxy + NO Reactions
086	1.12E+04	6.17E+03	-0.36	-1.00	ACO3 + NO = MO2 + NO2
087	1.12E+04	6.17E+03	-0.36	-1.00	TCO3 + NO = NO2 + #.92 HO2 + #.89 GLY + #.11 MGLY + #.05 ACO3 + #.95 CO + #2 XO2
079	1.12E+04	6.17E+03	-0.36	-1.00	MO2 + NO = HCHO + HO2 + NO2
080	1.12E+04	6.17E+03	-0.36	-1.00	HC3P + NO = #.69 ALD + #.26 KET + #.14 HCHO + #.03 ONIT + #.97 NO2 + #.97 HO2
081	1.12E+04	6.17E+03	-0.36	-1.00	HC5P + NO = #.36 ALD + #.76 KET + #.10 ONIT + #.90 NO2 + #.90 HO2
082	1.12E+04	6.17E+03	-0.36	-1.00	HC8P + NO = #.44 ALD + #1.05 KET + #.05 HCHO + #.24 ONIT + #.76 NO2 + #.76 HO2
083	1.12E+04	6.17E+03	-0.36	-1.00	OL2P + NO = #1.6 HCHO + HO2 + NO2 + #.2 ALD
084	1.12E+04	6.17E+03	-0.36	-1.00	OLTP + NO = ALD + HCHO + HO2 + NO2
085	1.12E+04	6.17E+03	-0.36	-1.00	OLIP + NO = HO2 + #1.45 ALD + #.28 HCHO + #.10 KET + NO2
088	1.12E+04	6.17E+03	-0.36	-1.00	TOLP + NO = NO2 + HO2 + #.724 MGLY + #.181 GLY + #.905 DCB
089	1.12E+04	6.17E+03	-0.36	-1.00	XYLP + NO = NO2 + HO2 + MGLY + DCB

(continued)

Table 2 (continued) - 5

Rxn. Label (a)	Kinetic Parameters (b)				Reactions (c)
	k(300)	A	Ea	B	
090	1.12E+04	6.17E+03	-0.36	-1.00	ETHP + NO = ALD + HO2 + NO2
091	1.12E+04	6.17E+03	-0.36	-1.00	KETP + NO = MGLY + NO2 + HO2
092	1.12E+04	6.17E+03	-0.36	-1.00	OLN + NO = HCHO + ALD + #2 NO2
150	1.12E+04	6.17E+03	-0.36	-1.00	XO2 + NO = NO2
					Organic Peroxy + HO2 Reactions
107	8.61E+03	1.13E+02	-2.58	-1.00	HO2 + MO2 = OP1
108		(Same k as 107)			HO2 + ETHP = OP2
109		(Same k as 107)			HO2 + HC3P = OP2
110		(Same k as 107)			HO2 + HC5P = OP2
111		(Same k as 107)			HO2 + HC8P = OP2
112		(Same k as 107)			HO2 + OL2P = OP2
113		(Same k as 107)			HO2 + OLTP = OP2
114		(Same k as 107)			HO2 + OLIP = OP2
115		(Same k as 107)			HO2 + KETP = OP2
117		(Same k as 107)			HO2 + TOLP = OP2
118		(Same k as 107)			HO2 + XYLP = OP2
120		(Same k as 107)			HO2 + OLN = ONIT
146		(Same k as 107)			HO2 + XO2 = OP2
116		(Same k as 107)			HO2 + ACO3 = PAA
119		(Same k as 107)			HO2 + TCO3 = OP2
					Organic Peroxy + ACO3 Reactions
142	3.64E+03	1.75E+03	-0.44	-1.00	ACO3 + ACO3 = #2 MO2
145	3.64E+03	1.75E+03	-0.44	-1.00	ACO3 + TCO3 = MO2 + #.92 HO2 + #.890 GLY + #.11 MGLY + #.05 ACO3 + #.950 CO + #2 XO2
130	2.93E+03	1.41E+03	-0.44	-1.00	MO2 + ACO3 = HCHO + #.5 HO2 + #.5 MO2 + #.5 ORA2
134	1.04E+03	4.99E+02	-0.44	-1.00	ETHP + ACO3 = ALD + #.5 HO2 + #.5 MO2 + #.5 ORA2
135	3.06E+02	1.47E+02	-0.44	-1.00	HC3P + ACO3 = #.2 ALD + #.8 KET + #.5 HO2 + #.5 MO2 + #.5 ORA2
136	2.57E+02	1.23E+02	-0.44	-1.00	HC5P + ACO3 = #.14 ALD + #.86 KET + #.5 HO2 + #.5 MO2 + #.5 ORA2
137	2.20E+02	1.06E+02	-0.44	-1.00	HC8P + ACO3 = #.10 ALD + #.9 KET + #.5 HO2 + #.5 MO2 + #.5 ORA2
138	1.04E+03	4.99E+02	-0.44	-1.00	OL2P + ACO3 = #.8 HCHO + #.6 ALD + #.5 HO2 + #.5 MO2 + #.5 ORA2
139	1.04E+03	4.99E+02	-0.44	-1.00	OLTP + ACO3 = ALD + #.5 HCHO + #.5 HO2 + #.5 MO2 + #.5 ORA2

(continued)

Table 2 (continued) - 6

Rxn. Label (a)	Kinetic Parameters (b) k(300)	A	Ea	B	Reactions (c)
140	1.28E+02	6.17E+01	-0.44	-1.00	OLIP + ACO3 = #.725 ALD + #.55 KET + #.14 HCHO + #.5 HO2 + #.5 MO2 + #.5 ORA2
141	1.28E+02	6.17E+01	-0.44	-1.00	KETP + ACO3 = MGLY + #.5 HO2 + #.5 MO2 + #.5 ORA2
143	1.28E+02	6.17E+01	-0.44	-1.00	ACO3 + TOLP = MO2 + #.8 MGLY + #.2 GLY + DCB + HO2
144	1.28E+02	6.17E+01	-0.44	-1.00	ACO3 + XYLP = MO2 + MGLY + DCB + HO2
148	1.28E+02	6.17E+01	-0.44	-1.00	XO2 + ACO3 = MO2
					Organic Peroxy + MO2 Reactions
121	5.81E+02	2.79E+02	-0.44	-1.00	MO2 + MO2 = #1.5 HCHO + HO2
122	4.28E+02	2.06E+02	-0.44	-1.00	MO2 + ETHP = #.75 HCHO + HO2 + #.75 ALD
123	1.28E+02	6.17E+01	-0.44	-1.00	MO2 + HC3P = #.75 HCHO + HO2 + #.15 ALD + #.60 KET
124	1.04E+02	4.99E+01	-0.44	-1.00	MO2 + HC5P = #.75 HCHO + HO2 + #.105 ALD + #.645 KET
125	8.86E+01	4.26E+01	-0.44	-1.00	MO2 + HC8P = #.75 HCHO + HO2 + #.075 ALD + #.675 KET
126	4.28E+02	2.06E+02	-0.44	-1.00	MO2 + OL2P = #1.55 HCHO + HO2 + #.35 ALD
127	4.28E+02	2.06E+02	-0.44	-1.00	MO2 + OLTP = #1.25 HCHO + HO2 + #.75 ALD
128	5.19E+01	2.50E+01	-0.44	-1.00	MO2 + OLIP = #.89 HCHO + HO2 + #.725 ALD + #.55 KET
129	5.19E+01	2.50E+01	-0.44	-1.00	MO2 + KETP = #.75 HCHO + HO2 + #.75 MGLY
131	5.19E+01	2.50E+01	-0.44	-1.00	MO2 + TOLP = #.976 HCHO + #1.9 HO2 + #.724 MGLY + #.181 GLY + #.905 DCB
132	5.19E+01	2.50E+01	-0.44	-1.00	MO2 + XYLP = HCHO + #2 HO2 + MGLY + DCB
133	2.93E+03	1.41E+03	-0.44	-1.00	MO2 + TCO3 = #.5 HCHO + #.5 ORA2 + #.46 HO2 + #.445 GLY + #.055 MGLY + #.025 ACO3 + #.475 CO + XO2
147	5.19E+01	2.50E+01	-0.44	-1.00	MO2 + XO2 = HCHO + HO2

(continued)

Table 2 (continued) - 7

Rxn. Label (a)	Kinetic Parameters (b) k(300)	A	Ea	B	Reactions (c)
					Other Organic Peroxy + Peroxy Reactions
149	1.10E+00	5.28E-01	-0.44	-1.00	XO2 + XO2 =
					XNO2 Reactions
151	1.12E+04	6.17E+03	-0.36	-1.00	XNO2 + NO2 = ONIT
152		(Same k as 107)			XNO2 + HO2 = OP2
153	5.19E+01	2.50E+01	-0.44	-1.00	XNO2 + MO2 = HCHO + HO2
154	1.28E+02	6.17E+01	-0.44	-1.00	XNO2 + ACO3 = MO2
155	1.10E+00	5.28E-01	-0.44	-1.00	XNO2 + XNO2 =

Notes:

(a) Reaction labels in this listing are the reaction sequence numbers used by Stockwell to implement this mechanism. Some reactions were re-arranged for the purpose of this listing. Some reactions were split into two reactions for implementation on SAPRC modeling software.

(b) Except as indicated otherwise, rate constants for reactions in this table are given by the expression

$$k = A\ (T/300)^{B}\ e^{-Ea/RT}$$

where k and A are in ppm, minute units, T is the temperature in degrees K, and R is 0.0019872 kcal deg^{-1} $mole^{-1}$. If the notation "Phot. Set" is used, then this is a photolysis reaction whose rate constant is calculated using the indicated set of absorption coefficients and quantum yields given in Table 3. If the notation "Falloff" is used, then this reaction is both temperature and pressure dependent, and its rate constant is given by

$$k = [(k_0\ M)\ /\ (1 + [k_0\ M\ /\ k_{inf}]\ )\ ]\ f^{g},$$

where

$$g = 1\ /\ [1 + (\log_{10}\ [k_0\ M\ /\ k_{inf}]\ /\ n)^{2}\ ],$$

M is the pressure in ppm, k_0 is the low pressure limiting rate constant calculated as a function of temperature from its

(continued)

corresponding A, Ea and B parameters given on the next line, k_{inf} is the high pressure limiting rate constant calculated from its parameters given on the line below that, and the parameters F and n are given as indicated in the line below that. If the notation "Equilibrium with" is used, the rate constant is calculated by multiplying the rate constant for the indicated reaction by the equilibrium constant, whose T=300 K value and temperature dependence parameters, analogous to A, Ea and B, are given on the following line.

(c) If a number preceded by a "#" appears on the list of reaction products, then the number is a product yield coefficient for the species whose name follows it. Otherwise the product yield is 1.0.

(d) These reactions are also used in the modified (RADM-M and RADM-P) versions of this mechanism.

Table 3. Absorption Coefficients and Quantum Yields Used in Versions of the RADM Gas-Phase Chemical Mechanism Evaluated in this Study

Data Used in the March 1988 and the Recommended Versions of the RADM Mechanism

Photolysis Set = NO2R

WL (nm)	Abs (cm^2)	QY	WL (nm)	Abs (cm^2)	QY	WL (nm)	Abs (cm^2)	QY
186.0	2.59E-19	1.000	187.8	2.72E-19	1.000	189.6	2.85E-19	1.000
191.4	2.73E-19	1.000	193.2	2.51E-19	1.000	195.1	2.44E-19	1.000
197.0	2.46E-19	1.000	199.0	2.46E-19	1.000	201.0	2.82E-19	1.000
203.0	2.92E-19	1.000	205.1	3.53E-19	1.000	207.3	3.74E-19	1.000
209.4	4.10E-19	1.000	211.6	4.36E-19	1.000	213.9	4.45E-19	1.000
216.2	4.60E-19	1.000	218.6	4.17E-19	1.000	221.0	4.54E-19	1.000
223.5	3.70E-19	1.000	226.0	3.89E-19	1.000	228.6	2.69E-19	1.000
231.2	2.76E-19	1.000	233.9	1.71E-19	1.000	236.7	1.62E-19	1.000
239.5	7.85E-20	1.000	242.4	6.12E-20	1.000	245.4	2.88E-20	1.000
248.4	2.13E-20	1.000	251.6	1.40E-20	1.000	254.8	1.49E-20	1.000
258.1	1.60E-20	1.000	261.4	1.80E-20	1.000	264.9	2.18E-20	1.000
268.5	2.72E-20	1.000	272.1	3.27E-20	1.000	275.9	4.10E-20	1.000
279.7	5.26E-20	1.000	283.7	6.27E-20	1.000	287.8	7.62E-20	1.000
292.0	9.39E-20	1.000	296.3	1.09E-19	1.000	300.5	1.26E-19	1.000
303.0	1.51E-19	1.000	304.0	1.56E-19	1.000	305.0	1.55E-19	1.000
306.0	1.53E-19	1.000	307.0	1.61E-19	1.000	308.0	1.65E-19	1.000
309.0	1.81E-19	1.000	310.0	1.83E-19	1.000	311.0	1.91E-19	1.000
312.0	2.03E-19	1.000	313.0	2.01E-19	1.000	314.0	1.99E-19	1.000
316.0	2.20E-19	1.000	320.0	2.50E-19	1.000	325.0	2.81E-19	1.000
330.0	3.04E-19	1.000	335.0	3.40E-19	1.000	340.0	3.84E-19	1.000
345.0	4.05E-19	1.000	350.0	4.46E-19	1.000	355.0	4.88E-19	1.000
360.0	4.94E-19	1.000	365.0	5.29E-19	1.000	370.0	5.40E-19	1.000
375.0	5.63E-19	1.000	380.0	5.61E-19	1.000	385.0	5.72E-19	0.997
390.0	6.00E-19	0.981	395.0	5.69E-19	0.922	400.0	6.18E-19	0.693
405.0	5.49E-19	0.356	410.0	5.98E-19	0.135	415.0	5.77E-19	0.060
420.0	0.00E-01	0.018						

Photolysis Set = O301DR

WL (nm)	Abs (cm^2)	QY	WL (nm)	Abs (cm^2)	QY	WL (nm)	Abs (cm^2)	QY
186.0	6.23E-19	0.900	187.8	5.76E-19	0.900	189.6	5.26E-19	0.900
191.4	4.75E-19	0.900	193.2	4.27E-19	0.900	195.1	3.82E-19	0.900
197.0	3.46E-19	0.900	199.0	3.22E-19	0.900	201.0	3.14E-19	0.900
203.0	3.27E-19	0.900	205.1	3.65E-19	0.900	207.3	4.37E-19	0.900
209.4	5.46E-19	0.900	211.6	7.05E-19	0.900	213.9	9.20E-19	0.900
216.2	1.20E-18	0.900	218.6	1.56E-18	0.900	221.0	2.00E-18	0.900
223.5	2.57E-18	0.900	226.0	3.24E-18	0.900	228.6	4.04E-18	0.900
231.2	4.94E-18	0.900	233.9	5.93E-18	0.900	236.7	7.01E-18	0.900
239.5	8.11E-18	0.900	242.4	9.20E-18	0.900	245.4	1.02E-17	0.900

(continued)

Table 3 (continued) - 2

WL (nm)	Abs (cm^2)	QY	WL (nm)	Abs (cm^2)	QY	WL (nm)	Abs (cm^2)	QY
248.4	1.10E-17	0.900	251.6	1.14E-17	0.900	254.8	1.16E-17	0.900
258.1	1.14E-17	0.900	261.4	1.08E-17	0.900	264.9	9.64E-18	0.900
268.5	8.35E-18	0.900	272.1	6.93E-18	0.900	275.9	5.43E-18	0.900
279.7	4.03E-18	0.900	283.7	2.79E-18	0.900	287.8	1.81E-18	0.900
292.0	1.11E-18	0.900	296.3	6.37E-19	0.900	300.5	3.63E-19	0.900
303.0	2.64E-19	0.900	304.0	2.33E-19	0.899	305.0	1.99E-19	0.872
306.0	1.79E-19	0.837	307.0	1.57E-19	0.789	308.0	1.36E-19	0.725
309.0	1.19E-19	0.639	310.0	1.03E-19	0.531	311.0	9.13E-20	0.413
312.0	8.01E-20	0.304	313.0	6.90E-20	0.216	314.0	6.33E-20	0.150
316.0	4.69E-20	0.065	320.0	2.65E-20	0.000			

Photolysis Set = 0303PR

WL (nm)	Abs (cm^2)	QY	WL (nm)	Abs (cm^2)	QY	WL (nm)	Abs (cm^2)	QY
186.0	6.23E-19	0.100	187.8	5.76E-19	0.100	189.6	5.26E-19	0.100
191.4	4.75E-19	0.100	193.2	4.27E-19	0.100	195.1	3.82E-19	0.100
197.0	3.46E-19	0.100	199.0	3.22E-19	0.100	201.0	3.14E-19	0.100
203.0	3.27E-19	0.100	205.1	3.65E-19	0.100	207.3	4.37E-19	0.100
209.4	5.46E-19	0.100	211.6	7.05E-19	0.100	213.9	9.20E-19	0.100
216.2	1.20E-18	0.100	218.6	1.56E-18	0.100	221.0	2.00E-18	0.100
223.5	2.57E-18	0.100	226.0	3.24E-18	0.100	228.6	4.04E-18	0.100
231.2	4.94E-18	0.100	233.9	5.93E-18	0.100	236.7	7.01E-18	0.100
239.5	8.11E-18	0.100	242.4	9.20E-18	0.100	245.4	1.02E-17	0.100
248.4	1.10E-17	0.100	251.6	1.14E-17	0.100	254.8	1.16E-17	0.100
258.1	1.14E-17	0.100	261.4	1.08E-17	0.100	264.9	9.64E-18	0.100
268.5	8.35E-18	0.100	272.1	6.93E-18	0.100	275.9	5.43E-18	0.100
279.7	4.03E-18	0.100	283.7	2.79E-18	0.100	287.8	1.81E-18	0.100
292.0	1.11E-18	0.100	296.3	6.37E-19	0.100	300.5	3.63E-19	0.100
303.0	2.64E-19	0.100	304.0	2.33E-19	0.101	305.0	1.99E-19	0.128
306.0	1.79E-19	0.163	307.0	1.57E-19	0.211	308.0	1.36E-19	0.275
309.0	1.19E-19	0.361	310.0	1.03E-19	0.469	311.0	9.13E-20	0.587
312.0	8.01E-20	0.696	313.0	6.90E-20	0.784	314.0	6.33E-20	0.850
316.0	4.69E-20	0.935	320.0	2.65E-20	1.000	325.0	1.30E-20	1.000
330.0	6.69E-21	1.000	335.0	3.06E-21	1.000	340.0	1.37E-21	1.000
345.0	7.21E-22	1.000	350.0	2.66E-22	1.000	355.0	1.09E-22	1.000
360.0	5.49E-23	1.000	365.0	0.00E-01	1.000	410.0	2.91E-23	1.000
415.0	3.14E-23	1.000	420.0	3.99E-23	1.000	425.0	6.54E-23	1.000
430.0	6.83E-23	1.000	435.0	8.66E-23	1.000	440.0	1.25E-22	1.000
445.0	1.49E-22	1.000	450.0	1.71E-22	1.000	455.0	2.12E-22	1.000
460.0	3.57E-22	1.000	465.0	3.68E-22	1.000	470.0	4.06E-22	1.000
475.0	4.89E-22	1.000	480.0	7.11E-22	1.000	485.0	8.43E-22	1.000
490.0	8.28E-22	1.000	495.0	9.09E-22	1.000	500.0	1.22E-21	1.000
505.0	1.62E-21	1.000	510.0	1.58E-21	1.000	515.0	1.60E-21	1.000
520.0	1.78E-21	1.000	525.0	2.07E-21	1.000	530.0	2.55E-21	1.000
535.0	2.74E-21	1.000	540.0	2.88E-21	1.000	545.0	3.07E-21	1.000
550.0	3.17E-21	1.000	555.0	3.36E-21	1.000	560.0	3.88E-21	1.000

(continued)

Table 3 (continued) - 3

WL (nm)	Abs (cm^2)	QY	WL (nm)	Abs (cm^2)	QY	WL (nm)	Abs (cm^2)	QY
565.0	4.31E-21	1.000	570.0	4.67E-21	1.000	575.0	4.75E-21	1.000
580.0	4.55E-21	1.000	585.0	4.35E-21	1.000	590.0	4.42E-21	1.000
595.0	4.61E-21	1.000	600.0	4.89E-21	1.000	605.0	4.84E-21	1.000
610.0	4.54E-21	1.000	615.0	4.24E-21	1.000	620.0	3.90E-21	1.000
625.0	3.60E-21	1.000	630.0	3.43E-21	1.000	635.0	3.17E-21	1.000
640.0	2.74E-21	1.000	644.8	2.61E-21	1.000	651.1	2.40E-21	1.000
660.0	2.07E-21	1.000	670.0	1.72E-21	1.000	680.0	1.37E-21	1.000
690.0	1.11E-21	1.000	700.0	9.13E-22	1.000	710.0	7.93E-22	1.000
720.0	6.40E-22	1.000	730.0	5.14E-22	1.000			

Photolysis Set = HONOR

311.0	2.50E-22	1.000	312.0	2.02E-21	1.000	313.0	3.97E-21	1.000
314.0	4.50E-21	1.000	316.0	5.26E-21	1.000	320.0	3.93E-20	1.000
325.0	3.93E-20	1.000	330.0	8.51E-20	1.000	335.0	6.31E-20	1.000
340.0	1.69E-19	1.000	345.0	1.14E-19	1.000	350.0	1.07E-19	1.000
355.0	2.58E-19	1.000	360.0	7.31E-20	1.000	365.0	1.84E-19	1.000
370.0	2.06E-19	1.000	375.0	3.71E-20	1.000	380.0	8.25E-20	1.000
385.0	1.46E-19	1.000	390.0	1.42E-20	1.000	395.0	0.00E-01	1.000

Photolysis Set = HNO3R

191.4	1.37E-17	1.000	193.2	1.22E-17	1.000	195.1	1.04E-17	1.000
197.0	8.54E-18	1.000	199.0	6.66E-18	1.000	201.0	5.12E-18	1.000
203.0	3.60E-18	1.000	205.1	2.48E-18	1.000	207.3	1.67E-18	1.000
209.4	9.93E-19	1.000	211.6	6.64E-19	1.000	213.9	3.78E-19	1.000
216.2	2.57E-19	1.000	218.6	1.65E-19	1.000	221.0	1.22E-19	1.000
223.5	9.10E-20	1.000	226.0	7.26E-20	1.000	228.6	5.77E-20	1.000
231.2	4.66E-20	1.000	233.9	3.68E-20	1.000	236.7	3.00E-20	1.000
239.5	2.48E-20	1.000	242.4	2.20E-20	1.000	245.4	2.03E-20	1.000
248.4	1.92E-20	1.000	251.6	1.90E-20	1.000	254.8	1.89E-20	1.000
258.1	1.87E-20	1.000	261.4	1.77E-20	1.000	264.9	1.67E-20	1.000
268.5	1.57E-20	1.000	272.1	1.40E-20	1.000	275.9	1.21E-20	1.000
279.7	1.01E-20	1.000	283.7	8.13E-21	1.000	287.8	6.17E-21	1.000
292.0	4.44E-21	1.000	296.3	2.95E-21	1.000	300.5	2.08E-21	1.000
303.0	1.74E-21	1.000	304.0	1.55E-21	1.000	305.0	1.39E-21	1.000
306.0	1.24E-21	1.000	307.0	1.09E-21	1.000	308.0	9.35E-22	1.000
309.0	7.85E-22	1.000	310.0	6.71E-22	1.000	311.0	5.93E-22	1.000
312.0	5.15E-22	1.000	313.0	4.37E-22	1.000	314.0	3.30E-22	1.000
316.0	2.00E-22	1.000	320.0	8.50E-23	1.000	325.0	3.50E-23	1.000
330.0	0.00E-01	1.000						

(continued)

Table 3 (continued) - 4

WL (nm)	Abs (cm^2)	QY	WL (nm)	Abs (cm^2)	QY	WL (nm)	Abs (cm^2)	QY
Photolysis Set = HNO4R								
189.6	1.00E-17	1.000	191.4	9.00E-18	1.000	193.2	7.60E-18	1.000
195.1	6.60E-18	1.000	197.0	5.60E-18	1.000	199.0	4.80E-18	1.000
201.0	4.00E-18	1.000	203.0	3.40E-18	1.000	205.1	2.90E-18	1.000
207.3	2.40E-18	1.000	209.4	2.10E-18	1.000	211.6	1.70E-18	1.000
213.9	1.50E-18	1.000	216.2	1.30E-18	1.000	218.6	1.10E-18	1.000
221.0	1.00E-18	1.000	223.5	9.00E-19	1.000	226.0	8.20E-19	1.000
228.6	7.50E-19	1.000	231.2	6.80E-19	1.000	233.9	6.50E-19	1.000
236.7	6.00E-19	1.000	239.5	5.50E-19	1.000	242.4	5.00E-19	1.000
245.4	4.40E-19	1.000	248.4	4.00E-19	1.000	251.6	3.50E-19	1.000
254.8	3.00E-19	1.000	258.1	2.70E-19	1.000	261.4	2.35E-19	1.000
264.9	2.00E-19	1.000	268.5	1.80E-19	1.000	272.1	1.55E-19	1.000
275.9	1.25E-19	1.000	279.7	9.00E-20	1.000	283.7	6.50E-20	1.000
287.8	4.50E-20	1.000	292.0	3.10E-20	1.000	296.3	2.10E-20	1.000
300.5	1.35E-20	1.000	303.0	1.10E-20	1.000	304.0	1.00E-20	1.000
305.0	9.00E-21	1.000	306.0	8.50E-21	1.000	307.0	7.70E-21	1.000
308.0	7.00E-21	1.000	309.0	6.60E-21	1.000	310.0	6.00E-21	1.000
311.0	5.50E-21	1.000	312.0	5.10E-21	1.000	313.0	4.50E-21	1.000
314.0	4.20E-21	1.000	316.0	3.30E-21	1.000	320.0	2.40E-21	1.000
325.0	1.50E-21	1.000	330.0	1.00E-21	1.000	335.0	0.00E-01	1.000
Photolysis Set = NO3NOR								
585.0	2.66E-18	0.032	590.0	4.74E-18	0.191	595.0	3.74E-18	0.350
600.0	2.69E-18	0.311	605.0	3.05E-18	0.272	610.0	1.51E-18	0.233
615.0	1.84E-18	0.194	620.0	4.61E-18	0.156	625.0	8.17E-18	0.117
630.0	4.89E-18	0.078	635.0	1.43E-18	0.039	640.0	1.08E-18	0.000
Photolysis Set = NO3NO2R								
405.0	2.80E-20	1.000	410.0	4.45E-20	1.000	415.0	5.35E-20	1.000
420.0	8.20E-20	1.000	425.0	1.05E-19	1.000	430.0	1.29E-19	1.000
435.0	1.84E-19	1.000	440.0	1.94E-19	1.000	445.0	2.23E-19	1.000
450.0	2.83E-19	1.000	455.0	3.35E-19	1.000	460.0	3.72E-19	1.000
465.0	4.34E-19	1.000	470.0	5.10E-19	1.000	475.0	6.03E-19	1.000
480.0	6.44E-19	1.000	485.0	6.86E-19	1.000	490.0	8.80E-19	1.000
495.0	9.67E-19	1.000	500.0	9.90E-19	1.000	505.0	1.09E-18	1.000
510.0	1.32E-18	1.000	515.0	1.40E-18	1.000	520.0	1.45E-18	1.000
525.0	1.49E-18	1.000	530.0	1.93E-18	1.000	535.0	2.04E-18	1.000
540.0	1.83E-18	1.000	545.0	1.82E-18	1.000	550.0	2.35E-18	1.000
555.0	2.68E-18	1.000	560.0	3.07E-18	1.000	565.0	2.54E-18	1.000
570.0	2.49E-18	1.000	575.0	2.61E-18	1.000	580.0	2.91E-18	1.000
585.0	2.66E-18	0.968	590.0	4.74E-18	0.809	595.0	3.74E-18	0.650
600.0	2.69E-18	0.578	605.0	3.05E-18	0.506	610.0	1.51E-18	0.433

(continued)

Table 3 (continued) - 5

WL (nm)	Abs (cm^2)	QY	WL (nm)	Abs (cm^2)	QY	WL (nm)	Abs (cm^2)	QY
615.0	1.84E-18	0.361	620.0	4.61E-18	0.289	625.0	8.17E-18	0.217
630.0	4.89E-18	0.144	635.0	1.43E-18	0.072	640.0	1.08E-18	0.000
Photolysis Set = H2O2R								
191.4	3.21E-19	1.000	193.2	3.00E-19	1.000	195.1	2.80E-19	1.000
197.0	5.27E-19	1.000	199.0	4.92E-19	1.000	201.0	4.61E-19	1.000
203.0	4.34E-19	1.000	205.1	4.07E-19	1.000	207.3	3.82E-19	1.000
209.4	3.56E-19	1.000	211.6	3.33E-19	1.000	213.9	3.10E-19	1.000
216.2	2.88E-19	1.000	218.6	2.67E-19	1.000	221.0	2.46E-19	1.000
223.5	2.26E-19	1.000	226.0	2.07E-19	1.000	228.6	1.89E-19	1.000
231.2	1.71E-19	1.000	233.9	1.55E-19	1.000	236.7	1.39E-19	1.000
239.5	1.25E-19	1.000	242.4	1.12E-19	1.000	245.4	9.93E-20	1.000
248.4	8.81E-20	1.000	251.6	7.76E-20	1.000	254.8	6.78E-20	1.000
258.1	5.80E-20	1.000	261.4	4.92E-20	1.000	264.9	4.21E-20	1.000
268.5	3.54E-20	1.000	272.1	2.96E-20	1.000	275.9	2.46E-20	1.000
279.7	2.02E-20	1.000	283.7	1.61E-20	1.000	287.8	1.29E-20	1.000
292.0	1.03E-20	1.000	296.3	8.16E-21	1.000	300.5	6.47E-21	1.000
303.0	5.59E-21	1.000	304.0	5.26E-21	1.000	305.0	4.93E-21	1.000
306.0	4.69E-21	1.000	307.0	4.46E-21	1.000	308.0	4.23E-21	1.000
309.0	4.00E-21	1.000	310.0	3.77E-21	1.000	311.0	3.58E-21	1.000
312.0	3.38E-21	1.000	313.0	3.19E-21	1.000	314.0	2.99E-21	1.000
316.0	2.65E-21	1.000	320.0	2.07E-21	1.000	325.0	1.53E-21	1.000
330.0	1.19E-21	1.000	335.0	9.36E-22	1.000	340.0	6.86E-22	1.000
345.0	5.03E-22	1.000	350.0	3.25E-22	1.000	355.0	0.00E-01	1.000
Photolysis Set = HCHOMR								
251.6	3.91E-22	0.480	254.8	1.18E-21	0.489	258.1	2.81E-21	0.494
261.4	5.06E-21	0.498	264.9	5.55E-21	0.495	268.5	9.35E-21	0.484
272.1	1.16E-20	0.457	275.9	1.60E-20	0.386	279.7	1.58E-20	0.342
283.7	2.27E-20	0.325	287.8	2.13E-20	0.306	292.0	2.26E-20	0.287
296.3	2.99E-20	0.270	300.5	1.52E-20	0.255	303.0	2.28E-20	0.249
304.0	6.33E-20	0.247	305.0	4.67E-20	0.246	306.0	4.50E-20	0.248
307.0	2.04E-20	0.251	308.0	1.41E-20	0.254	309.0	2.96E-20	0.257
310.0	1.75E-20	0.260	311.0	7.28E-21	0.264	312.0	1.34E-20	0.269
313.0	1.25E-20	0.273	314.0	3.92E-20	0.279	316.0	3.95E-20	0.310
320.0	1.53E-20	0.394	325.0	2.11E-20	0.508	330.0	1.92E-20	0.676
335.0	2.13E-21	0.754	340.0	1.63E-20	0.616	345.0	6.67E-21	0.471
350.0	1.52E-21	0.338	355.0	7.17E-21	0.198	360.0	9.07E-23	0.085
365.0	0.00E-01	0.005						

(continued)

Table 3 (continued) - 6

WL (nm)	Abs (cm^2)	QY	WL (nm)	Abs (cm^2)	QY	WL (nm)	Abs (cm^2)	QY
Photolysis Set = HCHORR								
251.6	3.91E-22	0.340	254.8	1.18E-21	0.323	258.1	2.81E-21	0.317
261.4	5.06E-21	0.319	264.9	5.55E-21	0.333	268.5	9.35E-21	0.365
272.1	1.16E-20	0.405	275.9	1.60E-20	0.456	279.7	1.58E-20	0.522
283.7	2.27E-20	0.606	287.8	2.13E-20	0.680	292.0	2.26E-20	0.724
296.3	2.99E-20	0.742	300.5	1.52E-20	0.750	303.0	2.28E-20	0.753
304.0	6.33E-20	0.754	305.0	4.67E-20	0.755	306.0	4.50E-20	0.754
307.0	2.04E-20	0.753	308.0	1.41E-20	0.752	309.0	2.96E-20	0.751
310.0	1.75E-20	0.749	311.0	7.28E-21	0.745	312.0	1.34E-20	0.740
313.0	1.25E-20	0.732	314.0	3.92E-20	0.723	316.0	3.95E-20	0.690
320.0	1.53E-20	0.593	325.0	2.11E-20	0.458	330.0	1.92E-20	0.305
335.0	2.13E-21	0.122	340.0	1.63E-20	0.003	345.0	6.67E-21	0.000
Photolysis Set = ALDR								
264.9	2.82E-20	0.340	268.5	3.25E-20	0.369	272.1	3.68E-20	0.421
275.9	4.01E-20	0.492	279.7	4.34E-20	0.557	283.7	4.50E-20	0.552
287.8	4.55E-20	0.531	292.0	4.43E-20	0.502	296.3	4.22E-20	0.463
300.5	3.90E-20	0.420	303.0	3.54E-20	0.383	304.0	3.41E-20	0.367
305.0	3.34E-20	0.351	306.0	3.27E-20	0.335	307.0	3.19E-20	0.319
308.0	3.11E-20	0.304	309.0	2.97E-20	0.288	310.0	2.81E-20	0.272
311.0	2.66E-20	0.255	312.0	2.50E-20	0.238	313.0	2.36E-20	0.221
314.0	2.25E-20	0.204	316.0	2.05E-20	0.169	320.0	1.57E-20	0.106
325.0	1.09E-20	0.050	330.0	6.43E-21	0.006	335.0	2.79E-21	0.000
Photolysis Set = OPR								
211.6	3.49E-19	1.000	213.9	3.14E-19	1.000	216.2	2.79E-19	1.000
218.6	2.42E-19	1.000	221.0	2.12E-19	1.000	223.5	1.92E-19	1.000
226.0	1.71E-19	1.000	228.6	1.50E-19	1.000	231.2	1.33E-19	1.000
233.9	1.19E-19	1.000	236.7	1.05E-19	1.000	239.5	9.07E-20	1.000
242.4	8.07E-20	1.000	245.4	7.18E-20	1.000	248.4	6.26E-20	1.000
251.6	5.48E-20	1.000	254.8	4.84E-20	1.000	258.1	4.19E-20	1.000
261.4	3.61E-20	1.000	264.9	3.16E-20	1.000	268.5	2.70E-20	1.000
272.1	2.29E-20	1.000	275.9	1.91E-20	1.000	279.7	1.54E-20	1.000
283.7	1.28E-20	1.000	287.8	1.03E-20	1.000	292.0	8.36E-21	1.000
296.3	6.98E-21	1.000	300.5	5.70E-21	1.000	303.0	5.08E-21	1.000
304.0	4.84E-21	1.000	305.0	4.60E-21	1.000	306.0	4.36E-21	1.000
307.0	4.12E-21	1.000	308.0	3.88E-21	1.000	309.0	3.64E-21	1.000
310.0	3.41E-21	1.000	311.0	3.25E-21	1.000	312.0	3.10E-21	1.000
313.0	2.95E-21	1.000	314.0	2.80E-21	1.000	316.0	2.50E-21	1.000
320.0	1.94E-21	1.000	325.0	1.50E-21	1.000	330.0	1.12E-21	1.000
335.0	8.50E-22	1.000	340.0	6.19E-22	1.000	345.0	5.00E-22	1.000
350.0	3.87E-22	1.000	355.0	2.00E-22	1.000	360.0	0.00E-01	1.000

(continued)

Table 3 (continued) - 7

WL (nm)	Abs (cm^2)	QY	WL (nm)	Abs (cm^2)	QY	WL (nm)	Abs (cm^2)	QY
Photolysis Set = PAAR								
191.4	8.98E-20	1.000	193.2	8.41E-20	1.000	195.1	7.84E-20	1.000
197.0	1.48E-19	1.000	199.0	1.38E-19	1.000	201.0	1.29E-19	1.000
203.0	1.21E-19	1.000	205.1	1.14E-19	1.000	207.3	1.07E-19	1.000
209.4	9.98E-20	1.000	211.6	9.32E-20	1.000	213.9	8.68E-20	1.000
216.2	8.07E-20	1.000	218.6	7.48E-20	1.000	221.0	6.90E-20	1.000
223.5	6.33E-20	1.000	226.0	5.79E-20	1.000	228.6	5.29E-20	1.000
231.2	4.80E-20	1.000	233.9	4.33E-20	1.000	236.7	3.90E-20	1.000
239.5	3.49E-20	1.000	242.4	3.13E-20	1.000	245.4	2.78E-20	1.000
248.4	2.47E-20	1.000	251.6	2.17E-20	1.000	254.8	1.90E-20	1.000
258.1	1.62E-20	1.000	261.4	1.38E-20	1.000	264.9	1.18E-20	1.000
268.5	9.91E-21	1.000	272.1	8.29E-21	1.000	275.9	6.90E-21	1.000
279.7	5.66E-21	1.000	283.7	4.52E-21	1.000	287.8	3.61E-21	1.000
292.0	2.88E-21	1.000	296.3	2.29E-21	1.000	300.5	1.81E-21	1.000
303.0	1.57E-21	1.000	304.0	1.47E-21	1.000	305.0	1.38E-21	1.000
306.0	1.31E-21	1.000	307.0	1.25E-21	1.000	308.0	1.18E-21	1.000
309.0	1.12E-21	1.000	310.0	1.06E-21	1.000	311.0	1.00E-21	1.000
312.0	9.47E-22	1.000	313.0	8.93E-22	1.000	314.0	8.38E-22	1.000
316.0	7.43E-22	1.000	320.0	5.81E-22	1.000	325.0	4.28E-22	1.000
330.0	3.32E-22	1.000	335.0	2.62E-22	1.000	340.0	1.92E-22	1.000
345.0	1.41E-22	1.000	350.0	9.10E-23	1.000	355.0	0.00E-01	1.000
Photolysis Set = KETR								
279.7	6.00E-20	0.077	283.7	5.80E-20	0.077	287.8	5.50E-20	0.077
292.0	5.10E-20	0.077	296.3	4.10E-20	0.077	300.5	3.20E-20	0.077
303.0	3.00E-20	0.077	304.0	2.80E-20	0.077	305.0	2.50E-20	0.077
306.0	2.30E-20	0.077	307.0	2.10E-20	0.077	308.0	1.90E-20	0.077
309.0	1.70E-20	0.077	310.0	1.50E-20	0.077	311.0	1.40E-20	0.077
312.0	1.20E-20	0.077	313.0	1.10E-20	0.077	314.0	1.00E-20	0.077
316.0	7.80E-21	0.077	320.0	3.90E-21	0.077	325.0	1.80E-21	0.077
330.0	0.00E-01	0.077						
Photolysis Set = GLY1R								
233.9	3.40E-21	1.000	236.7	4.01E-21	1.000	239.5	4.86E-21	1.000
242.4	5.73E-21	1.000	245.4	6.62E-21	1.000	248.4	7.54E-21	1.000
251.6	9.05E-21	1.000	254.8	1.12E-20	1.000	258.1	1.33E-20	1.000
261.4	1.62E-20	1.000	264.9	2.02E-20	1.000	268.5	2.24E-20	1.000
272.1	2.48E-20	1.000	275.9	2.76E-20	1.000	279.7	2.89E-20	1.000
283.7	3.18E-20	1.000	287.8	3.22E-20	1.000	292.0	3.21E-20	1.000
296.3	3.37E-20	1.000	300.5	3.43E-20	1.000	303.0	3.07E-20	1.000
304.0	2.90E-20	1.000	305.0	2.75E-20	1.000	306.0	2.72E-20	1.000
307.0	2.72E-20	1.000	308.0	2.72E-20	1.000	309.0	2.72E-20	1.000

(continued)

Table 3 (continued) - 8

WL (nm)	Abs (cm^2)	QY	WL (nm)	Abs (cm^2)	QY	WL (nm)	Abs (cm^2)	QY
310.0	2.73E-20	1.000	311.0	2.79E-20	1.000	312.0	2.83E-20	1.000
313.0	2.68E-20	1.000	314.0	2.49E-20	1.000	316.0	2.12E-20	1.000
320.0	1.51E-20	1.000	325.0	1.27E-20	1.000	330.0	1.42E-20	1.000
335.0	2.29E-20	1.000	340.0	3.58E-21	1.000	345.0	0.00E-01	1.000

Photolysis Set = GLY2R

355.0	2.86E-22	0.024	360.0	2.08E-21	0.024	365.0	3.44E-21	0.024
370.0	7.64E-21	0.024	375.0	1.07E-20	0.024	380.0	1.59E-20	0.024
385.0	1.66E-20	0.024	390.0	3.03E-20	0.024	395.0	2.63E-20	0.024
400.0	3.36E-20	0.024	405.0	3.66E-20	0.024	410.0	4.56E-20	0.024
415.0	6.43E-20	0.024	420.0	5.46E-20	0.024	425.0	9.22E-20	0.024
430.0	6.77E-20	0.024	435.0	5.99E-20	0.024	440.0	1.17E-19	0.024
445.0	7.15E-20	0.024	450.0	7.30E-20	0.024	455.0	2.01E-19	0.024
460.0	0.00E-01	0.024						

Photolysis Set = ONITR

264.9	2.91E-20	1.000	268.5	2.66E-20	1.000	272.1	2.37E-20	1.000
275.9	2.01E-20	1.000	279.7	1.64E-20	1.000	283.7	1.29E-20	1.000
287.8	9.92E-21	1.000	292.0	7.49E-21	1.000	296.3	5.62E-21	1.000
300.5	4.07E-21	1.000	303.0	3.28E-21	1.000	304.0	2.98E-21	1.000
305.0	2.68E-21	1.000	306.0	2.44E-21	1.000	307.0	2.21E-21	1.000
308.0	1.99E-21	1.000	309.0	1.76E-21	1.000	310.0	1.54E-21	1.000
311.0	1.38E-21	1.000	312.0	1.22E-21	1.000	313.0	1.07E-21	1.000
314.0	9.14E-22	1.000	316.0	6.87E-22	1.000	320.0	4.04E-22	1.000
325.0	1.90E-22	1.000	330.0	0.00E-01	1.000			

Data Used in the March 1988 Version of the RADM Mechanism, but Not in the Recommended Versions

Photolysis Set = MGLYR

233.9	1.23E-20	1.000	236.7	1.47E-20	1.000	239.5	1.69E-20	1.000
242.4	1.70E-20	1.000	245.4	1.67E-20	1.000	248.4	1.75E-20	1.000
251.6	1.80E-20	1.000	254.8	1.81E-20	1.000	258.1	1.89E-20	1.000
261.4	1.99E-20	1.000	264.9	2.12E-20	1.000	268.5	2.38E-20	1.000
272.1	2.61E-20	1.000	275.9	2.79E-20	1.000	279.7	2.96E-20	1.000
283.7	2.93E-20	1.000	287.8	2.93E-20	1.000	292.0	2.71E-20	1.000
296.3	2.32E-20	1.000	300.5	2.14E-20	1.000	303.0	1.93E-20	1.000
304.0	1.84E-20	1.000	305.0	1.75E-20	1.000	306.0	1.65E-20	1.000
307.0	1.55E-20	1.000	308.0	1.45E-20	1.000	309.0	1.35E-20	1.000
310.0	1.26E-20	1.000	311.0	1.23E-20	1.000	312.0	1.21E-20	1.000
313.0	1.19E-20	1.000	314.0	1.17E-20	1.000	316.0	1.04E-20	1.000
320.0	6.44E-21	1.000	325.0	4.00E-21	1.000	330.0	2.00E-21	1.000

(continued)

Table 3 (continued) - 9

WL (nm)	Abs (cm^2)	QY	WL (nm)	Abs (cm^2)	QY	WL (nm)	Abs (cm^2)	QY
335.0	2.50E-22	1.000	340.0	0.00E-01	1.000	355.0	7.23E-22	0.153
360.0	2.46E-21	0.153	365.0	4.00E-21	0.153	370.0	5.55E-21	0.153
375.0	8.00E-21	0.153	380.0	1.08E-20	0.153	385.0	1.51E-20	0.153
390.0	1.99E-20	0.153	395.0	2.40E-20	0.153	400.0	2.87E-20	0.153
405.0	3.75E-20	0.153	410.0	4.42E-20	0.153	415.0	4.82E-20	0.153
420.0	4.96E-20	0.153	425.0	4.97E-20	0.153	430.0	5.18E-20	0.153
435.0	5.87E-20	0.153	440.0	6.01E-20	0.153	445.0	6.06E-20	0.153
450.0	5.40E-20	0.153	455.0	2.97E-20	0.153	460.0	6.96E-21	0.153
465.0	2.00E-21	0.153	470.0	0.00E-01	0.153			

Photolysis Set = DCBR

186.0	2.59E-21	1.000	187.8	2.72E-21	1.000	189.6	2.85E-21	1.000
191.4	2.73E-21	1.000	193.2	2.51E-21	1.000	195.1	2.44E-21	1.000
197.0	2.46E-21	1.000	199.0	2.46E-21	1.000	201.0	2.82E-21	1.000
203.0	2.92E-21	1.000	205.1	3.53E-21	1.000	207.3	3.74E-21	1.000
209.4	4.10E-21	1.000	211.6	4.36E-21	1.000	213.9	4.45E-21	1.000
216.2	4.60E-21	1.000	218.6	4.17E-21	1.000	221.0	4.54E-21	1.000
223.5	3.70E-21	1.000	226.0	3.89E-21	1.000	228.6	2.69E-21	1.000
231.2	2.76E-21	1.000	233.9	1.71E-21	1.000	236.7	1.62E-21	1.000
239.5	7.85E-22	1.000	242.4	6.12E-22	1.000	245.4	2.88E-22	1.000
248.4	2.13E-22	1.000	251.6	1.40E-22	1.000	254.8	1.49E-22	1.000
258.1	1.60E-22	1.000	261.4	1.79E-22	1.000	264.9	2.18E-22	1.000
268.5	2.72E-22	1.000	272.1	3.27E-22	1.000	275.9	4.10E-22	1.000
279.7	5.26E-22	1.000	283.7	6.27E-22	1.000	287.8	7.62E-22	1.000
292.0	9.39E-22	1.000	296.3	1.09E-21	1.000	300.5	1.26E-21	1.000
303.0	1.51E-21	1.000	304.0	1.56E-21	1.000	305.0	1.55E-21	1.000
306.0	1.53E-21	1.000	307.0	1.61E-21	1.000	308.0	1.65E-21	1.000
309.0	1.81E-21	1.000	310.0	1.83E-21	1.000	311.0	1.91E-21	1.000
312.0	2.03E-21	1.000	313.0	2.01E-21	1.000	314.0	1.99E-21	1.000
316.0	2.20E-21	1.000	320.0	2.50E-21	1.000	325.0	2.81E-21	1.000
330.0	3.04E-21	1.000	335.0	3.40E-21	1.000	340.0	3.84E-21	1.000
345.0	4.05E-21	1.000	350.0	4.47E-21	1.000	355.0	4.88E-21	1.000
360.0	4.94E-21	1.000	365.0	5.29E-21	1.000	370.0	5.40E-21	1.000
375.0	5.63E-21	1.000	380.0	5.61E-21	1.000	385.0	5.72E-21	0.997
390.0	6.00E-21	0.981	395.0	5.69E-21	0.922	400.0	6.18E-21	0.693
405.0	5.49E-21	0.356	410.0	5.98E-21	0.135	415.0	5.77E-21	0.060
420.0	0.00E-01	0.018						

Data Used in the Recommended Versions of the RADM Mechanism, but Not in the March 1988 Version

Photolysis Set = MGLYRM

231.2	0.00E-01	1.000	233.9	1.23E-20	1.000	236.7	1.47E-20	1.000
239.5	1.69E-20	1.000	242.4	1.70E-20	1.000	245.4	1.67E-20	1.000

(continued)

Table 3 (continued) - 10

WL (nm)	Abs (cm^2)	QY	WL (nm)	Abs (cm^2)	QY	WL (nm)	Abs (cm^2)	QY
248.4	1.75E-20	1.000	251.6	1.80E-20	1.000	254.8	1.81E-20	1.000
258.1	1.89E-20	1.000	261.4	1.99E-20	1.000	264.9	2.12E-20	1.000
268.5	2.38E-20	1.000	272.1	2.61E-20	1.000	275.9	2.79E-20	1.000
279.7	2.96E-20	1.000	283.7	2.93E-20	1.000	287.8	2.93E-20	1.000
292.0	2.71E-20	1.000	296.3	2.32E-20	1.000	300.5	2.14E-20	1.000
303.0	1.93E-20	1.000	304.0	1.84E-20	1.000	305.0	1.75E-20	1.000
306.0	1.65E-20	1.000	307.0	1.55E-20	1.000	308.0	1.45E-20	1.000
309.0	1.35E-20	1.000	310.0	1.26E-20	1.000	311.0	1.23E-20	1.000
312.0	1.21E-20	1.000	313.0	1.19E-20	1.000	314.0	1.17E-20	1.000
316.0	1.04E-20	1.000	320.0	6.44E-21	1.000	325.0	4.00E-21	1.000
330.0	2.00E-21	1.000	335.0	2.50E-22	1.000	340.0	0.00E-01	1.000
345.0	0.00E-01	0.103	350.0	0.00E-01	0.103	355.0	7.23E-22	0.103
360.0	2.46E-21	0.103	365.0	4.00E-21	0.103	370.0	5.55E-21	0.103
375.0	8.00E-21	0.103	380.0	1.08E-20	0.103	385.0	1.51E-20	0.103
390.0	1.99E-20	0.103	395.0	2.40E-20	0.103	400.0	2.87E-20	0.103
405.0	3.75E-20	0.103	410.0	4.42E-20	0.103	415.0	4.82E-20	0.103
420.0	4.96E-20	0.103	425.0	4.97E-20	0.103	430.0	5.18E-20	0.103
435.0	5.87E-20	0.103	440.0	6.01E-20	0.103	445.0	6.06E-20	0.103
450.0	5.40E-20	0.103	455.0	2.97E-20	0.103	460.0	6.96E-21	0.103
465.0	2.00E-21	0.103	470.0	0.00E-01	0.103			

Photolysis Set = DCBRM

186.0	7.90E-20	1.000	187.8	7.90E-20	1.000	189.6	7.90E-20	1.000
191.4	7.90E-20	1.000	193.2	7.90E-20	1.000	195.1	7.90E-20	1.000
197.0	7.90E-20	1.000	199.0	7.90E-20	1.000	201.0	7.90E-20	1.000
203.0	7.90E-20	1.000	205.1	7.90E-20	1.000	207.3	7.90E-20	1.000
209.4	7.90E-20	1.000	211.6	7.90E-20	1.000	213.9	7.90E-20	1.000
216.2	7.90E-20	1.000	218.6	7.90E-20	1.000	221.0	7.90E-20	1.000
223.5	7.90E-20	1.000	226.0	7.90E-20	1.000	228.6	7.90E-20	1.000
231.2	7.90E-20	1.000	233.9	7.90E-20	1.000	236.7	7.90E-20	1.000
239.5	7.90E-20	1.000	242.4	7.90E-20	1.000	245.4	7.90E-20	1.000
248.4	7.90E-20	1.000	251.6	7.90E-20	1.000	254.8	7.90E-20	1.000
258.1	7.90E-20	1.000	261.4	7.90E-20	1.000	264.9	7.90E-20	1.000
268.5	7.90E-20	1.000	272.1	7.90E-20	1.000	275.9	7.90E-20	1.000
279.7	7.90E-20	1.000	283.7	7.90E-20	1.000	287.8	7.90E-20	1.000
292.0	7.90E-20	1.000	296.3	7.90E-20	1.000	300.5	7.90E-20	1.000
303.0	7.90E-20	1.000	304.0	7.90E-20	1.000	305.0	7.90E-20	1.000
306.0	7.90E-20	1.000	307.0	7.90E-20	1.000	308.0	7.90E-20	1.000
309.0	7.90E-20	1.000	310.0	7.90E-20	1.000	311.0	7.90E-20	1.000
312.0	7.90E-20	1.000	313.0	7.90E-20	1.000	314.0	7.90E-20	1.000
316.0	7.90E-20	1.000	320.0	7.90E-20	1.000	325.0	7.90E-20	1.000
330.0	7.90E-20	1.000	335.0	7.90E-20	1.000	340.0	7.90E-20	1.000
345.0	7.90E-20	1.000	350.0	7.90E-20	1.000	355.0	7.90E-20	0.500
360.0	7.90E-20	0.000	365.0	0.00E-01	0.000			

2.2 Recommended Modifications to the RADM Mechanism

The results of this evaluation study indicated that for the most part the March 1988 version of the RADM gas-phase chemical mechanism is chemically reasonable and performs as well as can reasonably be expected in simulating most of the available chamber data. However, there were aspects of the mechanism which we recommended be modified prior to its use in the RADM-II model. The results of the chamber simulations, discussed in Section 5, show that the performance of the RADM gas-phase mechanism in fitting results of aromatic-NO_x-air chamber experiments was not quite as good as should be expected given the performance of other current gas-phase chemical mechanisms. The test calculations described in Section 6.3 show that the representation of the higher alkanes could be condensed without significantly affecting model predictions. In addition, there were several other areas where it could be argued that minor modifications to the current mechanism might improve its chemical reasonableness. The recommended modifications to the RADM gas-phase chemical mechanism are described and justified below.

2.2.1 Recommended Modifications to the Aromatic Mechanism

There are major gaps in our understanding of the atmospheric reactions of aromatics, and the available laboratory data are not sufficient to serve as a basis for deriving models for the reactions of these compounds. Thus, we have no choice but to use simulations of environmental-chamber experiments as essentially the only means to judge otherwise chemically reasonable alternative assumptions concerning the unknown portions of the aromatics mechanisms. The performance of the RADM mechanism in simulating results of toluene-NO_x-air and xylene-NO_x-air environmental chamber runs, discussed in Section 5, indicated that there was room for improvement in this mechanism. The RADM mechanism was found to have considerably more scatter in the simulations of maximum ozone yields and rates of NO oxidation and O_3 formation than the SAPRC mechanism. By comparison, Jeffries (1989b) found that the Carbon Bond-IV mechanism -- a more condensed mechanism than RADM -- performed comparably to the SAPRC mechanism in simulating the aromatic runs, being somewhat better in simulating the UNC toluene runs, and somewhat worse in simulating UNC xylene runs. Thus by the criterion of performance in simulating the chamber data, the model used in the RADM mechanism to represent the unknown portions of the toluene and xylene mechanisms -- which is based largely on an earlier published aromatics mechanism (Lurmann et al., 1986) -- must be judged to be less reliable than the models used in the current SAPRC or Carbon Bond mechanisms. Since the mechanisms for toluene and xylene serve as the basis for the representation of all the aromatics hydrocarbons, it is clearly important that the RADM-II model incorporate mechanisms for these compounds that are as reliable as possible. For this reason, a major recommendation resulting from this study was that the aromatics photooxidation mechanism be modified to improve its performance in simulations of the toluene and xylene chamber data.

To address this concern, we investigated how the RADM mechanism might be modified to improve its performance in simulating the results of these chamber experiments. The modifications examined involved making the RADM aromatics mechanism more like the aromatics mechanism used in the current SAPRC mechanism (Carter et al., 1988). This approach was employed because (1) independent development of an entirely new aromatics mechanism was beyond the scope of this project; (2) we are familiar with the performance and implementation of the SAPRC aromatics model and know how to adjust it to optimize its ability to fit the chamber data; and (3) although the aromatics model in Carbon Bond IV also performs as satisfactorily in simulating chamber data, its use of lumped structure groups makes it less straightforward to implement in a lumped molecule mechanism such as RADM. In addition, we are less familiar with how to optimize the ability of the Carbon Bond mechanism to fit chamber data. However, it must be recognized that the SAPRC aromatics mechanism uses a highly idealized and simplified representation of the unknown aspects of aromatic reactions, and no claim is made that it is necessarily any more chemically reasonable than the aromatics representation used in any other current mechanism, including that in the RADM mechanism itself.

Two levels of modifications of the aromatic mechanism were examined in the course of this study: one in which the only changes involved parameter values, and the other where more extensive changes were made. The latter is the version of the modified aromatics mechanism which is designated as RADM-M and is listed in Section 2.3. The former is referred to as the "modified parameter" aromatics mechanism, which was recommended for implementation if more extensive changes in the mechanism were not feasible. It is designated as the RADM-P mechanism and is listed in Section 2.4. In the subsequent discussion, the modifications discussed for toluene refer to the reactions of the RADM model species TOL, and the modifications discussed for xylenes refer to reactions of the model species XYL. In both cases, the following parameter changes were recommended:

(1) It was recommended that the yields of methyl glyoxal (MGLY) and (for the modified parameter mechanism) glyoxal (GLY) be reduced to be more consistent with experimental yields of these products from toluene and m-xylene (Atkinson, 1989, and references therein). In addition, the yield of cresols (CSL) from toluene was increased slightly to be more consistent with the results of Gery et al. (1985) and Atkinson et al. (1989); this also resulted in somewhat improved fits of model simulations of maximum ozone yields in toluene-NO_x-air experiments. The specific changes in yields of these products are as follows:

	RADM	RADM-M and RADM-P
MGLY yield from TOLP	0.724	0.17
MGLY yield from XYLP	1.0	0.45
GLY yield form TOLP	0.181	0.16
CSL yield form TOL	0.16	0.25

(2) Although the available documentation of the derivation of photolysis rates to be used in the RADM mechanism (NCAR, 1987) states that the methylglyoxal quantum yields in the higher wavelength band are based on the data of Plum et al. (1983), the RADM mechanism actually uses higher quantum yield than indicated by those data. In particular, as shown in Table 3 (see photolysis file "MGLYR"), the RADM mechanism uses a wavelength-independent quantum yield of 0.153 for wavelengths above 350 nm, while the data of Plum et al. (1983) indicate that the quantum yield should be 0.107. We therefore recommended that the methylglyoxal quantum yields for these wavelengths be decreased to the lower value which is more consistent with the data of Plum et al. (1983). The modified sets of quantum yields recommended for methylglyoxal are listed in Table 3 (photolysis file "MGLYRM").

(3) The RADM mechanism uses the model species DCB to represent the uncharacterized aromatic ring fragmentation products. The photolysis

rates of these compounds, and the wavelengths where they photolyze, are unknown. In the RADM mechanism, the species DCB photolyzes at the same wavelengths as NO_2, but at a rate which is 10 times slower. The ratio to NO_2 is presumably based on results of simulations of chamber runs. However, in the development of the SAPRC mechanism, it was found that better performance in simulating the chamber data, especially runs carried out using a blacklight light source, could be obtained if it was assumed that this species photolyzes more rapidly, and photolyzes primarily at much lower wavelengths than those responsible for the photolysis of NO_2. Therefore, we recommended that the absorption coefficient, quantum yield products used in the SAPRC mechanism for the unknown aromatic fragmentation species be used in the RADM mechanism for DCB. This consists of assuming the absorption coefficient x quantum yield product is constant at 7.9×10^{-20} cm^2 $molecule^{-1}$, base e, at wavelengths of 350 nm or below, and decreases linearly to zero at 360 nm. This is essentially arbitrary, but allows good fits to aromatic-NO_x-air experiments carried out using a variety of light sources. The modified absorption coefficient x quantum yield products are listed in Table 3 (photolysis set "DCBRM").

(4) The yields of the DCB species from toluene and xylene were adjusted to optimize the fits of model simulations to results of selected SAPRC toluene-NO_x-air and m-xylene-NO_x-air experiments The approach employed, and the specific experiments whose results were utilized in the optimizations is the same as those used to derive the uncharacterized aromatic fragmentation product yields in the current SAPRC mechanism (Carter, 1988). The best fit DCB yields depended on the other changes made to the aromatic mechanism, which differed depending on whether changes other than just modifying parameter values were made. Thus, the optimum DCB yields for the modified parameter (RADM-P) mechanism are slightly different from those for the recommended (RADM-M) mechanism where other changes were made. These are indicated below:

	RADM	RADM-P	RADM-M
DCB yield from TOLP	0.905	0.70	0.68
DCB yield from XYLP	1.0	0.806	0.79

(5) The RADM mechanism uses an OH + XYL rate constant which was derived based on an analysis of total U. S. emissions data which we carried out during the initial review of the 1987 version of the RADM mechanism. However, since the time this initial analyses was carried out, the emissions assignments and rate constant estimates have been updated as a result of the work carried out for the California ARB (Carter, 1988), and there have also been some changes to methods used for aggregating emissions input into RADM. (See Section 3 of this report for a discussion of our analyses for aggregating emissions into RADM.) Therefore, an updated analysis of the emissions data was carried out for the purpose of developing our final recommendations in this regard, and the results are documented in Section 3.3. This updated analysis resulted in slight changes in the recommended OH radical rate constants for XYL and some of the other lumped species. In the recommended mechanisms, the A factor for the OH + XYL reaction was changed from 2.1×10^{-11} to 1.89×10^{-11} cm^3 $molecule^{-1}$ sec, to correspond better to the revised emissions analysis. This value was used in calculating the optimum DCB yields from XYLP, discussed above.

The modified product yields recommended for toluene and xylene given above actually refer to the yields of these products formed in the reaction of their corresponding peroxy radicals (TOLP and XYLP, respectively) with NO. The RADM mechanism also has these radical species reacting with HO_2, methyl peroxy (MO2), and acetyl peroxy (ACO3) radicals. The recommendations do not affect the species representing the products formed in the HO_2 reactions (which is the lumped higher hydroperoxide species OP2), but do affect the species formed in the other two reactions. For these reactions, the recommended product yields were derived based on assuming that the set of organic products formed from TOLP and XYLP are the same as those formed in the NO reaction, with the radical and MO2 or ACO3 product yields being determined based on assuming these reactions occur 50% via RO + RO + O_2 formation, and 50% via ROH formation. This may be somewhat arbitrary, but represents a systematic and self-consistent method for deriving product yields for the many peroxy radical species in this mechanism and, in view of our lack of knowledge of what the actual reactions and species are, appears to be as good as any other set of assumptions.

The above are the modifications recommended for the aromatic mechanism that involve only changes of parameter values, and thus are the modifications implemented in the RADM-P version of the mechanism. However, if more extensive modifications could be made, then it was recommended that the representation of the aromatic fragmentation products be simplified. Chamber simulations carried out in this study indicate that a simplified DCB mechanism, where the species TPAN and TCO3 are replaced by PAN and ACO3, respectively, and where GLY is eliminated, performs equally well, or even slightly better, in simulating the results of the chamber experiments, yet requires three fewer species. In view of the fact that the more complex "DCB" mechanism used in the evaluated RADM mechanism is based on theories of aromatic reactions (e.g., Atkinson et al. 1980) which are now known to be incorrect or at best incomplete (e.g., Atkinson, 1988 and references therein), that mechanism has no claim to greater chemical reasonableness than the more simplified representation that is recommended. The recommended simplifications are implemented in the RADM-M mechanism, and the specific changes involved are discussed below. (All these simplifications were implemented in the RADM-M mechanism before the optimum DCB yields were calculated.)

(1) Glyoxal (GLY) makes a relatively small contribution to the reactivity of aromatics compared to the much more reactive products methyl glyoxal (MGLY) and DCB. Thus, it is recommended that GLY be removed from the RADM mechanism, where it is formed only from TOL, and its contribution to reactivity be represented by having it lumped with the other aromatic fragmentation products which are represented by DCB. (The optimization of the yield of DCB from TOL in a mechanism where GLY is removed will automatically take its contribution to reactivity into account). Since glyoxal in itself is not (to our knowledge) of special significance to acid deposition, there is no reason to represent it explicitly in regional acid deposition models if its contribution to reactivity can be satisfactorily represented in other ways. If it is important, its formation from xylenes and other aromatics should also be included. We assume that this is not the case.

(2) The products of the reactions of DCB are assumed to be similar to those for the reactions of methyl glyoxal, and are represented as follows:

DCBX + HV = HO2 + CO + ACO3

DCBX + HO = ACO3

(DCB is renamed DCBX in the RADM-M mechanism to indicate that it reacts differently.) The photolysis reaction occurs with the same rate and spectral response as used in the modified parameter mechanism, which in turn is the same as that used in the SAPRC mechanism for unknown aromatic fragmentation products (as discussed above). The OH radical reaction is assumed to have the same rate constant as that for methyl glyoxal. The NO_3 radical reaction is unlikely to be a significant loss route for this species (or for NO_3), and is ignored. Although this simpler representation of DCB reactions is not necessarily any more chemically reasonable than that used in RADM or RADM-P, it has the significant advantage that it results in the removal of TCO3 and TPAN from the mechanism since the DCB reactions are the only source for these species in the evaluated RADM mechanism.

The removal of TPAN from the mechanism means that PAN is used to represent all types of PAN analogues that might be formed in the reactions of unidentified aromatic fragmentation products. This is not inconsistent with the general concept of the level of detail intended for this mechanism, since PAN is not represented explicitly in any case. In the RADM mechanism, the model species PAN represnts not only PAN, but PPN and other higher PAN analogues formed in non-aromatic systems. Thus, in the recommended modification for RADM-M, the higher PAN analogues (if any) formed from unknown aromatic fragmentation products are in effect lumped with the other higher PAN analogues. We see no a-priori reason why it is necessary to have separate representations of the higher PAN analogues formed from aromatics when this is not the case for those formed from alkanes, alkenes, and other species.

Comparisons of the performance of the RADM, the modified parameter RADM-P and the recommended RADM-M mechanisms in simulating the maximum ozone yields and rates of NO oxidation and ozone formation in the aromatic-NO_x-air experiments is shown in Figure 1. (See Section 4 for a discussion of how the simulations of the environmental chamber experiments were carried out, and see Section 5 for a more extensive discussion of the performance of the RADM and the RADM-M mechanisms in simulating these

```
                          RADM            RADM-P          RADM-M

                               Fits to Maximum Ozone
                         [Calculated - Experimental (ppm)]

   Model Low
       <  -0.33        :               :               :
 -0.33 -  -0.27        :5              :               :
 -0.27 -  -0.21        :2              :               :
 -0.21 -  -0.15        :               :               :
 -0.15 -  -0.09        :               :15             :15
 -0.09 -  -0.03        :14446          :24             :1246
 -0.03 -   0.03      --:11116         -:111111111446  -:11111111446
  0.03 -   0.09        :11111146       :116            :11366
  0.09 -   0.15        :16             :133466         :13334
  0.15 -   0.21        :1              :33             :
  0.21 -   0.27        :333            :3              :3
  0.27 -   0.33        :3              :               :
       >   0.33        :3              :               :
  Model High

                          Fits to Average d([O3]-[NO])/dt
                       [(Calculated - Experimental)/Calculated]

   Model Slow
       <  -1.00        :               :               :
 -1.00 -  -0.82        :               :               :
 -0.82 -  -0.64        :               :               :
 -0.64 -  -0.45        :125            :               :
 -0.45 -  -0.27        :               :11             :11
 -0.27 -  -0.09        :1144           :133            :133
 -0.09 -   0.09      --:13336         -:112334456     -:111112334456
  0.09 -   0.27        :1111113446     :11111366       :11366
  0.27 -   0.45        :1366           :1446           :1446
  0.45 -   0.64        :               :1              :1
  0.64 -   0.82        :1              :               :
  0.82 -   1.00        :               :1              :1
       >   1.00        :1              :               :
  Model Fast
```

Figure 1. Comparison of Fits of RADM and Modified RADM Simulations to Results of Toluene and Xylene-NO_x-Air Chamber Experiments.

Symbols:
1: EC Toluene
2: ITC Toluene
3: UNC Toluene
4: EC m-Xylene
5: ITC m-Xylene
6: UNC o-Xylene

Mechanisms:

RADM	March 1988 Mechanism
RADM-P	Recommended Parameter-only Modifications
RADM-M	Recommended Modifications

experiments). Both modified versions of RADM perform better than the current version in simulating these results, with fewer cases of large discrepancies and more cases of good fits being obtained. Despite its more condensed DCB mechanism, the more extensively modified RADM-M mechanism seems to be slightly better in its overall distribution of discrepancies than the version where only the parameters are modified, though the differences are probably not significant. It is significant, however, that the version of the mechanism with the more detailed (though not necessarily more accurate) representation of DCB mechanism performs no better in simulating the results of these experiments than does the version with three fewer species.

2.2.2 Condensed Higher Alkane Representation

One area where the RADM mechanism is more detailed than the current ADOM (Lurmann and Karamchandani, 1987), Carbon Bond (Gery et al., 1988), and other lumped mechanisms used in regional models is its representation of the reactions of the higher (C_{3+}) alkanes. RADM uses three lumped species to represent the C_{3+} alkanes (plus one additional species each to represent their peroxy radical intermediates), while both ADOM and Carbon Bond use only one lumped species for these compounds. Test calculations were carried out as part of this study to determine whether a moderate level of condensation of the RADM alkane mechanism, where the two higher alkane model species HC5 and HC8 were lumped together and represented by a single species, would have a significant effect on model predictions relative to the evaluated version. The results, given in detail in Section 6.4, indicate that using this condensation has insignificant effects on simulations of species of interest in regional modeling simulations for the wide range of chemical conditions examined. Because of this, we implemented this condensation in the RADM-M mechanism.

The OH radical rate constant and product yield parameters recommended for the new lumped higher alkane species were derived in a manner analogous to the derivation of the recommended parameters for the lumped higher alkane species in the current RADM mechanism, as discussed in Section 3.3.1 of this report. Specifically, values of average OH radical rate constants and product coefficients calculated for the aggregated emissions groups represented by HC5 and HC8 in the evaluated mechanism were further averaged, using reactivity weighing and relative molar emissions in the NAPAP total U.S. anthropogenic emissions inventory, to determine values for these parameters which are appropriate for this lumped HC5+HC8 alkane model species. The averages of the parameters, and the contributions of the various emissions groups to the values derived, are included with the tabulations given for the other RADM model species in Section 3.3.1. Since the average number of carbons calculated for this lumped species based on the NAPAP inventory is approximately 6.3, this new lumped model species is designated "HC6," to be consistent with the nomenclature used in the RADM mechanism. The listing of the RADM-M mechanism shows the reactions recommended for this model species, which replaces the model species HC5 and HC8 in the RADM and RADM-P mechanisms.

(Note that the specific kinetic and mechanistic parameters recommended for the new lumped "HC6" species based in the analysis in Section 3.3.1 are slightly different from those used in the sensitivity tests discussed in Section 6.4. This is because the parameters used in the sensitivity tests were derived based on those used for HC5 and HC8 in the RADM mechanism, for more straightforward comparison with that mechanism. As discussed below in Section 2.2.5, the mechanistic parameters for HC5 and HC8 in the evaluated mechanism are slightly different from those which are currently recommended and implemented in RADM-P.)

It is possible that it may not be much worse an approximation to lump HC3 with the higher alkane classes, as is done in the ADOM and (in effect) the Carbon Bond mechanisms. Test calculations carried out using the most recent SAPRC mechanism indicate that much more severe condensations of the alkane mechanisms can be employed without significantly affecting model predictions, provided the parameters for the lumped species are adjusted appropriately based on the mixture being represented. However, more severe approximations for alkane representation in RADM were not examined, and are not currently recommended.

2.2.3 Modifications to the XNO2 Reactions

The species "XNO2" is used in the RADM mechanism to represent the additional NO_x consumption caused by reactions of NO_3 radicals with dinitrophenols. As such, it actually represents a phenoxy-radical-like species. However, in the RADM mechanism, this species is represented as forming organic nitrates (ONIT) when it reacts with NO_2, forming organic hydroperoxides (OP2) when it reacts with HO_2, and reacting with MO2 and

ACO3 as if it were a peroxy radical. We believe that it is more chemically reasonable not to have it form ONIT or OP2 in its respective reactions with NO_2 and HO_2, and that it is equally chemically reasonable to use a simpler representation of its loss in the absence of NO_2 or HO_2. Therefore, modifications in this aspect of the mechanism are recommended for both improved chemical reasonableness and to simplify the mechanism. These modifications are implemented in the RADM-M mechanism, but could not be implemented into RADM-P.

The reaction of XNO2 with NO_2 actually represents the reaction of nitro-substituted phenoxy radicals with NO_2 to form dinitrophenols. These species probably condense into the aerosol phase and do not react; but if they react at all, it is estimated that the most likely process would be reaction with NO_3 to consume even more NO_x. However, the RADM mechanism in effect represents dinitrophenols as alkyl nitrates (ONIT), whose subsequent reactions tend to re-introduce NO_x into the system. For this reason, it is considered to be more chemically reasonable for the nitrogen in the XNO2 + NO_2 reaction to be "lost", rather than for it to re-appear as ONIT. Therefore, we recommend that the XNO2 + NO_2 reaction have no products, or, if there is a need to keep track of N-balance in the RADM simulations, its products be represented by some unreactive N-containing "counter" species.

The reaction of XNO2 with HO_2 represents a reaction of HO_2 with some type of phenoxy radical. The most likely organic product of such a reaction would be a phenol or nitrophenol, and not a hydroperoxide. Therefore, the use of OP2 as a product in this reaction is probably inappropriate. Since hydroperoxides are assumed to be involved in formation of acid deposition, we recommend that this source of OP2 be removed, and that the XNO2 + HO_2 reaction also have no reactive products.

The reactions used to represent the removal of XNO2 in those cases where it is formed in the absence of significant amounts of HO_2 and NO_2 are usually not important, since usually removal by NO_2 dominates, and the HO_2 reaction is probably adequate to represent its removal in most other cases. The use of peroxy-like reactions for this purpose is not necessarily inappropriate, but is essentially arbitrary. However, this representation introduces unnecessary complexity into the mechanism, probably making it more difficult to implement in "solvers" where the steady state approximation is used for XNO2. To simplify the mechanism and make it easier to implement, we recommend using a simple first-order loss process to represent the consumption of XNO2 in cases where levels of both HO_2 and NO_2 are low. The rate constant we chose for this process in RADM-M (2.0×10^{-4} sec^{-1}) is essentially arbitrary, and corresponds to the loss rate by reaction with 1 ppt of NO_2, or approximately 2 ppt of HO_2. Test calculations show that this simpler representation has essentially no effects on model predictions representative of conditions likely to occur in regional model simulations.

2.2.4 Omitted OLN Reactions

The RADM mechanism includes the reactions of MO2 and ACO3 with all the organic peroxy radical species in the mechanism except for OLN, the peroxy radical which is formed when NO_3 reacts with alkenes. This probably was an oversight, since there is no reason why OLN should be treated differently than the other organic peroxy radical species in this regard. Because under certain conditions at nighttime OLN can be the dominant peroxy radical, it is advisable that the OLN + OLN reaction be included in the mechanism, since that reaction might be its major sink under those conditions. Since the RADM development team were able to readily add these reactions to the mechanism being implemented into RADM (Stockwell, private communication, 1989), these changes are incorporated in the RADM-P as well as the RADM-M recommended modified mechanisms. The rate constants and mechanisms used for these reactions are those of Stockwell (private communication, 1988) derived for the "detailed radical" version of the RADM mechanism, given in Section 6.2.

2.2.5 Parameter Modifications Resulting from Updated Emissions Assignments

As indicated above and discussed in more detail in Section 3.3, kinetic, and in some cases product, yield parameters for a number of lumped species in the RADM mechanism are derived based on an analysis of the species they represent in the NAPAP total U.S. emissions inventory. The parameters used in the evaluated RADM mechanism for a number of these species are based on recommendations we made in this regard as part of our initial review of the 1987 version of the mechanism. However, an updated analysis of these data, discussed in Section 3.3 of this report, resulted in slight changes being recommended for several of these parameters. The specific changes which were recommended are given in the appropriate tabulations in Section 3.3, and are incorporated into both the recommended modified RADM-M and RADM-P mechanisms.

The recommended product yields given in the tables in Section 3.3 refer to yields under conditions where the reactions of peroxy radicals with NO dominate. The RADM mechanism also has peroxy radicals reacting with HO_2, MO2, and ACO3. The modified recommended product yields do not affect the products of the HO_2 reactions, since these are represented by separate hydroperoxide species. However, they do affect the products formed in the MO2 or ACO3 reactions. The products in those reactions were derived based on assuming that the products from MO2 and ACO3 are the same as in the RADM mechanism, and that the oxygenated products formed from the lumped peroxy radicals (e.g., HC3P, etc.) are the same as those formed in the NO reaction, excluding ONIT. In all cases, the radical yields were derived based on assuming the reactions occur 50% via RO + RO + O_2 formation, and 50% via ROH formation. This is the same approach as discussed above for TOLP and XYLP in the modified aromatics mechanisms and is in line with the representation for most of these reactions in other current mechanisms.

2.3 The Recommended Modified Mechanism (RADM-M)

The RADM-M mechanism is the version of the RADM mechanism which incorporates all the modifications recommended as a result of this study. It has the same inorganic reaction set and (except for the aromatic product species DCB and its PAN analogue and the rate of methyl glyoxal photolysis) the same mechanisms for reactive product species as employed in the RADM mechanism. Except for the lumping together of the two higher alkane classes and slight simplifications in mechanisms for some aromatic products, this mechanism represents the same level of condensation and chemical detail as employed in the RADM mechanism. However, results of test calculations representing the range of chemical conditions likely to be encountered in regional model simulations, given in Section 6.5 of this report, indicate that there are cases where these mechanisms can give significantly different predictions. These differences are attributed primarily to changes in the aromatics mechanism that were made to improve its performance in simulating results of chamber data. Other test calculations suggest that the other modifications, which are recommended primarily to yield a mechanism that is somewhat more compact and (in the case of reactions involving XNO2) somewhat more chemically reasonable, should have relatively little effect on predictions under most conditions.

The organic model species used in the RADM-M mechanism are listed in Table 4, and their reactions and thermal rate parameters are listed in Table 5. The inorganic species and their reactions and rate parameters are not included in these tables because they are the same as those listed for the RADM mechanism in Tables 1 and 2, respectively. The absorption coefficients and quantum yields used for the photolysis reactions in this mechanism are given in Table 3.

2.4 The Modified Parameter Mechanism (RADM-P)

The RADM-P mechanism is the version of the RADM mechanism which incorporates all the modifications recommended as a result of this study that can be implemented by changing only kinetic or product yield values. Because of practical difficulties involved in making the more extensive changes required to implement RADM-M, this is the version of the mechanism which is being implemented into the RADM-II model (Stockwell, private communication, 1989). This mechanism has the same number of species and (except for the three OLN reactions which were added) the same number of reactions as the March 1988 RADM mechanism, and thus represents almost exactly the same level of chemical detail and condensation. Its major modifications are the changes in parameters involved in the aromatic mechanisms which were made to improve its performance in simulating the chamber data. As with the RADM-M mechanism, test calculations discussed in Section 6.5 indicate that these changes result in cases where this mechanism can yield significantly different predictions in simulations representing conditions of regional model simulations. The other modifications concern the addition of the usually relatively unimportant OLN reactions and the minor changes in parameters for lumped species based on the updated analysis of the emissions data.

Table 4. Organic Model Species Employed in the Recommended Modified Version of the RADM Gas-Phase Chemical Mechanism (RADM-M)

Name	Description
Organic Hydrocarbons	
CH4	Methane
ETH	Ethane
HC3	C3+ Alkanes with kOH < 5 x 10^3 (a)
HC6	Alkanes with kOH > 0.5 x 10^4
OL2	Ethene
OLT	Terminal Monoalkenes
OLI	Internal Alkenes, Terpenes, Conjugated Dialkenes
ISO	Isoprene
TOL	Aromatic Hydrocarbons with kOH < 2 x 10^4
XYL	Aromatic Hydrocarbons wit kOH > 2 x 10^4
Organic Oxidation Products	
HCHO	Formaldehyde
ALD	Lumped Higher Aldehydes
KET	Ketones
MGLY	Methyl Glyoxal
DCBX	Uncharacterized Reactive Aromatic Fragmentation Products
CSL	Phenols and Cresols
PAN	Acyl Peroxy Nitrates
ONIT	Other Organic Nitrates (primarily alkyl nitrates)
OP1	Methyl Hydroperoxide
OP2	Higher Organic Hydroperoxides
ORA1	Formic Acid
ORA2	Higher Organic Acids (other than peroxy acetic acid)
PAA	Peroxy Acetic Acid
Organic Radicals	
MO2	Methyl Peroxy Radicals
ETHP	Ethyl Peroxy Radicals
HC3P	Peroxy Radicals from OH + HC3
HC6P	Peroxy Radicals from OH + HC6
OL2P	Peroxy Radicals from OH + Ethene
OLTP	Peroxy Radicals from OH + Isoprene and Terminal Alkenes
OLIP	Peroxy Radicals from OH + Internal Alkenes
KETP	Peroxy Radicals from OH + Ketones
TOLP	Peroxy Radicals from OH + Benzene and Monoalkyl Benzenes
XYLP	Peroxy Radicals from OH + Xylenes and More Reactive Aromatics
OLN	Peroxy Radicals from NO_3 + Alkenes

(continued)

Table 4 (continued) - 2

Name	Description
XO2	Chemical Operator Used to Account for NO-to-NO_2 conversions due to Secondarily Formed Organic Peroxy Radicals
ACO3	Acyl Peroxy Radicals
XNO2	Chemical Operator Used to Account for NO_x Loss Due to Reactions of NO_3 with Phenols and Cresols.

(a) kOH is the OH radical rate constant at 300 K in ppm^{-1} min^{-1}.

Table 5. Listing of the Organic Reactions in the Recommended Modified Version of the RADM Gas-Phase Chemical Mechanism (RADM-M)

Rxn. Label (a)	Kinetic Parameters (b)				Reactions (b)
	k(300)	A	Ea	B	
					Organic Photolysis Reactions
010	(Phot. Set = HCHOMR)				HCHO + HV = H2 + CO
011	(Phot. Set = HCHORR)				HCHO + HV = HO2 + HO2 + CO
012	(Phot. Set = ALDR)				ALD + HV = MO2 + HO2 + CO
013	(Phot. Set = OPR)				OP1 + HV = HCHO + HO2 + HO
014	(Phot. Set = OPR)				OP2 + HV = ALD + HO2 + HO
015	(Phot. Set = PAAR)				PAA + HV = MO2 + CO2 + HO
016	(Phot. Set = KETR)				KET + HV = ACO3 + ETHP
019	(Phot. Set = MGLYRM)				MGLY + HV = ACO3 + HO2 + CO
M01	(Phot. Set = DCBRM)				DCBX + HV = HO2 + CO + ACO3
021	(Phot. Set = ONITR)				ONIT + HV = #.20 ALD + #.80 KET + HO2 + NO2
					Organic + OH Reactions
051	1.29E+01	9.23E+02	2.54	1.00	CH4 + HO = MO2 + H2O
052	4.11E+02	1.81E+03	0.88	1.00	ETH + HO = ETHP + H2O
053	3.86E+03	2.33E+04	1.07	-1.00	HC3 + HO = #.83 HC3P + #.17 HO2 + #.009 HCHO + #.075 ALD + #.025 KET + H2O
M02	1.09E+04	3.86E+04	0.75	-1.00	HC6 + HO = HC6P + #.51 XO2 + H2O
056	1.24E+04	3.16E+03	-0.82	-1.00	OL2 + HO = OL2P
057	4.19E+04	7.81E+03	-1.00	-1.00	OLT + HO = OLTP
058	9.79E+04	1.57E+04	-1.09	-1.00	OLI + HO = OLIP
074	1.46E+05	3.74E+04	-0.81	-1.00	ISO + HO = OLTP
059	9.02E+03	3.08E+03	-0.64	-1.00	TOL + HO = #.76 TOLP + #.24 CSL + #.24 HO2
060	4.09E+04	2.77E+04	-0.23	-1.00	XYL + HO = #.83 XYLP + #.17 CSL + #.17 HO2
063	1.32E+04	1.32E+04	0.00	-1.00	HCHO + HO = HO2 + CO + H2O
064	2.37E+04	1.01E+04	-0.51	-1.00	ALD + HO = ACO3 + H2O
065	1.47E+03	1.76E+04	1.48	-1.00	KET + HO = KETP + H2O
067	2.50E+04	2.50E+04	0.00	-1.00	MGLY + HO = ACO3 + CO + H2O
M03	2.50E+04	2.50E+04	0.00	-1.00	DCBX + HO = ACO3
061	5.87E+04	5.87E+04	0.00	-1.00	CSL + HO = #.1 HO2 + #.9 XO2 + #.9 ACO3
062	5.28E+04	5.28E+04	0.00	-1.00	CSL + HO = CSL
069A	7.34E+03	7.34E+03	0.00	-1.00	OP1 + HO = MO2
069B	7.34E+03	7.34E+03	0.00	-1.00	HO + OP1 = HO + HCHO
070A	7.34E+03	7.34E+03	0.00	-1.00	OP2 + HO = HC3P
070B	7.34E+03	7.34E+03	0.00	-1.00	HO + OP2 = HO + ALD

(continued)

Table 5 (continued) - 2

Rxn. Label (a)	Kinetic Parameters (b)				Reactions (b)
	k(300)	A	Ea	B	
071	1.47E+04	1.47E+04	0.00	-1.00	PAA + HO = ACO3 + H2O
072	2.06E+02	9.06E+02	0.88	1.00	PAN + HO = HCHO + NO3 + XO2
073	3.76E+03	2.28E+04	1.07	-1.00	ONIT + HO = HC3P + NO2
					Organic + NO3 Reactions
093	9.23E-01	8.81E+02	4.09	-1.00	HCHO + NO3 = HO2 + HNO3 + CO
094	3.65E+00	2.06E+03	3.78	-1.00	ALD + NO3 = ACO3 + HNO3
096	3.65E+00	2.06E+03	3.78	-1.00	MGLY + NO3 = HNO3 + ACO3 + CO
098	3.23E+04	3.23E+04	0.00	-1.00	CSL + NO3 = HNO3 + XNO2 + #.5 CSL
099	1.72E-01	2.94E+03	5.81	-1.00	OL2 + NO3 = OLN
100	2.65E+01	1.47E+04	3.77	-1.00	OLT + NO3 = OLN
101	1.84E+03	4.74E+04	1.94	-1.00	OLI + NO3 = OLN
102	8.53E+02	8.53E+02	0.00	-1.00	ISO + NO3 = OLN
					Organic + O3 Reactions
103	2.72E-03	1.76E+01	5.23	-1.00	OL2 + O3 = HCHO + #.42 CO + #.4 ORA1 + #.12 HO2
104	1.74E-02	1.94E+01	4.18	-1.00	OLT + O3 = #.53 HCHO + #.50 ALD + #.33 CO + #.20 ORA1 + #.20 ORA2 + #.23 HO2 + #.22 MO2 + #.10 HO + #.06 CH4
105	2.43E-01	1.07E+01	2.26	-1.00	OLI + O3 = #.18 HCHO + #.72 ALD + #.10 KET + #.23 CO + #.06 ORA1 + #.29 ORA2 + #.09 CH4 + #.26 HO2 + #.14 HO + #.31 MO2
106	2.20E-02	1.81E+01	4.00	-1.00	ISO + O3 = #.53 HCHO + #.50 ALD + #.33 CO + #.20 ORA1 + #.20 ORA2 + #.23 HO2 + #.22 MO2 + #.10 HO
					Organic Peroxy + NO2 Reactions
075	7.52E+03	4.11E+03	-0.36	-1.00	ACO3 + NO2 = PAN
076	2.90E-02	1.17E+18	26.91	0.00	PAN = ACO3 + NO2
					Organic Peroxy + NO Reactions
086	1.12E+04	6.17E+03	-0.36	-1.00	ACO3 + NO = MO2 + NO2
079	1.12E+04	6.17E+03	-0.36	-1.00	MO2 + NO = HCHO + HO2 + NO2
080	1.12E+04	6.17E+03	-0.36	-1.00	HC3P + NO = #.75 ALD + #.25 KET + #.09 HCHO + #.036 ONIT + #.964 NO2 + #.964 HO2

(continued)

Table 5 (continued) - 3

Rxn. Label (a)	Kinetic Parameters (b) k(300)	A	Ea	B	Reactions (b)
M04	1.12E+04	6.17E+03	-0.36	-1.00	HC6P + NO = #.38 ALD + #.87 KET + #.15 ONIT + #.03 HCHO + #.85 NO2 + #.85 HO2
083	1.12E+04	6.17E+03	-0.36	-1.00	OL2P + NO = #1.6 HCHO + HO2 + NO2 + #.2 ALD
084	1.12E+04	6.17E+03	-0.36	-1.00	OLTP + NO = ALD + HCHO + HO2 + NO2
085	1.12E+04	6.17E+03	-0.36	-1.00	OLIP + NO = HO2 + #1.45 ALD + #.28 HCHO + #.10 KET + NO2
088	1.12E+04	6.17E+03	-0.36	-1.00	TOLP + NO = NO2 + HO2 + #.17 MGLY + #.68 DCBX
089	1.12E+04	6.17E+03	-0.36	-1.00	XYLP + NO = NO2 + HO2 + #.45 MGLY + #.79 DCBX
090	1.12E+04	6.17E+03	-0.36	-1.00	ETHP + NO = ALD + HO2 + NO2
091	1.12E+04	6.17E+03	-0.36	-1.00	KETP + NO = MGLY + NO2 + HO2
092	1.12E+04	6.17E+03	-0.36	-1.00	OLN + NO = HCHO + ALD + #2 NO2
150	1.12E+04	6.17E+03	-0.36	-1.00	XO2 + NO = NO2
					Organic Peroxy + HO2 Reactions
107	8.61E+03	1.13E+02	-2.58	-1.00	HO2 + MO2 = OP1
108		(Same k as 107)			HO2 + ETHP = OP2
109		(Same k as 107)			HO2 + HC3P = OP2
M05		(Same k as 107)			HO2 + HC6P = OP2
112		(Same k as 107)			HO2 + OL2P = OP2
113		(Same k as 107)			HO2 + OLTP = OP2
114		(Same k as 107)			HO2 + OLIP = OP2
115		(Same k as 107)			HO2 + KETP = OP2
117		(Same k as 107)			HO2 + TOLP = OP2
118		(Same k as 107)			HO2 + XYLP = OP2
120		(Same k as 107)			HO2 + OLN = ONIT
146		(Same k as 107)			HO2 + XO2 = OP2
116		(Same k as 107)			HO2 + ACO3 = PAA
					Organic Peroxy + ACO3 Reactions
142	3.64E+03	1.75E+03	-0.44	-1.00	ACO3 + ACO3 = #2 MO2
130	2.93E+03	1.41E+03	-0.44	-1.00	MO2 + ACO3 = HCHO + #.5 HO2 + #.5 MO2 + #.5 ORA2
134	1.04E+03	4.99E+02	-0.44	-1.00	ETHP + ACO3 = ALD + #.5 HO2 + #.5 MO2 + #.5 ORA2
135	3.06E+02	1.47E+02	-0.44	-1.00	HC3P + ACO3 = #.77 ALD + #.26 KET + #.09 HCHO + #.5 HO2 + #.5 MO2 + #.5 ORA2

(continued)

Table 5 (continued) - 4

Rxn. Label (a)	Kinetic Parameters (b)				Reactions (b)
	k(300)	A	Ea	B	
M06	2.57E+02	1.23E+02	-0.44	-1.00	HC6P + ACO3 = #.45 ALD + #1.02 KET + #.04 HCHO + #.5 HO2 + #.5 MO2 + #.5 ORA2
138	1.04E+03	4.99E+02	-0.44	-1.00	OL2P + ACO3 = #.8 HCHO + #.6 ALD + #.5 HO2 + #.5 MO2 + #.5 ORA2
139	1.04E+03	4.99E+02	-0.44	-1.00	OLTP + ACO3 = ALD + #.5 HCHO + #.5 HO2 + #.5 MO2 + #.5 ORA2
140	1.28E+02	6.17E+01	-0.44	-1.00	OLIP + ACO3 = #.725 ALD + #.55 KET + #.14 HCHO + #.5 HO2 + #.5 MO2 + #.5 ORA2
141	1.28E+02	6.17E+01	-0.44	-1.00	KETP + ACO3 = MGLY + #.5 HO2 + #.5 MO2 + #.5 ORA2
143	1.28E+02	6.17E+01	-0.44	-1.00	ACO3 + TOLP = #.17 MGLY + #.68 DCBX + #.5 HO2 + #.5 MO2 + #.5 ORA2
144	1.28E+02	6.17E+01	-0.44	-1.00	ACO3 + XYLP = #.45 MGLY + #.79 DCBX + #.5 HO2 + #.5 MO2 + #.5 ORA2
M07	1.28E+02	6.17E+01	-0.44	-1.00	OLN + ACO3 = HCHO + ALD + #.5 ORA2 + NO2 + #.5 MO2
148	1.28E+02	6.17E+01	-0.44	-1.00	XO2 + ACO3 = MO2
					Organic Peroxy + MO2 Reactions
121	5.81E+02	2.79E+02	-0.44	-1.00	MO2 + MO2 = #1.5 HCHO + HO2
122	4.28E+02	2.06E+02	-0.44	-1.00	MO2 + ETHP = #.75 HCHO + HO2 + #.75 ALD
123	1.28E+02	6.17E+01	-0.44	-1.00	MO2 + HC3P = #.84 HCHO + HO2 + #.77 ALD + #.26 KET
M08	1.04E+02	4.99E+01	-0.44	-1.00	MO2 + HC6P = #.79 HCHO + HO2 + #.45 ALD + #1.02 KET
126	4.28E+02	2.06E+02	-0.44	-1.00	MO2 + OL2P = #1.55 HCHO + HO2 + #.35 ALD
127	4.28E+02	2.06E+02	-0.44	-1.00	MO2 + OLTP = #1.25 HCHO + HO2 + #.75 ALD
128	5.19E+01	2.50E+01	-0.44	-1.00	MO2 + OLIP = #.89 HCHO + HO2 + #.725 ALD + #.55 KET
129	5.19E+01	2.50E+01	-0.44	-1.00	MO2 + KETP = #.75 HCHO + HO2 + #.75 MGLY
131	5.19E+01	2.50E+01	-0.44	-1.00	MO2 + TOLP = #.75 HCHO + HO2 + #.17 MGLY + #.68 DCBX
132	5.19E+01	2.50E+01	-0.44	-1.00	MO2 + XYLP = #.75 HCHO + HO2 + #.45 MGLY + #.79 DCBX

(continued)

Table 5 (continued) - 5

Rxn. Label (a)	Kinetic Parameters (b)				Reactions (b)
	k(300)	A	Ea	B	
M09	5.19E+01	2.50E+01	-0.44	-1.00	MO2 + OLN = #1.75 HCHO + #.5 HO2 + ALD + NO2
147	5.19E+01	2.50E+01	-0.44	-1.00	MO2 + XO2 = HCHO + HO2
					Other Organic Peroxy + Peroxy Reactions
149	1.10E+00	5.28E-01	-0.44	-1.00	XO2 + XO2 =
M10	1.10E+00	5.28E-01	-0.44	-1.00	OLN + OLN = #2 HCHO + #2 ALD + #2 NO2
					XNO2 Reactions
M11	1.12E+04	6.17E+03	-0.36	-1.00	XNO2 + NO2 = (Loss-of-NOx)
M12		(Same k as 107)			XNO2 + HO2 =
M13	1.20E-02	(No T Dependence)			XNO2 =

Notes:

(a) Reactions which correspond directly to reactions in the March 1988 RADM mechanism in Table 2 are given the same reaction labels as used for them in Table 2. Reactions that were added or significantly modified relative to the mechanism in Table 2 are indicated by the label "Mxx".

(b) See Footnotes (b) and (c) in Table 2 for a description of the formats used in the kinetic parameter and the reaction listings.

The model species used in the RADM-P mechanism are the same as those listed for the RADM mechanism in Table 1. The organic reactions and their thermal rate parameters for the RADM-P mechanism are listed in Table 6. The inorganic reactions and rate parameters are also the same as those of the mechanism listed in Table 2 and are thus not included in Table 6. The absorption coefficients and quantum yields used for the photolysis reactions in this mechanism are the same as used for the RADM-M mechanism and are given in Table 3. This mechanism was implemented by Stockwell on his modeling software at SUNY, and test calculations indicate that the mechanism implemented at SUNY is consistent with its implementation at SAPRC.

Table 6. Listing of the Organic Reactions in the Modified Parameter Version of the RADM Gas-Phase Chemical Mechanism (RADM-P)

Rxn. Label (a)	Kinetic Parameters (b)				Reactions (b)
	k(300)	A	Ea	B	
					Organic Photolysis Reactions
010	(Phot. Set = HCHOMR)				HCHO + HV = H2 + CO
011	(Phot. Set = HCHORR)				HCHO + HV = HO2 + HO2 + CO
012	(Phot. Set = ALDR)				ALD + HV = MO2 + HO2 + CO
013	(Phot. Set = OPR)				OP1 + HV = HCHO + HO2 + HO
014	(Phot. Set = OPR)				OP2 + HV = ALD + HO2 + HO
015	(Phot. Set = PAAR)				PAA + HV = MO2 + CO2 + HO
016	(Phot. Set = KETR)				KET + HV = ACO3 + ETHP
017	(Phot. Set = GLY2R)				GLY + HV = #.13 HCHO + #1.87 CO
018	(Phot. Set = GLY1R)				GLY + HV = #.45 HCHO + #1.55 CO + #.80 HO2
019	(Phot. Set = MGLYRM)				MGLY + HV = ACO3 + HO2 + CO
020	(Phot. Set = DCBRM)				DCB + HV = #.98 HO2 + #.02 ACO3 + TCO3
021	(Phot. Set = ONITR)				ONIT + HV = #.20 ALD + #.80 KET + HO2 + NO2
					Organic + OH Reactions
051	1.29E+01	9.23E+02	2.54	1.00	CH4 + HO = MO2 + H2O
052	4.11E+02	1.81E+03	0.88	1.00	ETH + HO = ETHP + H2O
053	3.86E+03	2.33E+04	1.07	-1.00	HC3 + HO = #.83 HC3P + #.17 HO2 + #.009 HCHO + #.075 ALD + #.025 KET + H2O
054	7.16E+03	2.54E+04	0.75	-1.00	HC5 + HO = HC5P + #.25 XO2 + H2O
055	1.51E+04	5.34E+04	0.75	-1.00	HC8 + HO = HC8P + #.75 XO2 + H2O
056	1.24E+04	3.16E+03	-0.82	-1.00	OL2 + HO = OL2P
057	4.19E+04	7.81E+03	-1.00	-1.00	OLT + HO = OLTP
058	9.79E+04	1.57E+04	-1.09	-1.00	OLI + HO = OLIP
074	1.46E+05	3.74E+04	-0.81	-1.00	ISO + HO = OLTP
059	9.02E+03	3.08E+03	-0.64	-1.00	TOL + HO = #.75 TOLP + #.25 CSL + #.25 HO2
060	4.09E+04	2.77E+04	-0.23	-1.00	XYL + HO = #.83 XYLP + #.17 CSL + #.17 HO2
063	1.32E+04	1.32E+04	0.00	-1.00	HCHO + HO = HO2 + CO + H2O
064	2.37E+04	1.01E+04	-0.51	-1.00	ALD + HO = ACO3 + H2O
065	1.47E+03	1.76E+04	1.48	-1.00	KET + HO = KETP + H2O
066	1.69E+04	1.69E+04	0.00	-1.00	GLY + HO = HO2 + #2 CO + H2O
067	2.50E+04	2.50E+04	0.00	-1.00	MGLY + HO = ACO3 + CO + H2O
061	5.87E+04	5.87E+04	0.00	-1.00	CSL + HO = #.1 HO2 + #.9 XO2 + #.9 TCO3

(continued)

Table 6 (continued) - 2

Rxn. Label (a)	Kinetic Parameters (b) k(300)	A	Ea	B	Reactions (b)
062	5.28E+04	5.28E+04	0.00	-1.00	CSL + HO = CSL
068	4.11E+04	4.11E+04	0.00	-1.00	DCB + HO = TCO3 + H2O
069A	7.34E+03	7.34E+03	0.00	-1.00	OP1 + HO = MO2
069B	7.34E+03	7.34E+03	0.00	-1.00	HO + OP1 = HO + HCHO
070A	7.34E+03	7.34E+03	0.00	-1.00	OP2 + HO = HC3P
070B	7.34E+03	7.34E+03	0.00	-1.00	HO + OP2 = HO + ALD
071	1.47E+04	1.47E+04	0.00	-1.00	PAA + HO = ACO3 + H2O
072	2.06E+02	9.06E+02	0.88	1.00	PAN + HO = HCHO + NO3 + XO2
073	3.76E+03	2.28E+04	1.07	-1.00	ONIT + HO = HC3P + NO2
					Organic + NO3 Reactions
093	9.23E-01	8.81E+02	4.09	-1.00	HCHO + NO3 = HO2 + HNO3 + CO
094	3.65E+00	2.06E+03	3.78	-1.00	ALD + NO3 = ACO3 + HNO3
095	9.23E-01	8.81E+02	4.09	-1.00	GLY + NO3 = HNO3 + HO2 + #2 CO
096	3.65E+00	2.06E+03	3.78	-1.00	MGLY + NO3 = HNO3 + ACO3 + CO
097	3.65E+00	2.06E+03	3.78	-1.00	DCB + NO3 = HNO3 + TCO3
098	3.23E+04	3.23E+04	0.00	-1.00	CSL + NO3 = HNO3 + XNO2 + #.5 CSL
099	1.72E-01	2.94E+03	5.81	-1.00	OL2 + NO3 = OLN
100	2.65E+01	1.47E+04	3.77	-1.00	OLT + NO3 = OLN
101	1.84E+03	4.74E+04	1.94	-1.00	OLI + NO3 = OLN
102	8.53E+02	8.53E+02	0.00	-1.00	ISO + NO3 = OLN
					Organic + O3 Reactions
103	2.72E-03	1.76E+01	5.23	-1.00	OL2 + O3 = HCHO + #.42 CO + #.4 ORA1 + #.12 HO2
104	1.74E-02	1.94E+01	4.18	-1.00	OLT + O3 = #.53 HCHO + #.50 ALD + #.33 CO + #.20 ORA1 + #.20 ORA2 + #.23 HO2 + #.22 MO2 + #.10 HO + #.06 CH4
105	2.43E-01	1.07E+01	2.26	-1.00	OLI + O3 = #.18 HCHO + #.72 ALD + #.10 KET + #.23 CO + #.06 ORA1 + #.29 ORA2 + #.09 CH4 + #.26 HO2 + #.14 HO + #.31 MO2
106	2.20E-02	1.81E+01	4.00	-1.00	ISO + O3 = #.53 HCHO + #.50 ALD + #.33 CO + #.20 ORA1 + #.20 ORA2 + #.23 HO2 + #.22 MO2 + #.10 HO
					Organic Peroxy + NO2 Reactions
075	7.52E+03	4.11E+03	-0.36	-1.00	ACO3 + NO2 = PAN
076	2.90E-02	1.17E+18	26.91	0.00	PAN = ACO3 + NO2

(continued)

Table 6 (continued) - 3

Rxn. Label (a)	Kinetic Parameters (b)				Reactions (b)
	k(300)	A	Ea	B	
077	6.90E+03	6.90E+03	0.00	-1.00	TCO3 + NO2 = TPAN
078	2.90E-02	1.17E+18	26.91	0.00	TPAN = TCO3 + NO2
					Organic Peroxy + NO Reactions
086	1.12E+04	6.17E+03	-0.36	-1.00	ACO3 + NO = MO2 + NO2
087	1.12E+04	6.17E+03	-0.36	-1.00	TCO3 + NO = NO2 + #.92 HO2 + #.89 GLY + #.11 MGLY + #.05 ACO3 + #.95 CO + #2 XO2
079	1.12E+04	6.17E+03	-0.36	-1.00	MO2 + NO = HCHO + HO2 + NO2
080	1.12E+04	6.17E+03	-0.36	-1.00	HC3P + NO = #.75 ALD + #.25 KET + #.09 HCHO + #.036 ONIT + #.964 NO2 + #.964 HO2
081	1.12E+04	6.17E+03	-0.36	-1.00	HC5P + NO = #.38 ALD + #.69 KET + #.08 ONIT + #.92 NO2 + #.92 HO2
082	1.12E+04	6.17E+03	-0.36	-1.00	HC8P + NO = #.35 ALD + #1.06 KET + #.04 HCHO + #.24 ONIT + #.76 NO2 + #.76 HO2
083	1.12E+04	6.17E+03	-0.36	-1.00	OL2P + NO = #1.6 HCHO + HO2 + NO2 + #.2 ALD
084	1.12E+04	6.17E+03	-0.36	-1.00	OLTP + NO = ALD + HCHO + HO2 + NO2
085	1.12E+04	6.17E+03	-0.36	-1.00	OLIP + NO = HO2 + #1.45 ALD + #.28 HCHO + #.10 KET + NO2
088	1.12E+04	6.17E+03	-0.36	-1.00	TOLP + NO = NO2 + HO2 + #.17 MGLY + #.16 GLY + #.70 DCB
089	1.12E+04	6.17E+03	-0.36	-1.00	XYLP + NO = NO2 + HO2 + #.45 MGLY + #.806 DCB
090	1.12E+04	6.17E+03	-0.36	-1.00	ETHP + NO = ALD + HO2 + NO2
091	1.12E+04	6.17E+03	-0.36	-1.00	KETP + NO = MGLY + NO2 + HO2
092	1.12E+04	6.17E+03	-0.36	-1.00	OLN + NO = HCHO + ALD + #2 NO2
153	1.12E+04	6.17E+03	-0.36	-1.00	XO2 + NO = NO2
					Organic Peroxy + HO2 Reactions
107	8.61E+03	1.13E+02	-2.58	-1.00	HO2 + MO2 = OP1
108		(Same k as 107)			HO2 + ETHP = OP2
109		(Same k as 107)			HO2 + HC3P = OP2
110		(Same k as 107)			HO2 + HC5P = OP2
111		(Same k as 107)			HO2 + HC8P = OP2
112		(Same k as 107)			HO2 + OL2P = OP2
113		(Same k as 107)			HO2 + OLTP = OP2
114		(Same k as 107)			HO2 + OLIP = OP2
115		(Same k as 107)			HO2 + KETP = OP2
117		(Same k as 107)			HO2 + TOLP = OP2

(continued)

Table 6 (continued) - 4

Rxn. Label (a)	Kinetic Parameters (b)				Reactions (b)
	k(300)	A	Ea	B	
118		(Same k as 107)			HO2 + XYLP = OP2
120		(Same k as 107)			HO2 + OLN = ONIT
149		(Same k as 107)			HO2 + XO2 = OP2
116		(Same k as 107)			HO2 + ACO3 = PAA
119		(Same k as 107)			HO2 + TCO3 = OP2
					Organic Peroxy + ACO3 Reactions
143	3.64E+03	1.75E+03	-0.44	-1.00	ACO3 + ACO3 = #2 MO2
146	3.64E+03	1.75E+03	-0.44	-1.00	ACO3 + TCO3 = MO2 + #.92 HO2 + #.890 GLY + #.11 MGLY + #.05 ACO3 + #.950 CO + #2 XO2
130	2.93E+03	1.41E+03	-0.44	-1.00	MO2 + ACO3 = HCHO + #.5 HO2 + #.5 MO2 + #.5 ORA2
133	2.93E+03	1.41E+03	-0.44	-1.00	MO2 + TCO3 = #.5 HCHO + #.5 ORA2 + #.46 HO2 + #.445 GLY + #.055 MGLY + #.025 ACO3 + #.475 CO + XO2
135	1.04E+03	4.99E+02	-0.44	-1.00	ETHP + ACO3 = ALD + #.5 HO2 + #.5 MO2 + #.5 ORA2
136	3.06E+02	1.47E+02	-0.44	-1.00	HC3P + ACO3 = #.77 ALD + #.26 KET + #.5 HO2 + #.5 MO2 + #.5 ORA2
137	2.57E+02	1.23E+02	-0.44	-1.00	HC5P + ACO3 = #.41 ALD + #.75 KET + #.5 HO2 + #.5 MO2 + #.5 ORA2
138	2.20E+02	1.06E+02	-0.44	-1.00	HC8P + ACO3 = #.46 ALD + #1.39 KET + #.5 HO2 + #.5 MO2 + #.5 ORA2
139	1.04E+03	4.99E+02	-0.44	-1.00	OL2P + ACO3 = #.8 HCHO + #.6 ALD + #.5 HO2 + #.5 MO2 + #.5 ORA2
140	1.04E+03	4.99E+02	-0.44	-1.00	OLTP + ACO3 = ALD + #.5 HCHO + #.5 HO2 + #.5 MO2 + #.5 ORA2
141	1.28E+02	6.17E+01	-0.44	-1.00	OLIP + ACO3 = #.725 ALD + #.55 KET + #.14 HCHO + #.5 HO2 + #.5 MO2 + #.5 ORA2
142	1.28E+02	6.17E+01	-0.44	-1.00	KETP + ACO3 = MGLY + #.5 HO2 + #.5 MO2 + #.5 ORA2
144	1.28E+02	6.17E+01	-0.44	-1.00	ACO3 + TOLP = MO2 + #.17 MGLY + #.16 GLY + #.70 DCB + HO2
145	1.28E+02	6.17E+01	-0.44	-1.00	ACO3 + XYLP = MO2 + #.45 MGLY + #.806 DCB + HO2
147	1.28E+02	6.17E+01	-0.44	-1.00	ACO3 + OLN = HCHO + ALD + #.5 ORA2 + NO2 + #.5 MO2

(continued)

Table 6 (continued) - 5

Rxn. Label (a)	Kinetic Parameters (b)				Reactions (b)
	k(300)	A	Ea	B	
151	1.28E+02	6.17E+01	-0.44	-1.00	XO2 + ACO3 = MO2
					Organic Peroxy + MO2 Reactions
121	5.81E+02	2.79E+02	-0.44	-1.00	MO2 + MO2 = #1.5 HCHO + HO2
122	4.28E+02	2.06E+02	-0.44	-1.00	MO2 + ETHP = #.75 HCHO + HO2 + #.75 ALD
123	1.28E+02	6.17E+01	-0.44	-1.00	MO2 + HC3P = #.84 HCHO + HO2 + #.77 ALD + #.26 KET
124	1.04E+02	4.99E+01	-0.44	-1.00	MO2 + HC5P = #.77 HCHO + HO2 + #.41 ALD + #.75 KET
125	8.86E+01	4.26E+01	-0.44	-1.00	MO2 + HC8P = #.80 HCHO + HO2 + #.46 ALD + #1.39 KET
126	4.28E+02	2.06E+02	-0.44	-1.00	MO2 + OL2P = #1.55 HCHO + HO2 + #.35 ALD
127	4.28E+02	2.06E+02	-0.44	-1.00	MO2 + OLTP = #1.25 HCHO + HO2 + #.75 ALD
128	5.19E+01	2.50E+01	-0.44	-1.00	MO2 + OLIP = #.89 HCHO + HO2 + #.725 ALD + #.55 KET
129	5.19E+01	2.50E+01	-0.44	-1.00	MO2 + KETP = #.75 HCHO + HO2 + #.75 MGLY
131	5.19E+01	2.50E+01	-0.44	-1.00	MO2 + TOLP = HCHO + #2 HO2 + #.17 MGLY + #.16 GLY + #.70 DCB
132	5.19E+01	2.50E+01	-0.44	-1.00	MO2 + XYLP = HCHO + #2 HO2 + #.45 MGLY + #.806 DCB
134	5.19E+01	2.50E+01	-0.44	-1.00	MO2 + OLN = #1.75 HCHO + #.5 HO2 + ALD + NO2
150	5.19E+01	2.50E+01	-0.44	-1.00	XO2 + MO2 = HCHO + HO2
					Other Organic Peroxy + Peroxy Reactions
148	1.10E+00	5.28E-01	-0.44	-1.00	OLN + OLN = #2 HCHO + #2 ALD + #2 NO2
152	1.10E+00	5.28E-01	-0.44	-1.00	XO2 + XO2 =
					XNO2 Reactions
154	1.12E+04	6.17E+03	-0.36	-1.00	XNO2 + NO2 = ONIT
155		(Same k as 107)			XNO2 + HO2 = OP2
156	5.19E+01	2.50E+01	-0.44	-1.00	XNO2 + MO2 = HCHO + HO2
157	1.28E+02	6.17E+01	-0.44	-1.00	XNO2 + ACO3 = MO2
158	1.10E+00	5.28E-01	-0.44	-1.00	XNO2 + XNO2 =

(continued)

Table 6 (continued) - 6

Notes:

(a) Reaction labels shown in this table are the reaction sequence number used by Stockwell to implement this mechanism at SUNY. Some reactions were re-arranged for the purpose of this listing. Some reactions were split into two reactions for implementation on SAPRC modeling software.

(b) See Footnotes (b) and (c) in Table 2 for a description of the formats used in the kinetic parameter and the reaction listings.

3. AGGREGATION AND REPRESENTATION OF ORGANIC EMISSIONS IN RADM

3.1 Introduction

The gas-phase reactions of volatile organic compounds (VOCs) are important in regional oxidant and acid deposition models for a number of reasons. They play a major role in the formation of oxidants on the local and regional scale, contribute to the generation (or inhibition) of the radicals responsible for converting sulphur oxides to sulphuric acid and nitrogen oxides to nitric acid, and are involved in the formation of peroxides. VOCs differ significantly in their effects on these processes, and the model must be able to represent these differences in reactivity with a reasonable degree of accuracy. This is a difficult problem, not only because there remain significant uncertainties in our knowledge of the atmospheric reactions of most types of VOCs, but also because the many hundreds (if not thousands) of different VOCs emitted into the atmosphere must be represented by only a limited number of model species. For example, the 1985 NAPAP inventory for anthropogenic emissions of VOCs in the United States (Wagner et al., 1986; Shareef et al., 1988) include emissions for over 600 different chemical compounds, while the gas-phase mechanism proposed for RADM-II has only 17 model species which are used to represent them. The methods used to represent these hundreds of compounds with the limited number of model species is therefore an important component of the gas-phase mechanism in RADM.

As part of the most recent update of the SAPRC gas-phase mechanism for oxidant models, we had previously, under funding from the California Air Resources Board, developed new VOC emissions processing procedures for representing in such models the large numbers of chemical species in detailed emissions inventories (Carter et al., 1988a,b). These procedures were designed to utilize, as much as possible, the chemical information available in the detailed VOC emissions inventories to derive the kinetic and mechanistic parameters for the model species. As part of this effort, kinetic and mechanistic parameters were assigned to the major categories of compounds used in current detailed emissions inventories. In addition, emissions processing software was developed to utilize these assignments to derive the parameters for the lumped model species which best correspond to those of the emissions profile being represented. Although the complexity of this new emissions processing system is such that it is not practical to utilize it in its current form in the RADM model, the procedures, data bases, and software developed in this effort could be utilized to recommend appropriate methods for representing VOC emissions in RADM.

Therefore, as part of this gas-phase mechanism evaluation program for RADM, we assisted the RADM team in the development of procedures for processing and representing VOC emissions for RADM-II. This effort has involved: (1) working with Dr. Paulette Middleton of the RADM team in the development of a new emissions processing and aggregation system for regional models which can be used with a variety of chemical mechanisms; (2) working with Stockwell and Middleton to determine how best to distribute the various VOC compounds in emissions inventories among the species used in the RADM mechanism; and (3) working with Stockwell in deriving the kinetic and mechanistic parameters for the lumped VOC species in the RADM mechanism which best represent those of the sets of emitted species they are intended to represent. The results of the first two efforts are discussed below in Section 3.2, and the results of the third are discussed in Section 3.3.

3.2 Aggregation of VOC Emissions Input for RADM

The current NAPAP inventory of VOC emissions in the RADM modeling region gives mass emissions of over 550 types of chemicals from several thousand different source categories throughout the United States. These detailed emissions data are not input into the RADM model directly, but instead must be aggregated into the much smaller number of VOC categories which are utilized in the model. Because of the extremely large size of the data bases involved, this is a very expensive procedure. In the past, the procedure has been to aggregate the detailed VOC emissions data into the species used by the model in a single step. Since the number and classification of VOC species in a model in general depends on the chemical mechanism used, the aggregation procedure must be carried out separately for each chemical mechanism, and once this procedure has been carried out, the representation of VOCs used in the mechanism cannot be readily modified.

Because there are currently available a number of chemical mechanisms which can be utilized in regional models, each in general using differing methods for aggregating VOC emissions, it would be advantageous to develop a procedure to aggregate the detailed emissions data into a more manageable data base which still contains all the information required by the different mechanisms, including mechanisms which may be developed in the future. To address this, Middleton proposed developing a two-step emissions aggregation process for the RADM model, where the detailed data are first aggregated into a manageable number of emissions categories which can be utilized by a variety of chemical mechanisms, and then these emission categories are further aggregated into the smaller set of VOC species which are directly input into the RADM mechanism. Since, in principle, only the second, much less expensive, aggregation step is necessarily mechanism-dependent, this means that this data base can be more readily utilized by alternative chemical mechanisms either for different types of applications, or for mechanism intercomparison studies. The development of the mechanism-independent VOC emissions classification scheme as it will be used for RADM, and recommended extensions to this scheme which are not yet implemented, are discussed below. Following that, the procedures developed for further aggregating these emissions into RADM model species are discussed.

3.2.1 Development of a Mechanism-Independent VOC Emissions Classification System

The primary objective in the development of a mechanism-independent VOC emissions aggregation scheme is to utilize a minimum number of chemical groupings while retaining, as much as possible, the types of chemical information needed to represent the various types of relevant impacts that VOCs might have on model simulations. These types of impacts, and their magnitudes on model outputs of interest, are referred to under the general term of "reactivity," where relevant measures of reactivity depend on the application of the model. Therefore, the objective in developing a general emissions classification scheme would be to organize the VOCs according to their reactivity where each class has compounds which are similar in all aspects of reactivity important for the model application. Since the aspects of reactivity which are of greatest interest depend on the application of the model, the most appropriate aggregation scheme will also be dependent on the intended application of the data.

In practice, if the number of categories which can be used is limited, compounds with different reactivity characteristics would have to be lumped together in the same category. Given a set number of categories, the extent to which reactivities should differ within a given class would depend on how important the compounds are expected to be in affecting the model, which in turn depends both on how much is emitted and on how reactive they are (i.e., on the magnitude of the effects of a given amount of the VOC on the relevant predictions of the model). For example, reactive compounds which are emitted in very large amounts (such as, for example, ethylene) should be in classes by themselves, and categories representing groups of relatively reactive types of compounds with significant amounts of emissions should represent relatively narrow ranges of reactivity. On the other hand, it is not worthwhile to have separate classes for reactive compounds of very low emissions; they can be grouped into classes which are closest to them in reactivity, even if the classes are not particularly close. Furthermore, compounds which are essentially unreactive for the purposes of the particular model application can be lumped together into a single "inert" category, regardless of how much may be emitted. However, a compound which is "inert" in one application may be reactive in another, so if the categorization scheme is to be used for several different applications, there may be more than one category which is treated as "inert" in a given type of application.

In the case of aggregation of emissions for models such as RADM, the relevant reactivity criteria concern reactivity with respect to oxidant formation and reactivity with respect to formation of acidic species. Reactivity with respect to oxidant formation is influenced by how rapidly the VOC reacts in the atmosphere, and, if it reacts sufficiently rapidly, by the nature of its reaction mechanism. Therefore, compounds which react sufficiently rapidly that they participate in the oxidant formation process, yet react at significantly different rates, should be placed in different reactivity categories, while compounds which do not react to a significant extent in the time frame of the model application can all be lumped together and be classified as "inert." If a VOC reacts, the nature of its reaction mechanism is also important, since different aspects of a

VOCs reaction can affect the system in different ways. For example, the reactions of a VOC can have a relatively direct effect on ozone formation by forming radicals which convert NO to NO_2 (which causes ozone formation in the presence of sunlight), and more indirectly (but often more significantly) by enhancing or inhibiting levels of the radicals which control the overall rate of the oxidant formation process, and by the formation of reactive organic products. For this reason, the emissions categorization scheme must not group together types of compounds with significantly different types of reaction mechanisms, even if they may react at similar rates. At a minimum, the classification scheme should include separate categories of compounds which are represented with different sets of reactions in current oxidant formation mechanisms. Finally, since the model is concerned with formation of acidic species, VOCs which are acids themselves should not be lumped into the same categories as those which are not.

Ideally, it would be desirable that the emissions aggregation scheme used for RADM and other oxidant and acid deposition models also be suitable for use with models concerned with global effects and the stratosphere. This would require the use of additional VOC categories. For global models, reactions occur on a much longer time scale, and thus many compounds classified as "inert" for regional model applications would have to be placed in separate "reactive" categories for global models. In addition, for models where the stratosphere is of interest, separate categories would have to be created for halogen-containing compounds which are transported to the stratosphere.

Unfortunately, current limitations in the software utilized by the EPA and its contractors for processing emissions input for RADM restrict the number of categories to 32. Our analysis indicates that this may be sufficient to convey the necessary reactivity information required for local and regional oxidant and acid deposition models using currently available chemical mechanisms, but is not sufficient to convey the necessary additional information required by global and stratospheric models. Therefore, it was determined that the initial emissions aggregation scheme to be developed for RADM would not contain the additional VOC categories required by such models.

An analysis of the total emissions into the contiguous United States of the approximately ~550 different types of VOCs in the NAPAP inventory was carried out to determine the most appropriate aggregation scheme, involving no more than 32 categories, to use for regional oxidant and acid rain models. This was carried out jointly by SAPRC as part of this program and by Middleton and co-workers at NCAR as part of the RADM development effort. NCAR determined the major overall characteristics of the classification scheme and the types of organics that had to be represented in separate classes because of their importance in the emissions inventory; they also had the final responsibility for the system which was developed. SAPRC provided guidance to NCAR in this task by analyzing the reactivity characteristics of the various types of VOCs in the inventory, and making recommendations as to how species should be classified based on their reactivity. This analysis utilized the kinetic and mechanistic assignments which were made for emitted VOC categories as part of its development of the new emissions processing system for the new California ARB model (Carter, 1988), together with new assignments which had to be made as part of this program for a number of major VOC categories which are on the NAPAP, but not the California inventories.

A number of emissions categories were assigned without direct consideration of reactivity, but based on considerations of importance of individual compounds in the total mass emissions, or on considerations of special chemical characteristics. In addition, special categories were created for emissions where there is information missing concerning their chemical characteristics. These are as follows:

(1) On the basis of total amounts of mass emitted into the United States, combined with considerations of their special chemical characteristics, eight individual compounds were determined to be sufficiently important that they should not be aggregated with other species, but should be in categories by themselves. These were methane, ethane, propane, ethene, propene, acetylene, formaldehyde, and acetone. Initially, it was also proposed that benzene, methanol, ethanol, isopropyl alcohol, perchloroethylene, and methyl chloroform be in their own categories because of large current or (in the case of methanol) possible future emissions; but it was decided that given the 32-class limitation there were an insufficient number of classes available for this purpose.

These compounds were lumped with other species either because they are relatively unreactive, or because their reactivities were judged to be fairly similar to those of other species. Note, however, that many of these compounds dominate the categories in which they were placed.

(2) Organic acids were lumped into their own separate category because of their obvious role in acidification. Their contribution to reactivity with respect to oxidant formation is minor, so it was not necessary to differentiate them further on this basis. Although the RADM mechanism represents formic acid separately from the higher organic acids, the emissions of formic acid in the NAPAP inventory are insufficient to justify utilization of a separate emissions category grouping just for this compound.

(3) Two aggregation categories were created for "chemical compounds" listed in the current detailed NAPAP (and California) emissions inventories which are not true compounds at all, but represent unspecified mixtures of compounds of ambiguous reactivity. The category "Alkane/Aromatic Mix" was used to represent emissions which are designated as "Naphtha," "Mineral Spirits," or "Lactol Spirits." These are solvents believed to consist primarily of C_{8+} alkanes and aromatics, but whose exact chemical compositions are unspecified. The category "Alkenes (Primary/Internal Mix)" was used to represent emissions designated as "C_n alkenes" (where $n \geq 4$), without reference to the location of the double bond. The location of the double bond significantly affects the reactivity of the alkene, and is a necessary basis for the reactivity classifications of these compounds.

(4) An "unreactive" category was included for compounds which are estimated to react too slowly to be important in affecting chemical transformations on the regional scale. Note, however, that many compounds in this category are not "unreactive" on a global scale or in the stratosphere.

(5) An "unidentified" category was included for unidentified VOCs. These constitute somewhat less than 6% of the mass in the NAPAP total U.S. anthropogenic emissions inventory.

(6) An "unassigned" category was included for those VOCs which were identified, but for which no reactivity assignments or classifications were made. As indicated above, as part of this and our previous ARB

program (Carter, 1988) we made mechanistic classifications and (where applicable) reactivity assignments for most of the detailed emissions categories in the California and NAPAP inventories. However, a number of compounds in the NAPAP inventory were not categorized because they both were very difficult to classify and had small total U.S. emissions. These "unassigned" compounds constitute less than 1% of the mass in the NAPAP total U.S. anthropogenic emissions inventory.

The above amounts to a total of 14 categories, leaving 18 categories available for all other types of compounds in a 32-category system. Based on considerations of differences in chemical reaction mechanisms, together with considerations of total amounts of different types of chemicals emitted, it was determined that the remaining categories should, at a minimum, differentiate between the following general types of chemicals (listed in order of mass emitted):

- Alkanes (other than methane, ethane, and propane)
- Aromatics
- "Others" (alcohols, ethers, alcohol ethers, esters, and other types of compounds which are generally represented as reacting analogously to alkanes in current mechanisms)
- Alkenes (other than ethene and groups of chemicals classified as "primary/internal mix")
- Haloalkenes
- Aldehydes (other than formaldehyde)
- Styrenes
- Phenols and Cresols

There are a number of other chemical classes emitted, but it was judged not to be worthwhile to assign them to separate groups because either the amounts emitted were too small or they were judged to be of minor reactivity with respect to oxidant or acid formation, and thus could be classified as "inert."

In the case of the first four groups listed above (alkanes, aromatics, "others," and alkenes), the variety of rates of reaction of the individual species are such that these groups needed to be further broken down on the basis of differences in reaction rates. At a minimum, the numbers of reactivity categories for each type of chemical should be such that there are at least as many as the number of lumped species which might be used for them in the models, and the criteria used to make the reactivity differentiations should also be compatible with those used in the models. Based on these considerations, the reactivity classifications were derived as follows:

Alkenes: Most current mechanisms differentiate between ethene, other terminal alkenes, and internal alkenes. This differentiation is therefore also used in the emissions categorization. As indicated above, ethene and propene are given emissions categories by themselves, so the differentiation of the mechanisms between ethene and other alkenes is already taken care of. The terminal alkenes other than propene are lumped into the group designated "alkenes (primary)," and the more reactive alkenes with internal double bonds are lumped into "alkenes (internal)."

However, certain "terminal" alkenes, such as 1,3-butadiene and beta-pinene have atmospheric reaction rates which are more typical of the internal alkenes, and lumping these into the "primary alkenes" group seemed to us to be inappropriate. To provide an objective criterion to determine the classification of these more reactive alkenes, all alkenes (other than ethene or propene) which react with OH radicals with rate constants less than 7.5×10^4 ppm^{-1} min^{-1} were assigned to the "primary" group, and alkenes with higher rate constants were assigned to the "internal" group. This rate constant lies well between the typical ranges for "ordinary" primary and internal alkenes, but results in the unusually reactive "primary" alkenes such as beta-pinene being grouped with the more reactive internal alkenes, which have more similar atmospheric reaction rates.

Note that this classification for the alkenes is appropriate for inventories which contain anthropogenic emissions only. If biogenic emissions are to be merged into the same scheme, then separate categories should be reserved for them. This is particularly important for regional modeling applications, since biogenics tend to dominate the mass emissions for large regions of the modeling domain. The biogenic emissions inventory includes species such as isoprene, alpha-pinene, other terpenes, and unidentified biogenics (Middleton, private communication, 1988), and, at a minimum, separate categories for each of these should be included in any merged emissions grouping system. However, in this discussion it is assumed that biogenic emissions are processed separately from anthropogenic emissions, and thus separate categories for biogenic emissions are not included in this scheme.

$\underline{C_{4+}\ \text{Alkanes}}$: The RADM mechanism uses three different species to represent the C_{4+} alkanes. Other mechanisms use fewer species for this purpose, and unlike the case for the alkenes, the mechanisms generally differ on how the lumped groups of alkanes are defined in the model. To allow for maximum flexibility in use with mechanisms with differing aggregation schemes for the alkanes, four different reactivity groups are used for the emitted C_{4+} alkanes, with (as indicated above) methane, ethane, and propane being in groups by themselves.

The criterion used in this aggregation scheme to determine the reactivity classifications for the alkanes is based solely on how rapidly they react in the atmosphere. This is an important factor in measuring reactivity, since it determines how much of the alkane which is emitted undergoes reaction and thus participates in chemical transformations. However, the rate of reaction is not the only factor affecting the reactivity of alkanes; aspects such as the alkyl nitrate yield in the reaction is also important (Carter and Atkinson, 1985, 1989). Nevertheless, at least to some extent the nitrate yields and other aspects are correlated with the size of the molecule, which in turn is correlated with how rapidly it reacts.

Alkanes are consumed in the atmosphere primarily by reaction with OH radicals, but the rate at which they react can vary significantly depending on the size of the alkane, and to a lesser extent on its structure. For example, the rate constants for n-butane and n-pentadecane, both important C_{4+} alkanes in the NAPAP inventory, have OH radical rate constants which differ by approximately an order of magnitude. 2,2-Dimethylbutane and cyclohexane have the same number of carbons, yet the latter reacts more than twice as rapidly as the former. Most other C_{4+} alkanes with significant emissions in the NAPAP inventory have rate constants between those of n-butane and n-pentadecane.

Based on an analysis of the amounts of alkanes with various ranges of rate constants in the available NAPAP total U.S. inventory, the four C_{4+} alkane reactivity classes are defined as follows (where kOH is the OH radical rate constant at T=300 K in units of ppm^{-1} min^{-1}):

(1) The group designated "alkanes (<0.5 react)," consists of all alkanes where kOH is less than 5 x 10^4 ppm^{-1} min^{-1}. This group is dominated by n-butane and isobutane, but also contains 2,2-dimethylbutane.

(2) The group designated "alkanes (0.5-1 react)," contains alkanes with kOH between 0.5 and 1 x 10^4 ppm^{-1} min^{-1}. It is dominated by pentanes and hexanes. This is the second largest group of alkanes in the NAPAP inventory in terms of estimated amount reacted in regional model simulations (see below).

(3) The group designated "alkanes (1-2 react)" consists of alkanes with kOH between 1 and 2 x 10^4 ppm^{-1} min^{-1}. It is dominated by n-heptane and other C_7-C_{10} isomers. This is the largest group of alkanes in terms of estimated amount reacted in regional model simulations.

(4) The group designated "alkanes (>2 react)" consists of alkanes with kOH greater than 2 x 10^4 ppm^{-1} min^{-1}. Almost 40% of the emissions of this group is accounted for by n-pentadecane, with the remainder being various C_{11+} acyclic or C_{9+} cyclic alkanes. Although this is the smallest group of C_{4+} alkanes in terms of estimated amount reacted, it still makes a non-negligible contribution to the emissions, consisting of over 3% of the mass of VOC emitted.

Aromatics: The aromatics, like the alkanes, are consumed in the atmosphere primarily by reaction with OH radicals, and it is the rate of this reaction which was used to define their reactivity classes. However, in terms of distribution of reaction rates and fractions of emitted aromatics estimated to react in regional model simulations, the aromatics tend to fall into three distinct groups. These groups also correspond reasonably well with how they are aggregated in current lumped kinetic mechanisms. These reactivity classifications are as follows:

(1) The lowest reactivity group is dominated by benzene, but also includes several halobenzenes which are also in the NAPAP inventory. The halobenzenes react somewhat slower than benzene, but not so slowly that they should be considered unreactive. Since there are not enough halobenzenes emitted to justify placing them in their own aggregation group, they are lumped with benzene.

(2) The middle reactivity aromatics group is designated "aromatics (<2 react)," and is defined as those aromatics which react with OH radicals more rapidly than benzene, but with rate constants of less than 2 x 10^4 ppm^{-1} min^{-1}. The compounds in this group have a relatively narrow range of kOH values, being around 0.8-1.2 x 10^4 ppm^{-1} min^{-1}, and consist entirely of toluene and other monoalkyl benzenes. Toluene is the dominant compound in this group, accounting for over 80% of the mass of such compounds emitted in the NAPAP inventory.

(3) The most reactive group of aromatics is designated "aromatics (>2 react)," and is defined as those aromatics which have kOH greater than 2 x 10^4 ppm^{-1} min^{-1}. This group consists primarily of di- and poly-alkyl benzenes, but it also includes naphthalenes and indans, which account for approximately 5% of the mass emissions into this group. This is the largest group of aromatics, both in terms of mass emissions and in terms of estimated amounts reacting in a model simulation. Almost 10% of the estimated number of moles of VOC reacted in a model simulation corresponds to compounds in this group.

It should be noted that had it been practical to include more than 32 groups in this total aggregation scheme, the most reactive aromatics group would have been broken down further with dialkylbenzenes, tri- and poly-alkylbenzenes, and naphthalenes and indans each being in their own groups. This would permit the scheme to be used with the most detailed version of the SAPRC/ERT mechanism described by Lurmann et al. (1987), which has separate model species for xylenes and trialkylbenzenes. In addition, smog chamber studies (Carter et al., 1987) indicate that the naphthalenes are much less reactive in NO_x-air irradiations than the di- and poly-alkylbenzenes, despite their high OH radical rate constants. However, this grouping corresponds to the lumping schemes used in the RADM and other chemical mechanisms in current regional models, which generally lump all polyalkylbenzenes with the xylenes. The emissions of the naphthalenes and the indans are not sufficient to justify creating a separate group for them in this 32-class scheme.

"Others": Compounds such as alcohols, ethers, alcohol ethers, and other compounds (primarily O-containing species which are not aldehydes, ketones, organic acids, and which do not contain aromatic rings or carbon-carbon double bonds) are lumped into the miscellaneous group designated "others." All these compounds are believed to react in the atmosphere primarily with OH radicals, and current kinetic mechanisms (including RADM) generally lump them with the alkanes. There is an insufficient number of available groups in the 32-class scheme to represent the variety of chemical types of this group separately, so they are aggregated into four reactivity classes based on their OH radical rate constants, using a method similar to that used for the alkanes. These categories are as follows:

(1) Compounds with OH radical rate constants less than 2.5 x 10^3 ppm^{-1} min^{-1} are lumped into the group designated "others (<0.25 react)." The major compounds in this group are methyl and ethyl acetates (~51% of the emitted mass in this group) and methanol (~40% of the emitted mass). Emissions of this class are relatively minor in the current NAPAP total U.S. inventory (consisting of less than 0.4% of the mass emitted and less than 0.2% of the estimated moles reacted), but these compounds are too reactive to be treated as "inert," and too unreactive to be lumped into the next highest reactivity "others" group. In addition, in view of the interest in using methanol as an alternative fuel, emissions into this class may become much more important in the future.

(2) Compounds with kOH values between 2.5 and approximately 5.0 x 10^3 ppm^{-1} min^{-1} are lumped into the group "others (0.25-0.5 react)." This group is dominated by ethanol, which accounts for over 85% of the mass of this group in the NAPAP total U.S. inventory. It is also non-negligible in terms of total emissions, accounting for almost 4% of the estimated moles of VOC reacted in the model simulations. [Subsequent to the development of this classification system, we revised our assignment of the OH radical rate parameters for ethanol to be consistent with the most recent recommendation of Atkinson (1989). This yields a 300 K rate constant which is slightly higher (by less than 1%) than the nominal upper limit rate constant for this group. However, ethanol was not re-assigned, since otherwise there would be no significant emissions for this group.]

(3) Compounds with kOH values between approximately 0.5 and 1.0 x 10^4 ppm^{-1} min^{-1} are lumped into the group "others (0.5-1 react)." The major compounds in this group are isopropyl alcohol (~60% of the mass) and propyl and higher acetates (~25%). This group accounts for an estimated 4-5% of the VOC mass reacted in model simulations.

(4) Compounds with kOH values higher than 1.0 x 10^4 ppm^{-1} min^{-1} are lumped into the group "others (>1 react)." The major compounds in this group consist of glycols and cellosolves and other alcohol ethers. [It also has very minor contributions by alkynes, allenes, and amines, which react within this rate constant range. In our opinion, these are not well represented by any of the other chemical classes in this aggregation scheme (for example, the alkynes and allenes are not lumped with the alkenes since they do not react significantly with ozone), and are not emitted in sufficient quantities to justify being in their own group.] The emissions of compounds in this group are small but non-negligible, accounting for approximately 1% of the mass emitted and 1-2% of the estimated moles reacted in the total U.S. inventory.

Summary of Emissions Groups: Table 7 gives a summary of all the groups in this 32-class aggregation scheme, and the total mass and molar emissions of compounds in each group of the current NAPAP inventory for total anthropogenic emissions in the contiguous United States. Note that the detailed emissions data bases give mass emissions, but these are aggregated into the 32-class scheme on a molar basis, with the number of moles of each type of emitted compound being calculated based on its molecular weight to determine its contribution to the aggregated emissions group. The table therefore also shows the percent contribution of each group to the total mass and molar emissions. Finally, to give an indication of the relative importance of the emissions of each category on model simulations, Table 7 also gives estimates of the number of moles of compounds in each group that is estimated to undergo chemical reaction in a 2-3 day RADM simulation. These latter estimates were made as indicated in footnotes to the table, and as discussed in the following section.

It can be seen that the most important group in terms of moles emitted is methane, accounting for almost 40% of the moles emitted in the inventory, but it accounts for less than 0.2% of the moles reacted. In terms of moles reacted, the most important single group is ethene, accounting for almost 21% of the moles reacted, followed by the middle reactivity C_{4+} alkane group and the high reactivity group of aromatics. Alkanes, aromatics, and alkenes account for ~80%, aldehydes and ketones for ~7%, and all other types of compounds for ~11% of the total estimated number of moles of VOC reacted. As indicated in Table 7, approximately 7%

Table 7. Summary of the Emissions Groupings Using the 32-Class Scheme, Amounts of Each Emitted in the NAPAP Total U.S. Inventory, and Estimated Amounts Reacted in Conditions Representative of RADM Applications

Emissions Group	----- Amounts Emitted			-----	Reacted (a)	
	M.Kg	%	K.Mole	%	K.Mole	%
C1-C2 Alkanes						
Methane	2.83	12.18	176.7	38.42	0.2	0.15
Ethane	0.46	1.98	15.3	3.33	0.7	0.41
Total	3.29	14.16	192.0	41.75	0.9	0.55
Higher Alkanes						
Propane	0.12	0.53	2.8	0.61	0.5	0.31
Alkanes (<0.5 react)	1.40	6.01	23.9	5.20	8.0	4.86
Alkanes (0.5-1 react)	2.03	8.72	25.5	5.53	13.2	8.06
Alkanes (1-2 react)	2.49	10.71	21.9	4.76	16.7	10.19
Alkanes (>2 react)	0.60	2.60	3.1	0.67	2.8	1.73
Alkane/Aromatic Mix (b)	0.25	1.06	1.8	0.38	1.6	0.98
Total	6.89	29.63	78.9	17.16	42.9	26.13
Ethene	1.27	5.45	45.2	9.82	33.9	20.65
Higher Alkenes						
Propene	0.44	1.91	10.6	2.29	10.5	6.37
Alkenes (primary)	0.33	1.42	4.6	1.00	4.6	2.78
Alkenes (internal)	0.76	3.28	11.0	2.38	11.0	6.68
Alkenes (mix)	0.20	0.85	1.9	0.41	1.9	1.13
Total	1.73	7.46	28.0	6.09	27.8	16.96
Aromatics						
Benzene, Halobenzenes	0.60	2.59	7.3	1.58	1.4	0.84
Aromatics (<2 react)	1.56	6.69	16.1	3.51	10.2	6.23
Aromatics (>2 react)	2.03	8.72	16.3	3.54	16.1	9.81
Phenols and Cresols	0.05	0.19	0.3	0.06	0.3	0.17
Styrenes	0.08	0.36	1.5	0.33	1.0	0.58
Total	4.31	18.55	41.5	9.02	29.0	17.64
Aldehydes and Ketones						
Formaldehyde	0.32	1.37	10.7	2.32	8.2	4.98
Higher Aldehydes	0.17	0.71	2.5	0.54	2.3	1.41
Acetone	0.21	0.90	3.6	0.79	0.1	0.08
Higher Ketones	0.20	0.85	2.2	0.48	0.3	0.20
Total	0.89	3.83	19.0	4.12	11.0	6.68
Miscellaneous						
Organic Acids (c)	0.04	0.17	0.3	0.07	0.0	0.00
Acetylene	0.36	1.56	14.0	3.04	1.7	1.01
Haloalkenes	0.52	2.24	2.1	0.46	0.1	0.04
Total	0.92	3.97	16.4	3.57	1.8	1.05

(continued)

Table 7 (continued) - 2

Emissions Group	----- Amounts Emitted -----				Reacted (a)	
	M.Kg	%	K.Mole	%	K.Mole	%
"Others"						
Others (<0.25 react)	0.10	0.42	2.0	0.43	0.3	0.17
Others (0.25-0.5 react)	0.80	3.44	16.7	3.63	6.3	3.85
Others (0.5-1 react)	0.88	3.76	12.5	2.73	7.7	4.67
Others (>1 react)	0.30	1.28	3.3	0.72	2.7	1.66
Total	2.08	8.90	34.7	7.53	16.9	10.34
Unreactive	0.35	1.50	4.3	0.94	0.0	0.00
Unknown/Unassigned						
Unidentified	1.36	5.83				
Unassigned	0.16	0.72				
Total	1.52	6.55				

(a) Estimated assuming reaction with OH radicals is the main consumption process for compounds in the groups, and assuming that the ratio of reacted to emitted compounds can be estimated by 1 - exp (-kOH x INTOH), where kOH is the average OH radical rate constant for compounds in the group, and INTOH is a parameter reflecting the effective integrated OH radical levels in the model simulation (Carter and Atkinson, 1989). The tabulated values are calculated assuming INTOH = 110 ppt-min, based on analyses of results of previous RADM model simulations (Stockwell, private communication, 1988), and the kOH values are weighed averages of those assigned for compounds in the groups (Carter, 1988). See Section 3.2.3.

(b) These are estimated to consist of approximately 90% alkanes and 10% aromatics (on a molar basis), so for the purpose of this summary they are counted as alkanes.

(c) Amount reacted using kOH of acetic acid, the major emitted organic acid in the NAPAP inventory.

of the mass in the current NAPAP total U.S. inventory is either unknown or unassigned.

3.2.2 Recommended Extensions to the VOC Emissions Classification System

The 32-class VOC classification system described in the previous section is the version which is being implemented for use with the RADM-II model. Although we consider this system to be satisfactory for this purpose, we have several recommendations, discussed below, for extending its utility for use with other mechanisms besides that which will be used in RADM-II, and for other types of models. All of these recommendations require updating the software currently used for aggregating detailed emissions data.

Use with the Carbon Bond Mechanism. The emissions aggregation system discussed above was designed primarily for use with mechanisms, such as that used in RADM, which represent reactions of emitted VOCs on a molecular level, where, in general, only one model species is used to represent the reaction of any type of emitted molecule. However, the Carbon Bond mechanism (Whitten et al., 1980; Gery et al., 1988), which is widely used in urban airshed modeling applications, represents portions of some types of molecules reacting independently, and thus requires at least some portions of the emissions to be aggregated in terms of reactive portions of molecules, rather than molecules as a whole. For that reason, this 32-class system, as described above, cannot be used in aggregating emissions input for models using the Carbon Bond mechanism. However, as indicated below, this limitation can be readily removed by adding two new emissions categories.

Although as originally conceived the Carbon Bond mechanism was radically different from molecularly-based mechanisms in its treatment of parts of molecules as reacting independently, in recent years the need for improved performance in simulating results of chamber experiments has required it to evolve more towards the molecularly-based mechanisms, with the latest version (Gery et al., 1988) using almost the same numbers and types of species to represent alkenes, aromatics, and oxygenates as other state-of-the art mechanisms. The principal remaining difference between the current version of Carbon Bond and the molecular-based mechanisms, is the use of a single-carbon model species called "paraffin bond" (PAR) to represent both the alkanes and the "extra" carbons on molecules which have more carbons than the species in the model representing them. In addition, the double bonds in some diolefins and other bifunctional compounds are represented as reacting independently. The present version of the emissions aggregation system does not contain the information necessary to determine the levels of the PAR model species or the contributions of bifunctional compounds to levels of alkene model species.

The deficiency with respect to aggregation of the "paraffin bond" species can be addressed by adding a separate category designated "reactive carbon," and using it to tabulate the total number of carbons in reactive emitted species. (The specific criterion used for "reactive" in this context would be determined by the criterion presently used when assigning contributions to PAR when aggregating emissions for Carbon Bond.) The levels of PAR emissions to use in the model could then be determined by subtracting from this number the number of carbons in the other model species used to represent the emissions. For example, if a simplified emissions inventory contained 1 mole each of n-butane, ethanol, and butyl benzene, then the corresponding emissions aggregation would include 1 mole each of "alkanes (0.25-0.5)," "others (0.25-0.5 react)," "Aromatic (<2 react)," and 16 moles of the special "reactive carbon" group (4 moles from n-butane, 2 from ethanol, and 10 from butyl benzene). In models using the Carbon Bond mechanism, the emissions group "Aromatic (<2 react)" would be represented by the seven-carbon species "TOL," and the "PAR" levels would be calculated by subtracting these 7 moles of reactive carbons already represented in TOL from the total of 16 moles of reactive carbon, yielding 9 moles of "PAR." Since the "alkanes" and "others" emissions in this inventory are already represented by "PAR," the aggregations in these groups are not used in determining input for models using this mechanism.

An analogous method could be used to account for the extra double bonds in polyfunctional alkenes. In this case, it is recommended that total terminal double bonds and total internal double bonds be aggregated into separate groups, since these are represented differently in the Carbon Bond mechanism.

In view of the extensive use of the Carbon Bond mechanism, it is perhaps surprising that this emissions aggregation system was not extended so it could be used for this mechanism. The principle reason for this appears to be that the software presently used to process the NAPAP emissions input data cannot be readily adapted to be able to distribute more than one detailed emissions class into more than one aggregated emissions [illegible]gory. Aggregation for Carbon Bond obviously requires this capability. This artificial limitation would presumably be addressed when the emissions processing software is upgraded.

Aggregation of Aromatics. The present 32-class scheme lumps the xylenes and other dialkylbenzenes, tri- and polyalkyl benzenes, and naphthalenes into a single group ("Aromatics >2 react"). This is satisfactory for use with the RADM and most other lumped mechanisms, which only uses a single model species (generally designated XYL) for these compounds. However, the most detailed version of the SAPRC/ERT mechanism (Lurmann et al., 1987) has a separate model species for the tri- and polyalkylbenzenes, and thus this grouping is not adequate for use with this mechanism. Splitting the "Aromatics (>2 react)" group into "Aromatics (2-4 react)" and "Aromatics (>4 react)," with the trialkylbenzenes and other aromatics which react faster than 4×10^4 ppm^{-1} min^{-1} being lumped into the latter group, would address this problem. Both of these groups would be significant in terms of amounts of emitted species, and thus aggregating them separately would not be inappropriate on that basis.

It would also be desirable to aggregate the naphthalenes and other tri- and poly-cyclic aromatics in separate groups from the alkylbenzenes. Environmental chamber and modeling studies carried out at SAPRC indicate that these species are much less reactive than alkylbenzenes, despite similar or higher OH radical rate constants (Carter et al., 1987). Therefore, lumping them with alkylbenzenes will result in models significantly overpredicting their reactivity in model simulations. On the other hand, the naphthalenes are relatively unimportant in terms of amounts emitted, contributing only approximately 0.4% of the mass emissions in the NAPAP total U.S. anthropogenic inventory. However, there may be special urban pollution cases where their contributions may be more important.

Use with Global and Stratospheric Models. As indicated above, this aggregation scheme was developed for use with local and regional oxidant and acid deposition models, and additional classes would have to be added for it to be used for other types of modeling applications. For example, global models may require more distinction among less reactive compounds, and stratospheric models would require halogenated compounds to be split out from the "unreactive" category, or perhaps separate categories tabulating the total numbers of Cl and Br atoms which reach the stratosphere. A discussion of the input requirements for such models is beyond the scope of this report.

3.2.3 Aggregation of Emissions into the RADM Mechanism

The gas-phase RADM mechanism contains 17 different model species which can be used to represent the reactions of various types of emitted reactive VOCs. These include five species for alkanes, four for alkenes, two for aromatics, two for aldehydes, one for ketones, one for phenols, and two for organic acids. As indicated above, the system developed for processing anthropogenic emissions input for the RADM model involves a two-step procedure where first the detailed emissions data, given in terms of mass emissions of over 550 compounds, are aggregated into molar emissions of 32 compounds judged to be similar in reactivity, and then these are further aggregated into molar emissions of the 16 species used in RADM. As part of this program, SAPRC was asked to make recommendations for how to aggregate emissions organized into the 32-class system into the species in the RADM mechanism. The system that was recommended, which we anticipate will be used in RADM, is summarized in this section.

The allocation of the 32 emissions groups to species in the RADM mechanism is summarized in Table 8. In many cases these allocations are reasonably obvious; cases that are less obvious are discussed below for the various types of chemicals. As indicated in the table, most of the emissions groups are represented by the RADM species on a simple mole-per-mole basis, with one mole of RADM species being used for each mole of compound emitted. However, in some cases, particularly those where emissions groups of significantly different reactivities have to be lumped together, "reactivity weighing" is employed. This involves use of a reactivity weighing factor in calculating the number of moles of model species from the moles of emitted species. The general principle of reactivity weighing will be discussed first, followed by a discussion of specific considerations involved for the various types of chemicals.

Table 8. Assignments of Emissions Groups to RADM Model Species

Emissions Class		Mix Fac. (a)	RADM Class	Weighing Factor (b,c)		
No.	Description			Factor	k(emit)	k(RADM)
1	Methane		CH4	1.0		
2	Ethane		ETH	1.0		
3	Propane		HC3	0.519	0.180	0.386
4	Alkanes (0.25-0.5 react)		HC3	0.964	0.369	0.386
5	Alkanes (0.5-1 react)		HC5	0.956	0.668	0.715
6	Alkanes (1-2 react)		HC8	0.945	1.315	1.507
7	Alkanes (>2 react		HC8	1.141	2.339	1.507
8	Alkane/Aromatic Mix	0.91	HC8	1.002	2.018	1.507
		0.09	XYL	0.090		
9	Ethene		OL2	1.0		
10	Propene		OLT	1.0		
11	Alkenes (Primary)		OLT	1.0		
12	Alkenes (Internal)		OLI	1.0		
13	Alkenes (Prim/Inter Mix)	0.50	OLT	0.500		
		0.50	OLI	0.500		
14	Benzene, Halobenzenes		TOL	0.293	0.185	0.902
15	Aromatics (<2 react)		TOL	1.0		
16	Aromatics (>2 react)		XYL	1.0		
17	Phenols and Cresols		CSL	1.0		
18	Styrenes	1.0	TOL	1.0		
		1.0	OLT	1.0		
19	Formaldehyde		HCHO	1.0		
20	Higher Aldehydes		ALD	1.0		
21	Acetone		KET	0.253	0.035	0.147
22	Higher Ketones		KET	1.0		
23	Organic Acids		ORA2	1.0		
24	Acetylene		HC3	0.343	0.115	0.386
25	Haloalkenes		HC3	0.078	0.025	0.386
26	Unreactive		-	1.0		
27	Others (<0.25 react)		HC3	0.404	0.137	0.386
28	Others (0.25-0.5 react)		HC3	1.215	0.496	0.386
29	Others (0.5-1. react)		HC5	1.075	0.801	0.715
30	Others (>1 react)		HC8	1.011	1.552	1.507

(a) Molar distribution of RADM species used for groups represented by more than one RADM species.

(b) "Factor" is number of moles of model species used to represent the emissions group. If reactivity weighing is not employed, the factor is 1.0 or "Mix Fac.," if applicable. If reactivity weighing is employed, these are given by

(continued)

Table 8 (continued) - 2

Factor = Mix Fac. (if applicable)
x (1-exp[-k(emit)xINTOH])/(1-exp[-k(RADM)xINTOH])

where k(emit) and k(RADM) are respectively the 300 K OH rate constants for the emissions group and the RADM species (given in the table in units of 10^4 ppm^{-1} min^{-1}), and INTOH is assigned a value of 110 ppt-min. See text.

(c) The tabulated k(RADM) values for the lumped alkane model species are for the RADM-P mechanism. The March 1988 RADM mechanism used k(RADM) values for HC3, HC5, and HC8 of 0.376, 0.786, and 1.655, respectively.

Reactivity Weighing. Reactivity weighing is used as a means to represent groups of compounds with similar reaction mechanisms, but with significantly differing reaction rates, with a single model species. It is based on the assumption that, at least for compounds with similar reaction mechanisms, the effects of emissions of different compounds on results of a model simulation is approximately proportional to the amount of compound which undergoes chemical reaction in the simulation. For example, if compound "A" reacts rapidly and essentially is all consumed in a model simulation, while compound "B" reacts more slowly and only half is consumed, then, under this approximation, emissions of 1 mole of "B" has the same effect as emissions of 0.5 moles of "A." If this is assumed, then the appropriate amount of model species to use to represent a given amount of emitted species would be such that the estimated amounts of each which react in the simulation are the same. Thus, for example, if an emissions group E is to be represented in a model simulation by model species M, then the reactivity weighing factor for E would be derived such that:

$$\begin{matrix}\text{Moles of M Reacting} \\ \text{in Simulation}\end{matrix} = \begin{matrix}\text{Moles of E Reacting} \\ \text{in Simulation}\end{matrix}$$

or

$$\begin{matrix}\text{Moles of M} \\ \text{used to} \\ \text{Represent E}\end{matrix} \times \begin{matrix}\text{Fraction} \\ \text{of M which} \\ \text{Reacts}\end{matrix} = \begin{matrix}\text{Moles of} \\ \text{E Emitted}\end{matrix} \times \begin{matrix}\text{Fraction} \\ \text{of E which} \\ \text{Reacts}\end{matrix}$$

Therefore,

$$\begin{matrix}\text{Reactivity} \\ \text{Weighing} \\ \text{Factor for E}\end{matrix} = \frac{\begin{matrix}\text{Moles of M} \\ \text{used to} \\ \text{Represent E}\end{matrix}}{\begin{matrix}\text{Moles of E} \\ \text{Emitted}\end{matrix}} = \frac{\begin{matrix}\text{Fraction} \\ \text{of E which} \\ \text{Reacts}\end{matrix}}{\begin{matrix}\text{Fraction} \\ \text{of M which} \\ \text{Reacts}\end{matrix}} \tag{I}$$

Thus, for example, if half of the emitted species is estimated to react under the conditions of a model simulation, and these species are represented by a more rapidly reacting model species where 75% is estimated to react under the same conditions, then the appropriate reactivity weighing factor would be 0.5/0.75 = 0.667.

The use of this reactivity weighing approach requires an ability to estimate fractions of emitted species which undergo reaction in representative model simulations. Such estimates are relatively straightforward for compounds which react in the atmosphere primarily with hydroxyl radicals, as is the case for most of the types of compounds where reactivity weighing is employed. For such compounds, we have shown that the fraction of compound which reacts in an airshed model simulation can be fit reasonably well by the following (Carter and Atkinson, 1989):

$$\frac{\text{Moles Compound Reacted}}{\text{Moles Compound Emitted}} = \left(1 - e^{-\,\text{kOH} \times \text{INTOH}}\right) \qquad \text{(II)}$$

where kOH is the OH radical rate constant and INTOH is a measure of the effective integrated OH radical levels under the conditions of the model simulation. (The above equation is exact if all the VOC is present at the beginning of the simulation, but is approximate otherwise.) If this approximation is employed, and if an emissions group E is to be represented by the model species M, then combining Equations (I) and (II) yields:

$$\begin{array}{l}\text{Reactivity}\\ \text{Weighing}\\ \text{Factor}\\ \text{for E}\end{array} = \begin{array}{l}\text{Moles of M}\\ \text{Representing}\\ \text{one mole of E}\end{array} = \frac{\left(1 - e^{-\,\text{kOH(e)} \times \text{INTOH}}\right)}{\left(1 - e^{-\,\text{kOH(m)} \times \text{INTOH}}\right)} \qquad \text{(III)}$$

where kOH(e) is the average OH radical rate constant for species in emissions group E, and kOH(m) is the OH radical rate constant used in the gas-phase mechanism for model species M. Note that if E and M are both rapidly reacting, then the reactivity weighing factor is always unity (and thus in effect reactivity weighing need not be employed); while if they both react slowly, then the reactivity factor is proportional to the ratio of the rate constants, and independent of the estimated INTOH parameter.

The appropriate value to use for INTOH in derivation of the reactivity weighing factors will depend on the conditions of the model simulation, since it is dependent on both the overall OH radical levels in the simulation, and the length of time the simulation is carried out. For

RADM simulations lasting 2-3 days, Stockwell and co-workers (Stockwell, private communication, 1988) estimate that an INTOH value of 110 ppt-min is appropriate. Therefore, that value is used in deriving our recommended weighing factors. Note that as indicated above the estimates of INTOH do not affect weighing for very rapidly or very slowly reacting compounds, but they do affect weighing factors for compounds of intermediate reactivity. A limited number of test calculations we have carried out with one-cell box models suggests that in practice the results of model simulations will not be highly sensitive to estimates of INTOH provided they are within reasonable limits. However, the recommended factors in Table 8 can be readily re-calculated for use in processing VOC emissions input for model simulations where an INTOH of 110 ppt-min is inappropriate. Smaller values may be more appropriate for 1-day urban simulations, while larger values may be appropriate for simulations of extended time periods.

The major parameters affecting the reactivity weighing factors are the OH radical rate constants assigned to the emissions groups and to the model species. The average T=300 K OH radical rate constants calculated for the emissions groups where reactivity weighing is recommended, and for the model species used to represent them in the RADM mechanism, are shown in Table 8. The former were calculated using the distributions of emissions in the current NAPAP total U.S. inventory, together with our assignments of OH radical rate constants for the various types of emitted compounds (Carter, 1988). The rate constants for several of the lumped model species in the RADM gas-phase mechanism vary depending on the version of the mechanism, since these were modified as a results of the recommendations made during this program. The table gives the rate constants for the version employing our final recommended values for the lumped model species which are discussed in the following section, since it is our understanding that our recommendations in this regard will be implemented into RADM.

This reactivity weighing approach is clearly not appropriate for lumping together species with different types of reaction mechanisms, since different types of mechanisms have been shown to have significantly different effects on results of model simulations, even if differences in reaction rates are taken into account (Carter and Atkinson, 1989). Furthermore, reactivity weighing is an approximation even for species with very similar reaction mechanisms, since differences in rates of reaction affect the distribution of where and when the compound reacts in the simulation. Rapidly reacting compounds react closer to the source areas, and slower reacting compounds have greater effects on remote regions. For this reason, it is not a good approximation to lump together species with very large differences in reaction rates. In addition, since the fractions of emitted compounds or model species which react will depend on the conditions of the model simulation, the weighing factors appropriate for one set of conditions may not necessarily be appropriate for others.

Clearly, the use of separate model species for compounds with appropriate reaction rates would be preferable to using reactivity weighing. However, when the number of species which can be used in the model is limited, as is the case for regional modeling applications, the use of reactivity weighing is preferable to options which are even more approximate. In particular, it is preferable to the options of either ignoring the effects of less reactive compounds for which there are no corresponding model species, or of representing emitted compounds with equal number of moles of model species of significantly different reactivity.

Representation of Alkanes and "Others" in RADM. The RADM mechanism employs five model species to represent reactions of the alkanes and species which are assumed to have alkane-like reaction mechanisms. Two of these species (CH4 and ETH) are used exclusively for methane and ethane, and the remaining three (HC3, HC5, and HC8) are lumped species representing the higher alkanes and the various types of species which are judged to be better represented by alkane model species than other species in the RADM mechanism. The nomenclature for HC3-HC8 is derived from the average number of carbons associated with each, as discussed in the following section.

As shown in Table 8, the miscellaneous groups of compounds aggregated into the "others" emissions groups are represented in RADM by lumped alkane model species. These "others" consist primarily of alcohols, ethers, and esters, though a variety of other reactive compounds, which are not considered appropriate for the other emissions groups, are included. Although except for the simple alcohols the reaction mechanisms of these compounds are uncertain, the major compounds in these groups are believed to react analogously to alkanes, reacting primarily with OH radicals, and probably forming similar types of oxygenated products.

Alkane model species are also used to represent acetylene and the haloalkenes. Although these are unsaturated compounds, the use of alkene model species to represent them is considered inappropriate because they react much slower with OH radicals than any of the alkene model species (Atkinson, 1986), and because their reaction with ozone is relatively much less important than is the case for most alkenes (Atkinson and Carter, 1984). They are thus lumped as alkanes by default because no other RADM model species is appropriate for them. The specific reaction mechanisms for these compounds are highly uncertain.

The allocation of lumped higher alkane model species to the various alkane and "others" reactivity groupings is shown in Table 8. These allocations were made such that each alkane emissions group (other than the "alkane/aromatic mix" group) is represented by only one RADM model species. In addition, the allocations were determined, as much as possible given the emissions groupings, (a) to minimize the range of reactivities of emissions groups represented by RADM species, and (b) to have the three higher lumped alkane RADM groups similar in their estimated numbers of moles reacted when representing the NAPAP U.S. inventory in RADM simulations. Since all three of the higher alkane RADM species represent two or more emissions groupings of differing reactivities, reactivity weighing is used in determining numbers of moles of RADM species representing these groups.

The group "alkane/aromatic mix" is used to represent the emissions in the NAPAP inventory which are characterized as mixtures with designations such as "mineral spirits," "naphtha," etc. Based on an analysis of detailed composition data for one type of mineral spirits (Weir et al., 1988), we estimate that these consist of approximately 91% C_7 and higher alkanes, with the remainder being aromatics. The average OH radical rate constant for the alkanes in this group is within the range used for the RADM species HC8, and thus these 91% of the molar emissions lumped in the "alkane/aromatic mix" group are represented by HC8, with reactivity weighing being employed. However, the extent to which the analysis used as a basis for this assignment is appropriate in representing the actual emissions lumped into this group is highly uncertain. This is an area where the emissions inventory needs to be improved.

Representation of Alkenes in RADM. The RADM mechanism employs four species to represent alkenes. Ethene (ETH) and isoprene (ISO) are represented explicitly, OLT represents propene and those alkenes which are lumped into the "alkenes (terminal)" emissions group, and OLI represents those lumped into "alkenes (internal)." As indicated above, the "alkenes (terminal)" group is defined as those alkenes, other than ethene, which react with OH radicals with rate constants less than 7.5×10^4 ppm^{-1} min^{-1} and includes most higher alkenes with only terminal double bonds. The "alkenes (internal)" group consists of alkenes, other than isoprene, which react with higher OH radical rate constants and consists of internal alkenes, dialkenes, and terpenes.

Other than isoprene and the "alkene (mixed)" emissions groups, which are special cases discussed below, the allocation of alkenes in the RADM mechanism corresponds almost exactly with that used in the emissions grouping. The only other exception is that, because of its high emissions, propene is treated separately in the emissions grouping, while in RADM it is lumped with the other "primary" alkenes. These correspondences are indicated in Table 8. As indicated there, no reactivity weighing is employed for alkene species. This is because the only case where more than one emissions group is aggregated into a RADM species are those represented by OLT, and these compounds react so rapidly that the reactivity weighing factor would be near unity (see Table 7).

The "alkene (mixed)" group consists of those emissions which are identified in the emissions inventories with terms such as "isomers of pentene," "C_{10} olefins," etc. It is not known to what extent these emissions consist of terminal alkenes (represented by OLT in RADM) or internal alkenes (represented by OLI), and we arbitrarily assume that they consist of equal amounts of each. Note, however, that in making allocations for the Carbon Bond and the CAL (SAPRC/ERT) mechanisms, Jeffries et al. (1989c) arbitrarily assumed that they were all terminal. This is another area where work is needed to improve the quality of the emissions inventories.

Because of the importance of isoprene in biogenic emissions, combined with the importance of biogenic emissions in regional model simulations, isoprene is treated explicitly in the RADM mechanism. However, its emissions are essentially negligible in the NAPAP anthropogenic inventory, and thus the RADM isoprene species (ISO) is not used in representing any of the anthropogenic emissions. (The small amount of isoprene in the anthropogenic inventory, consisting of only 0.001% of the mass emissions, is represented by OLI.) Thus, the RADM model species ISO is used only for biogenically emitted isoprene.

On the other hand, there is no RADM model species for terpenes, despite the fact that these are comparable in importance as isoprene in the biogenic inventory (Middleton, private communication, 1989). Thus, the biogenically emitted terpenes are represented by the same model species, OLI, which is used to represent anthropogenically emitted alkenes of similar reactivity. However, despite the potential importance of terpenes in regional model simulations, it is not clear whether there is any significant advantage to representing them separately in the model. Relatively little is known about their reaction mechanisms, other than their initial rates of reaction, which are in the range appropriate for OLI. Note that the model simulations of the chamber experiments (discussed in Section 5) indicate that representing at least one terpene, alpha-pinene, by OLI may not be inappropriate. As far as we are aware, there are no chamber data available to indicate how appropriate OLI is in representing the other terpenes.

Representation of Aromatics in RADM. The RADM mechanism uses three species to represent aromatic compounds. The most important of these are TOL, representing toluene, other monoalkylbenzenes, and lesser reactive aromatics, and XYL, representing xylenes, other di- and polyalkylbenzenes, and other aromatics which react more rapidly than the xylenes. In addition, the RADM mechanism includes the model species CSL, primarily to represent the phenol and cresol products formed in the reaction of TOL and XYL, but which can also be used to represent phenols and cresols which are emitted directly.

The allocations of the aromatic emissions groups to these three aromatic model species in RADM are shown in Table 8. Since there is no separate model species for benzene, the "benzene/halobenzene" emissions group is represented by the RADM species TOL, with reactivity weighing being employed to account for the differences in reaction rates for these species. The small amount of styrene emissions are represented by two RADM groups, with TOL being used to represent reaction at the aromatic group, and OLT being used to represent reaction at the double bond. (This is the only case where a version of the "lumped structure" approach is used with the RADM mechanism.) Most of the aromatics emitted are in the groups "aromatics (<2 react)," and "aromatics (>2 react)," which are represented by TOL and XYL, respectively. Since the mechanisms used for TOL and XYL are based primarily on those for the major species in these two groups (see following section), no reactivity weighing is employed in these cases.

As indicated above, the group "alkane/aromatic mix" is used to represent the emissions in the NAPAP inventory that are solvent mixtures which we estimate to consist of approximately 9% aromatics, with the remainder being alkanes. The average OH radical rate constant for the aromatics estimated to be in these mixtures is within the range used for the RADM species XYL, and thus these 9% of the molar emissions lumped in the "alkane/aromatic mix" group are represented by this species. No reactivity weighing is employed because these higher aromatic species react sufficiently rapidly that the reactivity weighing factors would be near unity.

Representation of Aldehydes, Ketones, and Organic Acids in RADM. The RADM mechanism includes the species HCHO for formaldehyde, ALD for higher aldehydes, KET for ketones, ORA1 for formic acid, and ORA2 for acetic acid. The aldehyde species corresponds directly to the aldehyde allocation in the emissions group, as shown in Table 8. The reactions used in the RADM mechanism for KET are based on estimated mechanisms for methyl ethyl ketone and higher ketones, and therefore KET is used to represent the "higher ketone" group directly, without reactivity weighing. There is no species in the RADM mechanism corresponding to acetone, so it is represented by the higher ketone model species, KET, using reactivity weighing. The organic acids are represented by ORA2, as discussed below.

Note that the use of reactivity weighing factors calculated using OH radical rate constants (as is the case for all those shown in Table 8) is not strictly valid when lumping acetone with the higher ketones, because these compounds (especially acetone) are consumed to a significant extent by photolysis. However, reactivity simulations we carried out using the

SAPRC mechanism (Carter, unpublished results, 1988) indicate that acetone is about 1/3 as reactive as the higher ketones in terms of effects on ozone formation, which is reasonably close to the reactivity difference estimated using OH radical rate constants. Since the reactivity weighing factor obtained using OH radical rate constants is reasonably consistent with the reactivity differences for the ketones indicated by modeling, the former is retained in our recommendations for consistency with the derivations of the factors for the other types of emitted species.

The representation of organic acids is the one case where the RADM mechanism is more detailed than the 32-class emissions aggregations. The mechanism has a separate species for formic acid and for higher organic acids, while the emissions scheme aggregates all organic acids into one group. However, the emissions of formic acid in the NAPAP total U.S. inventory is minor, accounting for only 2.5% of the mass of the organic acid emissions. For that reason, all the organic acid emissions are represented by ORA2 (higher organic acids) in the mechanism.

3.3 Derivation of Kinetic and Mechanistic Parameters for Lumped Model Species in RADM

As discussed in the previous section, the RADM mechanism includes a number of model species which are intended to represent aggregate mixtures of many different emitted VOCs. These include the lumped alkane species HC3, HC5, and HC8, the lumped aromatic species TOL and XYL (which, despite their names, actually represent a mixture of compounds), the lumped alkene species OLT and OLI, and the lumped oxygenate species ALD, KET, CSL, and ORA2, which are also used to represent various types of photooxidation products. As part of the RADM mechanism evaluation study, we evaluated the appropriateness of the reaction mechanisms used for these species to the specific groups of emitted compound each represents and made several recommendations in this regard. These recommendations, which have been adopted for the latest version of the RADM mechanism, are summarized in this section.

Lumped model species can be represented in molecularly-based mechanisms such as RADM either using the "surrogate species" or the "lumped molecule" approach. In the "surrogate species" approach, the mechanism of a typical or representative compound in the group is used to represent the reactions of all members of the group. For example, in the RADM mechanism (as in many others), the mechanism used for the species ALD, which represents the higher aldehydes, is based on that for acetaldehyde. In the "lumped molecule" approach, the reactions of a mixture of compounds is represented by a pseudo-molecule whose mechanisms are derived to represent an aggregate average of those of the sets of compounds they are used to represent. The former approach is most useful when one compound dominates in the lumped group, when there is only one compound in the group for which there is enough kinetic and mechanistic data available to derive or estimate a mechanism, or when the distribution of compounds in the group is unknown. The latter approach has the greatest potential for chemical accuracy, provided that there is sufficient information available concerning the distribution of compounds represented by the lumped group and relevant aspects of the reaction mechanisms of those compounds.

In the current RADM mechanism, the reactions of the lumped model species ALD, KET, CSL, ORA2, TOL, and (in part) XYL are based on the surrogate species approach, primarily because there is only limited information available concerning the mechanisms for more than a few examples of these types of compounds. On the other hand, the reactions used for the lumped alkane species HC3, HC5, and HC8, the lumped alkene species OLI and OLT, and (in part) the lumped higher aromatic species XYL are derived based on the lumped molecule approach. The derivation of the kinetic and mechanistic parameters for these lumped molecules was carried out at SAPRC as part of this RADM evaluation study, and were incorporated into the final recommended version of the RADM mechanism.

Tables 9 through 11 give the averages of the OH radical rate constant and other mechanistic parameters of relevance to RADM for the emitted species in the various emissions groups which are lumped as C3+ alkanes (Table 9), aromatic hydrocarbons (Table 10) and non-ethene alkenes (Table 11). The averages for the emissions groups were derived using the NAPAP total contiguous U.S. emissions inventory, and were computed based on the relative number of moles of the various types of species in each emissions group. No reactivity weighing of any kind was employed in computing these averages, because reactivity weighing is not employed when the emissions are aggregated into these groups. The tables also show the total number

Table 9. Averages of Parameters for Emissions Groups Lumped as C_{3+} Alkanes and for RADM Lumped Alkane Model Species, Derived Using the NAPAP Total U.S. Emissions Inventory

K.Moles	kOH	% Rct.	nC	---------		Products		---------	Description
Emit	(a)	(b)	(c)	ONIT	XO2	HCHO	ALD	KET	
Lumped as HC3									
23.9	0.369	45.6	4.02	0.07	0.48	0.16	0.61	0.50	Alkanes (0.25-0.50)
16.7	0.496	40.1	2.10	0.00	-0.87	0.02	0.98	0.04	Others (0.25-0.50)
14.0	0.115	9.5	2.00	0.00	-0.30	0.00	0.70	0.00	Acetylene
2.8	0.180	2.9	3.00	0.04	0.00	0.00	0.30	0.33	Propane
2.0	0.137	1.6	1.88	0.00	-0.63	0.69	0.12	0.19	Others (<0.25)
2.1	0.025	0.3	2.00	0.00	0.00	0.00	1.00	0.00	Haloalkenes
	0.386		2.99	0.03	-0.17	0.09	0.75	0.25	Recommended HC3 (d)
	0.376			0.03	-0.10	0.14	0.69	0.26	Initial RADM HC3 (e)
Lumped as HC5									
25.5	0.668	64.3	5.52	0.11	0.74	0.01	0.51	0.80	Alkanes (0.50-1.00)
12.5	0.801	35.7	3.43	0.02	-0.63	0.03	0.15	0.50	Others (0.50-1.00)
	0.715		4.77	0.08	0.25	0.02	0.38	0.69	Recommended HC5 (d)
	0.786			0.10	0.27	0.00	0.36	0.76	Initial RADM HC5 (e)
Lumped as HC8									
21.9	1.32	70.5	7.74	0.25	0.88	0.04	0.32	1.11	Alkanes (1.00-2.00)
3.1	2.34	12.0	12.38	0.34	1.10	0.06	0.20	1.39	Alkanes (>2.00)
3.3	1.55	11.5	2.87	0.02	-0.76	0.01	0.74	0.30	Others (>2.00)
1.6	2.02	6.0	10.04	0.30	1.34	0.12	0.37	1.31	Alkane/Aromatic Mix
	1.51		7.87	0.24	0.75	0.04	0.35	1.06	Recommended HC8 (d)
	1.66			0.24	0.78	0.05	0.44	1.05	Initial RADM HC8 (e)

(a) OH Radical rate constant in units of 10^4 ppm^{-1} min^{-1} at T = 300 K.

(b) Percent of estimated moles reacted for each lumped RADM group. Estimated by moles reacted = moles emitted x [1 - exp(-kOH x INTOH)], where INTOH = 110 ppt-min.

(c) Average number of carbons.

(d) Derived from averages for the emissions groups, as described in the text.

(e) Used in the March 1988 version of the RADM mechanism.

Table 10. Averages of Parameters for Emissions Groups Lumped as Aromatics and for RADM Lumped Aromatic Model Species, Derived Using the NAPAP Total U.S. Emissions Inventory

K.Moles Emit	kOH (a)	% Rct. (b)	nC (c)	Description
		Lumped as TOL		
16.1	0.919	84.9	7.26	Aromatics (<2.00)
7.3	0.185	11.1	6.00	Benzene, Halobenzenes
0.8	0.902	4.0	7.36	Styrenes
	0.918		7.13	Average for RADM TOL (d)
	0.902			Recommended RADM TOL (e)
	0.902			Initial RADM TOL (f)
		Lumped as XYL		
16.3	4.09	99.0	8.88	Aromatics (>2.00)
0.2	3.73	1.0	8.26	Alkane/Aromatic Mix
	4.09		8.87	Recommended for RADM XYL (d)
	4.54			Initial RADM XYL (f)

(a) OH Radical rate constant in units of 10^4 ppm^{-1} min^{-1} for T = 300 K.

(b) Percent contribution to the RADM group Reacted, estimated using Moles Reacted = Moles Emitted x [1 - exp(-kOH x INTOH)], where INTOH = 110 ppt min^{-1}.

(c) Average number of carbons.

(d) Derived from averages for the emissions groups.

(e) The OH radical rate constant for TOL used in the initial RADM mechanism is based on that for toluene. This is sufficiently close to the average for the emissions represented by TOL that no change is recommended.

(f) Used in the March 1988 version of the RADM mechanism.

Table 11. Averages of Parameters for Emissions Groups Lumped as Non-Ethene Alkenes and for RADM Lumped Non-Ethene Alkene Model Species, Derived Using the NAPAP Total U.S. Emissions Inventory

K.Moles Emit	% Rct. (a)	nC (b)	kOH (c)	kO3 (d)	kNO3 (e)	Structural Groups			Description
						$=CH_2$	$=CHR$	$=CR_2$	
Lumped as OLT									
10.6	62.6	3.00	3.82	1.74	14.4	1.00	1.00	0.00	Propene
4.6	27.3	4.74	4.72	1.67	24.1	1.00	0.99	0.01	Primary Alkenes
0.9	5.5	5.89	5.11	1.70	68.1	1.00	0.89	0.11	Mixed Alkenes
0.8	4.5		4.99	1.78	159.4	1.00	0.68	0.32	Styrenes
		3.50	4.19	1.73	26.5	1.00	0.98	0.02	Average for OLT (f)
			4.19	1.74	26.5	1.00	1.00	0.00	Recommended for OLT (g)
			3.82	1.74	23.3	1.00	1.00	0.00	Initial RADM OLT (h)
Lumped as OLI									
11.0	92.2	4.85	9.88	23.9	1944.	0.30	1.40	0.11	Internal Alkenes
0.9	7.8	5.89	9.11	29.0	578.	0.00	2.00	0.00	Mixed Alkenes
		4.93	9.82	24.3	1837.	0.28	1.44	0.10	Average for OLI (f)
		4.93	9.82	24.3	1837.	0.28	1.45	0.10	Recommended for OLI (g)
			9.24	30.2	1837.	0.28	1.45	0.10	Initial RADM OLI (h)

(a) Percent contribution to the RADM group reacted, estimated assuming all emitted alkenes are consumed through reaction.
(b) Average number of carbons.
(c) OH radical rate constant in units of 10^4 ppm^{-1} min^{-1} for T = 300 K.
(d) Ozone rate constant in units of 10^{-2} ppm^{-1} min^{-1} for T = 300 K.
(e) NO_3 radical rate constant in units of ppm^{-1} min^{-1} for T = 300 K.
(f) Derived from averages for the emissions groups.
(g) The average values for the structural group parameters are so close to the initial RADM values that no change is recommended.
(h) Used in the March 1988 version of the RADM mechanism.

of moles of each emissions group which were derived from the NAPAP total emissions inventory.

The estimated percent contributions of the various emissions groups to the reactivities of the lumped RADM groups used to represent them are also shown in Tables 9 through 11. In the case of the alkanes and aromatics, these contributions were computed based on the approximate amounts of each group expected to react in a model simulation, estimated as described above in the discussion of reactivity weighing [i.e., estimated using Equation (II), with INTOH = 110 ppt-min]. For non-ethene alkenes, these were estimated based on assuming all the emitted alkenes react in the model simulation as expected based on their relatively high OH radical rate constants and the fact that they are consumed non-negligibly by reaction with ozone as well. These percent contributions are then used to compute the recommended averages for the OH radical rate constants and for the other mechanistic parameters for the lumped RADM species.

It should be noted that as indicated in Section 2 the parameters for the evaluated RADM mechanism incorporated earlier recommendations we made for kinetic and mechanistic parameters for these species, based on an analysis similar to that described here. However, the emissions parameter data base at SAPRC was still undergoing development at the time these initial recommendations were made, and thus the final recommendations are slightly different. The parameter values used in the initially evaluated mechanism, derived based on this earlier analysis, are shown in the tables as "Initial RADM." Since the final recommendations have been implemented into the new version of the RADM-II mechanism, the derivation of the earlier recommendations is not discussed here.

The derivations of the values for the kinetic and mechanistic parameters shown in Tables 9 through 11, and the ways they are used in the RADM mechanism for the various types of lumped species are discussed below. In most cases, the parameters are based on the kinetic and mechanistic assignments we previously made for representing complex mixtures of emitted species in the SAPRC mechanism, which is documented elsewhere (Carter, 1988). However, in some cases, the product yield parameters had to be modified to be consistent with the set of product species used in the RADM mechanism.

3.3.1 Mechanistic Parameters for Lumped Alkanes

Alkanes react in the atmosphere primarily with OH radicals to form organic peroxy radicals. The peroxy radicals can react with NO to form NO_2, HO_2, and a variety of oxygenated products or they can react with NO to form organic nitrates. Techniques exist for estimating the rates of initial OH radical attack at various positions on the alkanes (Atkinson, 1986, 1987; Carter and Atkinson, 1985), and the branching ratios of the various reactions of the radicals subsequently formed (Carter and Atkinson, 1985). We have used these estimates to derive kinetic and mechanistic parameters for the major alkane species in the NAPAP inventory (Carter, 1988a). If the distribution of alkanes in the available NAPAP total U.S. emissions inventory can be considered to be generally representative, then these estimates can be used to derive average values for these parameters for the three alkane model species in RADM.

The mechanistic parameters for the alkanes, the ways in which they are estimated, and the ways in which they are implemented into the RADM mechanism, are as follows:

The OH Radical Rate Constants. Estimates of the OH radical rate constants at 300 K were made for the various types of emitted alkanes using the OH radical rate constant estimation technique of Atkinson (1987). These values were then used to derive rate constants at 300 K for the alkane species used in the model. No recommendation is made concerning the temperature dependence for these reactions, and the recommended modified RADM mechanism uses the same activation energies for these reactions as employed in the original RADM-II mechanism (NCAR 1987).

Organic Nitrate Yields. Organic nitrates are formed in alkane photooxidations by the reaction of peroxy radicals with NO, competing with the alternative reaction route involving conversion of NO to NO_2 and ultimate regeneration of radicals. The nitrate yield is an important parameter in alkane mechanisms since its formation represents a radical and NO_x sink. Note that by conservation of radicals and NO_x, the overall radical yield in the alkane photooxidation reaction is 1 minus the nitrate yield. These are estimated for the various types of alkanes in the inventory as described by Carter and Atkinson (1985), with parameters updated as given by Atkinson (1988) and Carter and Atkinson (1989b). Note that these estimates are based on assuming that alkyl nitrate formation occurs only during reaction of NO with unsubstituted peroxy radicals such as those formed immediately following the initial alkane + OH reaction, and not in the reactions of the hydroxy- or oxy-substituted radicals formed following the alkoxy radical isomerizations involved in the photooxidations of the long-chain alkanes (Carter and Atkinson, 1985). This is highly uncertain, and thus the simulated nitrate yields in the reactions of the higher alkanes may be underestimated.

The RADM mechanism represents the formation of alkyl nitrates in alkane systems by a two-step process. The first is the initial reaction with OH to form a peroxy radical. This radical then reacts with NO to form the lumped alkyl nitrate species (ONIT) in variable yields and HO_2 in yields of 1 minus the alkyl nitrate yield. For HC5 and HC8, the peroxy radical yield in the first reaction is unity, and thus the nitrate yield in the second reaction is the same as the nitrate yield derived in the emissions analysis. However, to represent the appropriate numbers of NO to NO_2 conversions as discussed below, the peroxy radical in the initial reaction of the lumped alkane HC3 has a less-than-unit yield, and thus the nitrate yield in the reaction of HC3's peroxy radical with NO is increased accordingly, to obtain the overall yield indicated in Table 9. The specifics of how nitrate formation and NO to NO_2 conversion is represented in the RADM mechanism is discussed below.

NO-to-NO_2 Conversions. The alkane photooxidation reactions involve the formation of organic peroxy radicals which convert varying amounts of NO to NO_2. The total amount of NO converted to NO_2 by these reactions is determined by a number of factors, including the alkyl nitrate yields and the overall number of isomerizations and decompositions of radicals which are involved in the photooxidation process. The number of these conversions have been estimated for the major types of alkanes in the emissions inventory (Carter, 1988) by using a computer program employing the peroxy- and alkoxy-radical branching ratio estimates of Carter and Atkinson (1985), as updated by Atkinson (1988). Analogous methods can be used for estimating NO-to-NO_2 conversions in species such as alcohols, esters, and others aggregated in the "others" categories which are lumped with alkanes in RADM, since generally they are predicted to form the same types of radical intermediates. Note, however, that the photooxidations of simple alcohols involve fewer NO-to-NO_2 conversions than do alkanes, since, unlike alkanes, photooxidations of alcohols do not involve formation of peroxy radicals.

In the RADM mechanism, the representation of NO to NO_2 conversions by peroxy radicals in the lumped alkane mechanism depends on the net number of conversions that are estimated to occur. If the emissions data indicate that an average of more than one NO is consumed per alkane reacted, then the reactions can be represented by

HCn + OH --> HCnP + a XO2
HCnP + NO --> b ONIT + (1-b) HO2 + (1-b) NO2 + oxygenated products
XO2 + NO --> NO2

where HCn is the lumped model species representing alkanes, HCnP is the lumped peroxy radical species associated with HCn, and XO2 is a "chemical operator" used to represent excess NO-to-NO_2 conversions. The parameter "a" in the above reaction is shown in Table 9 as the XO2 yield, and the parameter "b" indicates the organic nitrate (ONIT) yield. However, if the emitted species represented by the lumped alkane species "HCn" includes a large fraction of alcohols, whose reactions generate HO_2 and organic products without producing peroxy radicals and NO-to-NO_2 conversions, then there may be on the average less than one NO converted to NO_2 per alkane reacted. This is the case for the lumped species "HC3" in the present mechanism, and is indicated in Table 9 by a negative number for the parameter "a," the XO2 yield. In this case the reactions are represented by

HCn + OH --> (1+a) HCnP (where $a < 0$)
HCnP + NO --> b/(1+a) ONIT + (1-[b/(1+a)]) (HO2 + NO2)
+ oxygenated products.

Note that in both cases the parameter "b" reflects the total organic nitrate (ONIT) yield, and the total number of molecules of NO reacting per molecule of HCn consumed is a+1.

The above discussion concerns the case where reaction with NO is the major fate for organic peroxy radicals. The RADM mechanism also includes reactions of peroxy radicals with each other and with HO_2. The products formed in these reactions are not affected by the XO2 and the ONIT yields, though they are affected by the yields of the oxygenated organic products as discussed below.

Oxygenated Organic Products. The atmospheric photooxidation reactions of the alkanes in the presence of NO involve the formation of a variety of oxygenated products, including complex bi- and poly-functional species as well as simple aldehydes and ketones. The yields of these oxygenates can be estimated using the estimates of the relative rates for alkoxy radical decomposition, isomerization, and reaction with O_2 given by Carter and Atkinson (1985), and updated by Atkinson (1988). The computer program used to derive these estimates expresses the yields in terms of the oxygenated products used in the most detailed version of the current SAPRC mechanism. These products are HCHO (formaldehyde), CCHO (acetaldehyde), RCHO (C_3 and higher aldehydes), ACET (acetone), and MEK (methyl ethyl and higher ketones) (Carter, 1988). The RADM mechanism represents alkane oxygenated products using the model species HCHO (formaldehyde), ALD (higher aldehydes), and KET (ketones). The SAPRC representation is converted to RADM model species by using ALD to represent both CCHO and RCHO, using KET to represent MEK, and using 1/2 KET to represent ACET.

The yields shown in Table 9 for the products HCHO, ALD, and KET refer to their overall yields under conditions where reaction with NO is the major fate for organic peroxy radicals. As indicated above, the RADM mechanism also includes reactions of peroxy radicals with HO_2 and with other peroxy radicals. The RADM mechanism represents all peroxy + HO_2 reactions as forming lumped hydroperoxide species, which do not depend on the set of oxygenated products assumed when the reaction with NO dominates. When the peroxy radicals react with other peroxy radicals, the set of oxygenated organic products will in general be different from those formed in the reaction with NO, and organic nitrates will not be formed. However, no separate estimates were made concerning the set of organic products formed from peroxy + peroxy reactions; instead they were represented by the same set of products formed in the NO reaction, with the same relative yields, but their overall yields increased by a factor of b/(1-b) (where "b" is the ONIT yield) to account for the fact that organic nitrates are not formed. This is consistent with the way these reactions are represented in the SAPRC mechanism (Carter, 1988).

Mechanistic Parameters for Lumped Alkanes in the RADM-M Mechanism. As discussed in Section 2, one of the modifications we recommend for the RADM mechanism is that the two higher lumped alkane classes, HC5 and HC8, be combined into a single model species. This is because, as shown in Section 6.4, this condensation in the representation of the alkanes is unlikely to have significant impacts on predictions of species of interest in RADM applications and reduces the size of the mechanism by two species. The kinetic and mechanistic parameters for this new lumped species were derived in the same manner as discussed above. Table 12 gives the averages for the parameters for the emissions groups represented by this new lumped higher alkane species and the resulting averages calculated for the model species. As indicated in the table, the average number of carbons of the compounds it represents in the NAPAP inventory is 6.3, and thus the model species is designated "HC6." The parameters used for HC6 in the recommended RADM-M mechanism are based on the results of this analysis..

3.3.2 Mechanistic Parameters for Lumped Aromatics

The aromatic hydrocarbons are also consumed in the atmosphere primarily by reaction with OH radicals, and the rate constants for the reactions of most of the emitted aromatic species are known or can be estimated based on those for chemically similar species (Atkinson, 1986). OH radical rate constants for T=300 K were assigned for the major aromatic hydrocarbon species in the NAPAP total U.S. emissions inventory, and these values, combined with the relative molar emissions of aromatics in that inventory, were used to derive the weighed average rate constants shown in Table 10 for the various aromatic emissions groups and for the two aromatic model species in RADM. Note that the weighed average rate constant for the RADM species TOL is so close to that for toluene that use of the toluene rate constant is not inappropriate. However, because of polyalkyl benzenes, naphthalenes, and other higher aromatics represented by the RADM species XYL, the average rate constant derived for that species is higher than that for the xylenes.

We could not derive average values for the other mechanistic parameters for the aromatics in a manner analogous to that done for the alkanes because the mechanisms for aromatic reactions are highly uncertain. We must rely on chamber data, as discussed in Section 2.2.1, to derive these parameters.

Table 12. Averages of Parameters for Emissions Represented by the Combined Higher Alkane (HC5 + HC8) Model Species Recommended for the RADM-M Mechanism

K.Moles Emit	kOH (a)	% Rct. (b)	nC (c)	Products					Description
				ONIT	XO2	HCHO	ALD	KET	
Lumped as HC3									
21.9	1.315	37.8	7.74	0.25	0.88	0.04	0.32	1.11	Alkanes (1.00-2.00)
25.5	0.668	29.9	5.52	0.11	0.74	0.01	0.51	0.80	Alkanes (0.50-1.00)
12.5	0.801	16.6	3.43	0.02	-0.63	0.03	0.15	0.50	Others (0.50-1.00)
3.3	1.552	6.1	2.87	0.02	-0.76	0.01	0.74	0.30	Others (>2.00)
3.1	2.339	6.4	12.38	0.34	1.10	0.06	0.20	1.39	Alkanes (>2.00)
1.6	2.018	3.2	10.04	0.30	1.34	0.12	0.37	1.31	Alkane/Aromatic Mix
	1.088		6.26	0.15	0.51	0.03	0.38	0.87	Recommended HC6 (d)

(a) OH radical rate constant in units of 10^4 ppm^{-1} min^{-1} at T = 300 K.

(b) Percent of estimated moles reacted for each lumped RADM group. Estimated by moles reacted = moles emitted x [1 - exp(-kOH x INTOH)], where INTOH = 110 ppt-min.

(c) Average number of carbons.

(d) Derived from averages for the emissions groups, as described in the text.

3.3.3 Mechanistic Parameters for Lumped Alkenes

The RADM mechanism includes the reaction of alkenes with OH radicals, ozone, and NO_3 radicals. Rate constants were assigned for the major alkene species in the NAPAP total U. S. inventory based on experimental or estimated values (Carter, 1988, and references therein). Using these and the relative molar emissions in the NAPAP inventory, average rate constant values for the various lumped alkene emissions groups and for the RADM lumped alkene species OLT and OLI were derived. The results are shown in Table 11. The contributions of the emissions groups to the weighed averages for the lumped RADM species were calculated assuming that all the emitted alkenes represented in these groups are consumed during a model simulation.

The appropriate sets of organic products to use in alkene reaction mechanisms depend on the nature of the substituents around the double bond (Carter, 1988). For example, reactions of OH or NO_3 radicals with alkenes result in formation of formaldehyde from $=CH_2$ groups, higher aldehydes from =CHR groups (where R = alkyl), and ketones from $=CR_2$ groups, with analogous considerations being involved in determining the products in the ozone reactions (Carter, 1988). Table 11 shows the average number of substituents about the double bonds for the alkenes in the various emissions groups and for those represented by OLT and OLI in the RADM mechanism. (The number of substituents does not sum up to two for the "internal alkenes" emissions group because cycloalkenes are counted as having only one substituent about the double bond for the purpose of determining the organic product yields.) The recommended sets of products for the lumped internal alkene species (OLI) is based on the results of this analysis. Thus, for example, the reaction of OLI with OH radicals yields 0.28 HCHO + 1.45 ALD + 0.10 KET as the organic products, reflecting the weighed average numbers of $=CH_2$, =CHR, and $=CR_2$ substituents, respectively. In the case of the terminal alkenes (OLT), this analysis indicates that the continued use of propene (with one $=CH_2$ and one =CHR substituent) as the surrogate species for the terminal alkenes is appropriate.

4. EVALUATION AGAINST ENVIRONMENTAL CHAMBER DATA: CHARACTERIZATION AND LUMPING PROCEDURES

4.1 Introduction

An important step in the model design and evaluation process is evaluation of the gas phase chemistry against environmental chamber data. The gas phase chemistry module is one of the few modules in the atmospheric modeling system that can be independently tested against experimental data. The testing against chamber data is essential for, but not necessarily sufficient to, fully establishing the scientific validity of a mechanism for use in regional acid deposition modeling. The reason for this is that while a large data base of experiments exists for the $ROG/NO_x/O_3$ system under urban-like conditions, virtually no reliable data exist to test mechanisms' performance for other important species, such as sulfuric acid, nitric acid, hydrogen peroxide, organic peroxides, and organic acids, or for other important concentration regimes, such as the rural regime which is dominant in regional model applications. Nevertheless, the present chamber data base can be used to test the rate of NO_x oxidation and concentrations of ozone, peroxyacetylnitrate, and formaldehyde predicted by gas phase chemical mechanisms for urban conditions. This is important because these species are important in long-range transport and the regional model must simulate the chemistry of emissions as they are transported from urban areas to remote areas with sensitive receptors.

It is also important to recognize that even though the present data base does not allow for direct evaluation of model predictions for sulfuric acid and nitric acid, the testing protocol provides some indirect evidence for evaluation of performance for these species. First, accurate prediction of the rate of NO_x oxidation and ozone formation necessitate accurate predictions of OH radical concentrations. OH, according to present theory, is the sole gas-phase oxidant that converts SO_2 to sulfuric acid and NO_2 to nitric acid in the daylight hours. Second, since NO_x is primarily oxidized to nitric acid or PAN, the evaluation results for PAN provide some information on whether the mechanism is oxidizing NO_x to the correct species.

An evaluation of the March 1988 RADM, recommended modified RADM (RADM-M), and the recommended modified parameter (RADM-P) mechanisms against environmental chamber data was performed in this study. The objective of the evaluation was to assess the accuracy and precision of the mechanisms' predictions for ozone, PAN, formaldehyde, and the rate of NO_x oxidation. The approach for the evaluation involved simulating a large number of experiments (over 500) from four different chambers and statistically evaluating the mechanisms' performance.

Experimental data collected in the following chambers was used for the evaluation:

1) The SAPRC evacuable indoor chamber (EC),
2) The SAPRC indoor Teflon chamber (ITC),
3) The SAPRC outdoor Teflon chamber (OTC), and
4) The University of North Carolina outdoor chamber (UNC).

Only experiments with relatively complete data were employed in the evaluation. The specific sets of experiments used were those recommended for use in model evaluation by the experimentalists (Jeffries et al., 1985; Carter et al., 1986), with additional experiments added which were employed in more recent evaluations of the SAPRC mechanisms (Carter et al., 1987, 1988).

The results of the chamber simulations are described in Section 5. Before presenting these results, it is first necessary to indicate the assumptions made and procedures that were followed. Carrying out model simulations of environmental chamber experiments involves more than just implementing the chemical mechanism on a computer with the appropriate software, specifying the initial reactant concentrations, and then running the calculation. Before such simulations can be carried out, it is necessary to specify in the model input the appropriate conditions of the chamber experiments, including appropriate representation of such factors as temperature, light intensity and spectral characteristics, humidity, and chamber wall and contamination effects. In addition, for a lumped mechanism such as RADM, which does not contain explicit representation of all of the various types of organic compounds which are present in the experiments, appropriate procedures need to be established for representing the organics used in the chamber experiments with the species incorporated in the mechanism. These are discussed in this section.

4.2 Characterization of Chamber Conditions

In order to test chemical mechanisms against environmental chamber results, it is necessary to include in the model appropriate representations for chamber-dependent effects such as wall reactions and characteristics of the light source used during the experiments. The specific chamber-dependent aspects represented in the process of testing mechanisms are the following:

1) Light characterization;
2) Chamber-dependent radical sources;
3) Offgassing of NO_x from the walls;
4) Heterogeneous hydrolyses of N_2O_5 and NO_2;
5) Wall loss of ozone;
6) Excess NO oxidation caused by background organics;
7) Dilution rates; and
8) Characterization of temperature and humidity.

There is significant uncertainty regarding the most appropriate way to represent some of these aspects and different modeling groups have made different assumptions. As in our previous mechanism evaluation studies (Carter et al., 1986, 1987, 1988), the goal in this study was not to represent these effects exactly (since this is not possible given the current state of knowledge), but to represent these effects in the four chambers in a consistent manner and with the minimum number of empirical parameters required to be consistent with the available characterization data.

We had developed a comprehensive set of procedures and assumptions for representing these chamber- and run-dependent processes during the course of our previous mechanism evaluation studies (Carter et al., 1986, 1987). However, prior to conducting the evaluation, these procedures and assumptions were reviewed and updated where new data were available. Procedures for characterizing the SAPRC chambers were almost entirely adopted from those used in our previous evaluation studies (Carter et al., 1986, 1987) and therefore are only briefly summarized here. However, significant improvements were made in the procedures to characterize the light intensity and spectral distribution in the UNC chamber, based on the recent work carried out by Jeffries et al. (1989a). These changes in the light characterization for the UNC chamber necessitated other refinements in the characterization procedures for that chamber.

4.2.1 Light Characterization

The rates of the photolysis reactions in environmental chamber simulations are obviously important since these reactions supply the energy to drive the chemical transformations that the model is attempting to simulate. For both indoor and outdoor chamber simulations, photolysis rate constants were calculated using the following equation,

$$k^{phot}(t) = \sum_{\lambda} [\ J(\lambda,t)\ \sigma(\lambda)\ \phi(\lambda)\ ] \qquad \text{(I)}$$

where $k^{phot}(t)$ is a photolysis rate constant at time t, $J(\lambda,t)$ is the intensity at time t of the light source in a wavelength region centered at wavelength λ and $\sigma(\lambda)$ and $\phi(\lambda)$ are the absorption coefficient for the photolyzing species and the quantum yield for the photolysis reaction over that wavelength region. For each photolysis reaction, the values of the absorption coefficients and quantum yields are considered to be part of the homogeneous reaction mechanism (given in Section 2). On the other hand, the values $J(\lambda,t)$ are determined by the intensity and spectral distribution of the light source. Thus, specification of this parameter is part of the chamber-dependent input in the model simulations of the chamber experiments. The procedure used for deriving $J(\lambda,t)$ depends on whether the chamber is an indoor or an outdoor chamber.

Light Characterization for Indoor Chambers. The light intensities and spectral distributions used for the SAPRC EC and ITC are those discussed by Carter et al. (1986). These are believed to be reasonably well characterized and are assumed to be constant throughout each experiment. For both chambers, the light intensity is monitored by carrying out periodic NO_2 actinometry experiments, and the results of these are used to assign k_1 values for various groups of runs. For most experiments the values of the NO_2 photolysis rates (k_1) were in the range of 0.2 to 0.4

min^{-1}, with the values changing relatively slowly over time. Based on the observed variability of the k_1 measurements, the values assigned for individual runs are estimated to have an uncertainty of ~10% or less.

The ratios of rates of the other photolysis reactions to those for NO_2 are determined by the spectral distribution of the light source. For the experiments carried out in the SAPRC EC, the relative spectral distribution was measured during the course of each run, as described by Pitts et al. (1986). For runs carried out around the same time and with the same lamp, essentially the same spectral distribution was observed, though with some run-to-run variability; but over longer periods of time, systematic changes in the spectral distribution occurred, with the relative intensity in the UV region becoming progressively less. In the model testing, consecutive runs with similar measured spectral distributions were grouped together, and the averages of their measured spectral distributions were used for all the runs in the group. The sets of EC spectral distributions which were employed are summarized by Carter et al. (1986).

The relative spectral distribution for the blacklights used in the ITC was measured much less frequently, but the few measurements carried out indicate that it can be assumed to be essentially constant. The measured spectral distribution for this chamber is also given by Carter et al. (1986). Compared to the solar or EC spectral distributions, the ITC spectral distribution is relatively more intense in the ~330 - 370 micron region, but is much less intense for wavelengths greater than ~380 microns.

Light Characterization for Outdoor Chambers. The intensity and spectral distribution of the light source for the UNC and SAPRC OTC outdoor chambers, which consists of natural sunlight passing through the chamber walls, is more difficult to characterize. Both the intensity and spectral distribution of the light source depend on the time of day, the time of year, and the local meteorological conditions. Jeffries (1989a) recently completed an extensive experimental and theoretical study of the light characteristics inside and outside the UNC chamber and developed a model and a data base for deriving light intensities and spectral distributions as a function of time for each of the UNC chamber experiments whose data are available for model evaluation. This new UNC light characterization data base was employed in this study. In principle, the procedures employed to develop the UNC chamber light characterization data base could be employed to characterize the light in the SAPRC OTC runs, but there was insufficient time and resources available in this program to carry this out. Therefore, the methods used to represent OTC light characteristics in our previous mechanism evaluation studies, described by Carter et al. (1986), were also employed in this study.

The overall features of the methods used for light characterization for the OTC and the UNC chambers are summarized below. However, the reports of Jeffries et al. (1989a,d) (for the UNC chamber) or of Carter et al. (1986) (for the OTC) should be consulted for details.

Light Characterization of the SAPRC OTC. The light characterization data available for the OTC experiments consist of continual UV radiometer measurements of sunlight outside the chamber and, for many experiments, continual NO_2 actinometry (k_1) measurements made underneath the reaction bag, with the light passing in and out of the chamber before reaching the actinometer. Such data can be used to estimate how total light intensity is varying with time outside the chambers, but they give no direct indication of how the relative spectral distribution is varying, or (except to a limited extent for the k_1 measurements under the OTC) how the light intensity and spectral distribution inside the chamber may differ from that outside. Therefore, much of the light characterization input required for the OTC was derived based on theoretical calculations, assumptions and approximations which are discussed below.

The light intensities used in calculating the photolysis rate constants for a given OTC chamber experiment are given by $J(\lambda,t)$, which was calculated as a function of wavelength (λ) and time of day (t) according to the equation:

$$J(\lambda,t) = J_0(z[t']) \frac{UV(t)}{UV_0(z[t'])} f(\lambda,t) \qquad (II)$$

where z[t'] is the solar zenith angle at time t', which is our best estimate of the true solar time t of the experiment, $J_0(z[t'])$ is the theoretically-calculated clear-sky light intensity for the region associated with wavelength g, UV(t) is the experimental UV radiometer reading taken at time t during the experiment, $UV_0(z[t'])$ is the theoretically calculated clear-sky UV radiometer reading for z[t'], and $f(\lambda,t)$ is a correction factor to account for the effects of transmission of light through the chamber walls.

The clear-sky light intensities given by Peterson (1976) for his "best estimate" surface albedos were used to derive $J_0(\lambda,z[t'])$ for the OTC experiments. The values of J_0 used for a given wavelength and zenith angle were calculated using an empirical function fit to the data tabulated by Peterson (1976) as described by Carter et al. (1986). The solar zenith angle z(t') was calculated from the true solar time, the date, and the latitude of the SAPRC OTC (34.06 degrees) using the standard formula as employed by Carter et al. (1986). Because the clocks used during the outdoor chamber experiments were not always accurate (Carter et al., 1986), the difference between the clock time t and the true solar time t' were derived based on adjusting t-t' so that the experimental and the theoretically calculated UV curve shapes agreed. As expected, the time offsets did not vary randomly from run-to-run, but were generally the same for runs carried out around the same time period. For a few runs the light quality was so poor that it was not possible to determine t-t' using the light intensity data, and those runs were assumed to have the same time offset as observed in runs carried out at around the same time.

The experimentally measured UV data are used to take into account local meteorological factors which affect the light intensity entering the chamber as a function of time during the individual chamber experiments. As indicated in Equation (II), this is done by assuming that for any wavelength the ratio of the actual light intensity outside the chamber to J_0, the theoretical "clear sky" light intensity value, is the same as the ratio of the measured UV radiation intensity to UV_0, the calculated estimated "clear sky" UV values, which, like J_0, are assumed to be a function only of the solar zenith angle. These latter quantities are calculated from an empirical formula (Carter et al., 1986), which is expressed as:

$$UV_0 = f_{shape}(z) \lim_{z \to 0} (UV/k_1)^{expt}(0) \; k_1^{calc}(0) \tag{III}$$

where f_{shape} is an empirical function, normalized to unity for z=0, which was derived based on fits to the shapes of experimental UV vs time data obtained during SAPRC OTC and UNC outdoor chamber experiments on clear days; lim(z->0) $(UV/k_1)^{expt}(0)$ is the estimated z=0 ratio of UV intensity to the NO_2 photolysis rate (k_1) derived based on the empirical relationship between simultaneous experimental UV radiometer and k_1 measurements given as a function of zenith angle by Zafonte et al. (1977); and $k_1^{calc}(0)$ is the calculated NO_2 photolysis rate using the J_0 values for z=0.

At both the SAPRC and the UNC outdoor chamber laboratories the UV instrument is located outside the chamber, and thus does not directly measure the light intensity inside the chamber. In the case of the SAPRC OTC, which consists of a flexible Teflon bag held on a rope netting above a green indoor-outdoor carpet, the major cause for differences in light intensity between the inside and the outside of the chamber is assumed to be the attenuation of the light as it passes through the Teflon walls. The k_1 data taken during the OTC runs are used to obtain a rough indication of the magnitude of this attenuation, since the tube used to obtain these data is located underneath the reaction bag, and thus light reaching it passes through the chamber walls twice. A comparison of observed with theoretically calculated k_1 readings for these OTC runs (Carter et al., 1986) indicates that the light reaching the k_1 tube under the OTC is attenuated by a factor of ~1.44. Since the light has to pass through two Teflon surfaces (the top and the bottom of the chamber) before reaching the NO_2 actinometer, this corresponds to a suppression factor of 1.2 when passing through each wall of the chamber. Thus in modeling the OTC runs for this study, we use a wall transmission correction factor of 0.83 in equation (II) when calculating the light intensity.

This estimation that a simple 0.83 correction factor takes into account all the differences between the light intensity and spectral distribution inside the OTC and the theoretically calculated values is obviously subject to a number of uncertainties, since it does not take into account, for example, possibilities that the walls, or reflections from the surfaces and structures around the OTC may be changing the zenith angle dependences of the light intensity, or that attenuation and/or scattering of light as it passes through the walls may cause a change in the spectral distribution. These uncertainties are expected to be the greatest at the higher zenith angles, but for most SAPRC OTC runs the chamber is covered before 0900 PST and after 1500 or 1600 PST, so uncertainties associated with light characteristics at high zenith angles will not affect model simulations of most SAPRC OTC runs. Based on these considerations, we estimate that the light intensity inside the OTC is probably uncertain by ~15%; though this is a subjective estimate. The uncertainty is probably somewhat less at the wavelength region affecting the photolysis of NO_2, and probably somewhat greater at the lower wavelength region which affects the photolysis of aldehydes and the formation of $O(^1D)$ from O_3.

It should be noted that both the $k_1^{calc}(0)$ values used in Equation (III), and the comparison of observed and calculated k_1 values used in the derivation of the wall transmission correction factor depend on the set of absorption coefficients and quantum yields assumed for NO_2. However, these two factors have opposing effects on the calculation of the overall in-chamber light intensity in Equation (II), and thus the light intensities used in the model simulations are not sensitive to the sets of NO_2 absorption coefficients and quantum yields used in this analysis. At the time of the derivation of the data base used for the modeling of the OTC runs, we used the NO_2 absorption coefficient and quantum yields recommended by NASA (1985), which are somewhat different (yielding, for example, 7% lower calculated NO_2 photolysis rates for z=0) than those used in the current RADM (see Section 2) and SAPRC (Carter et al., 1988) mechanisms. However, since as indicated above these differences will tend to cancel out in the derivation of the overall light intensity, and since there are a number of much more significant uncertainties involved in this derivation, it was determined not to be productive to expend the significant effort required to re-derive the OTC light characterization data base using the updated NO_2 absorption coefficients and quantum yields. If the OTC light characterization data base is to be re-derived, it would be more appropriate to use the updated procedures developed by Jeffries (1989a) for re-deriving the UNC chamber light characterization data, as discussed below.

Updated Light Characterization of the UNC Chamber. In our previous mechanism evaluation studies (Carter et al., 1986, 1987), the light characterization input data used in the model simulations of the UNC outdoor chamber were derived in a manner similar to that described above for the SAPRC OTC. However, this previous light characterization for the UNC chamber was considered to be highly uncertain for a number of reasons. The particular uncertainties in UNC light characterization concerned the attenuation and reflection of light inside the chamber due to the Teflon walls of that chamber, the effects of enhancement of light due to the reflective chamber floor, the fact that (unlike the case for the OTC) irradiations in UNC chamber experiments begin with the sun very low in the sky, and evidence that at certain times in the past the UNC UV instrument was significantly out of calibration. Because of lack of data, highly uncertain and simplified assumptions had to be made in our previous mechanism evaluation studies concerning these effects (see Carter et al., 1986), such as, for example, assuming that effects of attenuation due to wall absorption and enhancement due to floor reflection exactly canceled out, and thus using a net chamber transmission factor of 1. In addition, correction factors for UV data when the instrument was apparently out of calibration were roughly estimated based on incomplete information. For these reasons, we determined that the light characterization model for the UNC chamber should be updated and improved as part of the effort carried out in this program.

For a number of years, Dr. Harvey Jeffries and co-workers at UNC have been working on developing new models for solar radiation and for light characteristics inside the UNC chamber (Jeffries et al., 1989a) and on developing correction factors for questionable light characterization data from past UNC chamber runs. Therefore, as a part of this program, the results of this effort have been utilized to develop a new data base for light characterization for use in modeling UNC chamber runs. The major part of the effort at UNC in developing and testing new light characterization models for solar radiation and radiation inside the UNC chamber were carried out under separate funding and is described elsewhere (Jeffries et al., 1989a). For this program, Jeffries and co-workers performed quality assurance and applied their best estimate corrections to the past UNC light characterization data, and, for each UNC chamber experiment whose results are currently available for modeling, derived sets of wavelength- and time-resolved light flux data for use in modeling the run. These consist of in-chamber actinic flux values for 91 wavelength intervals for each 16 minute interval in the runs. These data were then delivered to SAPRC in computer readable form, and the SAPRC chamber model simulation software was adopted to incorporate these data when simulating the UNC chamber runs.

A description of the models, data base, and procedures utilized to develop these run-specific light characterization data is given by Jeffries et al. (1989a) and is beyond the scope of this report. Briefly, the procedure involves the following:

(1) A spectral radiation transfer model is utilized to calculate clear-sky solar radiation fluxes outside the chamber. Its input includes: solar zenith angle; air pressure; total atmosphere ozone column; total atmosphere water vapor column; specification of atmospheric aerosol density, type, and optical properties; relative humidity; and spectral albedo of the surrounding surface.

(2) A broadband radiation transfer model is utilized to calculate clear-sky UV and TSR predictions, which can be directly compared with measured values taken during an experiment. Its input requirements are the same as the spectral radiation transfer model.

(3) A relatively simple cloud transmission model is utilized to account for the effects of clouds on surface level radiation fluxes and UV and TSR readings. Its input consists of ratios of cloudy-to-clear-sky UV and TSR values; these are derived by fitting calculated to observed UV and TSR readings for various time periods in the runs as indicated below. These ratios then account for the effects of clouds on the near UV and the higher wavelength spectral regions. No attempt is made to convert the broadband transmissions derived from the UV and TSR data into wavelength-dependent spectral transmissions in the current version of the UNC cloud model. However, Jeffries et al. (1989a) indicate that such a refinement is unlikely to have a significant effect if the clouds attenuate less than ~40% of the light intensity.

(4) Models for spectral transmission, reflection, and absorption of the FEP Teflon film used in the UNC chamber, for reflection of light off the floor of the chamber, and for other chamber-specific light effects are

utilized to calculate the light fluxes inside the chamber. Its inputs, besides those specifying characteristics of the chamber which remain constant, include the actinic fluxes outside the chamber for both the direct and diffuse components, the solar zenith angle, and transmission factors for the direct and the diffuse radiation. This model was developed and validated utilizing an extensive series of spectral flux and UV and broadband light intensity measurements made inside and outside the UNC chamber (Jeffries et al., 1989a).

For each run, the procedure for developing the run-specific in-chamber light fluxes involved the following: (1) Values of run-specific parameters such as humidity, total column ozone, etc., which are derived from meteorological observations, measurements made during the run, etc., and other available data bases are entered into the data base used by the models. (2) Other parameters required for calculation of out-of-chamber light fluxes, such as atmospheric aerosol parameters and broadband cloud transmission factors, are estimated based on time of year, meteorology, and past experience with the model and then are adjusted to yield acceptable fits of observed-to-calculated UV and TSR readings for the individual run. Cloud adjustment factors are derived for approximately three-hour intervals, which is a similar time resolution used to derive the analogous factors in the previous development of the UNC and OTC light characterization data base by Carter et al. (1986). The types of fits of calculated-to-observed UV and TSR data obtained after the application of this procedure are illustrated in sample plots given by Jeffries (1989d). (3) The UNC chamber transmission, absorption, and reflection model is then used to calculate the in-chamber light fluxes for each 16-minute interval of the run. These fluxes are incorporated into computer data sets (one for each run-day) which were then transmitted to SAPRC for use in modeling.

The updated UNC light characterization data were found to be different in a number of respects from the UNC light characterization data of Carter et al. (1986) which was employed in our previous modeling studies of this chamber. The major differences result from the use of the new inside-vs-outside chamber model, which predicts enhancement of light intensity at longer wavelengths due to floor reflection and suppression at shorter wavelengths due to light absorption by the walls. [As indicated above, because of lack of data, the Carter et al. (1986) model assumed that these effects canceled and thus the inside and outside fluxes were the same.] The magnitude of these chamber light effects depends on the time of day and on the relative amount of direct and diffuse radiation calculated by the outside radiation transfer model.

A comparison of the effects of changing from the previous light characterization of Carter et al. (1986) to this new light characterization is shown for several UNC chamber runs in Figures 2 through 4, where the former shows results for a formaldehyde-NO_x-air run, and the latter two show runs employing complex surrogate mixtures. [All these simulations used the Carter et al. (1986) set of assumptions for other chamber effects, though as discussed below some of the adjustable chamber effects parameters were subsequently modified in this study to be more consistent with simulations of characterization runs using the new light model.] As illustrated in Figure 2, the new characterization model tends to yield significantly better fits of formaldehyde decay rates in the formaldehyde-NO_x runs. However, in the case of this run the new model does not improve the fits to the initiation time for NO-to-NO_2 conversion, though the new model causes an overprediction of the initiation time, while in the old model it is underpredicted. These effects can be attributed to the suppression of UV intensity by the chamber walls at low zenith angles, which is represented in the new but not the old model. On the other hand, in many other types of runs, such as that shown in Figure 3, the new light characterization model results in higher predictions of maximum ozone yields, presumably due to the effects of assumed enhancement of light intensity caused by the chamber's reflective floor. This tendency of the new characterization model to increase predicted initiation times but also increase maximum ozone yields was the case to varying degrees for most of the UNC chamber runs modeled. However, for some runs, such as that shown in Figure 4, the effect of using different light characterization models was relatively small.

4.2.2 Representation of Other Chamber-Dependent Effects

Assumptions regarding chamber-dependent reactions and the presence of reactive background species have been recognized for a number of years as being important in affecting results of model simulations of chamber experiments. For example, it has been recognized for several years that overall rates of initiation in environmental chambers are

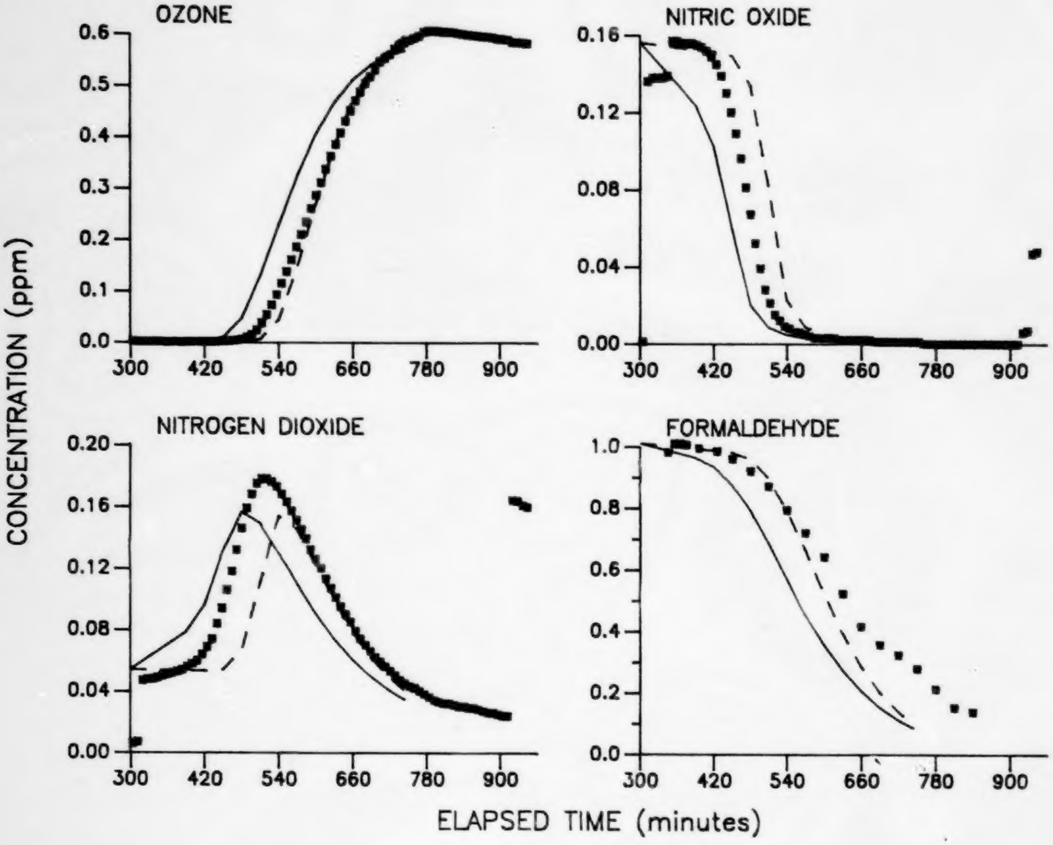

Figure 2. Experimental and Calculated Concentration-Time Plots for Selected Species in the UNC Formaldehyde-NO_x-Air Run AU0279B. [All calculations used the March 1988 RADM mechanism and the Carter et al. (1986) wall characterization model.]

——— Calculated Using the Carter et al. (1986) Light Model
- - - Calculated Using the New UNC Light Model
* Experimental Data

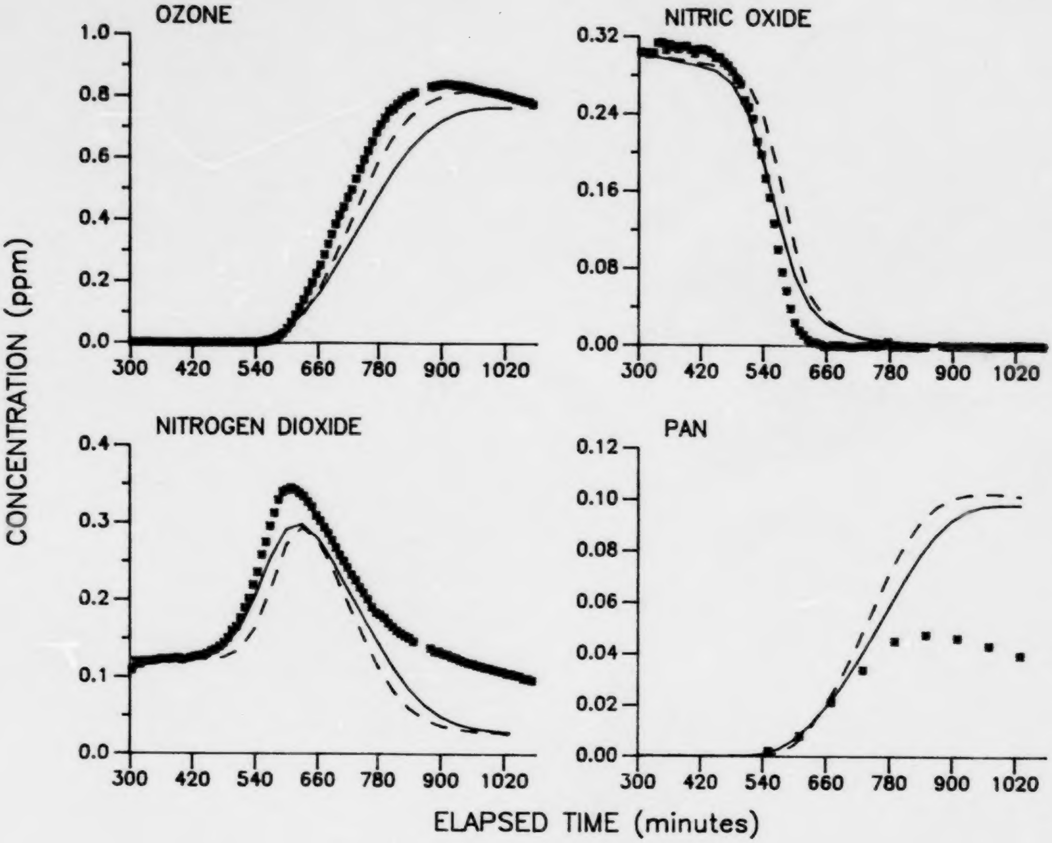

Figure 3. Experimental and Calculated Concentration-Time Plots for Selected Species in the UNC Complex Mixture-NO$_x$-Air Run ST1682B. [All calculations used the March 1988 RADM mechanism with adjusted OH rate constants for lumped hydrocarbon species and the Carter et al. (1986) wall characterization model.]

—— Calculated Using the Carter et al. (1986) Light Model
- - - Calculated Using the New UNC Light Model
* Experimental Data

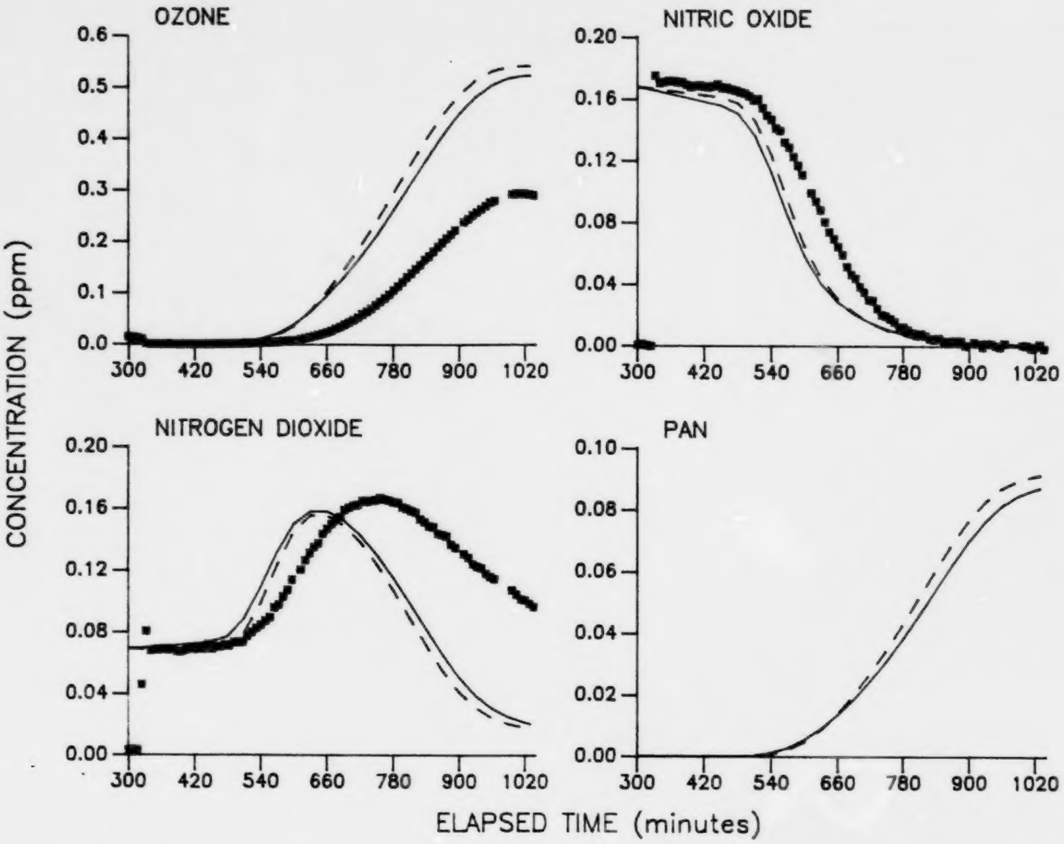

Figure 4. Experimental and Calculated Concentration-Time Plots for Selected Species in the UNC Complex Mixture-NO_x-Air Run ST2981R. [All calculations used the March 1988 RADM mechanism with adjusted OH rate constants for lumped hydrocarbon species and the Carter et al. (1986) wall characterization model.]

——— Calculated Using the Carter et al. (1986) Light Model
- - - Calculated Using the New UNC Light Model
* Experimental Data

higher than can be accounted for by known homogeneous processes (Carter et al., 1979a), and successful model simulations of chamber experiments have had to include provisions for "chamber radical sources," whose exact physical cause remains unknown or speculative. In addition, formation of PAN and ozone in acetaldehyde-air runs with no added NO_x has been observed in all four chambers whose data are modeled in this program (e.g., see Carter et al., 1986), indicating that offgassing of NO_x must be occurring from the walls of these chambers. Excess rates of NO oxidation observed in NO_x-air irradiations, and ozone formation in pure air irradiations indicate that unmeasured reactive organic species are also either offgassed from the chamber walls or present in the background air in environmental chamber experiments. Heterogeneous hydrolyses of NO_2 and N_2O_5 and wall losses of ozone are also known to occur. All of these need to be represented in model simulations of chamber experiments.

The methods we used in representing these chamber-dependent effects in the model simulations carried out in this study are summarized in this section. Methods used to represent other chamber- or run-specific conditions such as water concentration, temperature, or dilution in modeling runs from the various chambers are also summarized. The general approaches and types of assumptions employed in representing these effects is essentially the same as those described in Carter et al. (1986). That report should be consulted for detailed discussions of these effects and for the reasons why we chose to use the specific types of representations employed. Since the time of the Carter et al. (1986) report, we have made some minor modifications in the magnitude of the continuous, light-dependent portion of the chamber radical source used when modeling SAPRC ITC and OTC experiments (Carter et al., 1987) and in this study had to make more extensive modifications in the representation of chamber effects in the UNC chamber as a result of the changes in the UNC light characterization model. These changes to the UNC characterization model are discussed below, following the summary of the representation of the chamber-dependent parameters for the SAPRC chambers.

Representation of Chamber- or Run-Dependent Parameters in the SAPRC Chambers. Tables 13 through 15 summarize the methods and parameters used to represent chamber-dependent reactions, effects of offgasses or background species, and other chamber- or run-specific conditions for

Table 13. Summary of Chamber-Dependent Parameters Used in the Model Simulations of the SAPRC EC Chamber Runs

Parameter(s)	Value and Derivation
General Run Conditions	
Water Concentration	Based on measured temperature and humidity during the final pure air fill of the chamber. Typically 2.0×10^4 ppm.
Temperature	303 K. This is the typical average temperature in EC chamber runs.
Dilution	3.0×10^{-4} min^{-1} (Pitts et al., 1979).
Chamber Radical Sources	
Initial Nitrous Acid (HONO)	Initial HONO = 7% of the initial NO_2, based on measured or estimated initial HONO concentrations in EC tracer - NO_x air irradiations (Carter et al., 1982; Pitts et al., 1983).
$NO_2 \xrightarrow{wall} 0.5\ HONO + 0.5\ \text{loss of}\ NO_2$	Included to represent the dark formation of HONO from NO_2 observed in this chamber. Measured rate constant in the EC is 2.8×10^{-4} min^{-1} (Pitts et al., 1984).
$NO_2 + h\nu \xrightarrow{wall} 0.5\ HONO + 0.5\ \text{loss of}\ NO_2$	Included to represent the NO_2-dependent component of the continuous, light-dependent radical source in this chamber. Rate constant given by 2.16×10^{-3} $ppm^{-1} \times k_1$, where k_1 is the NO_2 photolysis rate. Derived based on results of tracer-NO_x-air irradiations (Carter et al., 1982; Pitts et al., 1983).
$h\nu \xrightarrow{wall} OH$	Included to represent the NO_2-independent component of the continuous, light-dependent radical source. Rate given by 0.39 ppb $\times k_1$, where k_1 is the NO_2 photolysis rate. Derived based on results of tracer-NO_x-air irradiations (Carter et al., 1982; Pitts et al., 1983).

(continued)

Table 13 (continued) - 2

Parameter(s)	Value and Derivation
NO_x Offgassing	
wall + hv -> NO_2	Rate given by 0.5 ppb x k_1, the NO_2 photolysis rate. Based on model simulations of the acetaldehyde-air run EC-253 (Carter et al., 1986).
Background Organics	
(none)	No representation of effects of background organics is used in model simulations of EC runs. (Carter et al., 1986).
Other Wall Reactions	
$O_3 \xrightarrow{\text{wall}}$ loss of O_3	First order loss rate of 1.1×10^{-3} min^{-1} is used, based on results of ozone dark decay experiments (Pitts et al., 1979; Carter et al., 1986).
$N_2O_5 \xrightarrow{\text{wall, } H_2O}$ Loss of N_2O_5	Rate constant given by $4.65 \times 10^{-3} + 7.21 \times 10^{-7} [H_2O]$ min^{-1}, based on measurements of N_2O_5 loss rates in the EC by Tuazon et al. (1983).

Table 14. Summary of Chamber-Dependent Parameters Used in the Model Simulations of the SAPRC ITC Chamber Runs

Parameter(s)	Value and Derivation
General Run Conditions	
Water Concentration	Based on measured temperature and humidity during the final pure air flush of the chamber. Typically 2.0×10^4 ppm.
Temperature	303 K. This is the typical average temperature in ITC chamber runs.
Dilution	No dilution is assumed to occur, due to flexible nature of chamber walls.
Chamber Radical Sources	
Initial Nitrous Acid (HONO)	Initial nitrous acid is assumed to be negligible in Teflon film chambers (Carter et al., 1986).
$NO_2 \xrightarrow{\text{wall}} 0.2\ HONO + 0.8$ loss of NO_2	Included to represent the dark formation of HONO from NO_2 observed in this chamber. The pseudo-first-order rate constant used for the ITC is 1.4×10^{-4} min^{-1}. This rate constant, and the assumed $HONO/NO_2$ stoichiometry, is based on studies of this process in a smaller, 4300-liter Teflon film chamber (Pitts et al., 1984), corrected for differences in chamber size (Carter et al., 1986).
$hv \xrightarrow{\text{wall}} OH$	This is the only process used to represent the continuous light-dependent component of the radical source in Teflon film chambers (Carter et al., 1986). The rate used is given by $k_{RS} \times k_1$, where k_1 is the NO_2 photolysis rate, and k_{RS} is determined by averaging, for each reaction bag, the radical input rates measured using tracer-NO_x-air irradiations (Carter et al., 1982). The k_{RS} values used in modeling ITC and OTC runs are given in Table 16.

(continued)

Table 14 (continued) - 2

Parameter(s)	Value and Derivation
NO_x Offgassing	
wall + hv -> NO_2	Rate given by 0.15 ppb x k_1, the NO_2 photolysis rate. Based on model simulations of acetaldehyde-air runs in this chamber.
Background Organics	
$OH \xrightarrow{wall} HO_2$	This "reaction" is used to simulate the effect of trace contamination by reactive organics which convert NO to NO_2. The rate constant used is 250 min^{-1}, based on model simulations of pure air irradiations (Carter et al., 1986).
Other Wall Reactions	
$O_3 \xrightarrow{wall}$ loss of O_3	First order loss rate of 1.3×10^{-4} min^{-1} is used, based on results of ozone dark decay experiments (Carter et al., 1986).
$N_2O_5 \xrightarrow{wall,\ H_2O}$ Loss of N_2O_5	Rate constant given by $2.5 \times 10^{-3} + 5.0 \times 10^{-8}$ [H_2O] min^{-1}, based on measurements of N_2O_5 loss rates in a smaller Teflon bag reactor by Tuazon et al. (1983), adjusted for differences in chamber sizes as discussed by Carter et al. (1986).

Table 15. Summary of Chamber-Dependent Parameters Used in the Model Simulations of the SAPRC OTC Chamber Runs

Parameter(s)	Value and Derivation
General Run Conditions	
Water Concentration	Derived based on continuous measurements of dew point and temperature data for runs where such data are available, as discussed by Carter et al. (1986). If such data are not available, a default water concentration of 5×10^{3} ppm was used. (OTC runs use unhumidified pure air, so the typical water concentration is relatively low.)
Temperature	Plots of measured temperatures against time were approximated by straight lines, which were used to derive the temperature as a function of time in the model simulations.
Dilution	No dilution is assumed to occur, due to flexible nature of the chamber walls.
Chamber Radical Sources	
Initial Nitrous Acid (HONO)	Initial nitrous acid is assumed to be negligible in Teflon film chambers (Carter et al., 1986).
$NO_2 \xrightarrow{wall} 0.2\ HONO + 0.8$ loss of NO_2	Included to represent the dark formation of HONO from NO_2 observed in Teflon bag chambers. The pseudo-first-order rate constant used for the OTC is 9.0×10^{-5} min^{-1}. This rate constant, and the assumed HONO/NO_2 stoichiometry, is based on studies of this process in a smaller, 4300-liter Teflon film chamber (Pitts et al., 1984), corrected for differences in chamber size (Carter et al., 1986).
$hv \xrightarrow{wall} OH$	This is the only process used to represent the continuous light-dependent component of the radical source in Teflon film chambers (Carter et al., 1986). The

(continued)

Table 15 (continued) - 2

Parameter(s)	Value and Derivation
	rate used is given by k_{RS} x k_1, where k_1 is the NO_2 photolysis rate, and k_{RS} is determined by averaging, for each reaction bag, the radical input rates measured using tracer-NO_x-air irradiations (Carter et al., 1982). The k_{RS} values used in modeling ITC and OTC runs are given in Table 16.
NO_x Offgassing	
wall + hv -> NO_2	Rate given by 0.1 ppb x k_1, the NO_2 photolysis rate. Based on model simulations of acetaldehyde-air runs in this chamber.
Background Organics	
$OH \xrightarrow{\text{wall}} HO_2$	This "reaction" is used to simulate the effect of trace contamination by reactive organics which convert NO to NO_2. The rate constant is assumed to be the same as used for ITC runs, which is 250 min^{-1}.
Other Wall Reactions	
$O_3 \xrightarrow{\text{wall}}$ loss of O_3	First order loss rate of 1.67×10^{-4} min^{-1} is used, based on results of ozone dark decay experiments (Carter et al., 1986).
$N_2O_5 \xrightarrow{\text{wall, } H_2O}$ Loss of N_2O_5	Rate constant given by $1.6 \times 10^{-3} + 3.0 \times 10^{-8}$ $[H_2O]$ min^{-1}, based on measurements of N_2O_5 loss rates in a smaller Teflon film reactor by Tuazon et al. (1983), adjusted for differences in chamber sizes as discussed by Carter et al. (1986).

experiments carried out in the SAPRC EC, ITC, or OTC. In the case of the ITC and the OTC, separate values of k_{RS}, the parameter used to determine the rate of light-induced continuous production of radicals from unknown sources, were employed for experiments using different reaction bags. These values were determined by averaging the results of radical tracer-NO_x-air experiments carried out with the different bags. [See Carter et al. (1982) for a discussion of tracer-NO_x-air experiments and measurements of chamber radical sources.] The averages of the measured values of these parameters for the various reaction bags and the k_{RS} values used in the model simulations are given in Table 16. Except for the use of separate values of k_{RS} for different Teflon reaction bags for ITC and OTC experiments, the representation of these chamber-dependent parameters and run-specific conditions for the SAPRC chambers is the same as that discussed by Carter et al. (1986).

The parameters shown in these tables are also the same as employed when evaluating the more recent version of the SAPRC gas-phase mechanism (Carter et al., 1988).

Representation of Chamber- and Run-Dependent Parameters in the UNC Chamber. Tables 17 and 18 summarize the methods used to represent the chamber- and run-dependent effects when modeling the UNC chamber runs during the course of this program. Table 17 indicates the general forms used for the representation of these effects and the values of the parameters which were not varied during this program [being in all cases the same as used by Carter et al. (1986)], while Table 18 gives the values of the parameters which were varied during the course of this study, as discussed below.

As discussed by Carter et al. (1986), values of several of the chamber-dependent parameters for the UNC and other chambers could be derived only as a result of model simulations of characterization runs which are particularly sensitive to these parameters. These are referred to as the "adjustable" chamber-dependent parameters. Since run-by-run optimization of uncharacterized parameters is incompatible with the objectives of using chamber data for mechanism testing, this adjustment must be done on a global basis, with the same sets of parameter values being used in modeling all of the runs from a given chamber. In the case of the UNC chamber, adjustable chamber-dependent parameters included k_{RS},

Table 16. Values of the Continuous Chamber Radical Input Parameter, k_{RS}, used in Modeling SAPRC ITC and OTC Chamber Runs, and Averages of Measured Values Used to Derive Them

Chamber	Inclusive Run Numbers	k_{RS} (ppb) Average Measured (a)	k_{RS} (ppb) Used in Model
ITC	450 - 503	0.16 ± 0.03	0.15
	532 - 563	0.44 ± 0.13	0.4
	621 - 638	0.21 ± 0.03	0.2
	692 - 734	0.61 ± 0.20	0.6
	737 - 789	0.49 ± 0.20	0.5
	793 - 832	0.36 ± 0.12	0.35
	859 - 893	0.28 ± 0.09	0.3
	924 - 970	0.25 ± 0.25	0.25
OTC	183 - 206	0.25 ± 0.19	0.25
	209 - 253	0.20 ± 0.09	0.2

(a) Runs carried out with new, unconditioned reaction bags or runs with anomalous results were not counted in the average.

Table 17. Summary of Chamber-Dependent Parameters Used in the Model Simulations of the UNC Chamber Runs

Parameter(s)	Value and Derivation
General Run Conditions	
Water Concentration	Derived based on continuous measurements of dew point and temperature data for runs where such data are available, as discussed by Carter et al. (1986). If such data are not available, a default water concentration of 2×10^4 ppm was used.
Temperature	Plots of measured temperatures against time were approximated by straight lines, which were used to derive the temperature as a function of time in the model simulations.
Dilution	Dilution rates of 2×10^{-4} min^{-1} were assumed, as discussed by Carter et al. (1986). No "dynamic dilution" experiments were modeled in this study.
Chamber Radical Sources	
Initial Nitrous Acid (HONO)	Initial nitrous acid is assumed to be negligible in Teflon film chambers (Carter et al., 1986).
$NO_2 \xrightarrow{wall} 0.2\ HONO + 0.8\ \text{loss of}\ NO_2$	Included to represent the dark formation of HONO from NO_2 observed in Teflon bag chambers. The pseudo-first-order rate constant used for the UNC chamber is 5.0×10^{-5} min^{-1}. This rate constant, and the assumed $HONO/NO_2$ stoichiometry, is based on studies of this process in a smaller, 4300-liter Teflon film chamber (Pitts et al., 1984), corrected for differences in chamber size (Carter et al., 1986).
$hv \xrightarrow{wall} OH$	This is the only process used to represent the continuous light-dependent component of the radical source in Teflon film chambers (Carter et al., 1986). The

(continued)

Table 17 (continued) - 2

Parameter(s)	Value and Derivation
	rate used is given by k_{RS} x k_1, where k_1 is the NO_2 photolysis rate, and k_{RS} was adjusted based on fits of model simulations to alkane-NO_x-air experiments. The values used for this parameter are are given in Table 18.
NO_x Offgassing	
wall + hv -> NO_2	Rate given by k_{EN} x k_1, the NO_2 photolysis rate, where k_{EN} was adjusted based on fits of model simulations to acetaldehyde-air experiments. The values used for this parameter are given in Table 18.
Background Organics	
$OH \xrightarrow{\text{wall}} HO_2$	This "reaction" is used to simulate the effect of trace contamination by reactive organics which convert NO to NO_2. The rate constant for this process, k_{XSHC}, was adjusted based primarily on fits of model simulations of pure air irradiations. The values used for this parameter are given in Table 18.
Other Wall Reactions	
$O_3 \xrightarrow{\text{wall}} \text{loss of } O_3$	First order loss rate of 1.43×10^{-4} min^{-1} is used, based on results of two ozone dark decay experiments (Carter et al., 1986).
$N_2O_5 \xrightarrow{\text{wall, } H_2O} \text{Loss of } N_2O_5$	Rate constant given by $9 \times 10^{-4} + 2 \times 10^{-8} [H_2O]\ min^{-1}$, based on measurements of N_2O_5 loss rates in a smaller Teflon film reactor by Tuazon et al. (1983), adjusted for differences in chamber sizes as discussed by Carter et al. (1986).

Table 18. Values of Adjustable Chamber-Dependent Parameters Employed in the Simulations of UNC Chamber Runs

Characterization Model	Temperature (K)	k_{RS} (ppb)	k_{EN} (ppb)	k_{XSHC} (min^{-1})
Original model (Carter et al., 1986)	All	0.30	0.30	500.
Re-adjusted. No temperature dependence	All	0.30	0.11	250.
Re-adjusted, with temperature dependence	$T < 290$	0.05	0.025	750.
	$290 < T < 300$	(a)	(a)	750.
	$T = 300$	0.10	0.050	750.
	$300 < T < 310$	(b)	(b)	750.
	$T > 310$	0.60	0.20	750.

(a) Obtained by linear interpolation between values given for T = 290 K and T = 300 K.

(b) Obtained by linear interpolation between values given for T = 300 K and T = 310 K.

which reflects the magnitude of the continuous radical source and which is adjusted so model simulations fit observed rates of NO oxidation and ozone formation in alkane-NO_x-air runs; k_{EN}, which reflects the NO_x offgassing rates and which is adjusted so simulations fit observed rates of ozone and PAN formation in acetaldehyde-air runs, and k_{XSHC}, which reflects the extent of excess NO-to-NO_2 conversions caused by reactive organic contaminants and which is determined based on fits to ozone formation rates observed in pure air photolyses. Since simulations of these characterization runs are affected at least to some extent by the full set of characterization parameters, this optimization has to be carried out in an iterative manner.

This use of model simulations to determine rates of some of the chamber-dependent processes means that the values derived will depend, at least to some extent, on the light characterization model used in the model simulations. Therefore, since the light characterization model for the UNC chamber was modified during this study, we also had to re-derive the adjustable chamber-dependent parameters used for modeling data in this chamber.

Figure 5 shows distribution plots of discrepancies between model predictions and experimental results for the chamber characterization runs used to derive the adjustable chamber-dependent parameters for the UNC chamber. These include distributions of fits to (1) maximum ozone yields in pure air irradiations, (2) changes in NO and NO_2 concentrations in NO_x-air and CO-NO_x-air experiments, (3) maximum ozone and PAN yields in acetaldehyde-air experiments, and (4) NO oxidation and ozone formation rates observed in alkane-NO_x-air runs. Also shown are fits to maximum ozone yields and NO oxidation and ozone formation rates in propene-NO_x-air runs; although modeling these runs was not used to derive the adjustable chamber-dependent parameters, the results of modeling these runs give a good indication of the overall performance and variability of the model in simulating a relatively large number of similar experiments carried out over a number of years.

Distributions of fits for five sets of model simulations are shown in Figure 5. The first four sets were all carried out using the latest SAPRC mechanism (Carter et al., 1988), but with varying light and chamber characterization models. The first set (designated "original") employed

Set	Mechanism	Light Model	Other Chamber Effects
1	SAPRC	Carter et al. (1986)	Carter et al. (1986)
2	SAPRC	New UNC Model	Carter et al. (1986)
3	SAPRC	New UNC Model	This work, T-independent k_{RS}, k_{EN}
4	SAPRC	New UNC Model	This work, T-dependent k_{RS}, k_{EN}
5	RADM	New UNC Model	This work, T-dependent k_{RS}, k_{EN}

```
-------------------------------------------------------------------------------------------
 Calculated-    -------------------- Pure Air Runs:  Maximum Ozone --------------------
 Experimental      Set 1           Set 2           Set 3          Set 4           Set 5
-------------------------------------------------------------------------------------------

        <  -0.33    :               :               :              :               :
  -0.33 -  -0.27    :               :               :              :               :
  -0.27 -  -0.21    :               :               :              :               :
  -0.21 -  -0.15    :               :               :              :               :
  -0.15 -  -0.09    :               :               :              :               :
  -0.09 -  -0.03    :               :               :1             :               :
  -0.03 -   0.03  --:111           -:1             -:11           -:111           -:111
   0.03 -   0.09    :               :11             :              :               :
   0.09 -   0.15    :               :               :              :               :
   0.15 -   0.21    :               :               :              :               :
   0.21 -   0.27    :               :               :              :               :
   0.27 -   0.33    :               :               :              :               :
        >   0.33    :               :               :              :               :

-------------------------------------------------------------------------------------------
```

Figure 5. Comparison of Results of UNC Characterization Simulations Using Various Mechanisms and Chamber and Light Characterization Models.

(continued)

Set	Mechanism	Light Model	Other Chamber Effects
1	SAPRC	Carter et al. (1986)	Carter et al. (1986)
2	SAPRC	New UNC Model	Carter et al. (1986)
3	SAPRC	New UNC Model	This work, T-independent k_{RS}, k_{EN}
4	SAPRC	New UNC Model	This work, T-dependent k_{RS}, k_{EN}
5	RADM	New UNC Model	This work, T-dependent k_{RS}, k_{EN}

```
----------------------------------------------------------------------------------------
Calculated-      - (1) Butane-NOx-Air and (2) Branched Alkane-NOx-Air:  Maximum Ozone  -
Experimental       Set 1          Set 2          Set 3          Set 4          Set 5
----------------------------------------------------------------------------------------

      <  -0.33    :1             :1             :1             :              :
-0.33 -  -0.27    :              :              :              :1             :1
-0.27 -  -0.21    :              :1             :              :              :
-0.21 -  -0.15    :1             :              :              :              :2
-0.15 -  -0.09    :1             :1             :11            :              :12
-0.09 -  -0.03    :1             :              :              :112           :1
-0.03 -   0.03  --:22           -:122          -:12           -:11           -:112
 0.03 -   0.09    :              :              :2             :2             :
 0.09 -   0.15    :              :              :              :1             :12
 0.15 -   0.21    :              :              :              :2             :
 0.21 -   0.27    :1             :              :              :2             :
 0.27 -   0.33    :12            :1             :1             :              :
      >   0.33    :2             :122           :122           :              :

----------------------------------------------------------------------------------------
(Calculated-      -------- (1) Butane-NOx-Air and (2) Branched Alkane-NOx-Air: ---------
Experimental)                Average Initial d(([O3] - [NO]))/dt
/Experimental       Set 1          Set 2          Set 3          Set 4          Set 5
----------------------------------------------------------------------------------------

      <  -1.00     :              :              :              :              :
-1.00 -  -0.82     :              :              :              :              :
-0.82 -  -0.64     :              :              :              :              :
-0.64 -  -0.45     :              :              :              :              :
-0.45 -  -0.27     :              :              :              :              :2
-0.27 -  -0.09     :111           :111           :11            :1112          :1112
-0.09 -   0.09   --:122          -:122          -:1122         -:1112         -:11122
 0.09 -   0.27     :              :              :              :22            :
 0.27 -   0.45     :              :12            :12            :              :
 0.45 -   0.64     :1122          :12            :1             :              :
 0.64 -   0.82     :              :              :2             :              :
 0.82 -   1.00     :              :              :              :              :
      >   1.00     :              :              :              :              :

----------------------------------------------------------------------------------------
```

Figure 5 (continued) - 2

Set	Mechanism	Light Model	Other Chamber Effects
1	SAPRC	Carter et al. (1986)	Carter et al. (1986)
2	SAPRC	New UNC Model	Carter et al. (1986)
3	SAPRC	New UNC Model	This work, T-independent k_{RS}, k_{EN}
4	SAPRC	New UNC Model	This work, T-dependent k_{RS}, k_{EN}
5	RADM	New UNC Model	This work, T-dependent k_{RS}, k_{EN}

```
------------------------------------------------------------------------------------------
Calculated-     ---------------  Acetaldehyde-Air Runs:  Maximum Ozone  ---------------
Experimental       Set 1         Set 2         Set 3         Set 4         Set 5
------------------------------------------------------------------------------------------

      <  -0.33   :             :             :             :             :
-0.33 -  -0.27   :             :             :             :             :
-0.27 -  -0.21   :             :             :             :             :
-0.21 -  -0.15   :             :             :             :             :
-0.15 -  -0.09   :             :             :             :             :11
-0.09 -  -0.03   :             :             :111          :1            :11
-0.03 -   0.03 --:1           -:            -:1           -:11111       -:11
 0.03 -   0.09   :111          :             :11           :             :
 0.09 -   0.15   :11           :1111         :             :             :
 0.15 -   0.21   :             :11           :             :             :
 0.21 -   0.27   :             :             :             :             :
 0.27 -   0.33   :             :             :             :             :
      >   0.33   :             :             :             :             :
```

```
------------------------------------------------------------------------------------------
(Calculated-     ----------------  Acetaldehyde-Air Runs:  Maximum PAN  ----------------
Experimental)
/Experimental      Set 1         Set 2         Set 3         Set 4         Set 5
------------------------------------------------------------------------------------------

      <  -0.50   :             :             :             :             :
-0.50 -  -0.41   :             :             :             :             :
-0.41 -  -0.32   :             :             :             :1            :1
-0.32 -  -0.23   :             :             :             :             :
-0.23 -  -0.14   :             :             :11           :             :
-0.14 -  -0.05   :             :             :1            :1            :
-0.05 -   0.05 --:            -:            -:            -:1           -:
 0.05 -   0.14   :             :             :1            :1            :11
 0.14 -   0.23   :1            :             :1            :11           :1
 0.23 -   0.32   :             :1            :             :             :1
 0.32 -   0.41   :             :             :             :             :1
 0.41 -   0.50   :1            :             :1            :             :
      >   0.50   :1111         :11111        :             :             :

------------------------------------------------------------------------------------------
```

Figure 5 (continued) - 3

Set	Mechanism	Light Model	Other Chamber Effects
1	SAPRC	Carter et al. (1986)	Carter et al. (1986)
2	SAPRC	New UNC Model	Carter et al. (1986)
3	SAPRC	New UNC Model	This work, T-independent k_{RS}, k_{EN}
4	SAPRC	New UNC Model	This work, T-dependent k_{RS}, k_{EN}
5	RADM	New UNC Model	This work, T-dependent k_{RS}, k_{EN}

```
-----------------------------------------------------------------------------------------
 Calculated-      -----  (1) NOx-Air and (2) CO-NOx-Air:  Change in NO/Initial NOx  ------
 Experimental      Set 1          Set 2          Set 3          Set 4          Set 5
-----------------------------------------------------------------------------------------

       <  -0.20    :22            :22            :22            :22            :22
 -0.20 -  -0.16    :              :              :              :              :
 -0.16 -  -0.13    :              :              :              :              :
 -0.13 -  -0.09    :              :              :2             :2             :2
 -0.09 -  -0.05    :122           :122           :12            :2             :2
 -0.05 -  -0.02    :1             :12            :122           :11122         :11122
 -0.02 -   0.02  --:22           -:22           -:22           -:11111122     -:11111122
  0.02 -   0.05    :11111112      :111111112     :111111111     :111           :111
  0.05 -   0.09    :1112          :11            :1             :              :
  0.09 -   0.13    :              :              :              :              :
  0.13 -   0.16    :              :              :              :              :
  0.16 -   0.20    :              :              :              :              :
       >   0.20    :              :              :              :              :

-----------------------------------------------------------------------------------------
 Calculated-      --------  NOx-Air and CO-NOx-Air:  Change in NO2/Initial NOx  ----------
 Experimental      Set 1          Set 2          Set 3          Set 4          Set 5
-----------------------------------------------------------------------------------------

       <  -0.20    :22            :22            :22            :22            :22
 -0.20 -  -0.16    :              :              :              :              :
 -0.16 -  -0.13    :              :              :              :              :
 -0.13 -  -0.09    :              :              :111           :              :
 -0.09 -  -0.05    :              :              :112           :112           :112
 -0.05 -  -0.02    :1             :111           :11122         :1111122       :1111122
 -0.02 -   0.02  --:11122        -:1112         -:1112         -:1122         -:1122
  0.02 -   0.05    :12            :111222        :12            :11            :11
  0.05 -   0.09    :1112          :112           :2             :12            :12
  0.09 -   0.13    :111122        :12            :              :              :
  0.13 -   0.16    :              :              :              :              :
  0.16 -   0.20    :              :              :              :              :
       >   0.20    :              :              :              :              :
-----------------------------------------------------------------------------------------
```

Figure 5 (continued) - 4

Set	Mechanism	Light Model	Other Chamber Effects
1	SAPRC	Carter et al. (1986)	Carter et al. (1986)
2	SAPRC	New UNC Model	Carter et al. (1986)
3	SAPRC	New UNC Model	This work, T-independent k_{RS}, k_{EN}
4	SAPRC	New UNC Model	This work, T-dependent k_{RS}, k_{EN}
5	RADM	New UNC Model	This work, T-dependent k_{RS}, k_{EN}

```
-----------------------------------------------------------------------------------
 Calculated-      ------------------  Propene-NOx-Air:  Maximum Ozone  -------------------
 Experimental       Set 1          Set 2          Set 3          Set 4          Set 5
-----------------------------------------------------------------------------------

       <  -0.33    :              :              :              :              :
 -0.33 -  -0.27    :              :              :              :              :
 -0.27 -  -0.21    :              :              :              :              :
 -0.21 -  -0.15    :111           :              :              :              :11
 -0.15 -  -0.09    :11            :11            :111           :11111         :111
 -0.09 -  -0.03    :11            :1111          :11            :1111          :11111
 -0.03 -   0.03  --:1111111      -:111          -:111111       -:11111        -:111
  0.03 -   0.09    :1111          :11111         :11111         :1             :111
  0.09 -   0.15    :11            :111           :111           :1111          :11
  0.15 -   0.21    :1             :1111          :11            :11            :1
  0.21 -   0.27    :1             :              :1             :1             :111
  0.27 -   0.33    :              :1             :              :              :
       >   0.33    :              :              :              :              :

-----------------------------------------------------------------------------------
(Calculated-      --------  Propene-NOx-Air:  Average Initial d(([O3] - [NO]))/dt  -------
Experimental)
/Experimental       Set 1          Set 2          Set 3          Set 4          Set 5
-----------------------------------------------------------------------------------

       <  -1.00    :              :              :              :              :
 -1.00 -  -0.82    :              :              :              :              :
 -0.82 -  -0.64    :              :              :              :              :
 -0.64 -  -0.45    :              :              :              :              :
 -0.45 -  -0.27    :              :              :              :              :
 -0.27 -  -0.09    :1111          :1111          :1111          :111111        :111111
 -0.09 -   0.09  --:11111111     -:11111111111 -:1111111111    -:111111111111-:1111111111111
  0.09 -   0.27    :1111111       :111           :1111          :11            :1
  0.27 -   0.45    :11            :111           :111           :1             :11
  0.45 -   0.64    :1             :1             :1             :              :
  0.64 -   0.82    :              :              :              :              :
  0.82 -   1.00    :              :              :              :              :
       >   1.00    :              :              :              :              :
-----------------------------------------------------------------------------------
```

Figure 5 (concluded) - 5

the Carter et al. (1986) model for both light characterization and chamber effects, and reflected our best estimates prior to this program. The second set employed the new UNC light characterization model but the original (Carter et al., 1986) model for the other chamber effects. The third and fourth sets employ the new UNC light model and two new sets of values for the adjustable chamber-dependent parameters, discussed below. The fifth set employed the same light and characterization input as the fourth set, but was carried out using the RADM mechanism.

Figure 5 shows that none of these chamber models yields close fits to experimental results for all of the characterization experiments modeled; there were always runs where significant discrepancies are obtained. This can be attributed to run-to-run variation of chamber effects due to unknown or uncontrolled factors. Improved fits could obviously be obtained by carrying out run-to-run optimization of the adjustable parameters, but such a procedure would not be consistent with our objectives. Until all significant chamber effects are identified and quantified so that they can be predictively modeled, the best that can be hoped for is that the biases and errors in the model simulations of these characterization runs is as small as possible.

A comparison of the first two sets of distributions in Figure 5 shows that updating the light characterization model without changing the representation of the other chamber effects tends to cause a slight increase in the tendency of the model to overpredict maximum ozone yields. Although this effect does not appear to be large, it has a non-negligible effect on the model performance statistics when simulating ozone yields in the full set of UNC chamber experiments. The updated light model with the old values of the adjustable parameters also results in significant overpredictions of PAN yields in acetaldehyde-air irradiations, indicating that the assumed value for the NO_x offgassing rate in the UNC chamber may be too high if the new light model is correct. The use of an apparently high NO_x offgassing rate in the chamber model could contribute to a tendency of the model to overpredict maximum ozone yields. On the other hand, use of the new light characterization model does not necessarily indicate that the assumed magnitudes of the chamber radical source need to be modified. The fits of model simulations to NO oxidation rates in alkane-NO_x-air experiments are sensitive to the representation of the chamber radical source, but use of the new light model without changing other parameters was found not to significantly degrade the performance of the model in simulating these results.

Better fits of model simulation to results of acetaldehyde-air experiments were obtained if the magnitude of the NO_x offgassing parameter k_{EN} was reduced by approximately a factor of three. This adjustment of k_{EN} required reducing by a factor of two the value of k_{XSHC}, the parameter measuring the amount of excess NO-to-NO_2 conversion caused by background or contaminant reactive organics, so the model would still fit the maximum ozone yields observed in the pure air irradiations. The third set of distributions shows the performance of the model after these minor modifications are made. It can be seen that these changes result is a significant improvement in terms of the overall biases in fits to ozone and PAN yields in the acetaldehyde-air runs and also a slight reduction of the tendency of the model to overpredict ozone yields in the propene-NO_x-air experiments.

The original chamber characterization model of Carter et al. (1986) neglected any effects of temperature on the magnitudes of the chamber radical source or the NO_x offgassing rate parameters, and these effects are also ignored in the re-adjusted model discussed above. However, in the process of re-assessing this chamber characterization model, we noted that there was a consistent tendency for the model to overpredict reactivity in runs with relatively low average temperatures (below ~290-300 K). This suggests that the chamber radical source in the UNC chamber may be temperature dependent. In addition, the modeling of the lower temperature acetaldehyde-air runs suggests a temperature dependence in the NO_x offgassing rates in that chamber. Therefore, we investigated whether using a modified chamber effects model with temperature dependences for the parameters k_{RS} and k_{EN} might result in reduced discrepancies in model simulations of the UNC chamber experiments.

The number of UNC characterization runs carried out at a variety of temperatures is not sufficient to unambiguously derive temperature dependencies for the radical source or for NO_x offgassing. Therefore, we tried a variety of assumed temperature dependencies to determine which would minimize the overall average error in the distribution of the fits to the runs used to characterize these effects. The model simulations suggested that runs with average temperatures below ~300 had significantly lower radical sources and NO_x offgassing rates than runs with the more typical average temperatures of ~300-305, but that runs with still higher average temperatures did not appear to have correspondingly higher radical sources. This suggests that these chamber effects increase relatively rapidly with temperature at temperatures below around 300 K, but increase slower at higher temperatures. To represent this, we assumed that k_{RS} and k_{EN} increased linearly with temperature both above and below 300 K, but that the rate of change is less in the higher temperature range. The dependences which we found gave the best fits of those we tried are given in Table 18. To obtain satisfactory fits to maximum ozone yields in the pure air irradiations, it was also necessary to use a larger value of k_{XSHC}. The last set of plots in Figure 5 show the distribution of fits obtained for the UNC characterization runs using this set of temperature-dependent chamber characterization parameters.

Figure 5 shows that using the temperature-dependent model for k_{RS} and k_{EN} yields somewhat better fits to ozone yields observed in the acetaldehyde-air experiments, and significantly better fits to NO oxidation rates and ozone yields in alkane-NO_x-air runs, compared to using the adjusted model where temperature dependences of these parameters are ignored. It also gives better distributions of fits to NO oxidation rates and ozone yields in the simulations of the propene runs. However, it should be noted that the number of runs useful for deriving temperature dependencies for the radical source and the NO_x offgassing rates in the UNC chamber is extremely limited, and thus the temperature dependencies derived for them in this study must be considered to be highly uncertain. In addition, there is uncertainty in the temperature dependencies of the reactions involved in PAN formation (Gery et al., 1988), and use of different assumptions in the mechanism in this regard, such as those employed in the latest Carbon Bond mechanism (Gery et al., 1988) may result in differences in the apparent temperature dependencies of k_{EN} being derived by model simulations of the acetaldehyde-air experiments. (On the other hand, this uncertainty in the temperature dependence of PAN formation reactions will have less of an impact on the values of k_{RS} which are derived from the model simulations of the alkane-NO_x-air experiments.) Nevertheless, because of this significantly better performance in the temperature-dependent chamber effects model in our simulations of these data, this is the model which was used in this study in simulating the UNC chamber runs for the evaluation of the RADM mechanism.

It should be emphasized that this derivation of adjustable chamber-dependent parameters by model simulation means that the parameters derived will depend on the chemical mechanism used for this purpose. In this study these parameters were derived primarily based on calculations using the latest SAPRC mechanism (Carter et al., 1988). This is because the SAPRC mechanism was used in our previous chamber characterization modeling work, and because the SAPRC mechanism has a more explicit representation of the reactions of the alkanes than does the RADM mechanism. In addition, since the RADM mechanism is being evaluated in this study, it was not considered to be in its final form at the time these chamber characterization calculations were being carried out. Ideally, the chamber characterization runs used to derive the adjustable parameters should only involve the "known" reactions, so differences in current mechanisms would not affect modeling of such runs. However, this is not yet entirely the case.

The differences between the RADM and the current SAPRC mechanism in modeling these UNC runs used for chamber characterization is shown in Figure 5, where the distributions of the fits calculated using these two mechanisms with the new UNC light and chamber characterization models can be compared. It can be seen that, as expected, there are essentially no differences between the mechanisms in the simulations of the pure air, NO_x-air, and CO-NO_x-air runs, but there are slight differences in the simulations of the propene-NO_x runs, and relatively larger differences in the simulations of the alkane-NO_x-air and the acetaldehyde-air runs. The differences in the simulations of the alkane-NO_x-air runs is expected since the RADM mechanism uses a more lumped representation of the alkanes than the SAPRC mechanism, and strictly speaking is not designed to be used for modeling such runs. The differences in the simulations of the acetaldehyde-air runs are due to differences between the mechanisms in the rate constants used for the decomposition and formation of PAN, which are such that PAN is predicted by the RADM mechanism to be more stable relative to NO_2 + acetyl peroxy radicals. This results in the RADM mechanism predicting lower ozone yields and higher PAN yields in acetaldehyde-air irradiations than predicted by the SAPRC mechanism. With the k_{RS} parameters adjusted to give optimum fits using the SAPRC mechanism, this results in the RADM mechanism underpredicting ozone and overpredicting PAN, relative to the experimental results. However, either increasing or decreasing k_{RS} from the optimum for the SAPRC mechanism would cause greater discrepancies for either PAN or ozone, respectively, with the RADM model. Because of this, it is considered to be unlikely that using the RADM mechanism to derive the adjustable chamber-dependent parameters would have yielded significantly different values than those used in this study.

4.3 Representation of Organics in Chamber Experiments

Many of the environmental chamber experiments used in this study include runs containing organic compounds, either singly or in mixtures, which are not represented explicitly in the RADM mechanism. The appropriate procedures for representing such compounds when simulating chamber experiments depends on the intended application of the mechanism being evaluated. If the mechanism is intended to be a fully detailed mechanism to test our ability to understand and predictively model the chemical system being simulated, or if the mechanism is to be used as a standard or "master mechanism" against which more condensed mechanisms will be compared, or if the mechanism is to be used to assess relative reactivities of individual organic compounds, then the approach should be to adjust the mechanism so that it represents the chemical conditions of the mixture being simulated as closely as possible. For example, the SAPRC detailed mechanism is designed to serve both as a basis for developing more condensed mechanisms and for use in reactivity assessment studies, and thus its evaluation involved adjusting the kinetic and mechanistic parameters for lumped model species based on the compounds in the experiments being simulated (Carter, 1988). If, on the other hand, the mechanism being evaluated is a condensed mechanism which is intended to be used as a component of a larger model such as RADM, then the appropriate procedure is to represent the compounds in the chamber experiments in the same way they would be represented when the mechanism is implemented in the larger model. Otherwise, the mechanism being evaluated in the chamber simulations is not the same as the mechanism which will be used in its intended application. Since the mechanism being evaluated in this study is intended to be a condensed mechanism for use as a component of the RADM-II model, and since as far as we are aware it is not anticipated it will be used as a basis for developing more condensed mechanisms or for assessing relative reactivities of different organics, it is obviously the latter approach that is appropriate for this study.

Therefore, the approach we used when simulating chamber experiments to evaluate the RADM mechanism was to process the organic input data in the chamber simulations in the same way that we anticipate the organic emissions data will be processed for input into the RADM-II model. The RADM emissions input processing procedure we anticipate will be used is the two-step procedure described in Section 3 of this report. This involves no adjustment of rate constants or mechanistic parameters in the mechanism -- these are the same regardless of the mixture being simulated. On the other hand, in some cases model species concentrations are adjusted to account for differences in reactivities between them and the input species they represent. The application of this procedure to the simulations of the chamber runs is briefly summarized below.

The first step in processing the organic input data involves aggregating, on a mole-per-mole basis, the individual chemicals into the 32-class emissions grouping discussed in Section 3.2.1. Table 7 in that section indicates how various types of chemicals are aggregated in this step. As indicated there, some of the groupings are determined based on the OH radical rate constants assumed for the individual organic compounds, and the specific sets of OH radical rate constants used in making these assignments in this study are those listed by Carter (1988a). Other than the UNC auto exhaust experiments, no experiments modeled in this study contained unknown or unidentified compounds. The initial organic concentrations used in the UNC auto exhaust experiments in our 1986 mechanism evaluation study (Carter et al., 1986) were also employed in this study. [The alkanes contained in these experiments are given in terms of the two lumped alkane classes, C_4-C_5 and C_{6+}. The lumped class C_4-C_5 was aggregated into emissions class "Alkanes (0.25-0.5 react)," and the lumped class C_{6+} was aggregated into "Alkanes (0.5-1 react)", based on the OH radical rate constants used for them in the SAPRC/ERT mechanism (Lurmann et al., 1987).] Therefore, there are no cases where chemicals in the chamber experiments were aggregated to the "unknown" or "unassigned" categories.

The organics aggregated into the emissions classes were then aggregated into the species in the RADM mechanism as discussed in Section 3.2.3 and as indicated in Table 8 in that section. Some emissions classes are aggregated on a mole-per-mole basis, while others are aggregated using "reactivity weighing," based on estimates of how much of the emissions class and the model species will react in the model simulation. Note, however, that the aggregation of classes based on "reactivity weighing" require use of the parameter "INTOH" in the derivation of the weighing factors. Since INTOH reflects the effective integrated radical levels in the simulation, it is a model input variable and not a parameter in the mechanism. As such, the weighing factors shown in Table 8, calculated using the INTOH value of 110 ppt-min, which was estimated to be appropriate for use in three-day RADM simulations (Stockwell, private communication, 1988), are not necessarily appropriate for use in the chamber simulations. Therefore, separate estimates for INTOH values were made for each chamber.

The INTOH values used for calculating reactivity weighing factors in the simulations of the chamber experiments carried out in this study were as follows:

Chamber	INTOH (ppt-min)
SAPRC EC	35
SAPRC ITC	40
SAPRC OTC	40
UNC	70

These were derived based on a rough analysis of average integrated OH radical levels in model simulations of one-day chamber experiments employing various complex mixtures of organics. (The model simulations employed either the SAPRC detailed mechanism, or the RADM mechanism with the rate constants of the lumped species adjusted based on the compounds present in the experiments -- the results were similar in either case.) The higher INTOH value for the UNC chamber can be attributed to the longer irradiation time used in that chamber, where runs start at sunrise and end at sunset, and are usually carried out in the summer. The SAPRC runs are usually limited to six hours.

Strictly speaking, the integrated OH radical levels, and thus the appropriate INTOH values, will depend on the type of experiment, with lower values for runs with high levels of radical inhibitors, etc., but this type of run-by-run analysis was not carried out. The simulations of only a relatively small number of runs are affected to any significant extent by reactivity weighing, since, of the experiments modeled in this study, reactivity weighing is of importance only for those containing significant amounts of methanol or benzene. For the other compounds in these experiments, the weighing factors are either unity or very close to unity. For this reason, we did not consider a comprehensive investigation of the most appropriate INTOH value to use in the chamber simulations to be worthwhile.

To provide an indication of the level of inaccuracy introduced into the model simulations by using this aggregation approach, a separate series of simulations of the chamber experiments was carried out where the rate constants for the lumped model species were adjusted for each experiment based on the compounds present. The rate constants which were subject to adjustment when this procedure was employed were those for the reactions of OH radicals with HC3, HC5, HC8, TOL, XYL, OLI, and OLT, and for the reactions of ozone and NO_3 radicals with OLI and OLT. The rate constants for the individual organics used when this procedure was employed are those assigned to the detailed model species in the latest SAPRC mechanism, as given by Carter (1988). In most cases, the results were not significantly different than when the standard RADM aggregation approach was employed, tending to indicate that the aggregation approach proposed for RADM is probably satisfactory. The results of these comparisons are given in more detail in Section 5.6.

5. EVALUATION AGAINST ENVIRONMENTAL CHAMBER DATA: RESULTS

The results of the simulations of the chamber experiments using the March 1988 and the recommended modified versions of the RADM mechanisms are described in this section. The organization of this evaluation against the chamber data is discussed first, then the measures of model performance are described, and finally the results of the evaluations are summarized and discussed. The results of the simulations using the March 1988 version of the RADM mechanism (designated simply as the "RADM" mechanism) are described first and in the most detail. Then the differences in the results of the simulations using the recommended modified (RADM-M) and the recommended modified parameter (RADM-P) versions of the mechanism are discussed.

Because of the large number (over 550) of chamber runs which were used in this evaluation, the discussion of the results of these simulations focuses primarily on statistical measures of model performance for the various groups of experiments. However, concentration-time plots for selected experiments are also shown for illustrative purposes. For a listing of all the individual experiments used in this evaluation, and for summaries of the performances of the mechanisms on a run-by-run basis, the reader is referred to Appendices A through C of this report. Appendix A lists all of the chamber experiments which were modeled in this study, together with their initial NO_x and organic concentrations, their average temperatures and water concentrations, and their maximum ozone yields and average initial rates of NO oxidation and ozone formation. (An "*" after the temperature or water concentration indicates that it was was not measured or that the data was unreliable, and the default for that chamber was used in the model calculations.) Appendix A also gives for each experiment the performance of the March 1988 RADM mechanism in simulating the maximum ozone yields and the average rates of NO oxidation and ozone formation. Appendices B and C give similar listings of the run-by-run performance of the RADM-M and RADM-P mechanisms, respectively, for all of the experiments whose results differed from those obtained with the RADM mechanism.

5.1 Organization of the Evaluation

The mechanism testing was organized in accordance with the hierarchy of species shown in Figure 6. This schematic shows the hierarchical nature and interdependence of the major components of atmospheric photochemical mechanisms. This hierarchy was recommended by the EPA Workshop on Evaluation and Documentation of Chemical Mechanisms (EPA, 1987) and has been used successfully in past evaluations. The mechanism testing followed this hierarchy, beginning with the lowest levels (i.e., the inorganic species) and proceeding to the highest level by stepwise addition of species with increasingly complex chemistry. The stepwise feature of this approach is designed to facilitate identification of the uncertain components of chemical mechanisms, and minimize the occurrence of compensating errors in the mechanisms and fortuitous agreement between models and chamber data. In concept, if a substantial disagreement between a model and data occurs at a high level in the hierarchy and the model has shown to perform well for experiments involving species lower in the hierarchy, then it is most likely that the new higher level chemistry is in error and not the whole mechanism.

The chamber data base was subdivided into six major groups for testing purposes. The first group included ~20 irradiations of pure air, NO_x-air, and carbon monoxide-NO_x-air mixtures. The purpose of simulating these experiments was to test the accuracy and precision of both the inorganic reactions in the mechanism and the assumptions used to represent chamber-dependent parameters. Since the level of organics is very low in these experiments, the rate of NO_x oxidation is very sensitive to chamber characteristics, such as the intensity and spectral distribution of radiation, the rates of radical offgassing from chamber walls, and the levels of background organic contaminants.

The second group of runs consisted of formaldehyde - air and acetaldehyde - air mixtures. These runs were simulated primarily to further test the submodels for the treatment of chamber effects. As discussed earlier, the acetaldehyde-air runs are particularly useful for testing how well NO_x offgassing from chamber walls is represented in the model.

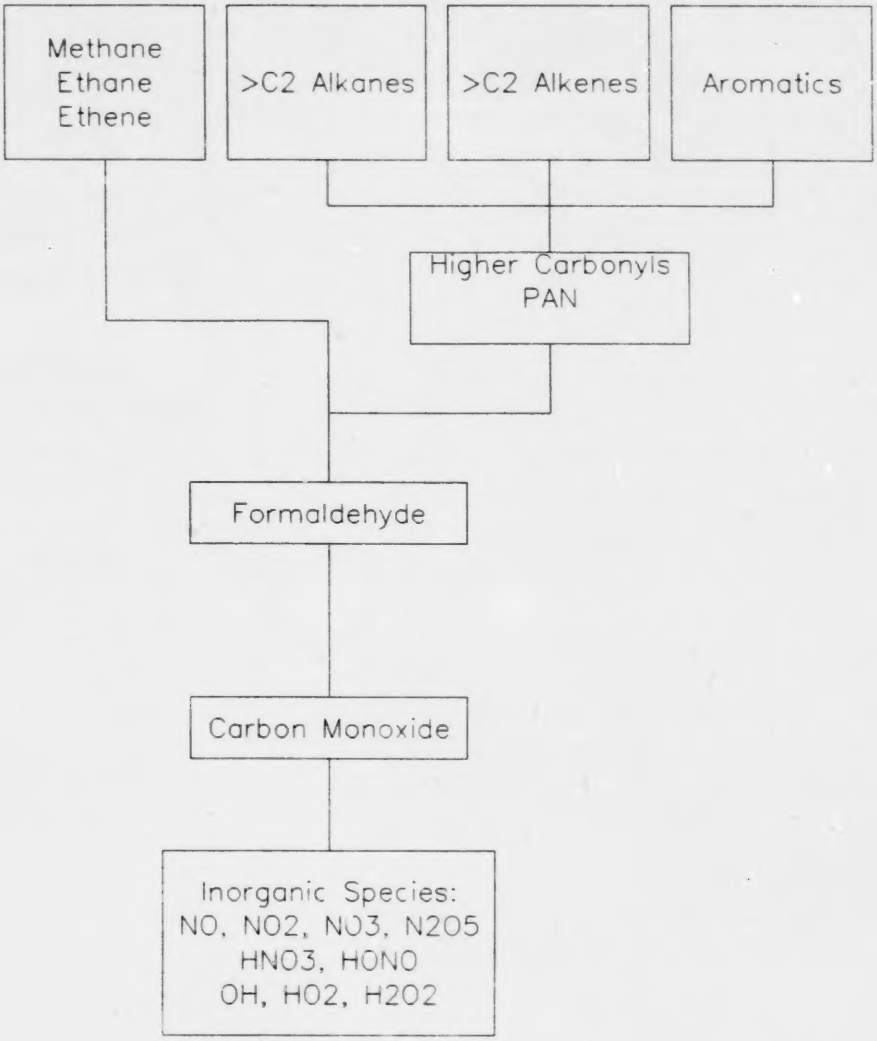
Methane
Ethane
Ethene
>C2 Alkanes
>C2 Alkenes
Aromatics
Higher Carbonyls
PAN
Formaldehyde
Carbon Monoxide
Inorganic Species:
NO, NO2, NO3, N2O5
HNO3, HONO
OH, HO2, H2O2

Figure 6. Hierarchy of Species for Mechanism Testing.

The third group consisted of ~20 single carbonyl - NO_x mixtures. These included runs with formaldehyde, acetaldehyde, propionaldehyde, acetone, or methyl ethyl ketone. These were simulated next to test the carbonyl chemistry, since the chemistry of the remaining compounds depends on these species.

The fourth groups consisted of the approximately 200 single hydrocarbon - NO_x experiments. The 91 alkene data sets included runs for ethene, propene, 1-butene, trans-2-butene, isobutene, 1-hexene, isoprene, and alpha-pinene. The 45 single alkane-NO_x data base included runs for ethane, n-butane, three branched alkanes (2,3-dimethylbutane, isopentane, and iso-octane), six long chain alkanes (n-pentane, n-hexane, n-heptane, n-octane, n-nonane, and n-pentadecane), and cyclohexane. The aromatic experiments included runs for benzene, toluene, m-xylene, o-xylene, mesitylene, tetralin, naphthalene, and dimethyl naphthalene. These were simulated to test the performance of the subgroups of hydrocarbon reactions incorporated into the mechanisms.

The fifth group consisted of ~40 runs for simple mixtures of organics and NO_x. By "simple mixtures" we mean mixtures of two or more organic species either from a given class (alkenes, alkanes, and aromatics) or from two classes, but not from all three classes. The simple mixture runs were simulated to test for compensating errors that might occur when compounds from different hydrocarbon classes in the mechanism were present.

The sixth group consisted of over 200 runs involving complex mixtures of organic species and NO_x, where one or more hydrocarbon species from each major class was included in the mixtures. These runs contained at least one alkene, alkane, and aromatic -- i.e., at least one representative from each of the major classes of organics. The majority of the mixtures included 3 to 8 organic species. However, some mixtures, such as those employing actual automobile exhaust, included a large number of compounds. The complex mixtures used in these experiments are surrogates for typical atmospheric mixtures of organics. (For this reason, they are also designated as "surrogate" runs.) The purpose of simulating a large number of runs of this type was to assess model performance as robustly as possible for the type of mixtures expected in atmospheric applications of the mechanism.

As indicated above, the mechanisms which were evaluated included the March 1988 version of the RADM mechanism, the recommended modified mechanism (RADM-M) and the recommended modified parameter mechanism (RADM-P). The evaluation of the March 1988 RADM mechanism is discussed in the most detail since evaluation of this mechanism was the primary focus of this study. The recommended modifications involve no changes in the lower portions of the hierarchy where only the inorganic reactions or the reactions of the carbonyls (other than the carbonyls formed only from the aromatics) are involved; therefore, the results discussed below for the RADM mechanism concerning the characterization and the carbonyl runs are applicable to the modified versions of the mechanism. The results of the evaluation for the runs containing compounds higher in the hierarchy are discussed separately for the three versions of the mechanism.

5.2 Measures of Model Performance

The rates of decay of precursor species and the rates of formation and the yields of key product species are important for assessing chemical mechanism performance. The selection of appropriate performance measures depends on the type of experiment. The most important distinction among experiments in this data base is whether or not significant amounts of ozone were observed. In simulations of the NO_x-air and CO-NO_x-air runs, which generally do not generate much ozone, the total changes in NO and NO_2 concentrations over the course of the experiments are the most useful measures of performance. These provide a coarse measure of the rate of precursor (NO) oxidation and product (NO_2) formation in these generally "slow" experiments.

In the organic-NO_x-air runs, where significant ozone is formed, the relative and absolute errors in the maximum ozone concentration and the average rate of change of $[O_3]$ minus [NO] during the first half of the time period to reach maximum experimental ozone are the most important measures of performance. The latter parameter (designated "$d([O_3]-[NO])/dt$" in the tabulations, and referred to variously as the "NO oxidation and ozone formation rate" or simply as the "NO oxidation rate") provides a relatively direct indication of the rate of NO oxidation by the peroxy radicals (HO_2, RO_2, and RCO_3) that are produced by the organics. This is illustrated using the kinetic rate equations for the important reactions of NO and ozone, as shown below:

$$NO_2 + hv \xrightarrow{O_2} NO + O_3 \qquad (1)$$

$$NO + O_3 \longrightarrow NO_2 + O_2 \qquad (2)$$

$$NO + RO_2 \longrightarrow NO_2 + HO_2 + \text{Carbonyls} \qquad (3)$$

where:

$$d([O_3])/dt = k_1\,[NO_2] - k_2\,[NO][O_3]$$

$$d([NO])/dt = k_1\,[NO_2] - k_2\,[NO][O_3] - k_3\,[NO][RO_2].$$

By subtraction, one obtains the rate of NO oxidation by peroxy radicals:

$$d([O_3]-[NO])/dt = k_3\,[NO][RO_2].$$

We have found this to be a robust measure of the overall timing of the simulations. When the rate of NO oxidation is slow, the time to the NO-NO_2 cross-over, the time to the NO_2 maximum, and the rates of organic precursor decay are almost always slow and vise-versa.

This measure is also a useful measure of the rate of ozone formation in experiments containing no initial NO_x, such as the pure air or carbonyl-air runs. However, in this case, it is referred to as $d[O_3]/dt$, or the average initial rate of ozone formation.

For experiments where formaldehyde and PAN are formed, the errors for the maximum predicted concentrations are also reported. These species are important intermediates and products in the photo-oxidation cycle. However, when evaluating a condensed mechanism such as RADM, it should be recognized that the model species called "PAN" actually refers to PAN + higher acyl peroxynitrates, and thus calculated "PAN" yields are not always directly comparable with experimental PAN measurements.

We have adopted an evaluation approach were we examine the errors in both the timing parameter and the maximum concentrations unpaired in time, rather than examining just the error in the predicted maximum concentrations at the time of the observed maximum (i.e., paired in time). While our approach is less stringent than the latter, it measures the aspects of performance which we believe are most important, i.e., the yields and timing of the simulations. The focus on maxima unpaired in time is also often used in evaluation of Eulerian photochemical models against ambient data (Burton, 1988).

In this study, the maximum ozone statistics were only compiled for those experiments where the maximum experimental ozone concentration exceeded 40 ppb. In experiments with lower ozone yields, relatively small errors and interferences in instrumental readings would constitute a relatively high percentage of the total yield and would not be a meaningful measurement of model performance. In addition, performance statistics on ozone yields for runs with less than approximately 40 ppb of ozone (approximately the global background) are not meaningful in the context of environmental chamber modeling where maximum ozone concentrations usually range from 100 to 1000 ppb.

The statistical parameters reported for each group and subgroups of runs are the mean experimental value, the mean calculated value, the mean bias, the mean normalized bias, the mean error (or gross error), and the mean normalized error. The latter are defined below in accordance with the American Meteorological Society's recommendations for air quality model evaluation (Fox, 1981).

$$\text{Mean Absolute Bias (ppb)} = \frac{1}{N} \sum_{i=1,N} (C_i - E_i)$$

$$\text{Mean Absolute Error (ppb)} = \frac{1}{N} \sum_{i=1,N} |C_i - E_i|$$

$$\text{Mean Normalized Bias (\%)} = \frac{100}{N} \sum_{i=1,N} \left[\frac{(C_i - E_i)}{0.5\,(C_i + E_i)}\right]$$

$$\text{Mean Normalized Error (\%)} = \frac{100}{N} \sum_{i=1,N} \left[\frac{|C_i - E_i|}{0.5\,(C_i + E_i)} \right]$$

where C_i = Calculated concentration, E_i = Experimental concentration, and the summations are over all N experiments in the group or subgroup. The standard deviations of the mean normalized bias is also reported.

In terms of our philosophy of evaluating models, we believe the testing should cover a wide range of conditions to "stress" the mechanism and to facilitate identification of situations where the mean bias and/or error are so large that one would have to reject the mechanism. A mechanism can be judged acceptable if it doesn't fail any of the tests. The performance levels at which one decides to accept or reject a mechanism are subjective. Nevertheless, it is useful to define such a criteria so that mechanism performance can be judged consistently. Our criteria for rejection is a mean normalized bias in excess of 20% and a mean normalized error in excess of 50%. These are referred to below at the minimum desired performance criteria. In addition, because the results for any one experiment are not nearly as meaningful as those for a group of experiments, one needs to determine the minimum number of experiments that must be simulated to determine whether or not a mechanism is performing satisfactorily. We believe a minimum of 10 to 15 experiments is needed to reasonably assess model performance for a particular type of run.

5.3 Performance on Characterization Runs

The performance of the RADM mechanism, combined with our current chamber effects submodels, in simulating the NO_x-air and CO-NO_x air runs is summarized in Table 19. Run-by-run summaries of these results are given in Appendix A. (These results are also applicable to the recommended modified versions of this mechanism.) This table (and Appendix A) shows the performance statistics for the total changes in NO and NO_2 concentrations during the runs. Figures 7 and 8 graphically compare the change in [NO] and [NO_2] for each run, respectively. In the NO_x-air runs, the model slightly underpredicts the absolute changes in NO and NO_2 concentrations, but in the CO-NO_x air runs, the model overpredicts the absolute changes in these values. On the average for all of these runs, the model overpredicts the changes in NO by 9% with an average error of

42% and underpredicts the changes in NO_2 by 10% with an average error of 45%. The graphical comparisons illustrate that the model performs well on the majority of these characterization runs. This suggests the combination of the chamber characterization procedures and the inorganic chemistry in the RADM mechanism provides moderately accurate predictions for these types of experiments. This is despite the fact that the chamber characterization model was derived using the SAPRC and not the RADM chemical mechanism. This level of performance is as good (or better) than reported elsewhere (Carter et al., 1986) and meets our desired performance criteria.

Table 19. Selected Performance Statistics in the RADM Simulations of the NO_x-Air, CO-NO_x-Air, Pure Air, and Carbonyl-Air Runs

Run Type	No. Runs	Experimental Avg. (sdev)	-Absolute-		-- Normalized --	
			Bias	Err.	Bias (%)	Err. (%)
		1) Change in NO (ppm). 2) Change in NO_2 (ppm)				
NO_x-Air	23	0.06 (0.49)	-0.004	0.038		
	23	-0.14 (0.56)	-0.005	0.025		
CO-NO_x-Air	13	-0.11 (0.10)	-0.016	0.019		
	13	0.06 (0.09)	0.005	0.018		
		1) Maximum Ozone (ppm) 2) Maximum Pan (ppb)				
Pure Air	6	0.11 (0.05)	-0.005	0.008	-4 (12)	9
Formaldehyde-Air	8	0.18 (0.06)	0.042	0.042	20 (13)	20
Acetaldehyde-Air	18	0.16 (0.16)	-0.014	0.039	-12 (30)	26
	18	19 (13)	3	6	19 (40)	34

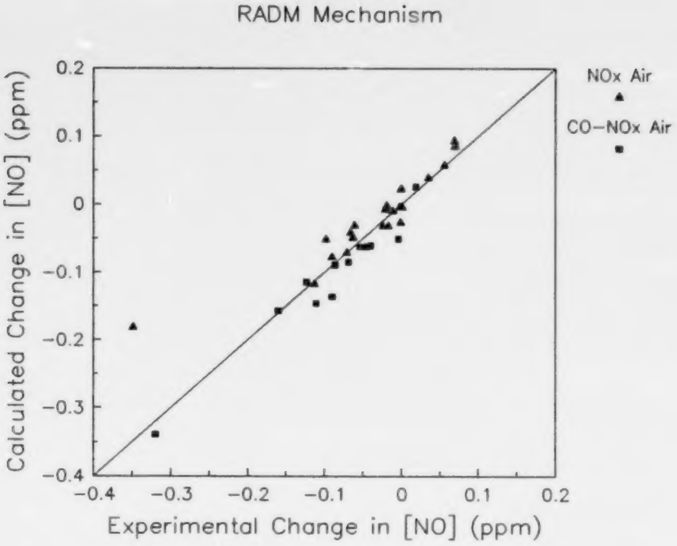

Figure 7. Calculated vs Experimental Changes in [NO] in NO_x-Air and $CO-NO_x$-Air Runs.

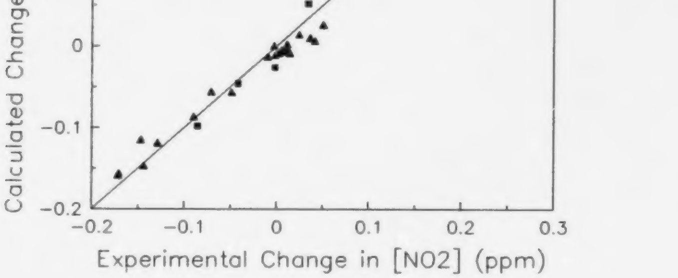

Figure 8. Calculated vs Experimental Changes in $[NO_2]$ in NO_x-Air and $CO-NO_x$-Air Runs.

The performance of the RADM mechanism and our chamber effects model in simulating ozone formation in pure air and carbonyl-air experiments is also summarized in Table 19. Run-by-run listings of these results are given in Appendix A. (Again, these results are also applicable to the recommended modified mechanisms.) As discussed in Section 4, the pure air runs primarily test the levels of background reactive organics and the rate of NO_x offgassing used in the chamber effects submodels. The carbonyl-air runs, especially the acetaldehyde-air runs, are good tests for the NO_x offgassing rates because the ozone and PAN predictions are very sensitive to NO_x offgassing. The performance statistic indicate that on the average there is relatively little bias and error (9%) in maximum ozone predictions for pure-air runs. Ozone concentrations are somewhat overpredicted in the formaldehyde-air and underpredicted in the acetaldehyde-air runs. The maximum PAN concentrations tend to be overpredicted in the acetaldehyde-air runs.

Comparisons of the calculated and experimental maximum ozone yields and ozone formation rates in the pure air and carbonyl-air runs are shown in Figures 9 and 10, respectively, and a histogram of the normalized biases in maximum ozone is shown in Figure 11. There is a fair amount of scatter in these fits with biases for ozone that are fairly evenly distributed between -40% and +50%. A plot of the error in maximum ozone vs. the initial HC/NO_x ratio is shown in Figure 12. There is no systematic dependence of the ozone prediction errors on this important ratio; this is a positive result since it probably means there is no systematic source of error in the mechanism. We suspect that the scatter is probably primarily due to uncontrolled or incompletely characterized chamber effects (Carter et al., 1986).

Overall, the RADM mechanism's performance on the pure-air and carbonyl-air is considered to be reasonably acceptable, given the uncertainties in the chamber characterization model.

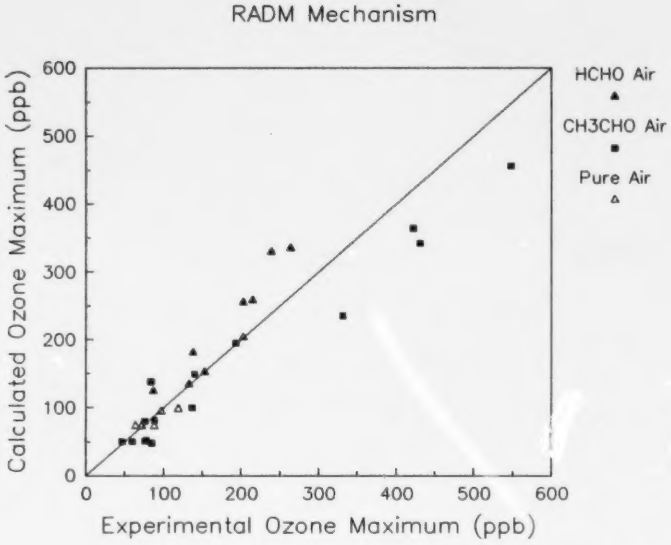

Figure 9. Calculated vs Experimental Maximum Ozone in the Pure Air and Carbonyl-Air Runs.

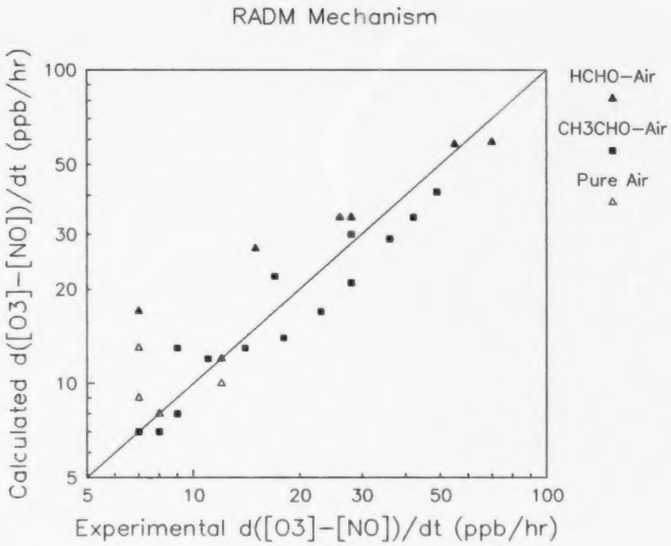

Figure 10. Calculated vs Experimental Rate of Ozone Formation in the Pure Air and Carbonyl-Air Runs.

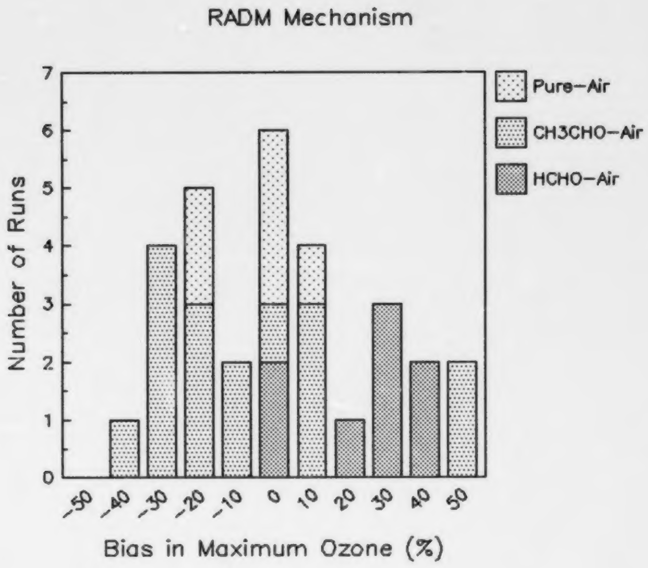

Figure 11. Histogram of Normalized Biases in Maximum Ozone in Pure Air and Carbonyl-Air Runs.

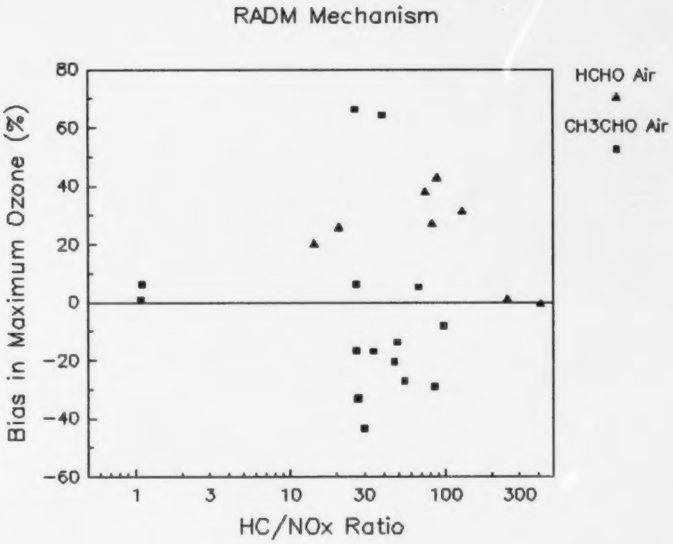

Figure 12. Normalized Biases in Maximum Ozone vs HC/NO$_x$ Ratios in Carbonyl-Air Runs.

5.4 Performance of the RADM Mechanism on Single Organic Runs

Model performance statistics for maximum ozone and the NO oxidation rate for the March 1988 RADM mechanism are shown in Table 20 for all of the organic-NO_x runs. Run-by-run listings of these results are given in Appendix A. In general, these results are applicable only to the March 1988 RADM mechanism. However, except for the aromatics-NO_x and (for the RADM-M mechanism) the C_{5+} akane-NO_x runs, the performance for the recommended modified mechanisms was found to be the same or very similar. The cases where the recommended modified mechanisms provide different results are discussed in Section 5.7.

In the following discussion, concentration-time plots for selected representative experiments will be presented. In all cases, the "*" symbols are used to designate experimental data, and solid lines are used to designate model calculations using the March 1988 RADM mechanism. (For experiments where the predictions of the recommended modified mechanisms are noticeably different, the plots also include results of model simulations using those mechanisms. These are indicated by dashed lines, with the longer dashes being for the RADM-P mechanism and the shorter dashes being for RADM-M.)

5.4.1 Carbonyl-NO_x Runs

Tabulations of the performance of the RADM mechanism in simulations of maximum ozone and NO oxidation rates for carbonyl-NO_x runs are given in Table 20, and graphical displays of these results are shown in Figures 13 through 16. The majority of runs in these groups are for formaldehyde. On the average, there is only +2% bias in the maximum ozone and the NO oxidation rate predictions for the formaldehyde runs. The error in the maximum ozone and timing parameter predictions are +21% and +13%, respectively, on the average. The performance of the RADM mechanism's formaldehyde chemistry is considered acceptable by the criteria discussed in Section 5.2.

The results for acetaldehyde runs show underprediction of both the maximum ozone (-37% mean bias) and the rate of NO_x oxidation (-18% mean bias). An example of one of the UNC Acetaldehyde-NO_x runs is shown in Figure 17. The ozone results for propionaldehyde, acetone, and methyl ethyl ketone show biases of -31%, +52%, and -19%. There does not appear

Table 20. Performance Statistics on Maximum Ozone and on NO Oxidation and Ozone Formation Rates in the Simulations of the Organic-NO_x-Air Runs Using the RADM Mechanism

Organic or Mixture	1) Statistics for Maximum Ozone (ppm) 2) Statistics for $d([O_3]-[NO])/dt$ (ppb/min)					
	No. Runs	Experimental Avg. (sdev)	Absolute Bias	Err.	-- Normalized -- Bias (%)	Err. (%)
Formaldehyde	15	0.47 (0.58)	0.03	0.09	2 (30)	21
	15	12.67 (27.92)	0.89	1.71	9 (22)	13
Acetaldehyde	5	0.60 (0.40)	-0.17	0.17	-37 (17)	37
	5	1.73 (0.29)	-0.29	0.29	-18 (11)	18
Propionaldehyde	2	0.84 (0.15)	-0.23	0.23	-31 (20)	31
	2	1.79 (0.05)	-0.41	0.41	-26 (1)	26
Acetone	1	0.23 (0.00)	0.16	0.16	52 (0)	52
	1	0.48 (0.00)	0.04	0.04	9 (0)	9
Methylethylketone	2	0.61 (0.06)	-0.11	0.11	-19 (1)	19
	2	1.19 (0.09)	0.27	0.27	19 (17)	19
Ethene	14	0.91 (0.20)	-0.09	0.16	-16 (30)	23
	14	5.23 (4.10)	-1.21	1.21	-27 (20)	27
Propene	49	0.61 (0.24)	0.03	0.09	5 (20)	15
	49	3.62 (2.60)	0.26	0.57	6 (19)	14
1-Butene	11	0.42 (0.26)	0.04	0.13	-2 (56)	45
	11	2.86 (2.18)	0.20	0.81	0 (32)	25
trans-2-Butene	4	0.28 (0.17)	-0.08	0.09	-52 (38)	54
	4	6.17 (2.80)	-1.50	1.68	-25 (26)	31
Isobutene	1	0.90 (0.00)	-0.19	0.19	-23 (0)	23
	1	8.84 (0.00)	-3.25	3.25	-45 (0)	45
1-Hexene	4	0.34 (0.25)	0.26	0.26	57 (25)	57
	4	1.57 (1.04)	2.95	2.95	82 (25)	82
Isoprene	13	0.72 (0.25)	-0.23	0.24	-42 (31)	43
	13	5.66 (4.06)	0.86	1.81	-2 (36)	26
a-Pinene	4	0.35 (0.11)	-0.03	0.08	-8 (35)	28
	4	0.97 (0.43)	0.09	0.17	4 (19)	14

(continued)

Table 20 (continued) - 2

1) Statistics for Maximum Ozone (ppm)
2) Statistics for $d([O_3]-[NO])/dt$ (ppb/min)

Organic or Mixture	No. Runs	Experimental Avg. (sdev)	Absolute Bias	Absolute Err.	-- Normalized -- Bias (%)	-- Normalized -- Err. (%)
Ethane	1	0.24 (0.00)	-0.04	0.04	-19 (0)	19
	1	1.32 (0.00)	0.08	0.08	6 (0)	6
n-Butane	27	0.31 (0.27)	0.02	0.13	0 (59)	46
	27	1.53 (0.98)	0.33	0.81	19 (50)	43
C4+ Br. Alkane	7	0.28 (0.18)	-0.05	0.10	-17 (67)	53
	7	0.93 (0.46)	-0.18	0.20	-22 (24)	26
C5+ n-Alkane	14	0.20 (0.15)	0.10	0.10	42 (28)	42
	14	1.15 (0.75)	0.22	0.35	24 (37)	34
Cycloalkane	4	0.05 (0.00)	0.01	0.02	33 (0)	33
	4	0.92 (0.12)	0.06	0.19	3 (29)	19
Benzene	6	0.29 (0.14)	0.08	0.08	22 (15)	22
	6	3.39 (2.30)	1.22	1.22	36 (19)	36
Toluene	20	0.34 (0.15)	0.09	0.12	24 (43)	33
	20	3.07 (1.87)	0.04	0.83	7 (34)	27
Xylene	10	0.44 (0.19)	-0.02	0.08	-4 (25)	18
	10	5.39 (4.14)	-0.41	1.28	0 (35)	25
Mesitylene	8	0.57 (0.26)	-0.18	0.22	-39 (50)	48
	6	9.50 (4.97)	-6.64	6.64	-93 (32)	93
Tetralin	5	0.29 (0.23)	0.11	0.13	-6 (62)	43
	5	11.89 (0.88)	12.58	12.73	106 (85)	119
Naphthalene	5	0.20 (0.08)	0.28	0.28	84 (40)	84
	5	1.59 (0.41)	7.04	7.04	134 (13)	134
2,3-Dimethylnaph.	4	0.32 (0.04)	-0.01	0.05	-6 (24)	17
	4	2.48 (0.51)	0.13	0.47	1 (24)	19
Simple Mixtures	40	0.49 (0.27)	-0.05	0.13	-12 (45)	34
	39	4.10 (4.06)	-0.87	1.09	-13 (26)	22
Simple Surrogates	36	0.37 (0.15)	0.02	0.05	7 (24)	15
	36	2.81 (1.61)	0.33	0.90	8 (38)	27

(continued)

Table 20 (continued) - 3

1) Statistics for Maximum Ozone (ppm)
2) Statistics for $d([O_3]-[NO])/dt$ (ppb/min)

Organic or Mixture	No. Runs	Experimental Avg. (sdev)	Absolute Bias	Absolute Err.	-- Normalized -- Bias (%)	-- Normalized -- Err. (%)
SAPRC 7-HC Surgs.	11	0.60 (0.17)	-0.01	0.04	0 (11)	8
	11	7.74 (5.16)	-0.38	0.65	-5 (12)	10
SAPRC 8-HC Surgs.	82	0.45 (0.27)	0.04	0.09	9 (26)	20
	82	2.81 (1.51)	-0.27	0.54	-10 (23)	19
UNC Misc. Surgs.	21	0.50 (0.17)	0.06	0.12	17 (40)	27
	21	1.32 (0.40)	0.00	0.13	2 (15)	11
UNC "Synurban"	11	0.37 (0.28)	0.13	0.13	39 (31)	39
	11	1.09 (0.47)	0.07	0.09	7 (8)	8
UNC "Synauto"	15	0.62 (0.18)	0.13	0.14	23 (17)	23
	15	1.81 (0.63)	0.02	0.28	2 (18)	14
UNC Auto Exhaust	28	0.57 (0.27)	0.06	0.09	8 (29)	19
	28	1.68 (0.61)	-0.08	0.19	-6 (15)	13
Syn. Jet Fuel	8	0.75 (0.10)	0.11	0.11	14 (12)	14
	8	3.47 (0.74)	0.38	0.61	11 (16)	16
Syn. Jet Exhaust	4	0.78 (0.13)	-0.09	0.09	-11 (8)	11
	4	6.66 (3.48)	-0.58	0.58	-8 (4)	8

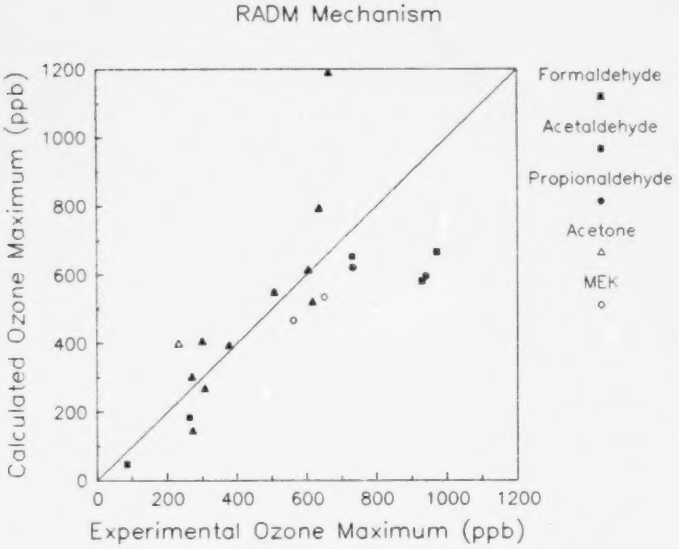

Figure 13. Calculated vs Experimental Maximum Ozone in Carbonyl-NO_x Runs.

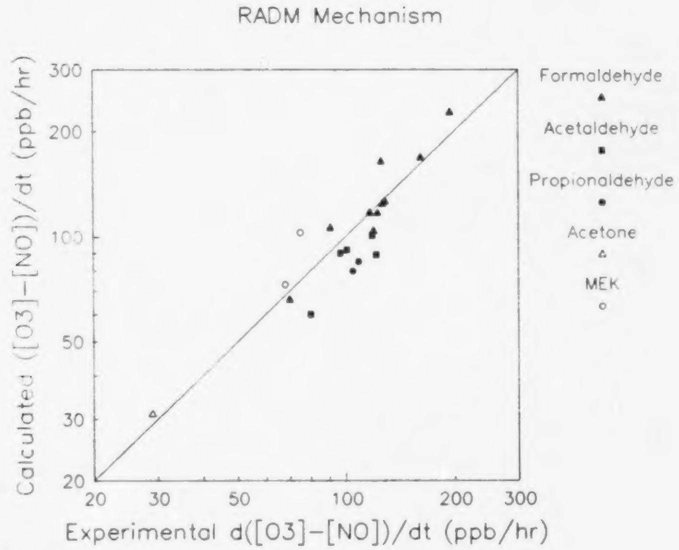

Figure 14. Calculated vs Experimental Rates of NO Oxidation and Ozone Formation in the Carbonyl-NO_x Runs.

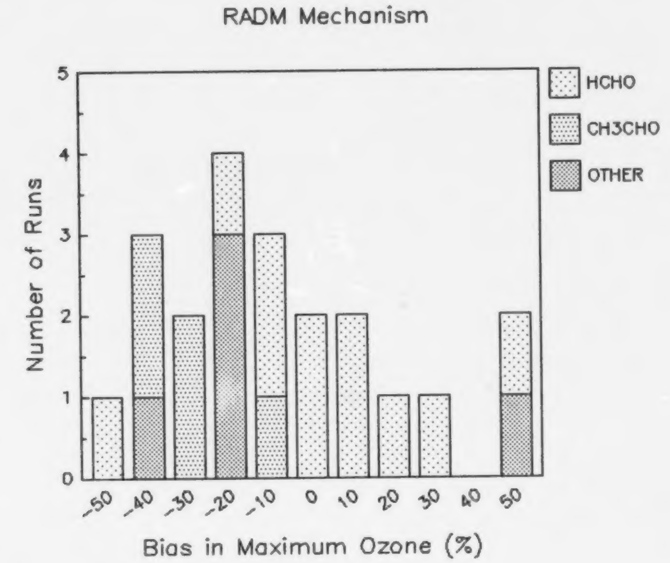

Figure 15. Histogram of Normalized Biases in Maximum Ozone in Carbonyl-NO_x Runs.

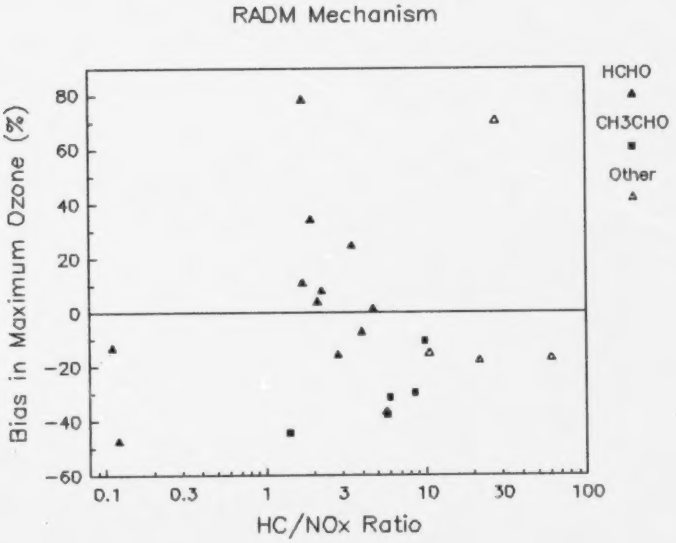

Figure 16. Normalized Bias in Maximum Ozone vs HC/NO_x Ratio in Carbonyl-NO_x-Runs.

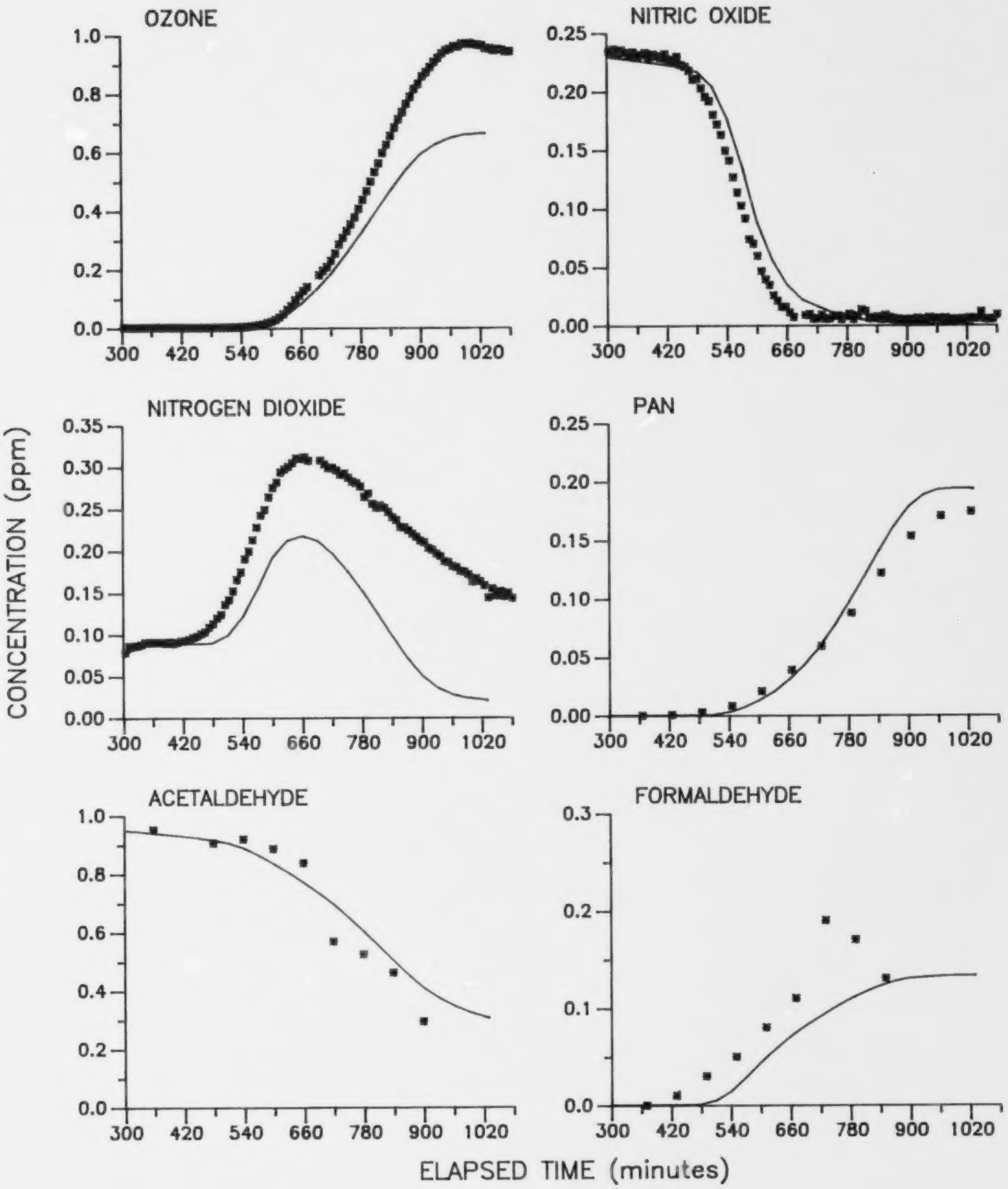

Figure 17. Experimental and Calculated Concentration-Time Plots for Selected Species in Simulations of UNC Acetaldehyde-NO_x Run AU2482B.

to be any systematic dependence of the errors on the initial HC/NO_x ratio. While the simulation results for the higher aldehydes and acetone do not meet our criteria for acceptable performance, there are too few runs with these compounds to draw meaningful conclusions regarding the adequacy of the chemistry. Nevertheless, we are concerned with the large biases for these simulations and recommend additional testing when more data become available.

5.4.2 Alkene-NO_x Runs

The result for tests of the RADM mechanism against the alkene-NO_x runs are shown in Table 20 and in Figures 18 through 21. Selected concentrations versus time plots for one of the best simulations of the UNC ethene-NO_x experiments are shown in Figure 22.

The statistics for ethene runs show a tendency for the mechanism to underpredict maximum ozone. On the average, it underpredicts the ozone by 16% with 23% error. Also, it underpredicts the rate of NO_x oxidation in ethene runs by 27% on the average. The RADM mechanism's underpredictions are primarily a result of its not including ethene's reaction with atomic oxygen, which we have found is important in these high concentration experiments. Test calculations where this reaction is included in the mechanism significantly improves its performance in simulating these results; with its performance being comparable to that of the SAPRC mechanisms (Carter et al., 1986; Carter, 1988). However, calculations using the set of test problems discussed in Section 6 of this report indicate that neglecting these reactions has a negligible effect under ambient conditions. For that reason, this reaction is not included in the recommended modified mechanisms. However, its omission does limit the range of validity of this mechanism to a concentration regime below that of these chamber experiments.

There are a large number of propene-NO_x runs in the data base and the RADM mechanism performs very well on these runs. Results from two typical propene-NO_x simulations are shown in Figures 23 and 24. The mechanism predicts the maximum ozone and rate of NO_x oxidation with a +5% bias and 15% error on the average. The results for 1-butene simulations also show a small mean bias (-2%), but the mean error (45%) is much higher than for the propene runs. Figure 25 shows a fairly typical simulation of a UNC 1-butene-NO_x experiment where the ozone is overpredicted by ~30%. (PAN is

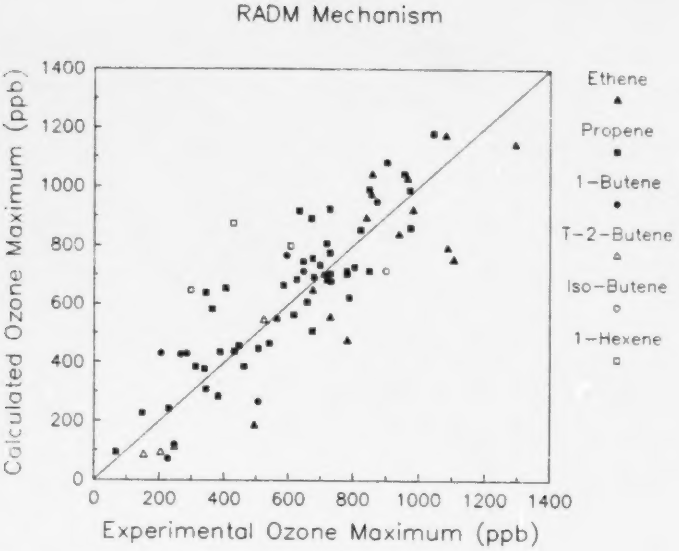

Figure 18. Calculated vs Experimental Maximum Ozone in the Alkene-NO_x Runs for the RADM Mechanism.

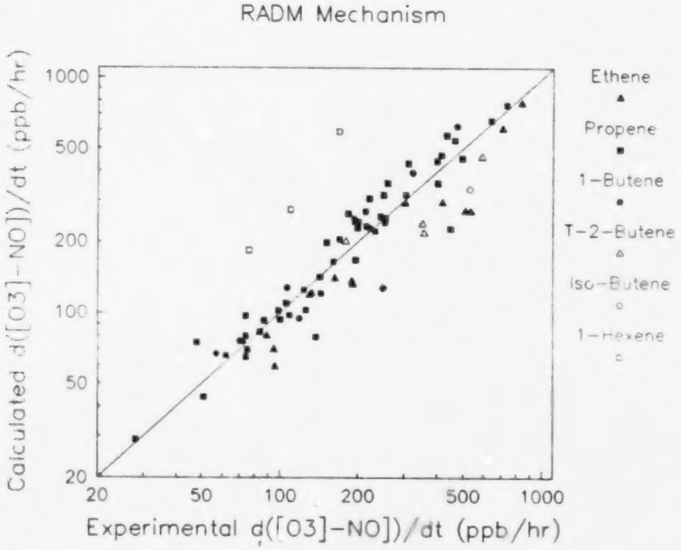

Figure 19. Calculated vs Experimental Rates of NO Oxidation and Ozone Formation in the Alkene-NO_x Runs for the RADM Mechanism.

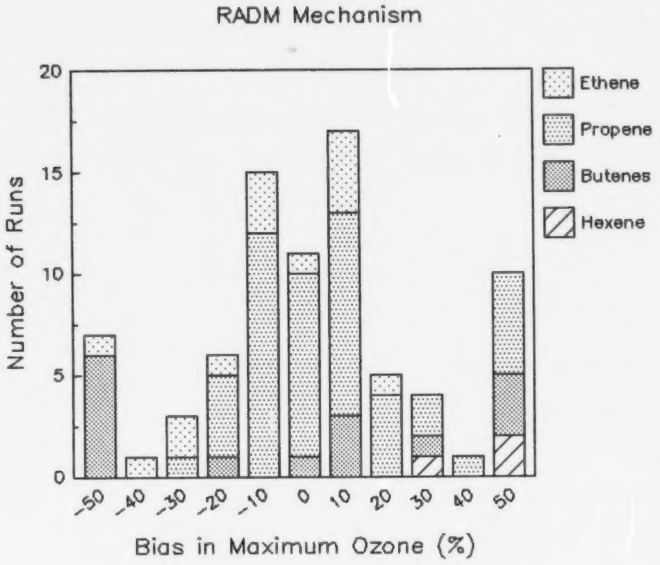

Figure 20. Histogram of Normalized Biases in Maximum Ozone in Alkene Runs for the RADM Mechanism.

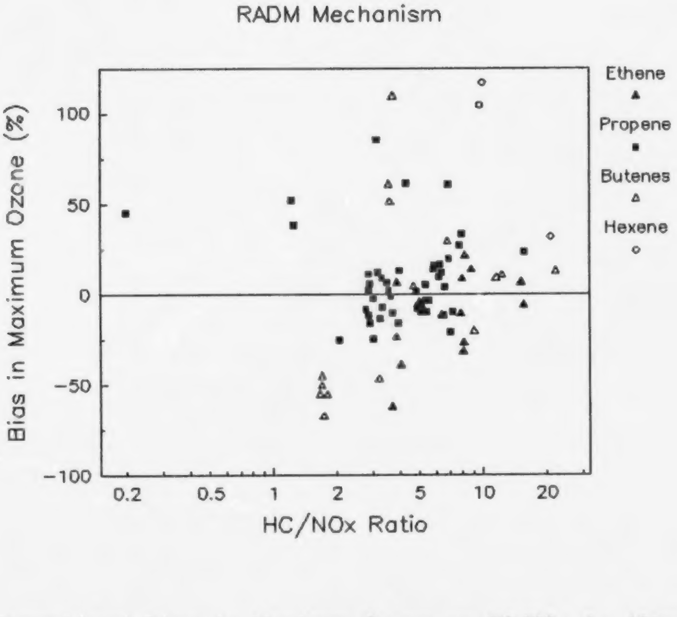

Figure 21. Normalized Bias in Maximum Ozone vs HC/NO_x in Alkene Runs for the RADM Mechanism.

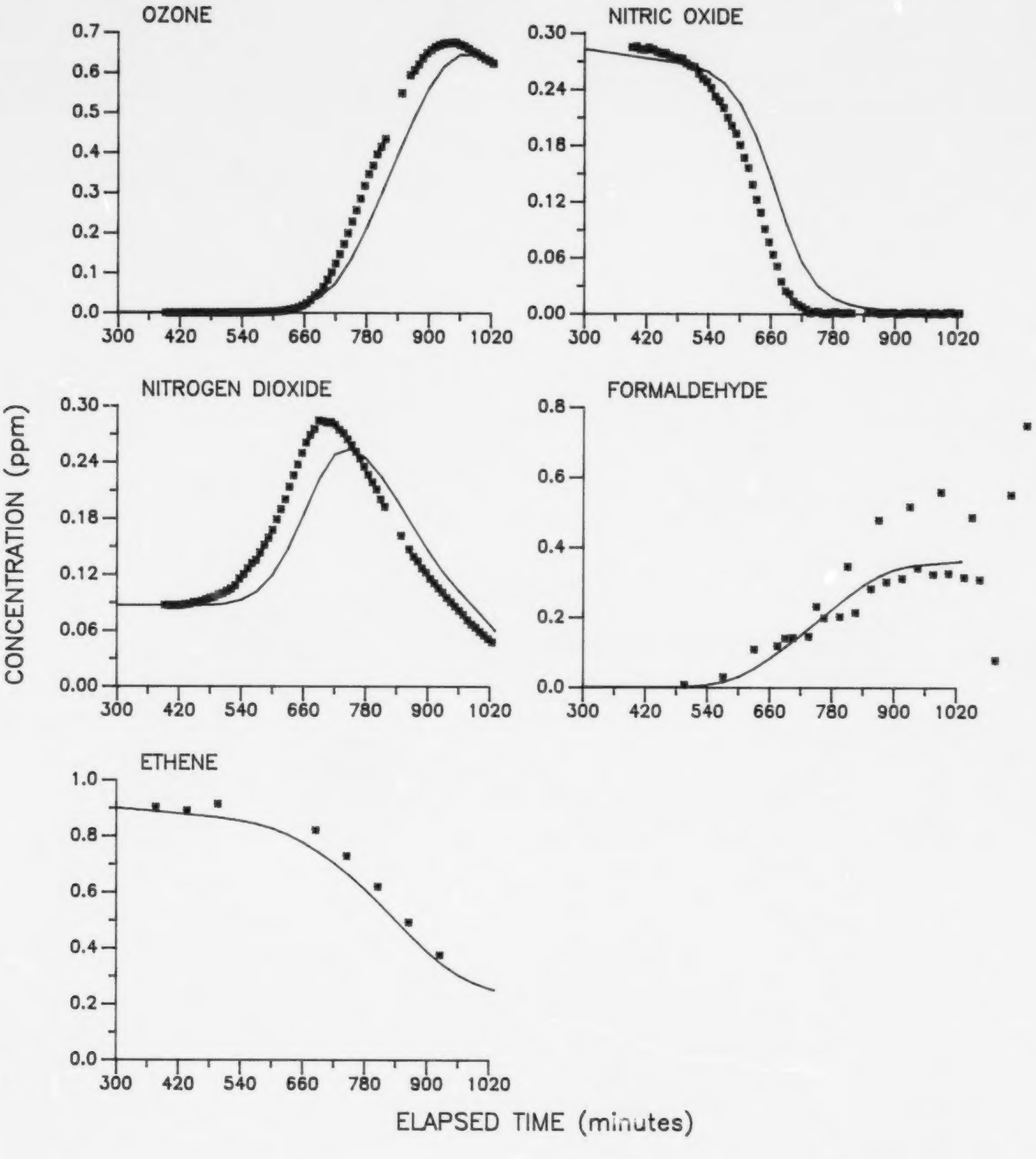

Figure 22. Experimental and Calculated Concentration-Time Plots for Selected Species in Simulations of UNC Ethene-NO_x Run OC0584B.

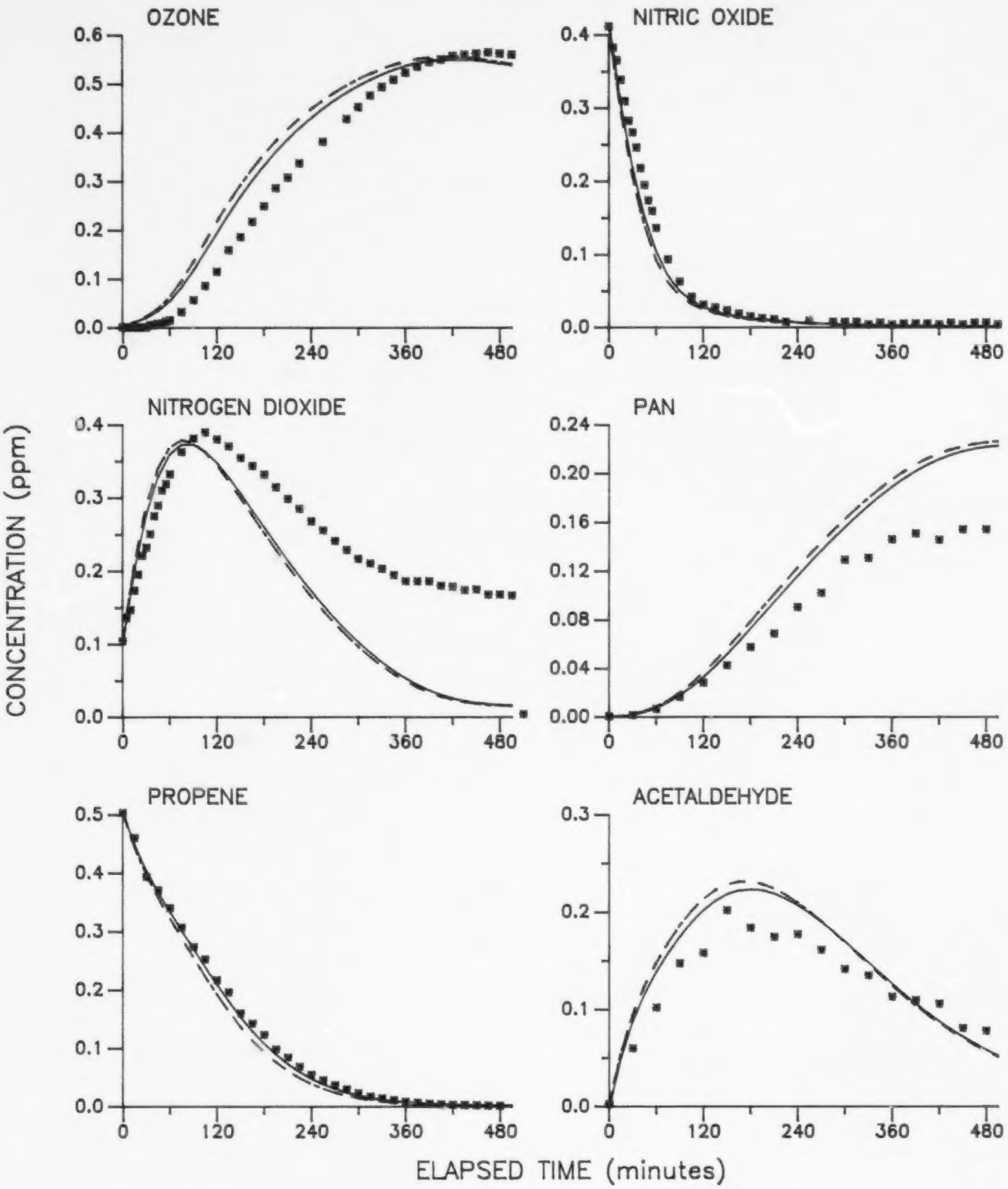

Figure 23. Experimental and Calculated Concentration-Time Plots for Selected Species in Simulations of the Propene-NO_x Run EC-216.

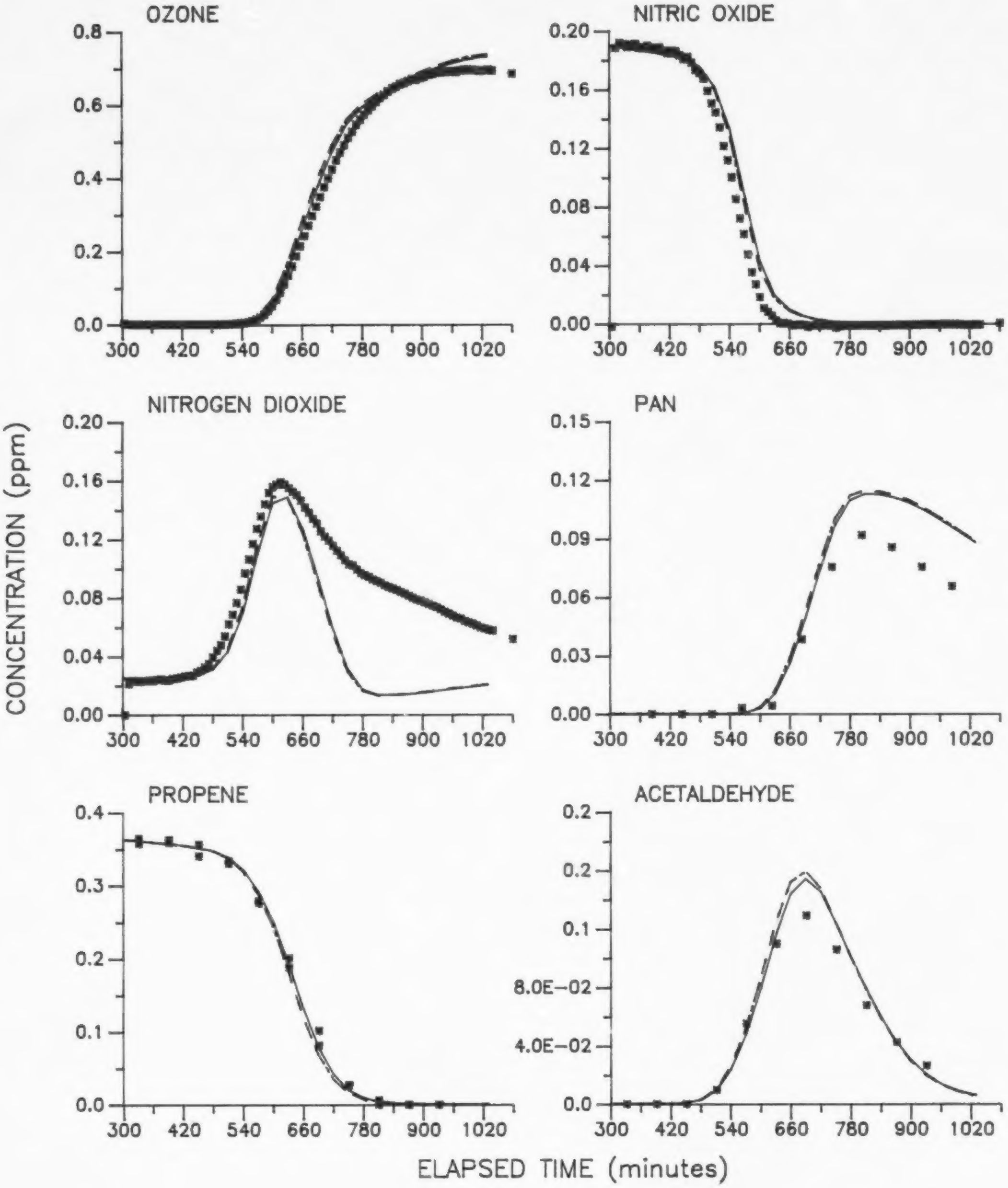

Figure 24. Experimental and Calculated Concentration-Time Plots for Selected Species in Simulations of UNC Propene-NO_x Run JL2983B.

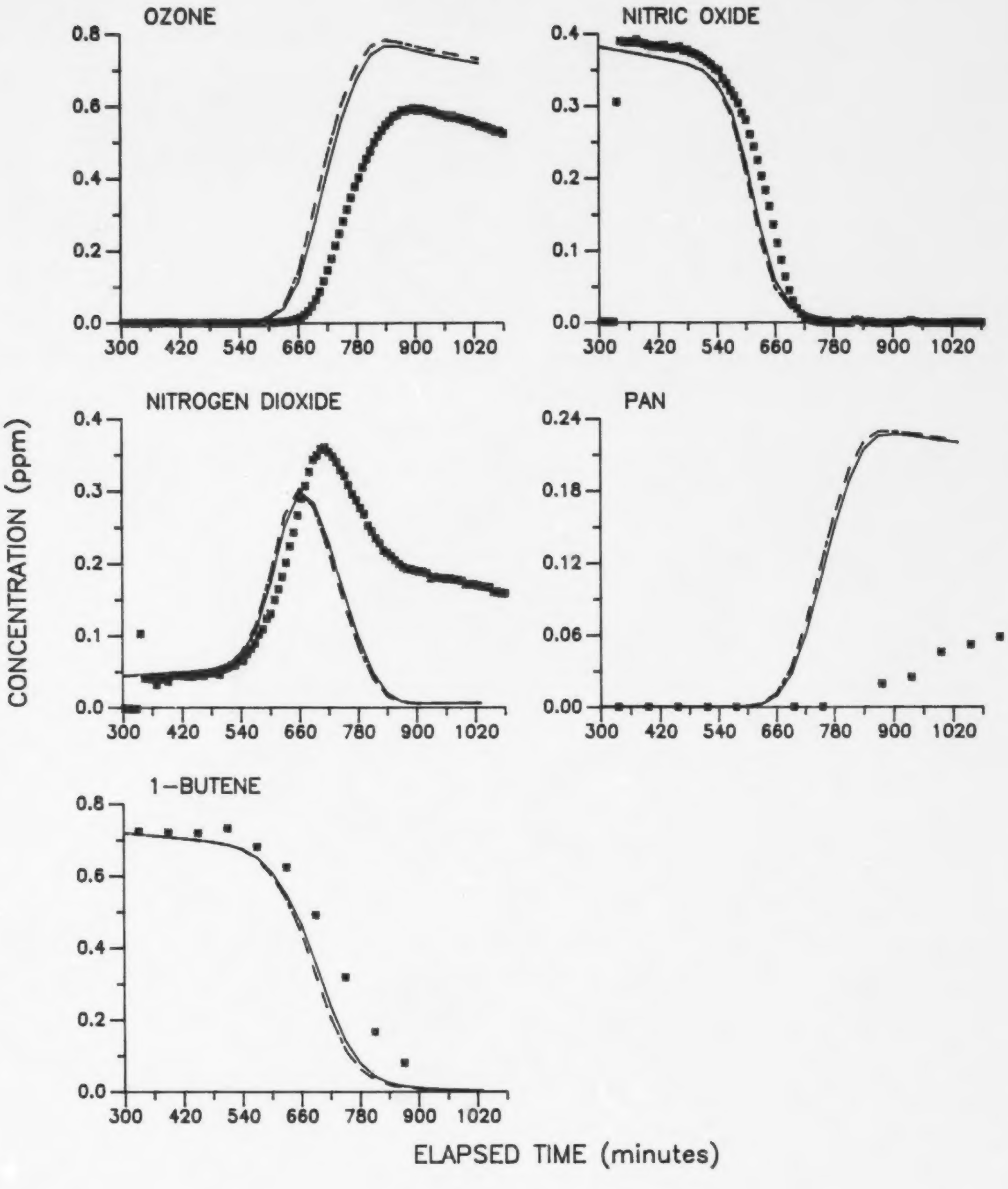

Figure 25. Experimental and Calculated Concentration-Time Plots for Selected Species in Simulations of UNC 1-Butene-NO_x Run ST2583B.

greatly overpredicted in this simulation because the model species PAN represents peroxypropionyl nitrate as well as PAN.) Figure 21 clearly shows that there is a lack of systematic dependence of the biases on the initial HC/NO_x ratios in these runs. There are a small number of runs for other butenes and 1-hexene. The mechanism's performance on these runs is poor. The ozone yields and rate of NO_x oxidation in the trans-2-butene and isobutene runs are underpredicted. Conversely, they are both overpredicted by almost 60% on the average in the 1-hexene runs.

Clearly, the propene portion of the mechanism perform well and easily meet the desired performance criteria. The 1-butene results also meet the criteria, although they are not as accurate. The internal alkene portion of the RADM mechanism do not perform well, but once again, this is based only on five experiments. The mechanism does not perform as well as other mechanisms in the simulations of the ethene runs because the concentration regime in these runs is beyond the range of validity of this mechanism. Test calculations show that if the $O(^3P)$ + ethene reaction were added, the mechanism would perform better in simulating the ethene runs.

5.4.3 Alkane-NO_x Runs

The model performance results for alkane-NO_x runs are shown in Table 20 and in Figures 26 through 29. Typical simulations of n-butane, n-octane, and 2,3-dimethylbutane experiments are shown in Figures 30 through 32, respectively. The simulation of the one ethane-NO_x system underpredicts the maximum ozone by 18%. For the butane experiments, the mechanism shows no bias but has a fairly large error of 46%. For the >C4 branched alkanes, the mean bias and error are -17% and 53%, respectively. However, for the >C4 long chain alkanes, the mean bias and error are both 42%. For the cyclohexane runs, the mechanism predicts ozone with a bias and error of 33% on the average. Overall, for all of the alkane experiments, the RADM mechanism is able to predict the maximum ozone with a relatively low bias but a relatively high error. The statistics for the rate of NO_x oxidation are only slightly better. Figures 26 through 29 confirm that there is a large amount of scatter in the results. Figure 29 shows that there does not appear to be any systematic dependence of the bias on initial HC/NO_x ratios, which is reassuring.

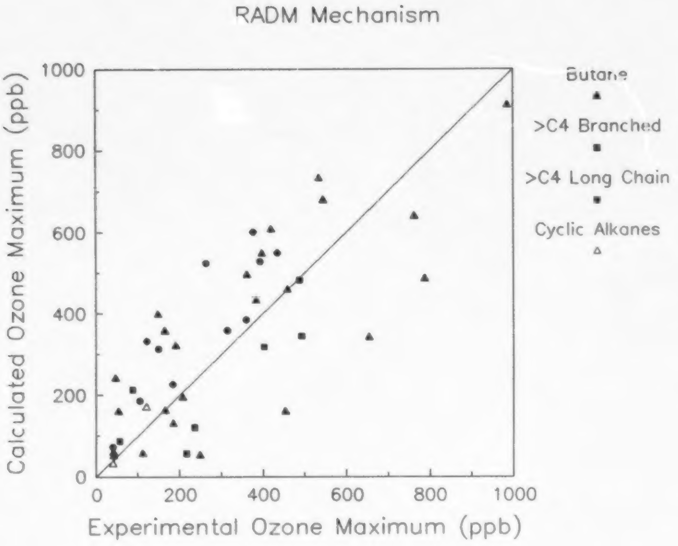

Figure 26. Calculated vs Experimental Maximum Ozone in the Alkane-NO_x Runs for the RADM Mechanism.

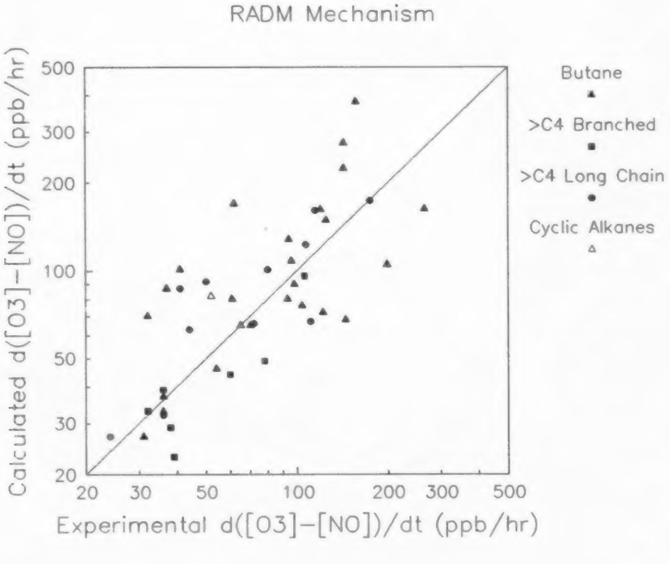

Figure 27. Calculated vs Experimental Rates of NO Oxidation and Ozone Formation in the Alkane-NO_x Runs for the RADM Mechanism.

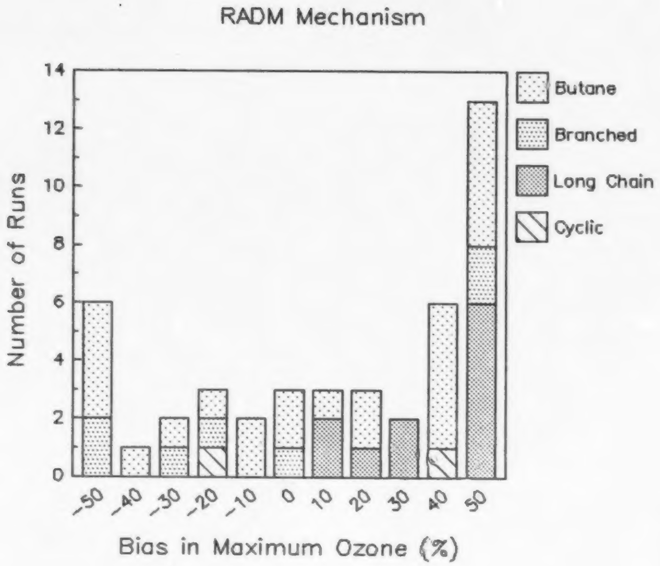

Figure 28. Histogram of Normalized Biases in Maximum Ozone in Alkane Runs for the RADM Mechanism.

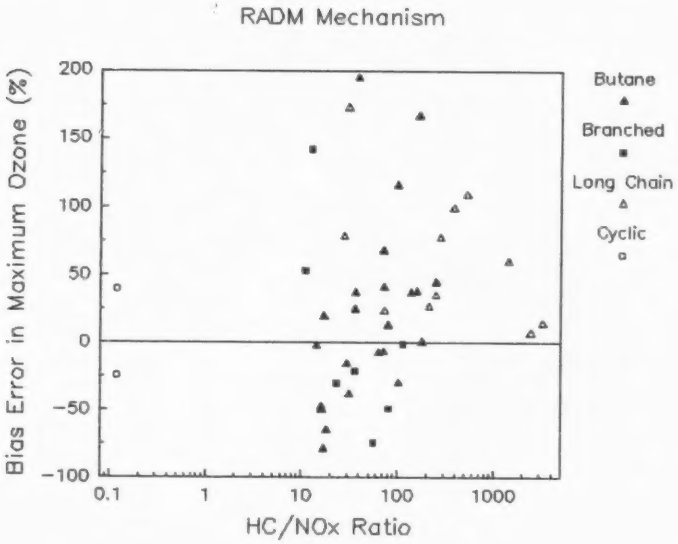

Figure 29. Normalized Bias in Maximum Ozone vs HC/NO_x in Alkane Runs for the RADM Mechanism.

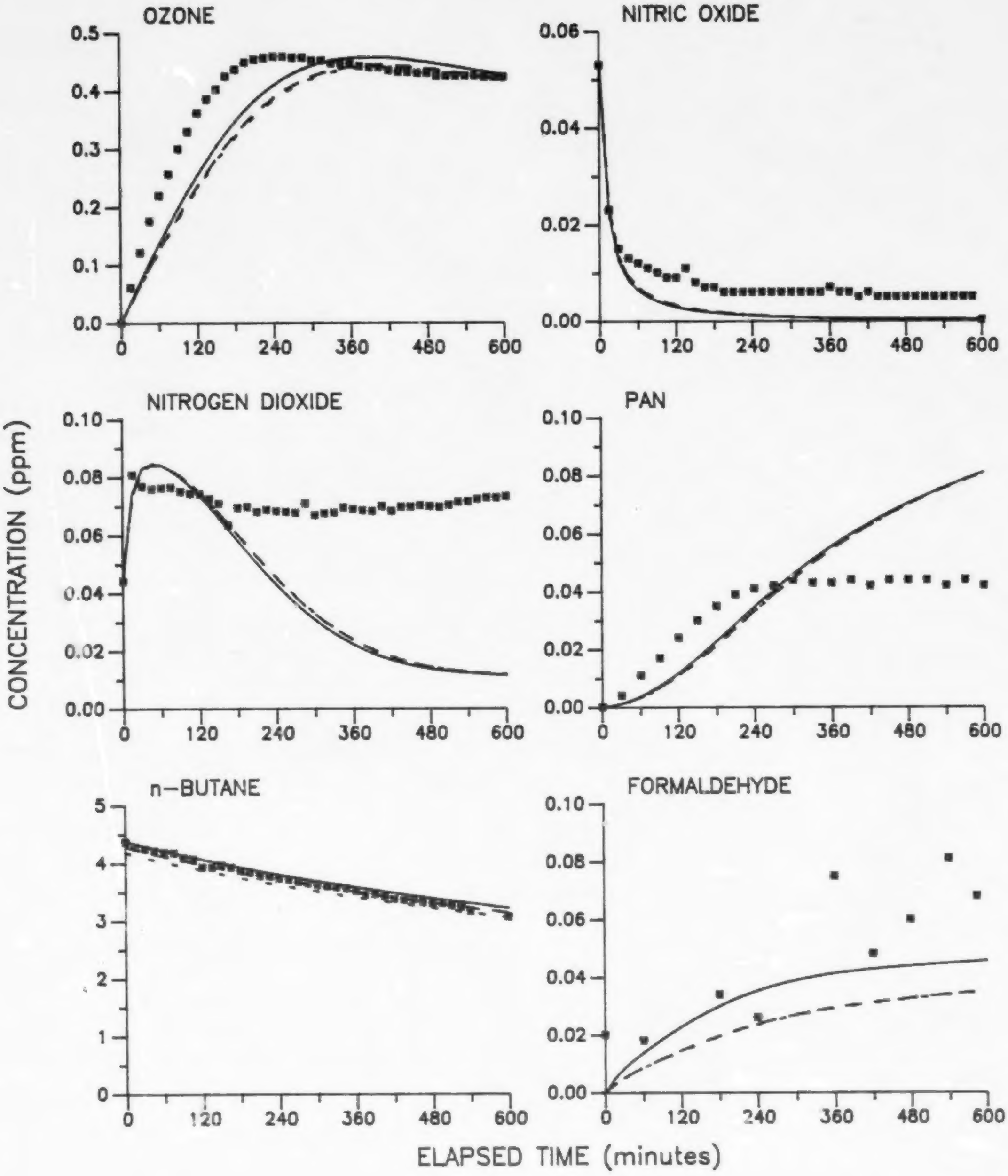

Figure 30. Experimental and Calculated Concentration-Time Plots for Selected Species in Simulations of n-Butane-NO_x Run EC-130.

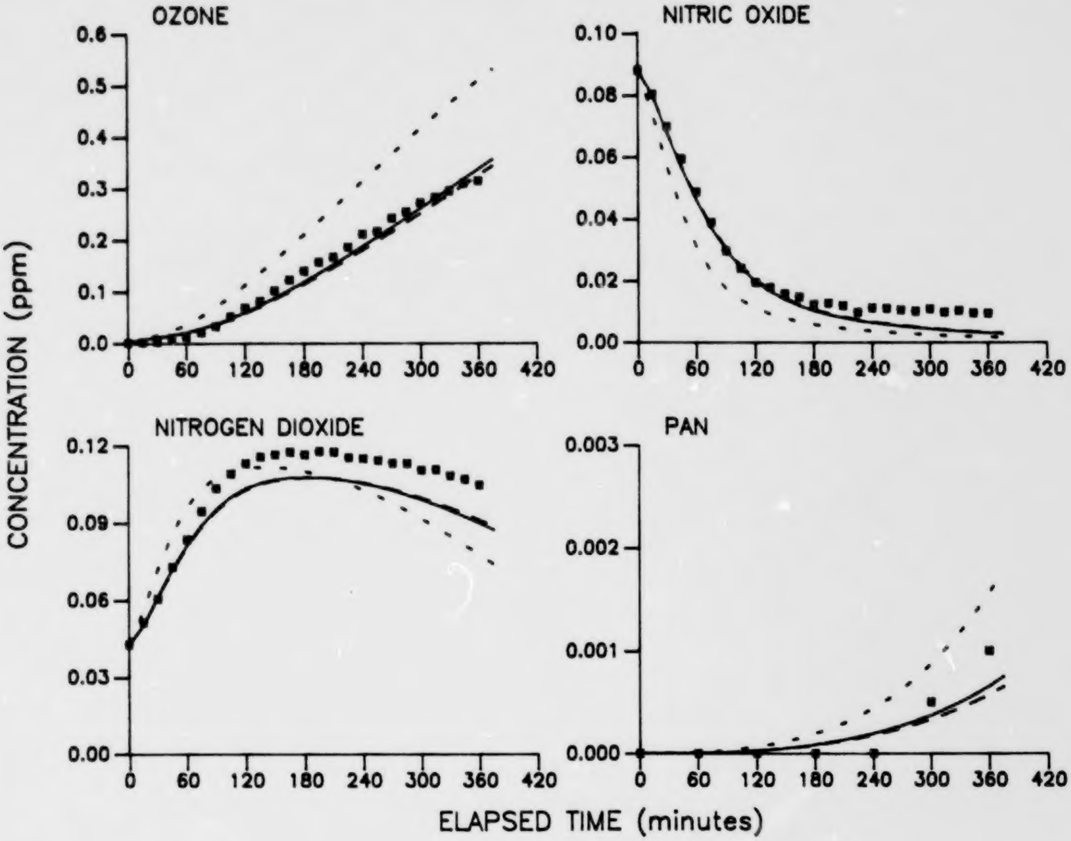

Figure 31. Experimental and Calculated Concentration-Time Plots for Selected Species in Simulations of n-Octane-NO_x Run ITC-552.

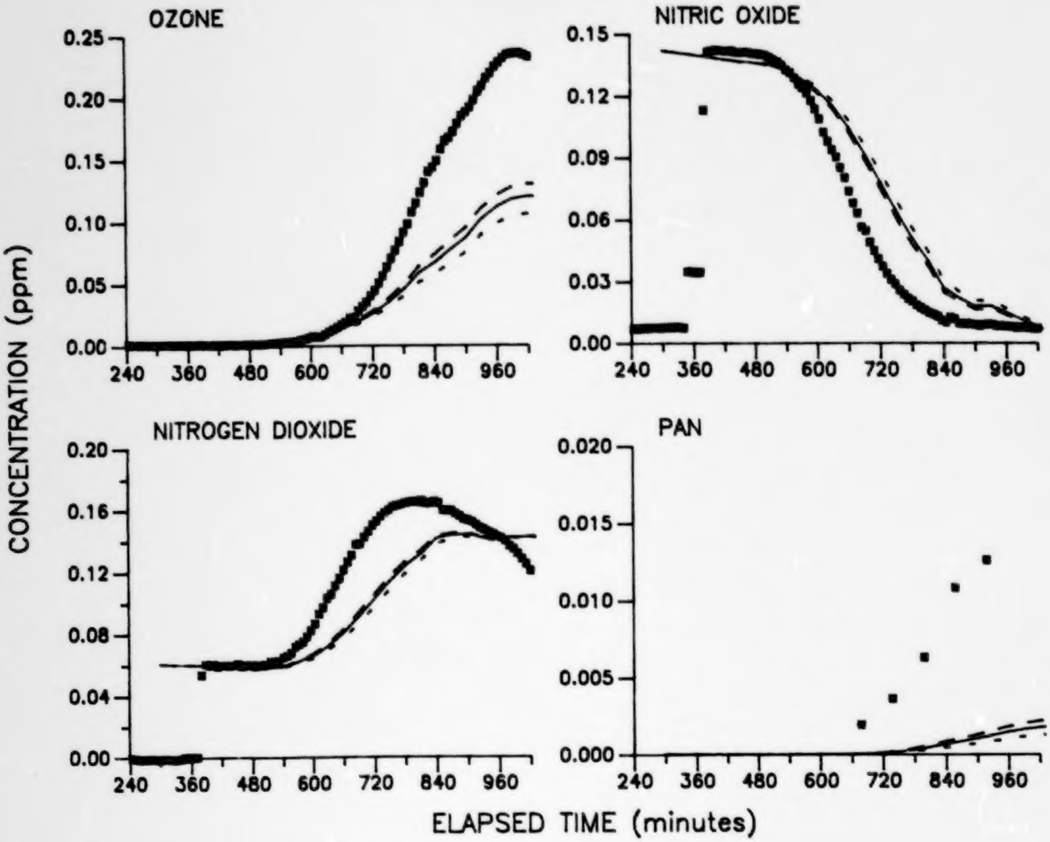

Figure 32. Experimental and Calculated Concentration-Time Plots for Selected Species in Simulations of UNC 2,3-Dimethylbutane -NO_x Run OC1789R.

We do not believe the large error in the results indicates that there is necessarily a problem in the mechanism because model simulations of alkane-NO_x runs are very sensitive to the chamber effects parameters. The variability in the chamber effects could account for a significant amount of the variability in the mechanism's predictions for alkane runs. As noted in previous evaluations (e.g., Carter et al., 1986), it is not possible to unambiguously evaluate the alkane portion of the mechanism on chamber data because of the uncertainties in chamber effects and variability. Therefore, within the limitations of the testing methodology, the alkane reactions appear to give acceptable predictions for ozone and the NO_x oxidation rate.

5.4.4 Aromatic-NO_x Runs

The model performance results for aromatic-NO_x runs are shown in Table 20 and in Figures 33 through 36. Typical simulations of runs employing benzene, toluene, m-xylene, o-xylene, or mesitylene are shown in Figures 37 through 42. The results indicate the RADM mechanism overpredicts the ozone yield in benzene and toluene runs by 22% and 24%, respectively, on the average. The mean error for the benzene and toluene runs are 22% and 33%, respectively. The mechanism performs better on xylene runs, with a mean bias and error of -4% and 18%. However, for the mesitylene runs, the mechanism underpredicts the maximum ozone by 39% on the average and has a mean error of 48%. This indicates the mechanism has a clear bias towards overpredicting ozone yields for the less reactive aromatic compounds and towards underpredicting ozone yields for the more reactive aromatic compounds. The biases in the rates of NO_x oxidation follow these same trends, although the discrepancy between the results for toluene and xylene is not as large. The results for other aromatic compounds are mixed. The mean biases on maximum ozone for tetralin and dimethyl naphthalene runs are small, each being -6%. However, the mean bias for naphthalene is +84%. This relatively poor level of performance for the other aromatics is not surprising since the mechanism was not designed with these types of compounds in mind. Overall, for all aromatic runs, the RADM mechanism predicts the maximum ozone with a low mean bias but a relatively high mean error.

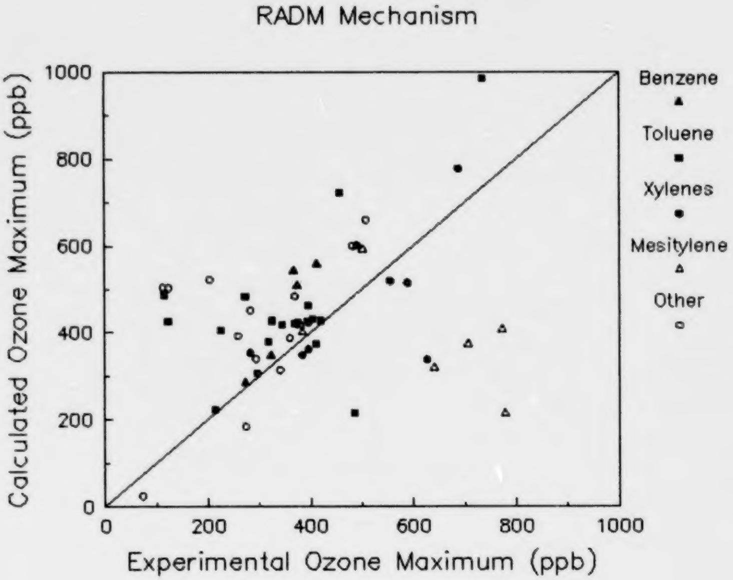

Figure 33. Calculated vs Experimental Maximum Ozone in the Aromatic-NO_x Runs for the RADM Mechanism.

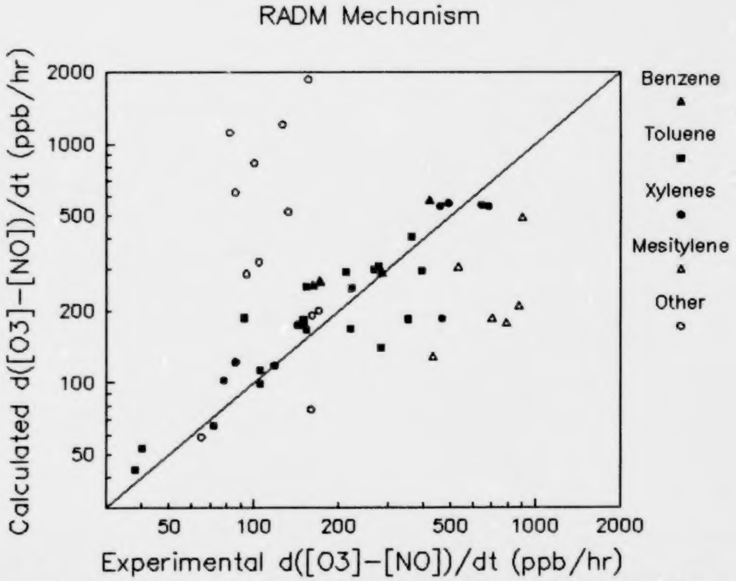

Figure 34. Calculated vs Experimental Rates of NO Oxidation and Ozone Formation in the Aromatic-NO_x Runs for the RADM Mechanism.

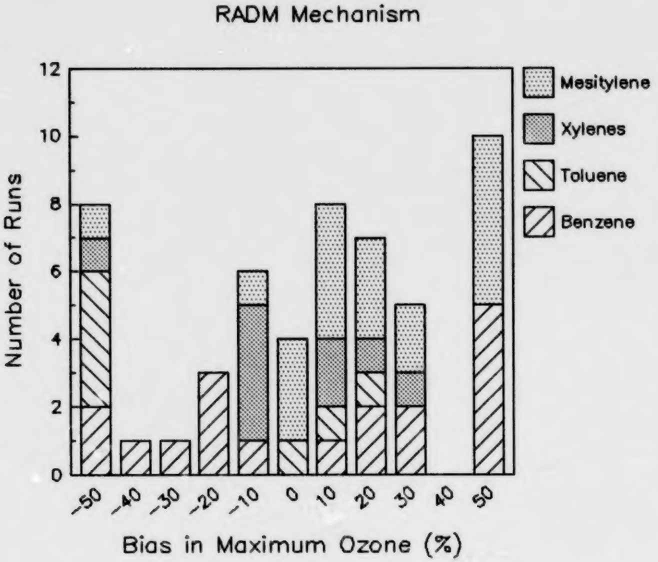

Figure 35. Histogram of Normalized Biases in Maximum Ozone in Aromatic Runs for the RADM Mechanism.

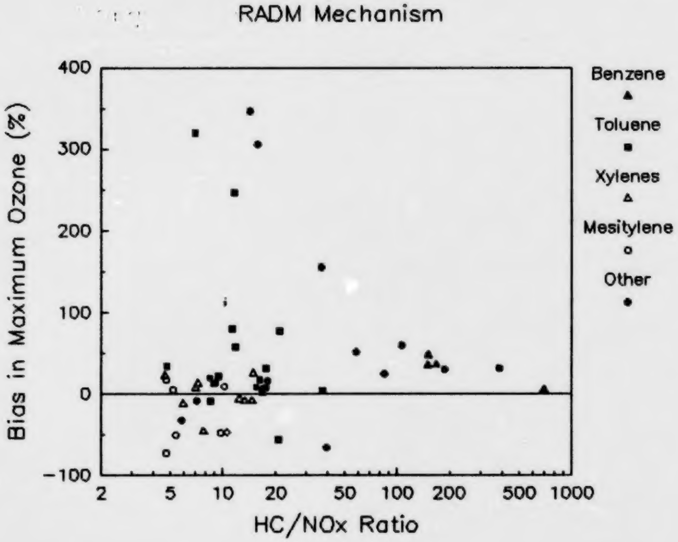

Figure 36. Normalized Bias in Maximum Ozone vs HC/NO_x in Aromatic Runs for the RADM Mechanism.

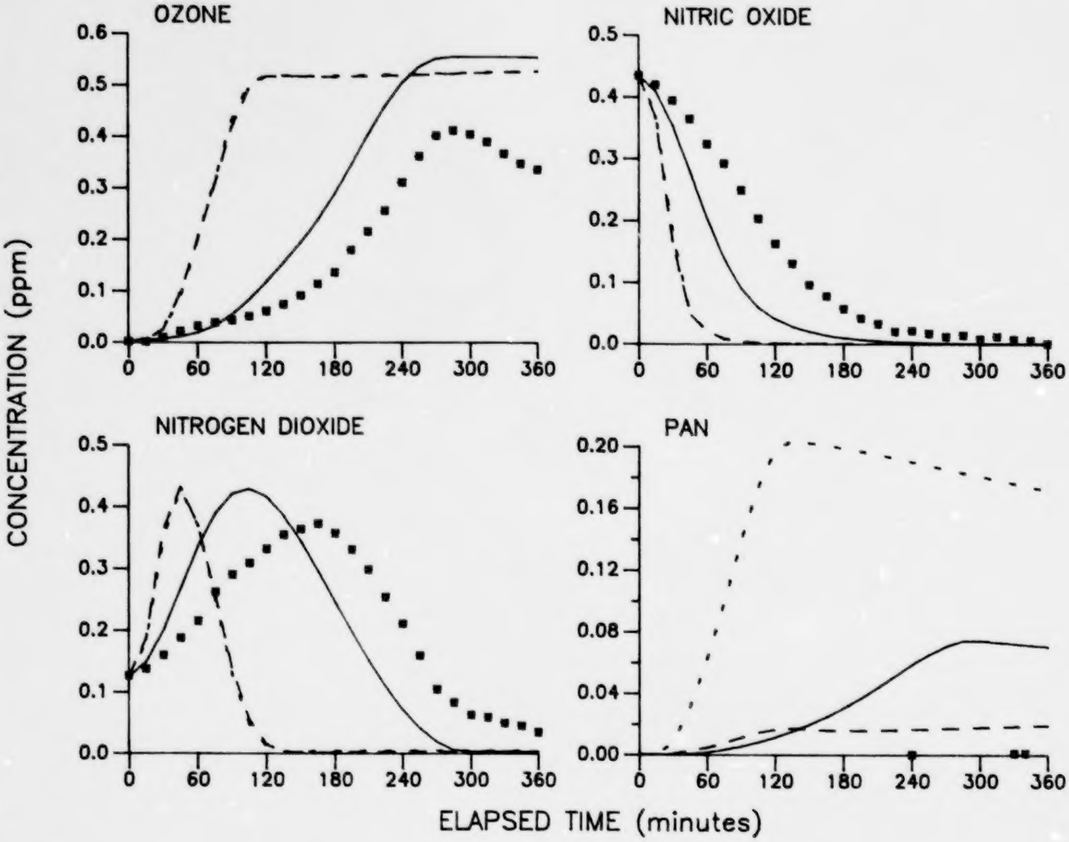

Figure 37. Experimental and Calculated Concentration-Time Plots for Selected Species in Simulations of the Benzene-NO_x Run ITC-562 (—— RADM, — — — RADM-P, - - - RADM-M).

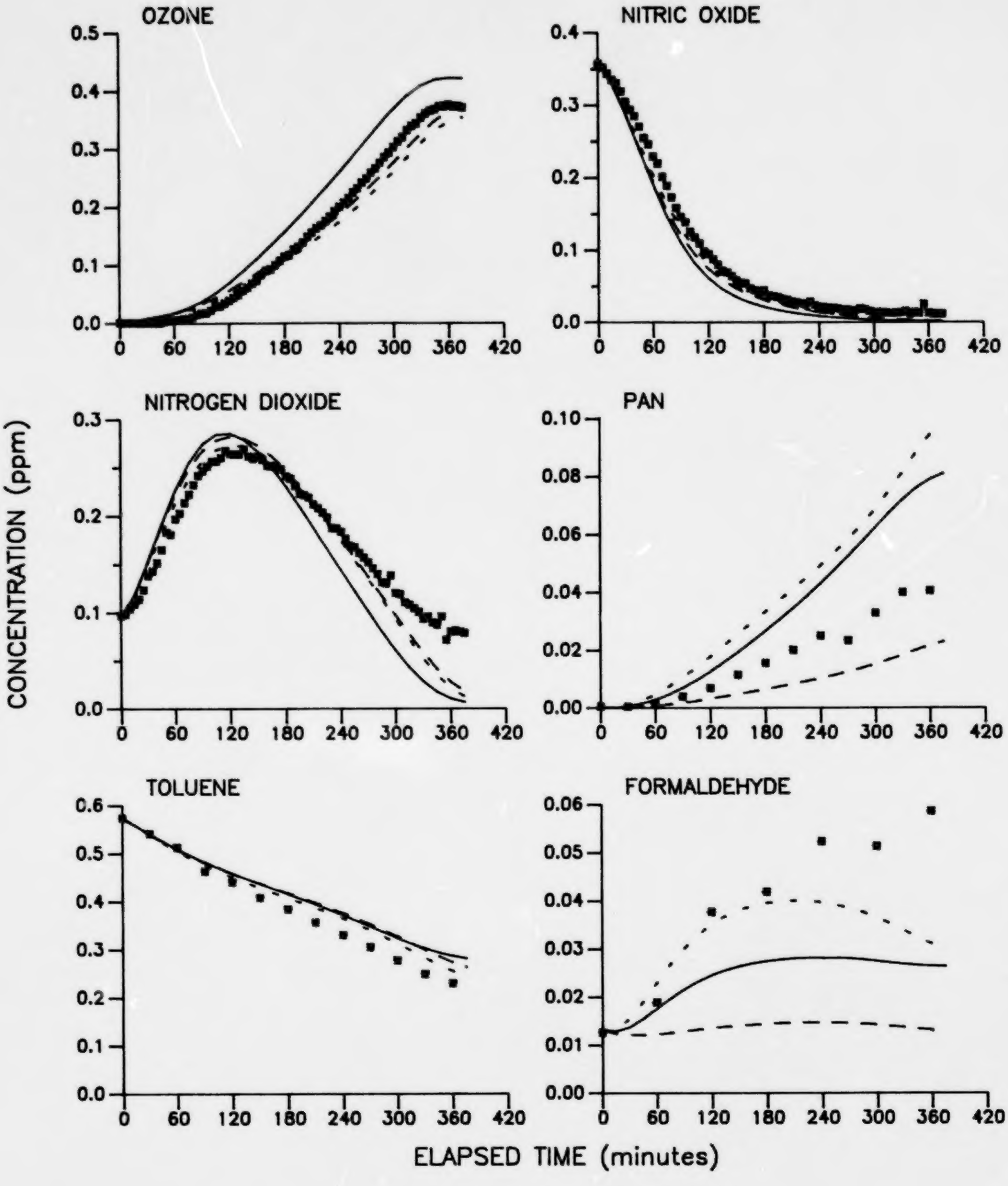

Figure 38. Experimental and Calculated Concentration-Time Plots for Selected Species in Simulations of the Toluene-NO_x Run EC-327.

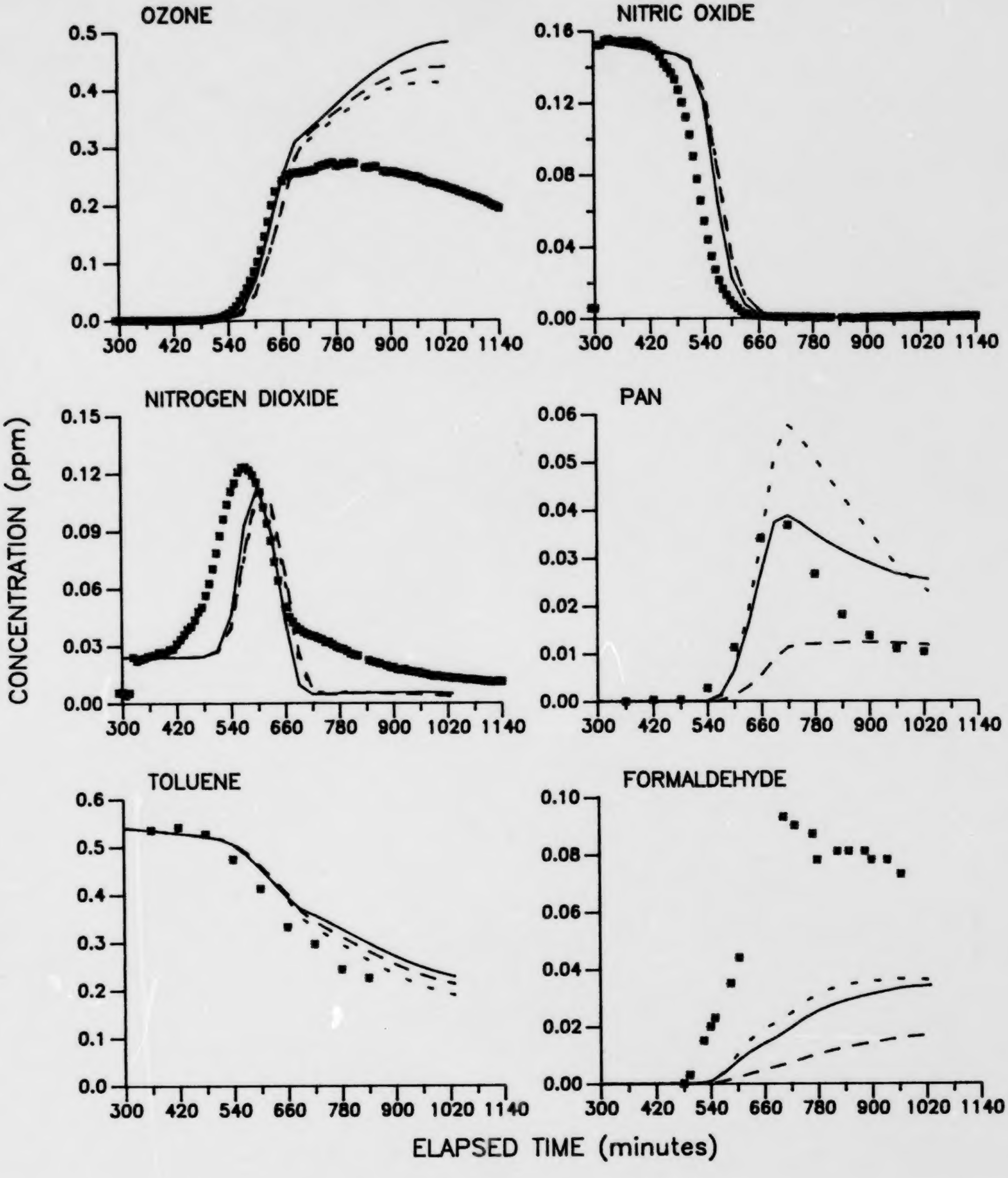

Figure 39. Experimental and Calculated Concentration-Time Plots for Selected Species in Simulations of the UNC Toluene-NO_x Run JL3080R.

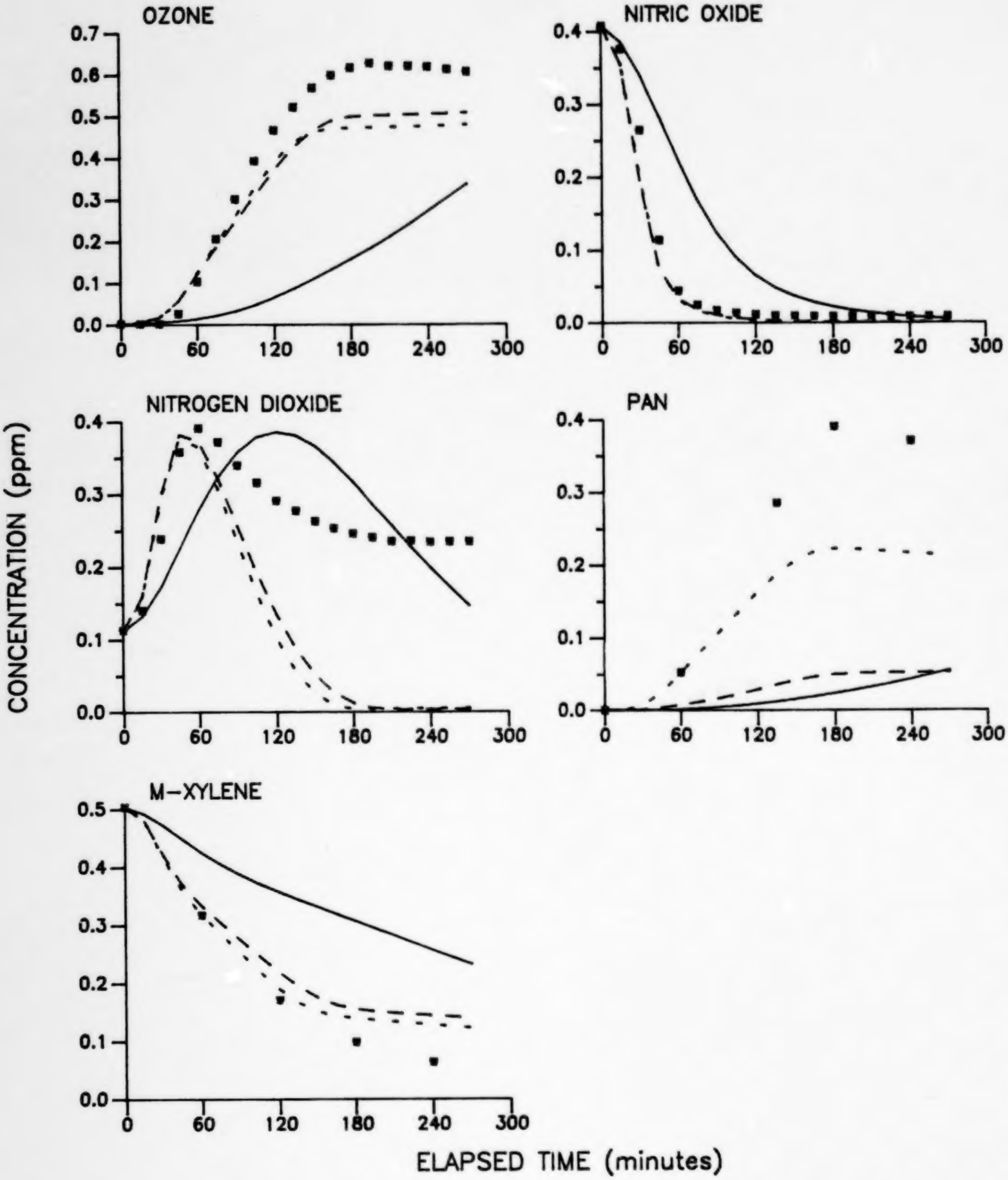

Figure 40. Experimental and Calculated Concentration-Time Plots for Selected Species in Simulations of the m-Xylene-NO_x Run ITC-702.

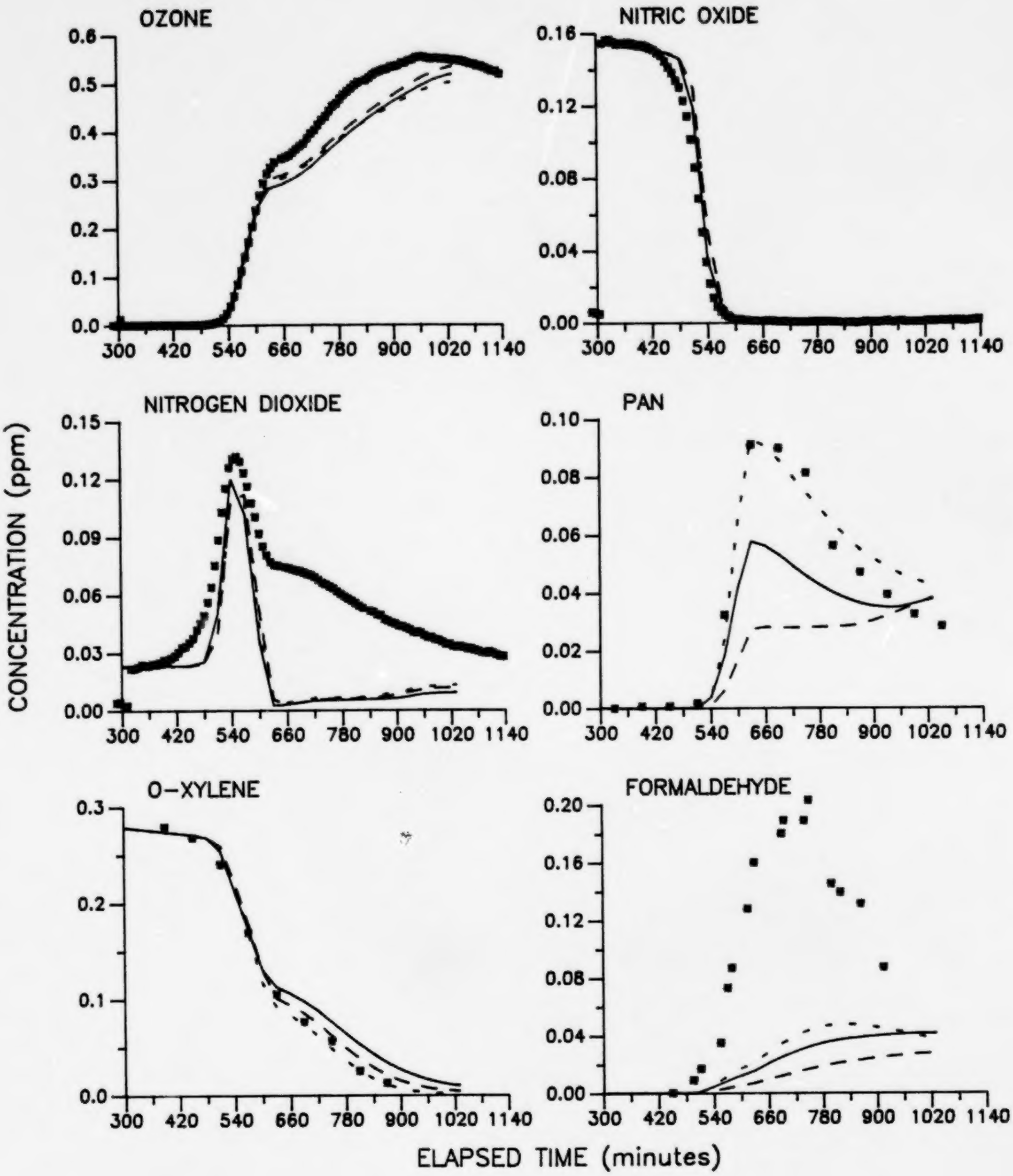

Figure 41. Experimental and Calculated Concentration-Time Plots for Selected Species in Simulations of the UNC o-Xylene-NO_x Run JL3080B.

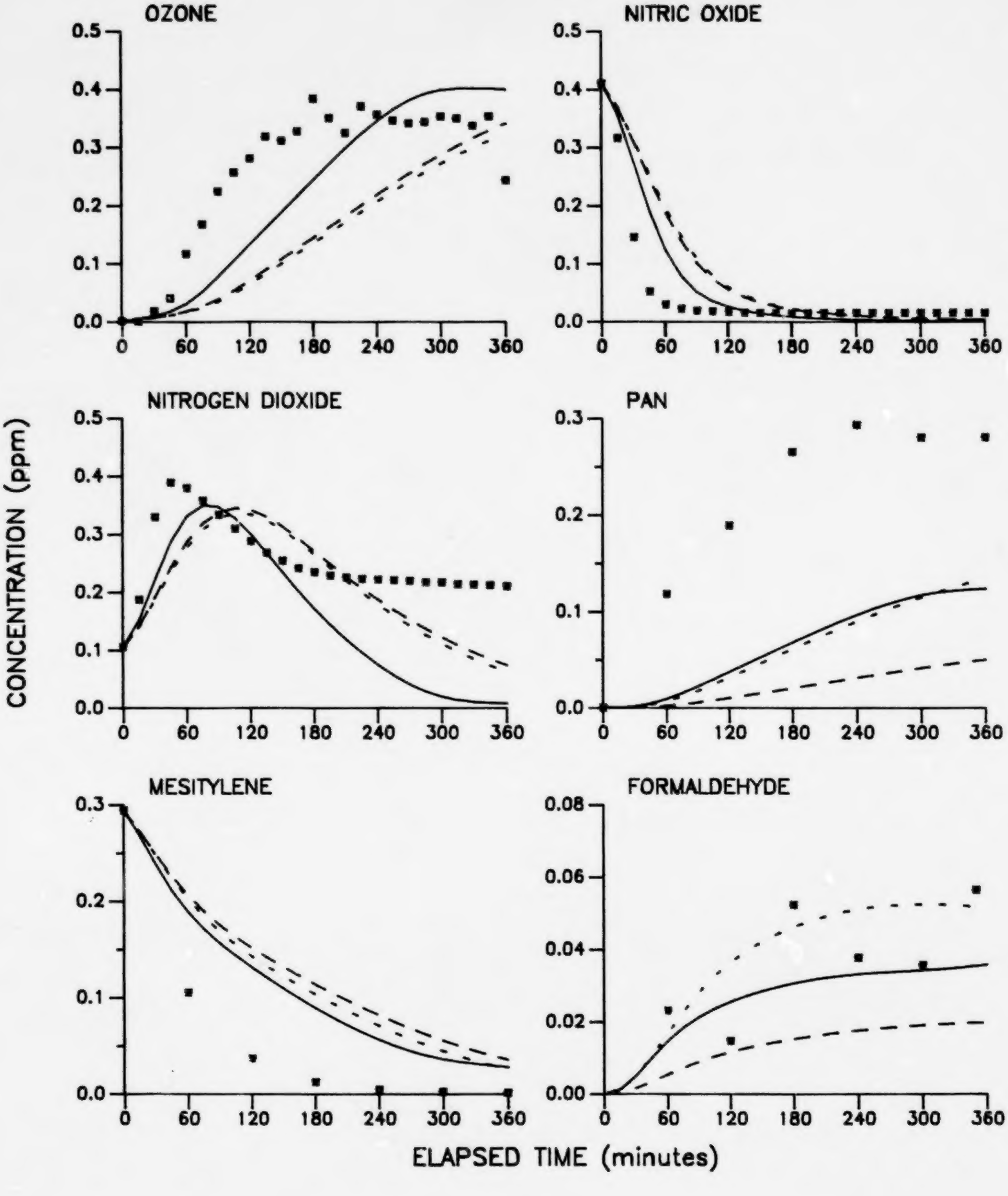

Figure 42. Experimental and Calculated Concentration-Time Plots for Selected Species in Simulations of the Mesitylene-NO_x Run EC-901.

Considering the uncertainties in the yields and subsequent reactions of the aromatic ring-opening products, this level of performance might be considered acceptable. However, unlike the alkanes, the modeling of aromatic runs should not be highly sensitive to uncertain chamber effects, and cases of generally poor performance can indicate problems with the mechanism. As discussed in Section 2, other mechanisms perform better in simulating results of these experiments, and there are several changes that can be made to the RADM aromatic mechanism which can reduce the error considerably and reduce the systematic bias in ozone yields between benzene and mesitylene. The modified RADM mechanisms, discussed in Section 5.7, perform better in simulating the results of these runs.

5.4.5 Natural Hydrocarbon Runs

The result of tests on experiments with two natural hydrocarbon species, isoprene and alpha-pinene, are shown in Table 20 and in Figures 43 through 46. Comparisons of predicted and observed concentration profiles for two isoprene runs and one alpha-pinene run are shown in Figures 47 through 49. Although there are some minor differences between the recommended modified and the March 1988 versions of the RADM mechanisms in their reactions of the natural hydrocarbons, these differences have no significant effect on the predictions for isoprene and only minor effects on predictions for alpha-pinene. (The most important difference is a slight change in the rate constant used for the reaction of ozone with OLI, the lumped model species which is used to represent alpha-pinene.) Therefore, the results discussed in this section are applicable to all three versions of the mechanism.

In the case of isoprene, the mechanism has a significant tendency to underpredict ozone yields, with an average bias of -42%. This level of performance does not meet the desired performance criteria. On the other hand, it has very little bias (-2%) in simulating the NO oxidation rate, and the error (26%) is only slightly higher than in the simulations of the propene runs. This mechanism represents isoprene explicitly, so in principle one should expect it to perform reasonably well in simulating this compound. However, although the RADM mechanism uses the appropriate rate constants for the initial atmospheric reactions of isoprene, it represents the products of these reactions with the same set of species

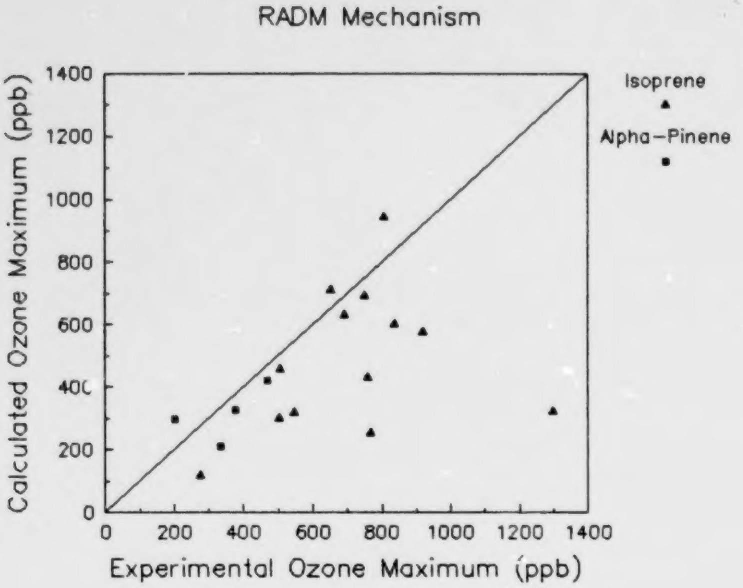

Figure 43. Calculated vs Experimental Maximum Ozone in the Natural Hydrocarbon Runs for the RADM Mechanism.

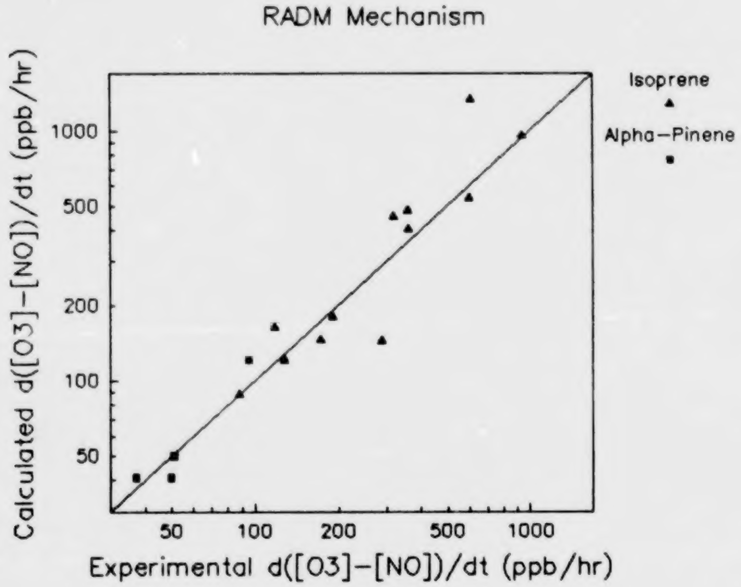

Figure 44. Calculated vs Experimental Rates of NO Oxidation and Ozone Formation in the Natural Hydrocarbon Runs for the RADM Mechanism.

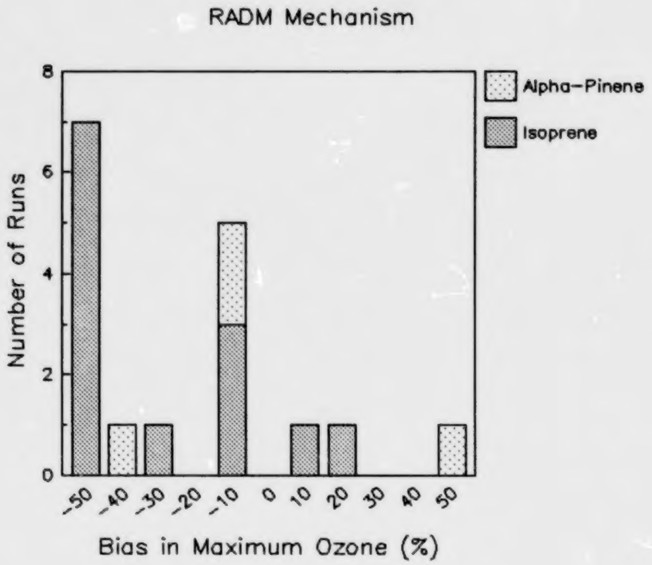

Figure 45. Histogram of Normalized Bias in Maximum Ozone in the Natural Hydrocarbon Runs for the RADM Mechanism.

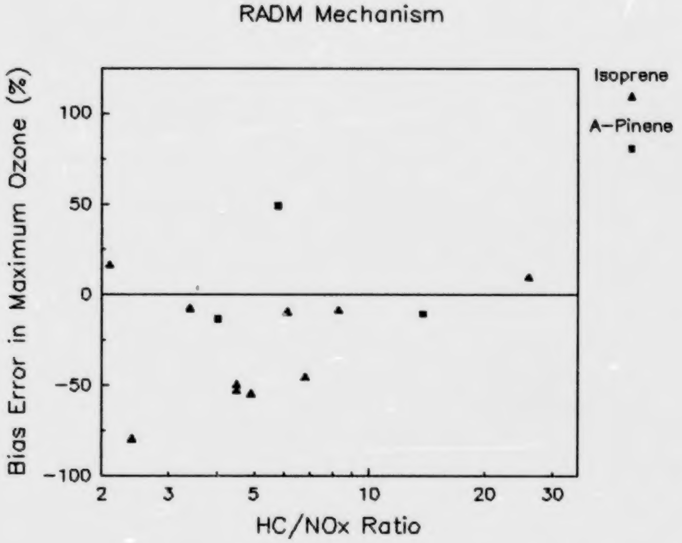

Figure 46. Normalized Bias in Maximum Ozone vs HC/NO$_x$ in the Natural Hydrocarbon for the RADM Mechanism.

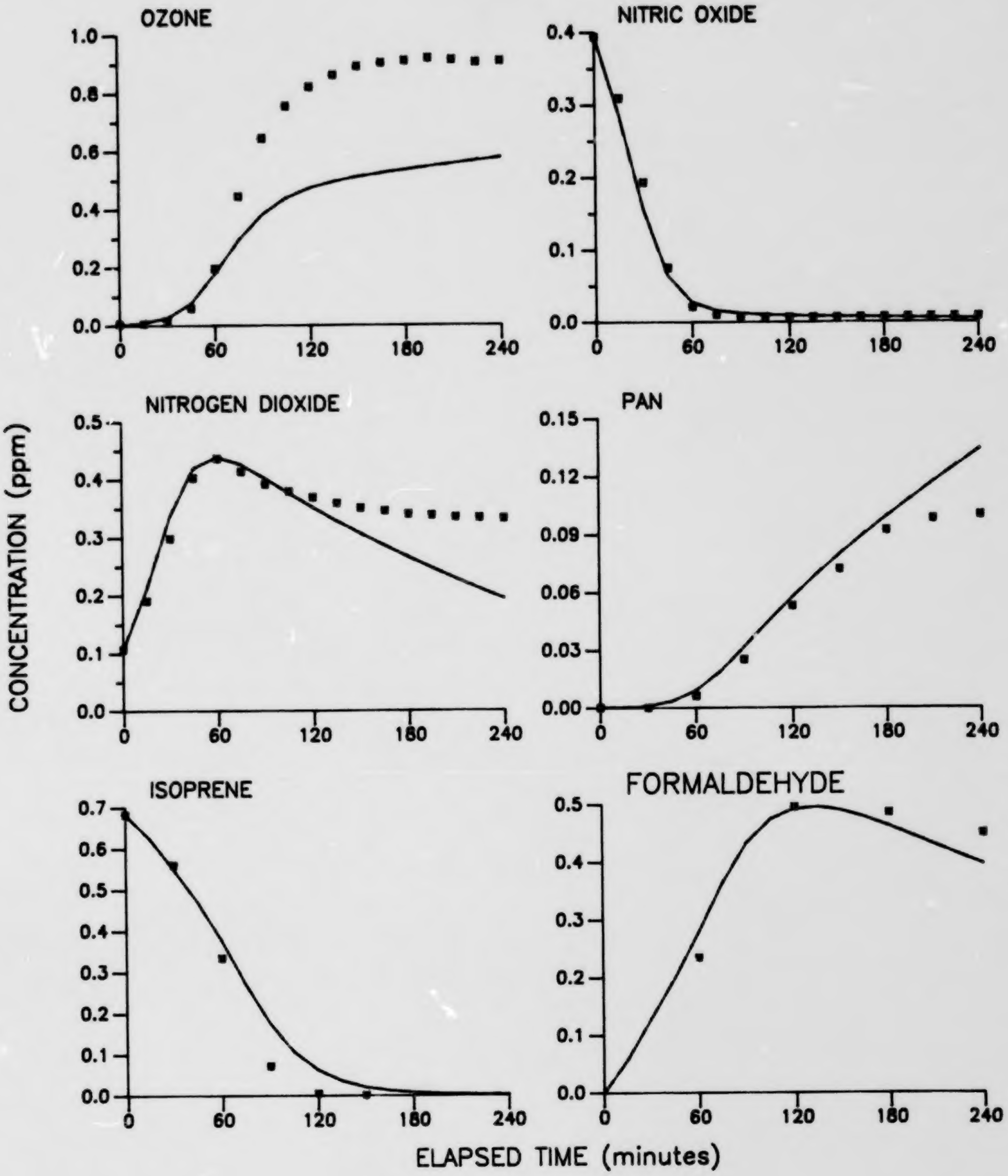

Figure 47. Experimental and Calculated Concentration-Time Plots for Selected Species in Simulations of the Isoprene-NO_x Run ITC-811.

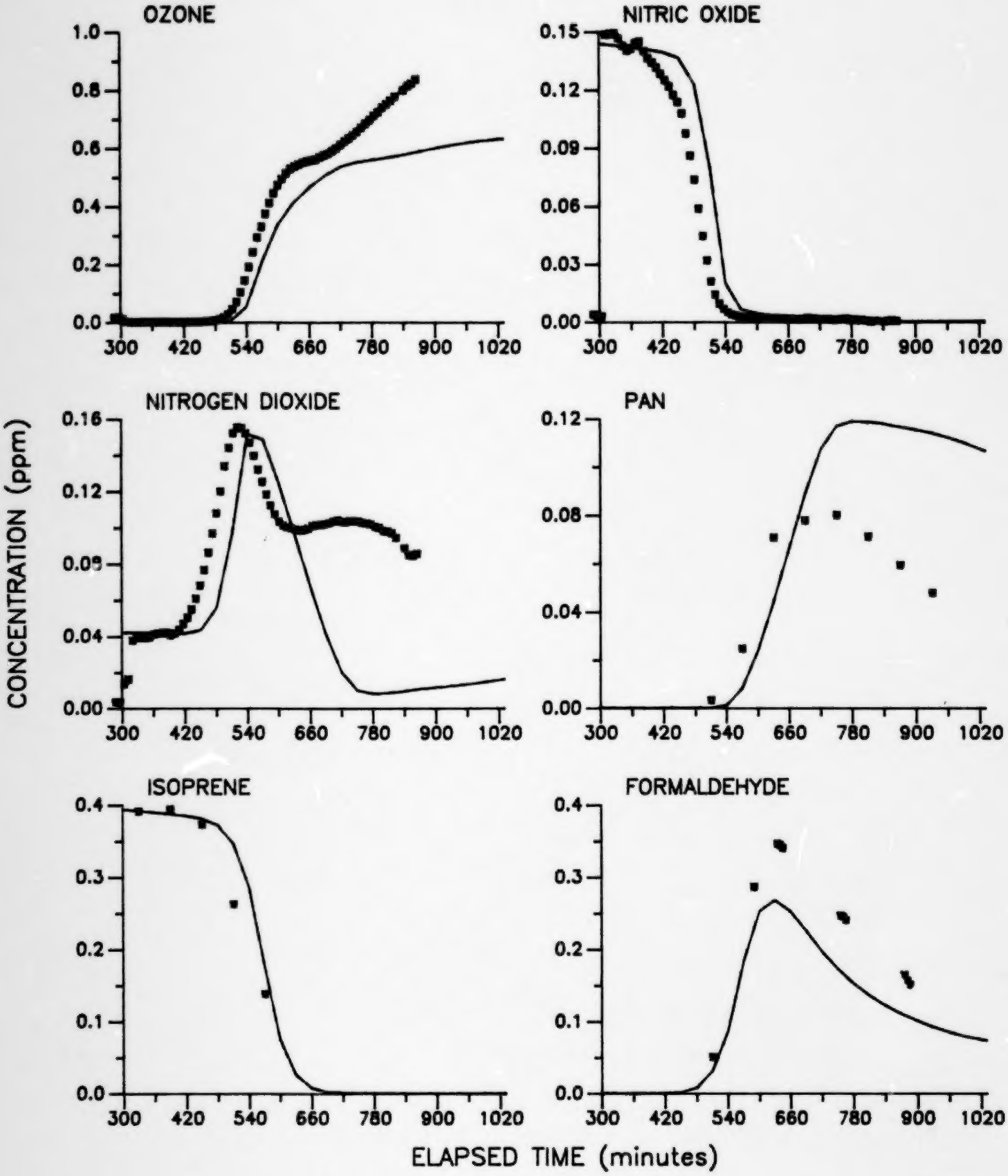

Figure 48. Experimental and Calculated Concentration-Time Plots for Selected Species in Simulations of the UNC Isoprene-NO_x Run JL1680B.

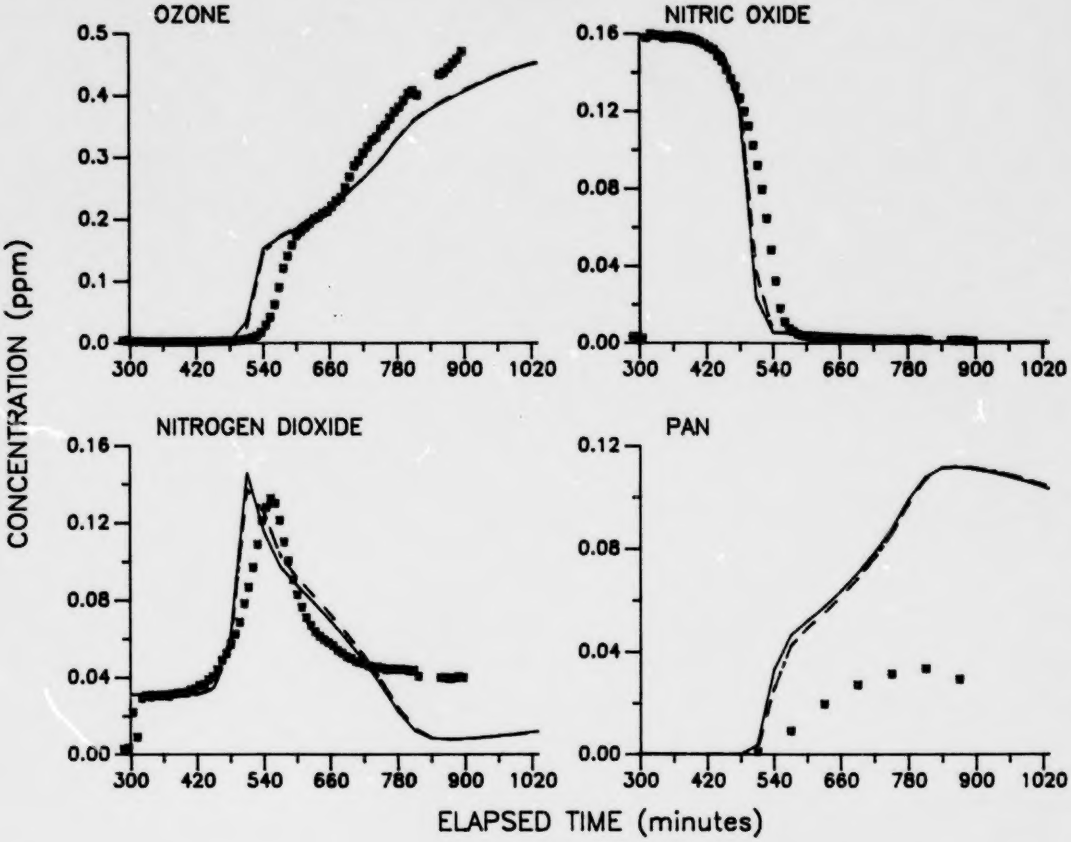

Figure 49. Experimental and Calculated Concentration-Time Plots for Selected Species in Simulations of the UNC α-Pinene-NO_x Run JL1580B.

used to represent the terminal alkenes. Preliminary results from our laboratories indicate that using mechanisms with more explicit representations of the reactions of isoprene's major products will result in somewhat better model performance, although there are still inconsistencies between the model and the data (Carter and Atkinson, unpublished SAPRC results). [In addition, approximately 40% of the products in the isoprene-OH reaction system have not been unidentified (Atkinson, unpublished SAPRC results).] Better performance of the RADM mechanism in simulating isoprene runs would probably require adding species to the mechanism to represent the reactions of isoprene's oxidation products, but the mechanism would still be uncertain.

The performance of the RADM mechanism in simulating the limited number of alpha-pinene runs, all carried out in the UNC chamber in July of 1980, is surprisingly good. The mean bias and error in the ozone maximum are -8% and 28%, respectively, while the bias and error in the NO oxidation rate are only +4% and 14%. (These four statistics are -8%, 27%, +2%, and 13%, respectively, for the RADM-P and RADM-M mechanisms.) This level of performance is perhaps fortuitous, since the atmospheric chemistry of alpha-pinene is not well understood and is represented by the same lumped model species (OLI) which is used to represent the internal olefins. Indeed, as discussed in Section 3.3, the rate constants and product yield parameters for this lumped species are derived based on analysis of anthropogenic emissions data, where the contribution of terpenes is negligible. Nevertheless, the alpha-pinene results for these four runs meet the desired performance criteria. Of course, these results do not necessarily indicate that the performance would be equally good for beta-pinene or the other terpenes.

5.4.6 Performance in Simulations of Formaldehyde Yields

Model performance statistics for the maximum formaldehyde concentrations are shown in Table 21. Comparisons of the individual calculated and experimental values for all of the single organic runs are shown in Figure 50. The maximum formaldehyde concentrations are underpredicted on the average in carbonyl, aromatic, and natural hydrocarbon runs and overpredicted by small amounts on the average in alkene and alkane runs. The mean errors in the prediction are large: on the order of 30 to 80% for most types of runs. Thus, there clearly is a

Table 21. Performance Statistics on Maximum Formaldehyde in the Simulations of the Organic-NO_x-Air Runs Using the RADM Mechanism

Compound or Mixture	No. Runs	Experimental(a) Avg. (sdev)	Absolute(a) Bias	Absolute(a) Err.	Normalized Bias (%)	Normalized Err. (%)
Acetaldehyde	5	0.17 (0.15)	-0.05	0.07	-5 (56)	44
Propionaldehyde	2	0.10 (0.01)	0.01	0.01	10 (17)	12
Ethene	14	0.86 (0.41)	-0.02	0.23	-9 (41)	34
Propene	39	0.36 (0.20)	0.00	0.10	4 (45)	33
1-Butene	8	0.32 (0.27)	0.10	0.10	21 (18)	22
trans-2-Butene	4	0.08 (0.06)	0.04	0.06	60 (58)	71
Isobutene	1	0.64	-0.02	0.02	-3	3
1-Hexene	4	0.33 (0.27)	0.30	0.30	76 (33)	76
Isoprene	13	0.30 (0.16)	0.01	0.12	-6 (59)	46
a-Pinene	2	0.08 (0.04)	-0.01	0.01	-24 (12)	24
n-Butane	21	0.04 (0.03)	0.01	0.03	35 (73)	70
C4+ Br. Alkane	5	0.03 (0.02)	-0.02	0.02	-75 (68)	91
C5+ n-Alkane	10	0.01 (0.01)	-0.01	0.01	-26 (110)	95
Cycloalkane	4	0.07 (0.12)	-0.06	0.06	-32 (133)	101
Toluene	20	0.09 (0.09)	-0.04	0.04	-48 (56)	54
Xylene	10	0.09 (0.05)	-0.05	0.05	-71 (51)	76
Mesitylene	8	0.09 (0.04)	-0.05	0.05	-75 (45)	75
Naphthalene	5	0.01 (0.01)	0.02	0.02	100 (64)	100
Simple Mixtures	34	0.25 (0.20)	0.02	0.09	-14 (56)	47
Simple Surrogates	7	0.13 (0.05)	-0.05	0.06	-45 (45)	56
SAPRC 7-HC Surgs.	11	0.38 (0.23)	0.09	0.09	18 (18)	21
SAPRC 8-HC Surgs.	82	0.18 (0.12)	-0.02	0.05	-1 (47)	35
UNC "Synurban"	11	0.12 (0.04)	-0.05	0.05	-55 (18)	55
UNC "Synauto"	13	0.16 (0.08)	0.02	0.03	13 (31)	24
UNC Auto Exhaust	28	0.18 (0.10)	-0.10	0.10	-68 (31)	70
Syn. Jet Fuel	8	0.05 (0.03)	-0.03	0.03	-58 (62)	67

(a) Concentrations in ppm.

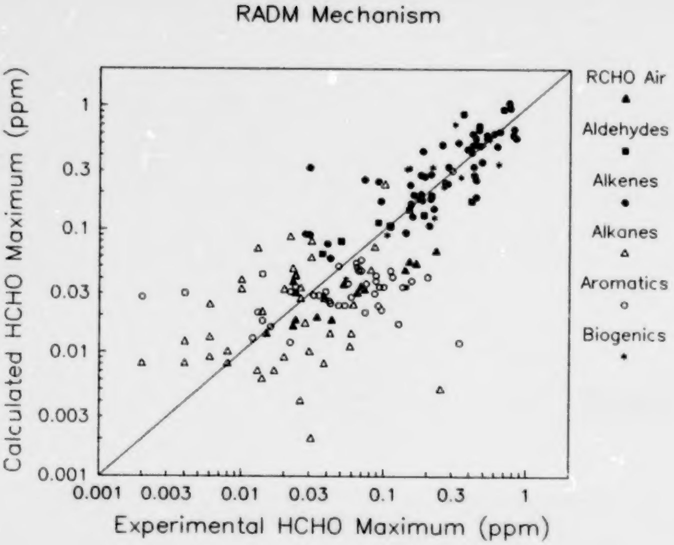

Figure 50. Calculated vs Experimental Maximum Formaldehyde in the Single Organic-NO_x Runs for the RADM Mechanism.

large amount of scatter in the formaldehyde predictions. While the accuracy of the measurements is questionable, especially at the low levels observed in some runs, it is unlikely that this is the primary cause of the poor comparisons in all cases. Formaldehyde is difficult to predict because it is both formed and destroyed in the photooxidation cycle. The RADM mechanism and other mechanisms (e.g., Carter et al., 1986) are not able to reproduce the observed formaldehyde levels well. If the same desired performance criteria that were used for ozone and rate of NO_x oxidation were used for formaldehyde, the mechanism would clearly be rejected. Fortunately, accurate prediction of formaldehyde is not the primary purpose of the mechanism.

5.4.7 Performance in Simulations of PAN Yields

Model performance statistics for the maximum PAN concentrations are shown in Table 22, and comparisons of the individual calculated and experimental values for all of the single organic runs are shown in Figure 51. These results show that the RADM mechanism predicts PAN well

Table 22. Performance Statistics on Maximum PAN in the Simulations of the Organic-NO_x-Air Runs Using the RADM Mechanism

Compound or Mixture	No. Runs	Experimental(a) Avg.	(sdev)	Absolute(a) Bias	Err.	Normalized Bias (%)		Err. (%)
Acetaldehyde	5	0.141	(0.088)	-0.002	0.020	-1	(18)	14
Propionaldehyde	2	0.052	(0.036)	0.129	0.129	110	(63)	110
Methylethylketone	1	0.070		-0.001	0.001	-1		1
Propene	46	0.142	(0.084)	0.044	0.051	28	(39)	34
1-Butene	7	0.039	(0.016)	0.054	0.055	64	(54)	69
trans-2-Butene	4	0.080	(0.044)	-0.004	0.014	-14	(25)	21
Isobutene	1	0.137		0.141	0.141	68		68
Isoprene	12	0.133	(0.082)	-0.029	0.080	-19	(85)	61
n-Butane	21	0.296	(1.012)	-0.257	0.294	17	(104)	89
C4+ Br. Alkane	6	0.226	(0.506)	-0.207	0.224	-44	(123)	104
C5+ n-Alkane	11	0.247	(0.814)	-0.243	0.247	7	(126)	98
Toluene	20	0.051	(0.036)	0.019	0.037	39	(65)	61
Xylene	10	0.125	(0.102)	-0.041	0.043	-24	(47)	26
Mesitylene	8	0.407	(0.189)	-0.317	0.317	-124	(40)	124
2,3-Dimethylnaph.	4	0.046	(0.019)	-0.001	0.015	-2	(44)	33
Simple Mixtures	38	0.081	(0.059)	0.018	0.033	14	(56)	48
Simple Surrogates	32	0.048	(0.020)	0.004	0.018	12	(57)	39
SAPRC 7-HC Surgs.	11	0.095	(0.047)	0.035	0.035	33	(13)	33
SAPRC 8-HC Surgs.	68	0.044	(0.030)	0.039	0.040	66	(34)	67
UNC Misc. Surgs.	12	0.055	(0.046)	0.007	0.024	33	(69)	55
UNC "Synurban"	10	0.024	(0.024)	0.012	0.012	48	(30)	49
UNC "Synauto"	15	0.054	(0.039)	0.014	0.029	30	(43)	44
UNC Auto Exhaust	28	0.047	(0.029)	-0.003	0.009	-14	(55)	36
Syn. Jet Exhaust	4	0.080	(0.031)	0.098	0.098	78	(13)	78

(a) Concentrations in ppm.

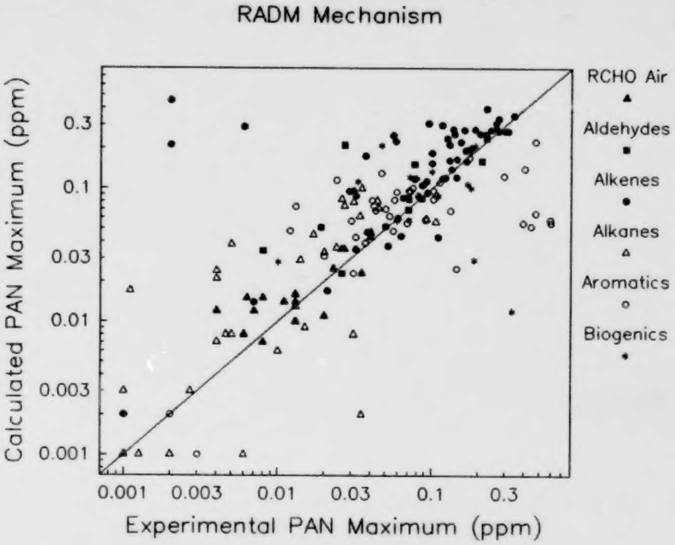

Figure 51. Calculated vs Experimental Maximum PAN in the Single Organic-NO_x Runs for the RADM Mechanism.

in acetaldehyde runs, but poorly in most other runs. The model overpredicts the PAN concentrations in most but not all types of runs, and there is also a large amount of scatter in the PAN predictions. The graphical comparisons confirm this. Cases of positive bias are at least partially explained by the fact that PAN is used in the mechanism as a surrogate for PAN plus many analogous organic peroxyacyl nitrate species. However, this is not expected to be a factor for the propene, isobutene and toluene runs. On the other hand, PAN is significantly underpredicted in the mesitylene runs, and is slightly underpredicted in the trans-2-butene, xylene, isoprene, and C4+ branched alkane runs (though with large mean errors in the latter two cases.) If the same desired performance criteria that were used for ozone and rate of NO_x oxidation were used for PAN, the mechanism would clearly be rejected. Given the partial mismatch between the species that mechanism predicts and what is measured, this criteria is probably too strict.

5.5 Performance of the RADM Mechanism on Runs with Organic Mixtures

Model performance statistics for maximum ozone and the NO oxidation rate for the March 1988 RADM mechanism are shown in Table 20 for the runs containing mixtures of organics. Run-by-run listings of these results are given in Appendix A. Graphical displays of these results are shown in Figure 52 through 55 for the simple mixture runs, and in Figures 56 through 61 for the complex and surrogate mixture runs. Concentration versus time profiles for a typical simple mixture run are shown in Figure 62, and similar plots are shown in Figures 63 through 75 for a variety of representative complex mixture simulations, including several multi-day simulations of ITC and OTC experiments. [These plots employ the same notation as those in the previous section -- the "*" symbols designate experimental data, solid lines designate data calculated using the March 1988 RADM mechanism, longer dashed lines designate results for the RADM-P mechanism, and shorter dashed lines are results for the RADM-M mechanism.] The results discussed in this section are applicable only to the March 1988 RADM mechanism, though the performance of the modified mechanisms in simulating experiments not containing aromatics are similar.

The results for the simple mixture runs show the mechanism tends to underpredict the maximum ozone by 12% on the average with a mean error of 34%. The NO_x oxidation rates are underpredicted by a similar amount on the average in these runs. The results for the surrogate mixture runs show overprediction of the maximum ozone by approximately 10% on the average with a mean error of approximately 20%. The mean bias and errors in the NO oxidation rates for these runs are slightly better than this on the average.

Since this data set has over 200 experiments for mixtures that include a wide range of organic compounds and range of hydrocarbon and NO_x concentrations, the evaluation statistics are fairly robust. The model performance statistics for ozone and NO_x oxidation rate are good, especially for the surrogate mixture runs. The mean error in ozone in the surrogate mixture simulations is less than that for most of the single organic compound simulations -- particularly the aromatics and alkanes. This suggests that there are some compensating errors in the mechanism, which is true of most photochemical reaction mechanisms. (Also, for runs with mixtures of organics, any error in the mechanism for any particular

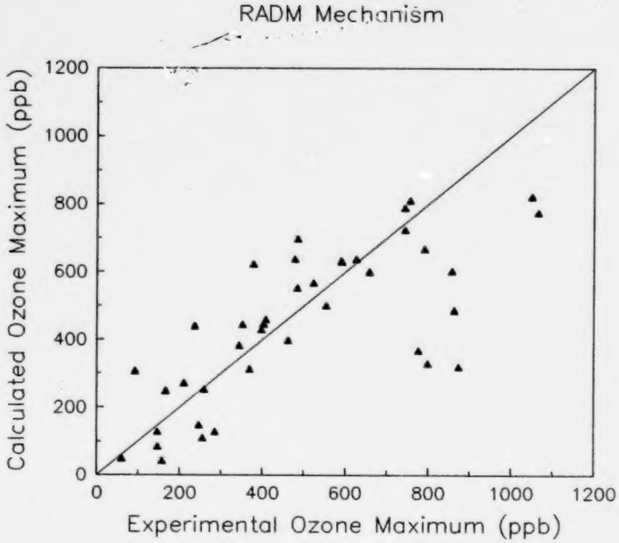

Figure 52. Calculated vs Experimental Maximum Ozone in the Simple Mixture Runs for the RADM Mechanism.

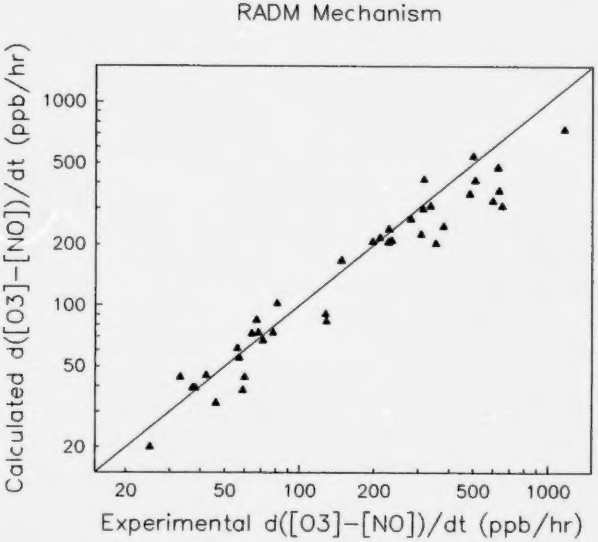

Figure 53. Calculated vs Experimental Rates of NO Oxidation and Ozone Formation in the Simple Mixture Runs for the RADM Mechanism.

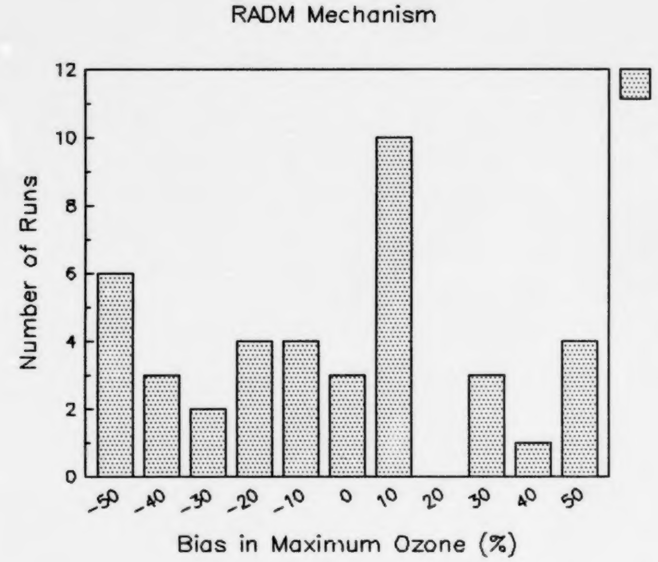

Figure 54. Histogram of Normalized Biases in Maximum Ozone in the Simple Mixture Runs for the RADM Mechanism.

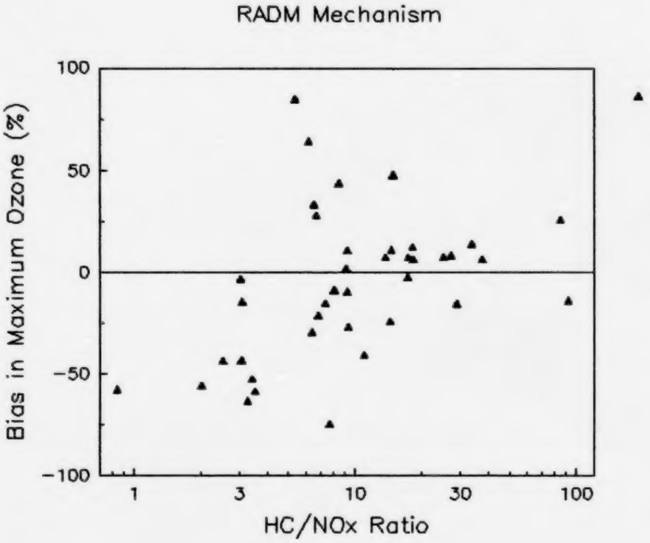

Figure 55. Normalized Bias in Maximum Ozone vs HC/NO_x in the Simple Mixture Runs for the RADM Mechanism.

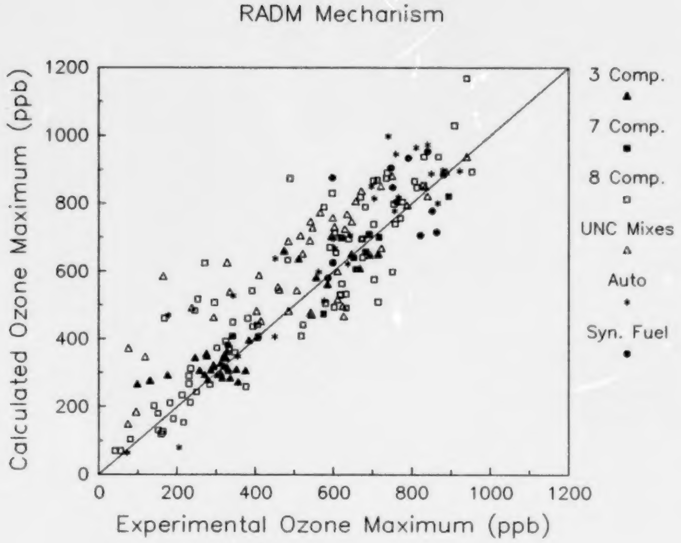

Figure 56. Calculated vs Experimental Maximum Ozone in the Surrogate Mixture Runs for the RADM Mechanism.

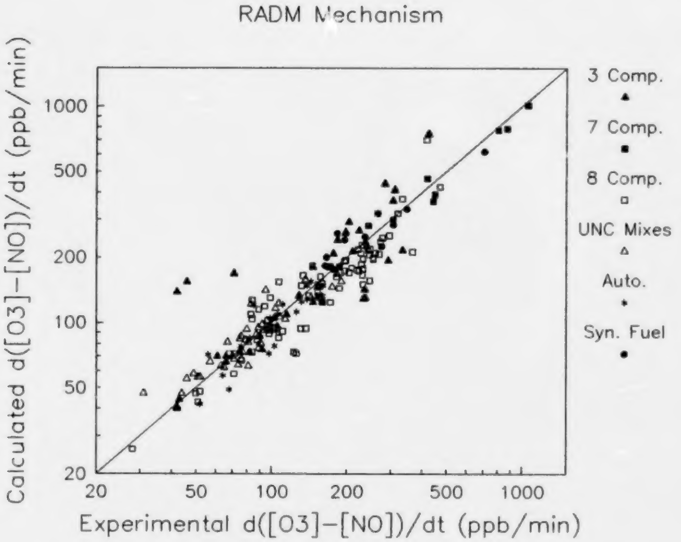

Figure 57. Calculated vs Experimental Rates of NO Oxidation and Ozone Formation in the Surrogate Mixture Runs for the RADM Mechanism.

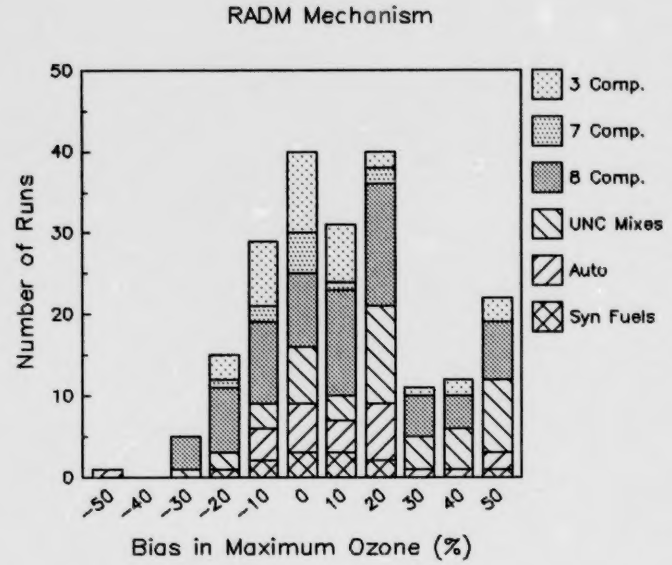

Figure 58. Histogram of Normalized Biases in Maximum Ozone in the Surrogate Mixture Runs for the RADM Mechanism.

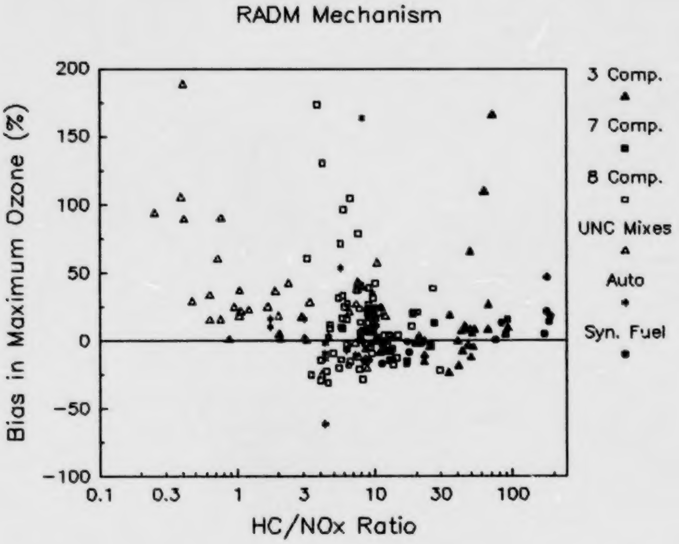

Figure 59. Normalized Bias in Maximum Ozone vs HC/NO_x in the Surrogate Mixture Runs for the RADM Mechanism.

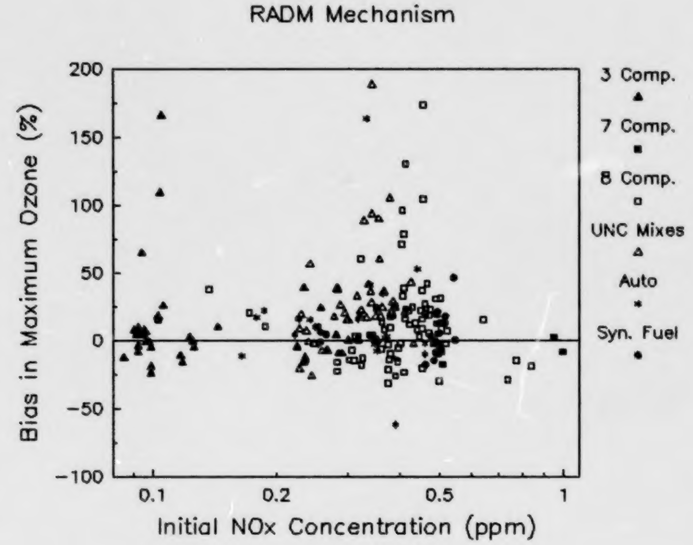

Figure 60. Normalized Bias in Maximum Ozone vs Initial NO_x in the Surrogate Mixture Runs for the RADM Mechanism.

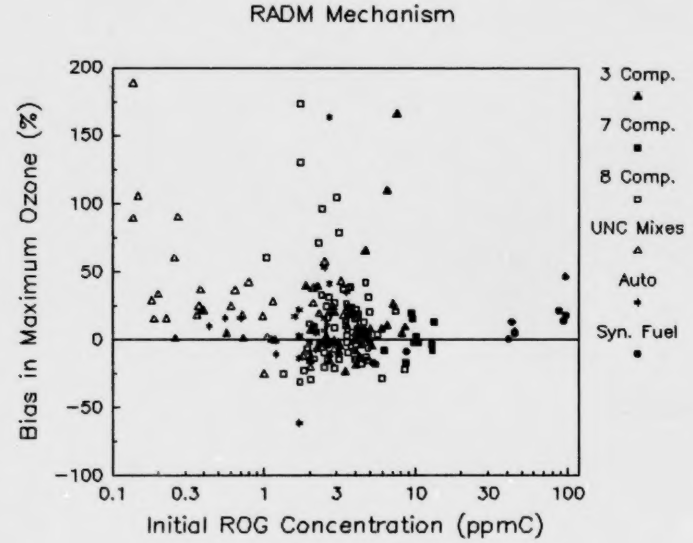

Figure 61. Normalized Bias in Maximum Ozone vs Initial HC in the Surrogate Mixture Runs for the RADM Mechanism.

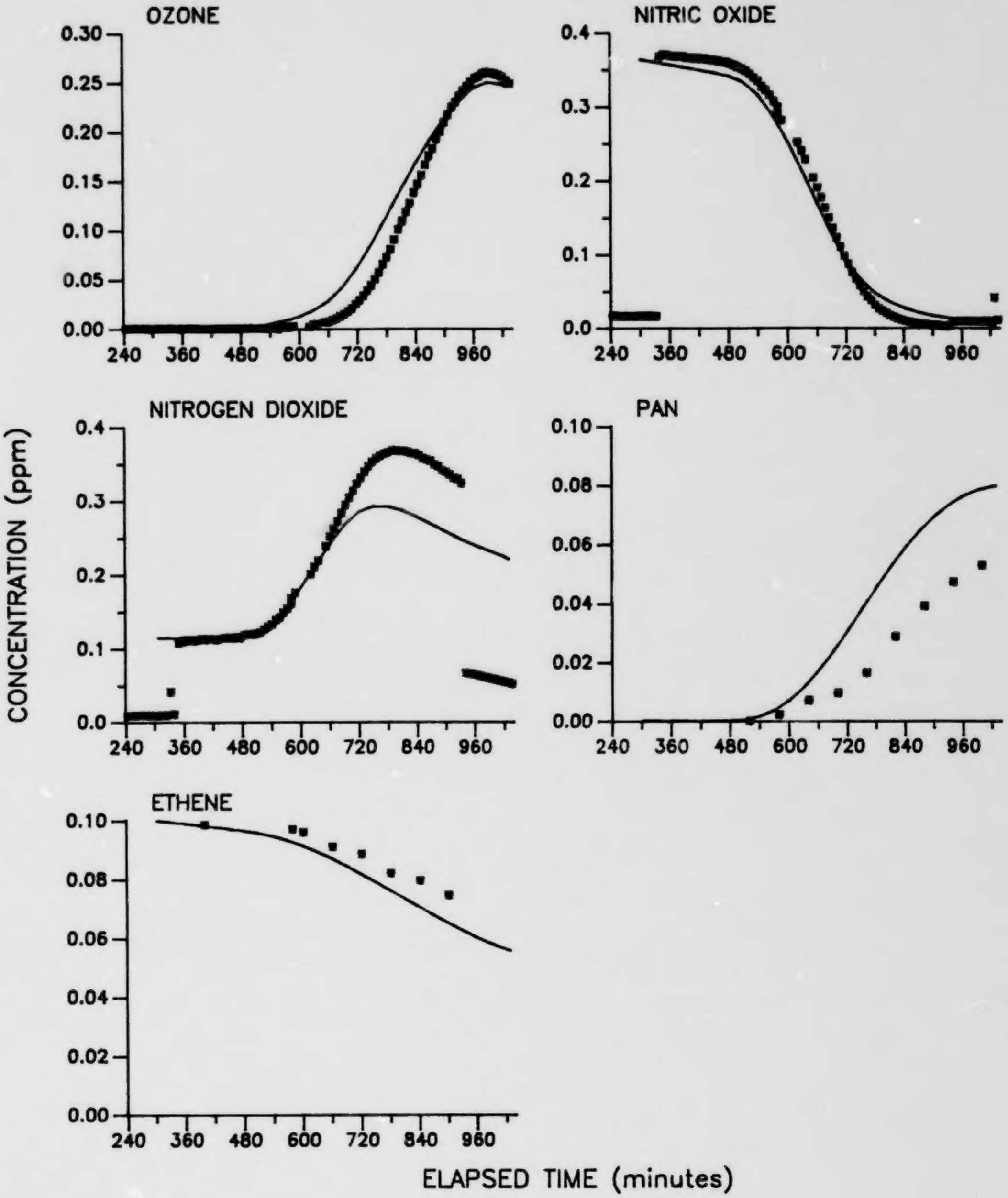

Figure 62. Experimental and Calculated Concentration-Time Plots for Selected Species in Simulations of the UNC Mixed Alkene Run OC1278R.

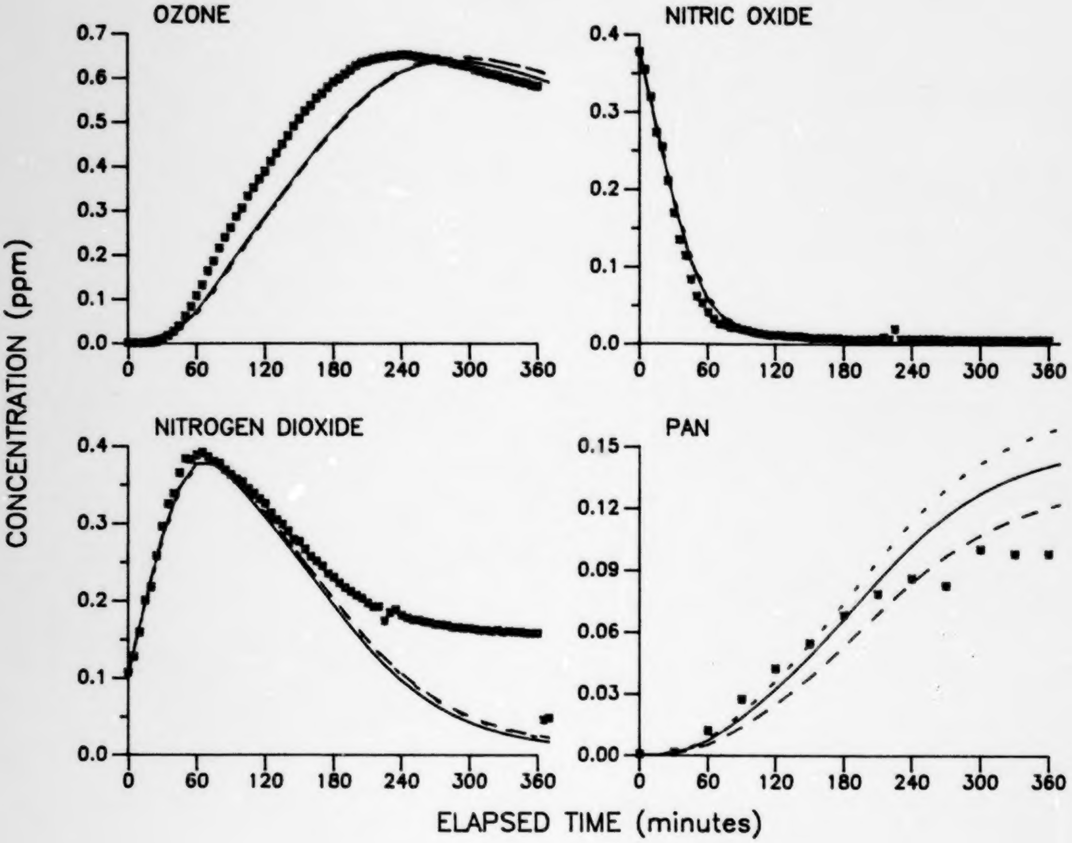

Figure 63. Experimental and Calculated Concentration-Time Plots for Selected Species in Simulations of the 7 Hydrocarbon Surrogate Run EC-237.

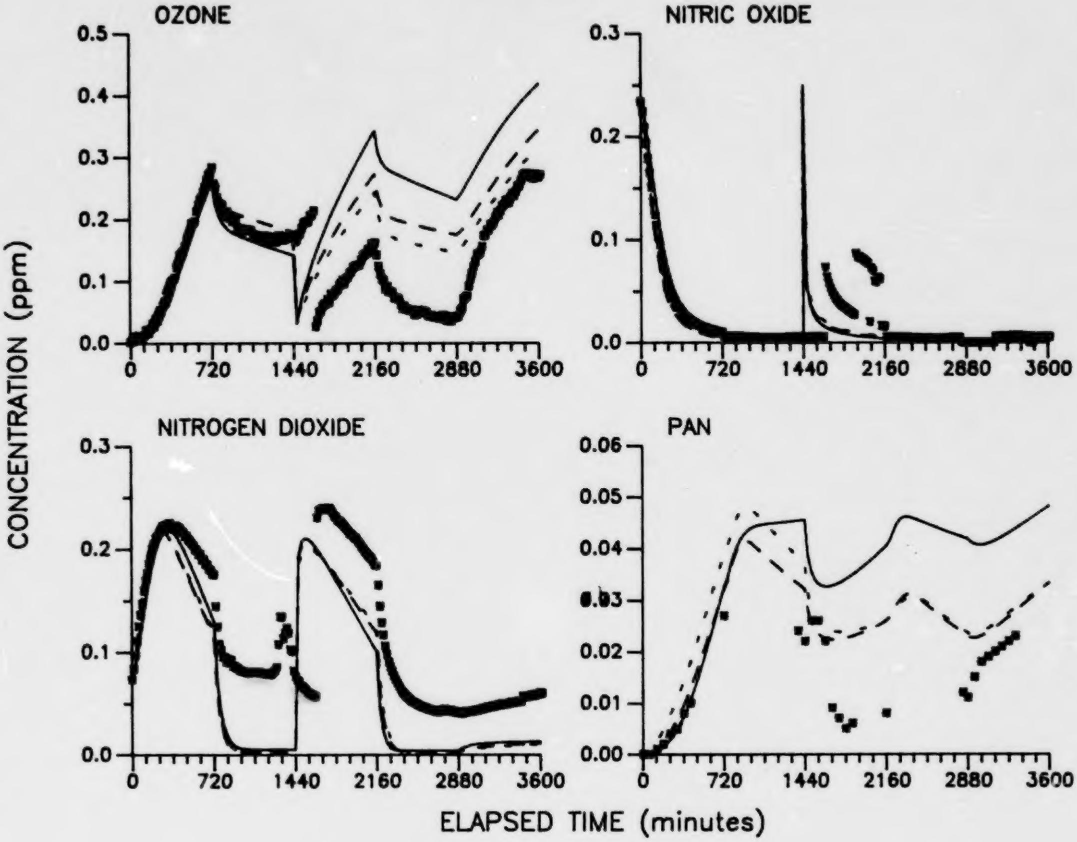

Figure 64. Experimental and Calculated Concentration-Time Plots for Selected Species in Simulations of the 8 Hydrocarbon Surrogate, Multi-Day Run ITC-630.

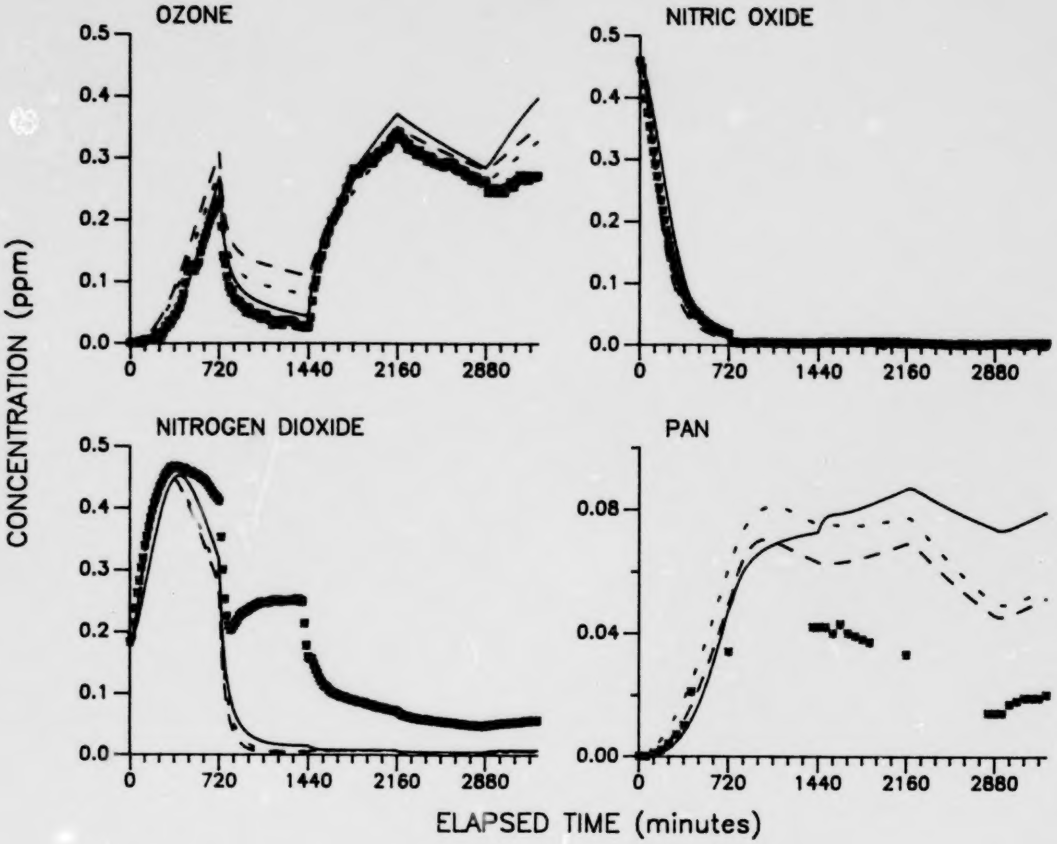

Figure 65. Experimental and Calculated Concentration-Time Plots for Selected Species in Simulations of the 8 Hydrocarbon Surrogate, Multi-Day Run ITC-633.

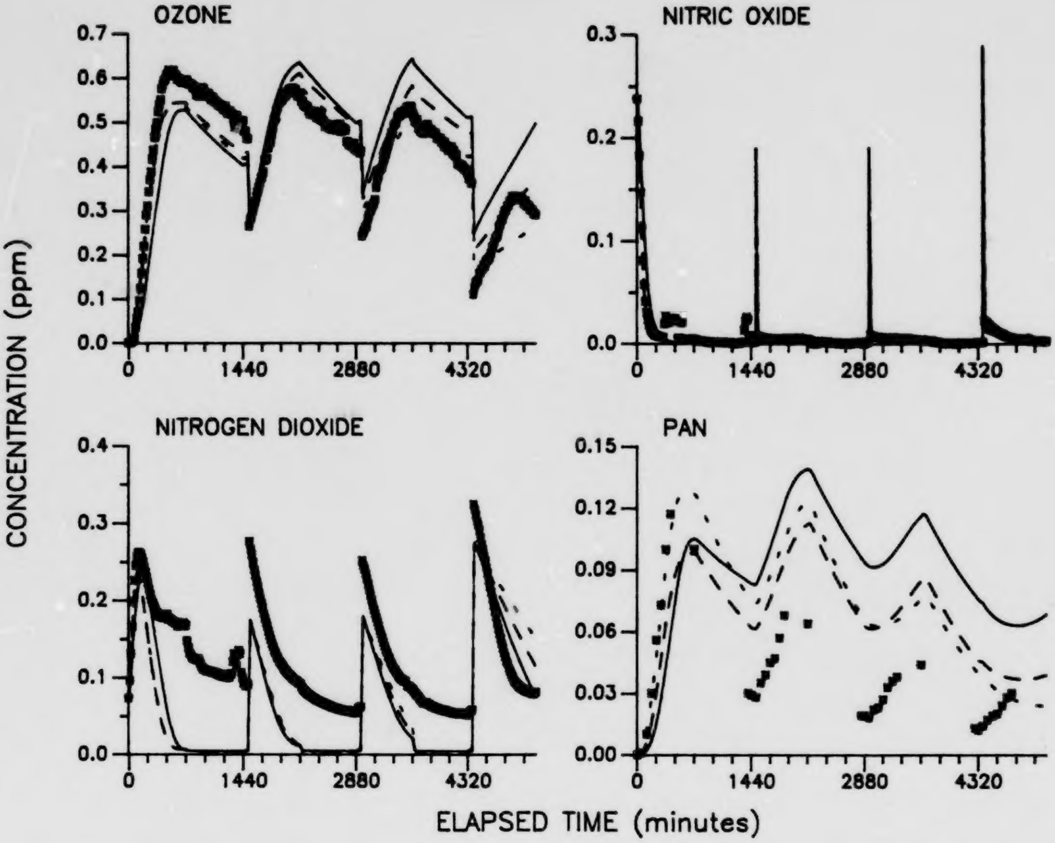

Figure 66. Experimental and Calculated Concentration-Time Plots for Selected Species in Simulations of the 8 Hydrocarbon Surrogate, Multi-Day Run ITC-637.

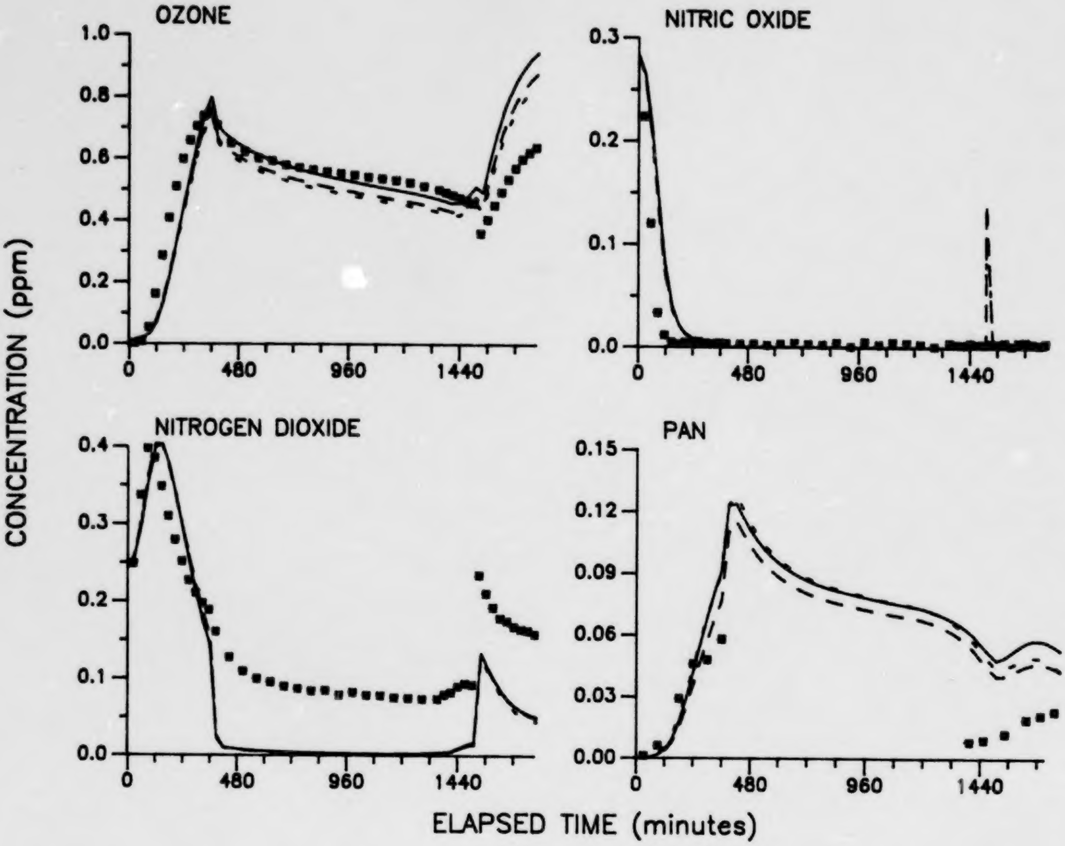

Figure 67. Experimental and Calculated Concentration-Time Plots for Selected Species in Simulations of the 8 Hydrocarbon Surrogate, Multi-Day Run OTC-192B

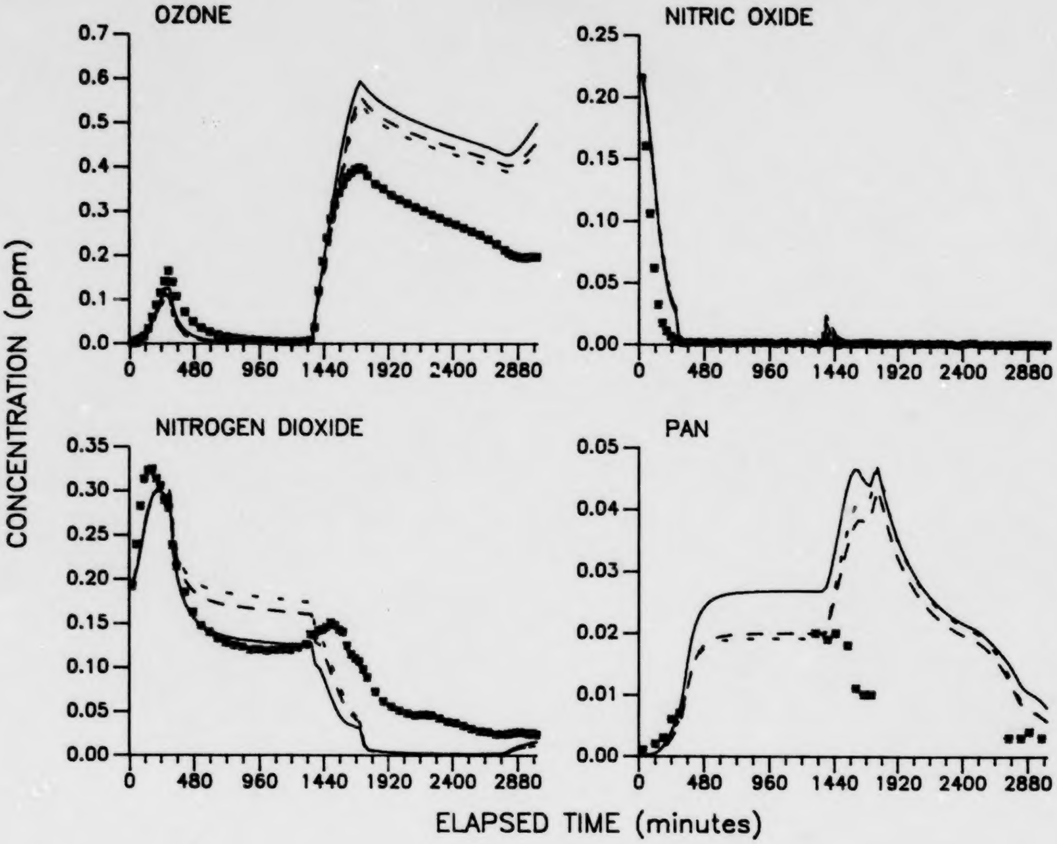

Figure 68. Experimental and Calculated Concentration-Time Plots for Selected Species in Simulations of the 8 Hydrocarbon Surrogate, Multi-Day Run OTC-195A.

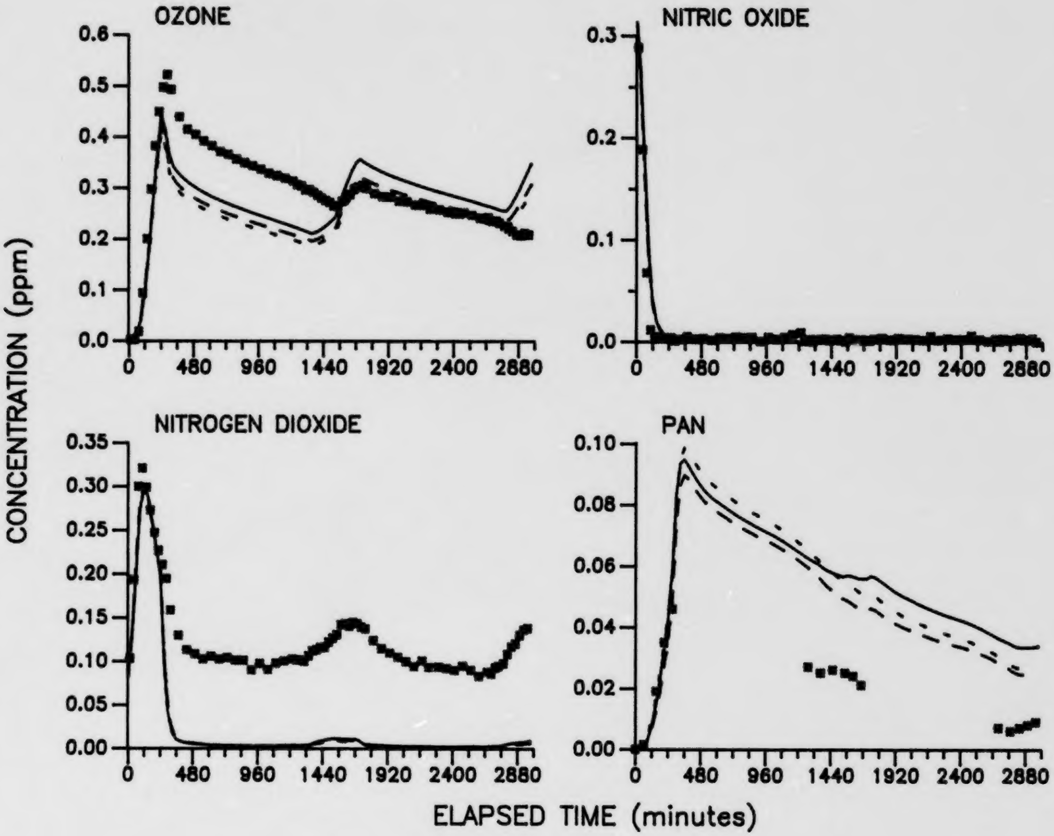

Figure 69. Experimental and Calculated Concentration-Time Plots for Selected Species in Simulations of the 8 Hydrocarbon Surrogate, Multi-Day Run OTC-202B.

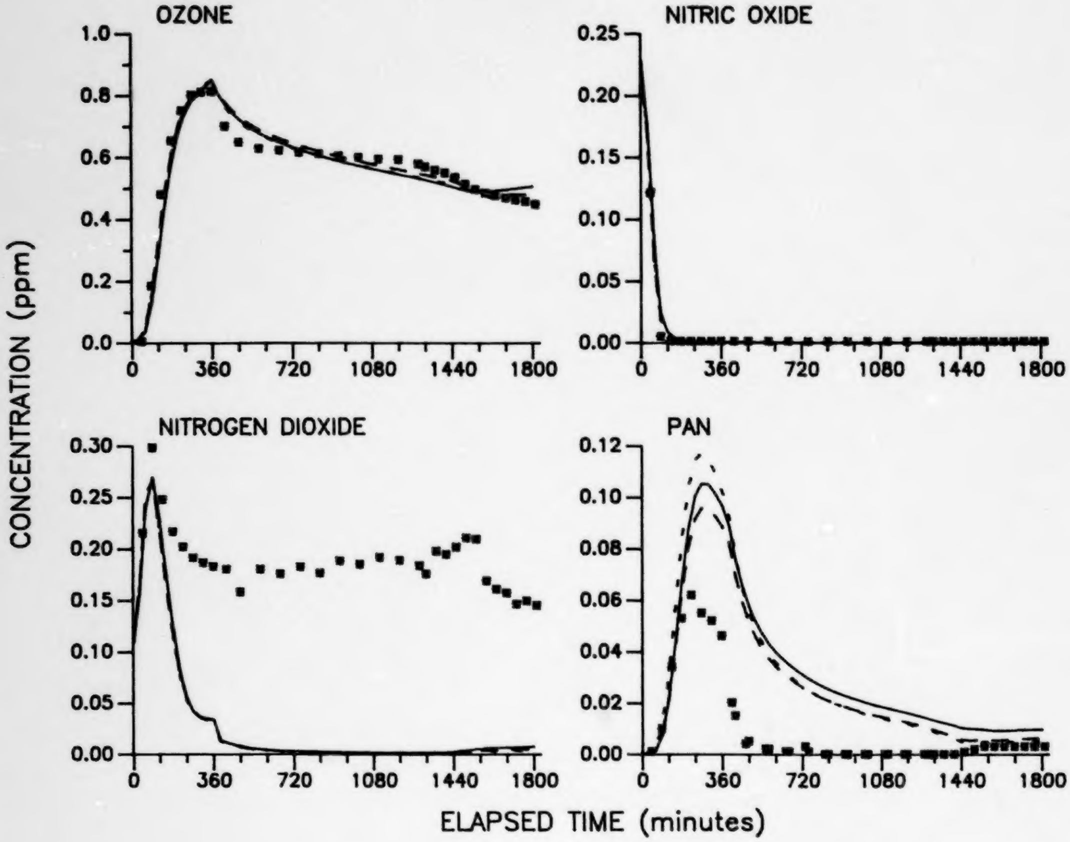

Figure 70. Experimental and Calculated Concentration-Time Plots for Selected Species in Simulations of the 8 Hydrocarbon Surrogate, Multi-Day Run OTC-224B.

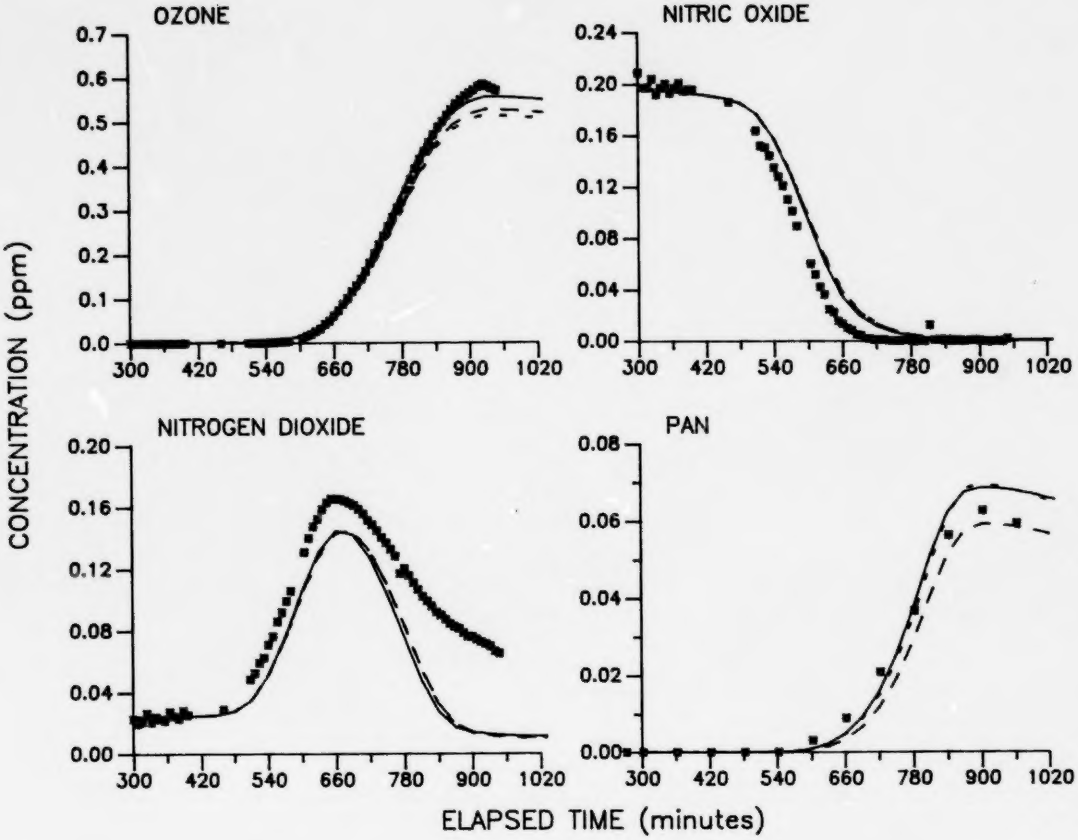

Figure 71. Experimental and Calculated Concentration-Time Plots for Selected Species in Simulations of the UNC 3 Hydrocarbon Surrogate Run JN1483R.

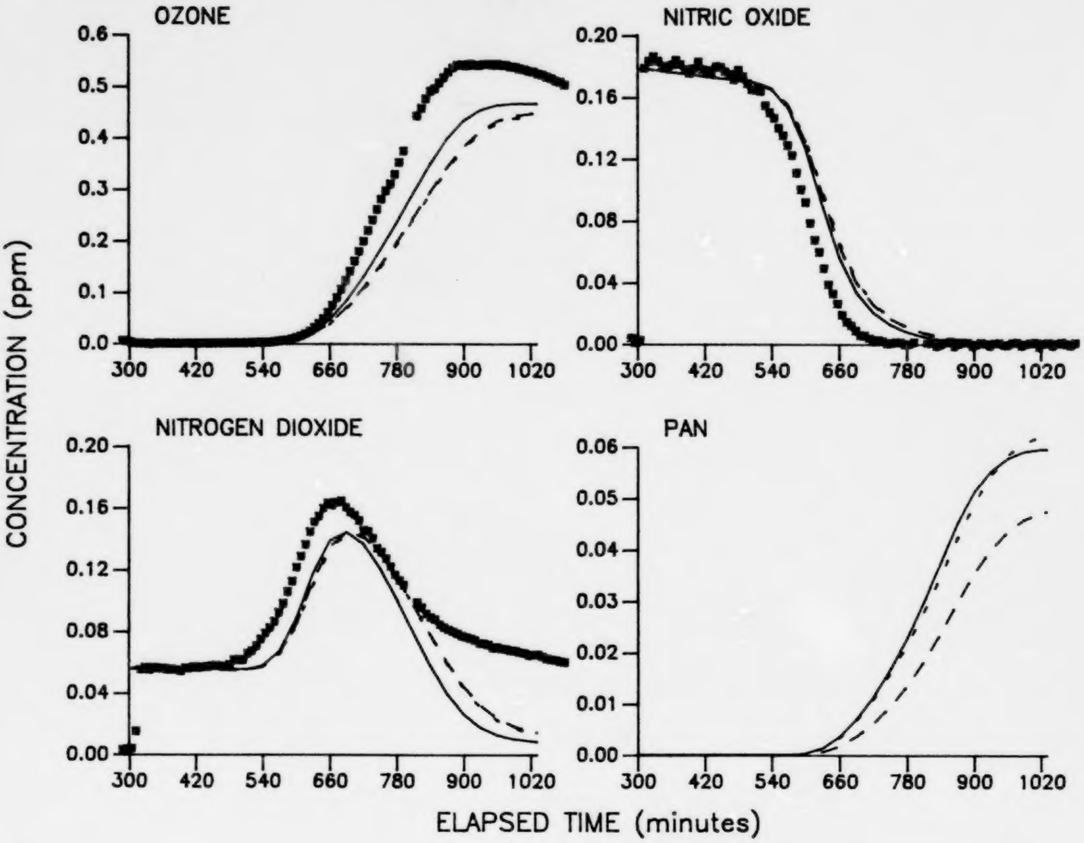

Figure 72. Experimental and Calculated Concentration-Time Plots for Selected Species in Simulations of the UNC Miscellaneous Surrogate Run AU2681B.

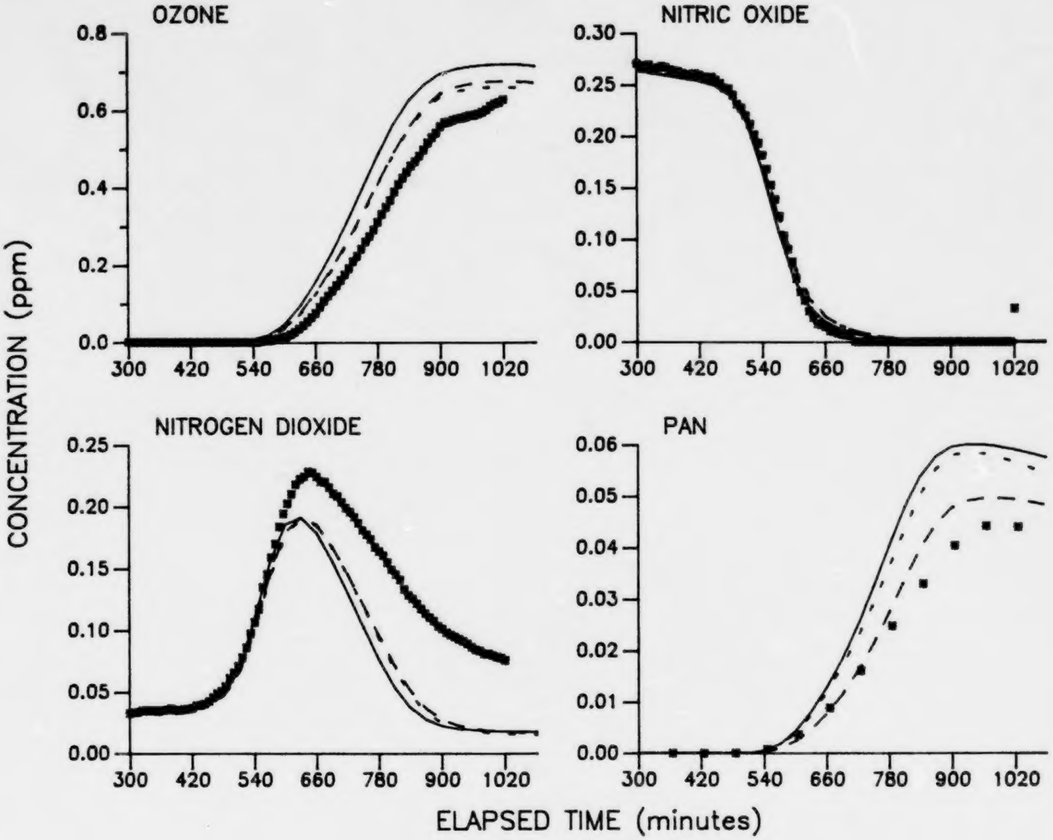

Figure 73. Experimental and Calculated Concentration-Time Plots for Selected Species in Simulations of the UNC Synurban Surrogate Run JN2685R.

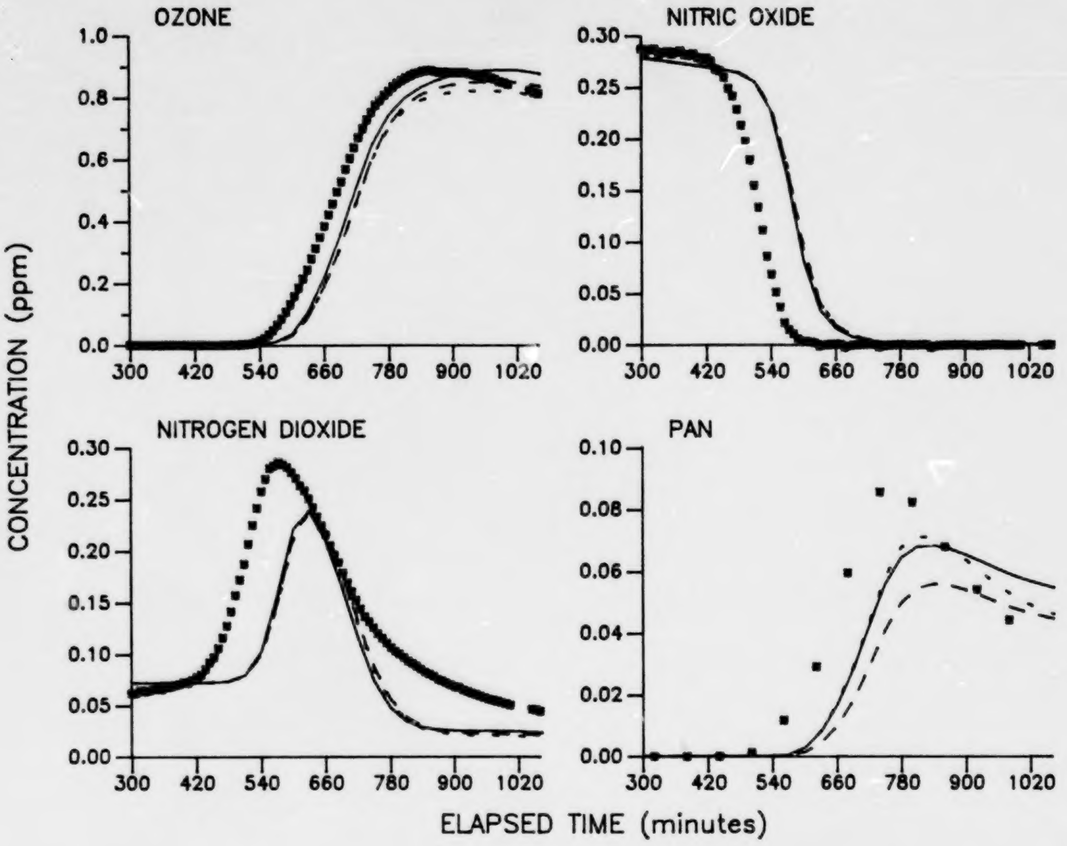

Figure 74. Experimental and Calculated Concentration-Time Plots for Selected Species in Simulations of the UNC Synauto Surrogate Run AU0684R.

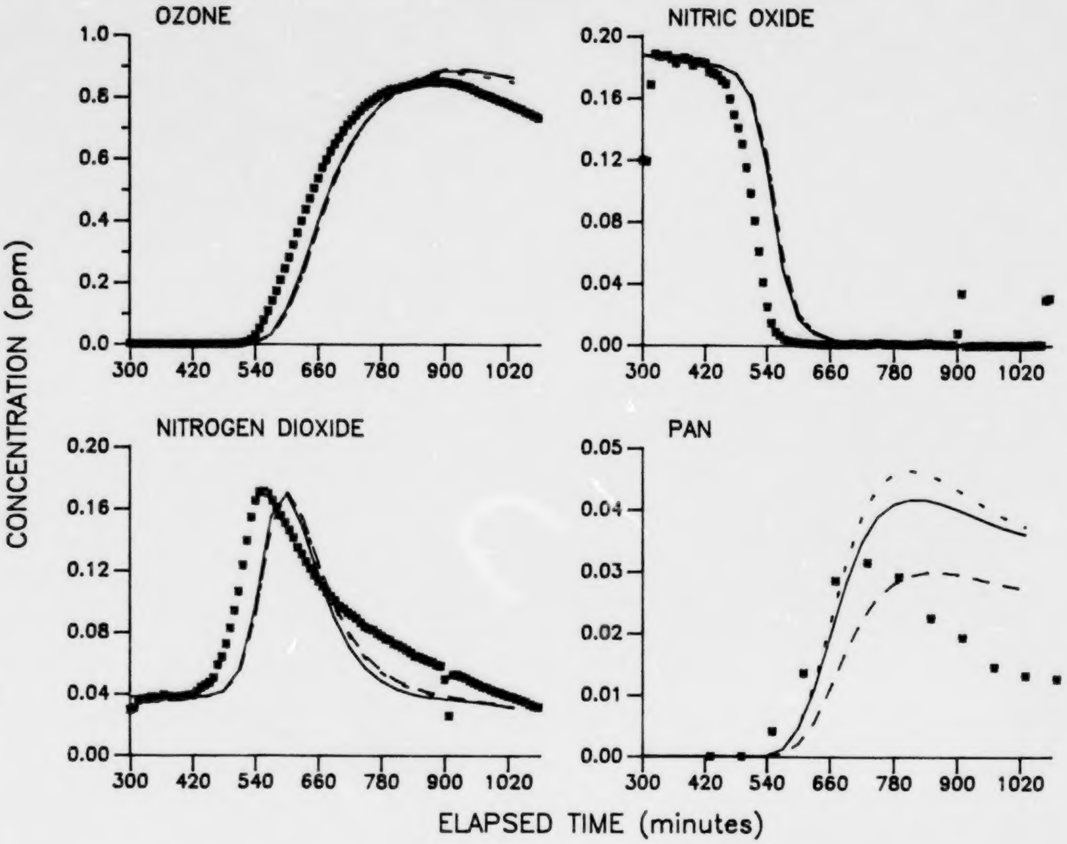

Figure 75. Experimental and Calculated Concentration-Time Plots for Selected Species in Simulations of the UNC Auto Exhaust Run AU1183R.

component would have a relatively smaller effect than would be the case in a run if that component were the only reactive organic present.) There does not appear to be any systematic bias in the results with respect to the initial HC to NO_x ratios, initial NO_x concentration, or initial HC concentrations. This is reassuring, but is not unexpected, considering that such a systematic bias was not observed for any of the groups of individual organics where one might expect such biases to be more evident.

The mechanism's performance on multi-day runs is comparable to that for single day runs, especially when good performance is achieved on the first day of the simulation. (See, for example, Figures 64 through 70.) If poor performance is achieved on the first day, then obviously the performance on the subsequent days would be even worse, since the starting conditions would be different.

Figures 76 and 77 compare the calculated and experimental formaldehyde maxima for the simple and complex mixture runs. The performance statistics are shown in Table 21. These results show that the RADM mechanism underpredicts the maximum formaldehyde on the average, though for most types of runs the mean biases are smaller in magnitude than the mean errors, which are typically on the order of 40-50%. The performance on formaldehyde in mixture runs is poorer than that found for single carbonyl and most types of alkene runs, but is better than the results for alkane and aromatic runs, on the average. The figures clearly show that for the runs with mixtures as well as those for the single compounds there is a large amount of scatter in the results and the mechanism is not able to reproduce the formaldehyde maxima very accurately. As already noted, however, the accuracy of the formaldehyde measurements is questionable.

Figures 78 and 79 compare the calculated and experimental PAN maxima for the simple and complex mixture runs. The performance statistics are shown in Table 22. Except for the UNC auto exhaust runs (whose chemical compositions are the most uncertain of all the runs), the RADM mechanism consistently overpredicts PAN in the mixture runs, with average biases ranging from 12 to over 66%. The mean error of these predictions are typically on the order of 40-60% or greater. The positive bias and large error is consistent with the results for single organic compound runs. A positive bias is expected since the PAN species in the mechanism is used

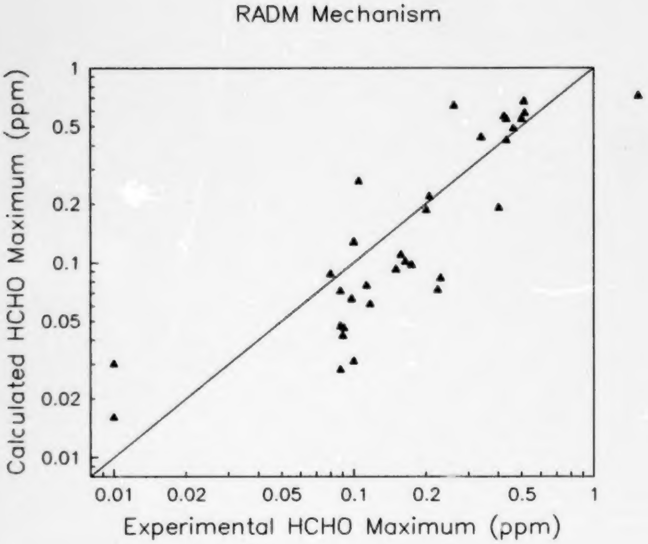

Figure 76. Calculated vs Experimental Maximum Formaldehyde in the Simple Mixture Runs for the RADM Mechanism.

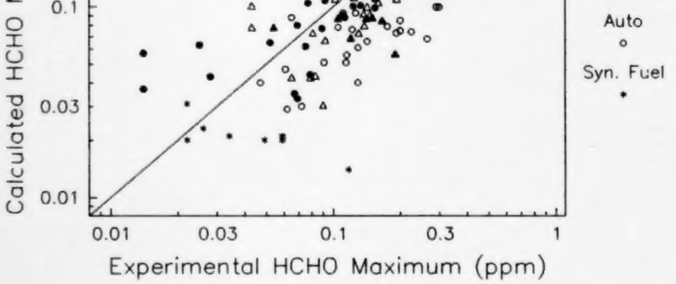

Figure 77. Calculated vs Experimental Maximum Formaldehyde in the Surrogate Mixture Runs for the RADM Mechanism.

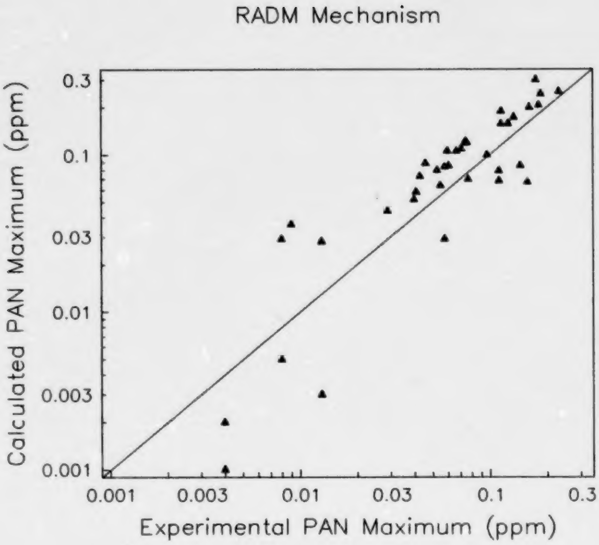

Figure 78. Calculated vs Experimental Maximum PAN in the Simple Mixture Runs for the RADM Mechanism.

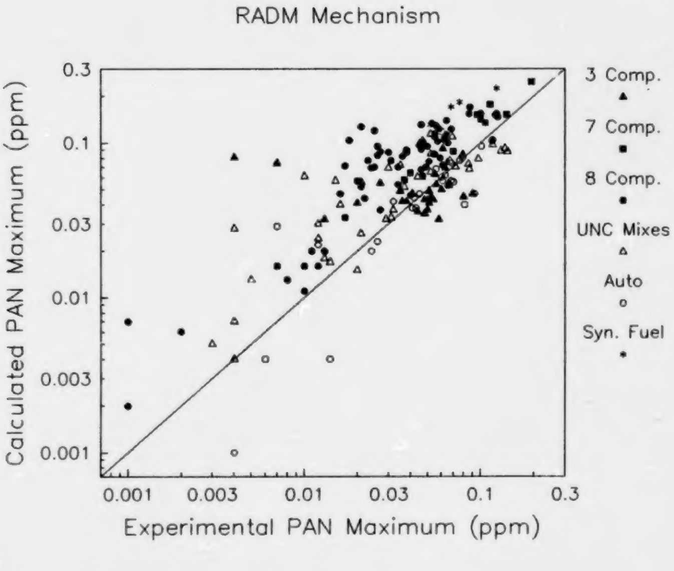

Figure 79. Calculated vs Experimental Maximum PAN in the Surrogate Mixture Runs for the RADM Mechanism.

to represent PAN plus numerous analogous organic nitrates. However, the magnitude of the bias, especially in the surrogate mixture runs, suggests the mechanism overpredicts the PAN and analogous species concentrations. This is of concern for regional acid deposition modeling because the model may underpredict nitric acid in the first few 100 km downwind of sources (i.e., if NO_x is oxidized disproportionately to PAN rather than HNO_3) and overestimate the distances for which nitrogen species are transported (since PAN is the long-range transport product of NO_x emissions).

5.6 Tests of the RADM VOC Aggregation Approach

As discussed in Section 4.3, the evaluation of the RADM mechanism involved processing organic input data in the simulations of the chamber experiments in a manner analogous to the expected procedure for processing of emissions input data for the RADM model. This involves, for example, representing some compounds by model species on a mole-per-mole basis, and others using "reactivity weighing," and not adjusting any parameters in the mechanism on a run-to-run basis. This is the appropriate procedure for evaluating the mechanism to be used in RADM, but in general it is not the one which would be expected to give the optimum fits of the model simulations to the experimental results. An alternative approach, which is appropriate for evaluations of detailed mechanisms or mechanisms to be used for assessment of relative reactivities, is to adjust parameters in the mechanism based on the mixtures being simulated. This latter procedure should in general result in the optimum performance of the model in simulating the experimental data; provided, of course, that errors in other aspects of the mechanism do not compensate for errors introduced using a more approximate representation.

Because of this, a comparison of the performance of the RADM mechanism using run-by-run adjustment of parameters with its performance using the standard evaluation procedure can give an indication of the level of inaccuracy introduced by using the RADM VOC aggregation procedure. To evaluate this, a separate set of simulations of the chamber experiments employing organics not explicitly represented in the RADM mechanism was carried out where the rate constants of the lumped model species were adjusted on a run-to-run basis to correspond to those of the compounds present in each experiment. The averages of the percent errors and biases in predictions of ozone yields and NO oxidation rates for groups of runs calculated for the RADM mechanism using this procedure are compared with the corresponding results for the standard evaluation in Table 23. Differences in ozone predictions for individual organic mixture runs are shown in Figure 80, where the maximum ozone yields calculated using this modified procedure are plotted against the yields calculated using the standard evaluation procedure.

The results shown in Table 23 and Figure 80 indicate that the two methods give very similar results for all types of mixture runs and for most single component runs. The differences are obviously greater for the single component runs; but, except for the one isobutene run and (to a lesser extent) the trimethylbenzene runs, the statistics for the simulations using the RADM VOC aggregation method are either about the same or somewhat better than the simulations where the rate constants are adjusted. Improvement of fits using the more approximate RADM VOC aggregation method relative to those obtained with adjusted rate constants is clearly a case of partial cancellation of errors. These results indicate that for realistic mixtures of organics likely to be encountered in regional modeling applications, any inaccuracies introduced by using the RADM VOC aggregation procedure discussed in Section 3 are likely to be small compared to inaccuracies introduced by other uncertainties in the mechanism.

5.7 Performance of the Recommended Modified Mechanisms

The recommended modified versions of the RADM mechanism, discussed in Section 2 of this report, were also evaluated against the chamber data. These mechanisms are the RADM-M, which incorporates all of the modifications we recommend as a result of this evaluation study, and the RADM-P, which primarily incorporates those recommendations involving only changes in parameter values. These mechanisms are the same as the March 1988 RADM mechanism in their inorganic and simple carbonyl reaction set, and thus the evaluation of the RADM mechanism for the characterization and carbonyl runs is also applicable to these mechanisms. However, both RADM-M and RADM-P have significant differences in their representation of aromatics, and in addition the RADM-M has a more condensed representation of the more rapidly reacting (generally C_{5+}) alkanes. The two mechanisms also have

Table 23. Comparison of Average Normalized Biases and Errors in Simulations of Chamber Experiments using the RADM Mechanism with Run-to-Run Adjustment of Rate Constants with Simulations using the Standard RADM VOC Aggregation Procedure

1) Adjusted Rate Constants
2) Standard VOC Aggregation

Compound or Mixture	Maximum Ozone (%) Bias	(sdev)	Err.	$d([O_3]-[NO])/dt$ (%) Bias	(sdev)	Err.
Propene	4	(19)	15	6	(18)	14
	5	(20)	15	6	(19)	14
1-Butene	5	(54)	45	9	(32)	29
	-2	(56)	45	0	(32)	25
trans-2-Butene	-52	(38)	54	-26	(26)	31
	-52	(38)	54	-25	(26)	31
Isobutene	-12	(0)	12	10	(0)	10
	-23	(0)	23	-45	(0)	45
1-Hexene	64	(26)	64	101	(30)	101
	57	(25)	57	82	(25)	82
a-Pinene	-12	(36)	29	-10	(10)	10
	-8	(35)	28	4	(19)	14
Ethane	-17	(0)	17	7	(0)	7
	-19	(0)	19	6	(0)	6
n-Butane	-1	(59)	46	18	(50)	43
	0	(59)	46	19	(50)	43
C4+ Br. Alkane	-12	(58)	44	-16	(20)	19
	-17	(67)	53	-22	(24)	26
C5+ n-Alkane	49	(34)	49	31	(36)	35
	42	(28)	42	24	(37)	34
Cycloalkane	34	(0)	34	5	(28)	17
	33	(0)	33	3	(29)	19
Benzene	22	(16)	22	28	(21)	31
	22	(15)	22	36	(19)	36
Toluene	24	(43)	33	6	(34)	26
	24	(43)	33	7	(34)	27

(continued)

Table 23 (continued) - 2

Compound or Mixture	1) Adjusted Rate Constants 2) Standard VOC Aggregation					
	Maximum Ozone (%)			$d([O_3]-[NO])/dt$ (%)		
	Bias	(sdev)	Err.	Bias	(sdev)	Err.
Xylene	-9	(30)	19	-19	(31)	20
	-4	(25)	18	0	(35)	25
Mesitylene	-21	(30)	30	-60	(39)	60
	-39	(50)	48	-93	(32)	93
Tetralin	-2	(56)	41	108	(85)	121
	-6	(62)	43	106	(85)	119
Naphthalene	82	(44)	82	118	(16)	118
	84	(40)	84	134	(13)	134
2,3-Dimethylnaph.	18	(15)	18	58	(28)	58
	-6	(24)	17	1	(24)	19
Simple Mixtures	-12	(45)	34	-13	(25)	22
	-12	(45)	34	-13	(26)	22
Simple Surrogates	10	(28)	17	7	(43)	30
	7	(24)	15	8	(38)	27
SAPRC 7-HC Surgs.	1	(11)	8	-9	(12)	12
	0	(11)	8	-5	(12)	10
SAPRC 8-HC Surgs.	12	(25)	21	-1	(24)	17
	9	(26)	20	-10	(23)	19
UNC Misc. Surgs.	14	(39)	27	1	(16)	12
	17	(40)	27	2	(15)	11
UNC "Synurban"	36	(30)	36	4	(9)	8
	39	(31)	39	7	(8)	8
UNC "Synauto"	22	(17)	23	0	(18)	14
	23	(17)	23	2	(18)	14
UNC Auto Exhaust	10	(29)	19	-3	(15)	12
	8	(29)	19	-6	(15)	13
Syn. Jet Fuel	10	(11)	11	35	(16)	35
	14	(12)	14	11	(16)	16
Syn. Jet Exhaust	-10	(8)	10	-15	(8)	15
	-11	(8)	11	-8	(4)	8

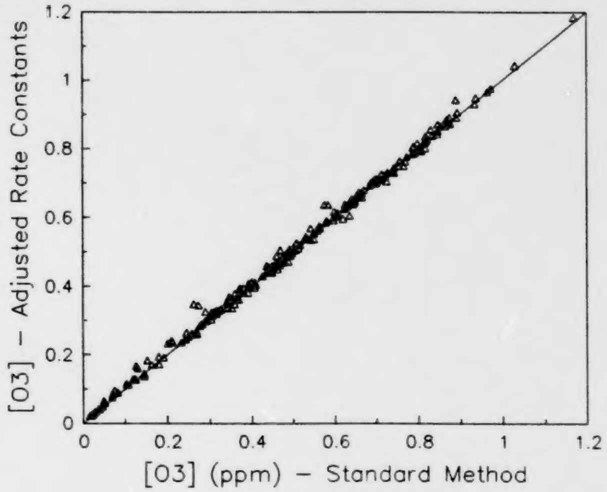

Figure 80. Plots of Maximum Ozone Yields in Simulations of Organic Mixture Experiments Using the RADM Mechanism with Run-to-Run Adjustment of Rate Constants Against Yields Calculated Using the Standard·RADM VOC Aggregation Procedure.

small differences in their reactions for the akenes and the less reactive C_{3+} alkanes. The evaluation calculations for these mechanisms were thus carried out for all the single and mixed organic-NO_x-air runs except those involving only simple carbonyls.

The summary statistics for the performance of the RADM-M and the RADM-P mechanisms in simulating maximum ozone yields and rates of NO oxidation and ozone formation are given in Tables 24 and 25; statistics for predictions of maximum formaldehyde are given in Tables 26 and 27; and statistics for predictions of maximum PAN are given in Tables 28 and 29. Table 30 shows comparisons of selected summary statistics for all three versions of the mechanism which were evaluated in this study. Figures 81 and 82 show plots of calculated vs experimental maximum ozone for the RADM-M and RADM-P mechanisms for the surrogate mixture runs; Figures 83 through 86 show similar plots for the alkane-NO_x and the aromatic-NO_x runs, respectively. Finally, Figures 23-25, 30-32, 37-42, 49 and 62-75 (presented earlier) give concentration-time profiles illustrating the performance of these mechanisms in simulating results of selected experiments where their predictions differed from the evaluated RADM mechanism. (Solid lines are for the RADM mechanism, longer dashed lines are for RADM-P, and shorter dashed lines are for RADM-M.) Run-by-run summaries of the performances of these mechanisms in simulating maximum ozone and NO oxidation rates are found in Appendix B for RADM-M and in Appendix C for RADM-P.

The differences between the predictions of the mechanisms for the alkene-NO_x and alkane-NO_x runs are relatively minor, as expected due to the relatively small changes in the mechanisms for these compounds. The RADM-M mechanism performs slightly worse than the other two for the higher alkane-NO_x runs because of its more condensed representation of these compounds. However, the test calculations discussed in Section 6.3 indicate that this should have relatively little effect in simulations of more realistic mixtures of organics.

Table 24. Performance Statistics on Maximum Ozone and NO Oxidation and Ozone Formation Rates in the Simulations of Organic-NO_x-Air Runs Using the RADM-M Mechanism

Organic or Mixture	1) Statistics for Maximum Ozone (ppb) 2) Statistics for $d([O_3]-[NO])/dt$ (ppb/min)					
	No. Runs	Experimental Avg. (sdev)	Absolute Bias	Absolute Err.	-- Normalized -- Bias (%)	-- Normalized -- Err. (%)
Ethene	14	0.91 (0.20)	-0.09	0.16	-16 (30)	23
	14	5.23 (4.10)	-1.21	1.21	-27 (20)	27
Propene	49	0.61 (0.24)	0.04	0.09	8 (20)	16
	49	3.62 (2.60)	0.53	0.76	11 (19)	17
1-Butene	11	0.42 (0.26)	0.05	0.14	2 (55)	45
	11	2.86 (2.18)	0.41	0.96	5 (32)	27
trans-2-Butene	4	0.28 (0.17)	-0.08	0.09	-53 (38)	54
	4	6.17 (2.80)	-1.68	1.76	-29 (24)	32
Isobutene	1	0.90 (0.00)	-0.17	0.17	-21 (0)	21
	1	8.84 (0.00)	-2.81	2.81	-38 (0)	38
1-Hexene	4	0.34 (0.25)	0.28	0.28	59 (26)	59
	4	1.57 (1.04)	3.32	3.32	88 (26)	88
Isoprene	13	0.72 (0.25)	-0.23	0.24	-42 (31)	43
	13	5.66 (4.06)	0.86	1.81	-2 (36)	26
a-Pinene	4	0.35 (0.11)	-0.03	0.08	-8 (34)	27
	4	0.97 (0.43)	0.06	0.15	2 (18)	13
Ethane	1	0.24 (0.00)	-0.04	0.04	-18 (0)	18
	1	1.32 (0.00)	0.09	0.09	7 (0)	7
n-Butane	27	0.31 (0.27)	-0.01	0.12	-10 (59)	47
	27	1.53 (0.98)	0.18	0.72	12 (49)	41
C4+ Br. Alkanes	7	0.28 (0.18)	-0.05	0.10	-17 (73)	58
	7	0.93 (0.46)	-0.21	0.23	-25 (25)	29
C5+ n-Alkanes	14	0.20 (0.15)	0.16	0.16	58 (39)	58
	14	1.15 (0.75)	0.42	0.56	38 (43)	46
Cycloalkanes	4	0.05 (0.00)	0.05	0.05	85 (0)	85
	4	0.92 (0.12)	0.36	0.41	25 (41)	31
Benzene	6	0.29 (0.14)	0.07	0.07	20 (13)	20
	6	3.39 (2.30)	6.11	6.11	92 (23)	92

(continued)

Table 24 (continued) - 2

1) Statistics for Maximum Ozone (ppb)
2) Statistics for $d([O_3]-[NO])/dt$ (ppb/min)

Organic or Mixture	No. Runs	Experimental Avg. (sdev)	Absolute		-- Normalized --	
			Bias	Err.	Bias (%)	Err. (%)
Toluene	20	0.34 (0.15)	0.03	0.06	13 (31)	21
	20	3.07 (1.87)	0.12	0.62	7 (31)	21
Xylene	10	0.44 (0.19)	-0.01	0.05	0 (16)	12
	10	5.39 (4.14)	0.67	0.96	17 (20)	20
Mesitylene	8	0.52 (0.26)	-0.13	0.14	-26 (19)	29
	6	9.50 (4.97)	-4.66	4.66	-57 (22)	57
Tetralin	5	0.29 (0.23)	0.23	0.23	57 (50)	57
	5	1.89 (0.88)	25.41	25.56	125 (91)	137
Naphthalene	5	0.20 (0.08)	0.33	0.33	93 (37)	93
	5	1.59 (0.41)	19.56	19.56	170 (8)	170
2,3-Dimethylnaph.	4	0.32 (0.04)	0.08	0.08	21 (17)	21
	4	2.48 (0.51)	3.90	3.90	79 (34)	79
Simple Mixtures	40	0.49 (0.27)	-0.06	0.12	-15 (43)	32
	39	4.10 (4.06)	-0.89	1.11	-15 (25)	23
Simple Surrogates	36	0.37 (0.15)	0.01	0.05	8 (24)	16
	36	2.81 (1.61)	1.08	1.32	28 (36)	36
SAPRC 7-HC Surgs.	11	0.60 (0.17)	0.00	0.04	0 (12)	8
	11	7.74 (5.16)	-0.55	0.72	-8 (12)	11
SAPRC 8-HC Surgs.	82	0.45 (0.27)	0.02	0.08	3 (26)	19
	82	2.81 (1.51)	-0.16	0.54	-5 (24)	19
UNC Misc. Surgs.	21	0.50 (0.17)	0.02	0.10	11 (40)	25
	21	1.32 (0.40)	-0.06	0.15	-3 (15)	12
UNC "Synurban"	11	0.37 (0.28)	0.06	0.07	22 (25)	24
	11	1.09 (0.47)	0.01	0.06	1 (9)	6
UNC "Synauto"	15	0.62 (0.18)	0.09	0.11	16 (17)	18
	15	1.81 (0.63)	-0.05	0.30	-2 (18)	16
UNC Auto Exhaust	28	0.57 (0.27)	0.04	0.10	1 (34)	23
	28	1.68 (0.61)	-0.14	0.21	-10 (15)	14
Syn. Jet Fuel	8	0.75 (0.10)	0.13	0.13	16 (11)	16
	8	3.47 (0.74)	8.22	8.22	107 (14)	107
Syn. Jet Exhaust	4	0.78 (0.13)	-0.07	0.08	-9 (8)	10
	4	6.66 (3.48)	0.06	0.33	3 (5)	5

Table 25. Performance Statistics on Maximum Ozone and NO Oxidation and Ozone Formation Rates in the Simulations of Organic-NO_x-Air Runs Using the RADM-P Mechanism

Organic or Mixture	1) Statistics for Maximum Ozone (ppb) 2) Statistics for $d([O_3]-[NO])/dt$ (ppb/min)					
	No. Runs	Experimental Avg. (sdev)	Absolute Bias	Absolute Err.	-- Normalized -- Bias (%)	-- Normalized -- Err. (%)
Ethene	14	0.91 (0.20)	-0.09	0.16	-16 (30)	23
	14	5.23 (4.10)	-1.21	1.21	-27 (20)	27
Propene	49	0.61 (0.24)	0.04	0.09	8 (20)	16
	49	3.62 (2.60)	0.53	0.76	11 (19)	17
1-Butene	11	0.42 (0.26)	0.05	0.14	2 (55)	45
	11	2.86 (2.18)	0.41	0.96	5 (32)	27
trans-2-Butene	4	0.28 (0.17)	-0.08	0.09	-53 (38)	54
	4	6.17 (2.80)	-1.68	1.76	-29 (24)	31
Isobutene	1	0.90 (0.00)	-0.17	0.17	-21 (0)	21
	1	8.84 (0.00)	-2.80	2.80	-38 (0)	38
1-Hexene	4	0.34 (0.25)	0.28	0.28	59 (26)	59
	4	1.57 (1.04)	3.33	3.33	88 (26)	88
Isoprene	13	0.72 (0.25)	-0.23	0.24	-42 (31)	43
	13	5.66 (4.06)	0.86	1.81	-2 (36)	26
a-Pinene	4	0.35 (0.11)	-0.03	0.08	-8 (34)	27
	4	0.97 (0.43)	0.06	0.15	2 (18)	13
Ethane	1	0.24 (0.00)	-0.04	0.04	-18 (0)	18
	1	1.32 (0.00)	0.10	0.10	7 (0)	7
n-Butane	27	0.31 (0.27)	-0.01	0.12	-8 (59)	47
	27	1.53 (0.98)	0.21	0.74	13 (49)	41
C4+ Br. Alkane	7	0.28 (0.18)	-0.06	0.09	-19 (62)	50
	7	0.93 (0.46)	-0.18	0.20	-22 (24)	25
C5+ n-Alkane	14	0.20 (0.15)	0.10	0.10	41 (27)	41
	14	1.15 (0.75)	0.27	0.40	25 (36)	35
Cycloalkanes	4	0.05 (0.00)	0.00	0.02	27 (0)	27
	4	0.92 (0.12)	0.03	0.21	-1 (31)	22
Benzene	6	0.29 (0.14)	0.07	0.07	19 (14)	19
	6	3.39 (2.30)	6.20	6.20	93 (24)	93

(continued)

Table 25 (continued) - 2

1) Statistics for Maximum Ozone (ppb)
2) Statistics for $d([O_3]-[NO])/dt$ (ppb/min)

Organic or Mixture	No. Runs	Experimental Avg. (sdev)	Absolute Bias	Absolute Err.	-- Normalized -- Bias (%)	-- Normalized -- Err. (%)
Toluene	20	0.34 (0.15)	0.05	0.07	17 (31)	22
	20	3.07 (1.87)	0.19	0.68	10 (31)	23
Xylene	10	0.44 (0.19)	0.02	0.06	5 (16)	12
	10	5.39 (4.14)	0.61	0.93	17 (21)	21
Mesitylene	8	0.52 (0.26)	-0.11	0.13	-21 (19)	25
	6	9.50 (4.97)	-4.63	4.63	-55 (22)	55
Tetralin	5	0.29 (0.23)	0.23	0.23	56 (49)	56
	5	1.89 (0.88)	25.16	25.30	125 (91)	137
Naphthalene	5	0.20 (0.08)	0.34	0.34	93 (38)	93
	5	1.59 (0.41)	19.27	19.27	170 (8)	170
2,3-Dimethylnaph.	4	0.32 (0.04)	0.10	0.10	26 (17)	26
	4	2.48 (0.51)	3.90	3.90	79 (32)	79
Simple Mixtures	40	0.49 (0.27)	-0.06	0.12	-14 (44)	32
	39	4.10 (4.06)	-0.87	1.10	-14 (25)	22
Simple Surrogates	36	0.37 (0.15)	0.02	0.05	9 (23)	16
	36	2.81 (1.61)	1.05	1.28	28 (36)	35
SAPRC 7-HC Surgs.	11	0.60 (0.17)	-0.01	0.04	-1 (12)	8
	11	7.74 (5.16)	-0.46	0.77	-6 (13)	12
SAPRC 8-HC Surgs.	82	0.45 (0.27)	0.03	0.08	5 (25)	19
	82	2.81 (1.51)	-0.10	0.54	-3 (25)	19
UNC Misc. Surgs.	21	0.50 (0.17)	0.02	0.10	10 (37)	24
	21	1.32 (0.40)	-0.06	0.14	-3 (15)	12
UNC "Synurban"	11	0.37 (0.28)	0.07	0.08	24 (25)	25
	11	1.09 (0.47)	0.02	0.06	2 (9)	6
UNC "Synauto"	15	0.62 (0.18)	0.10	0.12	18 (16)	19
	15	1.81 (0.63)	-0.04	0.29	-1 (18)	15
UNC Auto Exhaust	28	0.57 (0.27)	0.05	0.10	3 (34)	23
	28	1.68 (0.61)	-0.13	0.21	-9 (15)	14
Syn. Jet Fuel	8	0.75 (0.10)	0.12	0.12	15 (10)	15
	8	3.47 (0.74)	5.54	5.54	87 (17)	87
Syn. Jet Exhaust	4	0.78 (0.13)	-0.07	0.08	-9 (8)	10
	4	6.66 (3.48)	0.00	0.34	2 (5)	5

Table 26. Performance Statistics on Maximum Formaldehyde in the Simulations of Organic-NO_x-Air Runs Using the RADM-M Mechanism

Compound or	No.	Experimental(a)		Absolute(a)		Normalized	
Mixture	Runs	Avg.	(sdev)	Bias	Err.	Bias (%)	Err. (%)
Ethene	14	0.86	(0.41)	-0.02	0.23	-9 (41)	34
Propene	39	0.36	(0.20)	0.01	0.11	7 (45)	34
1-Butene	8	0.32	(0.27)	0.12	0.12	24 (19)	25
trans-2-Butene	4	0.08	(0.06)	0.04	0.06	59 (58)	70
Isobutene	1	0.64		0.00	0.00	-1	1
1-Hexene	4	0.33	(0.27)	0.32	0.32	79 (34)	79
Isoprene	13	0.30	(0.16)	0.01	0.12	-6 (60)	46
a-Pinene	2	0.08	(0.04)	-0.02	0.02	-25 (12)	25
n-Butane	21	0.04	(0.03)	0.01	0.03	14 (76)	65
C4+ Br. Alkane	5	0.03	(0.02)	-0.02	0.02	-57 (78)	87
C5+ n-Alkane	10	0.01	(0.01)	-0.01	0.01	-19 (101)	89
Cycloalkane	4	0.07	(0.12)	-0.06	0.07	-31 (135)	105
Toluene	20	0.09	(0.09)	-0.03	0.04	-26 (62)	48
Xylene	10	0.09	(0.05)	-0.04	0.05	-45 (68)	67
Mesitylene	8	0.09	(0.04)	-0.03	0.04	-30 (49)	44
Naphthalene	5	0.01	(0.01)	0.05	0.05	134 (43)	134
Simple Mixtures	34	0.25	(0.20)	0.02	0.09	-14 (53)	45
Simple Surrogates	7	0.13	(0.05)	-0.05	0.06	-45 (45)	55
SAPRC 7-HC Surgs.	11	0.38	(0.23)	0.10	0.10	18 (19)	22
SAPRC 8-HC Surgs.	82	0.18	(0.12)	-0.02	0.05	1 (48)	35
UNC "Synurban"	11	0.12	(0.04)	-0.05	0.05	-54 (18)	54
UNC "Synauto"	13	0.16	(0.08)	0.02	0.04	14 (31)	25
UNC Auto Exhaust	28	0.18	(0.10)	-0.10	0.10	-68 (31)	70
Syn. Jet Fuel	8	0.05	(0.03)	-0.01	0.03	-13 (67)	53

(a) Concentrations in ppm.

Table 27. Performance Statistics on Maximum Formaldehyde in the Simulations of Organic-NO_x-Air Runs Using the RADM-P Mechanism

Compound or Mixture	No. Runs	Experimental(a) Avg. (sdev)	Absolute(a) Bias	Absolute(a) Err.	Normalized Bias (%)	Normalized Err. (%)
Ethene	14	0.86 (0.41)	-0.02	0.23	-9 (41)	34
Propene	39	0.36 (0.20)	0.01	0.11	7 (45)	34
1-Butene	8	0.32 (0.27)	0.12	0.12	24 (19)	25
trans-2-Butene	4	0.08 (0.06)	0.04	0.06	59 (58)	70
Isobutene	1	0.64	0.00	0.00	-1	1
1-Hexene	4	0.33 (0.27)	0.32	0.32	79 (34)	79
Isoprene	13	0.30 (0.16)	0.01	0.12	-6 (60)	46
a-Pinene	2	0.08 (0.04)	-0.02	0.02	-25 (12)	25
n-Butane	21	0.04 (0.03)	0.01	0.03	14 (76)	65
C4+ Br. Alkane	5	0.03 (0.02)	-0.02	0.02	-74 (70)	92
C5+ n-Alkane	10	0.01 (0.01)	-0.01	0.01	-35 (106)	95
Cycloalkane	4	0.07 (0.12)	-0.06	0.06	-41 (128)	98
Toluene	20	0.09 (0.09)	-0.05	0.05	-90 (58)	91
Xylene	10	0.09 (0.05)	-0.07	0.07	-109 (56)	114
Mesitylene	8	0.09 (0.04)	-0.06	0.06	-101 (44)	101
Naphthalene	5	0.01 (0.01)	0.01	0.01	64 (75)	71
Simple Mixtures	34	0.25 (0.20)	0.02	0.09	-21 (62)	52
Simple Surrogates	7	0.13 (0.05)	-0.06	0.06	-50 (44)	59
SAPRC 7-HC Surgs.	11	0.38 (0.23)	0.09	0.10	17 (19)	21
SAPRC 8-HC Surgs.	82	0.18 (0.12)	-0.03	0.06	-4 (48)	36
UNC "Synurban"	11	0.12 (0.04)	-0.05	0.05	-61 (19)	61
UNC "Synauto"	13	0.16 (0.08)	0.01	0.03	9 (31)	24
UNC Auto Exhaust	28	0.18 (0.10)	-0.10	0.10	-74 (31)	75
Syn. Jet Fuel	8	0.05 (0.03)	-0.03	0.03	-75 (52)	75

(a) Concentrations in ppm.

Table 28. Performance Statistics on Maximum PAN in the Simulations of Organic-NO_x-Air Runs Using the RADM-M Mechanism

Compound or	No.	Experimental(a)		Absolute(a)		Normalized	
Mixture	Runs	Avg.	(sdev)	Bias	Err.	Bias (%)	Err. (%)
Propene	46	0.142	(0.084)	0.049	0.055	31 (39)	36
1-Butene	7	0.039	(0.016)	0.059	0.060	70 (50)	72
trans-2-Butene	4	0.080	(0.044)	-0.004	0.014	-14 (24)	21
Isobutene	1	0.137		0.140	0.140	68	68
1-Hexene	3	0.003	(0.003)	0.319	0.319	195 (4)	195
Isoprene	12	0.133	(0.082)	-0.029	0.080	-19 (85)	61
a-Pinene	2	0.022	(0.016)	0.048	0.048	100 (12)	100
n-Butane	21	0.296	(1.012)	-0.259	0.293	10 (105)	90
C4+ Br. Alkane	6	0.226	(0.506)	-0.208	0.223	-46 (119)	99
C5+ n-Alkane	11	0.247	(0.814)	-0.243	0.247	21 (129)	101
Cycloalkanes	4	0.002	(0.003)	-0.001	0.002	-112 (14)	112
Toluene	20	0.051	(0.036)	0.045	0.051	66 (43)	71
Xylene	10	0.125	(0.102)	0.025	0.059	35 (41)	46
Mesitylene	8	0.407	(0.189)	-0.230	0.230	-69 (27)	69
2,3-Dimethylnaph.	4	0.046	(0.019)	0.095	0.095	98 (28)	98
Simple Mixtures	38	0.081	(0.059)	0.023	0.037	18 (58)	51
Simple Surrogates	32	0.048	(0.020)	0.017	0.020	36 (51)	41
SAPRC 7-HC Surgs.	11	0.095	(0.047)	0.054	0.054	43 (12)	43
SAPRC 8-HC Surgs.	68	0.044	(0.030)	0.042	0.042	66 (35)	66
UNC Misc. Surgs.	12	0.055	(0.046)	0.011	0.019	35 (64)	48
UNC "Synurban"	10	0.024	(0.024)	0.010	0.010	31 (28)	37
UNC "Synauto"	15	0.054	(0.039)	0.018	0.030	29 (45)	41
UNC Auto Exhaust	28	0.047	(0.029)	0.000	0.011	-13 (60)	41
Syn. Jet Exhaust	4	0.080	(0.031)	0.117	0.117	87 (13)	87

(a) Concentrations in ppm.

Table 29. Performance Statistics on Maximum PAN in the Simulations of Organic-NO_x-Air Runs Using the RADM-P Mechanism

Compound or Mixture	No. Runs	Experimental(a) Avg.	(sdev)	Absolute(a) Bias	Err.	Normalized Bias (%)	Err. (%)
Propene	46	0.142	(0.084)	0.049	0.055	31 (39)	36
1-Butene	7	0.039	(0.016)	0.059	0.060	70 (50)	72
trans-2-Butene	4	0.080	(0.044)	-0.004	0.014	-14 (24)	21
Isobutene	1	0.137		0.140	0.140	68	68
1-Hexene	3	0.003	(0.003)	0.319	0.319	195 (4)	195
Isoprene	12	0.133	(0.082)	-0.029	0.080	-19 (85)	61
a-Pinene	2	0.022	(0.016)	0.048	0.048	100 (12)	100
n-Butane	21	0.296	(1.012)	-0.259	0.293	11 (105)	90
C4+ Br. Alkane	6	0.226	(0.506)	-0.206	0.224	-46 (124)	105
C5+ n-Alkane	11	0.247	(0.814)	-0.243	0.248	8 (132)	105
Cycloalkane	4	0.002	(0.003)	-0.002	0.002	-165 (8)	165
Toluene	20	0.051	(0.036)	-0.027	0.035	-64 (62)	82
Xylene	10	0.125	(0.102)	-0.073	0.073	-64 (40)	64
Mesitylene	8	0.407	(0.189)	-0.353	0.353	-147 (19)	147
2,3-Dimethylnaph.	4	0.046	(0.019)	-0.007	0.009	-16 (34)	24
Simple Mixtures	38	0.081	(0.059)	0.008	0.027	0 (55)	44
Simple Surrogates	32	0.048	(0.020)	0.002	0.017	9 (57)	38
SAPRC 7-HC Surgs.	11	0.095	(0.047)	0.009	0.019	13 (21)	20
SAPRC 8-HC Surgs.	68	0.044	(0.030)	0.032	0.033	54 (39)	57
UNC Misc. Surgs.	12	0.055	(0.046)	-0.005	0.023	5 (66)	54
UNC "Synurban"	10	0.024	(0.024)	0.005	0.005	15 (29)	25
UNC "Synauto"	15	0.054	(0.039)	0.003	0.027	10 (47)	41
UNC Auto Exhaust	28	0.047	(0.029)	-0.015	0.016	-44 (56)	56
Syn. Jet Exhaust	4	0.080	(0.031)	0.097	0.097	78 (14)	78

(a) Concentrations in ppm.

Table 30. Comparisons of Average Normalized Biases and Errors in Maximum Ozone and NO Oxidation Rates in the Simulations of Organic-NO_x-Air Runs Using the RADM, RADM-M, and RADM-P Mechanisms.

Organic or Mixture	Mechanism	Maximum Ozone (%)			$d([O_3]-[NO])/dt$ (%)		
		Bias	(sdev)	Err.	Bias	(sdev)	Err.
Ethene	RADM	-16	(30)	23	-27	(20)	27
	RADM-M	-16	(30)	23	-27	(20)	27
	RADM-P	-16	(30)	23	-27	(20)	27
Propene	RADM	5	(20)	15	6	(19)	14
	RADM-M	8	(20)	16	11	(19)	17
	RADM-P	8	(20)	16	11	(19)	17
1-Butene	RADM	-2	(56)	45	0	(32)	25
	RADM-M	2	(55)	45	5	(32)	27
	RADM-P	2	(55)	45	5	(32)	27
trans-2-Butene	RADM	-52	(38)	54	-25	(26)	31
	RADM-M	-53	(38)	54	-29	(24)	32
	RADM-P	-53	(38)	54	-29	(24)	31
Isobutene	RADM	-23	(0)	23	-45	(0)	45
	RADM-M	-21	(0)	21	-38	(0)	38
	RADM-P	-21	(0)	21	-38	(0)	38
1-Hexene	RADM	57	(25)	57	82	(25)	82
	RADM-M	59	(26)	59	88	(26)	88
	RADM-P	59	(26)	59	88	(26)	88
Isoprene	RADM	-42	(31)	43	-2	(36)	26
	RADM-M	-42	(31)	43	-2	(36)	26
	RADM-P	-42	(31)	43	-2	(36)	26
a-Pinene	RADM	-8	(35)	28	4	(19)	14
	RADM-M	-8	(34)	27	2	(18)	13
	RADM-P	-8	(34)	27	2	(18)	13
Ethane	RADM	-19	(0)	19	6	(0)	6
	RADM-M	-18	(0)	18	7	(0)	7
	RADM-P	-18	(0)	18	7	(0)	7
n-Butane	RADM	0	(59)	46	19	(50)	43
	RADM-M	-10	(59)	47	12	(49)	41
	RADM-P	-8	(59)	47	13	(49)	41
C4+ Br. Alkane	RADM	-17	(67)	53	-22	(24)	26
	RADM-M	-17	(73)	58	-25	(25)	29
	RADM-P	-19	(62)	50	-22	(24)	25

(continued)

Table 30 (continued) - 2

Organic or Mixture	Mechanism	Maximum Ozone (%)			$d([O_3]-[NO])/dt$ (%)		
		Bias	(sdev)	Err.	Bias	(sdev)	Err.
C5+ n-Alkane	RADM	42	(28)	42	24	(37)	34
	RADM-M	58	(39)	58	38	(43)	46
	RADM-P	41	(27)	41	25	(36)	35
Cycloalkane	RADM	33	(0)	33	3	(29)	19
	RADM-M	85	(0)	85	25	(41)	31
	RADM-P	27	(0)	27	-1	(31)	22
Benzene	RADM	22	(15)	22	36	(19)	36
	RADM-M	20	(13)	20	92	(23)	92
	RADM-P	19	(14)	19	93	(24)	93
Toluene	RADM	24	(43)	33	7	(34)	27
	RADM-M	13	(31)	21	7	(31)	21
	RADM-P	17	(31)	22	10	(31)	23
Xylene	RADM	-4	(25)	18	0	(35)	25
	RADM-M	0	(16)	12	17	(20)	20
	RADM-P	5	(16)	12	17	(21)	21
Mesitylene	RADM	-39	(50)	48	-93	(32)	93
	RADM-M	-26	(19)	29	-57	(22)	57
	RADM-P	-21	(19)	25	-55	(22)	55
Tetralin	RADM	-6	(62)	43	106	(85)	119
	RADM-M	57	(50)	57	125	(91)	137
	RADM-P	56	(49)	56	125	(91)	137
Naphthalene	RADM	84	(40)	84	134	(13)	134
	RADM-M	93	(37)	93	170	(8)	170
	RADM-P	93	(38)	93	170	(8)	170
2,3-Dimethylnaph.	RADM	-6	(24)	17	1	(24)	19
	RADM-M	21	(17)	21	79	(34)	79
	RADM-P	26	(17)	26	79	(32)	79
Simple Mixtures	RADM	-12	(45)	34	-13	(26)	22
	RADM-M	-15	(43)	32	-15	(25)	23
	RADM-P	-14	(44)	32	-14	(25)	22
Simple Surrogates	RADM	7	(24)	15	8	(38)	27
	RADM-M	8	(24)	16	28	(36)	36
	RADM-P	9	(23)	16	28	(36)	35

(continued)

Table 30 (continued) - 3

Organic or Mixture	Mechanism	Maximum Ozone (%)			d([O_3]-[NO])/dt (%)		
		Bias	(sdev)	Err.	Bias	(sdev)	Err.
SAPRC 7-HC Surgs.	RADM	0	(11)	8	-5	(12)	10
	RADM-M	0	(12)	8	-8	(12)	11
	RADM-P	-1	(12)	8	-6	(13)	12
SAPRC 8-HC Surgs.	RADM	9	(26)	20	-10	(23)	19
	RADM-M	3	(26)	19	-5	(24)	19
	RADM-P	5	(25)	19	-3	(25)	19
UNC Misc. Surgs.	RADM	17	(40)	27	2	(15)	11
	RADM-M	11	(40)	25	-3	(15)	12
	RADM-P	10	(37)	24	-3	(15)	12
UNC "Synurban"	RADM	39	(31)	39	7	(8)	8
	RADM-M	22	(25)	24	1	(9)	6
	RADM-P	24	(25)	25	2	(9)	6
UNC "Synauto"	RADM	23	(17)	23	2	(18)	14
	RADM-M	16	(17)	18	-2	(18)	16
	RADM-P	18	(16)	19	-1	(18)	15
UNC Auto Exhaust	RADM	8	(29)	19	-6	(15)	13
	RADM-M	1	(34)	23	-10	(15)	14
	RADM-P	3	(34)	23	-9	(15)	14
Syn. Jet Fuel	RADM	14	(12)	14	11	(16)	16
	RADM-M	16	(11)	16	107	(14)	107
	RADM-P	15	(10)	15	87	(17)	87
Syn. Jet Exhaust	RADM	-11	(8)	11	-8	(4)	8
	RADM-M	-9	(8)	10	3	(5)	5
	RADM-P	-9	(8)	10	2	(5)	5

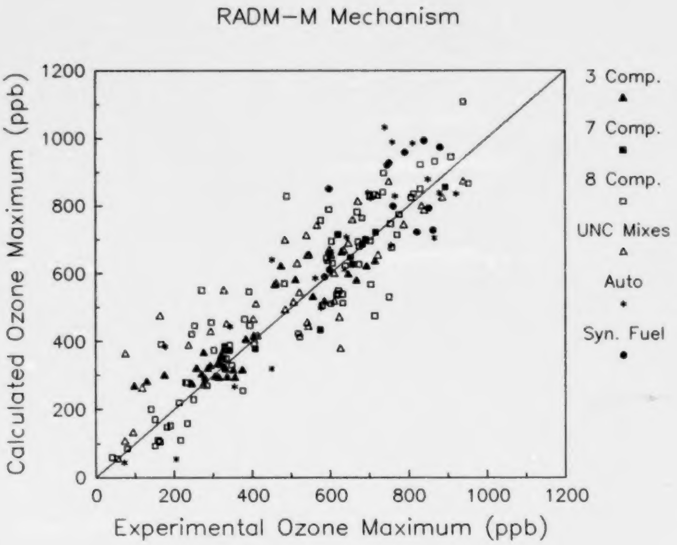

Figure 81. Calculated vs Experimental Maximum Ozone in the Surrogate Mixture Runs for the RADM-M Mechanism.

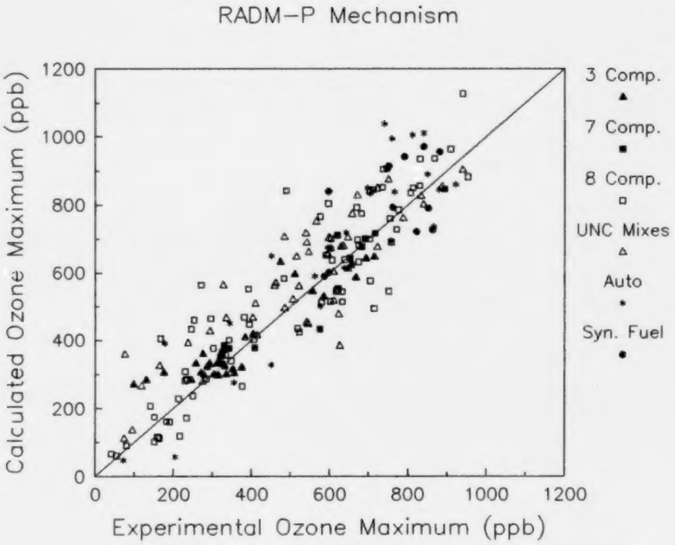

Figure 82. Calculated vs Experimental Maximum Ozone in the Surrogate Mixture Runs for the RADM-P Mechanism.

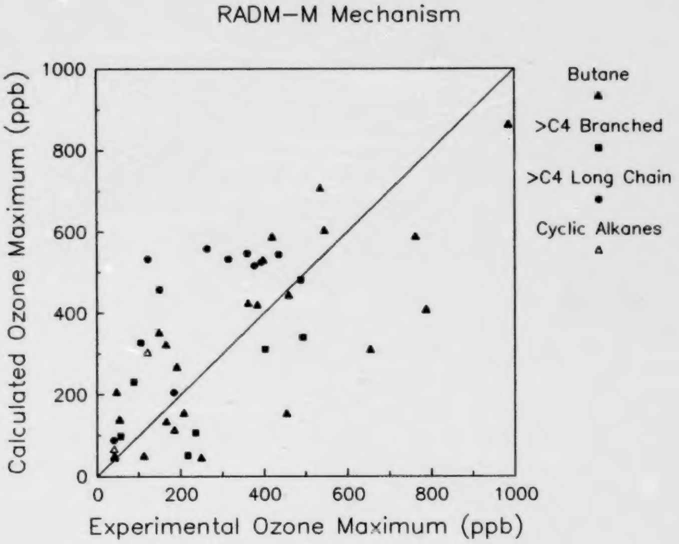

Figure 83. Calculated vs Experimental Maximum Ozone in the Alkane-NO_x Runs for the RADM-M Mechanism.

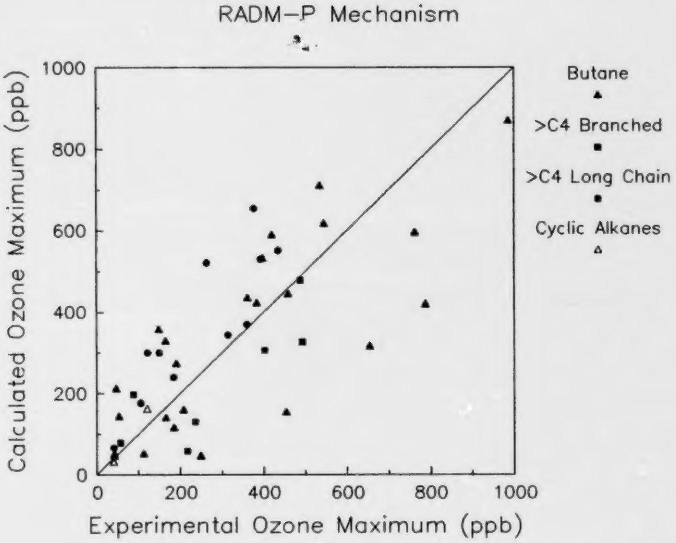

Figure 84. Calculated vs Experimental Maximum Ozone in the Alkane-NO_x Runs for the RADM-P Mechanism.

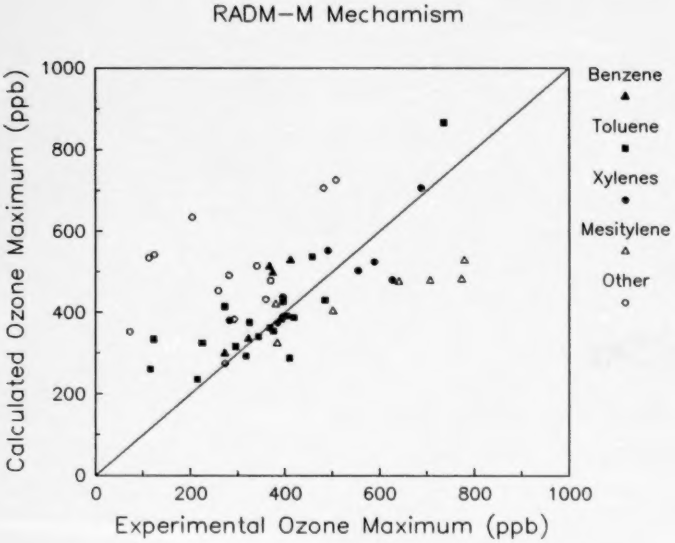

Figure 85. Calculated vs Experimental Maximum Ozone in the Aromatic-NO_x Runs for the RADM-M Mechanism.

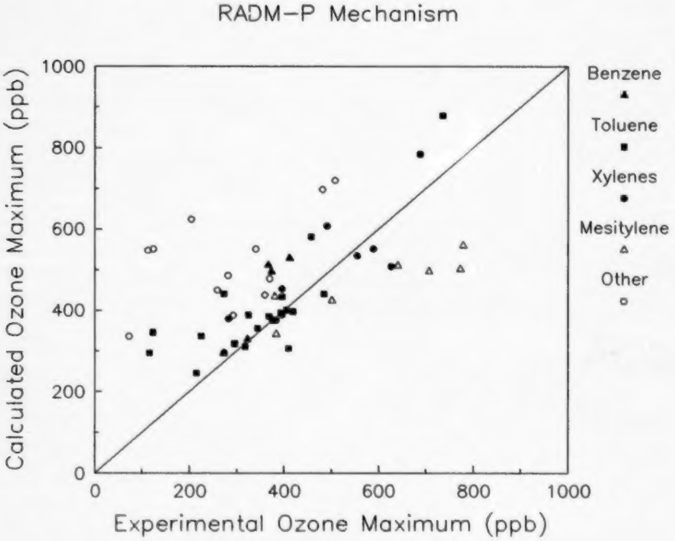

Figure 86. Calculated vs Experimental Maximum Ozone in the Aromatic-NO_x Runs for the RADM-P Mechanism.

The greatest differences between the March 1988 and the recommended modified mechanisms concern the aromatic chemistry. The RADM-M and RADM-P have significantly less scatter in the simulations of the toluene, xylene, and mesitylene-NO_x runs, and their biases in the simulations of the toluene and the mesitylene runs are also less. The apparently better biases of the RADM mechanism relative to RADM-M and RADM-P (Table 30) in the simulations of ozone yields and NO oxidation rates in the xylene runs are due in large part to cancellation of large and opposite errors in simulations of xylene runs carried out in the ITC compared to those carried out in other chambers. (See Figure 40 for the relative performances of these mechanisms in simulating an ITC xylene run, and Appendix A for a run-by-run listing showing the poor performance of the unmodified mechanism in simulating the xylene runs.) It is interesting to note that the differences between the mechanisms are the least in simulations of runs in the UNC chamber and the greatest in simulations of runs in the SAPRC ITC (see Figures 39 through 41 for examples).

Although the recommended modified mechanisms perform significantly better in the simulations of runs employing alkylbenzenes, they perform significantly worse in simulations of runs employing benzene or the naphthalenes, where they consistently overpredict reactivity. The overprediction of reactivities of these compounds is due to the fact that they are represented in the RADM mechanisms by model species (TOL and XYL) which are optimized to simulate toluene and xylenes. Toluene and xylenes are mechanistically much more reactive than benzene and naphthalenes (see Carter et al., 1987 for a discussion of this). The fact that benzene reacts slower than TOL is corrected for using "reactivity weighing," but, this does not correct for differences in mechanistic aspects of reactivity. The naphthalenes react more rapidly than XYL, and yet produce less ozone (Carter et al., 1987). Note that all of the runs with benzene and the naphthalenes were carried out in the SAPRC ITC (see Appendices A-C), where the unmodified mechanism significantly underpredicts the reactivities of alkylbenzene-NO_x runs. (Figure 40 is typical in this regard.) This underprediction for alkylbenzenes in the ITC tends to "correct" for the inappropriate use of TOL to represent benzene and XYL to represent naphthalenes, as shown, for example, in Figure 37 in the case of benzene. Modifying the TOL and XYL mechanism so they perform satisfactorily in simulations of ITC toluene and xylene runs thus causes the mechanism to be too reactive in the simulations of the ITC runs with the mechanistically less reactive aromatics. This modification is still appropriate, however, because alkylbenzenes are relatively more important than benzene or the naphthalenes in the ambient atmosphere.

With two exceptions, the RADM-M and RADM-P mechanisms perform comparably or better than the unmodified RADM mechanism in simulations of runs employing organic mixtures. The major exception concerns the simulations of the "synthetic jet fuel" runs, which were ITC runs containing relatively large amounts of naphthalenes. The other exception concerns the "simple surrogate" runs. This series is dominated by the large number of "mini-surrogate" runs carried out in the SAPRC ITC in 1982-83 (Atkinson et al., 1983), and all versions of the RADM mechanism, and the SAPRC mechanism as well (Carter, 1988), tend to consistently overpredict the NO oxidation rate. However, in most cases the statistical measures for performance on the runs employing mixtures is not significantly different for the three versions of the RADM mechanism.

The RADM-P and RADM-M mechanisms are comparable to the unmodified version in the predictions of formaldehyde. The mechanisms have greater differences in their predictions of PAN, with the RADM-M predicting slightly higher, and RADM-P predicting slightly lower, yields of this product for most, but not all, types of runs. The higher PAN predictions for RADM-M are probably mostly due to the lumping of the RADM's aromatic PAN-analog (TPAN) with PAN in the RADM-M mechanism. The causes for the different PAN predictions for RADM-P relative to RADM are less obvious, but must be due primarily to changes in the aromatics mechanisms, since that is the area where the two mechanisms differ the most.

Comparison of the ozone predictions of the modified mechanisms relative to the unmodified version is shown in Figures 87 and 88. These give plots of ozone yields calculated using RADM-M and RADM-P, respectively, against those calculated using the RADM mechanism for all of the chamber runs employing organic mixtures. It can be seen that while there are many experiments where the mechanisms give the same ozone predictions, there are cases where the modified mechanisms predict less ozone, and practically no cases where they tend to predict more. The tendency towards predicting less ozone in simulating these chamber experiments with

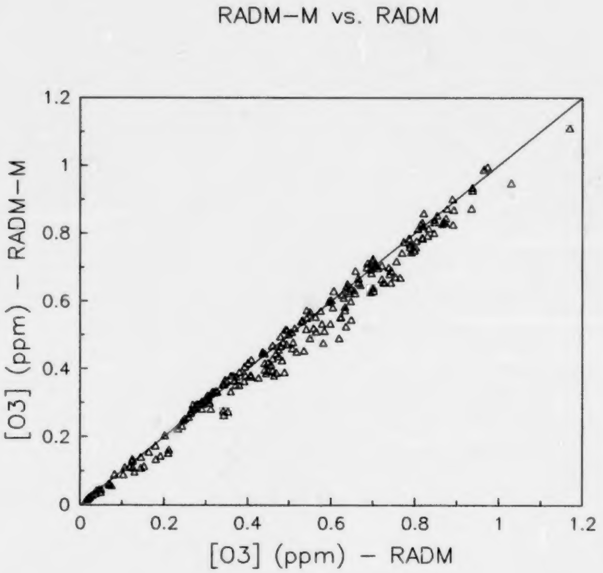

Figure 87. Comparisons of Maximum Ozone Calculated using the RADM-M and the Unmodified RADM Mechanisms for Simple and Surrogate Mixture Runs.

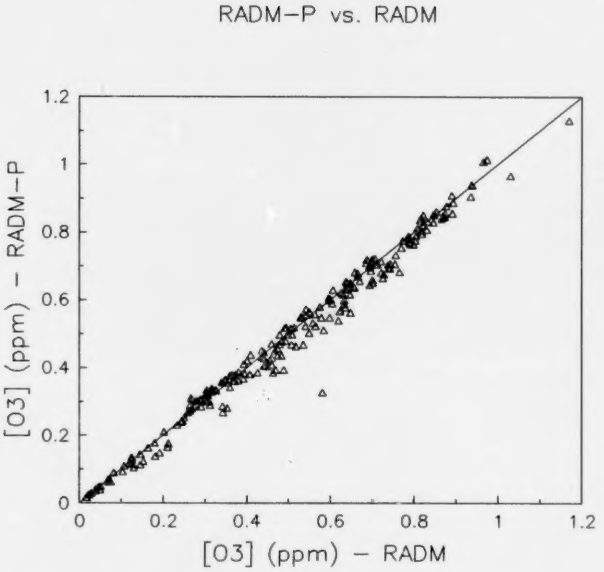

Figure 88. Comparisons of Maximum Ozone Calculated using the RADM-P and the Unmodified RADM Mechanisms for Simple and Surrogate Mixture Runs.

organic mixtures is slightly greater with RADM-M than RADM-P, though except for one run this difference is slight. This suggests that the recommended modifications on the average result in a slightly less reactive mechanism with respect to ozone formation. Differences between these mechanisms in simulations more directly representative of regional modeling applications are discussed in Section 6.

6. EVALUATION OF ALTERNATIVE CHEMICAL ASSUMPTIONS

An important task in the overall evaluation of a chemical mechanism is investigation of alternative versions of the mechanism that incorporate differing chemical approximations or degrees of chemical fidelity. In this study, we developed a series of 90 test problems representing a wide range of chemical conditions likely to be encountered in regional model simulations and used them to assess the effects of selected modifications of the mechanism on model predictions using the RADM mechanism. These included calculations to examine effects of using varying levels of details in representing peroxy radical reactions in the mechanism, calculations to determine the effects of using a more condensed representation of the reactions of the higher alkanes, and calculations to determine the differences in the predictions of the recommended modified versions of the RADM mechanism relative to the March 1988 version. The results of these tests are discussed in this section. Tests of several other mechanistic options were carried out during the course of this study and are referred to where appropriate in other portions of this report. The test problems developed in this study can serve as a basis for further studies of the effects of alternative chemical assumptions on regional model predictions and the future development of more condensed or efficient mechanisms for use in such models.

6.1 Test Problems for Sensitivity Analysis

A set of test problems that span the conditions of importance in regional acid deposition modeling is an essential component to any investigation of sensitivities of mechanism predictions to alternative formulations. If the set of conditions is not sufficiently comprehensive, then conditions where a set of alternative assumptions may be important may not be represented, resulting in the possibility of misleading conclusions regarding the sensitivity of model predictions to these assumptions. Several aspects of regional modeling must be considered in the selection of test problems. First, regional modeling involves transport of pollutants over long distances, so it is essential to use multi-day test problems. Second, the vertical domain of the regional models extends from the earth's surface to the tropopause. Atmospheric temperature, pressure, solar radiation intensity, and the radiation's spectral distribution vary significantly from the lower to the upper troposphere. The test conditions must address these variations. Third, the regional models are designed to simulate the chemical and physical evolution of emissions as they are transported from source areas to remote areas. Therefore, it is important for the test conditions to span the range of pollutant concentrations encountered in both urban and rural regions. This can be accomplished by varying the VOC and NO_x concentrations, VOC-to-NO_x ratio, and VOC composition.

The ideal framework in which to test alternative chemical mechanisms is in a three-dimensional transport model such as RADM using actual meteorological conditions. However, this approach is not practical because of the large computing resources needed for the transport model and the large effort required to both install an alternative mechanism in a transport model and develop mechanism specific speciated VOC emissions inventories. Even if this were practical, the fact that the meteorological inputs have only been developed for a small number of episodes limits the utility of this approach.

An alternative approach adopted here is to use a simple photochemical box model and exercise the model for a large number of cases that span the expected range of conditions encountered in actual regional modeling. The box modeling approach can sometimes produce unrealistic pollutant concentrations because of its simplistic treatment of transport. Nevertheless, it is well suited to investigating the relative differences in alternative chemical mechanisms. In fact, most mechanism comparisons have been performed with photochemical box models (Jeffries et al., 1981; Dunker, 1984; Leone and Seinfeld, 1985; Schafer and Seinfeld, 1985; Stockwell, 1986; Hough, 1987; Milford, 1988; Stockwell and Lurmann, 1989; Dodge, 1989).

The matrix of the test problems selected for the analysis involves a relatively small number of environmental conditions and a large number of chemical conditions. The rationale for this approach is that alternative mechanisms are expected to respond similarly to changes in environmental conditions and differently to variations in the chemical mixtures. The three sets of environmental conditions considered are shown in Table 31. These constant temperature cases include summer conditions at surface

Table 31. Environmental Conditions Used in Test Problems for Sensitivity Calculations

Parameter	Summer Surface	Winter Surface	Summer Aloft
Simulation Duration			
Start Time (LDT) (a)	0500	0500	0500
End Time on Last Day (LDT)	2000	2000	2000
Number of Days in Simulation (b)	2-5	3-5	3-5
Light Conditions (c)			
Date	June 21	December 21	June 21
Latitude (deg)	40	40	40
Elevation (km)	0	0	6
Meteorological Conditions			
Temperature (K)	298	273	248
Pressure (atm)	1	1	0.5
Rel. Humidity (%)	50	50	10
Water Vapor (ppm)	15,600	3,000	160
	LDT (m)	LDT (m)	
Inversion Height Schedule (d)	0539 800	0805 800	(Constant)
	1116 1116	1133 958	
	1501 1200	1352 1000	
Background Pollutant Concentrations (ppb) (e)			
O_3	20-40 (f)	20	0
CO	200	200	200
CH4	1800	1800	1800
Daytime Dry Deposition Velocities (cm/sec):			
O_3	0.6	0.3	0.0
SO_2	0.8	0.4	0.0
Sulfate	0.4	0.2	0.0
H_2O_2	1.6	0.8	0.0
NO2	0.4	0.2	0.0
PAN and Organic Nitrates (ONIT)	0.4	0.2	0.0
Organic peroxides (OP1 and OP2)	0.8	0.4	0.0
Organic Acids (ORA1 and ORA2)	0.8	0.4	0.0
HNO_3	3.0	1.5	0.0

(continued)

Table 31 (continued) - 2

(a) LDT = Local Daylight Time.

(b) Number of days of simulation depended on chemical conditions. See Table 34.

(c) Solar flux data output by the RADM radiation module was provided by Stockwell (private communication, 1988). The data were given in terms of actinic fluxes for 93 wavelength intervals between 280 and 735 nm for zenith angles of 0, 10, 20, 30, 40, 50, 60, 70, 78, and 86. These fluxes are available in computer readable form from the authors upon request. The zenith angle dependencies of these actinic fluxes for the various wavelength intervals were fit using a parameterized function similar to that used by Carter et al. (1986), which was then used to calculate the actinic flux at any given zenith angle in the simulation.

(d) Inversion height is constant at initial value shown at beginning of the day, then changed linearly with time to the values at the times indicated. The inversion height was constant at the final value for the remainder of the day. The inversion height schedule is based on a simplified approximation of the "characteristic curve" used in the OZIPM software (Gipson, 1984). The final inversion heights were determined to obtain the desired amount of dilution for each simulated day.

(e) "Background" species concentrations were added to the initial pollutant concentrations in the simulations, and (for the ground level simulations) are entrained into the air mass as the inversion height increases.

(f) 20 ppb background O_3 was used in the "rural" summer surface simulations with initial NO_x levels of 0.5 ppb. 40 ppb background ozone was used in all the other summer surface simulations.

elevation, winter conditions at surface elevation, and summer conditions at 6 km above the surface. The solar actinic fluxes used in the simulations of these conditions were obtained from the RADM radiation module (Stockwell, personal communication, 1988). Solar radiation for the simulations is based on the diurnal cycle at 40 degrees latitude in the summer and winter solstices. A small amount of dilution (25% per day in the winter case and 50% per day in the summer case) with relatively clean background air is included along with very approximate dry deposition velocities to inhibit build-up of unrealistically high concentrations. Only daytime dry deposition is included in the simulations. Nighttime deposition is assumed to be negligible.

All the winter surface and summer aloft simulations were "static" with respect to pollutant injection. All pollutants were assumed to be present initially, with no subsequent injection of pollutants other than background species entrained from aloft as the inversion height increased. "Static" and "dynamic" simulations were carried out for the summer surface conditions. In the "dynamic" simulations, no pollutants were present initially (other than the background species), and pollutants were injected at a constant flux (moles per unit area) throughout the simulation. Thus, four different types of environmental conditions are used in the simulations:

(1) Summer Surface - Static (designated "Summer Surface")
(2) Summer Surface - Dynamic (designated "Summer Dynamic")
(3) Winter Surface - Static (designated "Winter Surface")
(4) Summer Aloft - Static (designated "Summer Aloft")

The chemical conditions for these runs can be described as "rural" or "urban," with the former having the relatively low pollutant levels characteristic of rural conditions and the latter having the higher pollutant levels more typical of urban areas. For each type of chemical condition, the total NO_x and reactive organic (ROG) levels were varied over relatively wide ranges, and several different mixtures representing ROG pollutants were employed. The ROG mixtures employed in these simulations were chosen to represent typical ambient mixtures of varying composition and reactivity, with three different compositions used in the urban simulations and two used in the rural runs.

The three urban ROG composition profiles are based on 6-9 AM ambient urban samples collected by EPA/AREAL (under Bill Lonneman's direction) in 41 U.S. cities during 1984-1986. These hydrocarbon data have been thoroughly analyzed by Jeffries et al. (1989c) to derive the recommended carbon fractions for the "Carbon Bond" and the "CAL" mechanisms. The specific profiles used in these simulations are the average of the 773 samples collected in all of the cities (referred to as the "allcity" average), the average of the 8 samples collected in Washington, DC, during 1986 and the average of 9 samples collected in Beaumont, Texas during 1984. The latter two were selected because their composition and reactivity are most different from the average. The Beaumont profiles have unusually high alkane fractions and low aromatic and C3+ alkene fractions. The Washington DC profiles have unusually high levels of aromatics and low levels of alkanes. This data base does not contain aldehyde measurements, and for all three profiles we followed the standard assumption employed by the EPA and its contractors (e.g., EPA, 1984; Lurmann et al., 1987; Jeffries et al., 1989c) that urban ROG profiles consist of 5% aldehydes (on a carbon basis). This is based on an upper limit estimate derived from data collected in Los Angeles (Grosjean, 1983). It was assumed that these urban aldehydes consist of 60% formaldehyde and 40% acetaldehyde (on a carbon basis - as did Lurmann et al., 1987), which is slightly different than the 40% formaldehyde-60% acetaldehyde assumption employed by Jeffries et al. (1989c). Both assumptions are consistent with the available data. These three urban ROG surrogates are similar to those used in the mechanism comparison study recently carried out by Dodge (1989).

The ROG profiles employed in the rural simulations are based on 53 morning samples collected above the mixed layer by aircraft in four cities (Westburg and MacGregor, 1987). These measurements include aldehydes. These data have also been extensively analyzed by Jeffries et al. (1989c) for determination of typical ROG concentrations aloft. One of the two rural profiles is based on the average composition of these data. This is referred to as the "aloft" surrogate. The other rural surrogate is designed to represent air masses with significant biogenic hydrocarbon input. It has 46% isoprene (on a carbon basis), the same aldehyde levels as the aircraft data, and the remaining hydrocarbons apportioned based on the aircraft data. This is referred to as the "aloft+isoprene" surrogate.

The detailed compositions used for these five surrogate mixtures are given in Table 32. These were taken from the detailed data sets provided by Jeffries (private communication, 1988). As is the case with most ambient ROG samples, numerous assumptions were needed to assign the unidentified and ambiguously classified carbon into known species. These detailed profiles were converted to profiles of specific compounds (or groups of compounds assumed to have the same reactivity) based on (1) the assumptions employed by Jeffries et al. (1989c) concerning ambiguous classes of olefins and aromatics and concerning the classifications of species such as alkynes and styrenes, and (2) assuming the "unknown" data were hydrocarbons with the same distribution of species as the identified species in the profiles. These individual species were then converted into species in the RADM mechanism using the same set of procedures used in processing organic emissions input into the RADM-II model, discussed in Section 3. The distribution of RADM-II species for these five surrogates is given in Table 33. Note that in many cases the molar concentrations of the lumped RADM species do not add up exactly to the totals for the species they represent because of the use of "reactivity weighting" in the RADM emissions processing system (see Section 3).

Table 34 summarizes the conditions of all the test calculations, including the environmental conditions, the duration of the simulation, the ROG surrogate mixture, and the ROG and NO_x levels employed for each run. The minimum duration of the simulations was two days. The maximum duration was either five days or one day more than needed for complete consumption of the NO_x, whichever was less. With the exception of a few simulations at very low ROG/NO_x ratios, the simulations were carried out for a sufficient amount of time that the effects of alternative assumptions concerning the radical-radical reactions occurring in the absence of NO_x could be adequately tested. For the rural simulations, the ROG concentrations ranged from 10 to 100 ppbC, the NO_x concentrations from 0.5 to 5 ppb, and the initial ROG-to-NO_x ratio from 2 to 200. For the urban simulations, the ROG concentration ranged from 200 to 2000 ppbC, the NO_x concentration from 20 to 200 ppb, and the initial ROG-to-NO_x ratio from 2

Table 32. Compositions of ROG Surrogate Mixtures Used in Test Calculations

Compound and Emissions Group (a)	Composition (ppb Species/ppmC ROG Surrogate)				
	Allcity Average	Washington DC	Beaumont TX	Aloft	Aloft + Isop.
Ethane	20.78	24.33	38.15	111.06	54.42
Propane	15.47	11.35	27.40	48.47	23.91
Alkanes (0.25-0.50) (b)					
n-Butane	16.39	19.92	24.62	23.64	11.70
Isobutane	6.91	5.78	12.49	12.69	6.28
Neopentane	0.39	0.20	0.57	0.00	0.00
Unspeciated C4-C5 Alkanes	0.01	0.00	0.00	0.00	0.00
Alkanes (0.50-1.00)					
n-Pentane	6.81	5.37	8.50	7.14	3.54
Iso-Pentane	14.09	16.31	14.48	11.59	5.75
Cyclopentane	0.63	0.50	1.11	2.29	1.14
n-Hexane	2.94	1.98	4.03	2.02	1.00
2-Methyl Pentane	3.82	3.51	4.36	2.44	1.21
3-Methylpentane	2.74	3.03	3.00	1.32	0.66
2,3-Dimethyl Butane	1.01	1.17	1.08	0.57	0.28
Branched C6 Alkanes	0.89	1.84	0.72	0.00	0.00
Alkanes (1.00-2.00)					
Cyclohexane	0.84	0.27	1.38	0.45	0.22
C6 Cycloalkanes	1.66	1.43	2.15	0.86	0.43
n-Heptane	1.12	0.89	0.95	0.00	0.00
Branched C7 Alkanes	5.17	4.46	3.65	2.57	1.28
C7 Cycloalkanes	0.84	0.58	1.17	0.00	0.00
n-Octane	0.59	0.58	0.39	0.35	0.17
Branched C8 Alkanes	4.89	4.69	3.54	0.90	0.45
C8 Cycloalkanes	0.10	0.05	0.10	0.00	0.00
n-Nonane	0.46	0.42	0.33	0.00	0.00
Branched C9 Alkanes	1.92	1.82	1.71	0.00	0.00
n-Decane	0.63	0.90	0.33	0.00	0.00
Branched C10 Alkanes	1.38	0.96	1.26	0.00	0.00
Alkanes (>2.00)					
Branched C11 alkanes	0.55	1.09	0.20	0.00	0.00
Branched C12 Alkanes	0.13	0.18	0.11	0.00	0.00
Branched C13 Alkanes	0.00	0.00	0.00	0.00	0.00

(continued)

Table 32 (continued) - 2

Compound and Emissions Group (a)	Composition (ppb Species/ppmC ROG Surrogate)				
	Allcity Average	Washington DC	Beaumont TX	Aloft	Aloft + Isop.
Ethene	19.18	16.33	23.27	14.98	7.34
Propene	4.93	3.25	5.16	2.57	1.26
Other Terminal Monoalkenes					
1-Butene	2.49	2.56	1.78	0.00	0.00
1-Pentene	0.54	0.43	0.53	0.00	0.00
1-Hexene	0.21	0.13	0.09	0.00	0.00
2-Methyl-1-Butene	0.82	0.81	0.72	0.00	0.00
C4 Terminal Alkanes	1.72	0.25	1.33	0.00	0.00
C5 Terminal Alkanes	1.30	1.42	0.98	0.00	0.00
C6 Terminal Alkanes	0.51	0.31	0.47	0.00	0.00
C7 Terminal Alkanes	1.14	0.82	0.71	0.00	0.00
C8 Terminal Alkanes	0.40	0.40	0.20	0.00	0.00
C9 Terminal Alkanes	0.71	0.19	0.41	0.00	0.00
C10 Terminal Alkanes	0.03	0.15	0.01	0.00	0.00
C11 Terminal Alkanes	0.40	0.01	0.76	0.00	0.00
Internal Alkenes, Dienes, and Pinenes					
cis-2-Butene	0.79	0.64	0.81	0.00	0.00
trans-2-Butene	1.02	0.74	1.09	0.00	0.00
1,3-Butadiene	0.67	0.26	0.44	0.00	0.00
2-Methyl-2-Butene	0.11	0.00	0.03	0.00	0.00
C5 Terminal Alkenes	1.99	1.25	1.70	0.00	0.00
C6 Terminal Alkenes	0.93	0.61	0.72	0.00	0.00
C7 Terminal Alkenes	0.10	0.05	0.04	0.00	0.00
C8 Terminal Alkenes	0.02	0.00	0.03	0.00	0.00
a-Pinene	0.61	0.18	0.28	0.00	0.00
Benzene	3.43	3.58	2.31	4.07	2.02
Aromatics (<2.00)					
Toluene	8.19	11.18	4.09	4.87	2.42
Ethyl Benzene	1.23	1.61	0.71	0.88	0.44
Isopropyl Benzene	0.14	0.07	0.05	0.00	0.00
n-Propyl Benzene	0.28	0.39	0.18	0.00	0.00
Monoalkyl Benzenes	1.67	2.05	0.93	0.00	0.00

(continued)

Table 32 (continued) - 3

Compound and Emissions Group (a)	Composition (ppb Species/ppmC ROG Surrogate)				
	Allcity Average	Washington DC	Beaumont TX	Aloft	Aloft + Isop.
Aromatics (>2.00)					
m-Xylene	1.93	2.54	1.08	0.72	0.36
o-Xylene	1.53	2.37	0.72	2.03	1.01
p-Xylene	1.93	2.54	1.08	0.72	0.36
Dialkyl Benzenes	4.80	5.22	2.98	0.00	0.00
1,2,3-Trimethyl Benzene	2.88	4.03	1.41	0.00	0.00
Trialkyl Benzenes	1.92	1.89	1.44	0.00	0.00
Tetraalkyl Benzenes	0.18	0.11	0.10	0.00	0.00
Acetylene	11.43	10.55	4.82	8.99	4.41
Formaldehyde	30.00	30.00	30.00	74.86	74.86
Acetaldehyde	10.00	10.00	10.00	10.75	10.75
Isoprene	0.67	0.61	0.78	3.42	92.75

(a) "Emissions Group" is the group the individual compounds are lumped into during processing of emissions data (see Section 3). If a compound is given by itself (e.g., ethane), it is in an emissions group by itself. If more than one compound (or group of compounds) is lumped into an emissions group, [e.g., n-butane, isobutane, etc., in group "Alkanes (0.25-0.50)"], the individual compounds or groups are listed below the emissions group name.

(b) Quantities in parentheses refer to range of OH radical rate constants (in units of 10^4 ppm^{-1} min^{-1}) for compounds in the emissions group.

Table 33. Compositions of ROG Surrogates Used in the Test Calculations for the RADM Mechanism

RADM Species Name	Description (a)	Composition (ppb RADM Species/ppmC ROG)				
		Allcity Average	Washington DC	Beaumont TX	Aloft	Aloft + Isop.
ETH	Ethane	20.78	24.33	38.15	111.1	54.42
HC3	Alkanes (0.25-0.50)	35.54	35.22	53.33	64.63	31.93
HC5	Alkanes (0.50-1.00)	29.60	30.31	33.53	24.61	12.21
HC8	Alkanes (>1.00)	18.64	16.95	15.81	4.68	2.33
OL2	Ethene	19.18	16.33	23.27	14.98	7.34
OLT	Terminal Alkenes	15.21	10.73	13.15	2.65	1.27
OLI	Internal Alkenes	6.24	3.72	5.13	0.0	0.0
ISO	Isoprene	0.67	0.61	0.78	3.42	92.75
TOL	Aromatics (<2.00)	12.54	16.37	6.65	6.97	3.47
XYL	Aromatics (>2.00)	15.16	18.71	8.81	3.48	1.73
HCHO	Formaldehyde	30.00	30.00	30.00	74.86	74.86
ALD	Higher Aldehydes	10.00	10.00	10.00	10.75	10.75

(a) Quantities in parentheses for lumped higher alkanes and aromatics refer to OH radical rate constant ranges in units of 10^4 ppm^{-1} min^{-1}.

Table 34. Summary of Conditions of Test Calculations Used for Sensitivity Studies

No.	Environmental Condition	ROG Surrogate	Reactant Levels (a)			No. Days
			ROG	NO_x	ROG/NO_x	
		Rural Simulations				
1	Summer Surface	Aloft	10	0.5	20	3
2	Summer Surface	Aloft	33	0.5	66	3
3	Summer Surface	Aloft	100	0.5	200	3
4	Summer Surface	Aloft	10	1.7	6	2
5	Summer Surface	Aloft	33	1.7	20	2
6	Summer Surface	Aloft	100	1.7	60	2
7	Summer Surface	Aloft	10	5.0	2	3
8	Summer Surface	Aloft	33	5.0	7	3
9	Summer Surface	Aloft	100	5.0	20	3
10	Winter Surface	Aloft	10	1.7	6	5
11	Winter Surface	Aloft	33	1.7	20	4
12	Winter Surface	Aloft	100	1.7	60	3
13	Summer Aloft	Aloft	10	1.7	6	5
14	Summer Aloft	Aloft	33	1.7	20	4
15	Summer Aloft	Aloft	100	1.7	60	3
16	Summer Dynamic	Aloft	10	1.7	6	3
17	Summer Dynamic	Aloft	33	1.7	20	4
18	Summer Dynamic	Aloft	100	1.7	60	4
19	Summer Surface	Aloft+Isoprene	10	0.5	20	5
20	Summer Surface	Aloft+Isoprene	33	0.5	66	5
21	Summer Surface	Aloft+Isoprene	100	0.5	200	5
22	Summer Surface	Aloft+Isoprene	10	1.7	6	2
23	Summer Surface	Aloft+Isoprene	33	1.7	20	2
24	Summer Surface	Aloft+Isoprene	100	1.7	60	2
25	Summer Surface	Aloft+Isoprene	10	5.0	2	3
26	Summer Surface	Aloft+Isoprene	33	5.0	7	3
27	Summer Surface	Aloft+Isoprene	100	5.0	20	3
28	Winter Surface	Aloft+Isoprene	10	1.7	6	5
29	Winter Surface	Aloft+Isoprene	33	1.7	20	4
30	Winter Surface	Aloft+Isoprene	100	1.7	60	3
31	Summer Aloft	Aloft+Isoprene	10	1.7	6	5
32	Summer Aloft	Aloft+Isoprene	33	1.7	20	4
33	Summer Aloft	Aloft+Isoprene	100	1.7	60	3

(continued)

Table 34 (continued) - 2

No.	Environmental Condition	ROG Surrogate	Reactant Levels (a)			No. Days
			ROG	NO_x	ROG/NO_x	
34	Summer Dynamic	Aloft+Isoprene	10	1.7	6	3
35	Summer Dynamic	Aloft+Isoprene	33	1.7	20	4
36	Summer Dynamic	Aloft+Isoprene	100	1.7	60	4
		Urban Simulations				
37	Summer Surface	Allcity Avg.	200	67.	3	3
38	Summer Surface	Allcity Avg.	667	67.	10	3
39	Summer Surface	Allcity Avg.	2000	67.	30	2
40	Summer Surface	Allcity Avg.	200	20.	10	3
41	Summer Surface	Allcity Avg.	667	20.	33	2
42	Summer Surface	Allcity Avg.	2000	20.	100	2
43	Summer Surface	Allcity Avg.	200	100.	2	5
44	Summer Surface	Allcity Avg.	667	200.	3	3
45	Summer Surface	Allcity Avg.	2000	200.	10	3
46	Winter Surface	Allcity Avg.	200	67.	3	5
47	Winter Surface	Allcity Avg.	667	67.	10	5
48	Winter Surface	Allcity Avg.	2000	67.	30	4
49	Summer Aloft	Allcity Avg.	200	67.	3	5
50	Summer Aloft	Allcity Avg.	667	67.	10	4
51	Summer Aloft	Allcity Avg.	2000	67.	30	3
52	Summer Dynamic	Allcity Avg.	200	67.	3	5
53	Summer Dynamic	Allcity Avg.	667	67.	10	5
54	Summer Dynamic	Allcity Avg.	2000	67.	30	5
55	Summer Surface	Washington DC	200	67.	3	3
56	Summer Surface	Washington DC	667	67.	10	3
57	Summer Surface	Washington DC	2000	67.	30	2
58	Summer Surface	Washington DC	200	20.	10	3
59	Summer Surface	Washington DC	667	20.	33	2
60	Summer Surface	Washington DC	2000	20.	100	2
61	Summer Surface	Washington DC	200	100.	2	5
62	Summer Surface	Washington DC	667	200.	3	3
63	Summer Surface	Washington DC	2000	200.	10	3
64	Winter Surface	Washington DC	200	67.	3	5
65	Winter Surface	Washington DC	667	67.	10	5
66	Winter Surface	Washington DC	2000	67.	30	4

(continued)

Table 34 (continued) - 3

No.	Environmental Condition	ROG Surrogate	Reactant Levels (a)			No. Days
			ROG	NO_x	ROG/NO_x	
67	Summer Aloft	Washington DC	200	67.	3	5
68	Summer Aloft	Washington DC	667	67.	10	4
69	Summer Aloft	Washington DC	2000	67.	30	3
70	Summer Dynamic	Washington DC	200	67.	3	5
71	Summer Dynamic	Washington DC	667	67.	10	5
72	Summer Dynamic	Washington DC	2000	67.	30	5
73	Summer Surface	Beaumont TX	200	67.	3	3
74	Summer Surface	Beaumont TX	667	67.	10	3
75	Summer Surface	Beaumont TX	2000	67.	30	2
76	Summer Surface	Beaumont TX	200	20.	10	3
77	Summer Surface	Beaumont TX	667	20.	33	2
78	Summer Surface	Beaumont TX	2000	20.	100	2
79	Summer Surface	Beaumont TX	200	100.	2	5
80	Summer Surface	Beaumont TX	667	200.	3	3
81	Summer Surface	Beaumont TX	2000	200.	10	3
82	Winter Surface	Beaumont TX	200	67.	3	5
83	Winter Surface	Beaumont TX	667	67.	10	5
84	Winter Surface	Beaumont TX	2000	67.	30	4
85	Summer Aloft	Beaumont TX	200	67.	3	5
86	Summer Aloft	Beaumont TX	667	67.	10	4
87	Summer Aloft	Beaumont TX	2000	67.	30	3
88	Summer Dynamic	Beaumont TX	200	67.	3	5
89	Summer Dynamic	Beaumont TX	667	67.	10	5
90	Summer Dynamic	Beaumont TX	2000	67.	30	5

(a) For the static calculations ("summer surface," "winter surface," and "summer aloft"), the reactant levels refer to initial concentrations in ppbC (for ROG) or ppb (for NO_x), excluding background species. For the "summer dynamic" concentrations, the reactant levels refer to the increase in concentrations of ROG (in ppbC) or NO_x (in ppb) that would result following one day of continuous emissions if there were no chemical reaction and the inversion height remained constant at its initial level of 800 meters.

to 100. These combinations of ROG and NO_x adequately bracket probable atmospheric concentrations in most rural and urban areas. This set consists of a total of 90 simulations, 36 representing rural conditions and 54 representing urban pollution.

6.2 Presentation of Sensitivity Test Results

The results of test calculations using alternative mechanisms can be presented in a number of ways. Many sensitivity studies have used plots to compare concentrations of species of interest. While this is a useful approach when a relatively small number of test problems are used, it is less practical when the number of test cases is relatively large, as is the case in this study. This is analogous in some ways to the problems of summarizing the performance of a mechanism in simulating the results of a large number of chamber experiments. Therefore, in presenting the results of the test calculations, we use an approach similar to that used in the evaluation against the chamber data -- the results are presented in the form of tabulations of statistical measures of the comparisons of the mechanisms, with examples given for results of individual calculations which are of interest.

Statistics are tabulated for the following species, which are of known or potential interest in regional acid deposition model simulations (RADM model species name -- used in the tabulations -- are given in parentheses):

1. Ozone (O3);
2. Hydrogen Peroxide (H2O2);
3. Sulfuric Acid or Sulfates (SULF);
4. Nitric Acid (HNO3);
5. Formic Acid (ORA1);
6. Higher Organic Acids (ORA2);
7. Methyl Hydroperoxide (OP1);
8. Higher Organic Hydroperoxides (OP2);
9. Peroxy Acetic Acid (PAA); and
10. PAN and Higher Peroxy Nitrates (PAN).

Given the results of model calculations using two different models (one designated the "standard" calculation, and the other -- generally having a modification to the "standard" mechanism whose effect is being examined -- designated the "test" calculation), the following statistics are tabulated for each of these species for each of the test problems:

1. Maximum concentration for the standard calculation;
2. Percent change in the maximum concentration in the test calculation relative to the standard calculation;
3. Average concentration for the "standard" calculation;
4. Percent change in the average concentration in the test calculation relative to the standard calculation;
5. Percent change in the average concentration, relative to the maximum average concentration for the set (see below); and
6. The "Percent fit" statistic, calculated as discussed below.

The statistics are calculated for the entire time duration of these multi-day calculations. The first four of the above statistics are derived in the usual manner. A positive number means that the test calculation predicts a larger maximum or average than the standard calculation, while a negative number means it predicts a lower value. The tabulations indicate which of the mechanisms is used as the "standard" and which is used as the "test."

The fifth statistic, designated "% /Max" on the tabulations, is calculated for a given species in a given test calculation as follows:

$$\text{"\% /Max"} = 100 \times \frac{\begin{array}{c}\text{(Average Conc.,}\\ \text{Test Calc.)}\end{array} - \begin{array}{c}\text{(Average Conc.}\\ \text{Standard Calc.)}\end{array}}{\text{(Maximum of the Averages for the Group)}}$$

The purpose of this statistic is to obtain an indication of the changes in absolute concentrations of the species for an entire set of calculations. These are normalized to the maximum value for the set to allow for meaningful comparisons with predictions obtained for other species whose concentration may be quite different. Thus, if there is a large positive or negative magnitude in this statistic, it means that the two models are significantly different in their calculations of this species, and it is not a case of a large relative difference in the calculation of an insignificant concentration. For the purpose of calculating this statistic, the calculations are grouped into "rural" and "urban" problems. This is to account for the fact that concentration regimes for at least some of the species of interest might be different for these types of problems.

The sixth statistic, designated as "% Fit" on the tabulations, measures the overall differences in the simulations of the species on a point-by-point basis, paired in time. It is calculated by

$$\text{"\% Fit"} = \frac{\Sigma\ |T_i - S_i|}{0.5 \times \Sigma\ (T_i + S_i)}$$

where T_i and S_i are the concentrations of the species for the test and the standard calculation, respectively, at time "i," and the summations are over all the times where data are saved in the calculations, which is once every hour. The purpose of this statistic is to make evident differences in curve shapes which might still have similar average or maximum values.

6.3 Treatment of Peroxy Radical Reactions

Alkyl and acyl peroxy radicals are important intermediates in the gas-phase atmospheric reactions of organic compounds. In the presence of NO_x their major fates are reaction with NO and (for acyl peroxy radicals) with NO_2, and these reactions are important in affecting ozone formation. When NO_x levels are low, their major fates are reaction with HO_2 or with other peroxy radicals, and these reactions are important in affecting predictions of H_2O_2 and organic hydroperoxy species. Therefore, the appropriate representation of the reactions of these species is important in acid deposition models, where accurate predictions of both oxidant and hydroperoxide formation are essential. This includes appropriate representations of peroxy-peroxy radical reactions, since sensitivity calculations we have carried out previously (Carter et al., 1986) and more recent calculations carried out by Dodge (1989) indicate that they cannot be ignored. However, because of the relatively large number of organic peroxy species which must be included in even relatively condensed gas-phase atmospheric representations, almost all current mechanisms represent these peroxy-peroxy radical reactions in an approximate manner. The RADM mechanism is no exception in this regard.

As indicated in Section 2, the RADM mechanism has a relatively detailed representation of peroxy radicals, using separate species to represent peroxy radicals formed from most of the organic model species, and representing explicitly their reactions with NO, NO_2 (for acylperoxy radicals), HO_2, methyl peroxy radicals (MO2), and acetyl peroxy radicals (ACO3). However, this mechanism ignores all the reactions of organic peroxy radicals with organic peroxy radicals other than MO2 or ACO3. Stockwell (private communication) conducted test calculations which indicated that using only reactions with MO2 and ACO3 should be sufficient. However, the description and results of these tests have not been included with the available documentation of the mechanism. In view of the importance of peroxide and hydroperoxide predictions in acid deposition models, we felt that an independent test of the validity of this approximation in the RADM mechanism would be a useful component of this evaluation study.

On the other hand, it may well be that the RADM mechanism is more detailed in its representation of peroxy radical reactions than is necessary. The latest Carbon Bond (Gery et al., 1988) and SAPRC (Carter, 1989a) mechanisms, and the chemical mechanism for the ADOM model (Lurmann and Karamchandani, 1987) employ much more condensed representations of these reactions. These mechanisms do not have separate reactions for the many kinds of peroxy radical species; instead they use a limited number of chemical "operators" to represent the net effects of their reactions. The representations used in these other current mechanisms are too condensed to permit the separate representation of methyl hydroperoxide and the higher hydroperoxides which are utilized in the RADM mechanism. Since Stockwell (private communication) considers separate representation of methyl and the higher hydroperoxides to be important for RADM, the more condensed approaches which require that these be lumped together were not examined in this study.

However, an earlier version of the SAPRC mechanism (Carter et al., 1986) uses a less condensed representation which allows for separate representation of the two types of hydroperoxide species, and also allows for all the possible organic peroxy + organic peroxy reactions to be represented without using many more reactions than used for this purpose in the RADM mechanism. A detailed discussion of this approach is beyond the scope of this report (see Carter et al., 1986), but briefly it involves using chemical operators to account for total organic peroxy ("RO2") and acylperoxy ("RCO3") radical concentrations, and then using these to calculate rates of reactions of the individual organic peroxy radicals with themselves and all other organic peroxy radicals. This allows for all the possible radical combinations to be represented, but requires using the same rate constants for all these reactions. By contrast, the RADM mechanism is more approximate in the sense that it represents only a subset of the possible peroxy + peroxy reactions, but is more detailed in the sense that it uses separate estimated rate constants for the various individual reactions which it does include. Therefore, the effect of modifying the RADM mechanism so that it incorporates the SAPRC approach was also evaluated in this study.

In order to test effects of alternative approximation methods of representing the organic peroxy radical reactions, it is necessary to have a detailed representation against which to compare them. For this purpose, Stockwell (private communication, 1988) provided SAPRC with a "detailed radical" version of the RADM mechanism, which included all the possible combination reactions of the organic peroxy and acylperoxy species in the RADM mechanism. Other than the additional reactions of the organic peroxy and acylperoxy radical species with peroxy radical species other than MO2 and ACO3 (and the inclusion of the OLN + MO2 and OLN + ACO3 reactions), this mechanism was exactly the same as the March 1988 version of the RADM mechanism which was evaluated in this study. The approach Stockwell used to estimate the rate constants and products for these additional reactions was consistent with the approach used for the reactions in the March 1988 mechanism. Almost all of these additional reactions involve estimates which are highly uncertain, and in some cases we may have made different estimates were we required to independently derive such a mechanism. However, because this detailed mechanism and the March 1988 RADM mechanism are consistent with each other in their approaches to the chemistry, any differences between their predictions would reflect only the effects of the approximations in the RADM mechanism regarding the peroxy radical reactions. Therefore, the detailed radical mechanism provided by Stockwell was used without modification as the standard in this evaluation.

The organic peroxy + organic radical reactions in Stockwell's detailed radical mechanism, which was used as the standard mechanism in the tests of peroxy radical representations, are listed in Table 35. All the other reactions are the same as those listed in Table 2 in Section 2 of this report, excluding those indicated as "Organic Peroxy + MO2," "Organic Peroxy + ACO3," "Other Organic Peroxy + Peroxy" and "XNO2" reactions.

The reactions of organic species in the version of the RADM mechanism employing the approach of the 1986 SAPRC mechanism (Carter et al., 1986) are given in Table 36. All organic reactions have to be shown because there are modifications made throughout this portion of the mechanism. The inorganic reactions are the same as those used for all versions of the RADM mechanism and are given in Table 2. Except for the reactions involving organic peroxy radicals, this mechanism is the same as the March 1988 RADM mechanism. The major difference between this and the March 1988 RADM mechanism is that the chemical operators "[RO2]" and "[RCO3]" were added to represent total amounts of organic peroxy and acylperoxy radicals, respectively, and instead of reacting with MO2 and ACO3, the individual organic peroxy radicals are represented as reacting with these species. Reactions forming individual peroxy radicals were represented as also forming [RO2]. Reactions forming acetyl peroxy radicals (ACO3 or TCO3) were represented as also forming [RCO3]. Reactions of [RCO3] with NO_2 and [RO2] and [RCO3] with NO, HO_2, [RO2], and [RCO3] were added. The rate constants used for the [RO2] + [RO2], [RO2] + [RCO3], and [RCO3] + [RCO3] reactions were the same as those used in the SAPRC mechanisms (Carter et al., 1986; Carter, 1988) -- the RADM rate constants could not be used because the RADM reactions they replace have several different rate constants. The rate constants for the other [RO2] and [RCO3] reactions corresponded to those used in the RADM mechanism. The reactions for the individual peroxy radicals in this mechanism with NO, NO_2 (where applicable), and HO_2 are the same as in the RADM mechanism. The reactions of the peroxy radicals with [RO2] and [RCO3] are analogous to their reactions with MO2 and ACO3, respectively, in the RADM mechanism, except that (1)

Table 35. Organic Peroxy + Organic Peroxy Reactions Used in Stockwell's "Detailed Radical" Version of the RADM Mechanism

Rxn. Label	Kinetic Parameters (a)				Reactions (a,b)
	k(300)	A	Ea	B	
R001	5.81E+02	2.79E+02	-0.44	-1.00	MO2 + MO2 = #1.5 HCHO + HO2 + #.5 ROH
R002	4.28E+02	2.06E+02	-0.44	-1.00	MO2 + ETHP = #.75 HCHO + HO2 + #.75 ALD + #.5 ROH
R003	1.25E+02	6.02E+01	-0.44	-1.00	MO2 + HC3P = #.75 HCHO + HO2 + #.15 ALD + #.6 KET + #.5 ROH
R004	1.04E+02	4.99E+01	-0.44	-1.00	MO2 + HC5P = #.75 HCHO + HO2 + #.105 ALD + #.645 KET + #.5 ROH
R005	8.86E+01	4.26E+01	-0.44	-1.00	MO2 + HC8P = #.75 HCHO + HO2 + #.075 ALD + #.675 KET + #.5 ROH
R006	4.28E+02	2.06E+02	-0.44	-1.00	MO2 + OL2P = #1.550 HCHO + HO2 + #.350 ALD + #.5 ROH
R007	4.28E+02	2.06E+02	-0.44	-1.00	MO2 + OLTP = #1.25 HCHO + HO2 + #.75 ALD + #.5 ROH
R008	5.19E+01	2.50E+01	-0.44	-1.00	MO2 + OLIP = #.890 HCHO + HO2 + #.725 ALD + #.3 KET + #.5 ROH
R009	5.19E+01	2.50E+01	-0.44	-1.00	MO2 + KETP = #.75 HCHO + HO2 + #.75 MGLY + #.5 ROH
R010	5.19E+01	2.50E+01	-0.44	-1.00	MO2 + TOLP = #.75 HCHO + #1.405 HO2 + #.071 ALD + #.543 MGLY + #.274 ROH + #.181 GLY + #.905 DCB
R011	5.19E+01	2.50E+01	-0.44	-1.00	MO2 + XYLP = #.75 HCHO + #1.5 HO2 + #.75 MGLY + #.25 ROH + DCB
R012	5.19E+01	2.50E+01	-0.44	-1.00	MO2 + OLN = #1.75 HCHO + #.5 HO2 + ALD + #.25 ROH + NO2
R013	5.19E+01	2.50E+01	-0.44	-1.00	MO2 + XNO2 = #.75 HCHO + #.5 HO2 + #.25 ROH
R014	5.19E+01	2.50E+01	-0.44	-1.00	MO2 + XO2 = #.75 HCHO + #.5 HO2 + #.25 ROH
R015	2.93E+03	1.41E+03	-0.44	-1.00	MO2 + ACO3 = HCHO + #.5 HO2 + #.5 ORA2 + #.5 MO2
R016	2.93E+03	1.41E+03	-0.44	-1.00	MO2 + TCO3 = HCHO + #.96 HO2 + #.055 MGLY + #.5 ORA2 + #.445 GLY + #.025 ACO3 + XO2 + #.475 CO
R017	7.64E+01	3.67E+01	-0.44	-1.00	ETHP + ETHP = HO2 + #1.5 ALD + #.5 ROH
R018	4.58E+01	2.20E+01	-0.44	-1.00	ETHP + HC3P = HO2 + #.9 ALD + #.6 KET + #.5 ROH
R019	3.67E+01	1.76E+01	-0.44	-1.00	ETHP + HC5P = HO2 + #.855 ALD + #.645 KET + #.5 ROH

(continued)

Table 35 (continued) - 2

Rxn. Label	Kinetic Parameters (a)				Reactions (a,b)
	k(300)	A	Ea	B	
R020	3.05E+01	1.47E+01	-0.44	-1.00	ETHP + HC8P = HO2 + #.825 ALD + #.675 KET + #.5 ROH
R021	1.53E+02	7.34E+01	-0.44	-1.00	ETHP + OL2P = #.8 HCHO + HO2 + #1.1 ALD + #.5 ROH
R022	1.53E+02	7.34E+01	-0.44	-1.00	ETHP + OLTP = #.5 HCHO + HO2 + #1.5 ALD + #.5 ROH
R023	1.83E+01	8.81E+00	-0.44	-1.00	ETHP + OLIP = #.14 HCHO + HO2 + #1.475 ALD + #.3 KET + #.5 ROH
R024	1.83E+01	8.81E+00	-0.44	-1.00	ETHP + KETP = HO2 + #.75 ALD + #.75 MGLY + #.5 ROH
R025	1.83E+01	8.81E+00	-0.44	-1.00	ETHP + TOLP = #1.405 HO2 + #.821 ALD + #.543 MGLY + #.274 ROH + #.181 GLY + #.905 DCB
R026	1.83E+01	8.81E+00	-0.44	-1.00	ETHP + XYLP = #1.5 HO2 + #.75 ALD + #.75 MGLY + #.25 ROH + DCB
R027	1.83E+01	8.81E+00	-0.44	-1.00	ETHP + OLN = HCHO + #.5 HO2 + #1.75 ALD + #.25 ROH + NO2
R028	1.83E+01	8.81E+00	-0.44	-1.00	ETHP + XNO2 = #.5 HO2 + #.75 ALD + #.25 ROH
R029	1.83E+01	8.81E+00	-0.44	-1.00	ETHP + XO2 = #.5 HO2 + #.75 ALD + #.25 ROH
R030	1.04E+03	4.99E+02	-0.44	-1.00	ETHP + ACO3 = #.5 HO2 + ALD + #.5 ORA2 + #.5 MO2
R031	1.04E+03	4.99E+02	-0.44	-1.00	ETHP + TCO3 = #.96 HO2 + ALD + #.055 MGLY + #.5 ORA2 + #.445 GLY + #.025 ACO3 + XO2 + #.475 CO
R032	7.64E+01	3.67E+01	-0.44	-1.00	HC3P + HC3P = HO2 + #.3 ALD + #1.200 KET + #.5 ROH
R033	1.10E+01	5.28E+00	-0.44	-1.00	HC3P + HC5P = HO2 + #.255 ALD + #1.245 KET + #.5 ROH
R034	9.47E+00	4.55E+00	-0.44	-1.00	HC3P + HC8P = HO2 + #.225 ALD + #1.275 KET + #.5 ROH
R035	4.58E+01	2.20E+01	-0.44	-1.00	HC3P + OL2P = #.8 HCHO + HO2 + #.5 ALD + #.6 KET + #.5 ROH
R036	4.58E+01	2.20E+01	-0.44	-1.00	HC3P + OLTP = #.5 HCHO + HO2 + #.9 ALD + #.6 KET + #.5 ROH
R037	5.50E+00	2.64E+00	-0.44	-1.00	HC3P + OLIP = #.14 HCHO + HO2 + #.875 ALD + #.9 KET + #.5 ROH
R038	5.50E+00	2.64E+00	-0.44	-1.00	HC3P + KETP = HO2 + #.15 ALD + #.6 KET + #.75 MGLY + #.5 ROH
R039	5.50E+00	2.64E+00	-0.44	-1.00	HC3P + TOLP = #1.405 HO2 + #.221 ALD + #.6 KET +

(continued)

Table 35 (continued) - 3

Rxn. Label	Kinetic Parameters (a)				Reactions (a,b)
	k(300)	A	Ea	B	
					#.543 MGLY + #.274 ROH + #.181 GLY + #.905 DCB
R040	5.50E+00	2.64E+00	-0.44	-1.00	HC3P + XYLP = #1.5 HO2 + #.15 ALD + #.6 KET + #.75 MGLY + #.25 ROH + DCB
R041	5.50E+00	2.64E+00	-0.44	-1.00	HC3P + OLN = HCHO + #.5 HO2 + #1.150 ALD + #.6 KET + #.25 ROH + NO2
R042	5.50E+00	2.64E+00	-0.44	-1.00	HC3P + XNO2 = #.5 HO2 + #.15 ALD + #.6 KET + #.25 ROH
R043	5.50E+00	2.64E+00	-0.44	-1.00	HC3P + XO2 = #.5 HO2 + #.15 ALD + #.6 KET + #.25 ROH
R044	3.06E+02	1.47E+02	-0.44	-1.00	HC3P + ACO3 = #.5 HO2 + #.2 ALD + #.8 KET + #.5 ORA2 + #.5 MO2
R045	3.06E+02	1.47E+02	-0.44	-1.00	HC3P + TCO3 = #.96 HO2 + #.2 ALD + #.8 KET + #.055 MGLY + #.5 ORA2 + #.445 GLY + #.025 ACO3 + XO2 + #.475 CO
R046	7.64E+01	3.67E+01	-0.44	-1.00	HC5P + HC5P = HO2 + #.21 ALD + #1.290 KET + #.5 ROH
R047	7.64E+00	3.67E+00	-0.44	-1.00	HC5P + HC8P = HO2 + #.180 ALD + #1.320 KET + #.5 ROH
R048	3.67E+01	1.76E+01	-0.44	-1.00	HC5P + OL2P = #.8 HCHO + HO2 + #.455 ALD + #.645 KET + #.5 ROH
R049	3.67E+01	1.76E+01	-0.44	-1.00	HC5P + OLTP = #.5 HCHO + HO2 + #.855 ALD + #.645 KET + #.5 ROH
R050	4.58E+00	2.20E+00	-0.44	-1.00	HC5P + OLIP = #.14 HCHO + HO2 + #.830 ALD + #.945 KET + #.5 ROH
R051	4.58E+00	2.20E+00	-0.44	-1.00	HC5P + KETP = HO2 + #.105 ALD + #.645 KET + #.75 MGLY + #.5 ROH
R052	4.58E+00	2.20E+00	-0.44	-1.00	HC5P + TOLP = #1.405 HO2 + #.176 ALD + #.645 KET + #.543 MGLY + #.274 ROH + #.181 GLY + #.905 DCB
R053	4.58E+00	2.20E+00	-0.44	-1.00	HC5P + XYLP = #1.5 HO2 + #.105 ALD + #.645 KET + #.75 MGLY + #.25 ROH + DCB
R054	4.58E+00	2.20E+00	-0.44	-1.00	HC5P + OLN = HCHO + #.5 HO2 + #1.105 ALD + #.645 KET + #.25 ROH + NO2
R055	4.58E+00	2.20E+00	-0.44	-1.00	HC5P + XNO2 = #.5 HO2 + #.105 ALD + #.645 KET + #.25 ROH
R056	4.58E+00	2.20E+00	-0.44	-1.00	HC5P + XO2 = #.5 HO2 + #.105 ALD + #.645 KET + #.25 ROH

(continued)

Table 35 (continued) - 4

Rxn. Label	Kinetic Parameters (a)				Reactions (a,b)
	k(300)	A	Ea	B	
R057	2.57E+02	1.23E+02	-0.44	-1.00	HC5P + ACO3 = #.5 HO2 + #.14 ALD + #.860 KET + #.5 ORA2 + #.5 MO2
R058	2.57E+02	1.23E+02	-0.44	-1.00	HC5P + TCO3 = #.96 HO2 + #.14 ALD + #.860 KET + #.055 MGLY + #.5 ORA2 + #.445 GLY + #.025 ACO3 + XO2 + #.475 CO
R059	7.64E+01	3.67E+01	-0.44	-1.00	HC8P + HC8P = HO2 + #.15 ALD + #1.350 KET + #.5 ROH
R060	3.05E+01	1.47E+01	-0.44	-1.00	HC8P + OL2P = #.8 HCHO + HO2 + #.425 ALD + #.675 KET + #.5 ROH
R061	3.05E+01	1.47E+01	-0.44	-1.00	HC8P + OLTP = #.5 HCHO + HO2 + #.825 ALD + #.675 KET + #.5 ROH
R062	3.97E+00	1.91E+00	-0.44	-1.00	HC8P + OLIP = #.14 HCHO + HO2 + #.8 ALD + #.975 KET + #.5 ROH
R063	3.97E+00	1.91E+00	-0.44	-1.00	HC8P + KETP = HO2 + #.075 ALD + #.675 KET + #.75 MGLY + #.5 ROH
R064	3.97E+00	1.91E+00	-0.44	-1.00	HC8P + TOLP = #1.405 HO2 + #.146 ALD + #.675 KET + #.543 MGLY + #.274 ROH + #.181 GLY + #.905 DCB
R065	3.97E+00	1.91E+00	-0.44	-1.00	HC8P + XYLP = #1.5 HO2 + #.075 ALD + #.675 KET + #.75 MGLY + #.25 ROH + DCB
R066	3.97E+00	1.91E+00	-0.44	-1.00	HC8P + OLN = HCHO + #.5 HO2 + #1.075 ALD + #.675 KET + #.25 ROH + NO2
R067	3.97E+00	1.91E+00	-0.44	-1.00	HC8P + XNO2 = #.5 HO2 + #.075 ALD + #.675 KET + #.25 ROH
R068	3.97E+00	1.91E+00	-0.44	-1.00	HC8P + XO2 = #.5 HO2 + #.075 ALD + #.675 KET + #.25 ROH
R069	2.20E+02	1.06E+02	-0.44	-1.00	HC8P + ACO3 = #.5 HO2 + #.1 ALD + #.9 KET + #.5 ORA2 + #.5 MO2
R070	2.20E+02	1.06E+02	-0.44	-1.00	HC8P + TCO3 = #.96 HO2 + #.1 ALD + #.9 KET + #.055 MGLY + #.5 ORA2 + #.445 GLY + #.025 ACO3 + XO2 + #.475 CO
R071	7.64E+01	3.67E+01	-0.44	-1.00	OL2P + OL2P = #1.6 HCHO + HO2 + #.7 ALD + #.5 ROH
R072	1.53E+02	7.34E+01	-0.44	-1.00	OL2P + OLTP = #1.300 HCHO + HO2 + #1.1 ALD + #.5 ROH
R073	1.83E+01	8.81E+00	-0.44	-1.00	OL2P + OLIP = #.940 HCHO + HO2 + #1.075 ALD + #.3 KET + #.5 ROH

(continued)

Table 35 (continued) - 5

Rxn. Label	Kinetic Parameters (a)				Reactions (a,b)
	k(300)	A	Ea	B	
R074	1.83E+01	8.81E+00	-0.44	-1.00	OL2P + KETP = #.8 HCHO + HO2 + #.350 ALD + #.75 MGLY + #.5 ROH
R075	1.83E+01	8.81E+00	-0.44	-1.00	OL2P + TOLP = #.8 HCHO + #1.405 HO2 + #.421 ALD + #.543 MGLY + #.274 ROH + #.181 GLY + #.905 DCB
R076	1.83E+01	8.81E+00	-0.44	-1.00	OL2P + XYLP = #.8 HCHO + #1.5 HO2 + #.350 ALD + #.75 MGLY + #.25 ROH + DCB
R077	1.83E+01	8.81E+00	-0.44	-1.00	OL2P + OLN = #1.800 HCHO + #.5 HO2 + #1.350 ALD + #.25 ROH + NO2
R078	1.83E+01	8.81E+00	-0.44	-1.00	OL2P + XNO2 = #.8 HCHO + #.5 HO2 + #.350 ALD + #.25 ROH
R079	1.83E+01	8.81E+00	-0.44	-1.00	OL2P + XO2 = #.8 HCHO + #.5 HO2 + #.350 ALD + #.25 ROH
R080	1.04E+03	4.99E+02	-0.44	-1.00	OL2P + ACO3 = #.8 HCHO + #.5 HO2 + #.6 ALD + #.5 ORA2 + #.5 MO2
R081	1.04E+03	4.99E+02	-0.44	-1.00	OL2P + TCO3 = #.8 HCHO + #.96 HO2 + #.6 ALD + #.055 MGLY + #.5 ORA2 + #.445 GLY + #.025 ACO3 + XO2 + #.475 CO
R082	7.64E+01	3.67E+01	-0.44	-1.00	OLTP + OLTP = HCHO + HO2 + #1.5 ALD + #.5 ROH
R083	1.83E+01	8.81E+00	-0.44	-1.00	OLTP + OLIP = #.640 HCHO + HO2 + #1.475 ALD + #.3 KET + #.5 ROH
R084	1.83E+01	8.81E+00	-0.44	-1.00	OLTP + KETP = #.5 HCHO + HO2 + #.75 ALD + #.75 MGLY + #.5 ROH
R085	1.83E+01	8.81E+00	-0.44	-1.00	OLTP + TOLP = #.5 HCHO + #1.405 HO2 + #.821 ALD + #.543 MGLY + #.274 ROH + #.181 GLY + #.905 DCB
R086	1.83E+01	8.81E+00	-0.44	-1.00	OLTP + XYLP = #.5 HCHO + #1.5 HO2 + #.75 ALD + #.75 MGLY + #.25 ROH + DCB
R087	1.83E+01	8.81E+00	-0.44	-1.00	OLTP + OLN = #1.5 HCHO + #.5 HO2 + #1.75 ALD + #.25 ROH + NO2
R088	1.83E+01	8.81E+00	-0.44	-1.00	OLTP + XNO2 = #.5 HCHO + #.5 HO2 + #.75 ALD + #.25 ROH
R089	1.83E+01	8.81E+00	-0.44	-1.00	OLTP + XO2 = #.5 HCHO + #.5 HO2 + #.75 ALD + #.25 ROH
R090	1.04E+03	4.99E+02	-0.44	-1.00	OLTP + ACO3 = #.5 HCHO + #.5 HO2 + ALD + #.5 ORA2 + #.5 MO2

(continued)

Table 35 (continued) - 6

Rxn. Label	Kinetic Parameters (a)				Reactions (a,b)
	k(300)	A	Ea	B	
R091	1.04E+03	4.99E+02	-0.44	-1.00	OLTP + TCO3 = #.5 HCHO + #.96 HO2 + ALD + #.055 MGLY + #.5 ORA2 + #.445 GLY + #.025 ACO3 + XO2 + #.475 CO
R092	1.10E+00	5.28E-01	-0.44	-1.00	OLIP + OLIP = #.280 HCHO + HO2 + #1.450 ALD + #.6 KET + #.5 ROH
R093	2.23E+00	1.07E+00	-0.44	-1.00	OLIP + KETP = #.14 HCHO + HO2 + #.725 ALD + #.3 KET + #.75 MGLY + #.5 ROH
R094	2.23E+00	1.07E+00	-0.44	-1.00	OLIP + TOLP = #.14 HCHO + #1.405 HO2 + #.796 ALD + #.3 KET + #.543 MGLY + #.274 ROH + #.181 GLY + #.905 DCB
R095	2.23E+00	1.07E+00	-0.44	-1.00	OLIP + XYLP = #.14 HCHO + #1.5 HO2 + #.725 ALD + #.3 KET + #.75 MGLY + #.25 ROH + DCB
R096	2.23E+00	1.07E+00	-0.44	-1.00	OLIP + OLN = #1.140 HCHO + #.5 HO2 + #1.725 ALD + #.3 KET + #.25 ROH + NO2
R097	2.23E+00	1.07E+00	-0.44	-1.00	OLIP + XNO2 = #.14 HCHO + #.5 HO2 + #.725 ALD + #.3 KET + #.25 ROH
R098	2.23E+00	1.07E+00	-0.44	-1.00	OLIP + XO2 = #.14 HCHO + #.5 HO2 + #.725 ALD + #.3 KET + #.25 ROH
R099	1.28E+02	6.17E+01	-0.44	-1.00	OLIP + ACO3 = #.14 HCHO + #.5 HO2 + #.725 ALD + #.55 KET + #.5 ORA2 + #.5 MO2
R100	1.28E+02	6.17E+01	-0.44	-1.00	OLIP + TCO3 = #.14 HCHO + #.96 HO2 + #.725 ALD + #.55 KET + #.055 MGLY + #.5 ORA2 + #.445 GLY + #.025 ACO3 + XO2 + #.475 CO
R101	1.10E+00	5.28E-01	-0.44	-1.00	KETP + KETP = HO2 + #1.5 MGLY + #.5 ROH
R102	2.23E+00	1.07E+00	-0.44	-1.00	KETP + TOLP = #1.405 HO2 + #.071 ALD + #1.293 MGLY + #.274 ROH + #.181 GLY + #.905 DCB
R103	2.23E+00	1.07E+00	-0.44	-1.00	KETP + XYLP = #1.5 HO2 + #1.5 MGLY + #.25 ROH + DCB
R104	2.23E+00	1.07E+00	-0.44	-1.00	KETP + OLN = HCHO + #.5 HO2 + ALD + #.75 MGLY + #.25 ROH + NO2

(continued)

Table 35 (continued) - 7

Rxn. Label	Kinetic Parameters (a)				Reactions (a,b)
	k(300)	A	Ea	B	
R105	2.23E+00	1.07E+00	-0.44	-1.00	KETP + XNO2 = #.5 HO2 + #.75 MGLY + #.25 ROH
R106	2.23E+00	1.07E+00	-0.44	-1.00	KETP + XO2 = #.5 HO2 + #.75 MGLY + #.25 ROH
R107	1.28E+02	6.17E+01	-0.44	-1.00	KETP + ACO3 = #.5 HO2 + MGLY + #.5 ORA2 + #.5 MO2
R108	1.28E+02	6.17E+01	-0.44	-1.00	KETP + TCO3 = #.96 HO2 + #1.055 MGLY + #.5 ORA2 + #.445 GLY + #.025 ACO3 + XO2 + #.475 CO
R109	1.10E+00	5.28E-01	-0.44	-1.00	TOLP + TOLP = #1.810 HO2 + #.142 ALD + #1.448 MGLY + #.047 ROH + #.362 GLY + #1.810 DCB
R110	2.23E+00	1.07E+00	-0.44	-1.00	TOLP + XYLP = #1.905 HO2 + #.071 ALD + #1.655 MGLY + #.024 ROH + #.181 GLY + #1.905 DCB
R111	2.23E+00	1.07E+00	-0.44	-1.00	TOLP + OLN = HCHO + #.905 HO2 + #1.071 ALD + #.905 MGLY + #.024 ROH + #.181 GLY + #.905 DCB + NO2
R112	2.23E+00	1.07E+00	-0.44	-1.00	TOLP + XNO2 = #.905 HO2 + #.071 ALD + #.905 MGLY + #.024 ROH + #.181 GLY + #.905 DCB
R113	2.23E+00	1.07E+00	-0.44	-1.00	TOLP + XO2 = #.905 HO2 + #.071 ALD + #.905 MGLY + #.024 ROH + #.181 GLY + #.905 DCB
R114	1.28E+02	6.17E+01	-0.44	-1.00	TOLP + ACO3 = #.905 HO2 + #.095 ALD + #.724 MGLY + #.5 ORA2 + #.181 GLY + #.905 DCB + #.5 MO2
R115	1.28E+02	6.17E+01	-0.44	-1.00	TOLP + TCO3 = #1.365 HO2 + #.095 ALD + #.779 MGLY + #.5 ORA2 + #.626 GLY + #.905 DCB + #.025 ACO3 + XO2 + #.475 CO
R116	1.10E+00	5.28E-01	-0.44	-1.00	XYLP + XYLP = #2 HO2 + #2 MGLY + #2 DCB
R117	2.23E+00	1.07E+00	-0.44	-1.00	XYLP + OLN = HCHO + HO2 + ALD + #1.25 MGLY + DCB + NO2

(continued)

Table 35 (continued) - 8

Rxn. Label	Kinetic Parameters (a)				Reactions (a,b)
	k(300)	A	Ea	B	
R118	2.23E+00	1.07E+00	-0.44	-1.00	XYLP + XNO2 = HO2 + #1.25 MGLY + DCB
R119	2.23E+00	1.07E+00	-0.44	-1.00	XYLP + XO2 = HO2 + #1.25 MGLY + DCB
R120	1.28E+02	6.17E+01	-0.44	-1.00	XYLP + ACO3 = HO2 + MGLY + #.5 ORA2 + DCB + #.5 MO2
R121	1.28E+02	6.17E+01	-0.44	-1.00	XYLP + TCO3 = #1.46 HO2 + #1.055 MGLY + #.5 ORA2 + #.445 GLY + DCB + #.025 ACO3 + XO2 + #.475 CO
R122	1.10E+00	5.28E-01	-0.44	-1.00	OLN + OLN = #2 HCHO + #2 ALD + #2 NO2
R123	2.23E+00	1.07E+00	-0.44	-1.00	OLN + XNO2 = HCHO + ALD + NO2
R124	2.23E+00	1.07E+00	-0.44	-1.00	OLN + XO2 = HCHO + ALD + NO2
R125	1.28E+02	6.17E+01	-0.44	-1.00	OLN + ACO3 = HCHO + ALD + #.5 ORA2 + NO2 + #.5 MO2
R126	1.28E+02	6.17E+01	-0.44	-1.00	OLN + TCO3 = HCHO + #.46 HO2 + ALD + #.055 MGLY + #.5 ORA2 + #.445 GLY + #.025 ACO3 + XO2 + #.475 CO + NO2
R127	1.10E+00	5.28E-01	-0.44	-1.00	XNO2 + XNO2 =
R128	2.23E+00	1.07E+00	-0.44	-1.00	XNO2 + XO2 =
R129	1.28E+02	6.17E+01	-0.44	-1.00	XNO2 + ACO3 = #.5 ORA2 + #.5 MO2
R130	1.28E+02	6.17E+01	-0.44	-1.00	XNO2 + TCO3 = #.46 HO2 + #.055 MGLY + #.5 ORA2 + #.445 GLY + #.025 ACO3 + XO2 + #.475 CO
R131	1.10E+00	5.28E-01	-0.44	-1.00	XO2 + XO2 =
R132	1.28E+02	6.17E+01	-0.44	-1.00	XO2 + ACO3 = #.5 ORA2 + #.5 MO2
R133	1.28E+02	6.17E+01	-0.44	-1.00	XO2 + TCO3 = #.46 HO2 + #.055 MGLY + #.5 ORA2 + #.445 GLY + #.025 ACO3 + XO2 + #.475 CO
R134	3.67E+03	1.76E+03	-0.44	-1.00	ACO3 + ACO3 = #2 MO2
R135	7.33E+03	3.52E+03	-0.44	-1.00	ACO3 + TCO3 = #.920 HO2 + #.110 MGLY + #.890 GLY + #.05 ACO3 + #2 XO2 + #.950 CO + MO2
R136	3.67E+03	1.76E+03	-0.44	-1.00	TCO3 + TCO3 = #1.84 HO2 + #.220 MGLY + #1.780 GLY + #.1 ACO3 + #4 XO2 + #1.900 CO

(a) See Footnotes (b) and (c) in Table 2 for a description of the formats used in the kinetic parameter and the reaction listings.

(b) Note that ROH, a species not in the standard RADM mechanism, is shown as a product in some of these reactions. However, no reactions for it are included in this mechanism, so its formation has no effect.

Table 36. Listing of the Organic Reactions in the Modified RADM Mechanism Incorporating the 1986 SAPRC Approach for Representing Reactions of Organic Peroxy Radicals

Rxn. Label (a)	Kinetic Parameters (b)				Reactions (b)
	k(300)	A	Ea	B	
					Organic Photolysis Reactions
010	(Phot. Set = HCHOMR)				HCHO + HV = H2 + CO
011	(Phot. Set = HCHORR)				HCHO + HV = HO2 + HO2 + CO
012	(Phot. Set = ALDR)				ALD + HV = MO2 + HO2 + CO + [RO2]
013	(Phot. Set = OPR)				OP1 + HV = HCHO + HO2 + HO
014	(Phot. Set = OPR)				OP2 + HV = ALD + HO2 + HO
015	(Phot. Set = PAAR)				PAA + HV = MO2 + CO2 + HO + [RO2]
016	(Phot. Set = KETR)				KET + HV = ACO3 + [RCO3] + ETHP + [RO2]
017	(Phot. Set = GLY2R)				GLY + HV = #.13 HCHO + #1.87 CO
018	(Phot. Set = GLY1R)				GLY + HV = #.45 HCHO + #1.55 CO + #.80 HO2
019	(Phot. Set = MGLYR)				MGLY + HV = ACO3 + [RCO3] + HO2 + CO
020	(Phot. Set = DCBR)				DCB + HV = #.98 HO2 + #.02 ACO3 + TCO3 + #1.02 [RCO3]
021	(Phot. Set = ONITR)				ONIT + HV = #.20 ALD + #.80 KET + HO2 + NO2
					Organic + OH Reactions
051	1.29E+01	9.23E+02	2.54	1.00	CH4 + HO = MO2 + H2O + [RO2]
052	4.11E+02	1.81E+03	0.88	1.00	ETH + HO = ETHP + [RO2] + H2O
053	3.76E+03	2.28E+04	1.07	-1.00	HC3 + HO = #.90 "HC3P + [RO2]" + #.10 HO2 + #.014 HCHO + #.069 ALD + #.026 KET + H2O
054	7.86E+03	2.79E+04	0.75	-1.00	HC5 + HO = HC5P + #.27 XO2 + H2O + #1.27 [RO2]
055	1.66E+04	5.87E+04	0.75	-1.00	HC8 + HO = HC8P + #.78 XO2 + H2O + #1.78 [RO2]
056	1.24E+04	3.16E+03	-0.82	-1.00	OL2 + HO = OL2P + [RO2]
057	3.82E+04	7.12E+03	-1.00	-1.00	OLT + HO = OLTP + [RO2]
058	9.24E+04	1.48E+04	-1.09	-1.00	OLI + HO = OLIP + [RO2]
074	1.46E+05	3.74E+04	-0.81	-1.00	ISO + HO = OLTP + [RO2]
059	9.02E+03	3.08E+03	-0.64	-1.00	TOL + HO = #.84 "TOLP + [RO2]" + #.16 CSL + #.16 HO2
060	4.54E+04	3.08E+04	-0.23	-1.00	XYL + HO = #.83 "XYLP + [RO2]" + #.17 CSL + #.17 HO2
063	1.32E+04	1.32E+04	0.00	-1.00	HCHO + HO = HO2 + CO + H2O
064	2.37E+04	1.01E+04	-0.51	-1.00	ALD + HO = ACO3 + [RCO3] + H2O
065	1.47E+03	1.76E+04	1.48	-1.00	KET + HO = KETP + [RO2] + H2O

(continued)

Table 36 (continued) - 2

Rxn. Label (a)	Kinetic Parameters (b) k(300)	A	Ea	B	Reactions (b)
066	1.69E+04	1.69E+04	0.00	-1.00	GLY + HO = HO2 + #2 CO + H2O
067	2.50E+04	2.50E+04	0.00	-1.00	MGLY + HO = ACO3 + [RCO3] + CO + H2O
068	4.11E+04	4.11E+04	0.00	-1.00	DCB + HO = TCO3 + [RCO3] + H2O
061	5.87E+04	5.87E+04	0.00	-1.00	CSL + HO = #.1 HO2 + #.9 "XO2 + [RO2]" + #.9 "TCO3 + [RCO3]"
062	5.28E+04	5.28E+04	0.00	-1.00	CSL + HO = CSL
069	1.47E+04	1.47E+04	0.00	-1.00	OP1 + HO = #.5 "MO2 + [RO2]" + #.5 HCHO + #.5 HO
070	1.47E+04	1.47E+04	0.00	-1.00	OP2 + HO = #.5 "HC3P + [RO2]" + #.5 ALD + #.5 HO
071	1.47E+04	1.47E+04	0.00	-1.00	PAA + HO = ACO3 + [RCO3] + H2O
072	2.06E+02	9.06E+02	0.88	1.00	PAN + HO = HCHO + NO3 + XO2 + [RO2]
073	3.76E+03	2.28E+04	1.07	-1.00	ONIT + HO = HC3P + [RO2] + NO2
					Organic + NO3 Reactions
093	9.23E-01	8.81E+02	4.09	-1.00	HCHO + NO3 = HO2 + HNO3 + CO
094	3.65E+00	2.06E+03	3.78	-1.00	ALD + NO3 = ACO3 + [RCO3] + HNO3
095	9.23E-01	8.81E+02	4.09	-1.00	GLY + NO3 = HNO3 + HO2 + #2 CO
096	3.65E+00	2.06E+03	3.78	-1.00	MGLY + NO3 = HNO3 + ACO3 + [RCO3] + CO
097	3.65E+00	2.06E+03	3.78	-1.00	DCB + NO3 = HNO3 + TCO3 + [RCO3]
098	3.23E+04	3.23E+04	0.00	-1.00	CSL + NO3 = HNO3 + XNO2 + #.5 CSL
099	1.72E-01	2.94E+03	5.81	-1.00	OL2 + NO3 = OLN + [RO2]
100	2.33E+01	1.47E+04	3.84	-1.00	OLT + NO3 = OLN + [RO2]
101	1.84E+03	4.74E+04	1.94	-1.00	OLI + NO3 = OLN + [RO2]
102	8.53E+02	8.53E+02	0.00	-1.00	ISO + NO3 = OLN + [RO2]
					Organic + O3 Reactions
103	2.72E-03	1.76E+01	5.23	-1.00	OL2 + O3 = HCHO + #.42 CO + #.4 ORA1 + #.12 HO2
104	1.74E-02	1.94E+01	4.18	-1.00	OLT + O3 = #.53 HCHO + #.50 ALD + #.33 CO + #.20 ORA1 + #.20 ORA2 + #.23 HO2 + #.22 "MO2 + [RO2]" + #.10 HO + #.06 CH4
105	3.02E-01	1.33E+01	2.26	-1.00	OLI + O3 = #.18 HCHO + #.72 ALD + #.10 KET + #.23 CO + #.06 ORA1 + #.29 ORA2 + #.09 CH4 + #.26 HO2 + #.14 HO + #.31 "MO2 + [RO2]"

(continued)

Table 36 (continued) - 3

Rxn. Label (a)	Kinetic Parameters (b) k(300)	A	Ea	B	Reactions (b)
106	2.20E-02	1.81E+01	4.00	-1.00	ISO + O3 = #.53 HCHO + #.50 ALD + #.33 CO + #.20 ORA1 + #.20 ORA2 + #.23 HO2 + #.22 "MO2 + [RO2]" + #.10 HO
					Organic Peroxy + NO2 Reactions
M01	7.52E+03	4.11E+03	-0.36	-1.00	[RCO3] + NO2 = NO2
075		(Same k as M01)			ACO3 + NO2 = PAN
077		(Same k as M01)			TCO3 + NO2 = TPAN
076	2.90E-02	1.17E+18	26.91	0.00	PAN = ACO3 + [RCO3] + NO2
078	2.90E-02	1.17E+18	26.91	0.00	TPAN = TCO3 + [RCO3] + NO2
					Organic Peroxy + NO Reactions
M02	1.12E+04	6.17E+03	-0.36	-1.00	[RO2] + NO = NO
079		(Same k as M02)			MO2 + NO = HCHO + HO2 + NO2
080		(Same k as M02)			HC3P + NO = #.69 ALD + #.26 KET + #.14 HCHO + #.03 ONIT + #.97 NO2 + #.97 HO2
081		(Same k as M02)			HC5P + NO = #.36 ALD + #.76 KET + #.10 ONIT + #.90 NO2 + #.90 HO2
082		(Same k as M02)			HC8P + NO = #.44 ALD + #1.05 KET + #.05 HCHO + #.24 ONIT + #.76 NO2 + #.76 HO2
083		(Same k as M02)			OL2P + NO = #1.6 HCHO + HO2 + NO2 + #.2 ALD
084		(Same k as M02)			OLTP + NO = ALD + HCHO + HO2 + NO2
085		(Same k as M02)			OLIP + NO = HO2 + #1.45 ALD + #.28 HCHO + #.10 KET + NO2
088		(Same k as M02)			TOLP + NO = NO2 + HO2 + #.724 MGLY + #.181 GLY + #.905 DCB
089		(Same k as M02)			XYLP + NO = NO2 + HO2 + MGLY + DCB
090		(Same k as M02)			ETHP + NO = ALD + HO2 + NO2
091		(Same k as M02)			KETP + NO = MGLY + NO2 + HO2
092		(Same k as M02)			OLN + NO = HCHO + ALD + #2 NO2
150		(Same k as M02)			XO2 + NO = NO2
M03		(Same k as M02)			[RCO3] + NO = NO
086		(Same k as M02)			ACO3 + NO = MO2 + NO2 + [RO2]
087		(Same k as M02)			TCO3 + NO = NO2 + #.92 HO2 + #.89 GLY + #.11 MGLY +

(continued)

Table 36 (continued) - 4

Rxn. Label (a)	Kinetic Parameters (b)				Reactions (b)
	k(300)	A	Ea	B	
					#.05 "ACO3 + [RCO3]" + #.95 CO + #2 "XO2 + [RO2]"
					Organic Peroxy + HO2 Reactions
M04	8.61E+03	1.13E+02	-2.58	-1.00	HO2 + [RO2] = HO2
107		(Same k as M04)			HO2 + MO2 = OP1
108		(Same k as M04)			HO2 + ETHP = OP2
109		(Same k as M04)			HO2 + HC3P = OP2
110		(Same k as M04)			HO2 + HC5P = OP2
111		(Same k as M04)			HO2 + HC8P = OP2
112		(Same k as M04)			HO2 + OL2P = OP2
113		(Same k as M04)			HO2 + OLTP = OP2
114		(Same k as M04)			HO2 + OLIP = OP2
115		(Same k as M04)			HO2 + KETP = OP2
117		(Same k as M04)			HO2 + TOLP = OP2
118		(Same k as M04)			HO2 + XYLP = OP2
120		(Same k as M04)			HO2 + OLN = ONIT
146		(Same k as M04)			XO2 + HO2 = OP2
M05		(Same k as M04)			HO2 + [RCO3] = HO2
116		(Same k as M04)			HO2 + ACO3 = PAA
119		(Same k as M04)			HO2 + TCO3 = OP2
					Organic Peroxy + RO2 Reactions
M06	1.47E+00	1.47E+00	0.00	-1.00	[RO2] + [RO2] =
121		(Same k as M06)			MO2 + [RO2] = [RO2] + #.75 HCHO + #.5 HO2
122		(Same k as M06)			ETHP + [RO2] = [RO2] + #.75 ALD + #.5 HO2
123		(Same k as M06)			HC3P + [RO2] = [RO2] + #.15 ALD + #.6 KET + #.5 HO2
124		(Same k as M06)			HC5P + [RO2] = [RO2] + #.105 ALD + #.645 KET + #.5 HO2
125		(Same k as M06)			HC8P + [RO2] = [RO2] + #.075 ALD + #.675 KET + #.5 HO2
126		(Same k as M06)			OL2P + [RO2] = [RO2] + #.8 HCHO + #.35 ALD + #.5 HO2
127		(Same k as M06)			OLTP + [RO2] = [RO2] + #.5 HCHO + #.75 ALD + #.5 HO2
128		(Same k as M06)			OLIP + [RO2] = [RO2] + #.14 HCHO + #.725 ALD + #.55 KET + #.5 HO2
129		(Same k as M06)			KETP + [RO2] = [RO2] + #.75 MGLY + #.5 HO2

(continued)

Table 36 (continued) - 5

Rxn. Label (a)	Kinetic Parameters (b)				Reactions (b)
	k(300)	A	Ea	B	
131		(Same k as M06)			TOLP + [RO2] = [RO2] + #.23 HCHO + #1.4 HO2 + #.724 MGLY + #.181 GLY + #.905 DCB
132		(Same k as M06)			XYLP + [RO2] = [RO2] + #.25 HCHO + #1.5 HO2 + MGLY + DCB
M07		(Same k as M06)			OLN + [RO2] = [RO2] + HCHO + ALD + NO2
147		(Same k as M06)			XO2 + [RO2] = [RO2]
					Organic Peroxy + RCO3 Reactions
M08	2.93E+03	1.41E+03	-0.44	-1.00	[RCO3] + [RO2] =
M09		(Same k as M08)			MO2 + [RCO3] = [RCO3] + #.75 HCHO + #.5 HO2
134		(Same k as M08)			ETHP + [RCO3] = [RCO3] + #.75 ALD + #.5 HO2
135		(Same k as M08)			HC3P + [RCO3] = [RCO3] + #.15 ALD + #.6 KET + #.5 HO2
136		(Same k as M08)			HC5P + [RCO3] = [RCO3] + #.105 ALD + #.645 KET + #.5 HO2
137		(Same k as M08)			HC8P + [RCO3] = [RCO3] + #.075 ALD + #.675 KET + #.5 HO2
138		(Same k as M08)			OL2P + [RCO3] = [RCO3] + #.8 HCHO + #.35 ALD + #.5 HO2
139		(Same k as M08)			OLTP + [RCO3] = [RCO3] + #.5 HCHO + #.75 ALD + #.5 HO2
140		(Same k as M08)			OLIP + [RCO3] = [RCO3] + #.14 HCHO + #.725 ALD + #.55 KET + #.5 HO2
141		(Same k as M08)			KETP + [RCO3] = [RCO3] + #.75 MGLY + #.5 HO2
143		(Same k as M08)			TOLP + [RCO3] = [RCO3] + #.23 HCHO + #1.4 HO2 + #.724 MGLY + #.181 GLY + #.905 DCB
144		(Same k as M08)			XYLP + [RCO3] = [RCO3] + #.25 HCHO + #1.5 HO2 + MGLY + DCB
M10		(Same k as M08)			OLN + [RCO3] = [RCO3] + HCHO + ALD + NO2
148		(Same k as M08)			XO2 + [RCO3] = [RCO3]
130		(Same k as M08)			ACO3 + [RO2] = #1.5 [RO2] + #.5 MO2 + #.5 ORA2

(continued)

Table 36 (continued) - 6

Rxn. Label (a)	Kinetic Parameters (b) k(300)	A	Ea	B	Reactions (b)
133		(Same k as M08)			TCO3 + [RO2] = #2 [RO2] + #.5 ORA2 + #.46 HO2 + #.445 GLY + #.055 MGLY + #.025 "ACO3 + [RCO3]" + #.475 CO + XO2
M11	3.64E+03	1.75E+03	-0.44	-1.00	[RCO3] + [RCO3] =
142		(Same k as M11)			ACO3 + [RCO3] = [RCO3] + MO2 + [RO2]
145		(Same k as M11)			TCO3 + [RCO3] = [RCO3] + #.92 HO2 + #.890 GLY + #.11 MGLY + #.05 "ACO3 + [RCO3]" + #.950 CO + #2 "XO2 + [RO2]"
					XNO2 Reactions
151	1.12E+04	6.17E+03	-0.36	-1.00	XNO2 + NO2 = ONIT
152		(Same k as M04)			XNO2 + HO2 = OP2
153	5.19E+01	2.50E+01	-0.44	-1.00	XNO2 + [RO2] = [RO2]
154	1.28E+02	6.17E+01	-0.44	-1.00	XNO2 + [RCO3] = [RCO3]
155	1.10E+00	5.28E-01	-0.44	-1.00	XNO2 + XNO2 =

(a) Reactions which correspond directly with those in the standard RADM mechanism are given the same reaction labels as used for them in Table 2. Reactions which are added or significantly modified relative to that mechanism are indicated by the label "Mxx."

(b) See Footnotes (b) and (c) in Table 2 for a description of the formats used in the kinetic parameter and the reaction listings.

the products from MO2 and ACO3 are not included, (2) [RO2] or [RCO3] was included as a product as well as a reactant so the reactions with the individual radicals would be not counted as contributing to their consumption rate (since this is already accounted for in their reactions with [RO2] or [RCO3]), and (3) the rate constants for the corresponding reaction of [RO2] or [RCO3] are employed. Thus, other than the approximation approach used in lumping the organic peroxy + organic peroxy reactions, this mechanism was made to represent, as closely as possible, the chemical approaches used in the March 1988 and the detailed radical RADM mechanisms. Therefore, any differences found between the predictions using this and the other mechanisms should be due primarily to differences in the approximation approach.

Table 37 gives the results of the comparisons of the calculations using the March 1988 RADM mechanism (the "test set") relative to the calculations using the detailed radical mechanism (the "standard set") for the species of known or potential interest in RADM applications. The table gives the summary statistics for all the rural and the urban scenarios aggregated together, and the results for the individual calculations where the "% Fit" or some other percent change statistics is greater than 5%. (Thus, if the results for an individual test problem are not shown, then the two mechanisms gave predictions to within 5%.) With very few exceptions, the two mechanisms give almost exactly the same predictions. Even in the cases where they are the most different, the two mechanisms are generally within 5% of each other in predictions of maximum and average concentrations of O_3, H_2O_2, SULF, HNO_3, ORA1, ORA2, OP1, PAA, and PAN, and within 10% in predictions of OP2, excluding some cases where insignificantly low concentrations are predicted.

These results indicate that the approximation used in the evaluated mechanism, that all the organic peroxy + RO_2 reactions can be represented by reactions only with MO2, and that all the organic peroxy $+RCO_3$ reactions can be represented only by reactions with ACO3, is justified. This is consistent with the results of previous unpublished tests carried out by Stockwell (private communication).

Table 37. Results of Sensitivity Test Calculations Using the Evaluated RADM Mechanism as the Test Mechanism, Relative to the "Detailed Radical" Mechanism as the Standard

Test Problem (a)	Calculated Concentration (ppm) (b)					
	Maximum		Average			
Env Mix NO_x C/N	Standard	% Chg	Standard	% Chg	% /Max	% Fit
Rural O_3						
Maximum (c)	6.50E-02	0.8	4.96E-02	0.6	0.3	0.6
Average (d)		0.0		0.1	0.0	0.1
Avg. Abs. Value (e)		0.1		0.1	0.0	
Urban O_3						
Maximum (c)	3.47E-01	-1.6	2.22E-01	-1.0	-0.6	1.1
Average (d)		-0.2		-0.1	0.0	0.1
Avg. Abs. Value		0.2		0.2	0.1	
Rural H_2O_2						
Maximum (c)	2.41E-03	-2.2	1.85E-03	3.2	-1.5	3.1
Average (d)		0.1		0.2	0.0	0.3
Avg. Abs. Value (e)		0.7		0.5	0.1	
Urban H_2O_2						
Maximum (c)	1.48E-02	-16.5	1.20E-02	-13.3	-2.3	14.3
Average (d)		-1.4		-1.2	-0.2	1.0
Avg. Abs. Value (e)		1.5		1.4	0.2	
SA AC 67 3	2.58E-07	-14.9	1.06E-07	-13.3	0.0	14.3
SA DC 67 3	2.73E-07	-5.3	1.15E-07	-11.2	0.0	12.0
WS BT 67 3	2.05E-08	-16.5	6.64E-09	-5.1	0.0	12.3
Rural SULF						
Maximum (c)	2.20E-03	-1.4	1.53E-03	-1.3	0.6	1.3
Average (d)		0.0		0.1	0.0	0.2
Avg. Abs. Value (e)		0.5		0.4	0.0	
Urban SULF						
Maximum (c)	6.25E-03	-1.9	4.26E-03	-1.6	-0.3	1.6
Average (d)		-0.3		-0.2	0.0	0.2
Avg. Abs. Value (e)		0.4		0.3	0.0	

(continued)

Table 37 (continued) - 2

Test Problem (a)	Calculated Concentration (ppm) (b)					
	Maximum		Average			
Env Mix NO_x C/N	Standard	% Chg	Standard	% Chg	% /Max	% Fit
Rural HNO_3						
Maximum (c)	1.96E-03	3.1	9.86E-04	2.1	0.4	2.2
Average (d)		0.2		0.2	0.0	0.3
Avg. Abs. Value (e)		0.8		0.6	0.0	
Urban HNO_3						
Maximum (c)	8.44E-02	-4.6	3.36E-02	-2.9	-0.6	2.9
Average (d)		-0.5		-0.5	0.0	0.4
Avg. Abs. Value (e)		0.6		0.5	0.1	
Rural ORA1						
Maximum (c)	1.85E-04	5.1	1.38E-04	4.7	-0.7	4.6
Average (d)		0.1		0.1	0.0	0.3
Avg. Abs. Value (e)		0.7		0.7	0.0	
SA AL ~2 6	9.81E-08	5.1	7.85E-08	4.7	0.0	4.6
Urban ORA1						
Maximum (c)	4.52E-03	0.6	3.00E-03	0.5	0.2	0.5
Average (d)		0.1		0.1	0.0	0.1
Avg. Abs. Value (e)		0.2		0.1	0.0	
Rural ORA2						
Maximum (c)	2.68E-04	-4.5	2.10E-04	-8.2	-0.6	8.7
Average (d)		-0.7		-0.9	0.0	0.6
Avg. Abs. Value (e)		1.2		1.2	0.0	
WS AL ~2 20	2.55E-06	0.1	2.12E-06	-8.2	-0.1	8.7
SA AL ~2 60	2.12E-05	-4.5	1.02E-05	-5.6	-0.3	5.8
Urban ORA2						
Maximum (c)	6.46E-03	-5.3	3.52E-03	-3.9	-3.5	4.0
Average (d)		-1.6		-1.3	-0.3	0.8
Avg. Abs. Value (e)		1.6		1.3	0.3	
SS DC 300 10	5.87E-03	-5.3	3.16E-03	-3.9	-3.5	4.0

(continued)

Table 37 (continued) - 3

Test Problem (a)				Calculated Concentration (ppm) (b)					
				Maximum		Average			
Env	Mix	NO_x	C/N	Standard	% Chg	Standard	% Chg	% /Max	% Fit
Rural OP1									
Maximum (c)				1.72E-03	-3.1	1.25E-03	-3.3	-0.4	3.3
Average (d)					-0.2		-0.1	0.0	0.3
Avg. Abs. Value (e)					0.8		0.6	0.0	
Urban OP1									
Maximum (c)				1.38E-02	73.4	8.38E-03	57.3	-1.4	58.3
Average (d)					-0.6		-0.6	-0.2	1.9
Avg. Abs. Value (e)					3.6		2.8	0.2	
SA	AC	67	3	7.44E-07	-5.4	3.58E-07	-6.3	0.0	6.5
SA	DC	67	3	5.29E-07	73.4	2.55E-07	57.3	0.0	44.5
WS	BT	67	3	6.42E-07	-54.1	1.20E-07	-33.1	0.0	58.3
Rural OP2									
Maximum (c)				1.59E-03	-8.4	1.28E-03	-4.1	1.1	9.3
Average (d)					0.3		0.2	0.0	0.7
Avg. Abs. Value (e)					1.4		1.1	0.0	
WS	AL	~2	6	6.40E-06	5.9	3.78E-06	2.2	0.0	2.3
SA	AL	~2	6	5.32E-06	5.5	2.12E-06	3.1	0.0	3.4
WS	AI	~2	6	4.72E-06	-8.4	3.44E-06	-4.1	0.0	9.3
Urban OP2									
Maximum (c)				3.42E-02	2246.7	2.63E-02	1623.2	-1.9	178.7
Average (d)					56.8		39.8	-0.2	6.9
Avg. Abs. Value (e)					61.9		42.6	0.2	
SS	AC	67	10	3.66E-03	-9.9	1.65E-03	-3.6	-0.2	3.7
SS	AC	300	10	1.39E-02	-12.8	6.38E-03	-5.3	-1.3	5.5
WS	AC	67	3	4.29E-07	63.6	9.43E-08	54.2	0.0	44.9
WS	AC	67	10	1.74E-03	-5.4	1.03E-03	-4.5	-0.2	4.7
WS	AC	67	30	7.97E-03	-7.3	5.63E-03	-6.0	-1.3	6.2
SA	AC	67	3	7.20E-07	83.7	2.41E-07	101.7	0.0	67.2
SS	DC	67	10	4.28E-03	-11.1	1.88E-03	-4.4	-0.3	4.5
SS	DC	300	10	1.62E-02	-13.1	7.33E-03	-5.5	-1.5	5.7
WS	DC	67	3	4.36E-07	51.2	8.53E-08	50.3	0.0	40.9
WS	DC	67	10	2.07E-03	-6.7	1.24E-03	-5.7	-0.3	5.9
WS	DC	67	30	9.08E-03	-9.1	6.40E-03	-7.8	-1.9	8.1
SA	DC	67	3	6.50E-07	173.7	2.34E-07	149.8	0.0	86.8
SS	BT	67	10	2.31E-03	-9.3	1.29E-03	-2.9	-0.1	3.0
SS	BT	300	10	7.86E-03	-13.6	4.38E-03	-4.6	-0.8	4.7

(continued)

Table 37 (continued) - 4

Test Problem (a)				------- Calculated Concentration (ppm) (b) --------					
				--- Maximum ---		------- Average -------			
Env	Mix	NO_x	C/N	Standard	% Chg	Standard	% Chg	% /Max	% Fit
WS	BT	67	3	1.10E-07	2246.7	2.18E-08	1623.2	0.0	178.7
SA	BT	67	3	7.64E-08	582.8	4.90E-08	241.5	0.0	109.7
Rural PAA									
Maximum (c)				1.87E-03	-2.9	1.24E-03	3.2	-0.4	3.1
Average (d)					0.2		0.2	0.0	0.3
Avg. Abs. Value (e)					0.9		0.6	0.0	
Urban PAA									
Maximum (c)				1.05E-02	3.4	6.31E-03	3.5	1.1	3.5
Average (d)					0.5		0.4	0.1	0.6
Avg. Abs. Value (e)					0.9		0.8	0.1	
Rural PAN									
Maximum (c)				1.87E-03	2.1	1.26E-03	2.3	-0.5	2.5
Average (d)					0.0		0.3	0.0	0.4
Avg. Abs. Value (e)					0.4		0.6	0.0	
Urban PAN									
Maximum (c)				4.10E-02	0.9	3.28E-02	1.3	-0.4	2.3
Average (d)					0.1		0.1	0.0	0.3
Avg. Abs. Value (e)					0.2		0.3	0.0	

(a) The test problems are as indicated in Table 34. The following notation is employed: (1) "Env" = environmental condition, where SS = Summer surface, WS = Winter Surface, SA = Summer Aloft, and SD = Summer Dynamic. (2) "Mix" = ROG surrogate, where "AL" = aloft mixture, "AI" = aloft + isoprene, "AC" = allcity average, "DC" = Washington DC mixture, and "BT" = Beaumont, Texas, mixture. (3) "NO_x" is the effective NO_x level in ppb. (4) C/N is the ROG/NO_x ratio.

(b) See Section 6.2 for definitions of the statistical measures.

(c) The values given in the "standard" column are the highest maximum or average concentrations in the set of standard calculations. The values given in the "% Chg," "% /Max" and "% Fit" columns are the comparison statistics for the calculations where the two mechanisms are the most different.

(d) Average of the comparison statistics for all the calculations.

(e) Average of the absolute value for the comparison statistics for all the calculations.

The results of the test calculations comparing the version of the RADM mechanism employing the 1986 SAPRC peroxy radical representation with the detailed radical version are summarized in Table 38. As with the previous comparison, the detailed radical mechanism is used as the standard, and the results for individual test problems are shown only for those cases where differences are greater than 5%. For most of the species whose results are compared, this version of the RADM mechanism also gave predictions very close to those for the detailed radical version. However, this approximation did not perform as well in simulating the predictions of the detailed radical model for the higher organic peroxides (OP2) or the higher organic acids (ORA2) in some of the test problems, particularly for some of the urban cases. In the case of OP2, the approximate mechanism had a slight tendency (generally less than 5%) towards predicting lower levels of OP2 in those simulations where significant quantities are predicted, with a few cases of much higher relative predictions for some test problems where very low (sub-ppt) levels of OP2 are predicted. Since the large relative differences are generally restricted to cases where OP2 predictions are generally negligible, this is probably not a significant discrepancy. On the other hand, the disagreements for ORA2 are significant, since the approximate model predicted from 0-40% higher ORA2 levels in cases where its formation is non-negligible.

The discrepancies in the higher organic acid and (to a lesser extent) higher organic peroxide predictions can be attributed to the fact that the SAPRC approximation requires assuming the same rate constants for similar types of peroxy + peroxy reactions while the detailed model uses a variety of rate constants for these reactions. In particular, the most significant discrepancies for ORA2 are due to the fact that the RADM mechanism uses different rate constants for RCO_3 + RO_2 reactions depending on the nature of RO_2. These differences can be represented in the detailed RADM mechanism, but not in the version using the SAPRC approximation. If it is assumed that the rate constants for all RCO_3 + RO_2 reactions are the same, then the mechanism using the SAPRC approximation performs much better in simulating the ORA2 and OP2 results than the detailed version.

Table 38. Results of Sensitivity Test Calculations for the Version of the RADM Mechanism Using the 1986 SAPRC Peroxy Radical Representation as the Test Mechanism, Relative to the "Detailed Radical" Mechanism as the Standard

Test Problem (a)				Calculated Concentration (ppm) (b)					
				Maximum		Average			
Env	Mix	NO_x	C/N	Standard	% Chg	Standard	% Chg	% /Max	% Fit
Rural O_3									
Maximum (c)				6.50E-02	-1.0	4.96E-02	-1.1	-0.5	1.1
Average (d)					0.0		0.0	0.0	0.1
Avg. Abs. Value (e)					0.2		0.2	0.0	
Urban O_3									
Maximum (c)				3.47E-01	-2.3	2.22E-01	-2.1	-1.6	2.1
Average (d)					-0.7		-0.7	-0.2	0.5
Avg. Abs. Value (e)					0.8		0.7	0.2	
Rural H_2O_2									
Maximum (c)				2.41E-03	-4.4	1.85E-03	3.6	-1.6	3.5
Average (d)					-0.2		-0.3	-0.1	0.4
Avg. Abs. Value (e)					0.8		0.7	0.1	
Urban H_2O_2									
Maximum (c)				1.48E-02	-21.7	1.20E-02	-18.7	2.4	20.5
Average (d)					-1.1		-0.8	0.0	1.4
Avg. Abs. Value (e)					2.1		2.1	0.2	
SA	AC	67	3	2.58E-07	-21.7	1.06E-07	-17.3	0.0	19.0
WS	DC	67	3	3.12E-07	-15.8	3.93E-08	-12.4	0.0	13.7
SA	DC	67	3	2.73E-07	-16.1	1.15E-07	-18.7	0.0	20.5
WS	BT	67	3	2.05E-08	2.6	6.64E-09	12.9	0.0	12.3
Rural SULF									
Maximum (c)				2.20E-03	-2.4	1.53E-03	-1.5	0.3	1.5
Average (d)					-0.3		-0.2	0.0	0.2
Avg. Abs. Value (e)					0.6		0.5	0.0	
Urban SULF									
Maximum (c)				6.25E-03	-2.2	4.26E-03	1.3	-0.7	1.4
Average (d)					-0.1		0.1	0.0	0.3
Avg. Abs. Value (e)					0.4		0.5	0.1	

(continued)

Table 38 (continued) - 2

Test Problem (a)				Calculated Concentration (ppm) (b)					
				Maximum		Average			
Env	Mix	NO_x	C/N	Standard	% Chg	Standard	% Chg	% /Max	% Fit
Rural HNO_3									
Maximum (c)				1.96E-03	-4.1	9.86E-04	-2.9	-0.5	3.3
Average (d)					0.2		0.0	0.0	0.4
Avg. Abs. Value (e)					1.1		0.8	0.1	
Urban HNO_3									
Maximum (c)				8.44E-02	9.3	3.36E-02	5.6	-1.1	5.5
Average (d)					0.2		0.0	-0.1	0.5
Avg. Abs. Value (e)					1.0		0.7	0.1	
SD	AC	67	30	5.45E-03	9.3	2.61E-03	5.6	0.4	5.5
SD	DC	67	30	5.59E-03	6.6	2.68E-03	3.8	0.3	3.8
SD	BT	67	30	5.83E-03	8.0	2.79E-03	5.0	0.4	4.9
Rural ORA1									
Maximum (c)				1.85E-04	-6.6	1.38E-04	-5.7	1.3	5.9
Average (d)					-0.3		-0.2	0.0	0.4
Avg. Abs. Value (e)					1.1		1.0	0.0	
SA	AL	~2	20	5.12E-07	-5.1	3.79E-07	-4.1	0.0	4.2
SD	AI	~2	6	3.58E-06	-6.1	1.99E-06	-5.7	-0.1	5.9
SD	AI	~2	20	2.03E-05	-6.6	1.11E-05	-4.1	-0.3	4.3
Urban ORA1									
Maximum (c)				4.52E-03	-1.4	3.00E-03	-1.9	-0.6	1.1
Average (d)					-0.4		-0.3	-0.1	0.2
Avg. Abs. Value (e)					0.4		0.4	0.1	
SA	AL	~2	20	5.12E-07	-5.1	3.79E-07	-4.1	0.0	4.2
SD	AI	~2	6	3.58E-06	-6.1	1.99E-06	-5.7	-0.1	5.9
SD	AI	~2	20	2.03E-05	-6.6	1.11E-05	-4.1	-0.3	4.3
Rural ORA2									
Maximum (c)				2.68E-04	102.8	2.10E-04	116.1	20.0	73.4
Average (d)					25.5		24.8	1.5	8.2
Avg. Abs. Value (e)					25.5		24.8	1.5	
SS	AL	<1	20	3.80E-06	12.3	2.92E-06	13.2	0.2	12.3
SS	AL	<1	66	1.34E-05	33.5	1.04E-05	34.9	1.7	29.7

(continued)

Table 38 (continued) - 3

Test Problem (a)				Calculated Concentration (ppm) (b)					
				Maximum		Average			
Env	Mix	NO_x	C/N	Standard	% Chg	Standard	% Chg	% /Max	% Fit
SS	AL	<1	200	4.14E-05	71.2	3.15E-05	71.7	10.8	52.7
SS	AL	~2	6	7.68E-06	7.4	4.63E-06	6.3	0.1	6.2
SS	AL	~2	20	2.47E-05	25.7	1.58E-05	28.5	2.1	24.9
SS	AL	~2	60	7.19E-05	54.3	4.79E-05	59.0	13.4	45.5
SS	AL	5	2	6.21E-06	10.5	4.24E-06	10.8	0.2	10.2
SS	AL	5	7	2.23E-05	21.3	1.56E-05	20.3	1.5	18.4
SS	AL	5	20	7.44E-05	44.9	5.31E-05	42.3	10.7	34.9
WS	AL	~2	20	2.55E-06	13.4	2.12E-06	11.1	0.1	10.6
WS	AL	~2	60	1.18E-05	45.2	8.46E-06	33.3	1.3	28.7
SA	AL	~2	6	1.01E-07	16.5	4.03E-08	24.9	0.0	22.1
SA	AL	~2	20	1.33E-06	55.3	6.82E-07	63.7	0.2	48.3
SA	AL	~2	60	2.12E-05	102.8	1.02E-05	116.1	5.6	73.4
SD	AL	~2	6	2.44E-06	8.0	1.13E-06	7.6	0.0	7.3
SD	AL	~2	20	9.98E-06	23.8	5.02E-06	22.0	0.5	19.8
SD	AL	~2	60	3.04E-05	50.5	1.52E-05	46.1	3.3	37.5
SS	AI	<1	20	1.22E-05	9.2	6.37E-06	8.5	0.3	8.2
SS	AI	<1	66	5.39E-05	17.4	2.80E-05	17.1	2.3	15.8
SS	AI	<1	200	1.88E-04	26.8	1.06E-04	27.8	14.1	24.4
SS	AI	~2	20	6.62E-05	12.8	5.23E-05	10.7	2.7	10.2
SS	AI	~2	60	2.68E-04	22.6	2.10E-04	20.0	20.0	18.2
SS	AI	5	7	4.92E-05	9.3	3.37E-05	7.8	1.2	7.5
SS	AI	5	20	2.18E-04	19.6	1.37E-04	16.9	11.0	15.6
WS	AI	~2	6	1.06E-05	5.0	6.48E-06	4.9	0.2	4.8
WS	AI	~2	20	3.42E-05	8.9	2.50E-05	7.9	0.9	7.7
WS	AI	~2	60	1.80E-04	10.7	1.37E-04	9.8	6.4	9.4
SA	AI	~2	6	1.94E-07	7.9	1.59E-07	10.8	0.0	10.2
SA	AI	~2	20	6.55E-06	31.9	5.31E-06	31.3	0.8	27.1
SA	AI	~2	60	1.62E-04	39.3	7.78E-05	38.4	14.2	32.2
SD	AI	~2	6	6.37E-06	31.9	3.90E-06	16.9	0.3	15.6
SD	AI	~2	20	3.36E-05	31.9	1.94E-05	21.1	1.9	19.1
SD	AI	~2	60	1.24E-04	30.6	6.94E-05	24.5	8.1	21.8
Urban ORA2									
Maximum (c)				6.46E-03	82.4	3.52E-03	76.9	60.7	55.6
Average (d)					37.4		31.5	7.3	15.5
Avg. Abs. Value (e)					37.4		31.5	7.3	
SS	AC	20	10	4.22E-04	39.9	2.53E-04	33.6	2.4	28.8
SS	AC	20	33	1.44E-03	59.5	1.03E-03	54.4	15.8	42.9
SS	AC	20	100	4.19E-03	40.7	3.22E-03	38.5	35.2	32.4
SS	AC	67	3	2.05E-04	6.6	1.50E-04	14.8	0.6	13.9
SS	AC	67	10	1.79E-03	50.1	1.00E-03	47.1	13.4	38.2
SS	AC	67	30	4.94E-03	57.1	3.39E-03	52.8	50.8	41.9

(continued)

Table 38 (continued) - 4

Test Problem (a)				------- Calculated Concentration (ppm) (b) --------					
				--- Maximum ---		------- Average -------			
Env	Mix	NO_x	C/N	Standard	% Chg	Standard	% Chg	% /Max	% Fit
SS	AC	100	2	1.94E-04	0.6	1.04E-04	9.2	0.3	8.8
SS	AC	200	3	6.42E-04	46.9	4.66E-04	24.9	3.3	22.3
SS	AC	300	10	6.46E-03	54.7	3.52E-03	54.6	54.6	42.9
WS	AC	67	10	7.27E-04	1.9	5.02E-04	12.5	1.8	11.8
WS	AC	67	30	3.39E-03	8.0	2.29E-03	16.0	10.4	14.9
SA	AC	67	10	4.89E-04	37.7	3.79E-04	11.9	1.3	11.4
SA	AC	67	30	4.84E-03	47.5	3.09E-03	22.8	20.0	20.7
SD	AC	67	3	9.29E-05	26.4	5.28E-05	18.6	0.3	17.0
SD	AC	67	10	4.79E-04	68.4	2.55E-04	53.5	3.9	42.2
SD	AC	67	30	2.04E-03	66.6	1.09E-03	59.2	18.3	45.7
SS	DC	20	10	3.71E-04	53.0	2.17E-04	45.2	2.8	36.9
SS	DC	20	33	1.25E-03	76.4	8.51E-04	73.7	17.8	53.9
SS	DC	20	100	3.25E-03	58.6	2.44E-03	57.0	39.5	44.5
SS	DC	67	3	1.38E-04	43.4	1.07E-04	22.5	0.7	20.4
SS	DC	67	10	1.64E-03	60.8	9.02E-04	58.1	14.9	45.0
SS	DC	67	30	4.23E-03	75.2	2.78E-03	73.2	57.8	53.7
SS	DC	100	2	1.25E-04	27.1	8.09E-05	16.5	0.4	15.3
SS	DC	200	3	5.50E-04	59.1	3.45E-04	36.7	3.6	31.2
SS	DC	300	10	5.87E-03	67.4	3.16E-03	67.6	60.7	50.6
WS	DC	67	10	4.69E-04	18.8	3.46E-04	22.0	2.2	19.9
WS	DC	67	30	2.35E-03	17.4	1.64E-03	26.4	12.3	23.4
SA	DC	67	10	3.57E-04	60.6	2.34E-04	23.9	1.6	21.6
SA	DC	67	30	3.70E-03	64.4	2.11E-03	36.6	21.9	31.2
SD	DC	67	3	6.87E-05	31.0	3.84E-05	23.5	0.3	21.0
SD	DC	67	10	3.78E-04	78.2	1.98E-04	65.2	3.7	49.2
SD	DC	67	30	1.58E-03	82.4	8.33E-04	76.9	18.2	55.6
SS	BT	20	10	3.58E-04	34.5	2.20E-04	30.7	1.9	26.7
SS	BT	20	33	1.21E-03	51.2	8.41E-04	47.3	11.3	38.4
SS	BT	20	100	3.44E-03	39.0	2.63E-03	36.5	27.3	31.1
SS	BT	67	3	1.73E-04	10.7	1.31E-04	11.2	0.4	10.8
SS	BT	67	10	1.52E-03	40.9	8.62E-04	40.6	9.9	33.8
SS	BT	67	30	4.22E-03	51.5	2.78E-03	47.7	37.5	38.6
SS	BT	100	2	1.63E-04	0.1	8.17E-05	6.9	0.2	6.8
SS	BT	200	3	6.38E-04	34.0	3.99E-04	16.3	1.8	15.3
SS	BT	300	10	5.53E-03	45.3	3.00E-03	47.5	40.4	38.4
WS	BT	67	10	5.71E-04	0.2	3.81E-04	6.3	0.7	6.2
WS	BT	67	30	2.59E-03	4.9	1.75E-03	11.9	5.9	11.3
SA	BT	67	10	3.45E-04	22.4	2.98E-04	6.1	0.5	6.1
SA	BT	67	30	3.50E-03	44.1	2.24E-03	19.6	12.5	18.1
SD	BT	67	3	7.94E-05	24.9	4.49E-05	17.2	0.2	15.9
SD	BT	67	10	4.02E-04	65.7	2.12E-04	50.1	3.0	40.1
SD	BT	67	30	1.68E-03	65.6	8.83E-04	56.9	14.3	44.3

(continued)

Table 38 (continued) - 5

Test Problem (a)				Calculated Concentration (ppm) (b)					
				Maximum		Average			
Env	Mix	NO_x	C/N	Standard	% Chg	Standard	% Chg	% /Max	% Fit
Rural OP1									
Maximum (c)				1.72E-03	7.9	1.25E-03	56.9	1.9	13.8
Average (d)					2.9		2.8	0.2	1.3
Avg. Abs. Value (e)					3.5		3.2	0.2	
SS	AL	<1	20	4.01E-04	5.8	2.58E-04	3.7	0.8	3.6
SS	AL	<1	66	4.03E-04	5.0	2.85E-04	3.0	0.7	3.0
SS	AL	5	2	6.79E-04	7.8	3.62E-04	4.3	1.3	4.5
SS	AL	5	7	6.61E-04	7.5	3.84E-04	4.3	1.3	4.2
WS	AL	~2	20	4.24E-05	4.6	2.48E-05	5.5	0.1	5.4
SA	AL	~2	6	2.73E-05	-6.5	8.98E-06	-5.5	0.0	6.6
SS	AI	<1	20	4.08E-04	7.0	3.12E-04	4.3	1.1	4.5
SS	AI	5	2	6.97E-04	7.9	3.79E-04	4.1	1.3	4.1
SS	AI	5	7	6.95E-04	6.9	4.06E-04	3.4	1.1	3.4
WS	AI	~2	6	3.43E-05	2.2	1.89E-05	6.9	0.1	6.7
WS	AI	~2	60	2.63E-04	5.2	1.60E-04	15.0	1.9	13.8
Urban OP1									
Maximum (c)				1.38E-02	404.3	8.38E-03	417.2	3.9	135.1
Average (d)					29.7		31.3	0.1	8.9
Avg. Abs. Value (e)					30.0		31.8	0.2	
SS	AC	67	10	1.67E-03	7.5	1.11E-03	-1.1	-0.1	3.7
SS	AC	300	10	4.82E-03	12.5	2.95E-03	-0.7	-0.3	6.1
WS	AC	67	3	1.72E-06	78.5	3.74E-07	125.4	0.0	78.2
WS	AC	67	10	5.24E-04	6.3	3.21E-04	10.4	0.4	9.8
WS	AC	67	30	2.21E-03	4.0	1.55E-03	5.3	1.0	5.1
SA	AC	67	3	7.44E-07	286.3	3.58E-07	273.2	0.0	115.5
SA	AC	67	30	1.38E-02	9.0	8.38E-03	3.9	3.9	3.9
SS	DC	67	10	1.66E-03	8.6	1.12E-03	-1.4	-0.2	4.3
SS	DC	100	2	6.50E-04	6.1	2.88E-04	2.3	0.1	2.8
SS	DC	300	10	4.74E-03	14.7	3.00E-03	-0.5	-0.2	6.6
WS	DC	67	3	1.34E-06	197.9	2.92E-07	202.6	0.0	100.6
SA	DC	67	3	5.29E-07	237.4	2.55E-07	233.4	0.0	107.6
SA	DC	67	30	1.27E-02	9.1	7.52E-03	4.0	3.6	4.0
SS	BT	300	10	3.68E-03	6.0	2.37E-03	-0.6	-0.2	5.5
WS	BT	67	3	6.42E-07	258.6	1.20E-07	417.2	0.0	135.1
WS	BT	67	10	3.68E-04	8.7	1.79E-04	17.9	0.4	16.4
WS	BT	67	30	1.78E-03	3.1	1.18E-03	5.4	0.8	5.3
SA	BT	67	3	2.77E-07	404.3	1.53E-07	367.6	0.0	129.5
SA	BT	67	30	1.09E-02	8.5	6.42E-03	3.6	2.7	3.6

(continued)

Table 38 (continued) - 6

Test Problem (a)				Calculated Concentration (ppm) (b)					
				Maximum		Average			
Env	Mix	NO_x	C/N	Standard	% Chg	Standard	% Chg	% /Max	% Fit
Rural OP2									
Maximum (c)				1.59E-03	-7.5	1.28E-03	17.5	-1.3	16.0
Average (d)					-0.8		-0.6	-0.1	0.9
Avg. Abs. Value (e)					1.6		2.1	0.1	
SA	AL	~2	6	5.32E-06	-7.5	2.12E-06	-7.7	0.0	8.3
WS	AI	~2	6	4.72E-06	6.2	3.44E-06	17.5	0.0	16.0
Urban OP2									
Maximum (c)				3.42E-02	408.0	2.63E-02	311.2	-6.6	121.8
Average (d)					7.4		10.1	-0.8	9.5
Avg. Abs. Value (e)					24.7		23.2	0.8	
SS	AC	20	10	8.10E-04	-15.0	4.26E-04	-7.5	-0.1	7.8
SS	AC	20	33	5.97E-03	-8.3	4.23E-03	-8.3	-1.3	8.6
SS	AC	20	100	1.76E-02	-8.6	1.34E-02	-7.9	-4.0	8.3
SS	AC	67	10	3.66E-03	-27.4	1.65E-03	-14.8	-0.9	16.0
SS	AC	67	30	1.87E-02	-14.8	1.30E-02	-11.5	-5.7	12.2
SS	AC	200	3	1.55E-03	-3.1	6.95E-04	-6.2	-0.2	6.8
SS	AC	300	10	1.39E-02	-34.6	6.38E-03	-21.3	-5.2	23.8
WS	AC	67	3	4.29E-07	32.5	9.43E-08	36.5	0.0	36.5
WS	AC	67	10	1.74E-03	-12.2	1.03E-03	-11.1	-0.4	11.8
WS	AC	67	30	7.97E-03	-13.8	5.63E-03	-12.2	-2.6	13.0
SA	AC	67	3	7.20E-07	99.8	2.41E-07	125.5	0.0	77.1
SA	AC	67	10	4.08E-03	-2.9	2.43E-03	-0.9	-0.1	0.9
SA	AC	67	30	3.34E-02	-6.3	2.53E-02	-3.8	-3.7	3.9
SS	DC	20	10	9.23E-04	-16.8	4.67E-04	-7.7	-0.1	8.0
SS	DC	20	33	6.68E-03	-10.2	4.69E-03	-9.0	-1.6	9.5
SS	DC	20	100	1.86E-02	-9.3	1.42E-02	-8.5	-4.6	8.9
SS	DC	67	10	4.28E-03	-28.5	1.88E-03	-15.7	-1.1	17.1
SS	DC	67	30	2.09E-02	-15.3	1.45E-02	-12.0	-6.6	12.8
SS	DC	100	2	2.22E-04	-4.2	9.35E-05	-6.2	0.0	6.4
SS	DC	200	3	1.78E-03	-3.5	8.07E-04	-6.5	-0.2	7.0
SS	DC	300	10	1.62E-02	-34.0	7.33E-03	-21.5	-6.0	24.1
WS	DC	67	3	4.36E-07	62.2	8.53E-08	73.6	0.0	53.8
WS	DC	67	10	2.07E-03	-13.2	1.24E-03	-12.1	-0.6	12.9
WS	DC	67	30	9.08E-03	-15.2	6.40E-03	-13.6	-3.3	14.6
SA	DC	67	3	6.50E-07	140.9	2.34E-07	136.6	0.0	81.3
SA	DC	67	30	3.42E-02	-6.3	2.63E-02	-4.1	-4.1	4.2
SS	BT	20	10	6.05E-04	-12.7	3.81E-04	-6.1	-0.1	6.3
SS	BT	20	33	4.41E-03	-6.4	3.17E-03	-7.3	-0.9	7.6
SS	BT	20	100	1.44E-02	-6.8	1.10E-02	-7.0	-2.9	7.3

(continued)

Table 38 (continued) - 7

Test Problem (a)				Calculated Concentration (ppm) (b)					
				Maximum		Average			
Env	Mix	NO_x	C/N	Standard	% Chg	Standard	% Chg	% /Max	% Fit
SS	BT	67	10	2.31E-03	-28.1	1.29E-03	-13.8	-0.7	14.8
SS	BT	67	30	1.39E-02	-14.1	9.68E-03	-10.3	-3.8	10.9
SS	BT	200	3	8.26E-04	-6.8	3.29E-04	-9.4	-0.1	9.9
SS	BT	300	10	7.86E-03	-30.8	4.38E-03	-21.1	-3.5	23.5
WS	BT	67	3	1.10E-07	122.5	2.18E-08	215.1	0.0	103.7
WS	BT	67	10	1.02E-03	-8.5	4.80E-04	-7.2	-0.1	7.7
WS	BT	67	30	5.41E-03	-11.0	3.56E-03	-10.2	-1.4	10.7
SA	BT	67	3	7.64E-08	408.0	4.90E-08	311.2	0.0	121.8
SA	BT	67	30	2.76E-02	-5.5	2.01E-02	-2.7	-2.1	2.8
Rural PAA									
Maximum (c)				1.87E-03	-7.3	1.24E-03	-5.0	2.0	5.1
Average (d)					-0.2		-0.2	0.0	0.6
Avg. Abs. Value (e)					1.8		1.4	0.1	
WS	AL	~2	6	3.29E-06	-7.3	1.35E-06	-5.0	0.0	5.1
SA	AL	~2	6	3.34E-06	-7.0	1.13E-06	-0.4	0.0	1.7
Urban PAA									
Maximum (c)				1.05E-02	-12.3	6.31E-03	11.8	3.6	11.1
Average (d)					-1.0		-1.0	-0.1	1.6
Avg. Abs. Value (e)					3.0		2.4	0.3	
WS	AC	67	3	3.31E-08	-6.3	4.95E-09	-2.5	0.0	3.8
WS	AC	67	30	3.01E-03	9.0	1.91E-03	8.8	2.6	8.8
SA	AC	67	3	6.38E-08	-6.3	3.11E-08	-2.8	0.0	2.9
WS	DC	67	3	5.56E-08	-12.3	7.11E-09	-9.2	0.0	9.8
WS	DC	67	10	7.17E-04	5.6	4.32E-04	5.4	0.4	5.4
WS	DC	67	30	2.96E-03	11.8	1.93E-03	11.8	3.6	11.1
SA	DC	67	3	7.26E-08	-9.7	3.28E-08	-4.4	0.0	4.5
SS	BT	300	10	4.07E-03	-5.9	2.54E-03	-4.2	-1.7	5.4
WS	BT	67	30	2.51E-03	6.5	1.52E-03	6.6	1.6	6.5
SA	BT	67	30	7.94E-03	-6.2	4.45E-03	-2.2	-1.6	2.3
Rural PAN									
Maximum (c)				1.87E-03	-5.3	1.26E-03	-7.1	-1.8	9.3
Average (d)					-0.8		-0.8	0.0	1.0
Avg. Abs. Value (e)					1.0		2.2	0.1	
SD	AL	~2	60	7.41E-05	-2.2	3.37E-05	-5.6	-0.1	5.8
SD	AI	~2	6	2.04E-05	-5.3	7.42E-06	-6.7	0.0	7.3

(continued)

Table 38 (continued) - 8

Test Problem (a)				------- Calculated	Concentration (ppm) (b)				--------
				--- Maximum ---		------- Average -------			
Env	Mix	NO$_x$	C/N	Standard	% Chg	Standard	% Chg	% /Max	% Fit
SD	AI	~2	20	6.33E-05	1.8	2.57E-05	-7.1	-0.1	8.5
SD	AI	~2	60	1.34E-04	1.1	5.91E-05	-8.5	-0.4	9.3
Urban PAN									
Maximum (c)				4.10E-02	-6.6	3.28E-02	-8.5	-2.3	7.2
Average (d)					-1.3		-1.0	-0.1	1.0
Avg. Abs. Value (e)					1.3		1.4	0.2	
SD	AC	67	30	5.18E-03	-6.6	3.67E-03	-7.0	-0.8	7.2
SD	DC	67	30	4.97E-03	-5.0	3.51E-03	-5.5	-0.6	5.6
SD	BT	67	30	5.32E-03	-5.1	3.74E-03	-6.5	-0.7	6.7

(a) See Footnote (a) in Table 37 for a description of the notation used to indicate the test problems.

(b) See Section 6.2 for definitions of the statistical measures.

(c) The values given in the "standard" column are the highest maximum or average concentrations in the set of standard calculations. The values given in the "% Chg," "% /Max" and "% Fit" columns are the comparison statistics for the calculations where the two mechanisms are the most different.

(d) Average of the comparison statistics for all the calculations.

(e) Average of the absolute value for the comparison statistics for all the calculations.

The significance of this apparent failure of the SAPRC approximation to reproduce detailed model predictions of the higher organic acids depends upon the extent to which the detailed mechanism taken as the standard is assumed to represent reality. Had we developed the detailed radical mechanism for use in this evaluation, we would have estimated, based on the limited laboratory data available (Atkinson, 1989), that the rate constants for all the RO_2 + RCO_3 reactions were approximately the same, and thus the SAPRC radical approximation would have performed much better in reproducing the detailed model. It is clear that if there are variations in the RCO_3 + RO_2 rate constants to the extent assumed in the RADM mechanism, then the mechanisms utilizing the SAPRC approximation to represent peroxy radical + peroxy radical reactions will not perform satisfactorily in predicting yields of the higher organic acids. However, if the detailed model uses incorrect estimates for these rate constants -- which may well be the case since few have been measured -- the predictions of the detailed model may be even less reliable than the approximate one. No suitable data are available to test model predictions of organic acids.

In summary, the test calculations on the representation of peroxy + peroxy reactions tend to support the approach which is currently employed in the evaluated RADM mechanism. This does not mean, however, that it may not be possible to employ more efficient approaches involving fewer reactions and possibly fewer species. However, at the present time no alternatives in this regard are recommended for the RADM mechanism.

6.4 Lumping of Higher Alkanes

One area where the RADM mechanism is more detailed than most other current condensed mechanisms is its representation of the higher (C3+) alkanes. However, test calculations previously carried out using the latest SAPRC mechanism (Carter, 1988) indicate that relatively severe condensations of alkanes have relatively little effect on model predictions if the parameters and rate constants for the lumped species are adjusted appropriately based on the mixtures being represented. Therefore, as part of this study we carried out test calculations to determine whether a moderate level of condensation of the RADM mechanism, employing two lumped species to represent the C3+ alkanes rather than three, would have a significant effect on model predictions relative to the current version.

The condensation examined was to lump the species HC5 and HC8 and represent them by a single species, designated HC6. For direct comparison with the March 1988 RADM mechanism, the OH radical rate constant and product yield parameters for the new lumped species were determined by the averages of those for HC5 and HC8 in the March 1988 mechanism, weighed by the estimated relative numbers of moles of each reacting in RADM applications. These were derived using the total detailed U.S. emissions, and assuming an integrated OH radical parameter (INTOH) value of 110 ppt-min, using the methods and data bases discussed in Section 3.2. The reaction used for HC6 was,

$$\mathrm{HC6 + HO \dashrightarrow HC6P + 0.54\ XO2 + H2O}$$

where $k = 3.02 \times 10^{-11} \exp(-380/T)$ cm^3 $\mathrm{molecule}^{-1}$ sec^{-1}. The reactions used for HC6P, its associated peroxy peroxy radical, were

$$\begin{aligned}\mathrm{HC6P + NO \dashrightarrow}\ & \mathrm{0.4\ ALD + 0.91\ KET + \#.17\ ONIT + 0.03\ HCHO\ +} \\ & \mathrm{0.83\ NO2 + 0.83\ HO2}\end{aligned}$$

$$\mathrm{HC6P + HO2 \dashrightarrow OP2}$$

$$\mathrm{HC6P + ACO3 \dashrightarrow 0.12\ ALD + 0.88\ KET + 0.5\ HO2 + 0.5\ MO2 + 0.5\ ORA2}$$

$$\mathrm{HC6P + MO2 \dashrightarrow 0.75\ HCHO + HO2 + 0.089\ ALD + 0.66\ KET}$$

where their rate constants were the same as those used for HC5P and HC8P. The only other modifications made to the RADM mechanism was the removal of the reactions of HC5, HC5P, HC8, and HC8P.

(Note that the kinetic and product yield parameters used for HC6 and HC6P in the modified mechanism for the purpose of this test are slightly different from those used for this species in the RADM-M mechanism. The parameters in the latter mechanism are based on a more recent analysis of the emissions data than used to derive the parameters for the March 1988 version of the RADM mechanism used as the standard in this test. The parameters used in the test were derived to be consistent with those used in the standard mechanism for more direct comparison.)

A comparison of the predictions using this "condensed alkane" RADM mechanism with those of the standard mechanism in simulations of the 90 test problems is presented in Table 39. The results for individual test problems are shown only for those cases where differences are greater than 5%. These results show that despite the fact that these scenarios used five different ROG surrogates with four different profiles for the alkanes, this level of condensation had an almost insignificant effect on the simulations of the species of interest in regional oxidant or acid deposition models. There are only a few cases where relative discrepancies greater than 3% were observed, and in essentially all these cases the predicted concentrations of the species were very low.

It is on the basis of these results that we recommend that the RADM mechanism be condensed in its representation of these higher alkanes. It is possible that it may also be appropriate to lump HC3 with the higher alkane classes. However, more significant condensations of the RADM mechanism was considered to be beyond the scope of this evaluation program.

6.5 The Recommended vs. March 1988 RADM Mechanisms

As discussed in Section 2, as a result of the tests carried out in this program, we have recommended modifications in the RADM mechanism, relative to the March 1988, version which was evaluated in this study. The most important modifications in terms of effects on model performance concern changes in the representation of the unknown aspects of the aromatic photooxidation mechanism to improve the performance of the mechanism in simulating the results of aromatic - NO_x - air chamber experiments. Minor changes in rate constant and product yields are recommended for some of the lumped species based on the results of an updated analysis of emissions data as discussed in Section 3. Other minor changes are recommended for the representation of phenol and nitrophenol + NO_3 reactions to improve chemical reasonableness. In addition, as a result of the tests discussed in the previous section, we recommended that the two higher alkane species in the RADM mechanism be lumped together. All the

Table 39. Results of Sensitivity Test Calculations Using the Version of the RADM Mechanism with the Higher Alkane Species HC5 and HC8 Lumped Together, Relative to the Standard RADM Mechanism

Test Problem (a)	Calculated Concentration (ppm) (b)					
	Maximum		Average			
Env Mix NO$_x$ C/N	Standard	% Chg	Standard	% Chg	% /Max	% Fit
Rural O_3						
Maximum (c)	6.49E-02	-1.9	4.97E-02	-1.4	-0.6	1.4
Average (c)		-0.1		-0.2	0.0	0.1
Avg. Abs. Value (c)		0.2		0.2	0.0	
Urban O_3						
Maximum (c)	3.47E-01	1.6	2.23E-01	1.3	0.2	1.3
Average (c)		0.0		0.1	0.0	0.1
Avg. Abs. Value (c)		0.2		0.2	0.0	
Rural H_2O_2						
Maximum (c)	2.41E-03	2.8	1.82E-03	3.2	-1.5	3.3
Average (c)		-0.1		-0.1	0.0	0.3
Avg. Abs. Value (c)		0.6		0.6	0.1	
Urban H_2O_2						
Maximum (c)	1.48E-02	27.4	1.20E-02	11.1	-0.5	13.2
Average (c)		1.1		0.5	0.0	0.6
Avg. Abs. Value (c)		1.5		0.9	0.1	
SA DC 67 3	2.59E-07	5.1	1.02E-07	0.8	0.0	2.3
WS BT 67 3	1.71E-08	27.4	6.31E-09	11.1	0.0	13.2
SA BT 67 3	4.36E-08	20.2	3.47E-08	4.5	0.0	4.6
Rural SULF						
Maximum (c)	2.21E-03	-3.6	1.53E-03	-3.9	-1.0	3.9
Average (c)		-0.7		-0.7	0.0	0.4
Avg. Abs. Value (c)		0.9		0.8	0.1	
Urban SULF						
Maximum (c)	6.25E-03	-1.1	4.26E-03	-1.1	-0.5	1.1
Average (c)		-0.2		-0.1	0.0	0.2
Avg. Abs. Value (c)		0.4		0.3	0.1	

(continued)

Table 39 (continued) - 2

Test Problem (a)				------- Calculated Concentration (ppm) (b) --------					
				--- Maximum ---		------- Average -------			
Env	Mix	NO_x	C/N	Standard	% Chg	Standard	% Chg	% /Max	% Fit
Rural HNO_3									
Maximum (c)				1.95E-03	-3.8	9.87E-04	-6.9	-1.7	7.1
Average (c)					-1.3		-1.3	-0.1	0.6
Avg. Abs. Value (c)					1.4		1.4	0.1	
SS	AL	<1	200	6.48E-05	-3.6	2.68E-05	-6.9	-0.2	7.1
Urban HNO_3									
Maximum (c)				8.46E-02	-1.0	3.36E-02	-2.3	-0.6	0.9
Average (c)					-0.1		-0.1	0.0	0.2
Avg. Abs. Value (c)					0.3		0.2	0.0	
Rural ORA1									
Maximum (c)				1.84E-04	3.2	1.37E-04	2.7	0.4	2.6
Average (c)					0.4		0.4	0.0	0.3
Avg. Abs. Value (c)					0.7		0.7	0.0	
Urban ORA1									
Maximum (c)				4.53E-03	1.2	3.00E-03	1.0	0.7	1.0
Average (c)					0.3		0.3	0.1	0.2
Avg. Abs. Value (c)					0.4		0.3	0.1	
Rural ORA2									
Maximum (c)				2.68E-04	5.2	2.11E-04	5.2	1.1	5.1
Average (c)					0.9		1.0	0.1	0.6
Avg. Abs. Value (c)					1.5		1.3	0.1	
SA	AL	~2	20	1.29E-06	4.8	6.60E-07	5.2	0.0	5.1
SA	AL	~2	60	2.03E-05	5.2	9.61E-06	5.0	0.2	4.9
Urban ORA2									
Maximum (c)				6.19E-03	2.7	3.42E-03	1.1	0.7	1.1
Average (c)					0.3		0.3	0.1	0.3
Avg. Abs. Value (c)					0.5		0.4	0.1	

(continued)

Table 39 (continued) - 3

Test Problem (a)				Calculated Concentration (ppm) (b)					
				Maximum		Average			
Env	Mix	NO_x	C/N	Standard	% Chg	Standard	% Chg	% /Max	% Fit
Rural OP1									
Maximum (c)				1.70E-03	5.4	1.25E-03	5.0	0.9	4.9
Average (c)					0.2		0.5	0.0	0.4
Avg. Abs. Value (c)					0.8		0.7	0.0	
SA	AL	~2	20	8.48E-05	5.4	4.61E-05	5.0	0.2	4.9
Urban OP1									
Maximum (c)				1.37E-02	124.0	8.35E-03	56.5	0.8	56.8
Average (c)					1.7		0.8	0.0	1.6
Avg. Abs. Value (c)					3.8		2.5	0.0	
SA	AC	67	3	7.04E-07	-5.4	3.36E-07	-2.5	0.0	2.6
SA	DC	67	3	9.17E-07	-40.2	4.01E-07	-35.0	0.0	42.4
WS	BT	67	3	2.95E-07	124.0	8.04E-08	56.5	0.0	56.8
SA	BT	67	10	9.00E-04	5.4	3.05E-04	6.1	0.2	5.9
Rural OP2									
Maximum (c)				1.61E-03	16.2	1.30E-03	13.7	3.2	13.0
Average (c)					1.4		1.4	0.1	1.5
Avg. Abs. Value (c)					3.6		3.2	0.2	
SS	AL	<1	200	6.31E-04	5.7	4.39E-04	5.9	2.0	5.7
SS	AL	5	2	2.92E-05	-5.0	2.07E-05	-1.7	0.0	5.1
SS	AL	5	7	9.38E-05	-4.4	7.10E-05	-2.6	-0.1	2.8
WS	AL	~2	20	3.87E-05	8.1	2.56E-05	7.8	0.2	7.5
SA	AL	~2	6	5.61E-06	-7.8	2.19E-06	-5.6	0.0	7.2
SA	AL	~2	60	7.45E-04	6.5	6.60E-04	6.2	3.2	6.0
SD	AL	~2	6	2.33E-05	2.1	1.37E-05	5.0	0.1	4.9
WS	AI	~2	6	4.33E-06	16.2	3.30E-06	13.7	0.0	13.0
SA	AI	~2	6	2.71E-06	-5.9	1.40E-06	-7.5	0.0	8.3
Urban OP2									
Maximum (c)				3.40E-02	-85.6	2.61E-02	-90.6	1.5	165.4
Average (c)					-2.2		-2.3	0.1	4.3
Avg. Abs. Value (c)					4.3		4.6	0.1	
SS	AC	100	2	2.17E-04	-5.8	8.62E-05	-7.0	0.0	7.2
WS	AC	67	3	7.03E-07	9.3	1.45E-07	18.7	0.0	17.0
SS	DC	100	2	2.20E-04	-6.9	9.25E-05	-7.9	0.0	8.3

(continued)

Table 39 (continued) - 4

Test Problem (a)				------- Calculated Concentration (ppm) (b) --------					
				--- Maximum ---		------- Average -------			
Env	Mix	NO$_x$	C/N	Standard	% Chg	Standard	% Chg	% /Max	% Fit
WS	DC	67	3	6.60E-07	6.5	1.28E-07	7.4	0.0	11.1
SA	DC	67	3	1.78E-06	-17.1	5.85E-07	-13.7	0.0	23.1
SS	BT	200	3	8.21E-04	-5.5	3.24E-04	-0.8	0.0	3.9
WS	BT	67	3	2.58E-06	-85.6	3.76E-07	-90.6	0.0	165.4
SA	BT	67	3	5.22E-07	-34.3	1.67E-07	-31.0	0.0	38.1
SA	BT	67	10	3.10E-03	3.8	1.42E-03	5.3	0.3	5.2
Rural PAA									
Maximum (c)				1.86E-03	-5.9	1.24E-03	4.8	1.1	4.6
Average (c)					0.6		0.9	0.0	0.6
Avg. Abs. Value (c)					1.3		1.4	0.1	
SA	AL	~2	6	3.35E-06	-5.9	1.17E-06	-2.6	0.0	3.4
Urban PAA									
Maximum (c)				1.05E-02	6.6	6.33E-03	6.9	0.6	6.6
Average (c)					0.4		0.3	0.0	0.7
Avg. Abs. Value (c)					1.3		0.9	0.1	
SA	BT	67	3	1.65E-08	6.5	1.37E-08	2.1	0.0	2.1
SA	BT	67	10	6.45E-04	6.6	2.02E-04	6.9	0.2	6.6
Rural PAN									
Maximum (c)				1.87E-03	-3.5	1.26E-03	-6.1	-0.8	6.4
Average (c)					0.0		-0.2	0.0	0.5
Avg. Abs. Value (c)					0.7		0.9	0.0	
SS	AL	<1	200	1.19E-04	-3.5	2.89E-05	-6.1	-0.1	6.4
Urban PAN									
Maximum (c)				4.10E-02	2.1	3.28E-02	-1.7	0.4	2.6
Average (c)					0.1		0.0	0.0	0.3
Avg. Abs. Value (c)					0.4		0.3	0.0	

(a) See Footnote (a) in Table 37 for a description of the notation used to indicate the test problems.

(b) See Section 6.2 for a discussions of the specific measures of differences between the mechanisms.

(c) See footnotes (c-e) in Table 37 or 38 for a description of these quantities.

recommended changes are implemented in the RADM-M mechanism. The changes involving the aromatics mechanism and the updated parameters for the lumped species were implemented in the RADM-P mechanism, a version where only parameter values (for the most part) are changed. The modifications involved in the RADM-P mechanism have been accepted by the RADM team, and are being implemented into the RADM model (Stockwell, private communication, 1989).

Table 40 gives the summary statistics of the differences between the two modified RADM mechanisms and the March 1988 version in their predictions of the species of interest in the 90 test problems. (The March 1988 mechanism is taken as the "standard" for the purpose of this tabulation.) Tables 41 and 42 give the differences in the calculations of ozone and H_2O_2 for each of the individual sets of urban test calculations, and Figures 89 and 90 show comparisons of concentration-time plots for selected compounds for two such calculations. Figure 89 shows results calculated for the urban summer surface static simulation with initial NO_x of 67 ppb and ROG/NO_x ratio of 10, and Figure 90 shows the results calculated for winter surface conditions with the same pollutant levels. As with the plots in Section 5, the solid line designates results of calculations using the RADM mechanism, the longer dashes designate results calculated using RADM-P, and the shorter dashes indicate RADM-M results.

The results shown in Table 40 indicate that the recommended modified mechanisms can in some cases give quite different predictions for compounds of potential interest in RADM applications, especially for urban conditions. The greater sensitivities in the urban cases are expected since the most important modifications in the mechanism concerned the aromatics, which are relatively more important in urban conditions. The magnitudes of the differences depend on the conditions of the specific test problems, as shown in Tables 41 and 42 for the predictions of ozone and H_2O_2 for all the urban cases, and as shown in Figures 89 and 90 for summer vs. winter environments for one set of pollution conditions. In general, the modified mechanisms had a tendency to predict lower levels of ozone, hydroperoxides and organic acids than the March 1988 mechanism, with the effects on the peroxides and the acids being greater than the effects on ozone. In general, the test cases in Tables 41 and 42 that show the greatest differences in predictions for H_2O_2 are also the cases

Table 40. Summary of Results of Sensitivity Test Calculations Using the Recommended Modified (RADM-M) and the Recommended Modified Parameter (RADM-P) Mechanisms, Relative to the March 1988 RADM Mechanism as the Standard

Test Cases and Compound	--- RADM-M vs RADM (a) ---				--- RADM-P vs RADM (a) ---			
	Max. %Chg.	- Average - %Chg.	%/Max	% Fit	Max. %Chg.	- Average - %Chg.	%/Max	% Fit
Rural O_3								
Maximum	3.9	3.3	1.5	3.2	6.2	5.3	2.5	5.2
Average	0.0	-0.2	-0.1	0.2	0.2	0.1	0.0	0.2
Avg. Abs. Value	0.4	0.5	0.1		0.5	0.4	0.1	
Urban O_3								
Maximum	-34.8	-32.7	-9.0	39.2	-34.6	-27.9	9.9	32.5
Average	-3.0	-5.5	-0.9	5.4	-1.4	-3.4	-0.3	4.5
Avg. Abs. Value	6.7	7.3	1.5		6.0	6.1	1.2	
Rural H_2O_2								
Maximum	-9.3	-13.9	-4.0	14.8	-10.7	-15.1	-4.5	16.2
Average	-1.7	-2.1	-0.2	1.0	-1.5	-2.0	-0.2	1.0
Avg. Abs. Value	1.9	2.3	0.2		1.9	2.2	0.2	
Urban H_2O_2								
Maximum	-85.3	-72.9	-18.1	115.8	-89.3	-73.7	-17.8	117.9
Average	-17.5	-19.8	-1.8	14.9	-16.9	-19.1	-1.8	14.2
Avg. Abs. Value	17.6	19.8	1.8		17.0	19.1	1.8	
Rural SULF								
Maximum	5.9	6.1	2.0	5.9	7.4	7.7	2.5	7.4
Average	0.7	0.6	0.1	0.4	1.2	1.1	0.1	0.5
Avg. Abs. Value	1.0	1.0	0.1		1.4	1.3	0.1	
Urban SULF								
Maximum	-42.4	-32.9	-13.1	39.3	-42.8	-31.9	-13.2	38.0
Average	1.5	1.0	0.0	5.8	0.4	-0.1	-0.2	5.2
Avg. Abs. Value	10.8	8.6	1.2		9.4	7.6	1.1	
Rural HNO_3								
Maximum	7.8	6.8	3.0	6.5	10.0	9.0	3.9	8.6
Average	0.8	0.4	0.1	0.7	2.0	1.6	0.1	0.8
Avg. Abs. Value	1.8	1.3	0.1		2.1	1.7	0.2	
Urban HNO_3								
Maximum	-32.0	-31.3	-17.5	37.1	27.8	-28.5	15.9	33.2
Average	-0.1	0.8	-0.1	6.2	0.9	1.6	0.1	5.7
Avg. Abs. Value	9.7	7.8	1.6		8.9	7.6	1.5	

(continued)

Table 40 (continued) - 2

Test Cases and Compound	--- RADM-M vs RADM (a) ---				--- RADM-P vs RADM (a) ---			
	Max. %Chg.	- Average - %Chg.	%/Max	% Fit	Max. %Chg.	- Average - %Chg.	%/Max	% Fit
Rural ORA1								
Maximum	-6.7	-6.5	-0.5	6.7	-7.1	-6.6	-0.7	6.9
Average	-1.2	-1.2	0.0	0.6	-1.0	-1.0	0.0	0.5
Avg. Abs. Value	1.5	1.4	0.0		1.3	1.2	0.0	
Urban ORA1								
Maximum	-24.4	-21.6	-8.9	24.2	-19.3	-17.0	-6.4	18.6
Average	-8.9	-8.1	-1.2	5.3	-6.6	-6.0	-0.9	4.0
Avg. Abs. Value	8.9	8.1	1.2		6.6	6.1	0.9	
Rural ORA2								
Maximum	-28.5	-42.5	-1.9	53.7	-20.4	-21.1	-1.6	23.6
Average	-4.5	-5.1	-0.1	2.3	-4.6	-5.0	-0.1	2.2
Avg. Abs. Value	4.7	5.2	0.1		4.9	5.1	0.1	
Urban ORA2								
Maximum	-40.7	-29.3	-17.8	34.6	-39.1	-26.4	-16.4	30.6
Average	-13.2	-13.7	-2.2	8.9	-13.2	-13.6	-2.4	8.9
Avg. Abs. Value	13.2	13.7	2.2		13.2	13.6	2.4	
Rural OP1								
Maximum	-10.2	-15.3	-1.6	16.5	-12.8	-13.8	-3.2	14.8
Average	-0.7	-1.2	0.0	0.9	-1.9	-2.5	-0.1	1.2
Avg. Abs. Value	1.6	2.0	0.1		2.1	2.6	0.1	
Urban OP1								
Maximum	-79.9	-75.7	-15.3	121.8	-73.9	-69.0	-19.8	105.2
Average	-8.7	-15.0	-0.5	13.1	-18.7	-22.6	-1.8	16.6
Avg. Abs. Value	12.8	16.6	0.9		18.7	22.6	1.8	
Rural OP2								
Maximum	-28.1	-23.1	-9.8	26.1	35.7	-17.3	-7.6	18.9
Average	-14.1	-13.8	-0.6	6.1	-5.8	-6.4	-0.3	3.0
Avg. Abs. Value	14.3	13.8	0.6		7.8	7.0	0.3	
Urban OP2								
Maximum	191.3	-84.8	-28.6	157.5	900.4	748.8	-19.5	160.9
Average	-36.3	-40.5	-3.1	33.0	-6.2	-10.0	-1.5	20.8
Avg. Abs. Value	43.4	40.5	3.1		39.8	37.7	1.5	
Rural PAA								
Maximum	-14.8	-22.1	-1.4	16.9	-17.8	-21.0	-4.3	23.4
Average	-1.5	-1.5	0.0	1.2	-5.1	-6.1	-0.2	2.6
Avg. Abs. Value	2.1	2.7	0.1		5.1	6.1	0.2	

(continued)

Table 40 (continued) - 3

Test Cases and Compound	--- RADM-M vs RADM (a) ---				--- RADM-P vs RADM (a) ---			
	Max. %Chg.	- Average - %Chg.	- Average - %/Max	% Fit	Max. %Chg.	- Average - %Chg.	- Average - %/Max	% Fit
Urban PAA								
Maximum	-88.2	-73.4	-20.3	117.2	-91.1	-82.0	-37.3	139.8
Average	-13.4	-15.5	-0.6	12.7	-25.1	-27.2	-3.3	20.5
Avg. Abs. Value	15.8	17.1	1.3		25.1	27.2	3.3	
Rural PAN								
Maximum	9.2	9.5	6.8	9.1	-14.2	-14.2	-3.3	15.3
Average	2.4	0.3	0.1	1.2	-4.6	-4.6	-0.2	1.9
Avg. Abs. Value	2.8	1.6	0.2		4.6	4.6	0.2	
Urban PAN								
Maximum	-61.4	-39.3	30.7	61.4	-64.5	-51.6	-17.3	69.7
Average	3.4	-1.6	1.1	9.4	-17.8	-17.8	-1.7	13.0
Avg. Abs. Value	15.9	11.9	1.6		18.5	17.8	1.7	

(a) See Section 6.2 for a discussions of the specific measures of differences between the mechanisms. See footnotes (c-e) in Table 37 or 38 for a description of the quantities tabulated.

Table 41. Results of Sensitivity Test Calculations of Urban Ozone Formation Using the Recommended Modified (RADM-M) and the Recommended Modified Parameter (RADM-P) Mechanisms, Relative to the March 1988 Version of the RADM Mechanism as the Standard

Test	Problem (a)			Standard Conc (ppm)		--- RADM-M vs RADM (b) ---				--- RADM-P vs RADM (b) ---			
Env	Mix	NOx	C/N	Maximum	Average	Max.	- Average -		%	Max.	- Average -		%
						%Chg.	%Chg.	%/Max	Fit	%Chg.	%Chg.	%/Max	Fit
SS	AC	20	10	1.00E-01	7.06E-02	-3.8	-4.5	-1.4	4.6	-2.1	-2.6	-0.8	2.7
SS	AC	20	33	1.11E-01	9.32E-02	0.1	-0.7	-0.3	1.5	2.0	1.4	0.6	1.7
SS	AC	20	100	1.04E-01	8.68E-02	3.6	2.4	0.9	3.2	4.5	3.7	1.5	3.6
SS	AC	67	3	6.10E-02	4.89E-02	-0.8	-7.7	-1.7	7.9	0.7	-5.5	-1.2	6.1
SS	AC	67	10	1.86E-01	1.25E-01	-4.2	-6.3	-3.5	6.5	-2.0	-3.2	-1.8	3.3
SS	AC	67	30	1.94E-01	1.59E-01	0.4	-0.7	-0.5	2.1	2.3	1.6	1.1	2.3
SS	AC	100	2	6.62E-02	3.90E-02	-30.3	-19.2	-3.4	21.1	-30.1	-17.0	-3.0	18.4
SS	AC	200	3	9.94E-02	7.00E-02	13.1	-4.4	-1.4	18.8	13.8	-1.6	-0.5	17.6
SS	AC	200	10	3.44E-01	2.23E-01	-3.1	-6.6	-6.6	6.9	-0.7	-2.8	-2.8	2.8
WS	AC	67	3	2.00E-02	8.12E-03	0.0	-19.2	-0.7	21.1	0.0	-17.0	-0.6	18.4
WS	AC	67	10	5.48E-02	3.76E-02	9.6	4.8	0.8	10.4	10.3	5.8	1.0	10.6
WS	AC	67	30	1.55E-01	9.46E-02	2.7	3.3	1.4	3.4	2.8	3.5	1.5	3.7
SA	AC	67	3	7.93E-02	5.52E-02	-26.7	-26.8	-6.7	31.0	-22.5	-22.7	-5.6	25.6
SA	AC	67	10	2.37E-01	2.13E-01	-2.4	-5.8	-5.5	5.9	-0.3	-3.7	-3.6	3.8
SA	AC	67	30	2.05E-01	1.90E-01	7.8	8.1	6.9	7.9	9.6	9.9	8.5	9.5
SD	AC	67	3	8.46E-02	6.72E-02	-3.2	-2.6	-0.8	2.6	-1.7	-1.6	-0.5	1.6
SD	AC	67	10	1.11E-01	8.56E-02	-4.2	-3.2	-1.2	3.3	-1.4	-1.3	-0.5	1.3
SD	AC	67	30	1.19E-01	9.29E-02	-3.1	-1.6	-0.7	1.7	0.2	0.6	0.2	0.6
SS	DC	20	10	1.00E-01	7.08E-02	-4.4	-5.3	-1.7	5.5	-2.4	-3.1	-1.0	3.1
SS	DC	20	33	1.09E-01	9.18E-02	0.0	-1.0	-0.4	2.0	2.3	1.6	0.6	2.1
SS	DC	20	100	1.03E-01	8.63E-02	3.4	2.1	0.8	3.3	4.8	4.0	1.5	3.9
SS	DC	67	3	6.10E-02	4.97E-02	-1.7	-9.8	-2.2	10.2	0.1	-7.1	-1.6	7.3
SS	DC	67	10	1.85E-01	1.25E-01	-5.1	-7.7	-4.3	8.0	-2.4	-3.8	-2.1	3.9

(continued)

Table 41 (continued) - 2

Test	Problem (a)			Standard Conc (ppm)		--- RADM-M vs RADM (b) ---				--- RADM-P vs RADM (b) ---			
Env	Mix	NOx	C/N	Maximum	Average	Max. %Chg.	- Average - %Chg.	- Average - %/Max	% Fit	Max. %Chg.	- Average - %Chg.	- Average - %/Max	% Fit
SS	DC	67	30	1.89E-01	1.54E-01	0.1	-1.2	-0.8	2.6	2.5	1.7	1.2	2.5
SS	DC	100	2	7.07E-02	4.06E-02	-34.8	-22.8	-4.2	25.5	-34.6	-20.2	-3.7	22.3
SS	DC	200	3	9.65E-02	7.07E-02	14.7	-6.5	-2.1	22.3	15.4	-3.2	-1.0	20.6
SS	DC	200	10	3.38E-01	2.21E-01	-4.1	-8.2	-8.1	8.6	-1.0	-3.3	-3.3	3.4
WS	DC	67	3	2.00E-02	8.52E-03	0.0	-24.0	-0.9	27.1	0.0	-21.3	-0.8	23.7
WS	DC	67	10	5.26E-02	3.65E-02	14.1	8.3	1.4	14.7	14.8	9.5	1.6	14.8
WS	DC	67	30	1.50E-01	9.25E-02	3.8	4.5	1.9	4.5	4.0	4.3	2.0	4.9
SA	DC	67	3	8.08E-02	5.65E-02	-32.6	-32.7	-8.3	39.2	-27.8	-27.9	-7.1	32.5
SA	DC	67	10	2.32E-01	2.10E-01	-2.3	-6.1	-5.7	6.2	0.5	-3.4	-3.2	3.8
SA	DC	67	30	1.98E-01	1.85E-01	9.7	9.4	7.8	9.1	12.1	11.9	9.9	11.3
SD	DC	67	3	8.50E-02	6.76E-02	-4.1	-3.3	-1.0	3.3	-2.3	-2.1	-0.6	2.1
SD	DC	67	10	1.11E-01	8.55E-02	-5.1	-3.8	-1.5	3.9	-1.8	-1.5	-0.6	1.5
SD	DC	67	30	1.17E-01	9.20E-02	-3.9	-2.2	-0.9	2.3	0.2	0.6	0.2	0.6
SS	BT	20	10	9.63E-02	6.77E-02	-2.7	-3.0	-0.9	3.0	-1.7	-1.9	-0.6	1.9
SS	BT	20	33	1.16E-01	9.60E-02	-0.2	-0.7	-0.3	1.1	1.2	0.8	0.3	1.1
SS	BT	20	100	1.11E-01	9.34E-02	2.6	1.6	0.7	2.5	3.6	2.9	1.2	2.8
SS	BT	67	3	6.36E-02	4.54E-02	0.6	-4.0	-0.8	4.6	1.2	-2.9	-0.6	4.3
SS	BT	67	10	1.81E-01	1.19E-01	-3.6	-4.7	-2.5	4.8	-2.5	-3.1	-1.7	3.2
SS	BT	67	30	2.11E-01	1.70E-01	0.1	-0.7	-0.5	1.5	1.5	0.9	0.7	1.5
SS	BT	100	2	4.90E-02	3.19E-02	6.5	-3.2	-0.5	9.8	6.5	-2.3	-0.3	8.9
SS	BT	200	3	1.22E-01	6.82E-02	-31.2	-29.3	-9.0	34.0	-25.3	-24.1	-7.4	27.1
SS	BT	200	10	3.47E-01	2.16E-01	-3.5	-5.5	-5.4	5.7	-2.3	-3.5	-3.4	3.5
WS	BT	67	3	2.00E-02	6.19E-03	0.0	-9.6	-0.3	10.0	0.0	-8.4	-0.2	8.7
WS	BT	67	10	5.42E-02	3.48E-02	-14.1	-8.9	-1.4	9.3	-13.2	-8.2	-1.3	8.5
WS	BT	67	30	1.46E-01	8.80E-02	-2.0	-2.3	-0.9	2.4	-2.5	-2.8	-1.1	2.9

(continued)

Table 41 (continued) - 3

Test Env	Problem (a) Mix	NOx	C/N	Standard Conc (ppm) Maximum	Average	--- RADM-M vs RADM (b) --- Max. %Chg.	- Average - %Chg.	%/Max	% Fit	--- RADM-P vs RADM (b) --- Max. %Chg.	- Average - %Chg.	%/Max	% Fit
SA	BT	67	3	5.95E-02	4.00E-02	-17.0	-19.1	-3.4	21.1	-15.4	-17.0	-3.0	18.6
SA	BT	67	10	2.33E-01	1.98E-01	-2.3	-5.8	-5.1	5.9	-0.9	-4.6	-4.1	4.7
SA	BT	67	30	2.23E-01	2.07E-01	6.9	5.8	5.4	5.8	7.9	6.8	6.3	6.7
SD	BT	67	3	8.37E-02	6.62E-02	-2.2	-1.8	-0.5	1.8	-1.4	-1.2	-0.4	1.2
SD	BT	67	10	1.10E-01	8.45E-02	-2.8	-2.2	-0.8	2.2	-1.1	-1.0	-0.4	1.0
SD	BT	67	30	1.24E-01	9.56E-02	-2.3	-1.3	-0.6	1.4	0.0	0.2	0.1	0.2

(a) See Footnote (a) in Table 37 for a description of the notation used to indicate the test problems.

(b) See Section 6.2 for a discussions of the specific measures of differences between the mechanisms.

Table 42. Results of Sensitivity Test Calculations of Urban H_2O_2 Formation Using the Recommended Modified (RADM-M) and the Recommended Modified Parameter (RADM-P) Mechanisms, Relative to the March 1988 RADM Mechanism as the Standard

Test	Problem (a)			Standard Conc (ppm)		--- RADM-M vs RADM (b) ---				--- RADM-P vs RADM (b) ---			
Env	Mix	NOx	C/N	Maximum	Average	Max. %Chg.	- Average - %Chg.	%/Max	% Fit	Max. %Chg.	- Average - %Chg.	%/Max	% Fit
SS	AC	20	10	2.62E-03	1.86E-03	-6.1	-8.1	-1.3	8.4	-5.5	-7.8	-1.2	8.0
SS	AC	20	33	5.45E-03	3.86E-03	-5.0	-6.4	-2.1	6.7	-6.0	-6.7	-2.2	6.9
SS	AC	20	100	1.17E-02	8.16E-03	-2.3	-3.8	-2.6	4.0	-3.8	-5.0	-3.4	5.1
SS	AC	67	3	1.94E-03	9.12E-04	-4.8	-10.8	-0.8	11.3	-3.6	-9.3	-0.7	9.6
SS	AC	67	10	4.41E-03	3.12E-03	-11.3	-13.7	-3.6	14.7	-9.8	-12.7	-3.3	13.6
SS	AC	67	30	1.22E-02	8.56E-03	-5.7	-7.3	-5.2	7.7	-7.5	-8.4	-6.0	8.8
SS	AC	100	2	1.77E-03	7.61E-04	-12.6	-13.9	-0.9	14.9	-12.5	-12.9	-0.8	13.7
SS	AC	200	3	3.42E-03	1.57E-03	-18.7	-29.1	-3.8	33.6	-16.2	-23.0	-3.0	25.6
SS	AC	200	10	8.35E-03	5.90E-03	-15.0	-16.9	-8.3	18.5	-12.3	-15.4	-7.6	16.6
WS	AC	67	3	1.80E-07	2.92E-08	-81.9	-64.8	0.0	97.0	-80.5	-65.2	0.0	97.6
WS	AC	67	10	1.06E-03	6.27E-04	-27.7	-33.0	-1.7	39.4	-29.2	-33.8	-1.8	40.6
WS	AC	67	30	4.26E-03	3.03E-03	-11.1	-12.8	-3.2	13.7	-13.7	-15.5	-3.9	16.8
SA	AC	67	3	2.19E-07	9.15E-08	-77.4	-58.9	0.0	83.9	-75.6	-54.5	0.0	75.3
SA	AC	67	10	1.56E-03	1.08E-03	-32.8	-44.7	-4.0	57.2	-29.7	-42.0	-3.8	52.9
SA	AC	67	30	1.48E-02	1.20E-02	-16.1	-15.3	-15.3	16.6	-16.2	-15.2	-15.2	16.4
SD	AC	67	3	1.74E-03	1.03E-03	-7.5	-7.2	-0.6	7.4	-5.8	-6.5	-0.6	6.8
SD	AC	67	10	3.76E-03	2.29E-03	-8.2	-8.0	-1.5	8.3	-6.5	-7.2	-1.4	7.4
SD	AC	67	30	7.41E-03	4.67E-03	-6.9	-6.4	-2.5	6.7	-5.8	-6.1	-2.4	6.3
SS	DC	20	10	2.65E-03	1.89E-03	-7.5	-9.1	-1.4	9.5	-7.5	-9.4	-1.5	9.8
SS	DC	20	33	5.37E-03	3.81E-03	-5.5	-7.4	-2.3	7.7	-7.0	-7.6	-2.4	7.9
SS	DC	20	100	1.10E-02	7.68E-03	-3.0	-4.7	-3.0	4.9	-4.7	-5.8	-3.7	6.0
SS	DC	67	3	1.98E-03	9.28E-04	-7.1	-12.7	-1.0	13.5	-5.5	-11.1	-0.9	11.7
SS	DC	67	10	4.45E-03	3.19E-03	-13.3	-15.6	-4.2	16.9	-11.1	-14.4	-3.8	15.5

(continued)

Table 42 (continued) - 2

Test Env	Problem (a) Mix	NOx	C/N	Standard Conc (ppm) Maximum	Average	--- RADM-M vs RADM (b) --- Max. %Chg.	- Average - %Chg.	%/Max	% Fit	--- RADM-P vs RADM (b) --- Max. %Chg.	- Average - %Chg.	%/Max	% Fit
SS	DC	67	30	1.18E-02	8.32E-03	-6.5	-8.5	-5.9	9.0	-8.8	-9.8	-6.8	10.3
SS	DC	100	2	1.85E-03	8.11E-04	-16.8	-19.5	-1.3	21.4	-17.1	-18.8	-1.3	20.6
SS	DC	200	3	3.47E-03	1.60E-03	-20.9	-30.9	-4.1	36.1	-18.3	-23.6	-3.1	26.5
SS	DC	200	10	8.46E-03	6.08E-03	-17.9	-19.4	-9.8	21.5	-14.5	-17.4	-8.8	19.0
WS	DC	67	3	3.08E-07	3.89E-08	-85.3	-72.9	0.0	115.8	-89.3	-73.7	0.0	117.9
WS	DC	67	10	1.08E-03	6.55E-04	-28.8	-33.5	-1.8	40.1	-30.8	-34.9	-1.9	42.1
WS	DC	67	30	4.09E-03	2.96E-03	-13.3	-14.9	-3.7	16.1	-16.9	-18.6	-4.6	20.4
SA	DC	67	3	2.59E-07	1.02E-07	-81.9	-67.2	0.0	101.7	-81.4	-64.6	0.0	96.0
SA	DC	67	10	1.67E-03	1.22E-03	-40.6	-53.8	-5.5	73.3	-36.9	-51.1	-5.2	68.3
SA	DC	67	30	1.46E-02	1.18E-02	-19.7	-18.5	-18.1	20.3	-19.6	-18.2	-17.8	19.9
SD	DC	67	3	1.77E-03	1.05E-03	-9.1	-8.3	-0.7	8.7	-7.5	-7.8	-0.7	8.1
SD	DC	67	10	3.80E-03	2.32E-03	-9.5	-9.1	-1.8	9.5	-7.7	-8.0	-1.6	8.4
SD	DC	67	30	7.36E-03	4.66E-03	-8.4	-7.7	-3.0	8.0	-7.0	-7.2	-2.8	7.4
SS	BT	20	10	2.44E-03	1.65E-03	-4.5	-6.2	-0.9	6.4	-4.5	-6.2	-0.9	6.4
SS	BT	20	33	4.96E-03	3.51E-03	-4.1	-5.0	-1.5	5.2	-4.4	-4.8	-1.4	4.9
SS	BT	20	100	1.09E-02	7.64E-03	-2.4	-3.6	-2.3	3.7	-2.7	-3.4	-2.2	3.5
SS	BT	67	3	1.90E-03	8.08E-04	-2.3	-12.1	-0.8	12.6	-2.5	-11.3	-0.8	11.8
SS	BT	67	10	3.96E-03	2.54E-03	-8.3	-11.8	-2.5	12.5	-7.8	-11.7	-2.5	12.4
SS	BT	67	30	1.09E-02	7.62E-03	-5.2	-6.4	-4.1	6.6	-5.9	-6.4	-4.1	6.7
SS	BT	100	2	1.60E-03	6.67E-04	0.7	-8.3	-0.5	10.1	0.9	-7.4	-0.4	8.9
SS	BT	200	3	2.83E-03	8.98E-04	-25.1	-65.2	-4.9	94.8	-22.3	-63.4	-4.7	90.8
SS	BT	200	10	7.29E-03	4.47E-03	-11.7	-16.2	-6.0	17.6	-10.1	-15.2	-5.7	16.4
WS	BT	67	3	1.71E-08	6.31E-09	-42.6	-34.1	0.0	41.3	-31.7	-29.0	0.0	34.6
WS	BT	67	10	7.41E-04	3.57E-04	-12.0	-16.5	-0.5	17.9	-12.7	-16.9	-0.5	18.4
WS	BT	67	30	3.40E-03	2.23E-03	-4.1	-6.2	-1.1	6.4	-4.6	-7.0	-1.3	7.3

(continued)

Table 42 (continued) - 3

Test Problem (a)				Standard Conc (ppm)		--- RADMM-M vs RADM (b) ---				--- RADM-P vs RADM (b) ---			
Env	Mix	NOx	C/N	Maximum	Average	Max. %Chg.	- Average - %Chg.	%/Max	% Fit	Max. %Chg.	- Average - %Chg.	%/Max	% Fit
SA	BT	67	3	4.36E-08	3.47E-08	-30.7	-37.4	0.0	46.2	-30.2	-36.0	0.0	44.1
SA	BT	67	10	1.14E-03	6.21E-04	-17.5	-34.7	-1.8	41.7	-16.5	-34.8	-1.8	41.8
SA	BT	67	30	1.20E-02	9.78E-03	-13.5	-13.5	-11.0	14.4	-13.2	-13.0	-10.6	13.9
SD	BT	67	3	1.67E-03	9.66E-04	-6.0	-5.4	-0.4	5.5	-5.2	-5.2	-0.4	5.4
SD	BT	67	10	3.54E-03	2.11E-03	-6.0	-5.6	-1.0	5.8	-5.0	-5.3	-0.9	5.4
SD	BT	67	30	6.96E-03	4.31E-03	-5.0	-4.8	-1.7	4.9	-4.1	-4.4	-1.6	4.5

(a) See Footnote (a) in Table 37 for a description of the notation used to indicate the test problems.

(b) See Section 6.2 for a discussions of the specific measures of differences between the mechanisms.

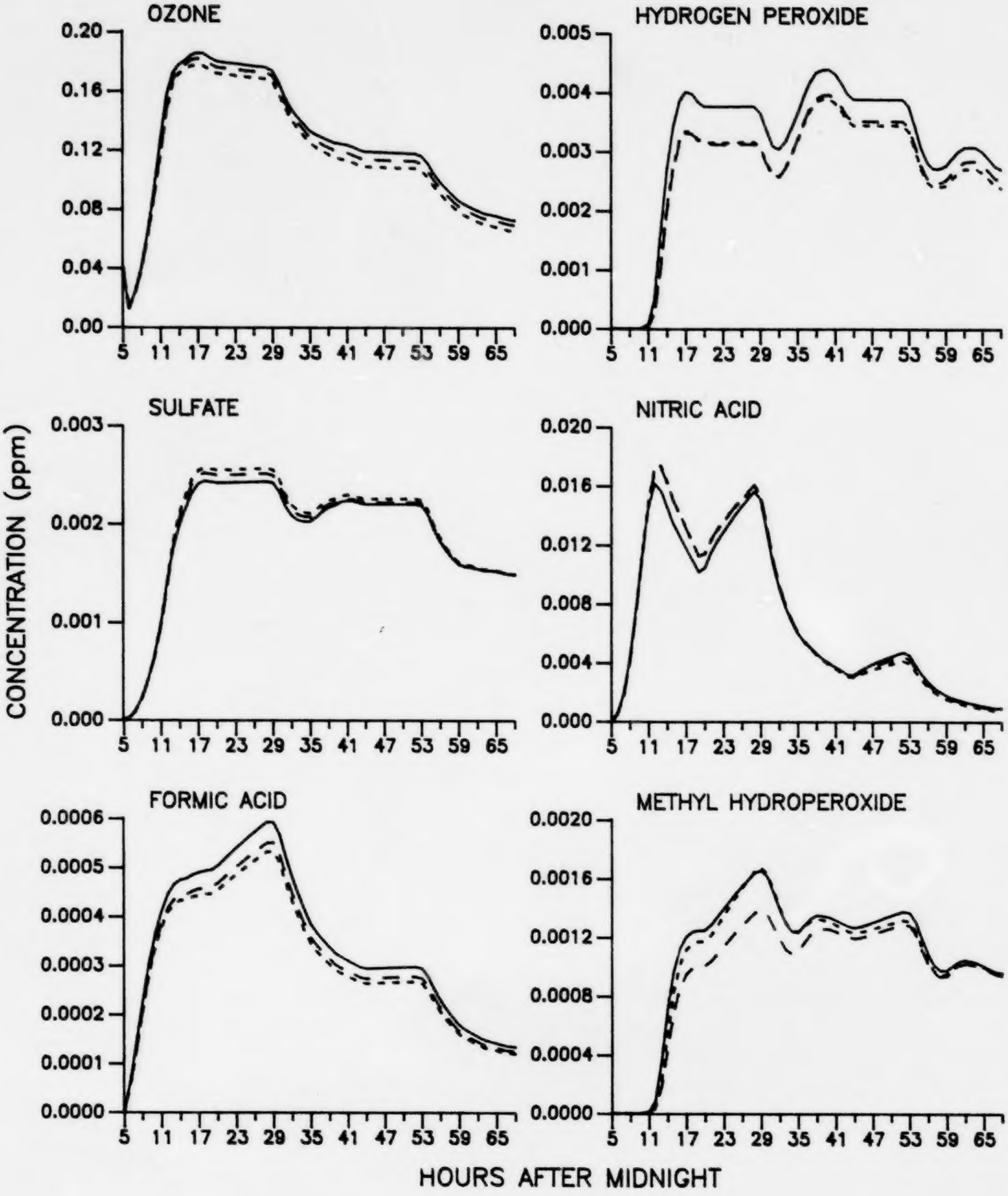

Figure 89. Concentration-Time Plots for Selected Species Calculated Using the RADM, RADM-M, and RADM-P Mechanisms for the Summer Surface Static Urban Test Problem with Initial NO_x of 67 ppb and a ROG/NO_x Ratio of 10.

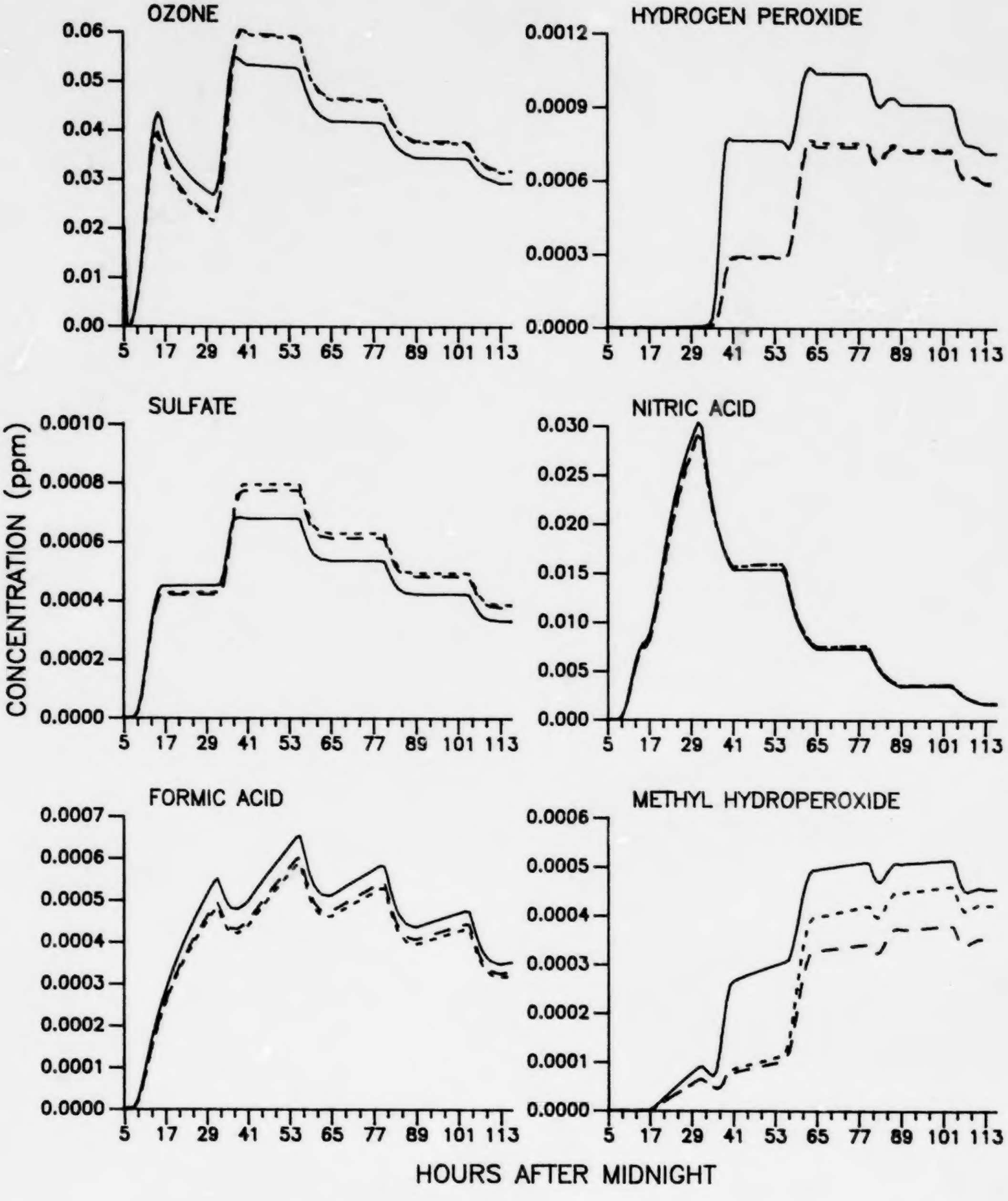

Figure 90. Concentration-Time Plots for Selected Species Calculated Using the RADM, RADM-M, and RADM-P Mechanisms for the Winter Surface Static Urban Test Problem with Initial NO_x of 67 ppb and a ROG/NO_x Ratio of 10.

where the predictions are most different for the other peroxides and the acid species. On the other hand, the modifications have much less of a consistent effect on predictions of nitric acid and sulfate, with positive as well as negative changes, and fewer cases with relatively large differences being observed.

As expected, the differences between the two versions of the recommended modified mechanisms are much less than the differences between the modified and the March 1988 mechanisms. The differences between the modified mechanisms in predictions of ozone, H_2O_2, sulfate, HNO_3, and the organic acids are generally minor, with discrepancies only being observed in predictions of peroxy or acid species in a few cases where their calculated concentrations are very low. There are some cases of non-negligible differences in predictions of the organic hydroperoxide species, peroxyacetic acid, and PAN. Since PAN is not represented explicitly in any of these mechanisms, and since there are no chamber data available to test predictions of organic hydroperoxide or acid species, there is no way of determining which of the two modified mechanisms is the more reliable in their predictions of these species. In view of the many chemical uncertainties in the mechanisms regarding reactions forming these species and the sensitivity of predictions to relatively small differences in the mechanisms, predictions for these species in regional model simulations should be viewed as highly uncertain.

These results indicate that the recommended modifications to the RADM mechanism may have a non-negligible impact on predictions of species of interest in regional modeling applications. Because the modified versions perform somewhat better in simulating the aromatic-NO_x-air chamber runs, predictions obtained with these mechanisms probably should be considered to be somewhat more reliable than those obtained with the March 1988 mechanism. On the other hand, it probably does not matter which of the two modified versions is adopted, except that the RADM-M version employs fewer species and thus is more efficient. The magnitude of the differences between the modified and the March 1988 mechanisms also gives us an approximate indication of the sensitivity of regional model predictions to the uncertain aspects of aromatics photooxidation chemistry, since that is the major aspect of the mechanism that was changed.

7. SUMMARY AND CONCLUSIONS

One of the more significant advances in regional acid deposition modeling in the 1980s has been the incorporation of gas phase chemical mechanisms that predict the formation of sulfate, nitric acid, ozone, organic nitrates, hydrogen peroxide, organic peroxide, and organic acids from emissions of SO_2, NO_x, and reactive organic gases (ROG). The gas-phase chemical mechanism is a particularly important component of regional acid deposition models because it controls the rates of radical and oxidant generation, which in turn controls the production rates of acidic species. The chemical mechanism is also the major potential source of nonlinearity in the relationships between acid deposition and emissions of SO_2 and NO_x. As such, it is one of the major reasons why control strategies for acid deposition cannot rely on analyses based on simple rollback, but require use of complex models such as RADM. Thus, it is particularly important that the gas-phase chemical mechanism used in such models be evaluated as comprehensively as possible, to assure that it represents the current state-of-the-science of atmospheric chemistry. In addition, since the RADM model is to be used for policy development, its major components such as the gas-phase chemical mechanism must be accepted as representing the best science by not only the technical community but by the public as a whole.

Peer review is the method presently used to assure the quality of scientific research. The essence of peer review is that the research be evaluated by experts in the field other than those who developed the research being considered. It is required before results are published in the most reputable scientific journals, and agencies such as the EPA periodically have peer review panels to assure the continuing quality of the research they support. Therefore, peer review is clearly an appropriate means to assure the quality and credibility of important components of the RADM model such as the gas-phase chemical mechanism. However, peer review as it is normally practiced does not lend itself to in-depth assessment of highly complex model components such as gas-phase atmospheric reaction mechanisms. Journal space is much too limited to permit in-depth discussion of the many components involved in such mechanisms, and thus they cannot be evaluated adequately by the reviewers. Peer review panels of agency research programs generally have relatively limited time to assess very broad areas of research and usually cannot be expected to carry out in-depth analyses of individual components. The study described in this report, however, is an in-depth peer review of an important model component -- the RADM gas-phase mechanism. The authors of this report have been involved for years in the development and evaluation of gas-phase mechanisms for use in airshed models, but had not participated in the development of the RADM gas-phase mechanism. Because of the many aspects involved in evaluating a chemical mechanism, including the need to test it against the results of over 500 environmental chamber experiments, this review took more than a year.

The results of this review indicated that for the most part the RADM mechanism represents the state of our present knowledge of atmospheric chemistry and performs as well as reasonably can be expected in simulating the results of environmental chamber experiments. However, the state of knowledge of atmospheric chemistry is constantly advancing, and over the course of this study, several sets of modifications to the RADM mechanism and its interface to the emissions inventory were identified and recommended. These recommendations and areas of suggested improvement are described in detail in the body of this report and are briefly summarized below. These recommendations do not involve major changes to the basic nature of the mechanism as conceived by its developers, but instead should be considered as refinements and enhancements to an already high quality product. However, we believe that the implementation of these recommendations will result in improvements in representation of several important aspects of the atmospheric chemistry of organic compounds.

As stated in the preface to this report, the developers of the RADM model cooperated fully with this review and actively participated in some of its elements. The principal developer of the RADM gas-phase mechanism kept us fully informed of the exact status of the mechanism as it underwent changes, evaluated our recommendations, and worked directly with us in those aspects of this evaluation where his participation proved most valuable. He and other members of the RADM team actively solicited our participation in the development of the emissions processing and aggregation methods, re-directing our efforts to this critical aspect of the implementation of the mechanism in the model. Without the high degree of interest and cooperation by the RADM team, this program could not have been nearly as successful as we believe it was. Most of the major recommendations developed during this evaluation were accepted for implementation in the RADM-II mechanism.

It should be emphasized that although we believe that the resulting RADM gas-phase mechanism and its associated emissions processing system represents the current state-of-the-science, this does not mean that there are no significant areas of uncertainty. There remain many important aspects of the gas-phase atmospheric reaction mechanisms of organics which are unknown and where basic laboratory research is still needed before reliable mechanisms representing them can be developed. The available environmental chamber data are not suitable for testing many critical aspects of the mechanism, particularly those of the peroxy and acid species which are of concern in acid deposition models. In addition, the need to represent the highly complex chemistry of the many hundreds of organic compounds emitted into the atmosphere with mechanisms using only limited numbers of species and reactions introduces uncertainties in model predictions whose effects are not fully understood. This is in addition to the uncertainties in the emissions inventories themselves, which -- particularly for biogenic emissions -- often dwarf the effects of any uncertainties in the chemical mechanism. Thus, users of regional models, even those such as RADM that contain the most up-to-date, thoroughly peer-reviewed gas-phase chemical mechanisms, must view their predictions with a certain amount of skepticism and with an appreciation of the magnitudes of the various uncertainties involved.

The scope of work for the study consisted of four major tasks. The research findings from each task are summarized below. Following that, we briefly summarize our recommendations for future work.

7.1 Evaluation of Kinetic and Mechanistic Parameters

At the time this study was initiated, the RADM mechanism was in a state of transition between the RADM-I and RADM-II versions of the mechanism. An initial review of the preliminary RADM-II mechanism was performed, and a number of changes in both the inorganic and organic reactions in the mechanism were recommended. A procedure was developed for determining rate constants and products for the reactions of lumped organic species based on the detailed speciation of the national emissions inventory. Many of these initial recommendations were adopted and incorporated into the March 1988 version of the RADM-II mechanism (referred to as the RADM). The comprehensive evaluation was carried out for this version of the RADM mechanism.

On the basis of testing the RADM mechanism against environmental chamber data, two alternate versions of the mechanism were developed and fully evaluated. The first alternate mechanism, referred to as the recommended modified RADM mechanism (RADM-M), offers the following features:

- Changes in the representation of the unknown aspects of the aromatic photooxidation mechanism which improve its performance in simulating chamber data and reduce the number of species needed;

- A more condensed representation of the >C3 alkanes which has comparable performance with fewer species;

- Some changes in rate constant and product yield parameters for lumped species to correspond more closely with the most recent analysis of national VOC emissions data;

- Correction of an error in the methylglyoxal quantum yields which resulted in overestimation of its photolysis rates;

- Addition of several reactions omitted from the NO_3 + alkene reaction system; and

- Revised representation of the reactions of nitrophenols which improves the chemical fidelity of the reactions.

Because implementation of the RADM mechanism was almost completed by the time the RADM-M was developed and evaluated, a second alternate mechanism was proposed that involved primarily changes in rate constants and product yields. This version is referred to as the recommended modified parameter version of the RADM (RADM-P). This incorporates:

- An improved aromatic oxidation mechanism which performs approximately as well as the RADM-M mechanism, but uses the larger number of species employed in the RADM mechanism;
- Some changes in rate constant and product yield parameters for lumped species to correspond more closely with the most recent analysis of national VOC emissions data;
- Reduced methylglyoxal quantum yields; and
- Addition of several reactions omitted from the NO_3 + alkene reaction system.

The RADM developers have adopted the modified parameter version of the mechanism and this version is now being implemented into the RADM transport model (Stockwell, private communication, 1989).

7.2 Development of the Linkage Between the VOC Emissions Inventory and the RADM Mechanism

In recent years, modelers have begun to appreciate fully the importance of carefully interfacing a chemical mechanism with VOC emission inventories. At the start of this program, only a very preliminary emission inventory interface had been developed for the RADM mechanism. At the request of the RADM developers, a large effort in this program was directed towards developing emissions aggregation procedures for use with the RADM model. A new two-step emissions aggregation system was developed for this purpose. The first step involved the aggregation of the detailed VOC emissions data into a 32-class mechanism-independent VOC grouping system based on reactivity and relative contributions to total emissions. The second step involved further aggregating these emissions groups into the more limited number of VOC species used in the RADM mechanism. This effort was carried out jointly as part of this program and as part of the RADM development effort.

The assignment of species in the emissions groups to the surrogate species used in the RADM mechanism involves use of a new reactivity weighing scheme. This scheme allows VOCs reacting at different rates, but with similar mechanisms, to be represented by the same model species. This is based on estimation of how much of the VOCs and the model surrogate undergo chemical reaction in the model simulation, and adjusting the amounts of the latter so they are approximately equal. Although approximate, the use of reactivity weighing is preferable to the alternatives of either ignoring compounds of low but non-negligible reactivity, or representing them by much more reactive model surrogates.

Another feature of this aggregation system is the use of detailed emissions data to derive the rate constants and product yield coefficients of lumped species in the mechanism based on those for the aggregate of compounds they will be representing. A software system recently developed as part of another program and the 1985 NAPAP anthropogenic emissions inventory were used for this purpose. This is considered a significant advancement that optimizes the linkage between the chemical mechanism and the emissions inventory.

7.3 Mechanism Evaluation Against Chamber Data

An important step in the model design and evaluation process is evaluation of the gas phase chemistry against environmental chamber data. The gas phase chemistry module is one of the few modules in the atmospheric modeling system that can be independently tested against experimental data. The present chamber data base, however, is not suitable for testing all aspects of the mechanism, particularly those involving predictions of acid or peroxy species or simulations of very low NO_x conditions that prevail in rural regions. The present chamber data base is best suited for testing the mechanism's predictions of ozone formation and rates of NO_x oxidation under urban conditions. To a lesser extent, the data can be used to test the mechanisms' ability to simulate formation of peroxyacetyl nitrate and formaldehyde under urban conditions. Simulation of urban-like conditions is important because urban areas represent the major sources of the pollutants which are transported to remote areas with sensitive receptors. Ozone, NO_x, PAN, and formaldehyde play critical roles in long-range transport.

It is also important to recognize that even though the present data base does not allow for direct evaluation of mechanisms' predictions for sulfuric acid and nitric acid, the testing protocol provides some indirect evidence for evaluation of performance for these species. First, accurate prediction of the rate of NO_x oxidation and ozone formation necessitate accurate predictions of OH radical concentrations. According to present theory, OH is the sole oxidant converting SO_2 to sulfuric acid and NO_2 to nitric acid in the daylight hours. Second, since NO_x is primarily oxidized to nitric acid or PAN, the evaluation results for PAN provide some information on whether the mechanism is oxidizing NO_x to the correct products. In general, if the model cannot at least simulate ozone and NO_x correctly in one-day smog chamber experiments, it certainly cannot be trusted to simulate accurately concentrations of these and other species under multi-day, long-range transport conditions.

A comprehensive evaluation of the RADM mechanism and the recommended modified versions of RADM mechanism against available environmental chamber data was performed in this study. The approach involved simulating a large number (~550) of experiments from four different chambers and statistically evaluating the mechanisms' performance. Experimental data collected in the following chambers was used for the evaluation:

- The SAPRC evacuable indoor chamber (EC),
- The SAPRC indoor Teflon chamber (ITC),
- The SAPRC outdoor Teflon chamber (OTC), and
- The University of North Carolina outdoor chamber (UNC).

Prior to conducting the evaluation, the procedures for characterizing chamber dependent processes were reviewed and updated where new data were available. A consistent set of procedures for representing these was used for all experiments from a given chamber. Organic compounds in experiments employing complex mixtures of organics were aggregated using the types of procedures which will be employed when the mechanism is used in RADM simulations. Thus there was no run-to-run adjust of chamber-dependent or mechanistic parameters employed in the evaluation protocol.

The major findings from the evaluation of the RADM, RADM-M, and RADM-P mechanisms against environmental chamber data are as follows.

- Testing against experiments using complex organic mixtures, that are surrogates for atmospheric VOC mixtures, showed that the RADM mechanism performs as well as other chemically up-to-date mechanisms (Lurmann et al., 1987; Gery et al., 1988; Carter, 1988). The mechanism is able to predict the maximum ozone and NO_x oxidation rate with a small bias and a mean error of 20% on the average. Even though the good performance on complex mixtures can in some cases be a result of partially compensating errors in the mechanism, the mechanism does provide ozone and NO_x oxidation rate predictions that are consistent with the available data. The performance of the two alternative versions of the RADM are comparable to that for the RADM on complex mixture simulations.

- Testing of the RADM mechanism against single organic-NO_x-air experimental data produced mixed results. With a few notable exceptions, the RADM mechanism performed as well as can reasonably be expected against experiments with the species for which the mechanism was designed. The areas where the predictions of the mechanism can be considered to be comparable to those of other current mechanism are as follows:
    - The predictions for experiments with formaldehyde and propene were reasonably good.
    - The predictions for acetaldehyde and methyl ethyl ketone systematically underpredicted ozone and NO_x oxidation rates, but there are too few experiments to draw definitive conclusions on the adequacy of this portion of the mechanism.
    - The mechanism has a bias towards underprediction of reactivity in ethene runs. This is due to the omission of a reaction which we found to be unimportant under conditions where the model will be applied. If this reaction is added to the mechanism, its performance in simulating these experiments is acceptable.
    - The mean error in the ozone predictions in the 1-butene runs are greater than is the case for propene, but the performance is considered acceptable.
    - The predictions for a limited number of trans-2-butene are poor. However, there are too few of these experiments to adequately test this portion of the mechanism.

- The mechanism had large errors in simulating results of alkane runs. This is not necessarily due to any failure in the mechanism, but to the extreme sensitivity of simulations of alkane-NO_x-air experiments to chamber effects which tend to vary unpredictably from run to run. Compared to the errors, the biases in the predictions of ozone and NO oxidation rates were relatively low.

The performance of the RADM-M and RADM-P mechanisms in simulating these experiments was similar. The only difference was that the RADM-M mechanism performed slightly worse in simulating some of the higher alkane runs because of its more condensed representation of these compounds.

- The performance of the RADM mechanism in tests against single aromatic species was not as good as that reported for other chemically up-to-date mechanisms. The testing showed that the aromatic reactions in the RADM mechanism have a bias towards overpredicting ozone and NO_x oxidation rates for the more slowly reacting compounds and underpredicting those same characteristics for the faster reacting compounds. This results in fairly large errors in ozone predictions on the average for toluene, xylenes, and mesitylene.

- The RADM-M and RADM-P mechanisms were designed to improve the performance of the mechanism in simulating the toluene, xylene, and mesitylene runs. This design objective was achieved. The performance of these mechanisms in simulating the results of aromatic runs was comparable to other current mechanisms.

- Because of the importance of biogenic emissions in regional model applications, the RADM mechanism has a separate species to represent isoprene. However, the performance of this mechanism in simulating isoprene experiments was not as good as those for some other alkenes. This is probably because the mechanism assumes that isoprene reacts to form the same photooxidation products that are formed when propene reacts. Improving the performance of the RADM mechanism in this regard would probably require adding additional species to the mechanism to represent these products. Research in this area is still underway at our laboratories, and thus no modifications in this area are recommended at the present time. The RADM-M and RADM-P therefore have the same isoprene mechanism as RADM and thus perform the same in simulating these experiments.

- On the other hand, the RADM mechanism performed surprisingly well in simulations of the limited number of α-pinene runs, despite the fact that it does not represent this compound explicitly. The RADM-M and RADM-P mechanisms perform similarly.

- The RADM mechanism's performance for species other than those for which it was designed, such as propionaldehyde, 1-hexene, benzene, naphthalenes, and tetralin was generally poor. Much better simulations of experiments employing those compounds can be obtained in mechanisms containing species designed to represent them. However, the level of performance of the RADM mechanism in this regard is certainly comparable to what one would expect from other condensed mechanisms designed for use in Eulerian atmospheric models. Satisfactory performance in simulating these compounds would probably require adding new species to the mechanism. This is probably not worthwhile given the relative contributions of these compounds to overall VOC reactivity in most regional model applications.

- The RADM, RADM-M, and RADM-P mechanisms do not predict maximum formaldehyde concentrations as accurately as they predict maximum ozone concentrations or NO oxidation rates. They tend to overpredict formaldehyde yields in alkene and alkane experiments and underpredict formaldehyde yields in experiments with single aromatic compounds and organic mixtures. The mean errors associated with the formaldehyde predictions are fairly large in alkane, aromatic, and organic mixture experiments. While one would like to see better formaldehyde predictions, this does not necessarily present a problem with respect to using the mechanisms for long-range transport and acid deposition modeling, especially given the uncertainty of the formaldehyde measurements.

- The mechanism consistently overpredicts measured PAN concentrations. This positive bias is expected since the species PAN is used in the mechanism to represent PAN plus numerous analogous organic nitrates. However, the magnitude of the bias, especially in the surrogate mixture runs, suggests the mechanism overpredicts the PAN and analogous species concentrations. This is of some concern for regional acid deposition modeling because the model may underpredict nitric acid in the first few 100 km downwind of sources (i.e., if NO_x is preferentially oxidized to PAN rather than HNO_3) and overpredict the distances for which nitrogen species are transported (since PAN is the long range transport product of NO_x emissions).

- Lastly, it is very unlikely that mechanisms could achieve the high level of performance on ozone and NO_x oxidation rates found in complex mixture runs without accurately simulating the production and destruction of the OH radical. These results indirectly suggest that the mechanisms are able to reasonably predict the OH concentrations and, therefore, the probable yields of nitric acid and sulfuric acid in daylight hours.

7.4 Sensitivity Testing of Alternate Mechanistic Assumption

Given the nonlinear couplings in mechanisms, it is often difficult to predict a-priori the conditions and species for which changes in mechanistic assumptions will have large effects. For this reason, it is particularly important in evaluating alternative mechanistic assumptions to make sure the testing is performed over a wide range of conditions. Testing of alternative mechanistic assumptions employing an insufficiently comprehensive range of conditions can often lead to misleading conclusions. Unfortunately, such testing can not rely on environmental chamber data alone because the chamber data do not cover all the species and conditions of interest for acid deposition modeling. To overcome this problem, a large number (~90) of test problems were developed in this program to represent a wide range of chemical conditions for purposes of evaluating selected mechanistic assumptions. Considerable thought and analysis went into the design of the test problems, and we believe they will be as useful in future mechanism evaluation programs as they have been in this program.

Based on our review of the kinetic and mechanistic assumptions employed in the RADM mechanism and the results of the evaluation against chamber data, a limited number of alternative chemical assumptions were identified for evaluation in sensitivity studies. The topics for investigation included:

- The effects of various levels of condensation of the peroxy-peroxy radical reactions in the RADM mechanism;

- The effects of condensation of the alkane reactions in the RADM-M mechanism; and

- The effects of the modifications incorporated into the RADM-M and RADM-P mechanisms on the predictions of species of interest in regional acid deposition models.

Testing was conducted to compare the RADM mechanism to an alternate version of the mechanism which included all possible peroxy-peroxy radical combinations. The results showed that even for hydrogen peroxide and organic peroxides, which are very sensitive to changes in the peroxy-peroxy radical reactions, the RADM mechanism's treatment of peroxy radicals is justified. Predicted concentrations of key species were almost identical for all test problems with the RADM mechanism and the detailed peroxy radical version of the RADM mechanism.

The method used to represent peroxy radical combinations in the RADM mechanism is clearly satisfactory, and no changes in this regard are recommended. However, tests were carried out to determine if a more condensed representation of peroxy-peroxy radical reactions could be used in the RADM model. The condensed representation did not yield predictions which agreed as closely with those obtained with the detailed radical mechanism, though the differences are probably not significant. The benefits of changing to the slightly more condensed peroxy-peroxy radical reactions scheme are not considered great enough to warrant the change.

Tests were carried out to determine if a more condensed representation of the reactions of alkanes could be employed in the RADM model. The results indicated there are no significant differences in model predictions if the two higher alkane classes in RADM are combined, provided the combined class has the appropriate mechanistic parameters. These results served as the basis for the representation of the alkanes in the recommended RADM-M mechanism.

Test calculations indicated that the versions of the RADM mechanism incorporating our recommended modifications (RADM-M and RADM-P) can in some cases be quite different from the original mechanism in predictions of species of interest in acid deposition models. The differences between the mechanisms tend to be the greatest in the simulations of urban conditions. These are due primarily to the recommended changes in the mechanisms for the aromatics. The modified mechanisms tended to predict slightly lower levels of ozone and in some cases significantly lower levels of peroxide or acid species under some conditions. On the other hand, the modifications had smaller effects on predictions of nitric acid or sulfate. This indicates that implementing the recommended changes in the mechanism might in some cases have non-negligible effects on results of regional model simulations.

The test calculations also indicate that the two recommended modified versions of the RADM mechanism are very close, but are not identical, to each other in their predictions of species of interest in regional acid deposition models. Their predictions of PAN and of the higher organic hydroperoxides and acids differed in some cases by 25% or more. Differences in predictions of PAN are expected because of different degrees of condensation in the two mechanisms -- PAN in RADM-M is used to represent the PAN analogues formed from the unknown aromatic photooxidation products, while RADM-P, like RADM, uses a separate species for these PAN analogues. In the case of the predictions of higher organic acids and hydroperoxides, the uncertainties concerning the rates and mechanisms of their formation are so great -- and the data suitable to test models for their predictions so inadequate -- that both mechanisms should probably be considered to be equally unreliable in this regard. Discrepancies on the order of 25% or even 50% are well within the uncertainty bounds for predictions of such species. Therefore, for all practical purposes the predictions of these two mechanisms can be considered to be essentially equivalent.

7.5 Recommendations

As indicated above, although we believe that the RADM gas-phase chemical mechanism, along with its emissions aggregation system, represents the current state-of-the-science, there remain significant uncertainties in this important model component. Therefore, continuing research is needed in areas related to its development and implementation. Our specific recommendations in this regard are given below. The longer term critical research needs will be discussed first, followed by a discussion of specific shorter-term research needs which became evident during the course of this program.

7.5.1 Longer Term Research Needs

The only way the gas-phase chemical mechanisms in airshed models can be tested in their entirety, but independently of the many other uncertainties in the models such as emissions, meteorology, etc., is by use of environmental chamber data. The presently available chamber data are suitable only for testing the ability of models to predict ozone formation and NO_x oxidation under the relatively high-NO_x conditions representative of the most polluted urban atmospheres. Even for this purpose, there are problems due to poorly characterized chamber effects. There is a critical need for chamber data suitable for testing mechanisms in the low-NO_x concentration regime important in regional and global models, and for testing their abilities to predict formation of peroxide and acidic species. Chamber wall effects are such that usable data of this type cannot be obtained using existing environmental chamber technology. This need can only be addressed by first carrying out research into new environmental chamber technologies and associated surface effects. This would require a significant commitment of resources. Unless such a commitment for long-term research is made, the present unsatisfactory situation will not change significantly.

There still remain many critical areas of uncertainties in our understanding of, and thus our ability to model, the gas-phase atmospheric chemistry of many classes of organics. The uncertainties associated with the chemistry of aromatics have been dwelt upon in "Recommendations" sections in reports such as this for at least a decade. The modifications we recommended to the RADM mechanism in this area are based on empirical curve-fits to chamber data which are largely outside the concentration regime even of urban conditions, and we have no way of knowing how accurately this largely empirical model will perform when extrapolated to ambient conditions. The situation with the higher alkanes only seems to be better because the present chamber data are unsuitable for indicating just how good or bad the present mechanisms really are. An additional area which is now recognized as being important is the mechanisms of the biogenic hydrocarbons. Recent work concerning isoprene indicates that its OH reaction mechanism is not as well understood as we once thought it was -- roughly 40% of the reaction routes are not accounted for by identified products. In addition, there are large and significant uncertainties in the mechanism for its reaction with ozone. Even less is known about the terpenes -- the fact that the RADM mechanism happens to be able to simulate the results of four α-pinene outdoor chamber experiments carried out within a one-month period is probably largely coincidental. It is unknown how well the model can simulate the reactions of other biogenically emitted species such as beta-pinene or other terpenes.

In some cases, important uncertainties can be addressed by applying presently available techniques to compounds which have not been adequately studied previously. An example of this concerns the non-isoprene biogenics, which is discussed in the next section. However, for compounds such as the aromatics, the higher alkanes, and even to some extent isoprene, we have probably approached the point where the experimental techniques traditionally used to study reaction mechanisms are unlikely to yield significant new information. It is clear that the aromatics and many other compounds of interest form products which cannot be quantitatively measured using present techniques. Many of these compounds appear to be highly labile and contribute significantly to the overall reactivities of the emitted organics. In the case of the higher alkanes, polyfunctional compounds are formed which probably do not remain in the gas phase. Until research laboratories interested in atmospheric reactions of organics have the type of equipment necessary to measure and study such compounds, significant further progress in this area is unlikely. For example, tandem MS equipment appears to be promising in this regard, but few research laboratories can afford such equipment, and those that have them apparently cannot afford to dedicate them to the long periods of time required for the types of fundamental research projects that are needed. Research into new types of equipment, and means of making them available for researchers for use in fundamental studies, is also needed. This is another area where significant new resources are needed if further progress is to be made.

The emissions inventories may not be as interesting scientifically as the subjects discussed above, but they probably represent the greatest area of uncertainty in the overall area of gas-phase chemistry in the models. Even if the gas-phase chemical mechanism were perfectly characterized, it would do us no good if we do not know the input rates of the species whose reactions are being modeled. The biogenic inventories are particularly uncertain; order-of-magnitude errors in the present inventories may well be the case. Until they are better characterized, it may well not be worth the effort to add new species in the model to better represent them. The anthropogenic emissions inventories also have significant uncertainties, particularly for the VOCs. If there are major errors in the anthropogenic inventory, it will not matter how accurate the mechanism is for the aromatics or other anthropogenic emissions. Improving the quality of these inventories may be a difficult and expensive process, but is is absolutely essential if airshed models are to be used for policy assessment purposes. This is an area which should be given top priority.

7.5.2 Shorter Term Needs

We believe that this program has resulted in an advance in the processing of emissions data for regional models. The aggregation of the huge detailed emissions data base into a manageable data set which can be used by a variety of models will permit for much more flexibility in using alternative chemical mechanisms and for carrying out model intercomparison studies. However, there is clearly need for further near-term work in this area. The first priority should be to improve the software presently used for processing the NAPAP emissions data bases. The software introduces artificial limits to the level of chemical accuracy and range of applicability in the emissions aggregation system; for example, the same aggregation process cannot be used for both the RADM and the widely-used Carbon Bond mechanism. In addition, some categories presently used in the VOC speciation source profiles are chemically ambiguous and need to be replaced by those which are not. Examples include "Mineral Spirits," which is not a compound but an uncharacterized mixture, and "C5 Olefins," which is a mixture of isomeric compounds with quite different reactivities. In some cases the speciation of the emissions sources may be highly uncertain. However, those responsible for compiling emissions profiles are in a better position to make estimates concerning the nature of these profiles than the chemical mechanism developers. These are not, strictly speaking, problems in the area of chemical mechanism development, but are areas where experts in atmospheric chemistry could well provide much needed guidance.

Another area where we believe this study has advanced the representation of VOC emissions in models is the use of model surrogates with parameters which are adjusted based on the set of compounds they represent. The RADM mechanism has been able to take advantage of some, but not all, of the recent advances in this area. Under funding for the California ARB, we developed software and procedures where mechanism parameters can be readily re-adjusted as emissions inventory change. However, at present the parameters in the RADM mechanism are fixed -- they were estimated based on the 1985 NAPAP anthropogenic inventory -- but cannot readily be changed if this inventory changes. It probably would not be too difficult to modify the RADM mechanism and the model software so that the parameters can be changed.

The representation of biogenically emitted alkenes is a particular concern in regional models. Although the RADM mechanism represents isoprene explicitly, its performance in simulating the chamber data is less than totally satisfactory. Probably it will be necessary to add new species to the model to represent isoprene's products satisfactorily. However, we were not able to complete our investigation of how best to represent isoprene in the mechanism within the time and funding limits of this program -- we are continuing work in this area under separate funding.

The terpenes are also important in the biogenic inventory, and research is needed on how best to represent them in the model. Chamber studies on the reactivities of the terpenes and possibly other biogenics under a wide range of conditions are clearly needed to test mechanism's abilities to simulate at least their effects on ozone formation and NO_x oxidation. In addition, such data are needed to assess the ozone formation reactivities of these compounds relative to anthropogenic VOC emissions. Until more data are available to test mechanisms for these compounds, no change in how they are represented in the RADM mechanism is warranted.

The scope of this study was such that we were unable to investigate effects of condensation in the mechanism as comprehensively as we had hoped at the time the program was conceived. We believe that research is still needed to investigate the appropriateness of the tradeoffs between condensation and chemical accuracy which are employed in RADM and other condensed chemical mechanisms. We also believe that the test problems developed in this program are well suited for this purpose. Examples of areas which need to be investigated concern the degree of condensation of the species used to represent reactive products. Preliminary studies of condensation methods we carried out for the SAPRC mechanism show that condensing the number of species used to represent primary emitted organics has less of an effect on model predictions than condensing the number of species used to represent reactive organic products. The RADM mechanism is relatively detailed in the number of species used to represent primary organic emissions, but is relatively condensed in its representation of reactive products. We did not investigate this problem as part of this program because by the time the other necessary tasks were completed, it was too late for the RADM team to consider implementing major changes in the mechanism for RADM-II. However, the possibility of such changes should be considered in time for the next major update of the RADM gas-phase chemical mechanism.

REFERENCES

Atkinson, R., W. P. L. Carter, K. R. Darnall, A. M. Winer, and J. N. Pitts, Jr. (1980), "A Smog Chamber and Modeling Study of the Gas Phase NO_x-Air Photooxidation of Toluene and the Cresols," Int J. Chem. Kinet., 12, 779-836.

Atkinson, R., W. P. L. Carter, and A. M. Winer (1983), "Evaluation of Hydrocarbon Reactivities for Use in Control Strategies," Final Report, California Air Resources Contract No. A0-105-32, May.

Atkinson, R. and W. P. L. Carter (1984), "Kinetics and Mechanisms of the Gas-Phase Reactions of Ozone with Organic Compounds Under Atmospheric Conditions," Chem. Rev., 84, 437-470.

Atkinson, R. (1986), "Kinetics and Mechanisms of the Gas Phase Reactions of the Hydroxyl Radical with Organic Compounds Under Atmospheric Conditions," Chem Rev., 86, 69-201.

Atkinson, R. (1987), "A Structure-Activity Relationship for the Estimation of Rate Constants for the Gas-Phase Reactions of OH Radicals with Organic Compounds," Int. J. Chem. Kinet., 19, 799-828.

Atkinson, R. (1988), "Gas-Phase Atmospheric Chemistry of Organic Compounds," Appendix A of Final Report, California Air Resources Board Contract No. A5-122-32, October.

Atkinson, R. (1989), "Gas-Phase Tropospheric Chemistry of Organic Compounds: A Review," Atmos. Environ., in press.

Atkinson, R., S. M. Aschmann, J. Arey, and W. P. L. Carter (1989), "Formation of Ring-Retaining Products from the OH Radical-Initiated Reactions of Benzene and Toluene," Int. J. Chem. Kinet., in press.

Burton, C. S. (1988), "Ozone Air Quality Models - Critical Review Discussion Papers," J. Air Poll. Cont. Assoc., 38, 1119-1128.

Carter, W. P. L., A. C. Lloyd, J. L. Sprung, and J. N. Pitts, Jr. (1979), "Computer Modeling of Smog Chamber Data: Progress in Validation of a Detailed Mechanism for the Photooxidation of Propene and n-Butane in Photochemical Smog," Int. J. Chem. Kinet, 11, 45-101.

Carter, W. P. L., R. Atkinson, A. M. Winer, and J. N. Pitts, Jr. (1982), "Experimental Investigation of Chamber-Dependent Radical Sources," Int. J. Chem Kinet., 14, 1071-1103.

Carter, W. P. L. and R. Atkinson (1985), "Atmospheric Chemistry of Alkanes," J. Atmos. Chem., 3, 377-405.

Carter, W. P. L., F. W. Lurmann, R. Atkinson, and A. C. Lloyd (1986), "Development and Testing of a Surrogate Species Chemical Reaction Mechanism," EPA-600/3-86-031, U.S. Environmental Protection Agency, Research Triangle Park, NC.

Carter, W. P. L., A. M. Winer, R. Atkinson, S. E. Heffron, M. P. Poe, and M. A. Goodman (1987), "Atmospheric Photochemical Modeling of Turbine Engine Fuels. Phase II. Computer Model Development," Report, USAF Contract No. F08635-83-0278, Engineering and Services Laboratory, Air Force Engineering and Services Center, Tyndall Air Force Base, Florida, August.

Carter, W. P. L. (1988a), "Documentation of a Gas Phase Photochemical Mechanism for Use in Airshed Modeling," Appendix B to Final Report, California Air Resources Board Contract No. A5-122-32, October.

Carter, W. P. L. (1988b) "Documentation for the SAPRC Atmospheric Photochemical Mechanism Preparation and Emissions Processing Programs for Implementation in Airshed Models," Appendix C to Final Report, California Air Resources Board Contract No. A5-122-32, October.

Carter, W. P. L. and R. Atkinson (1989a), "Alkyl Nitrate Formation from the Atmospheric Photooxidation of Alkanes: A Revised Estimation Method," J. Atmos. Chem., in press.

Carter, W. P. L. and R. Atkinson (1989b), "A Computer Modeling Study of Incremental Hydrocarbon Reactivity," Environ. Sci. Technol., in press.

Dodge, M. C. (1989), "A Comparison of Three Photochemical Reaction Mechanisms," J. Geophys. Res., 94, 5121-5136.

Dunker, A. M., S. Kumar, and P. H. Berzins (1984), "A Comparison of Chemical Mechanisms Used in Atmospheric Models," Atmos. Environ., 18, 311-321.

EPA (1984), "Guideline for Using the Carbon Bond Mechanism in City Specific EKMA," EPA-450/4-84-005, U.S. Environmental Protection Agency, Research Triangle Park, NC.

EPA (1987), "Workshop on Evaluation/Documentation of Chemical Mechanisms," EPA-600/9-87-024.

Fox, D. G. (1981), "Judging Air Quality Model Performance," Bull. Am. Meteorol. Soc., 62, 599-609.

Gery, M. W., D. L. Fox, J. E. Jeffries, L. Stockbuger, and W. S. Weathers (1985), "A Continuous Stirred Tank Reactor Investigation of the Gas-Phase Reactions of Hydroxyl Radicals and Toluene," Int. J. Chem. Kinet., 17, 931-955.

Gery, M. W., G. Z. Whitten, and J. P. Killus (1988), "Development and Testing of the CBM-IV For Urban and Regional Modeling," EPA/600/3-88/012, U.S. Environmental Protection Agency, Research Triangle Park, NC.

Gipson, G. L. (1984), "Users Manual for OZIPM-2: Ozone Isopleth Plotting With Optional Mechansims/Version 2," EPA-450/4-84-024, U.S. Environmental Protection Agency, Research Triangle Park, NC.

Grosjean, D. and K. Fung (1984), "Hydrocarbons and Carbonyls in Los Angeles Air," J. Air Poll. Control Assoc., 34, 537-543.

Hough, A. M. (1988), "An Intercomparison of Mechanism for the Production of Photochemical Oxidants," J. Geophys. Res., 93, 3789-3812.

Jeffries, H. E., K. G. Sexton, and C. N. Salmi (1981), "The Effects of Chemistry and Meteorology on Ozone Control Calculations Using Simple Trajectory Models and the EKMA Procedure," EPA-450/4-81-034, U.S. Environmental Protection Agency, Research Triangle Park, NC.

Jeffries, H. E., K. G. Sexton, R. M. Kamens, and M. S. Holleman (1985), Outdoor Smog Chamber Experiments to Test Photochemical Models: Phase II. EPA/600/3-85/029, U.S. Environmental Protection Agency, Research Triangle Park, NC.

Jeffries, H. E., K. G. Sexton, J. R. Arnold, and T. L. Kale (1989a), "Validation Testing of New Mechanisms with Outdoor Chamber Data. Volume 3: Calculation of Photochemical Reaction Photolysis Rates in the UNC Outdoor Chamber," EPA/600/3-89/010c, U.S. Environmental Protection Agency, Research Triangle Park, NC.

Jeffries, H. E., K. G. Sexton, J. R. Arnold, and T. L. Kale (1989b), "Validation Testing of New Mechanisms with Outdoor Chamber Data. Volume 1: Comparison of CB4 and CAL Mechanisms," EPA/600/3-89/010a, U.S. Environmental Protection Agency, Research Triangle Park, NC.

Jeffries, H. E., K. G. Sexton, and J. R. Arnold (1989c), "Validation Testing of New Mechanisms with Outdoor Chamber Data. Volume 2: Analysis of VOC Data for the CB4 and CAL Photochemical Mechanisms," EPA/600/3-89/010b, U.S. Environmental Protection Agency, Research Triangle Park, NC.

Jeffries, H. E., K. G. Sexton, J. R. Arnold, and T. L. Kale (1989d), "Validation Testing of New Mechanisms with Outdoor Chamber Data. Volume 4: Appendices to Photochemical Reaction Photolysis Rates in the UNC Outdoor Chamber," EPA/600/3-89/010d, U.S. Environmental Protection Agency, Research Triangle Park, NC.

Killus, J. P. and G. Z. Whitten (1982), "A New Carbon-Bond Mechanism for Air Quality Simulation Modeling," EPA-600/3-82-841, U.S. Environmental Protection Agency, Research Triangle Park, NC.

Leone, J. A. and J. H. Seinfeld (1984), "Evaluation of Chemical Reaction Mechanisms for Photochemical Smog Part II - Quantitative Evaluation of the Mechanisms," EPA-600/3-84-063, U.S. Environmental Protection Agency, Research Triangle Park, NC.

Lurmann, F. W., A. C. Lloyd, and R. Atkinson (1986), "A Chemical Mechanism for Use in Long-Range Transport/Acid Deposition Modeling," J. Geophys. Res. 91, 10905-10936.

Lurmann, F. W. and P. K. Karamchandani (1987), "An Updated Gas Phase Chemical Mechanism with Chlorine Chemistry for the TADAP Regional Model," Prepared for The Umweltbundesamt, West Germany, Environmental Research and Technology Document P-E142-201, September.

Lurmann, F. W., W. P. L. Carter, and L. A. Coyner (1987), "A Surrogate Species Chemical Reaction Mechanism for Urban-Scale Air Quality Simulation Models. Volume I - Adaptation of the Mechanism," EPA/600/3-87/014a, U.S. Environmental Protection Agency, Research Triangle Park, NC.

Milford, J. B. (1988), "Photochemical Air Pollution Control Strategy Development," Ph.D. Thesis, Carnegie Mellon Univ., Pittsburgh, PA.

NASA (1985), "Chemical Kinetics and Photochemical Data for Use in Stratospheric Modeling. Evaluation Number 7," JPL Publication 85-37, Jet Propulsion Laboratory, Pasadena, CA, July.

NASA (1987), "Chemical Kinetics and Photochemical Data for Use in Stratospheric Modeling. Evaluation Number 8," JPL Publication 87-41, Jet Propulsion Laboratory, Pasadena, CA, September.

NCAR (1987), "Development and Implementation of Chemical Mechanisms for the Regional Acid Deposition Model (RADM)," EPA Interagency Agreement DW49930144-01-4, U.S. Environmental Protection Agency, Research Triangle Park, NC.

Peterson, J. T. (1976), "Calculated Actinic Fluxes (290 - 700 nm) for Air Pollution Photochemistry Applications," EPA-600/4-76-025, U.S. Environmental Protection Agency.

Pitts, J. N., Jr., K. Darnall, W. P. L. Carter, A. M. Winer, and R. Atkinson (1979), "Mechanisms of Photochemical Reactions in Urban Air," EPA-600/3-79-110, U.S. Environmental Protection Agency.

Pitts, J. N., Jr., R. Atkinson, W. P. L. Carter, A. M. Winer, and E. C. Tuazon (1983), "Chemical Consequences of Air Quality Standard and of Control Implementation Programs," Final Report, California Air Resources Board Contract No. A1-030-32, April.

Pitts, J. N., Jr., E. Sanhueza, R. Atkinson, W. P. L. Carter, A. M. Winer, G. W. Harris, and C. N. Plum (1984), "An Investigation of the Dark Formation of Nitrous Acid in Environmental Chambers," Int. J. Chem. Kinet., 16, 919-939.

Plum, C. N., E. Sanhueza, R. Atkinson, W. P. L. Carter, and J. N. Pitts, Jr. (1983), "OH Radical Rate Constants and Photolysis Rates of Alpha-Dicarbonyls," Environ. Sci. Technol., 17, 479-484.

Shafer, T. B. and J. H. Seinfeld (1985), "Evaluation of Chemical Reaction Mechanisms for Photochemical Smog Part III - Sensitivity of EKMA to Chemical Mechanisms and Input Parameters," EPA-600/3-85-042. U.S. Environmental Protection Agency, Research Triangle Park, NC.

Shareef, G. S., W. A. Butler, L. A. Bravo, and M. B. Stockton (1988), "Air Emissions Species Manual Vol 1. Volatile Organic Compound Species Profiles," EPA-450/2-88-003a, U.S. Environmental Protection Agency, Research Triangle Park, NC.

Stockwell, W. R. (1986), "A Homogeneous Gas Phase Mechanism for Use in a Regional Acid Deposition Model," Atmos. Environ., 20, 1615-1632.

Stockwell, W. R. and F. W. Lurmann (1989), "Intercomparison of the ADOM and RADM Gas-Phase Chemical Mechanisms," State University of New York, Draft Report to the Electric Power Research Institute, Palo Alto, CA.

Tuazon, E. C., R. Atkinson, C. N. Plum, A. M. Winer, and J. N. Pitts, Jr. (1983), "The Reaction of Gas-Phase N_2O_5 with Water Vapor," Geophys. Res. Lett., 10, 953-956.

Wagner, J. K., R. A. Walters, L. J. Maiocco, and D. R. Neal (1986), "Development of the 1980 NAPAP Emissions Inventory," EPA-600/7-86-57a, U.S. Environmental Protection Agency, Research Triangle Park, NC.

Weir, B. R., A. S. Rosenbaum, L. A. Gardner, G. Z. Whitten and W. Carter (1988), "Architectural Coatings in the South Coast Air Basin: Survey, Reactivity, and Toxicity Evaluation," Final Report, South Coast Management District, SYSAPP-88/137, Systems Applications, Inc., San Rafael, CA, December.

Westburg, H. and L. MacGregor (1987), "Nonmethane Organic Carbon Concentrations in Air Masses Advected into Urban Areas in the United States," EPA-600/3-87/045, U.S. Environmental Protection Agency, Research Triangle Park, NC.

Whitten, G. Z., H. Hogo, and J. P. Killus (1980), "The Carbon-Bond Mechanism: A Condensed Kinetic Mechanism for Photochemical Smog," Environ. Sci. Technol., 14, 690-287.

Zafonte, L., P. L. Rieger, and J. R. Holmes (1977), Environ. Sci. Technol. 11, 483.

APPENDIX A

SELECTED RESULTS OF SIMULATIONS OF ALL EXPERIMENTS MODELED USING THE RADM MECHANISM

Appendix A. Selected Results of Simulations of All Experiments Modeled Using the RADM Mechanism.

Experiment	Initial Concentrations			Ave Temp	Ave H2O	Maximum Concentration OZONE			
	NOx (ppm)	HC (ppmC)	HC/NOx	(degK)	(ppm)	Expt (ppm)	Calc (ppm)	Calc -Expt (ppm)	Calc -Expt /Avg
1. Pure Air									
ITC940	0.02	0.0	0.0	303.0	20300.	0.072	0.073	0.001	0.01
ITC955	0.03	0.0	0.0	303.0	20300.	0.064	0.073	0.009	0.13
ITC1008	0.01	0.0	0.0	303.0	18200.	0.088	0.073	-0.014	-0.18
JN0682R	0.00	0.0	0.0	*	14200.	0.203	0.203	0.001	0.00
OC0684R	0.02	0.0	0.3	296.5	20000.*	0.097	0.094	-0.003	-0.04
OC0684B	0.02	0.0	0.3	296.5	20000.*	0.119	0.098	-0.021	-0.19
Group Average	0.02	0.0	0.1	300.4	18833.	0.107	0.102	-0.005	-0.04
S. Dev.	0.01	0.0	0.2	3.6	2404.	0.051	0.051	0.011	0.12
Avg. Abs. Value								0.008	0.09
S. Dev.								0.008	0.08

(continued)

Appendix A. Selected Results of Simulations of All Experiments Modeled Using the RADM Mechanism (continued).

Experiment	Initial Concentrations			Ave Temp	Ave H2O	Final - Init NO			Final - Init NO2-UNC		
	NOx (ppm)	HC (ppmC)	HC/NOx	(degK)	(ppm)	Expt (ppm)	Calc (ppm)	Calc -Expt (ppm)	Expt (ppm)	Calc (ppm)	Calc -Expt (ppm)
1. NOx-Air											
EC436	1.79	0.0	0.0	303.0	14900.	-0.098	-0.052	0.046	-0.071	-0.057	0.014
EC440	0.76	0.0	0.0	303.0	17500.	-0.063	-0.049	0.015	0.024	0.013	-0.011
EC442	0.58	0.0	0.1	303.0	21400.	0.069	0.093	0.024	-0.172	-0.160	0.012
EC457	0.50	0.0	0.1	303.0	19600.	-0.066	-0.042	0.023	0.008	-0.008	-0.017
EC464	0.19	0.0	0.2	303.0	19300.	-0.019	-0.002	0.016	-0.002	-0.012	-0.010
EC597	0.56	0.0	0.1	303.0	22000.	-0.061	-0.031	0.030	0.041	0.005	-0.036
EC599	3.40	0.0	0.0	303.0	20800.	2.276	1.878	-0.398	-2.685	-2.536	0.149
ITC695	0.50	0.0	0.1	303.0	20300.	-0.021	-0.008	0.014	0.011	0.001	-0.010
ITC826	0.90	0.8	0.9	303.0	17200.	-0.349	-0.182	0.167	0.263	0.135	-0.128
ITC882	0.70	0.0	0.0	303.0	17900.	-0.001	-0.027	-0.027	-0.010	-0.014	-0.003
OTC185	0.28	0.0	0.1	298.1	5000.*	-0.002	-0.004	-0.002	-0.003	-0.001	0.002
JN2782B	0.44	0.0	0.0	301.3	29300.	-0.113	-0.118	-0.005	0.050	0.025	-0.025
AU0282R	0.39	0.0	0.0	301.6	27700.	0.035	0.039	0.004	-0.129	-0.120	0.009
AU2082R	0.41	0.0	0.0	302.0	21000.	-0.011	-0.010	0.002	-0.049	-0.058	-0.009
AU2282R	0.46	0.0	0.0	300.0	25600.	0.000	0.022	0.023	-0.147	-0.116	0.031
AU2382R	0.43	0.0	0.0	302.8	20200.	0.056	0.057	0.001	-0.144	-0.148	-0.005
OC0882R	0.30	0.0	0.0	294.3	18100.	-0.024	-0.032	-0.008	0.005	-0.006	-0.011
OC0882B	0.30	0.0	0.0	294.3	18100.	-0.017	-0.032	-0.014	0.009	-0.005	-0.014
ST0582R	0.50	0.0	0.0	297.3	14300.	0.070	0.085	0.015	-0.171	-0.157	0.014
JL2483R	0.31	0.0	0.0	305.0	19600.	-0.047	-0.063	-0.015	0.011	-0.004	-0.015
JL2483B	0.48	0.0	0.0	305.0	19600.	-0.071	-0.071	0.000	0.014	-0.010	-0.024
JL2783B	0.43	0.0	0.0	300.7	20000.*	-0.090	-0.078	0.012	0.036	0.009	-0.027
AU0683B	0.37	0.0	0.0	304.2	20200.	0.001	-0.004	-0.005	-0.090	-0.088	0.002
Group Average	0.65	0.1	0.1	301.6	19548.	0.063	0.060	-0.004	-0.139	-0.144	-0.005
S. Dev.	0.68	0.2	0.2	3.0	4721.	0.490	0.401	0.094	0.563	0.526	0.045
Avg. Abs. Value						0.155	0.130	0.038	0.180	0.160	0.025
S. Dev.						0.468	0.383	0.085	0.551	0.521	0.037
2. CO-NOx											
ITC625	0.28	0.0	0.1	303.0	20300.	-0.069	-0.085	-0.016	0.068	0.078	0.010
ITC634	0.60	0.0	0.1	303.0	20300.	-0.040	-0.061	-0.021	0.034	0.052	0.017
OTC188	0.34	0.0	0.1	308.8	5000.*	-0.090	-0.136	-0.046	0.072	0.125	0.053
OTC201A	0.37	0.0	0.1	310.9	3880.	-0.160	-0.157	0.003	0.162	0.143	-0.019
OTC201B	0.76	0.0	0.1	310.8	3000.	-0.123	-0.115	0.008	0.096	0.100	0.004
JN2782R	0.45	0.0	0.0	301.3	29300.	-0.320	-0.339	-0.019	0.202	0.239	0.038
AU0282B	0.40	0.0	0.0	301.6	27700.	-0.054	-0.062	-0.008	-0.002	-0.026	-0.023
AU2082B	0.41	0.0	0.0	302.1	21000.	-0.111	-0.146	-0.035	0.072	0.076	0.004
AU2282B	0.46	0.0	0.0	300.0	25600.	-0.086	-0.089	-0.003	0.003	-0.009	-0.012
AU2382B	0.43	0.0	0.0	302.8	20200.	-0.004	-0.051	-0.047	-0.042	-0.046	-0.004
ST0582B	0.50	0.0	0.0	297.3	14300.	0.019	0.026	0.007	-0.086	-0.098	-0.012
JL2783R	0.47	0.0	0.0	302.8	20000.*	-0.289			0.214		

(continued)

Appendix A. Selected Results of Simulations of All Experiments Modeled Using the RADM Mechanism (continued).

Experiment	Initial Concentrations			Ave Temp	Ave H2O	Final - Init NO			Final - Init NO2-UNC		
	NOx (ppm)	HC (ppmC)	HC/NOx	(degK)	(ppm)	Expt (ppm)	Calc (ppm)	Calc -Expt (ppm)	Expt (ppm)	Calc (ppm)	Calc -Expt (ppm)
Group Average	0.45	0.0	0.0	303.7	17760.	-0.112	-0.110	-0.016	0.063	0.058	0.005
S. Dev.	0.12	0.0	0.0	4.1	8754.	0.099	0.092	0.020	0.089	0.097	0.024
Avg. Abs. Value						0.115	0.115	0.019	0.083	0.090	0.018
S. Dev.						0.095	0.085	0.017	0.069	0.064	0.015

(continued)

Appendix A. Selected Results of Simulations of All Experiments Modeled Using the RADM Mechanism (continued).

Experiment	Initial Concentrations			Ave Temp	Ave H2O	Maximum Concentration OZONE			
	NOx (ppm)	HC (ppmC)	HC/NOx	(degK)	(ppm)	Expt (ppm)	Calc (ppm)	Calc -Expt (ppm)	Calc -Expt /Avg
1. HCHO-Air									
EC250	0.02	0.3	14.5	303.0	17400.	0.215	0.258	0.043	0.18
EC255	0.02	0.3	20.4	303.0	15700.	0.203	0.255	0.052	0.23
JL1782R	0.01	0.5	71.2	303.3	14700.	0.239	0.329	0.090	0.32
JL1782B	0.01	0.6	86.0	303.3	14700.	0.264	0.335	0.071	0.24
OC0784R	0.00	0.4	96.1	292.6	20000.*	0.087	0.124	0.037	0.36
OC0784B	0.01	1.0	125.7	292.6	20000.*	0.138	0.181	0.043	0.27
OC1684R	0.00	0.4		299.7	20000.*	0.153	0.152	-0.001	-0.01
OC1684B	0.00	0.3		299.7	20000.*	0.133	0.134	0.000	0.00
Group Average	0.01	0.5	69.0	299.7	17813.	0.179	0.221	0.042	0.20
S. Dev.	0.01	0.2	43.8	4.6	2483.	0.061	0.085	0.031	0.13
Avg. Abs. Value								0.042	0.20
S. Dev.								0.031	0.13

(continued)

Appendix A. Selected Results of Simulations of All Experiments Modeled Using the RADM Mechanism (continued).

Experiment	Initial Concentrations NOx (ppm)	Initial Concentrations HC (ppmC)	Initial Concentrations HC/NOx	Ave Temp (degK)	Ave H2O (ppm)	Maximum Concentration OZONE Expt (ppm)	Maximum Concentration OZONE Calc (ppm)	Maximum Concentration OZONE Calc -Expt (ppm)	Maximum Concentration OZONE Calc -Expt /Avg	Maximum Concentration PAN Expt (ppm)	Maximum Concentration PAN Calc (ppm)	Maximum Concentration PAN Calc -Expt (ppm)	Maximum Concentration PAN Calc -Expt /Avg
1. Acetaldehyde-Air													
EC253	0.02	1.1	53.8	303.0	17100.	0.137	0.100	-0.036	-0.31	0.040	0.046	0.006	0.15
ITC627	0.03	0.8	26.1	303.0	20300.	0.060	0.050	-0.010	-0.19	0.013	0.014	0.001	0.10
ITC636	0.03	0.7	26.6	303.0	20300.	0.047	0.050	0.003		0.011	0.014	0.003	0.27
ITC825	0.01	0.8	55.3	303.0	17300.	0.037	0.017	-0.019		0.005	0.008	0.003	0.47
ITC957	0.04	1.1	27.6	303.0	20300.	0.076	0.051	-0.025	-0.40	0.013	0.016	0.004	0.25
ITC974	0.03	0.9	29.8	303.0	19000.	0.085	0.048	-0.037	-0.56	0.006	0.015	0.009	0.84
ITC1009	0.04	0.9	27.0	303.0	20100.	0.078	0.052	-0.026	-0.40	0.008	0.015	0.007	0.59
OTC200A	0.01	1.1	96.9	309.5	3950.	0.088	0.081	-0.007	-0.08	0.008	0.007	-0.001	-0.08
OTC200B	0.01	0.8	68.8	309.4	2870.	0.076	0.080	0.004	0.05	0.006	0.008	0.002	0.23
OTC206A	0.01	1.3	136.8	302.2	8740.	0.030	0.063	0.033		0.020	0.011	-0.009	-0.58
OTC206B	0.01	1.0	94.0	304.5	7840.	0.023	0.087	0.064		0.013	0.010	-0.003	-0.31
OTC234A	0.04	1.0	26.2	307.5	5000.*	0.083	0.138	0.055	0.50	0.004	0.012	0.008	0.97
OTC234B	0.04	1.5	39.3	307.7	5000.*	0.084	0.138	0.054	0.49	0.007	0.012	0.005	0.53
JL2683R	0.02	1.1	48.3	302.8	25900.	0.422	0.364	-0.057	-0.15	0.026	0.035	0.010	0.31
JL2683B	0.01	1.1	87.6	302.8	25900.	0.331	0.235	-0.096	-0.34	0.027	0.035	0.008	0.26
AU0483R	0.03	1.0	34.3	304.1	29300.	0.548	0.456	-0.092	-0.18	0.040	0.043	0.003	0.07
AU0483B	0.02	1.1	47.1	304.1	29300.	0.431	0.342	-0.090	-0.23	0.040	0.047	0.007	0.16
OC1584R	0.02	1.0	48.5	296.5	15200.	0.140	0.149	0.009	0.06	0.023	0.025	0.002	0.08
OC1584B	0.02	1.0	45.2	296.5	15200.	0.193	0.195	0.002	0.01	0.035	0.023	-0.012	-0.40
Group Average	0.02	1.0	53.6	303.6	16242.	0.156	0.142	-0.014	-0.12	0.018	0.021	0.003	0.20
S. Dev.	0.01	0.2	30.5	3.4	8541.	0.156	0.124	0.048	0.30	0.013	0.014	0.006	0.39
Avg. Abs. Value								0.038	0.26			0.005	0.35
S. Dev.								0.031	0.18			0.003	0.26

(continued)

Appendix A. Selected Results of Simulations of All Experiments Modeled Using the RADM Mechanism (continued).

Experiment	Initial Concentrations NOx (ppm)	HC (ppmC)	HC/NOx	Ave Temp (degK)	Ave H2O (ppm)	Maximum Concentration OZONE Expt (ppm)	Calc (ppm)	Calc -Expt (ppm)	Calc -Expt /Avg	Average Initial d([O3] - [NO])/dt Expt --	Calc (ppb/min)	Calc -Expt --	Calc -Expt /Avg
1. HCHO-NOx													
EC251	0.11	0.2	1.7	303.0	17600.	0.271	0.300	0.029	0.10	3.25	3.77	0.51	0.15
EC252	0.49	0.4	0.7	303.0	17100.	0.032	0.025	-0.007		1.94	2.13	0.19	0.09
EC389	4.75	9.1	1.9	303.0	2080.	0.002	0.031	0.029		50.01	50.67	0.66	0.01
EC391	4.43	17.7	4.0	303.0	2310.	2.371	2.190	-0.181	-0.08	102.89	97.24	-5.64	-0.06
EC392	8.05	9.5	1.2	303.0	877.	0.000	0.008	0.008		13.52	30.58	17.06	0.77
ITC864	0.54	0.1	0.1	303.0	16000.	0.001	0.017	0.017		0.60	0.71	0.11	0.17
OTC235A	0.56	0.1	0.1	299.2	4430.*	0.273	0.143	-0.130	-0.63	2.00	1.74	-0.26	-0.14
OTC235B	0.58	0.1	0.1	297.9	3940.*	0.308	0.267	-0.041	-0.14	2.16	2.09	-0.06	-0.03
AU0179B	0.35	1.0	2.8	308.2	19400.	0.618	0.519	-0.099	-0.17	2.06	1.96	-0.10	-0.05
AU0279B	0.21	1.0	4.7	307.2	20000.*	0.606	0.612	0.006	0.01	2.12	2.06	-0.07	-0.03
AU0479B	0.23	0.5	2.1	304.8	20800.	0.378	0.392	0.014	0.04	1.17	1.11	-0.06	-0.05
AU0579B	0.54	1.2	2.2	296.5	12500.	0.508	0.547	0.040	0.07	1.95	1.94	-0.01	0.00
JL2381B	0.43	1.5	3.5	306.1	20000.*	0.637	0.792	0.155	0.22	2.70	2.80	0.10	0.04
OC0984R	0.56	1.0	1.7	295.1	10900.	0.666	1.187	0.521	0.56	2.11	2.73	0.62	0.26
OC0984B	0.50	1.0	1.9	295.1	10900.	0.301	0.403	0.102	0.29	1.51	1.76	0.25	0.15
Group Average	1.49	2.9	1.9	301.9	11922.	0.465	0.496	0.031	0.02	12.67	13.55	0.89	0.09
S. Dev.	2.33	5.1	1.4	4.2	7438.	0.580	0.573	0.160	0.30	27.92	27.07	4.72	0.22
Avg. Abs. Value								0.092	0.21			1.71	0.13
S. Dev.								0.132	0.21			4.47	0.19
2. Acetaldehyde-NOx													
EC164	0.51	0.7	1.4	303.0	34000.	0.086	0.048	-0.037	-0.55	2.03	1.49	-0.54	-0.31
EC254	0.11	1.0	8.5	303.0	18900.	0.264	0.185	-0.079	-0.35	1.33	0.99	-0.33	-0.29
AU0179R	0.36	2.0	5.7	308.3	31300.	0.930	0.580	-0.350	-0.46	1.98	1.69	-0.29	-0.16
JN1482R	0.31	3.1	9.9	300.2*	22300.	0.731	0.653	-0.078	-0.11	1.62	1.50	-0.12	-0.08
AU2482B	0.32	1.9	6.0	304.0	17400.	0.972	0.665	-0.307	-0.37	1.68	1.54	-0.14	-0.09
Group Average	0.32	1.7	6.3	303.7	24780.	0.596	0.426	-0.170	-0.37	1.73	1.44	-0.29	-0.18
S. Dev.	0.14	1.0	3.2	2.9	7462.	0.401	0.289	0.146	0.17	0.29	0.26	0.17	0.11
Avg. Abs. Value								0.170	0.37			0.29	0.18
S. Dev.								0.146	0.17			0.17	0.11
3. Proprionaldehyde-NOx													
JN1482B	0.30	3.1	10.5	300.1*	18900.	0.733	0.621	-0.112	-0.17	1.75	1.34	-0.41	-0.27

(continued)

Experiment	Initial Concentrations			Ave Temp	Ave H2O	Maximum Concentration OZONE				Average Initial d([O3] - [NO])/dt			
	NOx (ppm)	HC (ppmC)	HC/NOx	(degK)	(ppm)	Expt (ppm)	Calc (ppm)	Calc -Expt (ppm)	Calc -Expt /Avg	Expt --	Calc (ppb/min)	Calc -Expt --	Calc -Expt /Avg
Group Average	0.32	2.5	8.0	302.1	18150.	0.837	0.608	-0.229	-0.31	1.79	1.38	-0.41	-0.26
S. Dev.	0.02	0.9	3.4	2.8	1061.	0.147	0.019	0.166	0.20	0.05	0.05	0.00	0.01
Avg. Abs. Value								0.229	0.31			0.41	0.26
S. Dev.								0.166	0.20			0.00	0.01
4. Acetone-NOx													
JN0480R	0.17	4.8	27.5	302.2	17700.	0.233	0.397	0.164	0.52	0.48	0.52	0.04	0.09
5. Methylethylketone-NOx													
OC2079R	0.22	13.6	60.5	295.3	27800.	0.563	0.466	-0.096	-0.19	1.25	1.71	0.46	0.31
JN0480B	0.18	3.8	21.6	302.2	18100.	0.652	0.534	-0.118	-0.20	1.13	1.21	0.08	0.07
Group Average	0.20	8.7	41.0	298.8	22950.	0.607	0.500	-0.107	-0.19	1.19	1.46	0.27	0.19
S. Dev.	0.03	6.9	27.5	4.9	6859.	0.063	0.048	0.015	0.01	0.09	0.35	0.26	0.17
Avg. Abs. Value								0.107	0.19			0.27	0.19
S. Dev.								0.015	0.01			0.26	0.17
6. Ethene-NOx													
EC142	0.48	1.9	4.1	303.0	26500.	0.782	0.474	-0.307	-0.49	3.20	2.20	-1.00	-0.37
EC143	0.50	4.1	8.1	303.0	22700.	1.087	0.791	-0.296	-0.32	8.50	4.51	-3.99	-0.61
EC156	0.50	4.0	8.0	303.0	29000.	1.105	0.751	-0.354	-0.38	8.89	4.50	-4.39	-0.66
EC285	1.01	3.9	3.9	303.0	20400.	0.840	0.892	0.052	0.06	5.05	4.89	-0.16	-0.03
EC286	0.94	7.5	8.0	303.0	20500.	1.081	1.171	0.090	0.08	11.76	10.13	-1.63	-0.15
EC287	0.53	8.0	15.1	303.0	19700.	0.965	1.026	0.061	0.06	13.89	13.00	-0.88	-0.07
ITC926	0.51	7.9	15.6	303.0	21100.	0.982	0.920	-0.062	-0.06	6.96	4.91	-2.05	-0.35
ITC936	0.50	3.9	7.8	303.0	20300.	0.940	0.838	-0.102	-0.11	2.72	2.34	-0.38	-0.15
AU0479R	0.23	0.9	3.9	298.9	32500.	0.729	0.554	-0.175	-0.27	1.60	0.99	-0.61	-0.47
AU0579R	0.64	4.1	6.4	292.4	29100.	1.294	1.142	-0.152	-0.12	3.17	2.27	-0.91	-0.33
OC0584R	0.36	3.2	8.8	297.3	20000.*	0.856	0.971	0.114	0.13	2.16	1.98	-0.18	-0.09
OC1184R	0.35	2.9	8.2	297.2	12700.	0.858	1.039	0.182	0.19	2.22	2.01	-0.21	-0.10
OC1284R	0.72	2.7	3.7	295.6	13600.	0.495	0.185	-0.310	-0.91	1.58	1.17	-0.41	-0.30
OC0584B	0.37	1.8	5.0	297.3	20000.*	0.675	0.646	-0.029	-0.04	1.48	1.33	-0.15	-0.11
Group Average	0.55	4.1	7.6	300.2	22007.	0.906	0.814	-0.092	-0.16	5.23	4.02	-1.21	-0.27
S. Dev.	0.22	2.3	3.8	3.6	5611.	0.204	0.275	0.179	0.30	4.10	3.53	1.39	0.20
Avg. Abs. Value								0.163	0.23			1.21	0.27
S. Dev.								0.111	0.24			1.39	0.20

(continued)

Appendix A. Selected Results of Simulations of All Experiments Modeled Using the RADM Mechanism (continued).

Experiment	Initial Concentrations NOx (ppm)	Initial Concentrations HC (ppmC)	Initial Concentrations HC/NOx	Ave Temp (degK)	Ave H2O (ppm)	Maximum Concentration OZONE Expt (ppm)	Maximum Concentration OZONE Calc (ppm)	Maximum Concentration OZONE Calc -Expt (ppm)	Maximum Concentration OZONE Calc -Expt /Avg	Average Initial d([O3] - [NO])/dt Expt --	Average Initial d([O3] - [NO])/dt Calc (ppb/min)	Average Initial d([O3] - [NO])/dt Calc -Expt --	Average Initial d([O3] - [NO])/dt Calc -Expt /Avg
7. Propene-NOx													
EC121	0.51	1.5	2.9	303.0	26500.	0.506	0.448	-0.057	-0.12	7.46	3.80	-3.66	-0.65
EC177	0.46	1.5	3.2	303.0	26900.	0.540	0.466	-0.074	-0.15	3.89	3.71	-0.18	-0.05
EC216	0.52	1.5	3.0	303.0	18100.	0.564	0.550	-0.014	-0.03	4.18	5.28	1.10	0.23
EC217	0.48	0.6	1.2	303.0	21400.	0.149	0.227	0.078	0.42	0.80	1.25	0.45	0.44
EC230	0.52	1.9	3.7	303.0	17200.	0.344	0.309	-0.035	-0.11	3.06	4.41	1.35	0.36
EC256	0.56	0.4	0.7	303.0	20200.	0.002	0.010	0.007		0.98	1.03	0.05	0.05
EC257	0.56	0.7	1.3	303.0	20000.	0.068	0.094	0.025	0.31	3.35	4.06	0.71	0.19
EC276	0.52	1.6	3.2	303.0	14500.	0.388	0.435	0.046	0.11	3.24	4.06	0.82	0.22
EC277	0.11	1.7	15.7	303.0	15700.	0.313	0.386	0.073	0.21	8.27	7.60	-0.67	-0.08
EC278	0.49	3.1	6.2	303.0	16100.	0.625	0.685	0.060	0.09	7.72	9.03	1.30	0.16
EC279	0.97	3.5	3.5	303.0	14200.	0.679	0.692	0.013	0.02	6.64	7.38	0.73	0.10
EC314	0.93	3.2	3.5	303.0	24000.	0.728	0.776	0.048	0.06	7.21	9.47	2.26	0.27
EC315	0.94	2.9	3.1	288.7	10600.	0.344	0.638	0.294	0.60	4.33	5.96	1.62	0.32
EC316	0.98	3.2	3.3	312.0	44900.	0.955	1.043	0.088	0.09	10.64	10.99	0.35	0.03
EC317	0.54	1.5	2.8	303.0	24200.	0.615	0.563	-0.052	-0.09	4.06	4.28	0.22	0.05
ITC693	0.49	3.5	7.2	303.0	20300.	0.779	0.702	-0.078	-0.11	5.07	5.29	0.23	0.04
ITC810	0.52	2.8	5.4	303.0	16800.	0.782	0.705	-0.078	-0.10	4.25	4.22	-0.03	-0.01
ITC860	0.52	3.0	5.8	303.0	17100.	0.585	0.665	0.081	0.13	3.57	4.50	0.94	0.23
ITC925	0.54	2.8	5.2	303.0	16300.	0.779	0.714	-0.065	-0.09	3.72	3.81	0.09	0.02
ITC938	0.52	2.8	5.3	303.0	19000.	0.729	0.704	-0.025	-0.03	3.61	3.91	0.30	0.08
ITC947	0.53	1.9	3.6	303.0	20300.	0.710	0.701	-0.009	-0.01	3.34	3.82	0.48	0.13
ITC960	0.50	2.8	5.5	303.0	20300.	0.721	0.697	-0.024	-0.03	4.23	4.05	-0.18	-0.04
OTC186	0.55	3.6	6.6	299.8	5000.*	0.822	0.853	0.030	0.04	5.16	7.22	2.06	0.33
OTC191	0.54	3.7	6.9	309.3	5000.*	0.903	1.082	0.179	0.18	12.18	12.79	0.61	0.05
OTC210	0.57	2.7	4.8	304.7	3720.*	0.972	0.989	0.017	0.02	6.70	5.95	-0.75	-0.12
OTC233	0.46	0.1	0.2	303.6	5000.*	0.633	0.918	0.285	0.37	3.69	5.12	1.43	0.32
OTC236	0.53	3.3	6.3	300.0	6510.*	0.848	0.990	0.142	0.15	6.91	7.83	0.93	0.13
JA1078R	0.46	3.1	6.9	265.1	20000.*	0.363	0.583	0.220	0.46	0.46	0.48	0.01	0.03
OC1278B	0.48	1.4	2.9	294.3	16300.	0.461	0.387	-0.074	-0.17	1.40	1.39	-0.01	-0.01
OC2078R	0.46	1.3	2.9	290.4	9590.	0.340	0.378	0.037	0.10	1.23	1.33	0.09	0.07
OC2078B	0.46	3.5	7.7	290.4	9560.	0.727	0.924	0.197	0.24	2.83	3.42	0.59	0.19
OC2178R	0.50	3.9	7.9	290.3	20000.*	0.670	0.893	0.223	0.29	2.53	3.32	0.79	0.27
OC2578B	0.44	1.3	2.9	288.4	12800.	0.230	0.243	0.013	0.05	1.03	1.10	0.07	0.06
JN1279R	0.50	1.0	2.1	293.5	20000.*	0.382	0.285	-0.097	-0.29	0.85	0.74	-0.11	-0.14
JN1279B	0.49	1.5	3.0	293.5	20000.*	0.673	0.508	-0.165	-0.28	1.24	1.09	-0.15	-0.13
JN1379R	0.45	2.9	6.5	294.9	20000.*	0.974	0.861	-0.113	-0.12	2.69	2.75	0.06	0.02
AU0279R	0.22	1.5	7.0	307.2	20000.*	0.788	0.622	-0.166	-0.24	2.41	2.01	-0.40	-0.18
AU2780B	0.48	1.9	4.0	302.2	28400.	1.044	1.180	0.136	0.12	3.26	2.79	-0.47	-0.16
ST0482B	0.23	1.1	4.9	300.5	11800.	0.658	0.607	-0.052	-0.08	1.46	1.54	0.08	0.06
ST1382B	0.33	1.1	3.3	302.6	24100.	0.731	0.678	-0.054	-0.08	1.69	1.57	-0.12	-0.07
JL1783R	0.27	1.1	3.9	307.2	29700.	0.848	0.713	-0.134	-0.17	2.10	1.72	-0.38	-0.20
JL2183R	0.22	1.1	5.0	308.5	23800.	0.804	0.725	-0.079	-0.10	1.76	1.83	0.07	0.04
JL2983B	0.21	1.1	5.3	303.1	23300.	0.697	0.733	0.037	0.05	1.66	1.70	0.04	0.03
JL3183R	0.21	1.1	5.1	305.0	19800.	0.719	0.682	-0.037	-0.05	1.81	1.62	-0.19	-0.11
ST2383B	0.38	1.6	4.3	292.5	23400.	0.405	0.654	0.250	0.47	1.23	1.62	0.39	0.28

(continued)

Appendix A. Selected Results of Simulations of All Experiments Modeled Using the RADM Mechanism (continued).

Experiment	Initial Concentrations NOx (ppm)	Initial Concentrations HC (ppmC)	Initial Concentrations HC/NOx	Ave Temp (degK)	Ave H2O (ppm)	Maximum Concentration OZONE Expt (ppm)	Maximum Concentration OZONE Calc (ppm)	Maximum Concentration OZONE Calc -Expt (ppm)	Maximum Concentration OZONE Calc -Expt /Avg	Average Initial d([O3] - [NO])/dt Expt --	Average Initial d([O3] - [NO])/dt Calc (ppb/min)	Average Initial d([O3] - [NO])/dt Calc -Expt --	Average Initial d([O3] - [NO])/dt Calc -Expt /Avg
OC0484B	0.36	1.0	2.9	296.7	20000.*	0.446	0.457	0.011	0.02	1.25	1.17	-0.08	-0.07
OC1184B	0.36	2.2	6.3	297.2	12700.	0.674	0.757	0.083	0.12	2.38	2.36	-0.02	-0.01
OC1284B	0.68	2.0	2.9	295.9	13500.	0.432	0.438	0.006	0.01	1.67	1.57	-0.10	-0.06
Group Average	0.49	2.1	4.6	299.9	18134.	0.608	0.635	0.026	0.05	3.62	3.88	0.26	0.06
S. Dev.	0.18	1.0	2.5	7.5	7349.	0.238	0.249	0.112	0.20	2.60	2.81	0.87	0.19
Avg. Abs. Value								0.087	0.15			0.57	0.14
S. Dev.								0.075	0.13			0.70	0.13
8. 1-Butene-NOx													
EC122	0.50	0.9	1.7	303.0	22000.	0.227	0.073	-0.154	-1.02	2.29	1.31	-0.98	-0.54
EC123	0.51	1.6	3.2	303.0	27200.	0.506	0.267	-0.238	-0.62	4.16	2.14	-2.02	-0.64
EC124	0.99	1.7	1.7	303.0	24500.	0.247	0.121	-0.126	-0.69	1.99	1.58	-0.41	-0.23
ITC927	0.31	3.8	12.3	303.0	19000.	0.646	0.712	0.066	0.10	3.24	4.19	0.95	0.26
ITC928	0.67	3.8	5.7	303.0	18400.	0.022	0.037	0.015		1.36	1.58	0.23	0.15
ITC930	0.32	7.2	22.2	303.0	21100.	0.717	0.807	0.090	0.12	7.91	10.39	2.49	0.27
ITC935	0.66	7.6	11.6	303.0	19700.	0.872	0.949	0.077	0.08	5.39	6.58	1.20	0.20
ST2383R	0.40	1.5	3.7	292.6	23400.	0.206	0.431	0.225	0.71	0.96	1.12	0.16	0.16
ST2583R	0.46	1.6	3.6	292.3	18800.	0.266	0.427	0.161	0.46	1.16	1.27	0.11	0.09
ST2583B	0.42	2.9	6.8	292.3	18900.	0.594	0.767	0.174	0.26	1.78	2.13	0.35	0.18
ST2783R	0.45	1.6	3.6	295.5	19400.	0.285	0.430	0.145	0.40	1.19	1.27	0.08	0.06
Group Average	0.52	3.1	6.9	299.4	21127.	0.417	0.457	0.039	-0.02	2.86	3.05	0.20	0.00
S. Dev.	0.20	2.3	6.2	5.0	2856.	0.263	0.316	0.150	0.56	2.18	2.95	1.16	0.32
Avg. Abs. Value								0.134	0.45			0.81	0.25
S. Dev.								0.068	0.31			0.81	0.18
9. trans-2-Butene-NOx													
EC146	0.51	0.9	1.8	303.0	26900.	0.247	0.109	-0.137	-0.77	5.87	3.99	-1.88	-0.38
EC147	0.98	1.7	1.7	303.0	22300.	0.154	0.084	-0.070	-0.59	9.83	7.66	-2.18	-0.25
EC157	0.53	0.9	1.7	303.0	27500.	0.205	0.091	-0.114	-0.77	5.96	3.64	-2.32	-0.48
ST2783B	0.43	2.0	4.7	295.5	19400.	0.523	0.544	0.021	0.04	3.00	3.36	0.35	0.11
Group Average	0.61	1.4	2.5	301.1	24025.	0.282	0.207	-0.075	-0.52	6.17	4.66	-1.50	-0.25
S. Dev.	0.25	0.6	1.5	3.7	3860.	0.165	0.225	0.070	0.38	2.80	2.01	1.25	0.26
Avg. Abs. Value								0.085	0.54			1.68	0.31
S. Dev.								0.051	0.35			0.90	0.16
10. Isobutene-NOx													
ITC694	0.51	4.6	9.1	303.0	20000.	0.900	0.714	-0.186	-0.23	8.84	5.59	-3.25	-0.45

(continued)

Appendix A. Selected Results of Simulations of All Experiments Modeled Using the RADM Mechanism (continued).

Experiment	Initial Concentrations			Ave Temp	Ave H2O	Maximum Concentration OZONE				Average Initial d([O3] - [NO])/dt			
	NOx (ppm)	HC (ppmC)	HC/NOx	(degK)	(ppm)	Expt (ppm)	Calc (ppm)	Calc -Expt (ppm)	Calc -Expt /Avg	Expt --	Calc (ppb/min)	Calc -Expt --	Calc -Expt /Avg
11. 1-Hexene-NOx													
ITC929	0.51	5.1	10.0	303.0	19000.	0.298	0.647	0.349	0.74	1.27	3.06	1.79	0.83
ITC931	0.49	10.3	21.1	303.0	20100.	0.606	0.799	0.193	0.27	2.82	9.84	7.02	1.11
ITC934	1.00	9.7	9.7	303.0	20300.	0.428	0.876	0.448	0.69	1.84	4.59	2.75	0.86
ITC937	0.99	0.1	0.1	303.0	20300.	0.007	0.047	0.040		0.33	0.56	0.22	0.50
Group Average	0.75	6.3	10.2	303.0	19925.	0.335	0.593	0.258	0.57	1.57	4.51	2.95	0.82
S. Dev.	0.28	4.8	8.6	0.0	624.	0.252	0.376	0.179	0.25	1.04	3.92	2.91	0.25
Avg. Abs. Value								0.258	0.57			2.95	0.82
S. Dev.								0.179	0.25			2.91	0.25
12. Isoprene-NOx													
EC520	0.49	2.2	4.5	303.0	13000.	0.503	0.300	-0.203	-0.50	5.30	7.56	2.26	0.35
EC522	0.92	2.3	2.4	303.0	13000.	0.276	0.118	-0.158	-0.80	6.00	6.75	0.76	0.12
EC524	0.96	4.7	4.9	303.0	13000.	0.759	0.429	-0.330	-0.55	15.57	15.94	0.37	0.02
EC525	0.54	4.5	8.3	303.0	13000.	0.691	0.630	-0.061	-0.09	10.13	22.16	12.03	0.75
EC527	0.50	2.2	4.5	303.0	13000.	0.547	0.317	-0.230	-0.53	5.97	7.95	1.97	0.28
ITC811	0.50	3.4	6.8	303.0	17300.	0.919	0.577	-0.341	-0.46	10.00	8.95	-1.05	-0.11
ITC812	0.52	1.8	3.4	303.0	17300.	0.768	0.253	-0.515	-1.01	4.86	2.42	-2.43	-0.67
JL1680R	0.18	4.6	26.0	305.0	30200.	0.652	0.712	0.060	0.09	3.18	3.00	-0.18	-0.06
JL1680B	0.18	6.4	36.6	301.9	26800.	0.837	0.600	-0.237	-0.33	2.88	2.43	-0.44	-0.17
JL1780R	0.46	1.0	2.1	305.6	27000.	0.806	0.420	-0.386	-0.63	1.96	1.36	-0.60	-0.36
JL1780B	0.47	2.6	5.5	302.8	25000.	1.298	0.835	-0.463	-0.43	4.20	2.87	-1.33	-0.38
JL2381R	0.43	1.4	3.4	306.1	20000.*	0.750	0.691	-0.058	-0.08	2.13	2.01	-0.12	-0.06
ST0981R	0.17	1.0	6.1	297.5	20000.*	0.506	0.457	-0.049	-0.10	1.46	1.45	-0.01	0.00
Group Average	0.49	2.9	8.8	303.1	19123.	0.716	0.488	-0.229	-0.42	5.66	6.53	0.86	-0.02
S. Dev.	0.25	1.7	10.4	2.1	6284.	0.246	0.208	0.174	0.31	4.06	6.29	3.58	0.36
Avg. Abs. Value								0.238	0.43			1.81	0.26
S. Dev.								0.160	0.29			3.18	0.24
13. a-Pinene-NOx													
JL1580R	0.18	1.1	5.8	302.4	30300.	0.201	0.299	0.098	0.39	0.61	0.69	0.08	0.12
JL1580B	0.19	2.6	13.8	299.6	29200.	0.470	0.420	-0.051	-0.11	1.59	2.02	0.43	0.24
JL2580R	0.25	1.0	4.0	302.4	31700.	0.377	0.326	-0.051	-0.14	0.84	0.83	-0.01	-0.01
JL2580B	0.25	0.3	1.4	300.1	26300.	0.334	0.211	-0.124	-0.45	0.84	0.69	-0.15	-0.20
Group Average	0.22	1.3	6.3	301.1	29375.	0.346	0.314	-0.032	-0.08	0.97	1.06	0.09	0.04
S. Dev.	0.04	1.0	5.3	1.5	2291.	0.112	0.086	0.093	0.35	0.43	0.64	0.25	0.19
Avg. Abs. Value								0.081	0.28			0.17	0.14
S. Dev.								0.036	0.17			0.18	0.10

(continued)

Appendix A. Selected Results of Simulations of All Experiments Modeled Using the RADM Mechanism (continued).

Experiment	Initial Concentrations			Ave Temp	Ave H2O	Maximum Concentration OZONE				Average Initial d([O3] - [NO])/dt			
	NOx (ppm)	HC (ppmC)	HC/NOx	(degK)	(ppm)	Expt (ppm)	Calc (ppm)	Calc -Expt (ppm)	Calc -Expt /Avg	Expt --	Calc (ppb/min)	Calc -Expt --	Calc -Expt /Avg
14. Ethane-NOx													
ITC999	0.09	45.4	534.1	303.0	20500.	0.243	0.202	-0.042	-0.19	1.32	1.41	0.08	0.06
15. n-Butane-NOx													
EC130	0.10	17.6	179.3	303.0	26200.	0.459	0.458	-0.001	0.00	4.41	2.72	-1.70	-0.48
EC133	0.50	8.6	17.1	303.0	27800.	0.249	0.052	-0.197	-1.31	2.42	1.13	-1.29	-0.73
EC134	0.51	8.3	16.3	303.0	20000.*	0.034	0.042	0.008		0.94	1.36	0.42	0.37
EC137	0.50	8.7	17.3	303.0	20000.*	0.042	0.050	0.008		1.02	1.33	0.32	0.27
EC162	0.51	8.2	16.3	303.0	27300.	0.112	0.056	-0.056	-0.67	1.73	1.27	-0.45	-0.30
EC163	0.49	9.0	18.3	303.0	28500.	0.454	0.158	-0.296	-0.97	3.31	1.74	-1.57	-0.62
EC168	0.49	8.0	16.2	303.0	20700.	0.655	0.340	-0.315	-0.63	2.03	1.21	-0.82	-0.51
EC178	0.10	7.8	79.6	303.0	20900.	0.384	0.432	0.049	0.12	1.61	1.80	0.20	0.12
EC304	0.47	17.1	36.7	303.0	26800.	0.362	0.494	0.132	0.31	2.09	2.49	0.40	0.17
EC305	0.10	15.7	159.7	303.0	25400.	0.398	0.547	0.149	0.32	2.39	3.74	1.35	0.44
EC306	0.19	25.8	138.2	302.6	24200.	0.535	0.731	0.196	0.31	2.38	4.59	2.21	0.63
EC307	0.10	25.8	252.9	303.0	29700.	0.420	0.606	0.186	0.36	2.61	6.34	3.74	0.83
EC308	0.48	16.2	33.6	288.7	8750.	0.047	0.240	0.193		1.04	2.84	1.80	0.93
EC309	0.47	17.2	36.3	310.9	12400.	0.545	0.678	0.133	0.22	2.00	2.69	0.70	0.30
ITC507	0.09	15.2	165.0	303.0	20300.	0.149	0.397	0.248	0.91	0.69	1.68	1.00	0.84
ITC533	0.12	11.9	99.8	303.0	20800.	0.165	0.356	0.191	0.73	0.61	1.45	0.84	0.82
ITC770	0.52	37.9	72.8	303.0	16800.	0.042	0.059	0.017		1.56	2.13	0.57	0.31
ITC939	0.51	14.8	28.9	303.0	20300.	0.017	0.028	0.011		0.36	0.68	0.32	0.61
ITC948	0.26	10.0	38.2	303.0	20300.	0.054	0.159	0.105	0.99	0.53	1.17	0.64	0.75
OTC211	0.55	42.8	77.5	300.1	3530.*	0.008	0.258	0.250		0.56	1.51	0.94	0.91
JL2178R	0.24	7.2	29.9	302.9	20000.*	0.763	0.639	-0.124	-0.18	1.17	1.09	-0.08	-0.07
JL2178B	0.24	15.4	63.9	302.9	20000.*	0.986	0.910	-0.077	-0.08	1.64	1.50	-0.13	-0.08
JL2278R	0.55	7.9	14.4	305.2	20000.*	0.166	0.161	-0.006	-0.03	0.90	0.77	-0.13	-0.16
JL2278B	0.55	17.5	31.5	305.2	20000.*	0.788	0.484	-0.304	-0.48	1.55	1.33	-0.22	-0.15
ST1879B	0.21	21.2	103.1	298.3	20000.*	0.185	0.129	-0.056	-0.36	0.51	0.45	-0.06	-0.13
OC0979R	0.21	14.6	71.0	297.2	15300.	0.191	0.320	0.129	0.51	0.60	0.62	0.03	0.04
OC1879B	0.20	14.3	71.8	295.0	28100.	0.208	0.193	-0.015	-0.08	0.60	0.54	-0.06	-0.11
Group Average	0.34	15.7	69.8	302.1	20892.	0.312	0.332	0.021	0.00	1.53	1.86	0.33	0.19
S. Dev.	0.18	8.8	61.6	3.8	6033.	0.268	0.245	0.163	0.59	0.98	1.32	1.13	0.50
Avg. Abs. Value								0.128	0.46			0.81	0.43
S. Dev.								0.101	0.36			0.84	0.29
16. C4+ Branched Alkane-NOx													
EC165	0.10	11.3	114.3	303.0	18600.	0.488	0.482	-0.006	-0.01	1.77	1.60	-0.16	-0.10

(continued)

Appendix A. Selected Results of Simulations of All Experiments Modeled Using the RADM Mechanism (continued).

Experiment	Initial Concentrations			Ave Temp	Ave H2O	Maximum Concentration OZONE				Average Initial d([O3] - [NO])/dt			
	NOx (ppm)	HC (ppmC)	HC/NOx	(degK)	(ppm)	Expt (ppm)	Calc (ppm)	Calc -Expt (ppm)	Calc -Expt /Avg	Expt --	Calc (ppb/min)	Calc -Expt --	Calc -Expt /Avg
EC171	0.10	3.5	35.7	303.0	19000.	0.403	0.318	-0.085	-0.24	1.30	0.82	-0.48	-0.46
OC1879R	0.20	16.4	81.9	295.0	28100.	0.236	0.120	-0.116	-0.65	0.64	0.49	-0.15	-0.27
OC2079B	0.22	12.6	56.5	295.3	27800.	0.217	0.056	-0.161	-1.18	0.66	0.38	-0.28	-0.54
AU1983R	0.38	4.7	12.6	307.1	21300.	0.088	0.213	0.125	0.83	0.61	0.66	0.05	0.08
AU1983B	0.37	4.1	10.9	307.1	21300.	0.057	0.087	0.030	0.41	0.53	0.55	0.02	0.04
Group Average	0.22	8.2	47.9	301.9	24143.	0.283	0.231	-0.052	-0.17	0.93	0.75	-0.18	-0.22
S. Dev.	0.11	5.2	38.7	5.0	5463.	0.181	0.157	0.106	0.67	0.46	0.41	0.19	0.24
Avg. Abs. Value								0.096	0.53			0.20	0.26
S. Dev.								0.059	0.39			0.16	0.19
17. C5+ n-Alkane-NOx													
EC135	0.10	20.4	212.7	303.0	25000.	0.435	0.549	0.114	0.23	2.92	2.89	-0.02	-0.01
OC0979B	0.21	15.1	73.3	297.2	15200.	0.184	0.226	0.042	0.21	0.59	0.53	-0.06	-0.11
EC131	0.10	24.6	251.1	303.0	25000.	0.393	0.528	0.135	0.29	1.92	2.69	0.77	0.33
ITC559	0.19	279.4	1441.1	303.0	20300.	0.377	0.601	0.224	0.46	1.79	2.05	0.26	0.14
ITC538	0.11	60.3	529.0	303.0	18900.	0.150	0.313	0.162	0.70	0.74	1.05	0.31	0.35
ITC540	0.11	274.8	2421.3	303.0	20300.	0.360	0.384	0.024	0.06	1.85	1.12	-0.73	-0.49
ITC552	0.13	428.8	3278.4	303.0	20300.	0.315	0.358	0.042	0.13	1.19	1.09	-0.10	-0.08
ITC761	0.52	75.2	145.9	303.0	17500.	0.030	0.036	0.006		1.08	1.27	0.19	0.16
ITC762	0.27	74.7	280.4	303.0	17000.	0.105	0.186	0.081	0.55	0.83	1.53	0.70	0.59
ITC763	0.28	7.7	27.7	303.0	17100.	0.041	0.073	0.032		0.68	1.45	0.77	0.72
ITC797	0.52	7.3	14.0	303.0	12200.	0.004	0.011	0.007		0.64	0.98	0.34	0.42
ST1879R	0.21	6.3	30.4	298.3	20000.*	0.122	0.332	0.210	0.92	0.40	0.45	0.05	0.12
EC155	0.10	37.3	385.1	303.0	26200.	0.264	0.524	0.260	0.66	1.33	1.69	0.36	0.24
ITC1001	0.11	2.4	22.4	303.0	17500.	0.036	0.078	0.042		0.15	0.43	0.28	0.97
Group Average	0.21	93.9	650.9	302.3	19464.	0.201	0.300	0.099	0.42	1.15	1.37	0.22	0.24
S. Dev.	0.14	133.5	1015.3	1.9	3919.	0.153	0.204	0.086	0.28	0.75	0.76	0.40	0.37
Avg. Abs. Value								0.099	0.42			0.35	0.34
S. Dev.								0.086	0.28			0.28	0.28
18. Methylcyclohexane-NOx													
ITC765	0.53	0.0	0.1	303.0	17900.	0.022	0.012	-0.010		0.86	0.70	-0.16	-0.20
ITC766	0.26	0.0	0.1	303.0	17100.	0.121	0.169	0.047	0.33	0.87	1.37	0.50	0.45
ITC767	0.55	0.1	0.1	303.0	17900.	0.041	0.031	-0.010		1.09	1.08	-0.01	-0.01
ITC800	0.54	0.0	0.1	303.0	17500.	0.015	0.011	-0.004		0.86	0.76	-0.09	-0.11
Group Average	0.47	0.0	0.1	303.0	17600.	0.050	0.056	0.006	0.33	0.92	0.98	0.06	0.03
S. Dev.	0.14	0.0	0.0	0.0	383.					0.12	0.31	0.30	0.29
Avg. Abs. Value								0.018	0.33			0.19	0.19
S. Dev.												0.22	0.19

(continued)

Appendix A. Selected Results of Simulations of All Experiments Modeled Using the RADM Mechanism (continued).

Experiment	Initial Concentrations NOx (ppm)	Initial Concentrations HC (ppmC)	Initial Concentrations HC/NOx	Ave Temp (degK)	Ave H2O (ppm)	Maximum Concentration OZONE Expt (ppm)	Maximum Concentration OZONE Calc (ppm)	Maximum Concentration OZONE Calc -Expt (ppm)	Maximum Concentration OZONE Calc -Expt /Avg	Average Initial d([O3] - [NO])/dt Expt --	Average Initial d([O3] - [NO])/dt Calc (ppb/min)	Average Initial d([O3] - [NO])/dt Calc -Expt --	Average Initial d([O3] - [NO])/dt Calc -Expt /Avg
19. Benzene-NOx													
ITC560	0.12	332.3	2874.4	303.0	17100.	0.323	0.347	0.024	0.07	7.01	9.61	2.59	0.31
ITC561	0.11	79.1	694.2	303.0	17600.	0.273	0.285	0.013	0.05	4.75	4.79	0.04	0.01
ITC562	0.56	83.8	149.7	303.0	18800.	0.412	0.556	0.144	0.30	2.85	4.40	1.55	0.43
ITC698	0.50	83.5	167.4	303.0	21900.	0.374	0.507	0.133	0.30	2.87	4.37	1.49	0.41
ITC710	0.55	83.6	151.0	303.0	21000.	0.367	0.542	0.176	0.39	2.70	4.21	1.51	0.44
ITC831	1.01	12.2	12.1	303.0	18300.	0.021	0.007	-0.014		0.17	0.30	0.13	0.56
Group Average	0.47	112.4	674.8	303.0	19117.	0.295	0.374	0.079	0.22	3.39	4.61	1.22	0.36
S. Dev.	0.33	111.3	1103.2	0.0	1920.	0.142	0.211	0.081	0.15	2.30	2.96	0.97	0.19
Avg. Abs. Value								0.084	0.22			1.22	0.36
S. Dev.								0.075	0.15			0.97	0.19
20. Toluene-NOx													
EC264	0.48	8.1	17.0	303.0	18900.	0.419	0.427	0.008	0.02	4.46	4.94	0.49	0.10
EC265	0.48	7.5	15.6	303.0	21900.	0.393	0.426	0.032	0.08	3.56	4.83	1.27	0.30
EC266	0.49	8.4	17.0	303.0	19400.	0.405	0.432	0.026	0.06	4.62	5.10	0.48	0.10
EC269	0.47	4.0	8.4	303.0	19100.	0.318	0.380	0.063	0.18	2.55	2.78	0.23	0.09
EC270	0.46	4.2	9.0	303.0	20000.	0.369	0.420	0.051	0.13	3.72	4.16	0.44	0.11
EC271	0.21	8.0	37.4	303.0	20500.	0.296	0.307	0.012	0.04	6.56	4.92	-1.64	-0.29
EC272	0.48	4.1	8.5	303.0	19400.	0.410	0.374	-0.036	-0.09	3.69	2.81	-0.88	-0.27
EC273	0.11	4.1	37.2	303.0	21200.	0.215	0.223	0.008	0.04	5.90	3.09	-2.81	-0.63
EC327	0.45	4.0	8.9	303.0	22400.	0.376	0.423	0.047	0.12	2.49	3.05	0.56	0.20
EC336	0.44	7.2	16.3	303.0	26900.	0.396	0.463	0.067	0.16	6.06	6.82	0.76	0.12
EC337	0.45	7.9	17.7	303.0	27000.	0.325	0.427	0.102	0.27	2.55	4.22	1.67	0.49
EC339	0.44	5.0	11.3	303.0	26800.	0.225	0.404	0.179	0.57	1.53	3.12	1.59	0.68
EC340	0.43	4.1	9.5	303.0	25900.	0.344	0.419	0.074	0.19	2.50	2.90	0.40	0.15
ITC699	0.51	10.5	20.8	303.0	20300.	0.485	0.215	-0.270	-0.77	4.72	2.34	-2.38	-0.67
ITC828	1.02	3.0	3.0	303.0	17200.	0.021	0.006	-0.015		0.49	0.88	0.39	0.57
JL3080R	0.18	3.9	21.3	304.5	35200.	0.273	0.484	0.210	0.56	1.20	1.10	-0.10	-0.08
AU2780R	0.48	2.3	4.8	302.2	32000.	0.736	0.985	0.249	0.29	1.76	1.65	-0.11	-0.06
AU2782B	0.43	3.0	7.0	301.7	24700.	0.116	0.487	0.371	1.23	0.63	0.72	0.08	0.12
OC2782R	0.39	4.5	11.7	289.8	19500.	0.123	0.426	0.303	1.10	0.66	0.88	0.22	0.28
AU0183R	0.39	4.6	11.8	306.1	23700.	0.458	0.722	0.264	0.45	1.75	1.88	0.13	0.07
Group Average	0.44	5.4	14.7	302.5	23100.	0.335	0.423	0.087	0.24	3.07	3.11	0.04	0.07
S. Dev.	0.18	2.3	9.2	3.1	4692.	0.154	0.190	0.143	0.43	1.87	1.68	1.17	0.34
Avg. Abs. Value								0.119	0.33			0.83	0.27
S. Dev.								0.116	0.36			0.80	0.22

21. Xylene-NOx

(continued)

Appendix A. Selected Results of Simulations of All Experiments Modeled Using the RADM Mechanism (continued).

Experiment	Initial Concentrations			Ave Temp	Ave H2O	Maximum Concentration OZONE				Average Initial d([O3] - [NO])/dt			
	NOx (ppm)	HC (ppmC)	HC/NOx	(degK)	(ppm)	Expt (ppm)	Calc (ppm)	Calc -Expt (ppm)	Calc -Expt /Avg	Expt --	Calc (ppb/min)	Calc -Expt --	Calc -Expt /Avg
EC343	0.28	4.2	14.9	303.0	29500.	0.283	0.354	0.071	0.22	8.18	9.39	1.21	0.14
EC344	0.67	4.0	5.9	303.0	28900.	0.589	0.515	-0.073	-0.13	10.72	9.23	-1.50	-0.15
EC345	0.28	3.7	13.3	303.0	25200.	0.396	0.362	-0.033	-0.09	11.35	9.13	-2.22	-0.22
EC346	0.26	3.9	14.8	303.0	25900.	0.384	0.349	-0.034	-0.09	7.65	9.14	1.49	0.18
ITC702	0.52	4.0	7.8	303.0	20300.	0.627	0.338	-0.289	-0.60	7.79	3.10	-4.69	-0.86
ITC827	1.07	1.2	1.1	303.0	14400.	0.021	0.009	-0.012		1.12	1.25	0.13	0.11
JL3080B	0.18	2.2	12.4	304.5	28000.	0.555	0.519	-0.036	-0.07	1.97	1.96	-0.01	0.00
AU2782R	0.43	2.0	4.6	301.7	24700.	0.491	0.601	0.111	0.20	1.31	1.69	0.38	0.26
OC2782B	0.39	2.8	7.0	289.8	19500.	0.396	0.422	0.026	0.06	1.43	2.04	0.61	0.35
AU0183B	0.37	2.7	7.2	306.0	23700.	0.688	0.777	0.089	0.12	2.39	2.91	0.52	0.20
Group Average	0.45	3.1	8.9	302.0	24010.	0.443	0.425	-0.018	-0.04	5.39	4.98	-0.41	0.00
S. Dev.	0.26	1.0	4.7	4.4	4737.	0.195	0.202	0.113	0.25	4.14	3.69	1.89	0.35
Avg. Abs. Value								0.077	0.18			1.28	0.25
S. Dev.								0.081	0.17			1.39	0.23
22. Mesitylene-NOx													
EC900	0.53	5.4	10.2	303.0	20000.*	0.381	0.417	0.036	0.09	3.85			
EC901	0.51	2.7	5.2	303.0	20000.*	0.384	0.402	0.019	0.05	8.88	5.07	-3.81	-0.55
EC903	1.00	4.7	4.7	303.0	20000.*	0.502	0.591	0.089	0.16	14.96	8.16	-6.80	-0.59
ITC703	0.50	5.3	10.6	303.0	21000.	0.707	0.373	-0.334	-0.62	14.59	3.49	-11.10	-1.23
ITC706	0.49	2.7	5.4	303.0	21000.	0.641	0.318	-0.322	-0.67	7.20	2.13	-5.08	-1.09
ITC709	0.99	4.7	4.7	303.0	21000.	0.779	0.214	-0.565	-1.14	11.74	3.10	-8.64	-1.16
ITC742	0.48	4.6	9.7	303.0	18100.	0.773	0.406	-0.367	-0.62	13.14	2.95	-10.20	-1.27
ITC826	0.90	0.8	0.9	303.0	17200.	0.022	0.007	-0.015		1.68	0.85	-0.83	-0.66
Group Average	0.68	3.9	6.4	303.0	19788.	0.524	0.341	-0.183	-0.39	9.50	3.68	-6.64	-0.93
S. Dev.	0.24	1.6	3.4	0.0	1419.	0.258	0.171	0.243	0.50	4.97	2.36	3.67	0.32
Avg. Abs. Value								0.218	0.48			6.64	0.93
S. Dev.								0.206	0.40			3.67	0.32
23. Tetralin-NOx													
ITC739	0.52	2.4	4.6	303.0	17900.	0.002	0.202	0.200		0.63	1.47	0.84	0.80
ITC747	0.50	93.2	187.4	303.0	17100.	0.508	0.659	0.150	0.26	2.73	31.12	28.40	1.68
ITC748	0.22	84.0	385.1	303.0	17500.	0.370	0.484	0.114	0.27	2.60	20.16	17.56	1.54
ITC750	0.53	44.5	84.6	303.0	17100.	0.482	0.599	0.117	0.22	2.10	18.59	16.48	1.59
ITC832	1.00	39.4	39.5	303.0	16800.	0.073	0.025	-0.048	-0.98	1.38	0.99	-0.38	-0.33
Group Average	0.55	52.7	140.2	303.0	17280.	0.287	0.394	0.107	-0.06	1.89	14.47	12.58	1.06
S. Dev.	0.28	36.7	153.2	0.0	427.	0.235	0.271	0.093	0.62	0.88	13.01	12.21	0.85
Avg. Abs. Value								0.126	0.43			12.73	1.19
S. Dev.								0.056	0.37			12.01	0.60

(continued)

Experiment	Initial Concentrations			Ave Temp	Ave H2O	Maximum Concentration OZONE				Average Initial d([O3] - [NO])/dt			
	NOx (ppm)	HC (ppmC)	HC/NOx	(degK)	(ppm)	Expt (ppm)	Calc (ppm)	Calc -Expt (ppm)	Calc -Expt /Avg	Expt --	Calc (ppb/min)	Calc -Expt --	Calc -Expt /Avg
24. Naphthalene-NOx													
ITC751	0.52	7.5	14.3	303.0	15100.	0.113	0.505	0.392	1.27	1.08	4.76	3.68	1.26
ITC755	0.24	14.1	58.3	303.0	17500.	0.259	0.392	0.132	0.41	1.57	8.68	7.11	1.39
ITC756	0.26	27.4	106.8	303.0	17200.	0.282	0.451	0.168	0.46	2.20	13.91	11.71	1.45
ITC798	0.53	19.4	36.8	303.0	16400.	0.204	0.521	0.317	0.88	1.66	10.47	8.80	1.45
ITC802	0.53	8.4	15.9	303.0	16800.	0.124	0.503	0.379	1.21	1.42	5.34	3.91	1.16
Group Average	0.42	15.4	46.4	303.0	16600.	0.196	0.474	0.278	0.84	1.59	8.63	7.04	1.34
S. Dev.	0.15	8.3	38.2	0.0	935.	0.077	0.053	0.120	0.40	0.41	3.78	3.39	0.13
Avg. Abs. Value								0.278	0.84			7.04	1.34
S. Dev.								0.120	0.40			3.39	0.13
25. 2,3-Dimethylnaphthalene-NOx													
ITC775	0.29	1.7	5.8	303.0	16800.	0.274	0.185	-0.089	-0.39	1.73	1.28	-0.44	-0.29
ITC771	0.26	4.8	18.0	303.0	20300.	0.293	0.339	0.045	0.14	2.67	3.20	0.53	0.18
ITC806	0.33	5.9	17.7	303.0	17100.	0.360	0.388	0.028	0.08	2.69	3.35	0.66	0.22
ITC774	0.56	4.0	7.1	303.0	22700.	0.341	0.313	-0.028	-0.08	2.84	2.61	-0.23	-0.08
Group Average	0.36	4.1	12.2	303.0	19225.	0.317	0.306	-0.011	-0.06	2.48	2.61	0.13	0.01
S. Dev.	0.14	1.8	6.6	0.0	2806.	0.040	0.087	0.061	0.24	0.51	0.94	0.55	0.24
Avg. Abs. Value								0.048	0.17			0.47	0.19
S. Dev.								0.029	0.15			0.18	0.09
26. Simple Mixture Runs													
EC144	0.51	4.7	9.3	303.0	24400.	1.065	0.773	-0.292	-0.32	10.53	6.09	-4.44	-0.53
EC145	0.99	3.4	3.4	303.0	24400.	0.777	0.365	-0.411	-0.72	5.11	3.71	-1.40	-0.32
EC160	0.99	3.2	3.3	303.0	29200.	0.874	0.316	-0.559	-0.94	5.86	3.37	-2.49	-0.54
EC149	0.99	2.0	2.0	303.0	29300.	0.286	0.125	-0.161	-0.78	10.83	5.12	-5.71	-0.72
EC150	1.00	3.5	3.5	303.0	29900.	0.799	0.327	-0.472	-0.84	6.30	4.07	-2.22	-0.43
EC151	2.06	5.2	2.5	303.0	30400.	0.147	0.082	-0.064	-0.56	8.43	6.84	-1.58	-0.21
EC152	0.50	3.7	7.3	303.0	26400.	0.791	0.665	-0.126	-0.17	10.41	7.93	-2.48	-0.27
EC153	0.97	6.6	6.8	303.0	25400.	1.050	0.820	-0.230	-0.25	19.23	12.23	-7.00	-0.44
EC161	0.51	3.2	6.4	303.0	36900.	0.857	0.600	-0.258	-0.35	9.94	5.42	-4.53	-0.59
OC1278R	0.48	1.4	3.0	294.3	16100.	0.260	0.250	-0.010	-0.04	1.14	1.22	0.08	0.07
OC2578R	0.44	1.4	3.1	288.4	12800.	0.147	0.125	-0.022	-0.16	0.94	1.01	0.07	0.07
AU0180R	0.56	0.5	0.8	304.9	23400.	0.256	0.107	-0.148	-0.82	0.98	0.64	-0.34	-0.42
AU1480R	0.47	1.4	3.0	305.2	34700.	0.863	0.484	-0.379	-0.56	2.13	1.39	-0.75	-0.42
EC166	0.10	9.2	92.0	303.0	27700.	0.462	0.395	-0.067	-0.16	2.11	1.50	-0.61	-0.34
EC172	0.10	2.8	28.9	303.0	21600.	0.369	0.310	-0.059	-0.17	1.00	0.73	-0.27	-0.31
ST0682R	0.46	2.8	6.2	299.1	22200.	0.378	0.619	0.240	0.48	1.11	1.40	0.29	0.23

(continued)

Appendix A. Selected Results of Simulations of All Experiments Modeled Using the RADM Mechanism (continued).

Experiment	Initial Concentrations NOx (ppm)	Initial Concentrations HC (ppmC)	Initial Concentrations HC/NOx	Ave Temp (degK)	Ave H2O (ppm)	Maximum Concentration OZONE Expt (ppm)	Maximum Concentration OZONE Calc (ppm)	Maximum Concentration OZONE Calc -Expt (ppm)	Maximum Concentration OZONE Calc -Expt /Avg	Average Initial d([O3] - [NO])/dt Expt --	Average Initial d([O3] - [NO])/dt Calc (ppb/min)	Average Initial d([O3] - [NO])/dt Calc -Expt --	Average Initial d([O3] - [NO])/dt Calc -Expt /Avg
EC106	0.50	9.2	18.3	303.0	20900.	0.592	0.626	0.033	0.05	3.80	3.95	0.15	0.04
EC113	0.11	9.5	85.0	303.0	19500.	0.352	0.441	0.089	0.23	5.26	6.93	1.67	0.27
EC114	1.00	17.3	17.3	303.0	28800.	0.744	0.721	-0.023	-0.03	8.03	5.89	-2.14	-0.31
EC115	0.51	12.7	25.2	303.0	22000.	0.590	0.630	0.040	0.06	3.78	3.41	-0.36	-0.10
EC116	0.49	18.6	37.6	303.0	27300.	0.743	0.786	0.044	0.06	8.28	8.99	0.70	0.08
EC335	0.44	7.7	17.4	303.0	24700.	0.398	0.426	0.027	0.07	4.64	4.43	-0.22	-0.05
EC329	0.45	4.2	9.2	303.0	27700.	0.403	0.444	0.041	0.10	3.27	3.43	0.16	0.05
EC330	0.29	4.3	14.6	303.0	26000.	0.344	0.380	0.036	0.10	3.91	3.47	-0.44	-0.12
EC334	0.45	8.1	18.2	303.0	27800.	0.408	0.456	0.048	0.11	5.59	5.14	-0.45	-0.08
EC338	0.45	15.0	33.7	303.0	27600.	0.484	0.549	0.065	0.13	5.19	4.96	-0.24	-0.05
EC328	0.45	12.1	27.1	303.0	27500.	0.523	0.564	0.041	0.08	3.50	3.58	0.08	0.02
JL1581R	0.27	2.3	8.4	304.6	20000.*	0.485	0.694	0.209	0.35	1.08	1.21	0.13	0.12
JL1881R	0.26	2.1	8.0	302.2	20000.*	0.658	0.597	-0.062	-0.10	1.31	1.21	-0.10	-0.08
ST2481R	0.23	1.6	6.7	292.2	12800.	0.211	0.269	0.058	0.24	0.62	0.65	0.03	0.05
AU2781R	0.23	2.1	9.2	299.6	30900.	0.554	0.498	-0.056	-0.11	0.95	0.92	-0.04	-0.04
OC0382R	0.25	2.7	11.0	297.2	21200.	0.247	0.145	-0.102	-0.52	0.76	0.55	-0.21	-0.32
OC0382B	0.25	1.9	7.7	296.9	21100.	0.158	0.039	-0.119	-1.21	0.62			
NV1582R	0.18	2.6	14.4	283.8	20000.*	0.061	0.046	-0.015	-0.29	0.42	0.34	-0.08	-0.22
JL2281R	0.26	2.4	9.1	302.3*	20000.*	0.626	0.635	0.009	0.01	1.18	1.12	-0.06	-0.05
JL2181B	0.24	1.3	5.4	304.2*	20000.*	0.237	0.437	0.200	0.59	0.63	0.64	0.01	0.02
NV1582B	0.18	2.7	14.9	283.8	20000.*	0.167	0.246	0.079	0.38	0.71	0.76	0.05	0.07
DE0782B	0.19	3.5	18.7	286.4	13400.	0.093	0.304	0.212	1.07	0.55	0.74	0.19	0.30
JN1379B	0.44	6.1	13.7	294.9	20000.*	0.756	0.808	0.052	0.07	2.44	2.77	0.33	0.13
Group Average	0.49	5.2	15.5	300.2	24160.	0.492	0.443	-0.049	-0.12	4.10	3.32	-0.87	-0.13
S. Dev.	0.37	4.5	19.2	5.7	5188.	0.270	0.226	0.183	0.45	4.06	2.76	1.81	0.26
Avg. Abs. Value								0.133	0.34			1.09	0.22
S. Dev.								0.134	0.32			1.68	0.18
27. 3-Component and "Mini" Surrogates													
ITC479	0.09	4.0	43.4	303.0	20300.	0.332	0.304	-0.028	-0.09	2.95	3.47	0.52	0.16
ITC584	0.10	4.0	40.7	303.0	20300.	0.375	0.303	-0.071	-0.21	3.05	2.80	-0.25	-0.08
ITC579	0.10	3.4	34.7	303.0	15800.	0.356	0.270	-0.086	-0.28	1.54	1.25	-0.28	-0.20
ITC472	0.10	3.6	35.1	303.0	13700.	0.258	0.304	0.046	0.16	1.72	1.75	0.03	0.02
ITC474	0.09	4.2	45.1	303.0	15600.	0.293	0.320	0.027	0.09	3.40	4.84	1.44	0.35
ITC581	0.09	4.3	50.0	303.0	16100.	0.352	0.307	-0.045	-0.14	3.74	4.41	0.67	0.17
ITC585	0.10	4.8	50.8	303.0	17100.	0.311	0.325	0.014	0.04	5.11	6.10	0.99	0.18
ITC478	0.10	5.0	52.6	303.0	18300.	0.320	0.344	0.024	0.07	4.73	7.30	2.58	0.43
ITC482	0.10	1.2	12.3	303.0	18300.	0.279	0.277	-0.002	-0.01	2.44	3.00	0.55	0.20
ITC488	0.09	6.0	66.2	303.0	19600.	0.293	0.315	0.021	0.07	3.06	4.00	0.94	0.27
ITC492	0.09	8.1	88.4	303.0	15000.	0.326	0.340	0.014	0.04	3.28	4.30	1.02	0.27
ITC494	0.09	8.5	92.5	303.0	21100.	0.321	0.349	0.027	0.08	3.30	4.36	1.06	0.28
ITC498	0.10	3.9	40.2	303.0	19300.	0.320	0.317	-0.003	-0.01	2.16	2.21	0.05	0.02
ITC500	0.10	4.1	42.7	303.0	18700.	0.286	0.305	0.019	0.06	5.18	6.84	1.65	0.28
ITC502	0.09	4.6	49.5	303.0	18100.	0.271	0.291	0.021	0.07	7.07	12.43	5.35	0.55

(continued)

Appendix A. Selected Results of Simulations of All Experiments Modeled Using the RADM Mechanism (continued).

Experiment	Initial Concentrations			Ave Temp	Ave H2O	Maximum Concentration OZONE				Average Initial d([O3] - [NO])/dt			
	NOx (ppm)	HC (ppmC)	HC/NOx	(degK)	(ppm)	Expt (ppm)	Calc (ppm)	Calc -Expt (ppm)	Calc -Expt /Avg	Expt --	Calc (ppb/min)	Calc -Expt --	Calc -Expt /Avg
ITC466	0.10	6.5	62.7	303.0	18200.	0.131	0.274	0.143	0.71	0.77	2.57	1.80	1.08
ITC468	0.09	4.6	49.0	303.0	18000.	0.176	0.290	0.114	0.49	1.19	2.80	1.61	0.81
ITC451	0.10	5.2	52.0	303.0	19800.	0.312	0.295	-0.016	-0.05	3.95	3.92	-0.03	-0.01
ITC455	0.09	4.4	47.8	303.0	20200.	0.304	0.292	-0.012	-0.04	3.52	3.55	0.03	0.01
ITC977	0.13	3.2	25.1	303.0	20900.	0.329	0.312	-0.017	-0.05	3.94	2.36	-1.58	-0.50
ITC985	0.12	2.7	22.9	303.0	20100.	0.336	0.282	-0.054	-0.17	3.95	2.17	-1.78	-0.58
ITC997	0.12	2.7	23.0	303.0	20100.	0.316	0.281	-0.035	-0.12	3.89	2.15	-1.74	-0.58
ITC979	0.12	2.9	23.1	303.0	20100.	0.404	0.401	-0.003	-0.01	4.88	3.21	-1.66	-0.41
ITC992	0.12	2.6	20.9	303.0	20900.	0.384	0.393	0.009	0.02	5.57	3.59	-1.99	-0.43
ITC981	0.14	6.5	45.0	303.0	19000.	0.328	0.360	0.033	0.10	2.56	2.43	-0.13	-0.05
ITC993	0.11	7.1	66.9	303.0	20100.	0.276	0.347	0.071	0.23	2.45	2.06	-0.39	-0.17
JL1581B	0.28	2.3	8.0	304.6	20000.*	0.474	0.657	0.184	0.32	1.10	1.17	0.07	0.06
ST2481B	0.23	1.9	8.1	292.2	14200.	0.246	0.342	0.095	0.32	0.71	0.73	0.02	0.03
JN0982B	0.28	3.1	11.0	299.7*	14300.	0.667	0.604	-0.063	-0.10	1.37	1.22	-0.15	-0.12
JN1483R	0.22	2.6	11.6	301.2	26100.	0.585	0.558	-0.027	-0.05	1.10	1.10	-0.01	0.00
JN2783B	0.26	2.9	11.1	305.1	24400.	0.511	0.633	0.123	0.21	1.01	1.16	0.15	0.13
AU1883B	0.28	0.6	2.0	303.0	23100.	0.556	0.578	0.023	0.04	0.70	0.66	-0.04	-0.05
AU2683R	0.32	2.6	8.1	302.2	26400.	0.646	0.647	0.001	0.00	1.24	1.21	-0.03	-0.03
JL1881B	0.27	2.3	8.5	303.2	20000.*	0.693	0.644	-0.049	-0.07	1.91	1.81	-0.10	-0.05
JN0982R	0.29	3.1	10.7	299.7*	14700.	0.714	0.647	-0.067	-0.10	1.77	1.60	-0.17	-0.10
Group Average	0.14	4.1	37.0	302.6	19061.	0.366	0.383	0.016	0.07	2.81	3.13	0.33	0.08
S. Dev.	0.08	1.9	23.7	2.0	3028.	0.148	0.134	0.066	0.24	1.61	2.28	1.37	0.38
Avg. Abs. Value								0.049	0.15			0.90	0.27
S. Dev.								0.047	0.19			1.07	0.28

28. SAPRC 7-Component Surrogates

Experiment	NOx (ppm)	HC (ppmC)	HC/NOx	Ave Temp (degK)	Ave H2O (ppm)	Ozone Expt (ppm)	Ozone Calc (ppm)	Calc -Expt (ppm)	Calc -Expt /Avg	Expt --	Calc (ppb/min)	Calc -Expt --	Calc -Expt /Avg
EC231	0.49	13.2	26.9	303.0	17400.	0.620	0.698	0.078	0.12	6.99	7.72	0.73	0.10
EC232	0.49	9.3	18.9	303.0	17100.	0.342	0.408	0.066	0.18	3.12	3.04	-0.08	-0.03
EC233	0.10	9.5	92.5	303.0	21400.	0.330	0.381	0.051	0.14	4.07	4.67	0.60	0.14
EC237	0.48	10.5	21.6	303.0	23200.	0.652	0.639	-0.013	-0.02	7.36	6.06	-1.30	-0.19
EC238	0.95	10.1	10.6	303.0	25400.	0.691	0.708	0.017	0.02	5.10	4.98	-0.12	-0.02
EC241	0.49	5.0	10.2	303.0	20700.	0.408	0.407	-0.001	0.00	2.87	3.03	0.16	0.06
EC242	0.50	12.9	25.6	303.0	24600.	0.682	0.658	-0.024	-0.04	17.53	16.87	-0.66	-0.04
EC243	0.50	9.7	19.5	303.0	16400.	0.716	0.700	-0.016	-0.02	14.50	13.10	-1.41	-0.10
EC245	1.00	12.9	12.9	303.0	20400.	0.894	0.821	-0.073	-0.08	13.41	12.91	-0.50	-0.04
EC246	0.51	8.6	17.0	303.0	22100.	0.574	0.474	-0.100	-0.19	2.65	2.09	-0.57	-0.24
EC247	0.51	6.2	12.2	303.0	22700.	0.657	0.606	-0.052	-0.08	7.49	6.49	-1.00	-0.14
Group Average	0.55	9.8	24.4	303.0	21036.	0.597	0.591	-0.006	0.00	7.74	7.36	-0.38	-0.05
S. Dev.	0.24	2.6	23.3	0.0	3020.	0.173	0.149	0.056	0.11	5.16	4.85	0.71	0.12
Avg. Abs. Value								0.044	0.08			0.65	0.10
S. Dev.								0.032	0.07			0.45	0.07

(continued)

Appendix A. Selected Results of Simulations of All Experiments Modeled Using the RADM Mechanism (continued).

Experiment	Initial Concentrations NOx (ppm)	HC (ppmC)	HC/NOx	Ave Temp (degK)	Ave H2O (ppm)	Maximum Concentration OZONE Expt (ppm)	Calc (ppm)	Calc -Expt (ppm)	Calc -Expt /Avg	Average Initial d([O3] - [NO])/dt Expt --	Calc (ppb/min)	Calc -Expt --	Calc -Expt /Avg
29. SAPRC 8-Component Surrogates													
ITC626	0.30	4.0	13.4	303.0	14300.	0.618	0.531	-0.087	-0.15	2.18	1.57	-0.60	-0.32
ITC630	0.31	1.9	6.3	303.0	16300.	0.284	0.265	-0.019	-0.07	0.86	0.80	-0.06	-0.07
ITC631	0.32	1.0	3.2	303.0	17500.	0.043	0.069	0.027		0.47	0.44	-0.03	-0.06
ITC633	0.64	4.0	6.2	303.0	16600.	0.231	0.267	0.036	0.14	1.26	1.12	-0.15	-0.12
ITC635	1.21	4.0	3.3	303.0	17500.	0.006	0.022	0.016		0.95	0.78	-0.17	-0.20
ITC637	0.31	4.0	12.8	303.0	16900.	0.617	0.529	-0.088	-0.15	2.31	1.57	-0.74	-0.38
ITC865	0.28	8.4	29.9	303.0	15100.	0.632	0.491	-0.141	-0.25	2.60	2.44	-0.15	-0.06
ITC867	0.28	4.8	17.2	303.0	14600.	0.631	0.532	-0.099	-0.17	2.23	2.75	0.52	0.21
ITC868	0.37	2.9	7.8	303.0	17100.	0.518	0.409	-0.109	-0.24	2.10	1.20	-0.90	-0.55
ITC871	0.37	1.7	4.6	303.0	14600.	0.376	0.259	-0.116	-0.37	1.18	0.97	-0.21	-0.20
ITC872	0.38	2.1	5.7	303.0	14600.	0.213	0.234	0.022	0.10	1.20	1.20	0.01	0.01
ITC873	0.39	1.3	3.4	303.0	14600.	0.160	0.119	-0.041	-0.29	0.85	0.71	-0.13	-0.17
ITC874	0.38	2.1	5.7	303.0	13200.	0.191	0.164	-0.026	-0.15	0.83	0.79	-0.04	-0.05
ITC877	0.38	2.3	6.2	303.0	14600.	0.250	0.243	-0.008	-0.03	1.14	1.19	0.05	0.04
ITC880	0.73	2.2	3.0	303.0	13700.	0.031	0.051	0.020		0.85	0.86	0.01	0.01
ITC881	0.73	2.3	3.1	303.0	14000.	0.012	0.037	0.025		1.03	0.99	-0.04	-0.04
ITC885	0.64	1.5	2.4	303.0	14600.	0.012	0.029	0.018		0.44	0.68	0.25	0.44
ITC886	0.73	2.3	3.1	303.0	20000.*	0.012	0.024	0.012		1.24	0.63	-0.61	-0.65
ITC888	0.33	4.7	14.5	303.0	18000.	0.579	0.505	-0.074	-0.14	1.65	1.53	-0.12	-0.08
ITC891	0.32	4.4	13.7	303.0	20000.*	0.602	0.494	-0.108	-0.20	2.67	2.07	-0.60	-0.25
OTC189A	0.45	3.3	7.4	295.4	5000.*	0.576	0.789	0.214	0.31	3.79	3.48	-0.31	-0.09
OTC189B	0.45	4.0	8.9	298.0	5000.*	0.712	0.869	0.157	0.20	3.70	3.63	-0.07	-0.02
OTC190A	0.41	3.8	9.2	302.7	5400.*	0.702	0.867	0.164	0.21	4.24	3.27	-0.98	-0.26
OTC190B	0.42	3.8	9.0	299.5	5410.*	0.669	0.818	0.149	0.20	3.73	2.88	-0.85	-0.26
OTC192A	0.47	4.2	8.9	297.8	5000.*	0.735	0.874	0.139	0.17	4.25	3.32	-0.93	-0.25
OTC192B	0.47	4.2	8.9	298.4	5000.*	0.754	0.798	0.045	0.06	3.84	2.77	-1.07	-0.32
OTC194A	0.38	7.4	19.3	296.1	5000.*	0.737	0.890	0.152	0.19	7.85	7.07	-0.78	-0.10
OTC194B	0.38	3.7	9.7	295.7	5000.*	0.603	0.713	0.110	0.17	2.95	2.93	-0.02	-0.01
OTC195A	0.41	1.8	4.5	351.6	4660.*	0.164	0.126	-0.038	-0.27	2.05	1.21	-0.84	-0.51
OTC195B	0.41	4.1	9.9	360.0	3180.*	0.681	0.789	0.108	0.15	4.14	3.66	-0.48	-0.12
OTC196B	0.41	3.7	9.1	337.5	5000.*	0.597	0.830	0.233	0.33	3.86	3.26	-0.60	-0.17
OTC197A	0.38	3.6	9.5	353.2	5000.*	0.621	0.563	-0.058	-0.10	4.12	2.59	-1.52	-0.45
OTC197B	0.77	3.1	4.1	358.0	5000.*	0.152	0.130	-0.021	-0.15	2.86	2.07	-0.80	-0.32
OTC198A	0.84	5.4	6.4	353.5	5000.*	0.704	0.575	-0.129	-0.20	6.09	3.54	-2.56	-0.53
OTC198B	0.40	3.7	9.4	347.5	5000.*	0.674	0.640	-0.034	-0.05	3.86	2.50	-1.36	-0.43
OTC199A	0.36	3.5	9.6	299.7	5000.*	0.591	0.670	0.079	0.12	3.86	2.95	-0.91	-0.27
OTC199B	0.37	3.5	9.6	298.9	5000.*	0.606	0.654	0.048	0.08	3.40	2.84	-0.56	-0.18
OTC202A	0.73	6.0	8.2	325.1	5000.*	0.714	0.509	-0.205	-0.34	6.95	11.67	4.71	0.51
OTC202B	0.40	2.6	6.7	324.1	4560.*	0.522	0.441	-0.080	-0.17	3.82	3.10	-0.72	-0.21
OTC203A	0.39	3.5	9.0	293.3	4850.*	0.231	0.291	0.060	0.23	2.34	2.21	-0.13	-0.06
OTC203B	0.19	3.5	18.5	293.7	4880.*	0.394	0.436	0.041	0.10	2.20	2.46	0.26	0.11
OTC204A	0.35	3.6	10.2	322.2	4330.*	0.302	0.373	0.071	0.21	3.27	3.20	-0.06	-0.02
OTC204B	0.17	3.5	20.3	348.8	4330.*	0.381	0.460	0.079	0.19	2.62	2.71	0.09	0.03
OTC205A	0.84	3.8	4.5	464.9	5000.*	0.039	0.075	0.035		4.85	2.16	-2.69	-0.77
OTC205B	0.14	3.6	26.5	433.4	5000.*	0.392	0.542	0.150	0.32	4.49	3.45	-1.04	-0.26

(continued)

Experiment	Initial Concentrations			Ave Temp	Ave H2O	Maximum Concentration OZONE				Average Initial d([O3] - [NO])/dt			
	NOx (ppm)	HC (ppmC)	HC/NOx	(degK)	(ppm)	Expt (ppm)	Calc (ppm)	Calc -Expt (ppm)	Calc -Expt /Avg	Expt --	Calc (ppb/min)	Calc -Expt --	Calc -Expt /Avg
OTC215B	0.44	4.1	9.3	293.4	4420.*	0.868	0.937	0.069	0.08	5.33	5.33	0.00	0.00
OTC217A	0.50	4.9	9.6	295.5	7460.*	0.483	0.633	0.151	0.27	2.55	2.51	-0.05	-0.02
OTC217B	0.51	4.6	9.0	294.2	7460.*	0.831	0.937	0.105	0.12	4.64	4.10	-0.54	-0.12
OTC221A	0.41	2.4	5.8	290.6	4460.*	0.235	0.312	0.077	0.28	1.63	1.48	-0.15	-0.09
OTC221B	0.42	2.0	4.7	288.8	4460.*	0.333	0.372	0.039	0.11	1.63	1.57	-0.06	-0.04
OTC222A	0.44	3.4	7.8	298.5	5000.*	0.909	1.030	0.121	0.12	3.83	3.80	-0.03	-0.01
OTC222B	0.43	2.6	6.0	296.1	5000.*	0.940	1.169	0.229	0.22	5.55	6.22	0.67	0.11
OTC223A	0.36	4.8	13.4	314.9	4270.*	0.953	0.893	-0.060	-0.06	4.55	3.94	-0.61	-0.14
OTC223B	0.40	3.5	8.8	314.7	4270.*	0.771	0.756	-0.015	-0.02	3.15	2.83	-0.32	-0.11
OTC224A	0.34	4.4	12.7	303.5	6410.*	0.776	0.804	0.029	0.04	3.67	2.92	-0.76	-0.23
OTC224B	0.34	4.3	12.6	303.8	6410.*	0.813	0.847	0.035	0.04	4.94	4.19	-0.75	-0.16
OTC226A	0.45	2.5	5.5	312.5	6840.*	0.751	0.598	-0.153	-0.23	3.12	2.40	-0.72	-0.26
OTC228A	0.41	2.4	6.0	293.2	5000.*	0.246	0.483	0.237	0.65	1.49	1.92	0.43	0.25
OTC228B	0.41	2.3	5.6	294.3	5000.*	0.296	0.507	0.211	0.53	1.79	2.57	0.78	0.36
OTC229A	0.46	3.0	6.6	295.7	5000.*	0.253	0.517	0.264	0.69	1.56	1.98	0.42	0.24
OTC229B	0.46	1.7	3.8	296.0	5000.*	0.168	0.460	0.292	0.93	1.38	1.82	0.44	0.28
OTC230A	0.41	3.1	7.6	297.9	5000.*	0.489	0.873	0.384	0.56	2.43	3.05	0.62	0.23
OTC230B	0.41	1.7	4.2	298.2	5000.*	0.271	0.624	0.353	0.79	1.66	2.16	0.50	0.26
OTC237A	0.52	4.3	8.2	292.3	3810.*	0.807	0.865	0.058	0.07	4.10	3.41	-0.69	-0.18
OTC237B	0.52	4.4	8.5	292.8	3810.*	0.757	0.739	-0.018	-0.02	3.48	2.98	-0.49	-0.15
OTC238A	0.50	2.9	5.8	292.5	4810.*	0.406	0.441	0.035	0.08	2.58	2.21	-0.37	-0.15
OTC238B	0.50	3.9	7.8	292.0	4810.*	0.702	0.738	0.036	0.05	4.06	3.58	-0.47	-0.12
OTC239A	0.49	2.7	5.4	290.2	5150.*	0.343	0.449	0.106	0.27	2.66	2.53	-0.12	-0.05
OTC239B	0.50	2.5	5.0	290.9	5150.*	0.234	0.212	-0.022	-0.10	1.85	1.51	-0.34	-0.20
OTC240A	0.50	1.8	3.6	93.4	6210.*	0.034	0.049	0.015		1.08	0.94	-0.14	-0.14
OTC240B	0.50	2.0	4.1	104.2	6210.*	0.217	0.153	-0.064	-0.35	1.79	1.42	-0.37	-0.23
OTC241A	0.32	4.7	14.8	290.7	4760.*	0.671	0.694	0.023	0.03	3.26	2.88	-0.38	-0.12
OTC241B	0.31	4.0	12.9	291.1	4760.*	0.674	0.696	0.022	0.03	3.30	3.23	-0.07	-0.02
OTC242A	0.45	2.6	5.8	302.0	4670.*	0.182	0.211	0.029	0.15	1.47	1.38	-0.09	-0.07
OTC242B	0.46	2.1	4.7	302.1	4670.*	0.639	0.694	0.055	0.08	3.04	2.72	-0.32	-0.11
OTC243A	0.47	4.7	10.0	276.5	4720.*	0.142	0.202	0.060	0.35	1.41	1.73	0.32	0.21
OTC243B	0.38	3.7	9.7	277.4	4720.*	0.152	0.180	0.028	0.17	1.40	2.11	0.71	0.40
OTC248A	0.48	3.7	7.7	271.6	5000.*	0.056	0.069	0.013	0.21	1.40	1.21	-0.19	-0.14
OTC248B	0.46	2.9	6.3	268.9	5000.*	0.081	0.103	0.022	0.24	1.61	1.70	0.09	0.05
OTC249A	0.48	5.6	11.8	286.9	3540.*	0.348	0.360	0.012	0.03	2.55	2.31	-0.24	-0.10
OTC249B	0.46	4.9	10.7	286.2	3540.*	0.325	0.392	0.067	0.19	2.83	2.99	0.16	0.06
Group Average	0.45	3.5	8.7	302.3	7630.	0.454	0.498	0.044	0.09	2.81	2.54	-0.27	-0.10
S. Dev.	0.16	1.3	4.9	43.6	4865.	0.272	0.291	0.111	0.26	1.51	1.59	0.82	0.23
Avg. Abs. Value								0.088	0.20			0.54	0.19
S. Dev.								0.081	0.18			0.67	0.16

30. UNC Miscellaneous Surrogates

Experiment	NOx (ppm)	HC (ppmC)	HC/NOx	Ave Temp (degK)	Ave H2O (ppm)	Expt (ppm)	Calc (ppm)	Calc -Expt (ppm)	Calc -Expt /Avg	Expt --	Calc (ppb/min)	Calc -Expt --	Calc -Expt /Avg
ST2081R	0.23	2.3	10.0	294.1	21900.	0.403	0.479	0.076	0.17	0.95	1.11	0.15	0.15
DE0782R	0.19	3.4	18.3	286.4	13400.	0.076	0.369	0.293	1.31	0.52	0.78	0.26	0.40

(continued)

Appendix A. Selected Results of Simulations of All Experiments Modeled Using the RADM Mechanism (continued).

Experiment	Initial Concentrations			Ave Temp	Ave H2O	Maximum Concentration OZONE				Average Initial d([O3] - [NO])/dt			
	NOx (ppm)	HC (ppmC)	HC/NOx	(degK)	(ppm)	Expt (ppm)	Calc (ppm)	Calc -Expt (ppm)	Calc -Expt /Avg	Expt --	Calc (ppb/min)	Calc -Expt --	Calc -Expt /Avg
AU2681B	0.24	2.0	8.5	295.7	27500.	0.544	0.468	-0.077	-0.15	1.22	1.07	-0.15	-0.13
AU2781B	0.23	2.0	8.8	296.4	25000.	0.623	0.493	-0.130	-0.23	1.27	1.13	-0.14	-0.12
ST0381R	0.24	1.8	7.6	301.0	23200.	0.541	0.474	-0.067	-0.13	1.48	1.27	-0.21	-0.15
ST1081R	0.25	2.8	11.3	297.9	22300.	0.610	0.596	-0.015	-0.02	1.59	1.60	0.00	0.00
ST2081B	0.23	2.1	9.2	292.6	15200.	0.414	0.449	0.035	0.08	1.06	1.05	-0.01	-0.01
JL2081B	0.42	1.8	4.3	305.0*	20000.*	0.165	0.581	0.417	1.12	0.82	0.97	0.16	0.17
ST1682R	0.43	3.2	7.5	304.4	23000.	0.410	0.584	0.174	0.35	1.28	1.21	-0.07	-0.06
JL2081R	0.41	2.7	6.6	305.0*	20000.*	0.635	0.765	0.130	0.19	1.55	1.53	-0.02	-0.01
JL2281B	0.26	2.9	11.2	302.3*	20000.*	0.722	0.665	-0.057	-0.08	1.80	1.76	-0.04	-0.02
OC1481R	0.28	3.3	11.9	291.3	9470.	0.462	0.542	0.080	0.16	1.53	1.64	0.11	0.07
ST1682B	0.43	3.1	7.2	304.4	23000.	0.840	0.817	-0.023	-0.03	2.39	2.17	-0.22	-0.10
ST2981R	0.24	2.5	10.3	293.7	18700.	0.294	0.460	0.166	0.44	0.76	0.91	0.15	0.18
ST2981B	0.24	2.5	10.4	291.6	14400.	0.485	0.479	-0.006	-0.01	1.35	1.36	0.01	0.01
OC1481B	0.29	2.9	9.9	288.9	10300.	0.458	0.550	0.091	0.18	1.48	1.58	0.10	0.07
ST0381B	0.23	2.0	8.6	297.9	16800.	0.611	0.513	-0.098	-0.17	1.70	1.57	-0.13	-0.08
ST1081B	0.24	1.0	4.1	295.3	17700.	0.626	0.463	-0.163	-0.30	1.36	1.06	-0.30	-0.25
JL0882R	0.29	2.1	7.3	304.2	16000.	0.598	0.754	0.156	0.23	1.25	1.41	0.16	0.12
JL0882B	0.28	2.1	7.4	304.2	16000.	0.541	0.743	0.201	0.31	1.12	1.36	0.24	0.19
Group Average	0.28	2.4	9.0	297.7	19018.	0.503	0.561	0.058	0.17	1.32	1.32	0.00	0.02
S. Dev.	0.08	0.6	3.0	5.8	4902.	0.175	0.122	0.145	0.40	0.40	0.33	0.16	0.15
Avg. Abs. Value								0.118	0.27			0.13	0.11
S. Dev.								0.099	0.33			0.09	0.10
31. UNC "Synurban" Surrogate													
AU2284R	0.32	0.4	1.2	302.7	8470.	0.657	0.802	0.145	0.20	1.61	1.70	0.09	0.06
AU2584R	0.34	0.1	0.3	302.0	22600.	0.075	0.145	0.070	0.64	0.70	0.66	-0.04	-0.05
AU2584B	0.33	0.1	0.4	302.0	22600.	0.096	0.181	0.085	0.61	0.69	0.68	-0.01	-0.01
ST0184R	0.31	0.2	0.6	302.5	9380.	0.546	0.725	0.179	0.28	1.32	1.39	0.07	0.05
ST0184B	0.30	0.2	0.8	302.5	9380.	0.646	0.743	0.097	0.14	1.72	1.66	-0.06	-0.03
ST0284R	0.34	0.1	0.4	304.6	19900.	0.119	0.343	0.224	0.97	0.73	0.78	0.05	0.07
ST0284B	0.33	0.1	0.3	304.5	19900.	0.020	0.192	0.172		0.40	0.51	0.11	0.24
JN2685R	0.30	0.2	0.6	303.6	16800.	0.629	0.721	0.093	0.14	1.34	1.54	0.20	0.14
JN2685B	0.30	0.3	0.9	303.6	16800.	0.788	0.791	0.003	0.00	1.74	1.93	0.19	0.10
JN2885R	0.38	0.1	0.4	299.8	11800.	0.238	0.488	0.250	0.69	0.85	0.94	0.09	0.10
JN2885B	0.39	0.2	0.5	299.8	11800.	0.275	0.353	0.078	0.25	0.87	0.92	0.06	0.06
Group Average	0.33	0.2	0.6	302.5	15403.	0.372	0.499	0.127	0.39	1.09	1.16	0.07	0.07
S. Dev.	0.03	0.1	0.3	1.6	5427.	0.284	0.265	0.074	0.31	0.47	0.50	0.08	0.08
Avg. Abs. Value								0.127	0.39			0.09	0.08
S. Dev.								0.074	0.31			0.06	0.06

32. UNC "Synauto" Surrogate

(continued)

Appendix A. Selected Results of Simulations of All Experiments Modeled Using the RADM Mechanism (continued).

Experiment	Initial Concentrations			Ave Temp	Ave H2O	Maximum Concentration OZONE				Average Initial d([O3] - [NO])/dt			
	NOx (ppm)	HC (ppmC)	HC/NOx	(degK)	(ppm)	Expt (ppm)	Calc (ppm)	Calc -Expt (ppm)	Calc -Expt /Avg	Expt --	Calc (ppb/min)	Calc -Expt --	Calc -Expt /Avg
AU0484R	0.37	0.4	1.0	307.5	34900.	0.515	0.701	0.186	0.31	1.45	1.46	0.01	0.01
AU0484B	0.36	0.3	0.8	307.5	34700.	0.328	0.622	0.294	0.62	1.16	1.17	0.01	0.01
AU0584R	0.36	0.3	0.7	307.1	44900.	0.335	0.535	0.200	0.46	1.08	1.03	-0.06	-0.05
AU0584B	0.35	0.4	1.0	307.2	44900.	0.595	0.700	0.105	0.16	1.48	1.44	-0.04	-0.03
AU0684R	0.35	0.7	2.1	307.6	36800.	0.887	0.891	0.004	0.00	2.53	2.17	-0.36	-0.15
AU0684B	0.35	1.1	3.2	307.6	36800.	0.940	0.935	-0.005	0.00	3.16	2.58	-0.58	-0.20
AU0784R	0.38	0.4	1.0	308.0	34700.	0.602	0.727	0.125	0.19	1.61	1.55	-0.06	-0.04
AU0884B	0.34	1.1	3.1	307.3	29000.	0.834	0.846	0.012	0.01	2.92	2.44	-0.48	-0.18
AU0984R	0.39	0.4	0.9	307.8	31500.	0.521	0.648	0.127	0.22	1.51	1.33	-0.18	-0.13
ST0884R	0.34	0.6	1.9	298.5	6920.	0.566	0.769	0.203	0.30	1.27	1.44	0.17	0.12
ST0884B	0.33	1.0	2.9	298.5	6920.	0.750	0.877	0.127	0.16	1.90	1.73	-0.18	-0.10
ST1784R	0.34	1.1	3.3	294.4	24800.	0.539	0.687	0.148	0.24	1.59	2.35	0.76	0.39
ST1784B	0.34	0.8	2.3	294.4	24800.	0.484	0.685	0.201	0.34	1.38	2.03	0.65	0.38
ST2184R	0.36	0.6	1.7	302.2	7350.	0.671	0.833	0.162	0.22	1.78	2.05	0.27	0.14
ST2184B	0.36	0.7	2.0	302.2	7350.	0.721	0.847	0.126	0.16	2.28	2.64	0.35	0.14
Group Average	0.35	0.7	1.9	303.9	27089.	0.619	0.754	0.134	0.23	1.81	1.83	0.02	0.02
S. Dev.	0.02	0.3	0.9	5.1	13697.	0.182	0.114	0.082	0.17	0.63	0.53	0.38	0.18
Avg. Abs. Value								0.135	0.23			0.28	0.14
S. Dev.								0.081	0.17			0.25	0.12
33. UNC Auto Exhaust													
OC0483B	0.25	0.4	1.7	299.7	18800.	0.642	0.706	0.064	0.10	1.86	2.02	0.17	0.09
OC0783R	0.33	2.7	8.1	295.5	21600.	0.178	0.469	0.291	0.90	0.94	1.18	0.24	0.23
OC0783B	0.34	2.7	7.9	295.4	21500.	0.451	0.637	0.186	0.34	1.41	2.00	0.59	0.34
JN2582R	0.65	0.6	0.9	301.1*	22700.	0.003	0.016	0.014		0.64	0.59	-0.05	-0.08
JN2582B	0.65	0.6	0.9	301.2*	22900.	0.003	0.018	0.014		0.68	0.59	-0.09	-0.14
JN2982R	0.24	2.5	10.3	303.1	30500.	0.704	0.814	0.109	0.14	2.32	2.14	-0.19	-0.08
JN2982B	0.25	2.5	9.8	303.1	30500.	0.766	0.817	0.052	0.07	2.67	2.21	-0.46	-0.19
JN3082R	0.32	2.8	8.7	302.5*	20000.*	0.811	0.965	0.154	0.17	2.55	2.46	-0.09	-0.04
JN3082B	0.32	0.6	1.7	302.3*	20000.*	0.840	0.973	0.133	0.15	2.68	2.46	-0.22	-0.08
JL0283B	0.19	1.7	9.1	304.0	24500.	0.697	0.850	0.153	0.20	1.65	1.75	0.09	0.06
JL0883B	0.37	1.7	4.6	299.5	21200.	0.879	0.898	0.019	0.02	1.76	1.52	-0.24	-0.15
ST2982B	0.39	1.7	4.3	295.7	24800.	0.205	0.079	-0.126	-0.89	1.12	0.82	-0.30	-0.31
OC0682R	0.46	2.0	4.3	300.2	16900.	0.355	0.348	-0.007	-0.02	1.37	1.23	-0.14	-0.11
AU1183R	0.22	2.2	9.9	306.8	21400.	0.850	0.887	0.036	0.04	2.55	2.19	-0.35	-0.15
AU1183B	0.23	0.7	3.1	306.9	21400.	0.601	0.696	0.096	0.15	1.26	1.29	0.03	0.03
JL0182R	0.37	3.5	9.6	299.5	27700.	0.740	0.998	0.258	0.30	2.31	2.47	0.16	0.07
JL0182B	0.35	3.6	10.2	299.3	27400.	0.759	0.946	0.187	0.22	2.41	2.59	0.18	0.07
AU0382R	0.44	2.5	5.7	302.6	27400.	0.344	0.527	0.183	0.42	1.26	1.27	0.01	0.01
AU0382B	0.16	1.2	7.3	302.6	27400.	0.576	0.513	-0.063	-0.11	1.06	0.95	-0.12	-0.12
ST1782R	0.26	2.2	8.6	300.1	27400.	0.562	0.598	0.036	0.06	1.63	1.19	-0.43	-0.31
ST1782B	0.25	2.4	9.5	300.1	27400.	0.637	0.621	-0.017	-0.03	1.72	1.30	-0.41	-0.27
ST2982R	0.39	1.7	4.4	295.7	24800.	0.073	0.063	-0.010	-0.14	0.86	0.70	-0.16	-0.20
OC0682B	0.46	2.0	4.3	300.2	16900.	0.450	0.406	-0.043	-0.10	1.49	1.34	-0.15	-0.11

(continued)

Appendix A. Selected Results of Simulations of All Experiments Modeled Using the RADM Mechanism (concluded).

Experiment	Initial Concentrations			Ave Temp	Ave H20	Maximum Concentration OZONE				Average Initial d([O3] - [NO])/dt			
	NOx (ppm)	HC (ppmC)	HC/NOx	(degK)	(ppm)	Expt (ppm)	Calc (ppm)	Calc -Expt (ppm)	Calc -Expt /Avg	Expt --	Calc (ppb/min)	Calc -Expt --	Calc -Expt /Avg
JL0883R	0.37	1.7	4.6	299.5	21200.	0.756	0.778	0.022	0.03	1.52	1.43	-0.09	-0.06
JL1583R	0.35	2.2	6.2	306.2	25700.	0.866	0.800	-0.066	-0.08	2.10	1.87	-0.23	-0.11
JL1583B	0.35	2.3	6.6	306.2	25700.	0.922	0.896	-0.026	-0.03	2.20	2.08	-0.12	-0.06
OC0483R	0.25	2.6	10.3	299.7	18800.	0.603	0.668	0.066	0.10	1.76	1.81	0.05	0.03
Group Average	0.34	2.0	6.5	301.2	23607.	0.567	0.632	0.065	0.08	1.68	1.60	-0.08	-0.06
S. Dev.	0.12	0.8	3.1	3.3	3802.	0.272	0.299	0.101	0.29	0.61	0.60	0.23	0.15
Avg. Abs. Value								0.090	0.19			0.19	0.13
S. Dev.								0.078	0.23			0.14	0.09
34. SAPRC Synthetic Jet Fuel													
ITC781	0.51	43.0	83.5	303.0	16600.	0.751	0.847	0.096	0.12	2.77	3.33	0.56	0.18
ITC784	0.50	88.0	177.6	303.0	16600.	0.746	0.905	0.160	0.19	3.93	4.15	0.22	0.05
ITC785	0.26	45.0	170.7	303.0	17900.	0.598	0.625	0.027	0.04	2.74	3.05	0.31	0.11
ITC805	0.52	98.0	189.5	303.0	17200.	0.791	0.934	0.144	0.17	3.27	4.02	0.75	0.21
ITC795	0.50	45.0	89.8	303.0	17900.	0.761	0.804	0.043	0.06	3.05	4.30	1.25	0.34
ITC796	0.54	97.0	178.9	303.0	17200.	0.597	0.876	0.279	0.38	4.43	5.31	0.88	0.18
ITC799	0.51	94.0	184.1	303.0	17200.	0.840	0.953	0.113	0.13	4.59	3.75	-0.84	-0.20
ITC801	0.55	41.0	75.1	303.0	17000.	0.881	0.885	0.004	0.00	2.98	2.94	-0.05	-0.02
Group Average	0.49	68.9	143.7	303.0	17200.	0.746	0.854	0.108	0.14	3.47	3.86	0.38	0.11
S. Dev.	0.09	27.3	50.8	0.0	499.	0.102	0.104	0.088	0.12	0.74	0.78	0.64	0.16
Avg. Abs. Value								0.108	0.14			0.61	0.16
S. Dev.								0.088	0.12			0.40	0.10
35. SAPRC Synthetic Jet Exhaust													
ITC963	0.49	4.4	9.1	303.0	19400.	0.822	0.705	-0.117	-0.15	4.00	3.72	-0.29	-0.07
ITC965	0.46	5.2	11.3	303.0	20000.	0.863	0.714	-0.149	-0.19	5.10	4.73	-0.37	-0.08
ITC967	0.26	4.4	17.2	303.0	18300.	0.586	0.580	-0.006	-0.01	5.79	5.59	-0.20	-0.04
ITC968	0.49	8.7	17.8	303.0	19400.	0.852	0.777	-0.075	-0.09	11.76	10.28	-1.48	-0.13
Group Average	0.42	5.7	13.8	303.0	19275.	0.781	0.694	-0.087	-0.11	6.66	6.08	-0.58	-0.08
S. Dev.	0.11	2.1	4.3	0.0	709.	0.131	0.082	0.062	0.08	3.48	2.90	0.60	0.04
Avg. Abs. Value								0.087	0.11			0.58	0.08
S. Dev.								0.062	0.08			0.60	0.04

APPENDIX B

SELECTED RESULTS OF SIMULATIONS OF ALL ORGANIC-NO_X EXPERIMENTS MODELED USING THE RADM-M MECHANISM

Appendix B. Selected Results of Simulations of Individual Organic-NOx-Air Experiments Using the RADM-M Mechanism.

Experiment	Initial Concentrations			Ave Temp	Ave H2O	Maximum Concentration OZONE				Average Initial d([O3] - [NO])/dt			
	NOx (ppm)	HC (ppmC)	HC/NOx	(degK)	(ppm)	Expt (ppm)	Calc (ppm)	Calc -Expt (ppm)	Calc -Expt /Avg	Expt --	Calc (ppb/min)	Calc -Expt --	Calc -Expt /Avg
1. Ethene-NOx													
EC142	0.48	1.9	4.1	303.0	26500.	0.782	0.475	-0.307	-0.49	3.20	2.20	-1.00	-0.37
EC143	0.50	4.1	8.1	303.0	22700.	1.087	0.791	-0.296	-0.32	8.50	4.51	-3.99	-0.61
EC156	0.50	4.0	8.0	303.0	29000.	1.105	0.751	-0.354	-0.38	8.89	4.50	-4.39	-0.66
EC285	1.01	3.9	3.9	303.0	20400.	0.840	0.892	0.052	0.06	5.05	4.89	-0.15	-0.03
EC286	0.94	7.5	8.0	303.0	20500.	1.081	1.172	0.091	0.08	11.76	10.13	-1.63	-0.15
EC287	0.53	8.0	15.1	303.0	19700.	0.965	1.026	0.061	0.06	13.89	13.00	-0.88	-0.07
ITC926	0.51	7.9	15.6	303.0	21100.	0.982	0.920	-0.062	-0.06	6.96	4.91	-2.05	-0.35
ITC936	0.50	3.9	7.8	303.0	20300.	0.940	0.838	-0.102	-0.11	2.72	2.34	-0.38	-0.15
AU0479R	0.23	0.9	3.9	298.9	32500.	0.729	0.554	-0.175	-0.27	1.60	0.99	-0.61	-0.47
AU0579R	0.64	4.1	6.4	292.4	29100.	1.294	1.142	-0.152	-0.12	3.17	2.27	-0.91	-0.33
OC0584R	0.36	3.2	8.8	297.3	20000.*	0.856	0.970	0.114	0.12	2.16	1.98	-0.18	-0.09
OC1184R	0.35	2.9	8.2	297.2	12700.	0.858	1.039	0.182	0.19	2.22	2.01	-0.21	-0.10
OC1284R	0.72	2.7	3.7	295.6	13600.	0.495	0.185	-0.310	-0.91	1.58	1.17	-0.41	-0.30
OC0584B	0.37	1.8	5.0	297.3	20000.*	0.675	0.646	-0.029	-0.04	1.48	1.33	-0.15	-0.11
Group Average	0.55	4.1	7.6	300.2	22007.	0.906	0.814	-0.092	-0.16	5.23	4.02	-1.21	-0.27
S. Dev.	0.22	2.3	3.8	3.6	5611.	0.204	0.275	0.179	0.30	4.10	3.53	1.39	0.20
Avg. Abs. Value								0.163	0.23			1.21	0.27
S. Dev.								0.111	0.24			1.39	0.20
2. Propene-NOx													
EC121	0.51	1.5	2.9	303.0	26500.	0.506	0.460	-0.046	-0.09	7.46	4.10	-3.36	-0.58
EC177	0.46	1.5	3.2	303.0	26900.	0.540	0.471	-0.069	-0.14	3.89	4.00	0.11	0.03
EC216	0.52	1.5	3.0	303.0	18100.	0.564	0.555	-0.009	-0.02	4.18	5.69	1.51	0.31
EC217	0.48	0.6	1.2	303.0	21400.	0.149	0.230	0.081	0.43	0.80	1.30	0.50	0.48
EC230	0.52	1.9	3.7	303.0	17200.	0.344	0.329	-0.015	-0.05	3.06	4.78	1.72	0.44
EC256	0.56	0.4	0.7	303.0	20200.	0.002	0.011	0.008		0.98	1.08	0.10	0.10
EC257	0.56	0.7	1.3	303.0	20000.	0.068	0.098	0.029	0.35	3.35	4.20	0.84	0.22
EC276	0.52	1.6	3.2	303.0	14500.	0.388	0.447	0.059	0.14	3.24	4.41	1.16	0.30
EC277	0.11	1.7	15.7	303.0	15700.	0.313	0.395	0.082	0.23	8.27	8.06	-0.21	-0.03
EC278	0.49	3.1	6.2	303.0	16100.	0.625	0.702	0.076	0.12	7.72	9.83	2.11	0.24
EC279	0.97	3.5	3.5	303.0	14200.	0.679	0.706	0.027	0.04	6.64	8.08	1.43	0.19
EC314	0.93	3.2	3.5	303.0	24000.	0.728	0.786	0.058	0.08	7.21	10.36	3.15	0.36
EC315	0.94	2.9	3.1	288.7	10600.	0.344	0.661	0.316	0.63	4.33	6.42	2.09	0.39
EC316	0.98	3.2	3.3	312.0	44900.	0.955	1.051	0.096	0.10	10.64	11.93	1.29	0.11
EC317	0.54	1.5	2.8	303.0	24200.	0.615	0.570	-0.046	-0.08	4.06	4.71	0.65	0.15
ITC693	0.49	3.5	7.2	303.0	20300.	0.779	0.718	-0.062	-0.08	5.07	5.72	0.65	0.12
ITC810	0.52	2.8	5.4	303.0	16800.	0.782	0.721	-0.061	-0.08	4.25	4.57	0.31	0.07
ITC860	0.52	3.0	5.8	303.0	17100.	0.585	0.680	0.096	0.15	3.57	4.88	1.31	0.31
ITC925	0.54	2.8	5.2	303.0	16300.	0.779	0.728	-0.051	-0.07	3.72	4.14	0.42	0.11
ITC938	0.52	2.8	5.3	303.0	19000.	0.729	0.719	-0.010	-0.01	3.61	4.24	0.63	0.16
ITC947	0.53	1.9	3.6	303.0	20300.	0.710	0.715	0.005	0.01	3.34	4.14	0.80	0.21
ITC960	0.50	2.8	5.5	303.0	20300.	0.721	0.712	-0.009	-0.01	4.23	4.40	0.17	0.04

(continued)

Appendix B. Selected Results of Simulations of Individual Organic-NOx-Air Experiments Using the RADM-M Mechanism (continued).

Experiment	Initial Concentrations NOx (ppm)	Initial Concentrations HC (ppmC)	Initial Concentrations HC/NOx	Ave Temp (degK)	Ave H2O (ppm)	Maximum Concentration OZONE Expt (ppm)	Maximum Concentration OZONE Calc (ppm)	Maximum Concentration OZONE Calc -Expt (ppm)	Maximum Concentration OZONE Calc -Expt /Avg	Average Initial d([O3] - [NO])/dt Expt --	Average Initial d([O3] - [NO])/dt Calc (ppb/min)	Average Initial d([O3] - [NO])/dt Calc -Expt --	Average Initial d([O3] - [NO])/dt Calc -Expt /Avg
OTC186	0.55	3.6	6.6	299.8	5000.*	0.822	0.939	0.117	0.13	5.16	7.81	2.65	0.41
OTC191	0.54	3.7	6.9	309.3	5000.*	0.903	1.155	0.252	0.24	12.18	13.94	1.77	0.14
OTC210	0.57	2.7	4.8	304.7	3720.*	0.972	1.006	0.034	0.03	6.70	6.36	-0.34	-0.05
OTC233	0.46	0.1	0.2	303.6	5000.*	0.633	0.934	0.301	0.38	3.69	5.50	1.81	0.39
OTC236	0.53	3.3	6.3	300.0	6510.*	0.848	1.015	0.167	0.18	6.91	8.41	1.50	0.20
JA1078R	0.46	3.1	6.9	265.1	20000.*	0.363	0.604	0.240	0.50	0.46	0.48	0.02	0.04
OC1278B	0.48	1.4	2.9	294.3	16300.	0.461	0.413	-0.048	-0.11	1.40	1.45	0.05	0.03
OC2078R	0.46	1.3	2.9	290.4	9590.	0.340	0.403	0.063	0.17	1.23	1.38	0.15	0.12
OC2078B	0.46	3.5	7.7	290.4	9560.	0.727	0.948	0.221	0.26	2.83	3.53	0.70	0.22
OC2178R	0.50	3.9	7.9	290.3	20000.*	0.670	0.913	0.243	0.31	2.53	3.44	0.91	0.31
OC2578B	0.44	1.3	2.9	288.4	12800.	0.230	0.269	0.039	0.16	1.03	1.15	0.12	0.11
JN1279R	0.50	1.0	2.1	293.5	20000.*	0.382	0.306	-0.076	-0.22	0.85	0.77	-0.09	-0.11
JN1279B	0.49	1.5	3.0	293.5	20000.*	0.673	0.515	-0.158	-0.27	1.24	1.10	-0.14	-0.12
JN1379R	0.45	2.9	6.5	294.9	20000.*	0.974	0.874	-0.099	-0.11	2.69	2.83	0.14	0.05
AU0279R	0.22	1.5	7.0	307.2	20000.*	0.788	0.632	-0.156	-0.22	2.41	2.06	-0.35	-0.16
AU2780B	0.48	1.9	4.0	302.2	28400.	1.044	1.183	0.139	0.12	3.26	2.84	-0.42	-0.14
ST0482B	0.23	1.1	4.9	300.5	11800.	0.658	0.614	-0.044	-0.07	1.46	1.59	0.13	0.08
ST1382B	0.33	1.1	3.3	302.6	24100.	0.731	0.687	-0.045	-0.06	1.69	1.61	-0.08	-0.05
JL1783R	0.27	1.1	3.9	307.2	29700.	0.848	0.720	-0.127	-0.16	2.10	1.75	-0.35	-0.18
JL2183R	0.22	1.1	5.0	308.5	23800.	0.804	0.731	-0.072	-0.09	1.76	1.87	0.10	0.06
JL2983B	0.21	1.1	5.3	303.1	23300.	0.697	0.739	0.042	0.06	1.66	1.74	0.08	0.05
JL3183R	0.21	1.1	5.1	305.0	19800.	0.719	0.687	-0.032	-0.05	1.81	1.67	-0.14	-0.08
ST2383B	0.38	1.6	4.3	292.5	23400.	0.405	0.666	0.261	0.49	1.23	1.67	0.44	0.31
OC0484R	0.36	2.1	5.9	296.8	20000.*	0.645	0.759	0.114	0.16	2.07	2.15	0.08	0.04
OC0484B	0.36	1.0	2.9	296.7	20000.*	0.446	0.474	0.029	0.06	1.25	1.21	-0.04	-0.04
OC1184B	0.36	2.2	6.3	297.2	12700.	0.674	0.772	0.098	0.14	2.38	2.45	0.06	0.03
OC1284B	0.68	2.0	2.9	295.9	13500.	0.432	0.471	0.039	0.09	1.67	1.64	-0.03	-0.02
Group Average	0.49	2.1	4.6	299.9	18134.	0.608	0.651	0.043	0.08	3.62	4.15	0.53	0.11
S. Dev.	0.18	1.0	2.5	7.5	7349.	0.238	0.253	0.117	0.20	2.60	3.08	1.01	0.19
Avg. Abs. Value								0.093	0.16			0.76	0.17
S. Dev.								0.081	0.14			0.85	0.14
3. 1-Butene-NOx													
EC122	0.50	0.9	1.7	303.0	22000.	0.227	0.081	-0.147	-0.95	2.29	1.40	-0.89	-0.48
EC123	0.51	1.6	3.2	303.0	27200.	0.506	0.280	-0.226	-0.58	4.16	2.30	-1.86	-0.58
EC124	0.99	1.7	1.7	303.0	24500.	0.247	0.132	-0.115	-0.61	1.99	1.71	-0.27	-0.15
ITC927	0.31	3.8	12.3	303.0	19000.	0.646	0.727	0.081	0.12	3.24	4.54	1.31	0.34
ITC928	0.67	3.8	5.7	303.0	18400.	0.022	0.045	0.023		1.36	1.69	0.34	0.22
ITC930	0.32	7.2	22.2	303.0	21100.	0.717	0.827	0.110	0.14	7.91	11.13	3.22	0.34
ITC935	0.66	7.6	11.6	303.0	19700.	0.872	0.972	0.100	0.11	5.39	7.15	1.76	0.28
ST2383R	0.40	1.5	3.7	292.6	23400.	0.206	0.451	0.244	0.74	0.96	1.15	0.20	0.19
ST2583R	0.46	1.6	3.6	292.3	18800.	0.266	0.449	0.182	0.51	1.16	1.31	0.15	0.12
ST2583B	0.42	2.9	6.8	292.3	18900.	0.594	0.783	0.190	0.28	1.78	2.19	0.41	0.21
ST2783R	0.45	1.6	3.6	295.5	19400.	0.285	0.452	0.167	0.45	1.19	1.31	0.12	0.10

(continued)

Appendix B. Selected Results of Simulations of Individual Organic-NOx-Air Experiments Using the RADM-M Mechanism (continued).

Experiment	Initial Concentrations			Ave Temp	Ave H2O	Maximum Concentration OZONE				Average Initial d([O3] - [NO])/dt			
	NOx (ppm)	HC (ppmC)	HC/NOx	(degK)	(ppm)	Expt (ppm)	Calc (ppm)	Calc -Expt (ppm)	Calc -Expt /Avg	Expt --	Calc (ppb/min)	Calc -Expt --	Calc -Expt /Avg
Group Average	0.52	3.1	6.9	299.4	21127.	0.417	0.472	0.055	0.02	2.86	3.26	0.41	0.05
S. Dev.	0.20	2.3	6.2	5.0	2856.	0.263	0.321	0.154	0.55	2.18	3.18	1.34	0.32
Avg. Abs. Value								0.144	0.45			0.96	0.27
S. Dev.								0.066	0.29			0.99	0.15
4. trans-2-Butene-NOx													
EC146	0.51	0.9	1.8	303.0	26900.	0.247	0.109	-0.138	-0.77	5.87	3.84	-2.02	-0.42
EC147	0.98	1.7	1.7	303.0	22300.	0.154	0.083	-0.071	-0.60	9.83	7.39	-2.45	-0.28
EC157	0.53	0.9	1.7	303.0	27500.	0.205	0.091	-0.114	-0.77	5.96	3.54	-2.42	-0.51
ST2783B	0.43	2.0	4.7	295.5	19400.	0.523	0.543	0.019	0.04	3.00	3.16	0.15	0.05
Group Average	0.61	1.4	2.5	301.1	24025.	0.282	0.207	-0.076	-0.53	6.17	4.48	-1.68	-0.29
S. Dev.	0.25	0.6	1.5	3.7	3860.	0.165	0.224	0.069	0.38	2.80	1.96	1.24	0.24
Avg. Abs. Value								0.085	0.54			1.76	0.32
S. Dev.								0.052	0.35			1.09	0.20
5. Isobutene-NOx													
ITC694	0.51	4.6	9.1	303.0	20000.	0.900	0.731	-0.169	-0.21	8.84	6.03	-2.81	-0.38
6. 1-Hexene-NOx													
ITC929	0.51	5.1	10.0	303.0	19000.	0.298	0.670	0.372	0.77	1.27	3.32	2.05	0.89
ITC931	0.49	10.3	21.1	303.0	20100.	0.606	0.819	0.213	0.30	2.82	10.67	7.84	1.16
ITC934	1.00	9.7	9.7	303.0	20300.	0.428	0.894	0.466	0.71	1.84	5.00	3.16	0.92
ITC937	0.99	0.1	0.1	303.0	20300.	0.007	0.060	0.053		0.33	0.57	0.24	0.52
Group Average	0.75	6.3	10.2	303.0	19925.	0.335	0.611	0.276	0.59	1.57	4.89	3.32	0.88
S. Dev.	0.28	4.8	8.6	0.0	624.	0.252	0.379	0.182	0.26	1.04	4.26	3.25	0.26
Avg. Abs. Value								0.276	0.59			3.32	0.88
S. Dev.								0.182	0.26			3.25	0.26
7. Isoprene-NOx													
EC520	0.49	2.2	4.5	303.0	13000.	0.503	0.300	-0.203	-0.50	5.30	7.57	2.26	0.35
EC522	0.92	2.3	2.4	303.0	13000.	0.276	0.118	-0.158	-0.80	6.00	6.75	0.76	0.12
EC524	0.96	4.7	4.9	303.0	13000.	0.759	0.430	-0.330	-0.55	15.57	15.94	0.37	0.02
EC525	0.54	4.5	8.3	303.0	13000.	0.691	0.630	-0.061	-0.09	10.13	22.16	12.03	0.75

(continued)

Appendix B. Selected Results of Simulations of Individual Organic-NOx-Air Experiments Using the RADM-M Mechanism (continued).

Experiment	Initial Concentrations			Ave Temp	Ave H2O	Maximum Concentration OZONE				Average Initial d([O3] - [NO])/dt			
	NOx (ppm)	HC (ppmC)	HC/NOx	(degK)	(ppm)	Expt (ppm)	Calc (ppm)	Calc -Expt (ppm)	Calc -Expt /Avg	Expt --	Calc (ppb/min)	Calc -Expt --	Calc -Expt /Avg
EC527	0.50	2.2	4.5	303.0	13000.	0.547	0.317	-0.230	-0.53	5.97	7.95	1.97	0.28
ITC811	0.50	3.4	6.8	303.0	17300.	0.919	0.577	-0.342	-0.46	10.00	8.95	-1.05	-0.11
ITC812	0.52	1.8	3.4	303.0	17300.	0.768	0.253	-0.515	-1.01	4.86	2.42	-2.43	-0.67
JL1680R	0.18	4.6	26.0	305.0	30200.	0.652	0.712	0.060	0.09	3.18	3.00	-0.18	-0.06
JL1680B	0.18	6.4	36.6	301.9	26800.	0.837	0.600	-0.237	-0.33	2.88	2.43	-0.44	-0.17
JL1780R	0.46	1.0	2.1	305.6	27000.	0.806	0.420	-0.386	-0.63	1.96	1.36	-0.60	-0.36
JL1780B	0.47	2.6	5.5	302.8	25000.	1.298	0.835	-0.463	-0.43	4.20	2.87	-1.33	-0.38
JL2381R	0.43	1.4	3.4	306.1	20000.*	0.750	0.691	-0.058	-0.08	2.13	2.01	-0.12	-0.06
ST0981R	0.17	1.0	6.1	297.5	20000.*	0.506	0.457	-0.049	-0.10	1.46	1.45	-0.01	0.00
Group Average	0.49	2.9	8.8	303.1	19123.	0.716	0.488	-0.229	-0.42	5.66	6.53	0.86	-0.02
S. Dev.	0.25	1.7	10.4	2.1	6284.	0.246	0.208	0.174	0.31	4.06	6.29	3.58	0.36
Avg. Abs. Value								0.238	0.43			1.81	0.26
S. Dev.								0.160	0.29			3.18	0.24
8. a-Pinene-NOx													
JL1580R	0.18	1.1	5.8	302.4	30300.	0.201	0.297	0.095	0.38	0.61	0.67	0.06	0.10
JL1580B	0.19	2.6	13.8	299.6	29200.	0.470	0.421	-0.049	-0.11	1.59	1.96	0.37	0.21
JL2580R	0.25	1.0	4.0	302.4	31700.	0.377	0.327	-0.050	-0.14	0.84	0.83	-0.02	-0.02
JL2580B	0.25	0.3	1.4	300.1	26300.	0.334	0.211	-0.123	-0.45	0.84	0.68	-0.16	-0.21
Group Average	0.22	1.3	6.3	301.1	29375.	0.346	0.314	-0.032	-0.08	0.97	1.03	0.06	0.02
S. Dev.	0.04	1.0	5.3	1.5	2291.	0.112	0.087	0.092	0.34	0.43	0.62	0.22	0.18
Avg. Abs. Value								0.079	0.27			0.15	0.13
S. Dev.								0.036	0.17			0.16	0.09
9. Ethane-NOx													
ITC999	0.09	45.4	534.1	303.0	20500.	0.243	0.203	-0.041	-0.18	1.32	1.42	0.09	0.07
10. n-Butane-NOx													
EC130	0.10	17.6	179.3	303.0	26200.	0.459	0.442	-0.017	-0.04	4.41	2.44	-1.97	-0.58
EC133	0.50	8.6	17.1	303.0	27800.	0.249	0.043	-0.206	-1.41	2.42	1.05	-1.37	-0.79
EC134	0.51	8.3	16.3	303.0	20000.*	0.034	0.036	0.002		0.94	1.27	0.33	0.30
EC137	0.50	8.7	17.3	303.0	20000.*	0.042	0.043	0.001		1.02	1.24	0.23	0.20
EC162	0.51	8.2	16.3	303.0	27300.	0.112	0.048	-0.064	-0.80	1.73	1.19	-0.54	-0.37
EC163	0.49	9.0	18.3	303.0	28500.	0.454	0.151	-0.304	-1.00	3.31	1.69	-1.62	-0.65
EC168	0.49	8.0	16.2	303.0	20700.	0.655	0.308	-0.347	-0.72	2.03	1.12	-0.91	-0.58
EC178	0.10	7.8	79.6	303.0	20900.	0.384	0.418	0.034	0.09	1.61	1.65	0.04	0.03
EC304	0.47	17.1	36.7	303.0	26800.	0.362	0.422	0.060	0.15	2.09	2.26	0.17	0.08

(continued)

Appendix B. Selected Results of Simulations of Individual Organic-NOx-Air Experiments Using the RADM-M Mechanism (continued).

Experiment	Initial Concentrations			Ave Temp	Ave H2O	Maximum Concentration OZONE				Average Initial d([O3] - [NO])/dt			
	NOx (ppm)	HC (ppmC)	HC/NOx	(degK)	(ppm)	Expt (ppm)	Calc (ppm)	Calc -Expt (ppm)	Calc -Expt /Avg	Expt --	Calc (ppb/min)	Calc -Expt --	Calc -Expt /Avg
EC305	0.10	15.7	159.7	303.0	25400.	0.398	0.528	0.130	0.28	2.39	3.38	0.99	0.34
EC306	0.19	25.8	138.2	302.6	24200.	0.535	0.705	0.170	0.27	2.38	4.12	1.74	0.54
EC307	0.10	25.8	252.9	303.0	29700.	0.420	0.585	0.165	0.33	2.61	5.81	3.20	0.76
EC308	0.48	16.2	33.6	288.7	8750.	0.047	0.204	0.157		1.04	2.54	1.51	0.84
EC309	0.47	17.2	36.3	310.9	12400.	0.545	0.601	0.056	0.10	2.00	2.42	0.42	0.19
ITC507	0.09	15.2	165.0	303.0	20300.	0.149	0.350	0.201	0.81	0.69	1.52	0.83	0.75
ITC533	0.12	11.9	99.8	303.0	20800.	0.165	0.321	0.156	0.64	0.61	1.33	0.72	0.75
ITC770	0.52	37.9	72.8	303.0	16800.	0.042	0.048	0.006		1.56	1.94	0.38	0.22
ITC939	0.51	14.8	28.9	303.0	20300.	0.017	0.025	0.008		0.36	0.63	0.27	0.55
ITC948	0.26	10.0	38.2	303.0	20300.	0.054	0.137	0.083	0.87	0.53	1.08	0.55	0.68
OTC211	0.55	42.8	77.5	300.1	3530.*	0.008	0.181	0.173		0.56	1.37	0.81	0.83
JL2178R	0.24	7.2	29.9	302.9	20000.*	0.763	0.586	-0.177	-0.26	1.17	1.05	-0.12	-0.11
JL2178B	0.24	15.4	63.9	302.9	20000.*	0.986	0.861	-0.125	-0.14	1.64	1.45	-0.19	-0.12
JL2278R	0.55	7.9	14.4	305.2	20000.*	0.166	0.132	-0.034	-0.23	0.90	0.75	-0.15	-0.18
JL2278B	0.55	17.5	31.5	305.2	20000.*	0.788	0.406	-0.382	-0.64	1.55	1.27	-0.28	-0.20
ST1879B	0.21	21.2	103.1	298.3	20000.*	0.185	0.111	-0.075	-0.50	0.51	0.43	-0.08	-0.17
OC0979R	0.21	14.6	71.0	297.2	15300.	0.191	0.266	0.075	0.33	0.60	0.59	-0.01	-0.01
OC1879B	0.20	14.3	71.8	295.0	28100.	0.208	0.153	-0.055	-0.30	0.60	0.51	-0.09	-0.16
Group Average	0.34	15.7	69.8	302.1	20892.	0.312	0.300	-0.011	-0.10	1.53	1.71	0.18	0.12
S. Dev.	0.18	8.8	61.6	3.8	6033.	0.268	0.233	0.161	0.59	0.98	1.19	1.04	0.49
Avg. Abs. Value								0.121	0.47			0.72	0.41
S. Dev.								0.104	0.36			0.76	0.28
11. C4+ Branched Alkane-NOx													
EC165	0.10	11.3	114.3	303.0	18600.	0.488	0.481	-0.008	-0.02	1.77	1.46	-0.30	-0.19
EC169	0.19	4.5	23.5	303.0	32900.	0.493	0.340	-0.153	-0.37	1.00	0.74	-0.26	-0.30
EC171	0.10	3.5	35.7	303.0	19000.	0.403	0.311	-0.092	-0.26	1.30	0.81	-0.50	-0.47
OC1879R	0.20	16.4	81.9	295.0	28100.	0.236	0.106	-0.130	-0.76	0.64	0.45	-0.18	-0.34
OC2079B	0.22	12.6	56.5	295.3	27800.	0.217	0.051	-0.165	-1.23	0.66	0.36	-0.30	-0.59
AU1983R	0.38	4.7	12.6	307.1	21300.	0.088	0.231	0.143	0.90	0.61	0.66	0.05	0.09
AU1983B	0.37	4.1	10.9	307.1	21300.	0.057	0.098	0.041	0.53	0.53	0.56	0.03	0.06
Group Average	0.22	8.2	47.9	301.9	24143.	0.283	0.231	-0.052	-0.17	0.93	0.72	-0.21	-0.25
S. Dev.	0.11	5.2	38.7	5.0	5463.	0.181	0.156	0.115	0.73	0.46	0.36	0.20	0.25
Avg. Abs. Value								0.105	0.58			0.23	0.29
S. Dev.								0.060	0.41			0.16	0.20
12. C5+ n-Alkane-NOx													
EC135	0.10	20.4	212.7	303.0	25000.	0.435	0.543	0.108	0.22	2.92	2.44	-0.47	-0.18
OC0979B	0.21	15.1	73.3	297.2	15200.	0.184	0.205	0.021	0.11	0.59	0.51	-0.08	-0.15
EC131	0.10	24.6	251.1	303.0	25000.	0.393	0.524	0.131	0.29	1.92	2.26	0.33	0.16
ITC559	0.19	279.4	1441.1	303.0	20300.	0.377	0.516	0.139	0.31	1.79	1.58	-0.21	-0.12

(continued)

Appendix B. Selected Results of Simulations of Individual Organic-NOx-Air Experiments Using the RADM-M Mechanism (continued).

Experiment	Initial Concentrations			Ave Temp	Ave H2O	Maximum Concentration OZONE				Average Initial d([O3] - [NO])/dt			
	NOx (ppm)	HC (ppmC)	HC/NOx	(degK)	(ppm)	Expt (ppm)	Calc (ppm)	Calc -Expt (ppm)	Calc -Expt /Avg	Expt --	Calc (ppb/min)	Calc -Expt --	Calc -Expt /Avg
ITC538	0.11	60.3	529.0	303.0	18900.	0.150	0.457	0.306	1.01	0.74	1.50	0.76	0.68
ITC540	0.11	274.8	2421.3	303.0	20300.	0.360	0.546	0.186	0.41	1.85	1.62	-0.24	-0.14
ITC552	0.13	428.8	3278.4	303.0	20300.	0.315	0.532	0.217	0.51	1.19	1.59	0.39	0.28
ITC761	0.52	75.2	145.9	303.0	17500.	0.030	0.079	0.049		1.08	1.85	0.77	0.53
ITC762	0.27	74.7	280.4	303.0	17000.	0.105	0.327	0.221	1.02	0.83	2.30	1.47	0.94
ITC763	0.28	7.7	27.7	303.0	17100.	0.041	0.088	0.047		0.68	1.78	1.10	0.89
ITC797	0.52	7.3	14.0	303.0	12200.	0.004	0.012	0.007		0.64	1.10	0.46	0.53
ST1879R	0.21	6.3	30.4	298.3	20000.*	0.122	0.532	0.410	1.25	0.40	0.51	0.11	0.23
EC155	0.10	37.3	385.1	303.0	26200.	0.264	0.558	0.294	0.72	1.33	2.42	1.09	0.58
ITC1001	0.11	2.4	22.4	303.0	17500.	0.036	0.084	0.049		0.15	0.49	0.34	1.06
Group Average	0.21	93.9	650.9	302.3	19464.	0.201	0.357	0.156	0.58	1.15	1.57	0.42	0.38
S. Dev.	0.14	133.5	1015.3	1.9	3919.	0.153	0.215	0.122	0.39	0.75	0.69	0.57	0.43
Avg. Abs. Value								0.156	0.58			0.56	0.46
S. Dev.								0.122	0.39			0.42	0.33
13. Methylcyclohexane-NOx													
ITC765	0.53	0.0	0.1	303.0	17900.	0.022	0.012	-0.010		0.86	0.77	-0.09	-0.12
ITC766	0.26	0.0	0.1	303.0	17100.	0.121	0.301	0.180	0.85	0.87	2.03	1.16	0.80
ITC767	0.55	0.1	0.1	303.0	17900.	0.041	0.064	0.022		1.09	1.48	0.39	0.30
ITC800	0.54	0.0	0.1	303.0	17500.	0.015	0.012	-0.003		0.86	0.85	0.00	0.00
Group Average	0.47	0.0	0.1	303.0	17600.	0.050	0.097	0.047	0.85	0.92	1.28	0.36	0.25
S. Dev.	0.14	0.0	0.0	0.0	383.					0.12	0.59	0.57	0.41
Avg. Abs. Value								0.054	0.85			0.41	0.31
S. Dev.												0.53	0.35
14. Benzene-NOx													
ITC560	0.12	332.3	2874.4	303.0	17100.	0.323	0.335	0.012	0.04	7.01	15.99	8.98	0.78
ITC561	0.11	79.1	694.2	303.0	17600.	0.273	0.299	0.026	0.09	4.75	10.63	5.88	0.76
ITC562	0.56	83.8	149.7	303.0	18800.	0.412	0.528	0.116	0.25	2.85	10.21	7.36	1.13
ITC698	0.50	83.5	167.4	303.0	21900.	0.374	0.497	0.123	0.28	2.87	10.16	7.29	1.12
ITC710	0.55	83.6	151.0	303.0	21000.	0.367	0.512	0.145	0.33	2.70	9.68	6.98	1.13
ITC831	1.01	12.2	12.1	303.0	18300.	0.021	0.009	-0.012		0.17	0.31	0.14	0.60
Group Average	0.47	112.4	674.8	303.0	19117.	0.295	0.363	0.068	0.20	3.39	9.50	6.11	0.92
S. Dev.	0.33	111.3	1103.2	0.0	1920.	0.142	0.199	0.067	0.13	2.30	5.08	3.08	0.23
Avg. Abs. Value								0.072	0.20			6.11	0.92
S. Dev.								0.062	0.13			3.08	0.23

(continued)

Appendix B. Selected Results of Simulations of Individual Organic-NOx-Air Experiments Using the RADM-M Mechanism (continued).

Experiment	Initial Concentrations			Ave Temp	Ave H2O	Maximum Concentration OZONE				Average Initial d([O3] - [NO])/dt			
	NOx (ppm)	HC (ppmC)	HC/NOx	(degK)	(ppm)	Expt (ppm)	Calc (ppm)	Calc -Expt (ppm)	Calc -Expt /Avg	Expt --	Calc (ppb/min)	Calc -Expt --	Calc -Expt /Avg
15. Toluene-NOx													
EC264	0.48	8.1	17.0	303.0	18900.	0.419	0.387	-0.032	-0.08	4.46	5.13	0.67	0.14
EC265	0.48	7.5	15.6	303.0	21900.	0.393	0.383	-0.010	-0.03	3.56	4.95	1.39	0.33
EC266	0.49	8.4	17.0	303.0	19400.	0.405	0.391	-0.014	-0.04	4.62	5.30	0.68	0.14
EC269	0.47	4.0	8.4	303.0	19100.	0.318	0.293	-0.025	-0.08	2.55	2.54	-0.01	0.00
EC270	0.46	4.2	9.0	303.0	20000.	0.369	0.362	-0.006	-0.02	3.72	3.94	0.21	0.06
EC271	0.21	8.0	37.4	303.0	20500.	0.296	0.316	0.021	0.07	6.56	5.59	-0.97	-0.16
EC272	0.48	4.1	8.5	303.0	19400.	0.410	0.288	-0.122	-0.35	3.69	2.52	-1.17	-0.38
EC273	0.11	4.1	37.2	303.0	21200.	0.215	0.236	0.021	0.09	5.90	3.47	-2.43	-0.52
EC327	0.45	4.0	8.9	303.0	22400.	0.376	0.354	-0.022	-0.06	2.49	2.63	0.14	0.05
EC336	0.44	7.2	16.3	303.0	26900.	0.396	0.426	0.030	0.07	6.06	6.61	0.55	0.09
EC337	0.45	7.9	17.7	303.0	27000.	0.325	0.375	0.050	0.14	2.55	3.99	1.44	0.44
EC339	0.44	5.0	11.3	303.0	26800.	0.225	0.325	0.101	0.37	1.53	2.88	1.35	0.61
EC340	0.43	4.1	9.5	303.0	25900.	0.344	0.341	-0.004	-0.01	2.50	2.47	-0.03	-0.01
ITC699	0.51	10.5	20.8	303.0	20300.	0.485	0.430	-0.055	-0.12	4.72	4.86	0.14	0.03
ITC828	1.02	3.0	3.0	303.0	17200.	0.021	0.007	-0.014		0.49	1.15	0.66	0.80
JL3080R	0.18	3.9	21.3	304.5	35200.	0.273	0.414	0.140	0.41	1.20	1.03	-0.16	-0.15
AU2780R	0.48	2.3	4.8	302.2	32000.	0.736	0.866	0.130	0.16	1.76	1.51	-0.25	-0.15
AU2782B	0.43	3.0	7.0	301.7	24700.	0.116	0.261	0.146	0.77	0.63	0.65	0.02	0.02
OC2782R	0.39	4.5	11.7	289.8	19500.	0.123	0.334	0.212	0.93	0.66	0.79	0.13	0.18
AU0183R	0.39	4.6	11.8	306.1	23700.	0.458	0.537	0.079	0.16	1.75	1.70	-0.06	-0.03
Group Average	0.44	5.4	14.7	302.5	23100.	0.335	0.366	0.031	0.13	3.07	3.19	0.12	0.07
S. Dev.	0.18	2.3	9.2	3.1	4692.	0.154	0.156	0.081	0.31	1.87	1.79	0.91	0.31
Avg. Abs. Value								0.062	0.21			0.62	0.21
S. Dev.								0.060	0.26			0.65	0.23
16. Xylene-NOx													
EC343	0.28	4.2	14.9	303.0	29500.	0.283	0.380	0.097	0.29	8.18	10.74	2.56	0.27
EC344	0.67	4.0	5.9	303.0	28900.	0.589	0.524	-0.065	-0.12	10.72	9.84	-0.88	-0.09
EC345	0.28	3.7	13.3	303.0	25200.	0.396	0.390	-0.006	-0.01	11.35	10.79	-0.55	-0.05
EC346	0.26	3.9	14.8	303.0	25900.	0.384	0.375	-0.009	-0.02	7.65	10.71	3.06	0.33
ITC702	0.52	4.0	7.8	303.0	20300.	0.627	0.480	-0.147	-0.26	7.79	8.20	0.42	0.05
ITC827	1.07	1.2	1.1	303.0	14400.	0.021	0.012	-0.009		1.12	1.97	0.84	0.55
JL3080B	0.18	2.2	12.4	304.5	28000.	0.555	0.503	-0.052	-0.10	1.97	1.95	-0.02	-0.01
AU2782R	0.43	2.0	4.6	301.7	24700.	0.491	0.552	0.061	0.12	1.31	1.63	0.32	0.22
OC2782B	0.39	2.8	7.0	289.8	19500.	0.396	0.438	0.042	0.10	1.43	1.97	0.54	0.32
AU0183B	0.37	2.7	7.2	306.0	23700.	0.688	0.706	0.018	0.03	2.39	2.76	0.37	0.14
Group Average	0.45	3.1	8.9	302.0	24010.	0.443	0.436	-0.007	0.00	5.39	6.06	0.67	0.17
S. Dev.	0.26	1.0	4.7	4.4	4737.	0.195	0.179	0.069	0.16	4.14	4.29	1.25	0.20
Avg. Abs. Value								0.050	0.12			0.96	0.20
S. Dev.								0.045	0.10			1.01	0.17

(continued)

Experiment	Initial Concentrations			Ave Temp	Ave H2O	Maximum Concentration OZONE				Average Initial d([O3] - [NO])/dt			
	NOx (ppm)	HC (ppmC)	HC/NOx	(degK)	(ppm)	Expt (ppm)	Calc (ppm)	Calc -Expt (ppm)	Calc -Expt /Avg	Expt --	Calc (ppb/min)	Calc -Expt --	Calc -Expt /Avg
17. Mesitylene-NOx													
EC900	0.53	5.4	10.2	303.0	20000.*	0.381	0.419	0.038	0.09	3.85			
EC901	0.51	2.7	5.2	303.0	20000.*	0.384	0.323	-0.061	-0.17	8.88	3.57	-5.32	-0.85
EC903	1.00	4.7	4.7	303.0	20000.*	0.502	0.403	-0.099	-0.22	14.96	5.63	-9.33	-0.91
ITC703	0.50	5.3	10.6	303.0	21000.	0.707	0.478	-0.229	-0.39	14.59	9.62	-4.97	-0.41
ITC706	0.49	2.7	5.4	303.0	21000.	0.641	0.475	-0.165	-0.30	7.2C	4.45	-2.75	-0.47
ITC709	0.99	4.7	4.7	303.0	21000.	0.779	0.528	-0.251	-0.38	11.74	7.09	-4.65	-0.49
ITC742	0.48	4.6	9.7	303.0	18100.	0.773	0.481	-0.293	-0.47	13.14	8.01	-5.13	-0.48
ITC826	0.90	0.8	0.9	303.0	17200.	0.022	0.008	-0.013		1.68	1.18	-0.49	-0.34
Group Average	0.68	3.9	6.4	303.0	19788.	0.524	0.389	-0.134	-0.26	9.50	5.65	-4.66	-0.57
S. Dev.	0.24	1.6	3.4	0.0	1419.	0.258	0.166	0.119	0.19	4.97	2.86	2.69	0.22
Avg. Abs. Value								0.144	0.29			4.66	0.57
S. Dev.								0.106	0.13			2.69	0.22
18. Tetralin-NOx													
ITC739	0.52	2.4	4.6	303.0	17900.	0.002	0.325	0.322		0.63	2.57	1.95	1.22
ITC747	0.50	93.2	187.4	303.0	17100.	0.508	0.726	0.217	0.35	2.73	54.85	52.12	1.81
ITC748	0.22	84.0	385.1	303.0	17500.	0.370	0.478	0.108	0.26	2.60	31.70	29.11	1.70
ITC750	0.53	44.5	84.6	303.0	17100.	0.482	0.706	0.224	0.38	2.10	46.35	44.25	1.83
ITC832	1.00	39.4	39.5	303.0	16800.	0.073	0.352	0.279	1.31	1.38	1.00	-0.37	-0.31
Group Average	0.55	52.7	140.2	303.0	17280.	0.287	0.517	0.230	0.57	1.89	27.30	25.41	1.25
S. Dev.	0.28	36.7	153.2	0.0	427.	0.235	0.190	0.081	0.50	0.88	24.72	23.96	0.91
Avg. Abs. Value								0.230	0.57			25.56	1.37
S. Dev.								0.081	0.50			23.77	0.64
19. Naphthalene-NOx													
ITC751	0.52	7.5	14.3	303.0	15100.	0.113	0.534	0.421	1.30	1.08	11.24	10.15	1.65
ITC755	0.24	14.1	58.3	303.0	17500.	0.259	0.453	0.193	0.54	1.57	22.32	20.75	1.74
ITC756	0.26	27.4	106.8	303.0	17200.	0.282	0.491	0.209	0.54	2.20	29.67	27.47	1.72
ITC798	0.53	19.4	36.8	303.0	16400.	0.204	0.634	0.430	1.03	1.66	29.98	28.32	1.79
ITC802	0.53	8.4	15.9	303.0	16800.	0.124	0.542	0.418	1.26	1.42	12.52	11.10	1.59
Group Average	0.42	15.4	46.4	303.0	16600.	0.196	0.531	0.334	0.93	1.59	21.15	19.56	1.70
S. Dev.	0.15	8.3	38.2	0.0	935.	0.077	0.068	0.122	0.37	0.41	9.01	8.67	0.08
Avg. Abs. Value								0.334	0.93			19.56	1.70
S. Dev.								0.122	0.37			8.67	0.08

(continued)

Experiment	Initial Concentrations NOx (ppm)	HC (ppmC)	HC/NOx	Ave Temp (degK)	Ave H2O (ppm)	Maximum Concentration OZONE Expt (ppm)	Calc (ppm)	Calc -Expt (ppm)	Calc -Expt /Avg	Average Initial d([O3] - [NO])/dt Expt --	Calc (ppb/min)	Calc -Expt --	Calc -Expt /Avg
20. 2,3-Dimethylnaphthalene-NOx													
ITC775	0.29	1.7	5.8	303.0	16800.	0.274	0.275	0.001	0.00	1.73	2.47	0.74	0.35
ITC771	0.26	4.8	18.0	303.0	20300.	0.293	0.383	0.090	0.27	2.67	8.32	5.65	1.03
ITC806	0.33	5.9	17.7	303.0	17100.	0.360	0.432	0.072	0.18	2.69	8.91	6.22	1.07
ITC774	0.56	4.0	7.1	303.0	22700.	0.341	0.514	0.174	0.41	2.84	5.82	2.98	0.69
Group Average	0.36	4.1	12.2	303.0	19225.	0.317	0.401	0.084	0.21	2.48	6.38	3.90	0.79
S. Dev.	0.14	1.8	6.6	0.0	2806.	0.040	0.100	0.071	0.17	0.51	2.93	2.54	0.34
Avg. Abs. Value								0.084	0.21			3.90	0.79
S. Dev.								0.071	0.17			2.54	0.34
21. Simple Mixture Runs													
EC144	0.51	4.7	9.3	303.0	24400.	1.065	0.772	-0.293	-0.32	10.53	6.15	-4.39	-0.53
EC145	0.99	3.4	3.4	303.0	24400.	0.777	0.376	-0.401	-0.70	5.11	3.84	-1.27	-0.28
EC160	0.99	3.2	3.3	303.0	29200.	0.874	0.326	-0.548	-0.91	5.86	3.48	-2.39	-0.51
EC149	0.99	2.0	2.0	303.0	29300.	0.286	0.131	-0.155	-0.74	10.83	5.20	-5.63	-0.70
EC150	1.00	3.5	3.5	303.0	29900.	0.799	0.329	-0.470	-0.83	6.30	4.12	-2.17	-0.42
EC151	2.06	5.2	2.5	303.0	30400.	0.147	0.086	-0.060	-0.52	8.43	7.04	-1.38	-0.18
EC152	0.50	3.7	7.3	303.0	26400.	0.791	0.665	-0.127	-0.17	10.41	7.84	-2.57	-0.28
EC153	0.97	6.6	6.8	303.0	25400.	1.050	0.817	-0.233	-0.25	19.23	11.91	-7.32	-0.47
EC161	0.51	3.2	6.4	303.0	36900.	0.857	0.599	-0.259	-0.36	9.94	5.43	-4.51	-0.59
OC1278R	0.48	1.4	3.0	294.3	16100.	0.260	0.250	-0.010	-0.04	1.14	1.22	0.08	0.07
OC2578R	0.44	1.4	3.1	288.4	12800.	0.147	0.125	-0.022	-0.16	0.94	1.01	0.07	0.07
AU0180R	0.56	0.5	0.8	304.9	23400.	0.256	0.107	-0.149	-0.82	0.98	0.64	-0.35	-0.43
AU1480R	0.47	1.4	3.0	305.2	34700.	0.863	0.474	-0.389	-0.58	2.13	1.37	-0.76	-0.44
EC166	0.10	9.2	92.0	303.0	27700.	0.462	0.377	-0.085	-0.20	2.11	1.37	-0.74	-0.42
EC172	0.10	2.8	28.9	303.0	21600.	0.369	0.297	-0.072	-0.22	1.00	0.70	-0.29	-0.35
ST0682R	0.46	2.8	6.2	299.1	22200.	0.378	0.487	0.108	0.25	1.11	1.27	0.16	0.13
ST0682B	0.45	2.9	6.5	299.1	22200.	0.478	0.522	0.044	0.09	1.35	1.58	0.23	0.15
EC106	0.50	9.2	18.3	303.0	20900.	0.592	0.614	0.021	0.04	3.80	4.05	0.25	0.06
EC113	0.11	9.5	85.0	303.0	19500.	0.352	0.441	0.089	0.22	5.26	7.06	1.81	0.29
EC114	1.00	17.3	17.3	303.0	28800.	0.744	0.702	-0.042	-0.06	8.03	6.07	-1.95	-0.28
EC115	0.51	12.7	25.2	303.0	22000.	0.590	0.606	0.016	0.03	3.78	3.40	-0.38	-0.10
EC116	0.49	18.6	37.6	303.0	27300.	0.743	0.782	0.039	0.05	8.28	9.25	0.97	0.11
EC335	0.44	7.7	17.4	303.0	24700.	0.398	0.370	-0.028	-0.07	4.64	4.21	-0.43	-0.10
EC329	0.45	4.2	9.2	303.0	27700.	0.403	0.384	-0.019	-0.05	3.27	3.16	-0.10	-0.03
EC330	0.29	4.3	14.6	303.0	26000.	0.344	0.348	0.004	0.01	3.91	3.44	-0.47	-0.13
EC334	0.45	8.1	18.2	303.0	27800.	0.408	0.409	0.001	0.00	5.59	4.99	-0.59	-0.11
EC338	0.45	15.0	33.7	303.0	27800.	0.484	0.487	0.003	0.01	5.19	4.71	-0.49	-0.10
EC328	0.45	12.1	27.1	303.0	27500.	0.523	0.507	-0.016	-0.03	3.50	3.23	-0.27	-0.08
JL1581R	0.27	2.3	8.4	304.6	20000.*	0.485	0.691	0.206	0.35	1.08	1.23	0.15	0.13
JL1881R	0.26	2.1	8.0	303.2	20000.*	0.658	0.594	-0.065	-0.10	1.31	1.23	-0.08	-0.06
ST2481R	0.23	1.6	6.7	292.2	22800.	0.211	0.276	0.065	0.27	0.62	0.67	0.05	0.08
AU2781R	0.23	2.1	9.2	299.5	30900.	0.554	0.498	-0.056	-0.11	0.95	0.92	-0.03	-0.03

(continued)

Appendix B. Selected Results of Simulations of Individual Organic-NOx-Air Experiments Using the RADM-M Mechanism (continued).

Experiment	Initial Concentrations			Ave Temp	Ave H2O	Maximum Concentration OZONE				Average Initial d([O3] - [NO])/dt			
	NOx (ppm)	HC (ppmC)	HC/NOx	(degK)	(ppm)	Expt (ppm)	Calc (ppm)	Calc -Expt (ppm)	Calc -Expt /Avg	Expt --	Calc (ppb/min)	Calc -Expt --	Calc -Expt /Avg
OC0382R	0.25	2.7	11.0	297.2	21200.	0.247	0.137	-0.110	-0.57	0.76	0.54	-0.22	-0.33
OC0382B	0.25	1.9	7.7	296.9	21100.	0.158	0.038	-0.120	-1.22	0.62			
NV1582R	0.18	2.6	14.4	283.8	20000.*	0.061	0.042	-0.019	-0.36	0.42	0.33	-0.09	-0.24
JL2281R	0.26	2.4	9.1	302.3*	20000.*	0.626	0.638	0.012	0.02	1.18	1.12	-0.06	-0.05
JL2181B	0.24	1.3	5.4	304.2*	20000.*	0.237	0.441	0.204	0.60	0.63	0.65	0.01	0.02
NV1582B	0.18	2.7	14.9	283.8	20000.*	0.167	0.245	0.079	0.38	0.71	0.74	0.03	0.05
DE0782B	0.19	3.5	18.7	286.4	13400.	0.093	0.303	0.210	1.06	0.55	0.71	0.17	0.27
JN1379B	0.44	6.1	13.7	294.9	20000.*	0.756	0.809	0.053	0.07	2.44	2.78	0.33	0.13
Group Average	0.49	5.2	15.5	300.2	24160.	0.492	0.428	-0.065	-0.15	4.10	3.30	-0.89	-0.15
S. Dev.	0.37	4.5	19.2	5.7	5188.	0.270	0.220	0.172	0.43	4.06	2.76	1.82	0.25
Avg. Abs. Value								0.123	0.32			1.11	0.23
S. Dev.								0.136	0.32			1.69	0.18
22. 3-Component and "Mini" Surrogates													
ITC479	0.09	4.0	43.4	303.0	20300.	0.332	0.317	-0.015	-0.05	2.95	4.81	1.87	0.48
ITC584	0.10	4.0	40.7	303.0	20300.	0.375	0.314	-0.060	-0.18	3.05	3.95	0.90	0.26
ITC579	0.10	3.4	34.7	303.0	15800.	0.356	0.292	-0.064	-0.20	1.54	2.14	0.61	0.33
ITC472	0.10	3.6	35.1	303.0	13700.	0.258	0.319	0.061	0.21	1.72	3.01	1.30	0.55
ITC474	0.09	4.2	45.1	303.0	15600.	0.293	0.327	0.034	0.11	3.40	6.10	2.70	0.57
ITC581	0.09	4.3	50.0	303.0	16100.	0.352	0.313	-0.039	-0.12	3.74	5.30	1.56	0.35
ITC585	0.10	4.8	50.8	303.0	17100.	0.311	0.332	0.021	0.07	5.11	7.00	1.89	0.31
ITC478	0.10	5.0	52.6	303.0	18300.	0.320	0.351	0.031	0.09	4.73	8.20	3.48	0.54
ITC482	0.10	1.2	12.3	303.0	18300.	0.279	0.292	0.013	0.05	2.44	4.41	1.97	0.57
ITC488	0.09	6.0	66.2	303.0	19600.	0.293	0.327	0.034	0.11	3.06	5.18	2.12	0.51
ITC492	0.09	8.1	88.4	303.0	15000.	0.326	0.350	0.024	0.07	3.28	5.40	2.12	0.49
ITC494	0.09	8.5	92.5	303.0	21100.	0.321	0.358	0.036	0.11	3.30	5.34	2.04	0.47
ITC498	0.10	3.9	40.2	303.0	19300.	0.320	0.330	0.009	0.03	2.16	3.63	1.47	0.51
ITC500	0.10	4.1	42.7	303.0	18700.	0.286	0.318	0.031	0.10	5.18	7.42	2.23	0.35
ITC502	0.09	4.6	49.5	303.0	18100.	0.271	0.302	0.031	0.11	7.07	12.32	5.25	0.54
ITC462	0.11	7.5	71.3	303.0	18300.	0.099	0.267	0.168	0.92	0.70	2.49	1.79	1.12
ITC466	0.10	6.5	62.7	303.0	18200.	0.131	0.280	0.149	0.72	0.77	2.93	2.16	1.17
ITC468	0.09	4.6	49.0	303.0	18000.	0.176	0.299	0.123	0.52	1.19	3.46	2.27	0.98
ITC451	0.10	5.2	52.0	303.0	19800.	0.312	0.294	-0.018	-0.06	3.95	5.68	1.73	0.36
ITC455	0.09	4.4	47.8	303.0	20200.	0.304	0.295	-0.008	-0.03	3.52	5.08	1.56	0.36
ITC977	0.13	3.2	25.1	303.0	20900.	0.329	0.324	-0.006	-0.02	3.94	3.51	-0.43	-0.12
ITC985	0.12	2.7	22.9	303.0	20100.	0.336	0.294	-0.042	-0.13	3.95	3.32	-0.63	-0.17
ITC997	0.12	2.7	23.0	303.0	20100.	0.316	0.292	-0.024	-0.08	3.89	3.27	-0.61	-0.17
ITC979	0.12	2.9	23.1	303.0	20100.	0.404	0.414	0.010	0.02	4.88	4.11	-0.77	-0.17
ITC992	0.12	2.6	20.9	303.0	20900.	0.384	0.404	0.020	0.05	5.57	4.49	-1.08	-0.22
ITC981	0.14	6.5	45.0	303.0	19000.	0.328	0.377	0.049	0.14	2.56	3.73	1.17	0.37
ITC993	0.11	7.1	66.9	303.0	20100.	0.276	0.365	0.089	0.28	2.45	3.21	0.76	0.27
JL1581B	0.28	2.3	8.0	304.6	20000.*	0.474	0.619	0.145	0.27	1.10	1.15	0.05	0.05
ST2481B	0.23	1.9	8.1	292.2	14200.	0.246	0.274	0.028	0.11	0.71	0.70	-0.01	-0.01

(continued)

Appendix B. Selected Results of Simulations of Individual Organic-NOx-Air Experiments Using the RADM-M Mechanism (continued).

Experiment	Initial Concentrations NOx (ppm)	HC (ppmC)	HC/NOx	Ave Temp (degK)	Ave H2O (ppm)	Maximum Concentration OZONE Expt (ppm)	Calc (ppm)	Calc -Expt (ppm)	Calc -Expt /Avg	Average Initial d([O3] - [NO])/dt Expt --	Calc (ppb/min)	Calc -Expt --	Calc -Expt /Avg
JN0982B	0.28	3.1	11.0	299.7*	14300.	0.667	0.578	-0.089	-0.14	1.37	1.19	-0.18	-0.14
JN1483R	0.22	2.6	11.6	301.2	26100.	0.585	0.516	-0.069	-0.13	1.10	1.06	-0.04	-0.04
JN2783B	0.26	2.9	11.1	305.1	24400.	0.511	0.579	0.069	0.13	1.01	1.12	0.11	0.10
AU1883B	0.28	0.6	2.0	303.0	23100.	0.556	0.530	-0.025	-0.05	0.70	0.65	-0.05	-0.07
AU2683R	0.32	2.6	8.1	302.2	26400.	0.646	0.596	-0.050	-0.08	1.24	1.17	-0.07	-0.06
JL1881B	0.27	2.3	8.5	303.2	20000.*	0.693	0.620	-0.073	-0.11	1.91	1.76	-0.15	-0.08
JN0982R	0.29	3.1	10.7	299.7*	14700.	0.714	0.634	-0.080	-0.12	1.77	1.55	-0.22	-0.13
Group Average	0.14	4.1	37.0	302.6	19061.	0.366	0.380	0.014	0.08	2.81	3.88	1.08	0.28
S. Dev.	0.08	1.9	23.7	2.0	3028.	0.148	0.117	0.065	0.24	1.61	2.44	1.36	0.36
Avg. Abs. Value								0.051	0.16			1.32	0.36
S. Dev.								0.042	0.19			1.13	0.28
23. SAPRC 7-Component Surrogates													
EC231	0.49	13.2	26.9	303.0	17400.	0.620	0.715	0.094	0.14	6.99	7.67	0.68	0.09
EC232	0.49	9.3	18.9	303.0	17100.	0.342	0.374	0.032	0.09	3.12	2.91	-0.21	-0.07
EC233	0.10	9.5	92.5	303.0	21400.	0.330	0.386	0.056	0.16	4.07	4.34	0.27	0.06
EC237	0.48	10.5	21.6	303.0	23200.	0.652	0.648	-0.004	-0.01	7.36	5.89	-1.47	-0.22
EC238	0.95	10.1	10.6	303.0	25400.	0.691	0.701	0.010	0.01	5.10	4.71	-0.39	-0.08
EC241	0.49	5.0	10.2	303.0	20700.	0.408	0.378	-0.030	-0.08	2.87	2.90	0.03	0.01
EC242	0.50	12.9	25.6	303.0	24600.	0.682	0.686	0.004	0.01	17.53	16.65	-0.88	-0.05
EC243	0.50	9.7	19.5	303.0	16400.	0.716	0.722	0.006	0.01	14.50	12.77	-1.74	-0.13
EC245	1.00	12.9	12.9	303.0	20400.	0.894	0.856	-0.038	-0.04	13.41	12.82	-0.59	-0.05
EC246	0.51	8.6	17.0	303.0	22100.	0.574	0.434	-0.140	-0.28	2.65	1.95	-0.70	-0.30
EC247	0.51	6.2	12.2	303.0	22700.	0.657	0.627	-0.030	-0.05	7.49	6.49	-1.00	-0.14
Group Average	0.55	9.8	24.4	303.0	21036.	0.597	0.593	-0.004	0.00	7.74	7.19	-0.55	-0.08
S. Dev.	0.24	2.6	23.3	0.0	3020.	0.173	0.170	0.060	0.12	5.16	4.83	0.73	0.12
Avg. Abs. Value								0.041	0.08			0.72	0.11
S. Dev.								0.043	0.08			0.53	0.09
24. SAPRC 8-Component Surrogates													
ITC626	0.30	4.0	13.4	303.0	14300.	0.618	0.540	-0.078	-0.13	2.18	2.26	0.09	0.04
ITC630	0.31	1.9	6.3	303.0	16300.	0.284	0.270	-0.014	-0.05	0.86	1.00	0.14	0.15
ITC631	0.32	1.0	3.2	303.0	17500.	0.043	0.059	0.016		0.47	0.52	0.05	0.10
ITC633	0.64	4.0	6.2	303.0	16600.	0.231	0.279	0.048	0.19	1.26	1.50	0.24	0.17
ITC635	1.21	4.0	3.3	303.0	17500.	0.006	0.018	0.013		0.95	1.00	0.05	0.05
ITC637	0.31	4.0	12.8	303.0	16900.	0.617	0.537	-0.080	-0.14	2.31	2.24	-0.07	-0.03
ITC865	0.28	8.4	29.9	303.0	15100.	0.632	0.513	-0.120	-0.21	2.60	3.43	0.84	0.28

(continued)

Appendix B. Selected Results of Simulations of Individual Organic-NOx-Air Experiments Using the RADM-M Mechanism (continued).

Experiment	Initial Concentrations			Ave Temp	Ave H2O	Maximum Concentration OZONE				Average Initial d([O3] - [NO])/dt			
	NOx (ppm)	HC (ppmC)	HC/NOx	(degK)	(ppm)	Expt (ppm)	Calc (ppm)	Calc -Expt (ppm)	Calc -Expt /Avg	Expt --	Calc (ppb/min)	Calc -Expt --	Calc -Expt /Avg
ITC867	0.28	4.8	17.2	303.0	14600.	0.631	0.539	-0.092	-0.16	2.23	3.37	1.15	0.41
ITC868	0.37	2.9	7.8	303.0	17100.	0.518	0.423	-0.095	-0.20	2.10	1.41	-0.68	-0.39
ITC871	0.37	1.7	4.6	303.0	14600.	0.376	0.255	-0.121	-0.38	1.18	1.09	-0.10	-0.09
ITC872	0.38	2.1	5.7	303.0	14600.	0.213	0.220	0.007	0.03	1.20	1.33	0.13	0.10
ITC873	0.39	1.3	3.4	303.0	14600.	0.160	0.109	-0.051	-0.38	0.85	0.78	-0.07	-0.09
ITC874	0.38	2.1	5.7	303.0	13200.	0.191	0.152	-0.038	-0.22	0.83	0.85	0.02	0.03
ITC877	0.38	2.3	6.2	303.0	14600.	0.250	0.229	-0.022	-0.09	1.14	1.31	0.17	0.14
ITC880	0.73	2.2	3.0	303.0	13700.	0.031	0.042	0.011		0.85	0.96	0.11	0.12
ITC881	0.73	2.3	3.1	303.0	14000.	0.012	0.030	0.018		1.03	1.08	0.04	0.04
ITC885	0.64	1.5	2.4	303.0	14600.	0.012	0.025	0.013		0.44	0.76	0.33	0.54
ITC886	0.73	2.3	3.1	303.0	20000.*	0.012	0.021	0.009		1.24	0.69	-0.55	-0.57
ITC888	0.33	4.7	14.5	303.0	18000.	0.579	0.505	-0.074	-0.14	1.65	1.84	0.19	0.11
ITC891	0.32	4.4	13.7	303.0	20000.*	0.602	0.511	-0.091	-0.16	2.67	2.84	0.17	0.06
OTC189A	0.45	3.3	7.4	295.4	5000.*	0.576	0.757	0.181	0.27	3.79	3.55	-0.24	-0.07
OTC189B	0.45	4.0	8.9	298.0	5000.*	0.712	0.833	0.121	0.16	3.70	3.67	-0.03	-0.01
OTC190A	0.41	3.8	9.2	302.7	5400.*	0.702	0.828	0.126	0.16	4.24	3.30	-0.95	-0.25
OTC190B	0.42	3.8	9.0	299.5	5410.*	0.669	0.782	0.113	0.16	3.73	2.90	-0.83	-0.25
OTC192A	0.47	4.2	8.9	297.8	5000.*	0.735	0.841	0.106	0.13	4.25	3.35	-0.91	-0.24
OTC192B	0.47	4.2	8.9	298.4	5000.*	0.754	0.747	-0.007	-0.01	3.84	2.75	-1.09	-0.33
OTC194A	0.38	7.4	19.3	296.1	5000.*	0.737	0.897	0.160	0.20	7.85	7.55	-0.31	-0.04
OTC194B	0.38	3.7	9.7	295.7	5000.*	0.603	0.695	0.091	0.14	2.95	3.00	0.05	0.02
OTC195A	0.41	1.8	4.5	351.6	4660.*	0.164	0.105	-0.059	-0.44	2.05	1.16	-0.89	-0.55
OTC195B	0.41	4.1	9.9	360.0	3180.*	0.681	0.764	0.083	0.11	4.14	3.73	-0.40	-0.10
OTC196B	0.41	3.7	9.1	337.5	5000.*	0.597	0.789	0.192	0.28	3.86	3.30	-0.56	-0.16
OTC197A	0.38	3.6	9.5	353.2	5000.*	0.621	0.549	-0.072	-0.12	4.12	2.63	-1.48	-0.44
OTC197B	0.77	3.1	4.1	358.0	5000.*	0.152	0.093	-0.059	-0.48	2.86	2.02	-0.84	-0.34
OTC198A	0.84	5.4	6.4	353.5	5000.*	0.704	0.568	-0.136	-0.21	6.09	3.63	-2.46	-0.51
OTC198B	0.40	3.7	9.4	347.5	5000.*	0.674	0.627	-0.047	-0.07	3.86	2.55	-1.31	-0.41
OTC199A	0.36	3.5	9.6	299.7	5000.*	0.591	0.645	0.054	0.09	3.86	3.00	-0.86	-0.25
OTC199B	0.37	3.5	9.6	298.9	5000.*	0.606	0.630	0.024	0.04	3.40	2.88	-0.52	-0.17
OTC202A	0.73	6.0	8.2	325.1	5000.*	0.714	0.475	-0.239	-0.40	6.95	12.47	5.52	0.57
OTC202B	0.40	2.6	6.7	324.1	4560.*	0.522	0.413	-0.109	-0.23	3.82	3.10	-0.72	-0.21
OTC203A	0.39	3.5	9.0	293.3	4850.*	0.231	0.279	0.048	0.19	2.34	2.29	-0.05	-0.02
OTC203B	0.19	3.5	18.5	293.7	4880.*	0.394	0.447	0.053	0.12	2.20	2.61	0.41	0.17
OTC204A	0.35	3.6	10.2	322.2	4330.*	0.302	0.374	0.071	0.21	3.27	3.36	0.09	0.03
OTC204B	0.17	3.5	20.3	348.8	4330.*	0.381	0.465	0.084	0.20	2.62	2.86	0.24	0.09
OTC205A	0.84	3.8	4.5	464.9	5000.*	0.039	0.054	0.015		4.85	2.09	-2.76	-0.80
OTC205B	0.14	3.6	26.5	433.4	5000.*	0.392	0.546	0.154	0.33	4.49	3.64	-0.85	-0.21
OTC215A	0.45	3.5	7.8	293.1	4420.*	0.830	0.850	0.020	0.02	4.33	3.61	-0.72	-0.18
OTC215B	0.44	4.1	9.3	293.4	4420.*	0.868	0.931	0.063	0.07	5.33	5.48	0.15	0.03
OTC217A	0.50	4.9	9.6	295.5	7460.*	0.483	0.570	0.087	0.17	2.55	2.47	-0.08	-0.03
OTC217B	0.51	4.6	9.0	294.2	7460.*	0.831	0.922	0.091	0.10	4.64	4.24	-0.40	-0.09
OTC221A	0.41	2.4	5.8	290.6	4460.*	0.235	0.279	0.044	0.17	1.63	1.48	-0.14	-0.09
OTC221B	0.42	2.0	4.7	288.8	4460.*	0.333	0.349	0.016	0.05	1.63	1.59	-0.04	-0.03
OTC222A	0.44	3.4	7.8	298.5	5000.*	0.909	0.945	0.036	0.04	3.83	3.67	-0.16	-0.04

(continued)

Appendix B. Selected Results of Simulations of Individual Organic-NOx-Air Experiments Using the RADM-M Mechanism (continued).

Experiment	Initial Concentrations NOx (ppm)	HC (ppmC)	HC/NOx	Ave Temp (degK)	Ave H2O (ppm)	Maximum Concentration OZONE Expt (ppm)	Calc (ppm)	Calc -Expt (ppm)	Calc -Expt /Avg	Average Initial d([O3] - [NO])/dt Expt --	Calc (ppb/min)	Calc -Expt --	Calc -Expt /Avg
OTC222B	0.43	2.6	6.0	296.1	5000.*	0.940	1.107	0.167	0.16	5.55	6.17	0.62	0.11
OTC223A	0.36	4.8	13.4	314.9	4270.*	0.953	0.866	-0.086	-0.10	4.55	4.08	-0.47	-0.11
OTC223B	0.40	3.5	8.8	314.7	4270.*	0.771	0.714	-0.057	-0.08	3.15	2.83	-0.33	-0.11
OTC224A	0.34	4.4	12.7	303.5	6410.*	0.776	0.774	-0.002	0.00	3.67	2.91	-0.76	-0.23
OTC224B	0.34	4.3	12.6	303.8	6410.*	0.813	0.836	0.023	0.03	4.94	4.41	-0.53	-0.11
OTC226A	0.45	2.5	5.5	312.5	6840.*	0.751	0.530	-0.221	-0.35	3.12	2.32	-0.80	-0.29
OTC228A	0.41	2.4	6.0	293.2	5000.*	0.246	0.421	0.175	0.52	1.49	1.92	0.43	0.25
OTC228B	0.41	2.3	5.6	294.3	5000.*	0.296	0.456	0.160	0.43	1.79	2.56	0.77	0.36
OTC229A	0.46	3.0	6.6	295.7	5000.*	0.253	0.446	0.193	0.55	1.56	1.96	0.40	0.23
OTC229B	0.46	1.7	3.8	296.0	5000.*	0.168	0.391	0.223	0.80	1.38	1.83	0.45	0.28
OTC230A	0.41	3.1	7.6	297.9	5000.*	0.489	0.828	0.339	0.52	2.43	3.07	0.64	0.23
OTC230B	0.41	1.7	4.2	298.2	5000.*	0.271	0.550	0.279	0.68	1.66	2.16	0.50	0.26
OTC237A	0.52	4.3	8.2	292.3	3810.*	0.807	0.825	0.018	0.02	4.10	3.39	-0.71	-0.19
OTC237B	0.52	4.4	8.5	292.8	3810.*	0.757	0.676	-0.081	-0.11	3.48	2.92	-0.56	-0.17
OTC238A	0.50	2.9	5.8	292.5	4810.*	0.406	0.393	-0.013	-0.03	2.58	2.18	-0.40	-0.17
OTC238B	0.50	3.9	7.8	292.0	4810.*	0.702	0.696	-0.006	-0.01	4.06	3.56	-0.49	-0.13
OTC239A	0.49	2.7	5.4	290.2	5150.*	0.343	0.390	0.047	0.13	2.66	2.49	-0.16	-0.06
OTC239B	0.50	2.5	5.0	290.9	5150.*	0.234	0.159	-0.075	-0.38	1.85	1.46	-0.39	-0.24
OTC240A	0.50	1.8	3.6	93.4	6210.*	0.034	0.034	0.000		1.08	0.90	-0.18	-0.18
OTC240B	0.50	2.0	4.1	104.2	6210.*	0.217	0.110	-0.107	-0.65	1.79	1.36	-0.43	-0.28
OTC241A	0.32	4.7	14.8	290.7	4760.*	0.671	0.693	0.022	0.03	3.26	2.94	-0.32	-0.10
OTC241B	0.31	4.0	12.9	291.1	4760.*	0.674	0.679	0.005	0.01	3.30	3.26	-0.05	-0.01
OTC242A	0.45	2.6	5.8	302.0	4670.*	0.182	0.148	-0.034	-0.20	1.47	1.31	-0.17	-0.12
OTC242B	0.46	2.1	4.7	302.1	4670.*	0.639	0.623	-0.016	-0.03	3.04	2.64	-0.40	-0.14
OTC243A	0.47	4.7	10.0	276.5	4720.*	0.142	0.201	0.059	0.34	1.41	1.78	0.37	0.23
OTC243B	0.38	3.7	9.7	277.4	4720.*	0.152	0.171	0.019	0.11	1.40	2.14	0.74	0.42
OTC248A	0.48	3.7	7.7	271.6	5000.*	0.056	0.055	-0.001	-0.03	1.40	1.20	-0.20	-0.16
OTC248B	0.46	2.9	6.3	268.9	5000.*	0.081	0.085	0.004	0.05	1.61	1.69	0.08	0.05
OTC249A	0.48	5.6	11.8	286.9	3540.*	0.348	0.330	-0.018	-0.05	2.55	2.29	-0.26	-0.11
OTC249B	0.46	4.9	10.7	286.2	3540.*	0.325	0.360	0.035	0.10	2.83	2.97	0.14	0.05
Group Average	0.45	3.5	8.7	302.3	7630.	0.454	0.474	0.020	0.03	2.81	2.65	-0.16	-0.05
S. Dev.	0.16	1.3	4.9	43.6	4865.	0.272	0.284	0.102	0.26	1.51	1.65	0.89	0.24
Avg. Abs. Value								0.076	0.19			0.54	0.19
S. Dev.								0.070	0.17			0.73	0.16
25. UNC Miscellaneous Surrogates													
ST2081R	0.23	2.3	10.0	294.1	21900.	0.403	0.463	0.059	0.14	0.95	1.05	0.10	0.10
DE0782R	0.19	3.4	18.3	286.4	13400.	0.076	0.361	0.285	1.30	0.52	0.74	0.22	0.35
AU2681R	0.24	2.0	8.4	298.8	25500.	0.506	0.514	0.007	0.01	1.18	1.08	-0.11	-0.09
AU2681B	0.24	2.0	8.5	295.7	27500.	0.544	0.442	-0.102	-0.21	1.22	1.00	-0.22	-0.20
AU2781B	0.23	2.0	8.8	296.4	25000.	0.623	0.469	-0.153	-0.28	1.27	1.07	-0.21	-0.18
ST0381R	0.24	1.8	7.6	301.0	23200.	0.541	0.453	-0.088	-0.18	1.48	1.22	-0.26	-0.19
ST1081R	0.25	2.8	11.3	297.9	22300.	0.610	0.598	-0.012	-0.02	1.59	1.54	-0.05	-0.03
ST2081B	0.23	2.1	9.2	292.6	15200.	0.414	0.415	0.000	0.00	1.06	0.98	-0.07	-0.07

(continued)

Appendix B. Selected Results of Simulations of Individual Organic-NOx-Air Experiments Using the RADM-M Mechanism (continued).

Experiment	Initial Concentrations			Ave Temp	Ave H2O	Maximum Concentration OZONE				Average Initial d([O3] - [NO])/dt			
	NOx (ppm)	HC (ppmC)	HC/NOx	(degK)	(ppm)	Expt (ppm)	Calc (ppm)	Calc -Expt (ppm)	Calc -Expt /Avg	Expt --	Calc (ppb/min)	Calc -Expt --	Calc -Expt /Avg
JL2081B	0.42	1.8	4.3	305.0*	20000.*	0.165	0.473	0.308	0.97	0.82	0.94	0.12	0.14
ST1682R	0.43	3.2	7.5	304.4	23000.	0.410	0.508	0.098	0.21	1.28	1.17	-0.12	-0.09
JL2081R	0.41	2.7	6.6	305.0*	20000.*	0.635	0.666	0.031	0.05	1.55	1.43	-0.12	-0.08
JL2281B	0.26	2.9	11.2	302.3*	20000.*	0.722	0.652	-0.070	-0.10	1.80	1.70	-0.10	-0.06
OC1481R	0.28	3.3	11.9	291.3	9470.	0.462	0.570	0.108	0.21	1.53	1.56	0.04	0.02
ST1682B	0.43	3.1	7.2	304.4	23000.	0.840	0.784	-0.055	-0.07	2.39	2.08	-0.32	-0.14
ST2981R	0.24	2.5	10.3	293.7	18700.	0.294	0.427	0.134	0.37	0.76	0.88	0.12	0.15
ST2981B	0.24	2.5	10.4	291.6	14400.	0.485	0.492	0.008	0.02	1.35	1.29	-0.06	-0.04
OC1481B	0.29	2.9	9.9	288.9	10300.	0.458	0.564	0.106	0.21	1.48	1.50	0.02	0.02
ST0381B	0.23	2.0	8.6	297.9	16800.	0.611	0.517	-0.093	-0.17	1.70	1.55	-0.15	-0.09
ST1081B	0.24	1.0	4.1	295.3	17700.	0.626	0.376	-0.250	-0.50	1.36	0.95	-0.41	-0.35
JL0882R	0.29	2.1	7.3	304.2	16000.	0.598	0.668	0.070	0.11	1.25	1.33	0.09	0.07
JL0882B	0.28	2.1	7.4	304.2	16000.	0.541	0.651	0.110	0.18	1.12	1.29	0.17	0.14
Group Average	0.28	2.4	9.0	297.7	19018.	0.503	0.527	0.024	0.11	1.32	1.25	-0.06	-0.03
S. Dev.	0.08	0.6	3.0	5.8	4902.	0.175	0.110	0.134	0.40	0.40	0.32	0.17	0.15
Avg. Abs. Value								0.102	0.25			0.15	0.12
S. Dev.								0.086	0.32			0.10	0.09
26. UNC "Synurban" Surrogate													
AU2284R	0.32	0.4	1.2	302.7	8470.	0.657	0.756	0.099	0.14	1.61	1.63	0.02	0.01
AU2584R	0.34	0.1	0.3	302.0	22600.	0.075	0.105	0.030	0.33	0.70	0.64	-0.06	-0.10
AU2584B	0.33	0.1	0.4	302.0	22600.	0.096	0.130	0.034	0.30	0.69	0.65	-0.04	-0.06
ST0184R	0.31	0.2	0.6	302.5	9380.	0.546	0.653	0.107	0.18	1.32	1.30	-0.02	-0.01
ST0184B	0.30	0.2	0.8	302.5	9380.	0.646	0.687	0.041	0.06	1.72	1.57	-0.15	-0.09
ST0284R	0.34	0.1	0.4	304.6	19900.	0.119	0.261	0.142	0.74	0.73	0.75	0.02	0.02
ST0284B	0.33	0.1	0.3	304.5	19900.	0.020	0.140	0.120		0.40	0.49	0.09	0.21
JN2685R	0.30	0.2	0.6	303.6	16800.	0.629	0.662	0.034	0.05	1.34	1.45	0.11	0.08
JN2685B	0.30	0.3	0.9	303.6	16800.	0.788	0.742	-0.046	-0.06	1.74	1.84	0.10	0.06
JN2885R	0.38	0.1	0.4	299.8	11800.	0.238	0.387	0.148	0.47	0.85	0.88	0.03	0.04
JN2885B	0.39	0.2	0.5	299.8	11800.	0.275	0.271	-0.004	-0.01	0.87	0.87	0.00	0.01
Group Average	0.33	0.2	0.6	302.5	15403.	0.372	0.436	0.064	0.22	1.09	1.10	0.01	0.01
S. Dev.	0.03	0.1	0.3	1.6	5427.	0.284	0.266	0.063	0.25	0.47	0.47	0.08	0.09
Avg. Abs. Value								0.073	0.24			0.06	0.06
S. Dev.								0.051	0.23			0.05	0.06

(continued)

Appendix B. Selected Results of Simulations of Individual Organic-NOx-Air Experiments Using the RADM-M Mechanism (continued).

Experiment	Initial Concentrations			Ave Temp	Ave H2O	Maximum Concentration OZONE				Average Initial d([O3] - [NO])/dt			
	NOx (ppm)	HC (ppmC)	HC/NOx	(degK)	(ppm)	Expt (ppm)	Calc (ppm)	Calc -Expt (ppm)	Calc -Expt /Avg	Expt --	Calc (ppb/min)	Calc -Expt --	Calc -Expt /Avg
27. UNC "Synauto" Surrogate													
AU0484R	0.37	0.4	1.0	307.5	34900.	0.515	0.627	0.112	0.20	1.45	1.37	-0.08	-0.06
AU0484B	0.36	0.3	0.8	307.5	34700.	0.328	0.548	0.220	0.50	1.16	1.11	-0.06	-0.05
AU0584R	0.36	0.3	0.7	307.1	44900.	0.335	0.450	0.115	0.29	1.08	0.97	-0.12	-0.11
AU0584B	0.35	0.4	1.0	307.2	44900.	0.595	0.636	0.042	0.07	1.48	1.37	-0.11	-0.08
AU0684R	0.35	0.7	2.1	307.6	36800.	0.887	0.823	-0.064	-0.07	2.53	2.10	-0.43	-0.19
AU0684B	0.35	1.1	3.2	307.6	36800.	0.940	0.870	-0.070	-0.08	3.16	2.52	-0.64	-0.22
AU0784R	0.38	0.4	1.0	308.0	34700.	0.602	0.651	0.049	0.08	1.61	1.46	-0.15	-0.10
AU0884B	0.34	1.1	3.1	307.3	29000.	0.834	0.798	-0.035	-0.04	2.92	2.39	-0.52	-0.20
AU0984R	0.39	0.4	0.9	307.8	31500.	0.521	0.541	0.021	0.04	1.51	1.25	-0.26	-0.19
ST0884R	0.34	0.6	1.9	298.5	6920.	0.566	0.740	0.174	0.27	1.27	1.38	0.11	0.08
ST0884B	0.33	1.0	2.9	298.5	6920.	0.750	0.869	0.119	0.15	1.90	1.69	-0.21	-0.12
ST1784R	0.34	1.1	3.3	294.4	24800.	0.539	0.710	0.171	0.27	1.59	2.25	0.67	0.35
ST1784B	0.34	0.8	2.3	294.4	24800.	0.484	0.696	0.212	0.36	1.38	1.95	0.57	0.34
ST2184R	0.36	0.6	1.7	302.2	7350.	0.671	0.811	0.141	0.19	1.78	2.00	0.22	0.11
ST2184B	0.36	0.7	2.0	302.2	7350.	0.721	0.829	0.108	0.14	2.28	2.61	0.33	0.13
Group Average	0.35	0.7	1.9	303.9	27089.	0.619	0.707	0.088	0.16	1.81	1.76	-0.05	-0.02
S. Dev.	0.02	0.3	0.9	5.1	13697.	0.182	0.130	0.094	0.17	0.63	0.54	0.37	0.18
Avg. Abs. Value								0.110	0.18			0.30	0.16
S. Dev.								0.064	0.13			0.21	0.09
28. UNC Auto Exhaust													
OC0483B	0.25	0.4	1.7	299.7	18800.	0.642	0.708	0.066	0.10	1.86	1.97	0.12	0.06
OC0783R	0.33	2.7	8.1	295.5	21600.	0.178	0.385	0.207	0.73	0.94	1.11	0.18	0.17
OC0783B	0.34	2.7	7.9	295.4	21500.	0.451	0.640	0.190	0.35	1.41	1.92	0.51	0.30
JN2582R	0.65	0.6	0.9	301.1*	22700.	0.003	0.012	0.010		0.64	0.57	-0.07	-0.11
JN2582B	0.65	0.6	0.9	301.2*	22900.	0.003	0.013	0.010		0.68	0.57	-0.11	-0.18
JN2982R	0.24	2.5	10.3	303.1	30500.	0.704	0.823	0.119	0.16	2.32	2.10	-0.22	-0.10
JN2982B	0.25	2.5	9.8	303.1	30500.	0.766	0.829	0.063	0.08	2.67	2.18	-0.49	-0.20
JN3082R	0.32	2.8	8.7	302.5*	20000.*	0.811	0.985	0.174	0.19	2.55	2.41	-0.14	-0.05
JN3082B	0.32	0.6	1.7	302.3*	20000.*	0.840	0.992	0.151	0.17	2.68	2.41	-0.27	-0.11
JL0283B	0.19	1.7	9.1	304.0	24500.	0.697	0.839	0.141	0.18	1.65	1.72	0.07	0.04
JL0883B	0.37	1.7	4.6	299.5	21200.	0.879	0.838	-0.041	-0.05	1.76	1.43	-0.33	-0.21
ST2982B	0.39	1.7	4.3	295.7	24800.	0.205	0.054	-0.151	-1.17	1.12	0.75	-0.38	-0.40
OC0682R	0.46	2.0	4.3	300.2	16900.	0.355	0.267	-0.088	-0.28	1.37	1.17	-0.20	-0.16
AU1183R	0.22	2.2	9.9	306.8	21400.	0.850	0.878	0.028	0.03	2.55	2.16	-0.39	-0.17
AU1183B	0.23	0.7	3.1	306.9	21400.	0.601	0.665	0.065	0.10	1.26	1.25	-0.01	-0.01
JL0182R	0.37	3.5	9.6	299.5	27700.	0.740	1.032	0.292	0.33	2.31	2.41	0.09	0.04
JL0182B	0.35	3.6	10.2	299.3	27400.	0.759	0.989	0.230	0.26	2.41	2.53	0.12	0.05

(continued)

Appendix B. Selected Results of Simulations of Individual Organic-NOx-Air Experiments Using the RADM-M Mechanism (continued).

Experiment	Initial Concentrations			Ave Temp	Ave H2O	Maximum Concentration OZONE				Average Initial d([03] - [NO])/dt			
	NOx (ppm)	HC (ppmC)	HC/NOx	(degK)	(ppm)	Expt (ppm)	Calc (ppm)	Calc -Expt (ppm)	Calc -Expt /Avg	Expt --	Calc (ppb/min)	Calc -Expt --	Calc -Expt /Avg
AU0382R	0.44	2.5	5.7	302.6	27400.	0.344	0.444	0.100	0.25	1.26	1.22	-0.03	-0.03
AU0382B	0.16	1.2	7.3	302.6	27400.	0.576	0.498	-0.078	-0.15	1.06	0.92	-0.14	-0.14
ST1782R	0.26	2.2	8.6	300.1	27400.	0.562	0.586	0.024	0.04	1.63	1.15	-0.47	-0.34
ST1782B	0.25	2.4	9.5	300.1	27400.	0.637	0.612	-0.025	-0.04	1.72	1.27	-0.45	-0.30
ST2982R	0.39	1.7	4.4	295.7	24800.	0.073	0.044	-0.029	-0.49	0.86	0.68	-0.19	-0.24
OC0682B	0.46	2.0	4.3	300.2	16900.	0.450	0.319	-0.131	-0.34	1.49	1.26	-0.23	-0.17
JL0283R	0.18	1.6	9.0	304.0	24500.	0.595	0.658	0.063	0.10	1.37	1.37	0.00	0.00
JL0883R	0.37	1.7	4.6	299.5	21200.	0.756	0.683	-0.073	-0.10	1.52	1.31	-0.21	-0.15
JL1583R	0.35	2.2	6.2	306.2	25700.	0.866	0.705	-0.161	-0.20	2.10	1.73	-0.36	-0.19
JL1583B	0.35	2.3	6.6	306.2	25700.	0.922	0.836	-0.086	-0.10	2.20	1.98	-0.22	-0.10
OC0483R	0.25	2.6	10.3	299.7	18800.	0.603	0.657	0.055	0.09	1.76	1.74	-0.02	-0.01
Group Average	0.34	2.0	6.5	301.2	23607.	0.567	0.607	0.040	0.01	1.68	1.55	-0.14	-0.10
S. Dev.	0.12	0.8	3.1	3.3	3802.	0.272	0.310	0.119	0.34	0.61	0.59	0.23	0.15
Avg. Abs. Value								0.102	0.23			0.21	0.14
S. Dev.								0.072	0.25			0.15	0.11
29. SAPRC Synthetic Jet Fuel													
ITC781	0.51	43.0	83.5	303.0	16600.	0.751	0.927	0.176	0.21	2.77	9.61	6.84	1.10
ITC784	0.50	88.0	177.6	303.0	16600.	0.746	0.921	0.176	0.21	3.93	13.15	9.22	1.08
ITC785	0.26	45.0	170.7	303.0	17900.	0.598	0.611	0.013	0.02	2.74	8.64	5.90	1.04
ITC805	0.52	98.0	189.5	303.0	17200.	0.791	0.959	0.169	0.19	3.27	12.47	9.21	1.17
ITC795	0.50	45.0	89.8	303.0	17900.	0.761	0.799	0.038	0.05	3.05	13.25	10.19	1.25
ITC796	0.54	97.0	178.9	303.0	17200.	0.597	0.851	0.254	0.35	4.43	17.30	12.86	1.18
ITC799	0.51	94.0	184.1	303.0	17200.	0.840	0.993	0.152	0.17	4.59	11.31	6.72	0.85
ITC801	0.55	41.0	75.1	303.0	17000.	0.881	0.974	0.093	0.10	2.98	7.82	4.84	0.90
Group Average	0.49	68.9	143.7	303.0	17200.	0.746	0.880	0.134	0.16	3.47	11.69	8.22	1.07
S. Dev.	0.09	27.3	50.8	0.0	499.	0.102	0.126	0.080	0.11	0.74	3.06	2.63	0.14
Avg. Abs. Value								0.134	0.16			8.22	1.07
S. Dev.								0.080	0.11			2.63	0.14
30. SAPRC Synthetic Jet Exhaust													
ITC963	0.49	4.4	9.1	303.0	19400.	0.822	0.722	-0.100	-0.13	4.00	4.16	0.16	0.04
ITC965	0.46	5.2	11.3	303.0	20000.	0.863	0.728	-0.135	-0.17	5.10	5.31	0.21	0.04
ITC967	0.26	4.4	17.2	303.0	18300.	0.586	0.591	0.005	0.01	5.79	6.21	0.42	0.07
ITC968	0.49	8.7	17.8	303.0	19400.	0.852	0.793	-0.059	-0.07	11.76	11.21	-0.55	-0.05
Group Average	0.42	5.7	13.8	303.0	19275.	0.781	0.708	-0.072	-0.09	6.66	6.72	0.06	0.03
S. Dev.	0.11	2.1	4.3	0.0	709.	0.131	0.084	0.060	0.08	3.48	3.11	0.42	0.05
Avg. Abs. Value								0.075	0.10			0.33	0.05
S. Dev.								0.056	0.07			0.18	0.01

APPENDIX C

SELECTED RESULTS OF SIMULATIONS OF ALL ORGANIC-NO_X EXPERIMENTS MODELED USING THE RADM-P MECHANISM

Appendix C. Selected Results of Simulations of Individual Organic-NOx-Air Experiments Using the RADM-P Mechanism.

Experiment	Initial Concentrations			Ave Temp	Ave H2O	Maximum Concentration OZONE				Average Initial d([O3] - [NO])/dt			
	NOx (ppm)	HC (ppmC)	HC/NOx	(degK)	(ppm)	Expt (ppm)	Calc (ppm)	Calc -Expt (ppm)	Calc -Expt /Avg	Expt --	Calc (ppb/min)	Calc -Expt --	Calc -Expt /Avg
1. Ethene-NOx													
EC142	0.48	1.9	4.1	303.0	26500.	0.782	0.474	-0.307	-0.49	3.20	2.20	-1.00	-0.37
EC143	0.50	4.1	8.1	303.0	22700.	1.087	0.791	-0.296	-0.32	8.50	4.51	-4.00	-0.61
EC156	0.50	4.0	8.0	303.0	29000.	1.105	0.751	-0.354	-0.38	8.89	4.50	-4.39	-0.66
EC285	1.01	3.9	3.9	303.0	20400.	0.840	0.892	0.052	0.06	5.05	4.89	-0.15	-0.03
EC286	0.94	7.5	8.0	303.0	20500.	1.081	1.171	0.090	0.08	11.76	10.14	-1.63	-0.15
EC287	0.53	8.0	15.1	303.0	19700.	0.965	1.026	0.061	0.06	13.89	13.01	-0.88	-0.07
ITC926	0.51	7.9	15.6	303.0	21100.	0.982	0.921	-0.061	-0.06	6.96	4.92	-2.05	-0.34
ITC936	0.50	3.9	7.8	303.0	20300.	0.940	0.839	-0.101	-0.11	2.72	2.35	-0.37	-0.15
AU0479R	0.23	0.9	3.9	298.9	32500.	0.729	0.554	-0.175	-0.27	1.60	0.99	-0.61	-0.47
AU0579R	0.64	4.1	6.4	292.4	29100.	1.294	1.142	-0.152	-0.12	3.17	2.27	-0.91	-0.33
OC0584R	0.36	3.2	8.8	297.3	20000.*	0.856	0.970	0.114	0.12	2.16	1.98	-0.18	-0.09
OC1184R	0.35	2.9	8.2	297.2	12700.	0.858	1.039	0.181	0.19	2.22	2.01	-0.21	-0.10
OC1284R	0.72	2.7	3.7	295.6	13600.	0.495	0.185	-0.310	-0.91	1.58	1.17	-0.41	-0.30
OC0584B	0.37	1.8	5.0	297.3	20000.*	0.675	0.646	-0.029	-0.04	1.48	1.33	-0.15	-0.11
Group Average	0.55	4.1	7.6	300.2	22007.	0.906	0.814	-0.092	-0.16	5.23	4.02	-1.21	-0.27
S. Dev.	0.22	2.3	3.8	3.6	5611.	0.204	0.275	0.179	0.30	4.10	3.53	1.39	0.20
Avg. Abs. Value								0.163	0.23			1.21	0.27
S. Dev.								0.111	0.24			1.39	0.20
2. Propene-NOx													
EC121	0.51	1.5	2.9	303.0	26500.	0.506	0.460	-0.046	-0.09	7.46	4.10	-3.36	-0.58
EC177	0.46	1.5	3.2	303.0	26900.	0.540	0.471	-0.069	-0.14	3.89	4.00	0.11	0.03
EC216	0.52	1.5	3.0	303.0	18100.	0.564	0.555	-0.009	-0.02	4.18	5.69	1.51	0.31
EC217	0.48	0.6	1.2	303.0	21400.	0.149	0.230	0.081	0.43	0.80	1.30	0.50	0.48
EC230	0.52	1.9	3.7	303.0	17200.	0.344	0.329	-0.015	-0.05	3.06	4.78	1.72	0.44
EC256	0.56	0.4	0.7	303.0	20200.	0.002	0.011	0.008		0.98	1.08	0.10	0.10
EC257	0.56	0.7	1.3	303.0	20000.	0.068	0.098	0.029	0.35	3.35	4.20	0.84	0.22
EC276	0.52	1.6	3.2	303.0	14500.	0.388	0.447	0.059	0.14	3.24	4.41	1.16	0.30
EC277	0.11	1.7	15.7	303.0	15700.	0.313	0.395	0.082	0.23	8.27	8.06	-0.21	-0.03
EC278	0.49	3.1	6.2	303.0	16100.	0.625	0.702	0.076	0.12	7.72	9.84	2.11	0.24
EC279	0.97	3.5	3.5	303.0	14200.	0.679	0.706	0.027	0.04	6.64	8.08	1.43	0.19
EC314	0.93	3.2	3.5	303.0	24000.	0.728	0.786	0.058	0.08	7.21	10.36	3.15	0.36
EC315	0.94	2.9	3.1	288.7	10600.	0.344	0.661	0.316	0.63	4.33	6.43	2.09	0.39
EC316	0.98	3.2	3.3	312.0	44900.	0.955	1.051	0.096	0.10	10.64	11.93	1.29	0.11
EC317	0.54	1.5	2.8	303.0	24200.	0.615	0.570	-0.045	-0.08	4.06	4.71	0.65	0.15
ITC693	0.49	3.5	7.2	303.0	20300.	0.779	0.718	-0.061	-0.08	5.07	5.72	0.66	0.12
ITC810	0.52	2.8	5.4	303.0	16800.	0.782	0.721	-0.061	-0.08	4.25	4.57	0.32	0.07
ITC860	0.52	3.0	5.8	303.0	17100.	0.585	0.681	0.096	0.15	3.57	4.88	1.31	0.31
ITC925	0.54	2.8	5.2	303.0	16300.	0.779	0.728	-0.051	-0.07	3.72	4.14	0.42	0.11
ITC938	0.52	2.8	5.3	303.0	19000.	0.729	0.719	-0.010	-0.01	3.61	4.24	0.63	0.16
ITC947	0.53	1.9	3.6	303.0	20300.	0.710	0.715	0.005	0.01	3.34	4.15	0.81	0.22
ITC960	0.50	2.8	5.5	303.0	20300.	0.721	0.712	-0.009	-0.01	4.23	4.40	0.17	0.04

(continued)

Appendix C. Selected Results of Simulations of Individual Organic-NOx-Air Experiments Using the RADM-P Mechanism (continued).

Experiment	Initial Concentrations			Ave Temp	Ave H2O	Maximum Concentration OZONE				Average Initial d([O3] - [NO])/dt			
	NOx (ppm)	HC (ppmC)	HC/NOx	(degK)	(ppm)	Expt (ppm)	Calc (ppm)	Calc -Expt (ppm)	Calc -Expt /Avg	Expt --	Calc (ppb/min)	Calc -Expt --	Calc -Expt /Avg
OTC186	0.55	3.6	6.6	299.8	5000.*	0.822	0.939	0.117	0.13	5.16	7.81	2.65	0.41
OTC191	0.54	3.7	6.9	309.3	5000.*	0.903	1.155	0.252	0.24	12.18	13.94	1.77	0.14
OTC210	0.57	2.7	4.8	304.7	3720.*	0.972	1.006	0.034	0.03	6.70	6.36	-0.34	-0.05
OTC233	0.46	0.1	0.2	303.6	5000.*	0.633	0.934	0.301	0.38	3.69	5.50	1.81	0.39
OTC236	0.53	3.3	6.3	300.0	6510.*	0.848	1.015	0.167	0.18	6.91	8.41	1.50	0.20
JA1078R	0.46	3.1	6.9	265.1	20000.*	0.363	0.604	0.240	0.50	0.46	0.48	0.02	0.04
OC1278B	0.48	1.4	2.9	294.3	16300.	0.461	0.413	-0.049	-0.11	1.40	1.45	0.05	0.03
OC2078R	0.46	1.3	2.9	290.4	9590.	0.340	0.403	0.063	0.17	1.23	1.38	0.15	0.12
OC2078B	0.46	3.5	7.7	290.4	9560.	0.727	0.948	0.221	0.26	2.83	3.53	0.70	0.22
OC2178R	0.50	3.9	7.9	290.3	20000.*	0.670	0.913	0.243	0.31	2.53	3.44	0.91	0.31
OC2578B	0.44	1.3	2.9	288.4	12800.	0.230	0.269	0.039	0.15	1.03	1.15	0.12	0.11
JN1279R	0.50	1.0	2.1	293.5	20000.*	0.382	0.306	-0.076	-0.22	0.85	0.77	-0.09	-0.11
JN1279B	0.49	1.5	3.0	293.5	20000.*	0.673	0.515	-0.158	-0.27	1.24	1.10	-0.14	-0.12
JN1379R	0.45	2.9	6.5	294.9	20000.*	0.974	0.874	-0.099	-0.11	2.69	2.83	0.14	0.05
AU0279R	0.22	1.5	7.0	307.2	20000.*	0.788	0.632	-0.156	-0.22	2.41	2.06	-0.35	-0.16
AU2780B	0.48	1.9	4.0	302.2	28400.	1.044	1.183	0.139	0.12	3.26	2.84	-0.42	-0.14
ST0482B	0.23	1.1	4.9	300.5	11800.	0.658	0.614	-0.044	-0.07	1.46	1.59	0.13	0.08
ST1382B	0.33	1.1	3.3	302.6	24100.	0.731	0.687	-0.045	-0.06	1.69	1.61	-0.08	-0.05
JL1783R	0.27	1.1	3.9	307.2	29700.	0.848	0.720	-0.127	-0.16	2.10	1.75	-0.35	-0.18
JL2183R	0.22	1.1	5.0	308.5	23800.	0.804	0.731	-0.073	-0.09	1.76	1.87	0.10	0.06
JL2983B	0.21	1.1	5.3	303.1	23300.	0.697	0.739	0.042	0.06	1.66	1.74	0.08	0.05
JL3183R	0.21	1.1	5.1	305.0	19800.	0.719	0.687	-0.032	-0.05	1.81	1.67	-0.14	-0.08
ST2383B	0.38	1.6	4.3	292.5	23400.	0.405	0.666	0.261	0.49	1.23	1.67	0.44	0.31
OC0484R	0.36	2.1	5.9	296.8	20000.*	0.645	0.759	0.114	0.16	2.07	2.15	0.08	0.04
OC0484B	0.36	1.0	2.9	296.7	20000.*	0.446	0.474	0.029	0.06	1.25	1.21	-0.04	-0.04
OC1184B	0.36	2.2	6.3	297.2	12700.	0.674	0.772	0.098	0.14	2.38	2.45	0.06	0.03
OC1284B	0.68	2.0	2.9	295.9	13500.	0.432	0.471	0.039	0.09	1.67	1.64	-0.03	-0.02
Group Average	0.49	2.1	4.6	299.9	18134.	0.608	0.651	0.043	0.08	3.62	4.15	0.53	0.11
S. Dev.	0.18	1.0	2.5	7.5	7349.	0.238	0.254	0.117	0.20	2.60	3.08	1.01	0.19
Avg. Abs. Value								0.093	0.16			0.76	0.17
S. Dev.								0.081	0.14			0.85	0.14
3. 1-Butene-NOx													
EC122	0.50	0.9	1.7	303.0	22000.	0.227	0.081	-0.147	-0.95	2.29	1.40	-0.89	-0.48
EC123	0.51	1.6	3.2	303.0	27200.	0.506	0.280	-0.226	-0.58	4.16	2.30	-1.86	-0.58
EC124	0.99	1.7	1.7	303.0	24500.	0.247	0.132	-0.115	-0.61	1.99	1.71	-0.27	-0.15
ITC927	0.31	3.8	12.3	303.0	19000.	0.646	0.728	0.082	0.12	3.24	4.54	1.31	0.34
ITC928	0.67	3.8	5.7	303.0	18400.	0.022	0.045	0.023		1.36	1.69	0.34	0.22
ITC930	0.32	7.2	22.2	303.0	21100.	0.717	0.827	0.110	0.14	7.91	11.12	3.21	0.34
ITC935	0.66	7.6	11.6	303.0	19700.	0.872	0.972	0.100	0.11	5.39	7.16	1.77	0.28
ST2383R	0.40	1.5	3.7	292.6	23400.	0.206	0.451	0.245	0.74	0.96	1.15	0.20	0.19
ST2583R	0.46	1.6	3.6	292.3	18800.	0.266	0.449	0.182	0.51	1.16	1.31	0.15	0.12
ST2583B	0.42	2.9	6.8	292.3	18900.	0.594	0.783	0.190	0.28	1.78	2.19	0.41	0.21
ST2783R	0.45	1.6	3.6	295.5	19400.	0.285	0.452	0.167	0.45	1.19	1.31	0.12	0.10

(continued)

Appendix C. Selected Results of Simulations of Individual Organic-NOx-Air Experiments Using the RADM-P Mechanism (continued).

Experiment	Initial Concentrations			Ave Temp	Ave H2O	Maximum Concentration OZONE				Average Initial d([O3] - [NO])/dt			
	NOx (ppm)	HC (ppmC)	HC/NOx	(degK)	(ppm)	Expt (ppm)	Calc (ppm)	Calc -Expt (ppm)	Calc -Expt /Avg	Expt --	Calc (ppb/min)	Calc -Expt --	Calc -Expt /Avg
Group Average	0.52	3.1	6.9	299.4	21127.	0.417	0.473	0.055	0.02	2.86	3.26	0.41	0.05
S. Dev.	0.20	2.3	6.2	5.0	2856.	0.263	0.321	0.154	0.55	2.18	3.18	1.34	0.32
Avg. Abs. Value								0.144	0.45			0.96	0.27
S. Dev.								0.066	0.29			0.99	0.15
4. trans-2-Butene-NOx													
EC146	0.51	0.9	1.8	303.0	26900.	0.247	0.109	-0.138	-0.77	5.87	3.85	-2.02	-0.42
EC147	0.98	1.7	1.7	303.0	22300.	0.154	0.083	-0.071	-0.60	9.83	7.39	-2.45	-0.28
EC157	0.53	0.9	1.7	303.0	27500.	0.205	0.091	-0.114	-0.77	5.96	3.54	-2.42	-0.51
ST27838	0.43	2.0	4.7	295.5	19400.	0.523	0.543	0.019	0.04	3.00	3.16	0.15	0.05
Group Average	0.61	1.4	2.5	301.1	24025.	0.282	0.207	-0.076	-0.53	6.17	4.48	-1.68	-0.29
S. Dev.	0.25	0.6	1.5	3.7	3860.	0.165	0.224	0.069	0.38	2.80	1.96	1.24	0.24
Avg. Abs. Value								0.085	0.54			1.76	0.31
S. Dev.								0.052	0.35			1.09	0.20
5. Isobutene-NOx													
ITC694	0.51	4.6	9.1	303.0	20000.	0.900	0.731	-0.169	-0.21	8.84	6.04	-2.80	-0.38
6. 1-Hexene-NOx													
ITC929	0.51	5.1	10.0	303.0	19000.	0.298	0.670	0.372	0.77	1.27	3.33	2.06	0.89
ITC931	0.49	10.3	21.1	303.0	20100.	0.606	0.819	0.213	0.30	2.82	10.67	7.85	1.16
ITC934	1.00	9.7	9.7	303.0	20300.	0.428	0.895	0.467	0.71	1.84	5.00	3.16	0.93
ITC937	0.99	0.1	0.1	303.0	20300.	0.007	0.060	0.053		0.33	0.57	0.24	0.52
Group Average	0.75	6.3	10.2	303.0	19925.	0.335	0.611	0.276	0.59	1.57	4.89	3.33	0.88
S. Dev.	0.28	4.8	8.6	0.0	624.	0.252	0.379	0.182	0.26	1.04	4.26	3.25	0.26
Avg. Abs. Value								0.276	0.59			3.33	0.88
S. Dev.								0.182	0.26			3.25	0.26
7. Isoprene-NOx													
EC520	0.49	2.2	4.5	303.0	13000.	0.503	0.300	-0.203	-0.50	5.30	7.56	2.26	0.35
EC522	0.92	2.3	2.4	303.0	13000.	0.276	0.118	-0.158	-0.80	6.00	6.75	0.76	0.12
EC524	0.96	4.7	4.9	303.0	13000.	0.759	0.430	-0.330	-0.55	15.57	15.93	0.37	0.02
EC525	0.54	4.5	8.3	303.0	13000.	0.691	0.630	-0.061	-0.09	10.13	22.16	12.04	0.75

(continued)

Appendix C. Selected Results of Simulations of Individual Organic-NOx-Air Experiments Using the RADM-P Mechanism (continued).

Experiment	Initial Concentrations			Ave Temp	Ave H2O	Maximum Concentration OZONE				Average Initial d([O3] - [NO])/dt			
	NOx (ppm)	HC (ppmC)	HC/NOx	(degK)	(ppm)	Expt (ppm)	Calc (ppm)	Calc -Expt (ppm)	Calc -Expt /Avg	Expt --	Calc (ppb/min)	Calc -Expt --	Calc -Expt /Avg
EC527	0.50	2.2	4.5	303.0	13000.	0.547	0.317	-0.230	-0.53	5.97	7.95	1.97	0.28
ITC811	0.50	3.4	6.8	303.0	17300.	0.919	0.578	-0.341	-0.46	10.00	8.96	-1.04	-0.11
ITC812	0.52	1.8	3.4	303.0	17300.	0.768	0.253	-0.515	-1.01	4.86	2.43	-2.43	-0.67
JL1680R	0.18	4.6	26.0	305.0	30200.	0.652	0.712	0.060	0.09	3.18	3.00	-0.18	-0.06
JL1680B	0.18	6.4	36.6	301.9	26800.	0.837	0.600	-0.237	-0.33	2.88	2.43	-0.44	-0.17
JL1780R	0.46	1.0	2.1	305.6	27000.	0.806	0.420	-0.386	-0.63	1.96	1.36	-0.60	-0.36
JL1780B	0.47	2.6	5.5	302.8	25000.	1.298	0.835	-0.463	-0.43	4.20	2.87	-1.33	-0.38
JL2381R	0.43	1.4	3.4	306.1	20000.*	0.750	0.691	-0.058	-0.08	2.13	2.01	-0.12	-0.06
ST0981R	0.17	1.0	6.1	297.5	20000.*	0.506	0.457	-0.049	-0.10	1.46	1.45	-0.01	0.00
Group Average	0.49	2.9	8.8	303.1	19123.	0.716	0.488	-0.228	-0.42	5.66	6.53	0.86	-0.02
S. Dev.	0.25	1.7	10.4	2.1	6284.	0.246	0.208	0.174	0.31	4.06	6.29	3.58	0.36
Avg. Abs. Value								0.238	0.43			1.81	0.26
S. Dev.								0.160	0.29			3.18	0.24
8. a-Pinene-NOx													
JL1580R	0.18	1.1	5.8	302.4	30300.	0.201	0.297	0.095	0.38	0.61	0.67	0.06	0.10
JL1580B	0.19	2.6	13.8	299.6	29200.	0.470	0.421	-0.049	-0.11	1.59	1.96	0.37	0.21
JL2580R	0.25	1.0	4.0	302.4	31700.	0.377	0.327	-0.050	-0.14	0.84	0.83	-0.02	-0.02
JL2580B	0.25	0.3	1.4	300.1	26300.	0.334	0.211	-0.123	-0.45	0.84	0.68	-0.16	-0.21
Group Average	0.22	1.3	6.3	301.1	29375.	0.346	0.314	-0.032	-0.08	0.97	1.03	0.06	0.02
S. Dev.	0.04	1.0	5.3	1.5	2291.	0.112	0.087	0.091	0.34	0.43	0.62	0.22	0.18
Avg. Abs. Value								0.079	0.27			0.15	0.13
S. Dev.								0.036	0.17			0.16	0.09
9. Ethane-NOx													
ITC999	0.09	45.4	534.1	303.0	20500.	0.243	0.203	-0.040	-0.18	1.32	1.42	0.10	0.07
10. n-Butane-NOx													
EC130	0.10	17.6	179.3	303.0	26200.	0.459	0.444	-0.015	-0.03	4.41	2.49	-1.93	-0.56
EC133	0.50	8.6	17.1	303.0	27800.	0.249	0.045	-0.204	-1.38	2.42	1.07	-1.35	-0.77
EC134	0.51	8.3	16.3	303.0	20000.*	0.034	0.038	0.004		0.94	1.30	0.36	0.32
EC137	0.50	8.7	17.3	303.0	20000.*	0.042	0.044	0.002		1.02	1.27	0.25	0.22
EC162	0.51	8.2	16.3	303.0	27300.	0.112	0.050	-0.062	-0.76	1.73	1.21	-0.51	-0.35
EC163	0.49	9.0	18.3	303.0	28500.	0.454	0.152	-0.302	-0.99	3.31	1.71	-1.60	-0.64
EC168	0.49	8.0	16.2	303.0	20700.	0.655	0.315	-0.340	-0.70	2.03	1.14	-0.89	-0.56
EC178	0.10	7.8	79.6	303.0	20900.	0.384	0.421	0.037	0.09	1.61	1.68	0.07	0.04
EC304	0.47	17.1	36.7	303.0	26800.	0.362	0.434	0.073	0.18	2.09	2.31	0.22	0.10

(continued)

Appendix C. Selected Results of Simulations of Individual Organic-NOx-Air Experiments Using the RADM-P Mechanism (continued).

Experiment	Initial Concentrations			Ave Temp	Ave H2O	Maximum Concentration OZONE				Average Initial d([O3] - [NO])/dt			
	NOx (ppm)	HC (ppmC)	HC/NOx	(degK)	(ppm)	Expt (ppm)	Calc (ppm)	Calc -Expt (ppm)	Calc -Expt /Avg	Expt --	Calc (ppb/min)	Calc -Expt --	Calc -Expt /Avg
EC305	0.10	15.7	159.7	303.0	25400.	0.398	0.531	0.133	0.29	2.39	3.43	1.04	0.36
EC306	0.19	25.8	138.2	302.6	24200.	0.535	0.709	0.174	0.28	2.38	4.20	1.82	0.55
EC307	0.10	25.8	252.9	303.0	29700.	0.420	0.588	0.168	0.33	2.61	5.89	3.28	0.77
EC308	0.48	16.2	33.6	288.7	8750.	0.047	0.210	0.164		1.04	2.62	1.59	0.87
EC309	0.47	17.2	36.3	310.9	12400.	0.545	0.616	0.071	0.12	2.00	2.48	0.48	0.22
ITC507	0.09	15.2	165.0	303.0	20300.	0.149	0.356	0.207	0.82	0.69	1.54	0.85	0.77
ITC533	0.12	11.9	99.8	303.0	20800.	0.165	0.327	0.162	0.66	0.61	1.36	0.75	0.76
ITC770	0.52	37.9	72.8	303.0	16800.	0.042	0.050	0.008		1.56	1.98	0.42	0.24
ITC939	0.51	14.8	28.9	303.0	20300.	0.017	0.025	0.008		0.36	0.65	0.28	0.56
ITC948	0.26	10.0	38.2	303.0	20300.	0.054	0.141	0.087	0.89	0.53	1.10	0.57	0.70
OTC211	0.55	42.8	77.5	300.1	3530.*	0.008	0.190	0.182		0.56	1.40	0.83	0.85
JL2178R	0.24	7.2	29.9	302.9	20000.*	0.763	0.594	-0.168	-0.25	1.17	1.06	-0.11	-0.10
JL2178B	0.24	15.4	63.9	302.9	20000.*	0.986	0.868	-0.119	-0.13	1.64	1.46	-0.18	-0.12
JL2278R	0.55	7.9	14.4	305.2	20000.*	0.166	0.138	-0.028	-0.18	0.90	0.75	-0.15	-0.18
JL2278B	0.55	17.5	31.5	305.2	20000.*	0.788	0.418	-0.369	-0.61	1.55	1.28	-0.27	-0.19
ST1879B	0.21	21.2	103.1	298.3	20000.*	0.185	0.114	-0.072	-0.48	0.51	0.43	-0.08	-0.16
OC0979R	0.21	14.6	71.0	297.2	15300.	0.191	0.272	0.081	0.35	0.60	0.59	0.00	0.00
OC1879B	0.20	14.3	71.8	295.0	28100.	0.208	0.158	-0.050	-0.27	0.60	0.52	-0.09	-0.16
Group Average	0.34	15.7	69.8	302.1	20892.	0.312	0.305	-0.006	-0.08	1.53	1.74	0.21	0.13
S. Dev.	0.18	8.8	61.6	3.8	6033.	0.268	0.235	0.160	0.59	0.98	1.21	1.05	0.49
Avg. Abs. Value								0.122	0.47			0.74	0.41
S. Dev.								0.102	0.36			0.77	0.28
11. C4+ Branched Alkane-NOx													
EC165	0.10	11.3	114.3	303.0	18600.	0.488	0.479	-0.009	-0.02	1.77	1.65	-0.12	-0.07
EC169	0.19	4.5	23.5	303.0	32900.	0.493	0.326	-0.168	-0.41	1.00	0.70	-0.30	-0.35
EC171	0.10	3.5	35.7	303.0	19000.	0.403	0.306	-0.097	-0.27	1.30	0.79	-0.51	-0.49
OC1879R	0.20	16.4	81.9	295.0	28100.	0.236	0.130	-0.106	-0.58	0.64	0.50	-0.13	-0.23
OC2079B	0.22	12.6	56.5	295.3	27800.	0.217	0.058	-0.158	-1.15	0.66	0.39	-0.27	-0.52
AU1983R	0.38	4.7	12.6	307.1	21300.	0.088	0.197	0.109	0.77	0.61	0.65	0.05	0.07
AU1983B	0.37	4.1	10.9	307.1	21300.	0.057	0.078	0.020	0.30	0.53	0.55	0.02	0.03
Group Average	0.22	8.2	47.9	301.9	24143.	0.283	0.225	-0.058	-0.19	0.93	0.75	-0.18	-0.22
S. Dev.	0.11	5.2	38.7	5.0	5463.	0.181	0.153	0.102	0.62	0.46	0.42	0.20	0.24
Avg. Abs. Value								0.095	0.50			0.20	0.25
S. Dev.								0.061	0.37			0.17	0.20
12. C5+ n-Alkane-NOx													
EC135	0.10	20.4	212.7	303.0	25000.	0.435	0.552	0.117	0.24	2.92	3.16	0.25	0.08
OC0979B	0.21	15.1	73.3	297.2	15200.	0.184	0.240	0.056	0.26	0.59	0.55	-0.05	-0.08
EC131	0.10	24.6	251.1	303.0	25000.	0.393	0.530	0.137	0.30	1.92	2.95	1.03	0.42
ITC559	0.19	279.4	1441.1	303.0	20300.	0.377	0.654	0.277	0.54	1.79	2.46	0.67	0.32

(continued)

Appendix C. Selected Results of Simulations of Individual Organic-NOx-Air Experiments Using the RADM-P Mechanism (continued).

Experiment	Initial Concentrations NOx (ppm)	Initial Concentrations HC (ppmC)	Initial Concentrations HC/NOx	Ave Temp (degK)	Ave H2O (ppm)	Maximum Concentration OZONE Expt (ppm)	Maximum Concentration OZONE Calc (ppm)	Maximum Concentration OZONE Calc -Expt (ppm)	Maximum Concentration OZONE Calc -Expt /Avg	Average Initial d([O3] - [NO])/dt Expt --	Average Initial d([O3] - [NO])/dt Calc (ppb/min)	Average Initial d([O3] - [NO])/dt Calc -Expt --	Average Initial d([O3] - [NO])/dt Calc -Expt /Avg
ITC538	0.11	60.3	529.0	303.0	18900.	0.150	0.300	0.150	0.67	0.74	1.03	0.29	0.33
ITC540	0.11	274.8	2421.3	303.0	20300.	0.360	0.370	0.010	0.03	1.85	1.10	-0.76	-0.51
ITC552	0.13	428.8	3278.4	303.0	20300.	0.315	0.344	0.029	0.09	1.19	1.07	-0.12	-0.11
ITC761	0.52	75.2	145.9	303.0	17500.	0.030	0.033	0.003		1.08	1.23	0.16	0.14
ITC762	0.27	74.7	280.4	303.0	17000.	0.105	0.176	0.071	0.50	0.83	1.51	0.68	0.58
ITC763	0.28	7.7	27.7	303.0	17100.	0.041	0.066	0.025		0.68	1.40	0.72	0.69
ITC797	0.52	7.3	14.0	303.0	12200.	0.004	0.010	0.006		0.64	0.93	0.29	0.37
ST1879R	0.21	6.3	30.4	298.3	20000.*	0.122	0.300	0.179	0.85	0.40	0.44	0.04	0.10
EC155	0.10	37.3	385.1	303.0	26200.	0.264	0.521	0.257	0.65	1.33	1.65	0.32	0.22
ITC1001	0.11	2.4	22.4	303.0	17500.	0.036	0.073	0.037		0.15	0.42	0.27	0.95
Group Average	0.21	93.9	650.9	302.3	19464.	0.201	0.298	0.097	0.41	1.15	1.42	0.27	0.25
S. Dev.	0.14	133.5	1015.3	1.9	3919.	0.153	0.211	0.092	0.27	0.75	0.87	0.44	0.36
Avg. Abs. Value								0.097	0.41			0.40	0.35
S. Dev.								0.092	0.27			0.31	0.26
13. Methylcyclohexane-NOx													
ITC765	0.53	0.0	0.1	303.0	17900.	0.022	0.011	-0.011		0.86	0.86	-0.20	-0.26
ITC766	0.26	0.0	0.1	303.0	17100.	0.121	0.159	0.038	0.27	0.87	1.34	0.48	0.43
ITC767	0.55	0.1	0.1	303.0	17900.	0.041	0.029	-0.012		1.09	1.05	-0.04	-0.03
ITC800	0.54	0.0	0.1	303.0	17500.	0.015	0.010	-0.004		0.86	0.72	-0.13	-0.17
Group Average	0.47	0.0	0.1	303.0	17600.	0.050	0.052	0.002	0.27	0.92	0.95	0.03	-0.01
S. Dev.	0.14	0.0	0.0	0.0	383.					0.12	0.32	0.31	0.31
Avg. Abs. Value								0.016	0.27			0.21	0.22
S. Dev.												0.19	0.17
14. Benzene-NOx													
ITC560	0.12	332.3	2874.4	303.0	17100.	0.323	0.329	0.006	0.02	7.01	15.95	8.94	0.78
ITC561	0.11	79.1	694.2	303.0	17600.	0.273	0.294	0.021	0.08	4.75	10.53	5.78	0.76
ITC562	0.56	83.8	149.7	303.0	18800.	0.412	0.528	0.116	0.25	2.85	10.45	7.60	1.14
ITC698	0.50	83.5	167.4	303.0	21900.	0.374	0.495	0.121	0.28	2.87	10.39	7.52	1.13
ITC710	0.55	83.6	151.0	303.0	21000.	0.367	0.512	0.145	0.33	2.70	9.92	7.22	1.14
ITC831	1.01	12.2	12.1	303.0	18300.	0.021	0.010	-0.011		0.17	0.32	0.15	0.61
Group Average	0.47	112.4	674.8	303.0	19117.	0.295	0.361	0.066	0.19	3.39	9.59	6.20	0.93
S. Dev.	0.33	111.3	1103.2	0.0	1920.	0.142	0.199	0.068	0.14	2.30	5.08	3.13	0.24
Avg. Abs. Value								0.070	0.19			6.20	0.93
S. Dev.								0.064	0.14			3.13	0.24

(continued)

Appendix C. Selected Results of Simulations of Individual Organic-NOx-Air Experiments Using the RADM-P Mechanism (continued).

Experiment	Initial Concentrations			Ave Temp	Ave H2O	Maximum Concentration OZONE				Average Initial d([O3] - [NO])/dt			
	NOx (ppm)	HC (ppmC)	HC/NOx	(degK)	(ppm)	Expt (ppm)	Calc (ppm)	Calc -Expt (ppm)	Calc -Expt /Avg	Expt --	Calc (ppb/min)	Calc -Expt --	Calc -Expt /Avg
15. Toluene-NOx													
EC264	0.48	8.1	17.0	303.0	18900.	0.419	0.397	-0.022	-0.05	4.46	5.24	0.79	0.16
EC265	0.48	7.5	15.6	303.0	21900.	0.393	0.395	0.001	0.00	3.56	5.07	1.52	0.35
EC266	0.49	8.4	17.0	303.0	19400.	0.405	0.401	-0.004	-0.01	4.62	5.43	0.81	0.16
EC269	0.47	4.0	8.4	303.0	19100.	0.318	0.311	-0.006	-0.02	2.55	2.67	0.12	0.05
EC270	0.46	4.2	9.0	303.0	20000.	0.369	0.385	0.016	0.04	3.72	4.12	0.39	0.10
EC271	0.21	8.0	37.4	303.0	20500.	0.296	0.318	0.023	0.07	6.56	5.58	-0.99	-0.16
EC272	0.48	4.1	8.5	303.0	19400.	0.410	0.306	-0.105	-0.29	3.69	2.65	-1.04	-0.33
EC273	0.11	4.1	37.2	303.0	21200.	0.215	0.245	0.030	0.13	5.90	3.46	-2.44	-0.52
EC327	0.45	4.0	8.9	303.0	22400.	0.376	0.376	0.000	0.00	2.49	2.76	0.27	0.10
EC336	0.44	7.2	16.3	303.0	26900.	0.396	0.434	0.039	0.09	6.06	6.76	0.70	0.11
EC337	0.45	7.9	17.7	303.0	27000.	0.325	0.389	0.064	0.18	2.55	4.11	1.56	0.47
EC339	0.44	5.0	11.3	303.0	26800.	0.225	0.337	0.112	0.40	1.53	2.99	1.46	0.64
EC340	0.43	4.1	9.5	303.0	25900.	0.344	0.356	0.012	0.03	2.50	2.59	0.09	0.03
ITC699	0.51	10.5	20.8	303.0	20300.	0.485	0.441	-0.043	-0.09	4.72	4.88	0.15	0.03
ITC828	1.02	3.0	3.0	303.0	17200.	0.021	0.008	-0.013		0.49	1.21	0.72	0.85
JL3080R	0.18	3.9	21.3	304.5	35200.	0.273	0.441	0.167	0.47	1.20	1.04	-0.16	-0.14
AU2780R	0.48	2.3	4.8	302.2	32000.	0.736	0.879	0.143	0.18	1.76	1.53	-0.23	-0.14
AU2782B	0.43	3.0	7.0	301.7	24700.	0.116	0.295	0.180	0.87	0.63	0.67	0.03	0.05
OC2782R	0.39	4.5	11.7	289.8	19500.	0.123	0.346	0.223	0.95	0.66	0.81	0.15	0.20
AU0183R	0.39	4.6	11.8	306.1	23700.	0.458	0.581	0.123	0.24	1.75	1.72	-0.03	-0.02
Group Average	0.44	5.4	14.7	302.5	23100.	0.335	0.382	0.047	0.17	3.07	3.26	0.19	0.10
S. Dev.	0.18	2.3	9.2	3.1	4692.	0.154	0.159	0.084	0.31	1.87	1.81	0.94	0.31
Avg. Abs. Value								0.066	0.22			0.68	0.23
S. Dev.								0.069	0.28			0.66	0.23
16. Xylene-NOx													
EC343	0.28	4.2	14.9	303.0	29500.	0.283	0.380	0.096	0.29	8.16	10.60	2.41	0.26
EC344	0.67	4.0	5.9	303.0	28900.	0.589	0.552	-0.037	-0.06	10.72	9.93	-0.79	-0.08
EC345	0.28	3.7	13.3	303.0	25200.	0.396	0.389	-0.007	-0.02	11.35	10.59	-0.76	-0.07
EC346	0.26	3.9	14.8	303.0	25900.	0.384	0.376	-0.007	-0.02	7.65	10.49	2.84	0.31
ITC702	0.52	4.0	7.8	303.0	20300.	0.627	0.509	-0.118	-0.21	7.79	8.09	0.30	0.04
ITC827	1.07	1.2	1.1	303.0	14400.	0.021	0.013	-0.007		1.12	2.08	0.96	0.60
JL3080B	0.18	2.2	12.4	304.5	28000.	0.555	0.535	-0.019	-0.04	1.97	1.93	-0.04	-0.02
AU2782R	0.43	2.0	4.6	301.7	24700.	0.491	0.608	0.117	0.21	1.31	1.64	0.33	0.22
OC2782B	0.39	2.8	7.0	289.8	19500.	0.396	0.453	0.057	0.13	1.43	1.97	0.54	0.32
AU0183B	0.37	2.7	7.2	306.0	23700.	0.688	0.784	0.096	0.13	2.39	2.75	0.36	0.14
Group Average	0.45	3.1	8.9	302.0	24010.	0.443	0.460	0.017	0.05	5.39	6.01	0.61	0.17
S. Dev.	0.26	1.0	4.7	4.4	4737.	0.195	0.200	0.073	0.16	4.14	4.22	1.19	0.21
Avg. Abs. Value								0.056	0.12			0.93	0.21
S. Dev.								0.047	0.10			0.94	0.18

(continued)

Experiment	Initial Concentrations			Ave Temp	Ave H2O	Maximum Concentration OZONE				Average Initial d([O3] - [NO])/dt			
	NOx (ppm)	HC (ppmC)	HC/NOx	(degK)	(ppm)	Expt (ppm)	Calc (ppm)	Calc -Expt (ppm)	Calc -Expt /Avg	Expt --	Calc (ppb/min)	Calc -Expt --	Calc -Expt /Avg
17. Mesitylene-NOx													
EC900	0.53	5.4	10.2	303.0	20000.*	0.381	0.434	0.053	0.13	3.85			
EC901	0.51	2.7	5.2	303.0	20000.*	0.384	0.341	-0.042	-0.12	8.88	3.72	-5.17	-0.82
EC903	1.00	4.7	4.7	303.0	20000.*	0.502	0.424	-0.078	-0.17	14.96	5.88	-9.08	-0.87
ITC703	0.50	5.3	10.6	303.0	21000.	0.707	0.496	-0.211	-0.35	14.59	9.40	-5.19	-0.43
ITC706	0.49	2.7	5.4	303.0	21000.	0.641	0.510	-0.130	-0.23	7.20	4.48	-2.72	-0.47
ITC709	0.99	4.7	4.7	303.0	21000.	0.779	0.560	-0.219	-0.33	11.74	7.21	-4.53	-0.48
ITC742	0.48	4.6	9.7	303.0	18100.	0.773	0.502	-0.271	-0.42	13.14	7.77	-5.37	-0.51
ITC826	0.90	0.8	0.9	303.0	17200.	0.022	0.009	-0.013		1.68	1.29	-0.39	-0.26
Group Average	0.68	3.9	6.4	303.0	19788.	0.524	0.410	-0.114	-0.21	9.50	5.68	-4.63	-0.55
S. Dev.	0.24	1.6	3.4	0.0	1419.	0.258	0.175	0.113	0.19	4.97	2.74	2.66	0.22
Avg. Abs. Value								0.127	0.25			4.63	0.55
S. Dev.								0.096	0.12			2.66	0.22
18. Tetralin-NOx													
ITC739	0.52	2.4	4.6	303.0	17900.	0.002	0.358	0.356		0.63	2.64	2.02	1.23
ITC747	0.50	93.2	187.4	303.0	17100.	0.508	0.720	0.211	0.34	2.73	54.42	51.69	1.81
ITC748	0.22	84.0	385.1	303.0	17500.	0.370	0.478	0.108	0.26	2.60	31.58	28.98	1.70
ITC750	0.53	44.5	84.6	303.0	17100.	0.482	0.697	0.215	0.36	2.10	45.57	43.46	1.82
ITC832	1.00	39.4	39.5	303.0	16800.	0.073	0.336	0.263	1.29	1.38	1.00	-0.37	-0.31
Group Average	0.55	52.7	140.2	303.0	17280.	0.287	0.518	0.231	0.56	1.89	27.04	25.16	1.25
S. Dev.	0.28	36.7	153.2	0.0	427.	0.235	0.182	0.090	0.49	0.88	24.42	23.67	0.91
Avg. Abs. Value								0.231	0.56			25.30	1.37
S. Dev.								0.090	0.49			23.47	0.64
19. Naphthalene-NOx													
ITC751	0.52	7.5	14.3	303.0	15100.	0.113	0.548	0.436	1.32	1.08	11.27	10.18	1.65
ITC755	0.24	14.1	58.3	303.0	17500.	0.259	0.450	0.191	0.54	1.57	21.78	20.22	1.73
ITC756	0.26	27.4	106.8	303.0	17200.	0.282	0.486	0.203	0.53	2.20	29.17	26.97	1.72
ITC798	0.53	19.4	36.8	303.0	16400.	0.204	0.624	0.421	1.02	1.66	29.50	27.84	1.79
ITC802	0.53	8.4	15.9	303.0	16800.	0.124	0.551	0.427	1.27	1.42	12.55	11.13	1.59
Group Average	0.42	15.4	46.4	303.0	16600.	0.196	0.532	0.335	0.93	1.59	20.85	19.27	1.70
S. Dev.	0.15	8.3	38.2	0.0	935.	0.077	0.067	0.127	0.38	0.41	8.74	8.40	0.08
Avg. Abs. Value								0.335	0.93			19.27	1.70
S. Dev.								0.127	0.38			8.40	0.08

(continued)

Appendix C. Selected Results of Simulations of Individual Organic-NOx-Air Experiments Using the RADM-P Mechanism (continued).

Experiment	Initial Concentrations			Ave Temp	Ave H2O	Maximum Concentration OZONE				Average Initial d([O3] - [NO])/dt			
	NOx (ppm)	HC (ppmC)	HC/NOx	(degK)	(ppm)	Expt (ppm)	Calc (ppm)	Calc -Expt (ppm)	Calc -Expt /Avg	Expt --	Calc (ppb/min)	Calc -Expt --	Calc -Expt /Avg
20. 2,3-Dimethylnaphthalene-NOx													
ITC775	0.29	1.7	5.8	303.0	16800.	0.274	0.296	0.022	0.08	1.73	2.53	0.81	0.38
ITC771	0.26	4.8	18.0	303.0	20300.	0.293	0.388	0.095	0.28	2.67	8.26	5.59	1.02
ITC806	0.33	5.9	17.7	303.0	17100.	0.360	0.438	0.079	0.20	2.69	8.80	6.11	1.06
ITC774	0.56	4.0	7.1	303.0	22700.	0.341	0.551	0.210	0.47	2.84	5.92	3.09	0.70
Group Average	0.36	4.1	12.2	303.0	19225.	0.317	0.418	0.101	0.26	2.48	6.38	3.90	0.79
S. Dev.	0.14	1.8	6.6	0.0	2806.	0.040	0.106	0.079	0.17	0.51	2.85	2.45	0.32
Avg. Abs. Value								0.101	0.26			3.90	0.79
S. Dev.								0.079	0.17			2.45	0.32
21. Simple Mixture Runs													
EC144	0.51	4.7	9.3	303.0	24400.	1.065	0.772	-0.293	-0.32	10.53	6.15	-4.39	-0.53
EC145	0.99	3.4	3.4	303.0	24400.	0.777	0.376	-0.401	-0.70	5.11	3.84	-1.27	-0.28
EC160	0.99	3.2	3.3	303.0	29200.	0.874	0.326	-0.548	-0.91	5.86	3.48	-2.39	-0.51
EC149	0.99	2.0	2.0	303.0	29300.	0.286	0.131	-0.155	-0.74	10.83	5.21	-5.63	-0.70
EC150	1.00	3.5	3.5	303.0	29900.	0.799	0.329	-0.470	-0.83	6.30	4.12	-2.18	-0.42
EC151	2.06	5.2	2.5	303.0	30400.	0.147	0.086	-0.060	-0.52	8.43	7.05	-1.38	-0.18
EC152	0.50	3.7	7.3	303.0	26400.	0.791	0.665	-0.127	-0.17	10.41	7.84	-2.57	-0.28
EC153	0.97	6.6	6.8	303.0	25400.	1.050	0.817	-0.233	-0.25	19.23	11.91	-7.32	-0.47
EC161	0.51	3.2	6.4	303.0	36900.	0.857	0.599	-0.259	-0.36	9.94	5.43	-4.52	-0.59
OC1278R	0.48	1.4	3.0	294.3	16100.	0.260	0.250	-0.010	-0.04	1.14	1.22	0.08	0.07
OC2578R	0.44	1.4	3.1	288.4	12800.	0.147	0.125	-0.022	-0.16	0.94	1.01	0.07	0.07
AU0180R	0.56	0.5	0.8	304.9	23400.	0.256	0.107	-0.149	-0.82	0.98	0.64	-0.35	-0.43
AU1480R	0.47	1.4	3.0	305.2	34700.	0.863	0.474	-0.389	-0.58	2.13	1.37	-0.76	-0.44
EC166	0.10	9.2	92.0	303.0	27700.	0.462	0.379	-0.083	-0.20	2.11	1.41	-0.70	-0.39
EC172	0.10	2.8	28.9	303.0	21600.	0.369	0.297	-0.072	-0.22	1.00	0.70	-0.30	-0.35
ST0682R	0.46	2.8	6.2	299.1	22200.	0.378	0.536	0.158	0.34	1.11	1.29	0.18	0.15
ST0682B	0.45	2.9	6.5	299.1	22200.	0.478	0.574	0.096	0.18	1.35	1.59	0.24	0.16
EC106	0.50	9.2	18.3	303.0	20900.	0.592	0.617	0.025	0.04	3.80	4.08	0.28	0.07
EC113	0.11	9.5	85.0	303.0	19500.	0.352	0.442	0.090	0.23	5.26	7.09	1.83	0.30
EC114	1.00	17.3	17.3	303.0	28800.	0.744	0.710	-0.034	-0.05	8.03	6.11	-1.91	-0.27
EC115	0.51	12.7	25.2	303.0	22000.	0.590	0.612	0.021	0.04	3.78	3.44	-0.34	-0.09
EC116	0.49	18.6	37.6	303.0	27300.	0.743	0.785	0.042	0.06	8.28	9.30	1.01	0.12
EC335	0.44	7.7	17.4	303.0	24700.	0.398	0.383	-0.015	-0.04	4.64	4.31	-0.33	-0.07
EC329	0.45	4.2	9.2	303.0	27700.	0.403	0.406	0.002	0.01	3.27	3.27	0.00	0.00
EC330	0.29	4.3	14.6	303.0	26000.	0.344	0.359	0.015	0.04	3.91	3.50	-0.41	-0.11
EC334	0.45	8.1	18.2	303.0	27800.	0.408	0.420	0.012	0.03	5.59	5.09	-0.50	-0.09
EC338	0.45	15.0	33.7	303.0	27800.	0.484	0.499	0.016	0.03	5.19	4.78	-0.41	-0.08
EC328	0.45	12.1	27.1	303.0	27500.	0.523	0.520	-0.002	0.00	3.50	3.31	-0.19	-0.06
JL1581R	0.27	2.3	8.4	304.6	20000.*	0.485	0.693	0.208	0.35	1.08	1.23	0.15	0.13
JL1881R	0.26	2.1	8.0	303.2	20000.*	0.658	0.596	-0.063	-0.10	1.31	1.23	-0.08	-0.06
ST2481R	0.23	1.6	6.7	292.2	22800.	0.211	0.277	0.066	0.27	0.62	0.67	0.05	0.08
AU2781R	0.23	2.1	9.2	299.5	30900.	0.554	0.496	-0.058	-0.11	0.95	0.92	-0.03	-0.03

(continued)

Appendix C. Selected Results of Simulations of Individual Organic-NOx-Air Experiments Using the RADM-P Mechanism (continued).

Experiment	Initial Concentrations NOx (ppm)	HC (ppmC)	HC/NOx	Ave Temp (degK)	Ave H2O (ppm)	Maximum Concentration OZONE Expt (ppm)	Calc (ppm)	Calc -Expt (ppm)	Calc -Expt /Avg	Average Initial d([O3] - [NO])/dt Expt --	Calc (ppb/min)	Calc -Expt --	Calc -Expt /Avg
OC0382R	0.25	2.7	11.0	297.2	21200.	0.247	0.141	-0.106	-0.55	0.76	0.55	-0.21	-0.32
OC0382B	0.25	1.9	7.7	296.9	21100.	0.158	0.038	-0.120	-1.23	0.62			
NV1582R	0.18	2.6	14.4	283.8	20000.*	0.061	0.045	-0.016	-0.30	0.42	0.34	-0.08	-0.22
JL2281R	0.26	2.4	9.1	302.3*	20000.*	0.626	0.628	0.002	0.00	1.18	1.11	-0.06	-0.06
JL2181B	0.24	1.3	5.4	304.2*	20000.*	0.237	0.428	0.191	0.58	0.63	0.64	0.01	0.02
NV1582B	0.18	2.7	14.9	283.8	20000.*	0.167	0.240	0.073	0.36	0.71	0.74	0.04	0.05
DE0782B	0.19	3.5	18.7	286.4	13400.	0.093	0.296	0.203	1.05	0.55	0.72	0.18	0.28
JN1379B	0.44	6.1	13.7	294.9	20000.*	0.756	0.809	0.053	0.07	2.44	2.78	0.34	0.13
Group Average	0.49	5.2	15.5	300.2	24160.	0.492	0.432	-0.060	-0.14	4.10	3.32	-0.87	-0.14
S. Dev.	0.37	4.5	19.2	5.7	5188.	0.270	0.221	0.175	0.44	4.06	2.77	1.83	0.25
Avg. Abs. Value								0.124	0.32			1.10	0.22
S. Dev.								0.136	0.32			1.69	0.18
22. 3-Component and "Mini" Surrogates													
ITC479	0.09	4.0	43.4	303.0	20300.	0.332	0.323	-0.009	-0.03	2.95	4.79	1.84	0.48
ITC584	0.10	4.0	40.7	303.0	20300.	0.375	0.320	-0.055	-0.16	3.05	3.93	0.88	0.25
ITC579	0.10	3.4	34.7	303.0	15800.	0.356	0.303	-0.054	-0.16	1.54	2.14	0.61	0.33
ITC472	0.10	3.6	35.1	303.0	13700.	0.258	0.331	0.073	0.25	1.72	3.02	1.31	0.55
ITC474	0.09	4.2	45.1	303.0	15600.	0.293	0.329	0.036	0.12	3.40	6.08	2.69	0.57
ITC581	0.09	4.3	50.0	303.0	16100.	0.352	0.315	-0.037	-0.11	3.74	5.28	1.54	0.34
ITC585	0.10	4.8	50.8	303.0	17100.	0.311	0.332	0.021	0.07	5.11	6.98	1.88	0.31
ITC478	0.10	5.0	52.6	303.0	18300.	0.320	0.352	0.032	0.09	4.73	8.19	3.46	0.54
ITC482	0.10	1.2	12.3	303.0	18300.	0.279	0.298	0.019	0.07	2.44	4.39	1.94	0.57
ITC488	0.09	6.0	66.2	303.0	19600.	0.293	0.332	0.039	0.12	3.06	5.17	2.10	0.51
ITC492	0.09	8.1	88.4	303.0	15000.	0.326	0.355	0.029	0.09	3.28	5.39	2.11	0.49
ITC494	0.09	8.5	92.5	303.0	21100.	0.321	0.363	0.041	0.12	3.30	5.33	2.03	0.47
ITC498	0.10	3.9	40.2	303.0	19300.	0.320	0.336	0.016	0.05	2.16	3.60	1.45	0.50
ITC500	0.10	4.1	42.7	303.0	18700.	0.286	0.322	0.036	0.12	5.18	7.40	2.22	0.35
ITC502	0.09	4.6	49.5	303.0	18100.	0.271	0.304	0.034	0.12	7.07	12.30	5.23	0.54
ITC462	0.11	7.5	71.3	303.0	18300.	0.099	0.269	0.170	0.92	0.70	2.51	1.81	1.13
ITC466	0.10	6.5	62.7	303.0	18200.	0.131	0.283	0.152	0.73	0.77	2.96	2.19	1.17
ITC468	0.09	4.6	49.0	303.0	18000.	0.176	0.304	0.128	0.53	1.19	3.48	2.29	0.98
ITC451	0.10	5.2	52.0	303.0	19800.	0.312	0.296	-0.016	-0.05	3.95	5.63	1.68	0.35
ITC455	0.09	4.4	47.8	303.0	20200.	0.304	0.300	-0.004	-0.01	3.52	5.05	1.52	0.36
ITC977	0.13	3.2	25.1	303.0	20900.	0.329	0.330	0.001	0.00	3.94	3.50	-0.44	-0.12
ITC985	0.12	2.7	22.9	303.0	20100.	0.336	0.300	-0.036	-0.11	3.95	3.31	-0.65	-0.18
ITC997	0.12	2.7	23.0	303.0	20100.	0.316	0.298	-0.018	-0.06	3.89	3.26	-0.63	-0.18
ITC979	0.12	2.9	23.1	303.0	20100.	0.404	0.418	0.014	0.03	4.88	4.09	-0.78	-0.17
ITC992	0.12	2.6	20.9	303.0	20900.	0.384	0.407	0.023	0.06	5.57	4.47	-1.10	-0.22
ITC981	0.14	6.5	45.0	303.0	19000.	0.328	0.375	0.047	0.13	2.56	3.33	0.77	0.26
ITC993	0.11	7.1	66.9	303.0	20100.	0.276	0.359	0.083	0.26	2.45	2.71	0.25	0.10
JL1581B	0.28	2.3	8.0	304.6	20000.*	0.474	0.632	0.158	0.29	1.10	1.16	0.06	0.05
ST2481B	0.23	1.9	8.1	292.2	14200.	0.246	0.283	0.037	0.14	0.71	0.71	0.00	0.00

(continued)

Appendix C. Selected Results of Simulations of Individual Organic-NOx-Air Experiments Using the RADM-P Mechanism (continued).

Experiment	Initial Concentrations			Ave Temp	Ave H2O	Maximum Concentration OZONE				Average Initial d([O3] - [NO])/dt			
	NOx (ppm)	HC (ppmC)	HC/NOx	(degK)	(ppm)	Expt (ppm)	Calc (ppm)	Calc -Expt (ppm)	Calc -Expt /Avg	Expt --	Calc (ppb/min)	Calc -Expt --	Calc -Expt /Avg
JN0982B	0.28	3.1	11.0	299.7*	14300.	0.667	0.586	-0.081	-0.13	1.37	1.20	-0.17	-0.13
JN1483R	0.22	2.6	11.6	301.2	26100.	0.585	0.529	-0.056	-0.10	1.10	1.07	-0.03	-0.03
JN2783B	0.26	2.9	11.1	305.1	24400.	0.511	0.596	0.085	0.15	1.01	1.13	0.12	0.11
AU1883B	0.28	0.6	2.0	303.0	23100.	0.556	0.545	-0.011	-0.02	0.70	0.65	-0.05	-0.07
AU2683R	0.32	2.6	8.1	302.2	26400.	0.646	0.612	-0.035	-0.05	1.24	1.18	-0.07	-0.05
JL1881B	0.27	2.3	8.5	303.2	20000.*	0.693	0.643	-0.050	-0.08	1.91	1.76	-0.15	-0.08
JN0982R	0.29	3.1	10.7	299.7*	14700.	0.714	0.647	-0.068	-0.10	1.77	1.56	-0.21	-0.13
Group Average	0.14	4.1	37.0	302.6	19061.	0.366	0.387	0.021	0.09	2.81	3.85	1.05	0.28
S. Dev.	0.08	1.9	23.7	2.0	3028.	0.148	0.121	0.063	0.23	1.61	2.43	1.36	0.36
Avg. Abs. Value								0.050	0.16			1.28	0.35
S. Dev.								0.043	0.19			1.14	0.29
23. SAPRC 7-Component Surrogates													
EC231	0.49	13.2	26.9	303.0	17400.	0.620	0.711	0.090	0.14	6.99	7.96	0.97	0.13
EC232	0.49	9.3	18.9	303.0	17100.	0.342	0.377	0.035	0.10	3.12	3.03	-0.09	-0.03
EC233	0.10	9.5	92.5	303.0	21400.	0.330	0.385	0.056	0.16	4.07	4.73	0.66	0.15
EC237	0.48	10.5	21.6	303.0	23200.	0.652	0.645	-0.007	-0.01	7.36	5.98	-1.38	-0.21
EC238	0.95	10.1	10.6	303.0	25400.	0.691	0.701	0.010	0.01	5.10	4.79	-0.31	-0.06
EC241	0.49	5.0	10.2	303.0	20700.	0.408	0.378	-0.030	-0.08	2.87	2.94	0.08	0.03
EC242	0.50	12.9	25.6	303.0	24600.	0.682	0.678	-0.003	-0.01	17.53	16.62	-0.91	-0.05
EC243	0.50	9.7	19.5	303.0	16400.	0.716	0.717	0.001	0.00	14.50	12.74	-1.76	-0.13
EC245	1.00	12.9	12.9	303.0	20400.	0.894	0.847	-0.047	-0.05	13.41	12.84	-0.57	-0.04
EC246	0.51	8.6	17.0	303.0	22100.	0.574	0.433	-0.141	-0.28	2.65	1.97	-0.68	-0.29
EC247	0.51	6.2	12.2	303.0	22700.	0.657	0.625	-0.032	-0.05	7.49	6.48	-1.01	-0.14
Group Average	0.55	9.8	24.4	303.0	21036.	0.597	0.591	-0.006	-0.01	7.74	7.28	-0.46	-0.06
S. Dev.	0.24	2.6	23.3	0.0	3020.	0.173	0.167	0.060	0.12	5.16	4.78	0.83	0.13
Avg. Abs. Value								0.041	0.08			0.77	0.12
S. Dev.								0.043	0.08			0.52	0.08
24. SAPRC 8-Component Surrogates													
ITC626	0.30	4.0	13.4	303.0	14300.	0.618	0.548	-0.070	-0.12	2.18	2.32	0.14	0.06
ITC630	0.31	1.9	6.3	303.0	16300.	0.284	0.287	0.003	0.01	0.86	1.04	0.18	0.19
ITC631	0.32	1.0	3.2	303.0	17500.	0.043	0.066	0.023		0.47	0.54	0.07	0.15
ITC633	0.64	4.0	6.2	303.0	16600.	0.231	0.308	0.077	0.28	1.26	1.58	0.31	0.22
ITC635	1.21	4.0	3.3	303.0	17500.	0.006	0.021	0.015		0.95	1.05	0.09	0.09
ITC637	0.31	4.0	12.8	303.0	16900.	0.617	0.545	-0.072	-0.12	2.31	2.30	-0.01	0.00
ITC865	0.28	8.4	29.9	303.0	15100.	0.632	0.514	-0.118	-0.21	2.60	3.51	0.91	0.30

(continued)

Appendix C. Selected Results of Simulations of Individual Organic-NOx-Air Experiments Using the RADM-P Mechanism (continued).

Experiment	Initial Concentrations			Ave Temp	Ave H2O	Maximum Concentration OZONE				Average Initial d([O3] - [NO])/dt			
	NOx (ppm)	HC (ppmC)	HC/NOx	(degK)	(ppm)	Expt (ppm)	Calc (ppm)	Calc -Expt (ppm)	Calc -Expt /Avg	Expt --	Calc (ppb/min)	Calc -Expt --	Calc -Expt /Avg
ITC867	0.28	4.8	17.2	303.0	14600.	0.631	0.544	-0.088	-0.15	2.23	3.41	1.19	0.42
ITC868	0.37	2.9	7.8	303.0	17100.	0.518	0.435	-0.083	-0.17	2.10	1.46	-0.64	-0.36
ITC871	0.37	1.7	4.6	303.0	14600.	0.376	0.265	-0.111	-0.35	1.18	1.12	-0.06	-0.05
ITC872	0.38	2.1	5.7	303.0	14600.	0.213	0.228	0.015	0.07	1.20	1.36	0.16	0.13
ITC873	0.39	1.3	3.4	303.0	14600.	0.160	0.115	-0.045	-0.33	0.85	0.80	-0.05	-0.06
ITC874	0.38	2.1	5.7	303.0	13200.	0.191	0.160	-0.031	-0.18	0.83	0.88	0.05	0.06
ITC877	0.38	2.3	6.2	303.0	14600.	0.250	0.237	-0.013	-0.05	1.14	1.34	0.20	0.16
ITC880	0.73	2.2	3.0	303.0	13700.	0.031	0.046	0.016		0.85	0.99	0.14	0.15
ITC881	0.73	2.3	3.1	303.0	14000.	0.012	0.033	0.021		1.03	1.10	0.07	0.06
ITC885	0.64	1.5	2.4	303.0	14600.	0.012	0.027	0.015		0.44	0.78	0.35	0.57
ITC886	0.73	2.3	3.1	303.0	20000.*	0.012	0.022	0.010		1.24	0.70	-0.54	-0.55
ITC888	0.33	4.7	14.5	303.0	18000.	0.579	0.512	-0.068	-0.12	1.65	1.89	0.24	0.14
ITC891	0.32	4.4	13.7	303.0	20000.*	0.602	0.515	-0.087	-0.16	2.67	2.91	0.23	0.08
OTC189A	0.45	3.3	7.4	295.4	5000.*	0.576	0.766	0.190	0.28	3.79	3.62	-0.17	-0.05
OTC189B	0.45	4.0	8.9	298.0	5000.*	0.712	0.845	0.132	0.17	3.70	3.74	0.04	0.01
OTC190A	0.41	3.8	9.2	302.7	5400.*	0.702	0.841	0.138	0.18	4.24	3.35	-0.89	-0.23
OTC190B	0.42	3.8	9.0	299.5	5410.*	0.669	0.793	0.124	0.17	3.73	2.94	-0.79	-0.24
OTC192A	0.47	4.2	8.9	297.8	5000.*	0.735	0.852	0.117	0.15	4.25	3.41	-0.85	-0.22
OTC192B	0.47	4.2	8.9	298.4	5000.*	0.754	0.760	0.006	0.01	3.84	2.80	-1.05	-0.31
OTC194A	0.38	7.4	19.3	296.1	5000.*	0.737	0.905	0.167	0.20	7.85	7.71	-0.14	-0.02
OTC194B	0.38	3.7	9.7	295.7	5000.*	0.603	0.701	0.098	0.15	2.95	3.04	0.09	0.03
OTC195A	0.41	1.8	4.5	351.6	4660.*	0.164	0.112	-0.052	-0.38	2.05	1.20	-0.85	-0.52
OTC195B	0.41	4.1	9.9	360.0	3180.*	0.681	0.775	0.095	0.13	4.14	3.83	-0.31	-0.08
OTC196B	0.41	3.7	9.1	337.5	5000.*	0.597	0.804	0.206	0.29	3.86	3.37	-0.49	-0.14
OTC197A	0.38	3.6	9.5	353.2	5000.*	0.621	0.554	-0.068	-0.12	4.12	2.66	-1.46	-0.43
OTC197B	0.77	3.1	4.1	358.0	5000.*	0.152	0.102	-0.049	-0.39	2.86	2.07	-0.79	-0.32
OTC198A	0.84	5.4	6.4	353.5	5000.*	0.704	0.576	-0.128	-0.20	6.09	3.69	-2.40	-0.49
OTC198B	0.40	3.7	9.4	347.5	5000.*	0.674	0.633	-0.041	-0.06	3.86	2.58	-1.28	-0.40
OTC199A	0.36	3.5	9.6	299.7	5000.*	0.591	0.653	0.062	0.10	3.86	3.05	-0.81	-0.23
OTC199B	0.37	3.5	9.6	298.9	5000.*	0.606	0.638	0.032	0.05	3.40	2.92	-0.47	-0.15
OTC202A	0.73	6.0	8.2	325.1	5000.*	0.714	0.494	-0.220	-0.37	6.95	13.77	6.81	0.66
OTC202B	0.40	2.6	6.7	324.1	4560.*	0.522	0.424	-0.098	-0.21	3.82	3.17	-0.65	-0.19
OTC203A	0.39	3.5	9.0	293.3	4850.*	0.231	0.282	0.051	0.20	2.34	2.36	0.02	0.01
OTC203B	0.19	3.5	18.5	293.7	4880.*	0.394	0.447	0.053	0.13	2.20	2.65	0.45	0.19
OTC204A	0.35	3.6	10.2	322.2	4330.*	0.302	0.377	0.075	0.22	3.27	3.48	0.21	0.06
OTC204B	0.17	3.5	20.3	348.8	4330.*	0.381	0.468	0.087	0.21	2.62	2.91	0.29	0.11
OTC205A	0.84	3.8	4.5	464.9	5000.*	0.039	0.060	0.021		4.85	2.16	-2.70	-0.77
OTC205B	0.14	3.6	26.5	433.4	5000.*	0.392	0.552	0.160	0.34	4.49	3.71	-0.78	-0.19
OTC215A	0.45	3.5	7.8	293.1	4420.*	0.830	0.857	0.027	0.03	4.33	3.65	-0.68	-0.17
OTC215B	0.44	4.1	9.3	293.4	4420.*	0.868	0.937	0.069	0.08	5.33	5.49	0.16	0.03
OTC217A	0.50	4.9	9.6	295.5	7460.*	0.483	0.584	0.101	0.19	2.55	2.52	-0.03	-0.01
OTC217B	0.51	4.6	9.0	294.2	7460.*	0.831	0.935	0.104	0.12	4.64	4.30	-0.34	-0.08
OTC221A	0.41	2.4	5.8	290.6	4460.*	0.235	0.286	0.051	0.20	1.63	1.50	-0.12	-0.08
OTC221B	0.42	2.0	4.7	288.8	4460.*	0.333	0.357	0.024	0.07	1.63	1.60	-0.03	-0.02
OTC222A	0.44	3.4	7.8	298.5	5000.*	0.909	0.964	0.055	0.06	3.83	3.75	-0.09	-0.02

(continued)

Appendix C. Selected Results of Simulations of Individual Organic-NOx-Air Experiments Using the RADM-P Mechanism (continued).

Experiment	Initial Concentrations			Ave Temp	Ave H2O	Maximum Concentration OZONE				Average Initial d([O3] - [NO])/dt			
	NOx (ppm)	HC (ppmC)	HC/NOx	(degK)	(ppm)	Expt (ppm)	Calc (ppm)	Calc -Expt (ppm)	Calc -Expt /Avg	Expt --	Calc (ppb/min)	Calc -Expt --	Calc -Expt /Avg
OTC222B	0.43	2.6	6.0	296.1	5000.*	0.940	1.127	0.187	0.18	5.55	6.25	0.70	0.12
OTC223A	0.36	4.8	13.4	314.9	4270.*	0.953	0.883	-0.069	-0.08	4.55	4.15	-0.41	-0.09
OTC223B	0.40	3.5	8.8	314.7	4270.*	0.771	0.729	-0.043	-0.06	3.15	2.88	-0.27	-0.09
OTC224A	0.34	4.4	12.7	303.5	6410.*	0.776	0.786	0.010	0.01	3.67	2.96	-0.71	-0.21
OTC224B	0.34	4.3	12.6	303.8	6410.*	0.813	0.850	0.038	0.05	4.94	4.48	-0.47	-0.10
OTC226A	0.45	2.5	5.5	312.5	6840.*	0.751	0.545	-0.205	-0.32	3.12	2.37	-0.75	-0.27
OTC228A	0.41	2.4	6.0	293.2	5000.*	0.246	0.433	0.187	0.55	1.49	1.96	0.47	0.27
OTC228B	0.41	2.3	5.6	294.3	5000.*	0.296	0.464	0.168	0.44	1.79	2.60	0.81	0.37
OTC229A	0.46	3.0	6.6	295.7	5000.*	0.253	0.460	0.207	0.58	1.56	2.01	0.45	0.25
OTC229B	0.46	1.7	3.8	296.0	5000.*	0.168	0.405	0.237	0.83	1.38	1.87	0.49	0.30
OTC230A	0.41	3.1	7.6	297.9	5000.*	0.489	0.842	0.353	0.53	2.43	3.14	0.71	0.25
OTC230B	0.41	1.7	4.2	298.2	5000.*	0.271	0.564	0.293	0.70	1.66	2.21	0.55	0.29
OTC237A	0.52	4.3	8.2	292.3	3810.*	0.807	0.836	0.029	0.03	4.10	3.46	-0.64	-0.17
OTC237B	0.52	4.4	8.5	292.8	3810.*	0.757	0.691	-0.066	-0.09	3.48	2.97	-0.50	-0.16
OTC238A	0.50	2.9	5.8	292.5	4810.*	0.406	0.403	-0.003	-0.01	2.58	2.22	-0.36	-0.15
OTC238B	0.50	3.9	7.8	292.0	4810.*	0.702	0.700	-0.002	0.00	4.06	3.60	-0.46	-0.12
OTC239A	0.49	2.7	5.4	290.2	5150.*	0.343	0.401	0.058	0.15	2.66	2.54	-0.12	-0.05
OTC239B	0.50	2.5	5.0	290.9	5150.*	0.234	0.172	-0.062	-0.31	1.85	1.49	-0.35	-0.21
OTC240A	0.50	1.8	3.6	93.4	6210.*	0.034	0.037	0.003		1.08	0.92	-0.16	-0.16
OTC240B	0.50	2.0	4.1	104.2	6210.*	0.217	0.119	-0.098	-0.58	1.79	1.39	-0.40	-0.25
OTC241A	0.32	4.7	14.8	290.7	4760.*	0.671	0.698	0.027	0.04	3.26	2.99	-0.28	-0.09
OTC241B	0.31	4.0	12.9	291.1	4760.*	0.674	0.683	0.009	0.01	3.30	3.27	-0.03	-0.01
OTC242A	0.45	2.6	5.8	302.0	4670.*	0.182	0.161	-0.021	-0.12	1.47	1.35	-0.13	-0.09
OTC242B	0.46	2.1	4.7	302.1	4670.*	0.639	0.640	0.001	0.00	3.04	2.70	-0.33	-0.12
OTC243A	0.47	4.7	10.0	276.5	4720.*	0.142	0.207	0.065	0.37	1.41	1.84	0.43	0.27
OTC243B	0.38	3.7	9.7	277.4	4720.*	0.152	0.174	0.022	0.13	1.40	2.18	0.77	0.43
OTC248A	0.48	3.7	7.7	271.6	5000.*	0.056	0.060	0.004	0.06	1.40	1.24	-0.16	-0.13
OTC248B	0.46	2.9	6.3	268.9	5000.*	0.081	0.090	0.009	0.10	1.61	1.73	0.11	0.07
OTC249A	0.48	5.6	11.8	286.9	3540.*	0.348	0.340	-0.008	-0.02	2.55	2.36	-0.19	-0.08
OTC249B	0.46	4.9	10.7	286.2	3540.*	0.325	0.365	0.040	0.12	2.83	3.02	0.19	0.07
Group Average	0.45	3.5	8.7	302.3	7630.	0.454	0.483	0.029	0.05	2.81	2.71	-0.10	-0.03
S. Dev.	0.16	1.3	4.9	43.6	4865.	0.272	0.286	0.103	0.25	1.51	1.76	1.00	0.25
Avg. Abs. Value								0.078	0.19			0.54	0.19
S. Dev.								0.072	0.17			0.84	0.16
25. UNC Miscellaneous Surrogates													
ST2081R	0.23	2.3	10.0	294.1	21900.	0.403	0.466	0.062	0.14	0.95	1.06	0.10	0.10
DE0782R	0.19	3.4	18.3	286.4	13400.	0.076	0.357	0.281	1.30	0.52	0.75	0.23	0.36
AU2681R	0.24	2.0	8.4	298.8	25500.	0.506	0.520	0.014	0.03	1.18	1.08	-0.10	-0.09
AU2681B	0.24	2.0	8.5	295.7	27500.	0.544	0.448	-0.096	-0.19	1.22	1.01	-0.21	-0.19
AU2781B	0.23	2.0	8.8	296.4	25000.	0.623	0.476	-0.147	-0.27	1.27	1.07	-0.20	-0.17
ST0381R	0.24	1.8	7.6	301.0	23200.	0.541	0.452	-0.089	-0.18	1.48	1.22	-0.26	-0.19
ST1081R	0.25	2.8	11.3	297.9	22300.	0.610	0.603	-0.008	-0.01	1.59	1.54	-0.05	-0.03
ST2081B	0.23	2.1	9.2	292.6	15200.	0.414	0.414	0.000	0.00	1.06	0.99	-0.07	-0.07

(continued)

Appendix C. Selected Results of Simulations of Individual Organic-NOx-Air Experiments Using the RADM-P Mechanism (continued).

Experiment	Initial Concentrations			Ave Temp	Ave H2O	Maximum Concentration OZONE				Average Initial d([O3] - [NO])/dt			
	NOx (ppm)	HC (ppmC)	HC/NOx	(degK)	(ppm)	Expt (ppm)	Calc (ppm)	Calc -Expt (ppm)	Calc -Expt /Avg	Expt --	Calc (ppb/min)	Calc -Expt --	Calc -Expt /Avg
JL2081B	0.42	1.8	4.3	305.0*	20000.*	0.165	0.325	0.160	0.66	0.82	0.82	0.01	0.01
ST1682R	0.43	3.2	7.5	304.4	23000.	0.410	0.508	0.099	0.22	1.28	1.17	-0.11	-0.09
JL2081R	0.41	2.7	6.6	305.0*	20000.*	0.635	0.679	0.043	0.07	1.55	1.44	-0.11	-0.07
JL2281B	0.26	2.9	11.2	302.3*	20000.*	0.722	0.675	-0.047	-0.07	1.80	1.70	-0.10	-0.06
OC1481R	0.28	3.3	11.9	291.3	9470.	0.462	0.569	0.108	0.21	1.53	1.57	0.04	0.03
ST1682B	0.43	3.1	7.2	304.4	23000.	0.840	0.800	-0.040	-0.05	2.39	2.08	-0.31	-0.14
ST2981R	0.24	2.5	10.3	293.7	18700.	0.294	0.426	0.132	0.37	0.76	0.88	0.12	0.15
ST298[illegible]B	0.24	2.5	10.4	291.6	14400.	0.485	0.494	0.009	0.02	1.35	1.30	-0.05	-0.04
OC1481B	0.29	2.9	9.9	288.9	10300.	0.458	0.561	0.102	0.20	1.48	1.51	0.03	0.02
ST0381B	0.23	2.0	8.6	297.9	16800.	0.611	0.516	-0.095	-0.17	1.70	1.55	-0.15	-0.09
ST1081B	0.24	1.0	4.1	295.3	17700.	0.626	0.382	-0.244	-0.48	1.36	0.96	-0.40	-0.34
JL0882R	0.29	2.1	7.3	304.2	16000.	0.598	0.703	0.105	0.16	1.25	1.35	0.10	0.08
JL0882B	0.28	2.1	7.4	304.2	16000.	0.541	0.689	0.147	0.24	1.12	1.30	0.18	0.15
Group Average	0.28	2.4	9.0	297.7	19018.	0.503	0.527	0.024	0.10	1.32	1.26	-0.06	-0.03
S. Dev.	0.08	0.6	3.0	5.8	4902.	0.175	0.126	0.121	0.37	0.40	0.33	0.16	0.15
Avg. Abs. Value								0.097	0.24			0.14	0.12
S. Dev.								0.073	0.29			0.10	0.10
26. UNC "Synurban" Surrogate													
AU2284R	0.32	0.4	1.2	302.7	8470.	0.657	0.773	0.116	0.16	1.61	1.63	0.03	0.02
AU2584R	0.34	0.1	0.3	302.0	22600.	0.075	0.109	0.034	0.37	0.70	0.64	-0.06	-0.09
AU2584B	0.33	0.1	0.4	302.0	22600.	0.096	0.135	0.039	0.33	0.69	0.66	-0.03	-0.05
ST0184R	0.31	0.2	0.6	302.5	9380.	0.546	0.661	0.115	0.19	1.32	1.31	-0.01	-0.01
ST0184B	0.30	0.2	0.8	302.5	9380.	0.646	0.704	0.058	0.09	1.72	1.58	-0.14	-0.08
ST0284R	0.34	0.1	0.4	304.6	19900.	0.119	0.265	0.146	0.76	0.73	0.76	0.02	0.03
ST0284B	0.33	0.1	0.3	304.5	19900.	0.020	0.144	0.124		0.40	0.50	0.10	0.22
JN2685R	0.30	0.2	0.6	303.6	16800.	0.629	0.677	0.049	0.07	1.34	1.46	0.12	0.09
JN2685B	0.30	0.3	0.9	303.6	16800.	0.788	0.761	-0.027	-0.03	1.74	1.85	0.11	0.06
JN2885R	0.38	0.1	0.4	299.8	11800.	0.238	0.391	0.153	0.49	0.85	0.89	0.04	0.05
JN2885B	0.39	0.2	0.5	299.8	11800.	0.275	0.278	0.003	0.01	0.87	0.88	0.01	0.01
Group Average	0.33	0.2	0.6	302.5	15403.	0.372	0.445	0.074	0.24	1.09	1.11	0.02	0.02
S. Dev.	0.03	0.1	0.3	1.6	5427.	0.284	0.272	0.060	0.25	0.47	0.47	0.08	0.09
Avg. Abs. Value								0.078	0.25			0.06	0.06
S. Dev.								0.053	0.24			0.05	0.06

(continued)

Appendix C. Selected Results of Simulations of Individual Organic-NOx-Air Experiments Using the RADM-P Mechanism (continued).

Experiment	Initial Concentrations NOx (ppm)	HC (ppmC)	HC/NOx	Ave Temp (degK)	Ave H2O (ppm)	Maximum Concentration OZONE Expt (ppm)	Calc (ppm)	Calc -Expt (ppm)	Calc -Expt /Avg	Average Initial d([O3] - [NO])/dt Expt --	Calc (ppb/min)	Calc -Expt --	Calc -Expt /Avg
27. UNC "Synauto" Surrogate													
AU0484R	0.37	0.4	1.0	307.5	34900.	0.515	0.648	0.133	0.23	1.45	1.38	-0.06	-0.04
AU0484B	0.36	0.3	0.8	307.5	34700.	0.328	0.562	0.234	0.53	1.16	1.12	-0.04	-0.04
AU0584R	0.36	0.3	0.7	307.1	44900.	0.335	0.465	0.130	0.33	1.08	0.98	-0.10	-0.10
AU0584B	0.35	0.4	1.0	307.2	44900.	0.595	0.656	0.062	0.10	1.48	1.38	-0.10	-0.07
AU0684R	0.35	0.7	2.1	307.6	36800.	0.887	0.853	-0.035	-0.04	2.53	2.10	-0.43	-0.18
AU0684B	0.35	1.1	3.2	307.6	36800.	0.940	0.902	-0.037	-0.04	3.16	2.52	-0.64	-0.22
AU0784R	0.38	0.4	1.0	308.0	34700.	0.602	0.672	0.070	0.11	1.61	1.48	-0.13	-0.09
AU0884B	0.34	1.1	3.1	307.3	29000.	0.834	0.825	-0.009	-0.01	2.92	2.39	-0.52	-0.20
AU0984R	0.39	0.4	0.9	307.8	31500.	0.521	0.559	0.039	0.07	1.51	1.26	-0.25	-0.18
ST0884R	0.34	0.6	1.9	298.5	6920.	0.566	0.751	0.185	0.28	1.27	1.38	0.11	0.08
ST0884B	0.33	1.0	2.9	298.5	6920.	0.750	0.874	0.123	0.15	1.90	1.69	-0.21	-0.12
ST1784R	0.34	1.1	3.3	294.4	24800.	0.539	0.716	0.177	0.28	1.59	2.26	0.67	0.35
ST1784B	0.34	0.8	2.3	294.4	24800.	0.484	0.705	0.222	0.37	1.38	1.95	0.58	0.35
ST2184R	0.36	0.6	1.7	302.2	7350.	0.671	0.827	0.157	0.21	1.78	2.01	0.22	0.12
ST2184B	0.36	0.7	2.0	302.2	7350.	0.721	0.848	0.126	0.16	2.28	2.61	0.32	0.13
Group Average	0.35	0.7	1.9	303.9	27089.	0.619	0.724	0.105	0.18	1.81	1.77	-0.04	-0.01
S. Dev.	0.02	0.3	0.9	5.1	13697.	0.182	0.131	0.087	0.16	0.63	0.53	0.37	0.18
Avg. Abs. Value								0.116	0.19			0.29	0.15
S. Dev.								0.071	0.14			0.22	0.10
28. UNC Auto Exhaust													
OC0483B	0.25	0.4	1.7	299.7	18800.	0.642	0.719	0.077	0.11	1.86	1.97	0.12	0.06
OC0783R	0.33	2.7	8.1	295.5	21600.	0.178	0.391	0.213	0.75	0.94	1.13	0.19	0.18
OC0783B	0.34	2.7	7.9	295.4	21500.	0.451	0.650	0.199	0.36	1.41	1.93	0.52	0.31
JN2582R	0.65	0.6	0.9	301.1*	22700.	0.003	0.013	0.010		0.64	0.58	-0.06	-0.10
JN2582B	0.65	0.6	0.9	301.2*	22900.	0.003	0.014	0.011		0.68	0.58	-0.10	-0.17
JN2982R	0.24	2.5	10.3	303.1	30500.	0.704	0.833	0.128	0.17	2.32	2.10	-0.22	-0.10
JN2982B	0.25	2.5	9.8	303.1	30500.	0.766	0.839	0.073	0.09	2.67	2.18	-0.50	-0.20
JN3082R	0.32	2.8	8.7	302.5*	20000.*	0.811	1.005	0.194	0.21	2.55	2.40	-0.15	-0.06
JN3082B	0.32	0.6	1.7	302.3*	20000.*	0.840	1.011	0.170	0.18	2.68	2.40	-0.28	-0.11
JL0283B	0.19	1.7	9.1	304.0	24500.	0.697	0.850	0.152	0.20	1.65	1.72	0.07	0.04
JL0883B	0.37	1.7	4.6	299.5	21200.	0.879	0.845	-0.034	-0.04	1.76	1.44	-0.32	-0.20
ST2982B	0.39	1.7	4.3	295.7	24800.	0.205	0.057	-0.148	-1.13	1.12	0.76	-0.36	-0.38
OC0682R	0.46	2.0	4.3	300.2	16900.	0.355	0.276	-0.079	-0.25	1.37	1.18	-0.19	-0.15
AU1183R	0.22	2.2	9.9	306.8	21400.	0.850	0.890	0.040	0.05	2.55	2.15	-0.39	-0.17
AU1183B	0.23	0.7	3.1	306.9	21400.	0.601	0.673	0.072	0.11	1.26	1.25	0.00	0.00
JL0182R	0.37	3.5	9.6	299.5	27700.	0.740	1.038	0.298	0.34	2.31	2.40	0.09	0.04
JL0182B	0.35	3.6	10.2	299.3	27400.	0.759	0.995	0.236	0.27	2.41	2.52	0.11	0.05

(continued)

Appendix C. Selected Results of Simulations of Individual Organic-NOx-Air Experiments Using the RADM-P Mechanism (concluded).

Experiment	Initial Concentrations NOx (ppm)	Initial Concentrations HC (ppmC)	Initial Concentrations HC/NOx	Ave Temp (degK)	Ave H2O (ppm)	Maximum Concentration OZONE Expt (ppm)	Maximum Concentration OZONE Calc (ppm)	Maximum Concentration OZONE Calc -Expt (ppm)	Maximum Concentration OZONE Calc -Expt /Avg	Average Initial d([O3] - [NO])/dt Expt --	Average Initial d([O3] - [NO])/dt Calc (ppb/min)	Average Initial d([O3] - [NO])/dt Calc -Expt --	Average Initial d([O3] - [NO])/dt Calc -Expt /Avg
AU0382R	0.44	2.5	5.7	302.6	27400.	0.344	0.450	0.106	0.27	1.26	1.23	-0.02	-0.02
AU0382B	0.16	1.2	7.3	302.6	27400.	0.576	0.501	-0.074	-0.14	1.06	0.93	-0.14	-0.14
ST1782R	0.26	2.2	8.6	300.1	27400.	0.562	0.590	0.028	0.05	1.63	1.16	-0.47	-0.34
ST1782B	0.25	2.4	9.5	300.1	27400.	0.637	0.616	-0.021	-0.03	1.72	1.27	-0.45	-0.30
ST2982R	0.39	1.7	4.4	295.7	24800.	0.073	0.047	-0.026	-0.44	0.86	0.68	-0.18	-0.23
OC0682B	0.46	2.0	4.3	300.2	16900.	0.450	0.328	-0.121	-0.31	1.49	1.27	-0.22	-0.16
JL0283R	0.18	1.6	9.0	304.0	24500.	0.595	0.675	0.080	0.13	1.37	1.37	0.00	0.00
JL0883R	0.37	1.7	4.6	299.5	21200.	0.756	0.694	-0.062	-0.09	1.52	1.32	-0.20	-0.14
JL1583R	0.35	2.2	6.2	306.2	25700.	0.866	0.737	-0.129	-0.16	2.10	1.75	-0.35	-0.18
JL1583B	0.35	2.3	6.6	306.2	25700.	0.922	0.860	-0.062	-0.07	2.20	1.99	-0.21	-0.10
OC0483R	0.25	2.6	10.3	299.7	18800.	0.603	0.672	0.069	0.11	1.76	1.75	-0.02	-0.01
Group Average	0.34	2.0	6.5	301.2	23607.	0.567	0.617	0.050	0.03	1.68	1.55	-0.13	-0.09
S. Dev.	0.12	0.8	3.1	3.3	3802.	0.272	0.314	0.119	0.34	0.61	0.59	0.23	0.15
Avg. Abs. Value								0.104	0.23			0.21	0.14
S. Dev.								0.074	0.24			0.15	0.10
29. SAPRC Synthetic Jet Fuel													
ITC781	0.51	43.0	83.5	303.0	16600.	0.751	0.914	0.163	0.20	2.77	7.54	4.77	0.92
ITC784	0.50	88.0	177.6	303.0	16600.	0.746	0.906	0.160	0.19	3.93	9.86	5.93	0.86
ITC785	0.26	45.0	170.7	303.0	17900.	0.598	0.602	0.004	0.01	2.74	6.65	3.91	0.83
ITC805	0.52	98.0	189.5	303.0	17200.	0.791	0.942	0.151	0.17	3.27	9.39	6.12	0.97
ITC795	0.50	45.0	89.8	303.0	17900.	0.761	0.794	0.033	0.04	3.05	10.78	7.72	1.12
ITC796	0.54	97.0	178.9	303.0	17200.	0.597	0.840	0.242	0.34	4.43	13.31	8.88	1.00
ITC799	0.51	94.0	184.1	303.0	17200.	0.840	0.972	0.131	0.15	4.59	8.44	3.86	0.59
ITC801	0.55	41.0	75.1	303.0	17000.	0.881	0.957	0.076	0.08	2.98	6.14	3.16	0.69
Group Average	0.49	68.9	143.7	303.0	17200.	0.746	0.866	0.120	0.15	3.47	9.01	5.54	0.87
S. Dev.	0.09	27.3	50.8	0.0	499.	0.102	0.122	0.078	0.10	0.74	2.35	2.01	0.17
Avg. Abs. Value								0.120	0.15			5.54	0.87
S. Dev.								0.078	0.10			2.01	0.17
30. SAPRC Synthetic Jet Exhaust													
ITC963	0.49	4.4	9.1	303.0	19400.	0.822	0.722	-0.100	-0.13	4.00	4.15	0.14	0.03
ITC965	0.46	5.2	11.3	303.0	20000.	0.863	0.728	-0.135	-0.17	5.10	5.28	0.18	0.03
ITC967	0.26	4.4	17.2	303.0	18300.	0.586	0.591	0.005	0.01	5.79	6.14	0.35	0.06
ITC968	0.49	8.7	17.8	303.0	19400.	0.852	0.791	-0.061	-0.07	11.76	11.08	-0.68	-0.06
Group Average	0.42	5.7	13.8	303.0	19275.	0.781	0.708	-0.073	-0.09	6.66	6.66	0.00	0.02
S. Dev.	0.11	2.1	4.3	0.0	709.	0.131	0.084	0.060	0.08	3.48	3.06	0.46	0.05
Avg. Abs. Value								0.075	0.10			0.34	0.05
S. Dev.								0.056	0.07			0.24	0.01